Novel Molecular Si(II) Precursors for Synthesis of the First Compounds with Metal-Silicon Triple Bonds

Dissertation

Submitted in fulfillment of the degree

doctor rerum naturalium

(Dr. rer. nat)

of

The Faculty of Mathematics and Natural Sciences

of

The Rheinische Friedrich-Wilhelms-University of Bonn

by

Dipl.-Chem. Oleg Chernov

born in Belgorod, Russia

Bonn, April 2012

Angefertigt mit Genehmigung der Mathematisch-Naturwissenschaftlichen Fakultät der Rheinischen Friedrich-Wilhelms-Universität Bonn

1st	Examiner:	Prof. Dr. A. C. Filippou
2nd	Examiner:	Prof. Dr. J. Beck
3rd	Examiner:	Prof. Dr. A. Gansäuer
4th	Examiner:	Prof. Dr. M. Wagner

Date of dissertation defense: 21. September 2012
Publication year: 2012

Acknowledgements

First, I would like to thank Prof. Dr. Alexander C. Filippou for giving me the opportunity to work in his research group, for his guidance, helpful advices and the thorough evaluation of my thesis including various suggestions for amendments.

I am obliged to many of my colleagues, without their help this dissertation would not have been possible:

Dr. Gregor Schnakenburg for the X-ray diffraction measurements, quantum chemical calculations and of course for correcting the draft of the disertation.

Gabriele Hofer, Katrin Puffler, Kerstin Kühnel-Lysek, Bernhard Beile and Dietmar Kühlmorgen for the synthesis of starting materials and everyday help.

Dr. Jürgen Tirée for his great help in organization of the experimental work.

All of my students, who contributed to my research: Volker Adam, Martin Speer, Jana Haag, Klaas Remmerssen.

Dr. Nils Weidemann for his useful advices and some of precious starting materials.

Dr. Sebastian Schwieger for solving some of my X-ray structures

The NMR department: Karin Prochnicki, Claus Schmidt, Hannelore Spitz and Dr. Wilfried Hoffbauer.

Dr. Sabine Rings and her colleagues for the elemental analysis measurements.

Dr. Burhanshah Lewall for the cyclic voltammetry studies.

Dr. Maurice van Gastel for the EPR measurements in the MPI Mülheim.

Dr. Eckhard Bill and Bernd Mienert for the Mössbauer measurements in the MPI Mülheim.

Phillip Malcho for proofreading the draft of the thesis.

All the group members for the friendly atmosphere, support and help.

For the things we have to learn before we can do, we learn by doing.

Aristotle

Table of Content

1 Introduction

1.1 Silylenes

According to the IUPAC nomenclature, "silylene" is a “generic name for H_2Si: and substitution derivatives thereof, containing an electrically neutral bivalent silicon atom with two non-bonding electrons”.[1] The definition is analogous to that of carbenes.[2]

Silylenes are bent molecules. The silicon center has only 6 valence electrons and is electron-deficient. The geometry and electronic configuration of silylenes (SiXY; X, Y = F–I, H, CH_3, OR etc.) were the subjects of numerous investigations.[3, 4] The experimentally found geometry of silylenes compares well with the results of quantum chemical calculations.[4] Elementary silylenes are diamagnetic species, because of the high singlet-triplet energy gap. Thus, they feature an empty orbital and a non-bonding lone pair of electrons (Figure 1). The electronic unsaturation coupled with the low coordination number predetermines the high reactivity of silylenes. Thus, e.g. the half-life times of the most stable SiF_2 is 150 sec at 0.1 Torr.[5, 6] The reactivity of silylenes is significantly diminished when electron density is donated to the empty orbital, either by direct coordination of a donor or by conjugation with other filled orbitals.

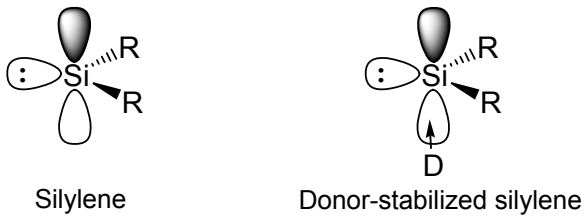

Figure 1: A silylene and a donor-stabilized silylene

Generation of elementary silylenes SiXY (X,Y = F–I, H, CH_3, OR)

The preparation of $(SiCl_2)_n$ upon reduction of $SiCl_4$ with hydrogen in electric discharge was reported as early as in 1937.[7] It was postulated that the initially formed gaseous $SiCl_2$ had rapidly polymerized to produce $(SiCl_2)_n$.[7] In 1938, emission bands of dichlorosilylene, generated by the action of electric discharge on $SiCl_4$ in the gas phase, were reported.[8] The early studies were conducted mostly on elementary silylenes, such as SiH_2, $SiMe_2$, SiF_2 and

$SiCl_2$.[9-11] Various approaches for generation of silylenes were developed, some of them are summarized in Scheme 1.

Redox reactions	Reference
$SiX_4 + Si \xrightarrow[X = F–I]{1000–1500\ °C} 2\ :SiX_2$	X = F[5]; Cl[12] Br[13]; I[14, 15]
$2\ CuCl + Si \longrightarrow 2\ Cu + :SiCl_2$	[16]
$Me_2SiCl_2 + 2\ K/Na \xrightarrow{260–280\ °C} 2\ KCl + :SiMe_2$	[17]
$SiCl_4 + H_2 \longrightarrow 2\ HCl + :SiCl_2$	[18]
Thermal decomposition (disproportionation)	
$Si_2F_6 \xrightarrow{700\ °C} SiF_4 + :SiF_2$	[19]
$MeO(SiMe_2)_2OMe \xrightarrow{225\ °C} Me_2Si(OMe)_2 + :SiMe_2$	[20]
$HSiCl_3 \xrightarrow{> 1000\ °C} HCl + :SiCl_2$	[18]
$SiX_4 \xrightarrow{> 900\ °C} SiX_2 + X_2$	X = Cl[21]; I[14]
$MeSiH_3 \xrightarrow{h\nu} H_2 + :SiHMe$	[22]

Scheme 1: Generation of transient silylenes.

The high reactivity of silylenes was demonstrated by a series of reactions. The most characteristic are: polymerization, insertion into σ-bonds and reactions with unsaturated compounds.[9] The presence of an empty orbital allows the coordination of Lewis bases to silylenes. A number of adducts of transient silylenes with ethers, amines, CO, CS were characterized by IR and UV-vis spectroscopy in solid matrixes at low temperatures.[23] The first room temperature stable silylene-isonitrile adducts have been isolated in 1997 by Okazaki et al.: SiMes(Tbt)←:C=NR (Tbt = -C_6H_2-2,4,6-$(CH(SiMe_3)_2)_3$; Mes = -C_6H_2-2,4,6-Me_3; R = -C_6H_2-2,4,6-*t*Bu_3, -C_6H_2-2,4,6-*i*Pr_3, Tbt).[24]

Disproportionation of silanes

The based-catalyzed disproportionation of silanes can proceed rapidly already at ambient temperatures. It is considered to involve silylene intermediates.[25, 26] For example, the

reaction of Si_2Cl_6 with 2,2′-bipiridyne (bipy) in pentane leads to the formation of a 1:1 Lewis base-adduct of hexachlorodisilane. However, in tetrahydrofuran the formation of $SiCl_4$(bipy) and $SiCl_2(bipy)_2$ was observed (Scheme 2).[27] The dark green formal adduct of dichlorosilylene $SiCl_2(bipy)_2$ was earlier prepared by the reaction of $SiCl_4$(bipy) with Li_2[bipy].[28] On the basis of variable temperature EPR studies $SiCl_2(bipy)_2$ was suggested to be a *cis*- octahedral complex, featuring two η^2-coordinated bipyridil radical anions.[29] The base-catalyzed disproportionation of Si_2Cl_6 including the putative formation of the intermediate $SiCl_2$ has been also reported.[30]

The disproportionation of 1,1,2,2-chloro-1,2-dimethyldisilane in the gas phase at about 500 °C leads to the formation of SiClMe.[31] The same disproportionation in the presence of 1-methylimidazole in solution results in the formation of $MeSiCl_3$ and several products of the insertion of SiClMe fragment into the Si–Cl bonds of the starting material.[25] The suggested mechanism includes the intermediate formation of the donor-stabilized silylene SiClMe (Scheme 2). The formation of donor-stabilized $SiCl_2$ upon disproportionation of Si_2Cl_6 is also supported by recent findings.[26]

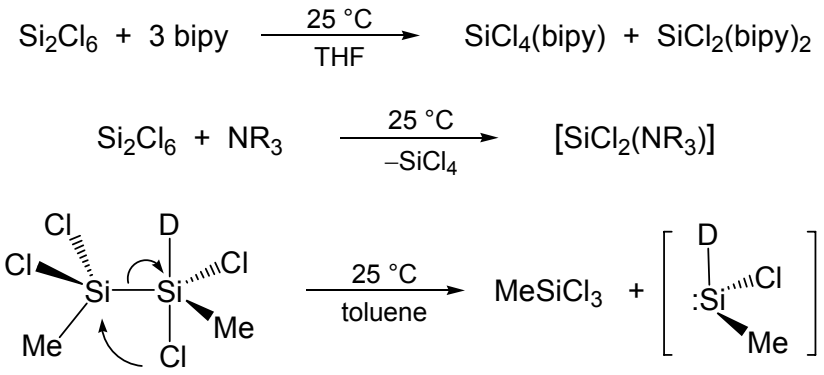

Scheme 2: Base-induced disproportionation of disilanes. D = 1-methylimidazole.

Recently, the disproportionation of Si_2Cl_6 by tertiary amines was studied. The mechanism, including the intermediate formation of the $Si_2Cl_6(NR_3)$ adduct and its disproportionation to $SiCl_4$ and $SiCl_2(NR_3)$ was proposed on the basis of calculations. Interestingly, by H,Si-correlation NMR spectroscopy, the putative intermediate $SiCl_2(NMe_2Et)$ was observed in solution at –10 °C (δ = 42.7 ppm).[26] Generation of $SiCl_2$ upon decomposition of $Me_3GeSiCl_3$ at RT and trapping reaction with a phosphaalkene was also reported.[32]

Silylenoids

In analogy to the carbenoids, the silylenoids can be defined as «complexed silylenes, that display the reactivity characteristics of silylenes, either directly or by acting as sources of silylenes».[33]

Wiberg et al. reported, that substituted halosilyl anions decompose already at low temperatures, forming halosilylenes R*SiX (Scheme 3) or disubstituted silylenes $SiR*_2$ (R* = -Si(*t*Bu)$_3$; X = Cl. Br, I).[34] The intermediacy of silylenes was deduced on the basis of their reactivity. Silylenes R*SiX (X = H, Me, Ph, Br) were also generated upon thermolysis of the corresponding silanes $R*_2SiX_2$ and characterized by trapping reactions.[34]

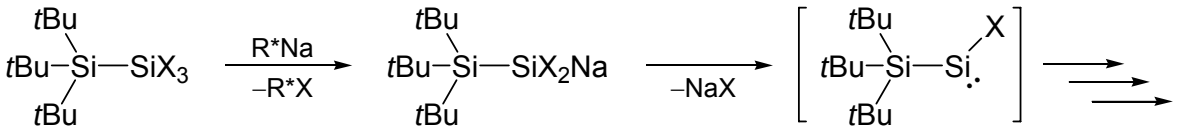

Scheme 3: Formation of organohalosilylenes from silylenoids. R* = -Si(*t*Bu)$_3$; Cl, Br, I.

Reduction of $(Me_3Si)_3C–SiBr_3$ with lithium naphtalenide in THF at –78 °C afforded an orange compound of unknown structure. The trapping reactions were consistent with the formation of the bromosilylene $(Me_3Si)_3C–SiBr$.[35] However, the ^{29}Si NMR shift of **1** along with DFT calculations suggested that the product of the reaction is a silylenoid **1**·LiBr (Scheme 4).

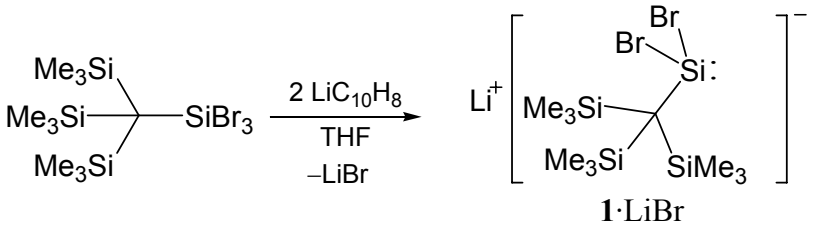

Scheme 4: Reduction of tribromotris(trimethylsilyl)methylsilane.

The Benkeser reagent

The Benkeser reaction is the hydrogenation of aromatic hydrocarbons or alkenes with calcium or lithium in the presence of amines, named in the honor of R. A. Benkeser, the inventor of the reaction.[36] R. A. Benkeser is also known for his research of the chemical properties of the mixture of trichlorosilane and a tertiary amine *(Benkeser reagent)*.[37] Thus, a mixture of $SiHCl_3$ with R_3N (typically *n*Pr$_3$N) was successfully employed for the hydrosilylation of alkynes,[38] reduction of polyhalo compounds,[39] reduction of carbonyl group of aldehydes,

ketones and acylchlorides to substituted alkyltrichlorosilanes,[40] silylation of organic halides,[41] and reduction of imines to amines.[42] The reactive intermediate in the reactions was suggested to be the trichlorosilyl anion $SiCl_3^-$, generated according to Scheme 5.[37]

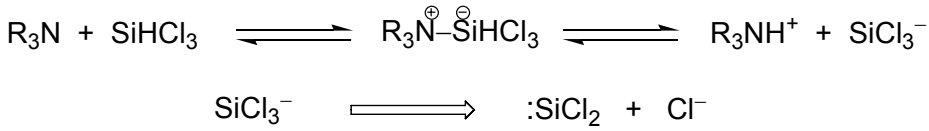

Scheme 5: The reaction of tertiary amines with trichlorosilane. $SiCl_3^-$ as a source of $SiCl_2$.

The formation of the trichlorosilyl anion was evidenced by ^{1}H NMR spectroscopy. Thus, addition of nPr$_3$N to trichlorosilane in acetonitrile leads to gradual rise of the signal of the ammonium ion nPr$_3$NH$^+$ and disappearance of the signal of $SiHCl_3$.[43] The trichlorosilyl anion can be considered as a silylenoid which upon elimination of the chloride anion forms dichlorosilylene $SiCl_2$ (Scheme 5). The intermediacy of $SiCl_2$ in the above mentioned reactions was considered, however, the experimental results indicated that such species were not involved.[37]

The mixture of $SiHCl_3$ and DABCO (1,4-diazabicyclo[2,2,2]octane) or DBU (1,8-diazabicyclo[5.4.0]undec-7-ene) was later used for preparation of silicon containing N-heterocycles starting from diazabutadienes. The reactions were suggested to proceed via the $SiCl_3^-$ intermediate ($SiCl_2$-synthon).[44] The reactions of tertiary amines with trichlorosilane are closely related to the recently reported NHC-induced dehydrochlorination of $SiHCl_3$, leading to an NHC-stabilized dichlorosilylene $SiCl_2$(IDipp).[45] Our investigations on related systems will be presented in section 2.1.2, p. 44.

Stable Si(II) compounds

Several comprehensive reviews covered the recent developments in the chemistry of low-valent silicon compounds.[46, 47] Here the most characteristic examples will be presented.

The first stable Si(II) compound – decamethylsilicocene – was isolated in 1989 in the group of P. Jutzi.[48] The compound was synthesized from the corresponding dihalide upon reduction with alkali metals (Scheme 6).

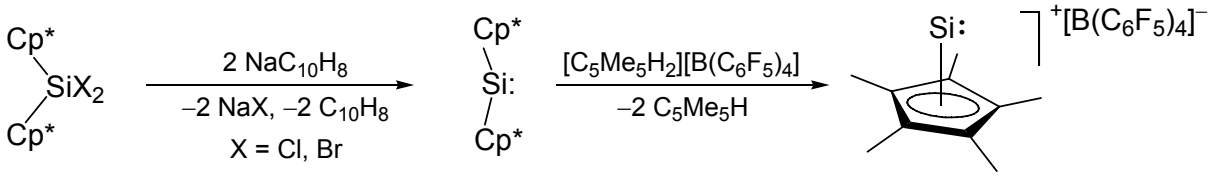

Scheme 6: Decamethylsilicocene – the first stable Si(II) compound.[48, 49]

The cyclopentadienyl ligands are η^5-coordinated. In the solid state two geometrical isomers of the compound were found. The first isomer features coplanar Cp* rings and is isotypical to decamethylferrocene, the second isomer has a bent structure. However, the compound exhibits a bent structure in the gas phase according to gas electron diffraction. Decamethylsilicocene features a very unusual chemical ^{29}Si NMR shift at –392.0 ppm, because of the two η^5-Cp* ligands.

Protonation of the decamethylsilicocene with $[C_5Me_5H_2][B(C_6F_5)_4]$ led to the formation of an unprecedented π-complex of a divalent silicon atom (Scheme 6).[1] The complex features a η^5-coordinated pentametylcyclopentadienyl ligand and a naked silicon center.[49] The Cp^*Si^+ fragment is reactive towards nucleophiles. Thus, the reaction of the cation with $K[Cp^*Fe(CO)_2]$ afforded the first metallasilylene $[Cp(CO)_2Fe–Si(\eta^3\text{-}Cp^*)]$; treatment with lithium salts of substituted cyclopentadienes led to the unsymmetrically substituted sandwich complexes.[50, 51]

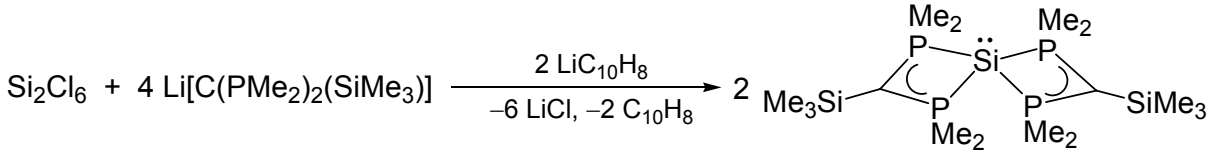

Scheme 7: Synthesis of tetraphosphino-substituted donor-stabilized silylene.[52]

In 1990 a four-coordinate stable Si(II) compound was reported by Karsch et al. (Scheme 7).[52] The silicon center exhibits a pseudo-trigonal bypyramidal geometry, suggesting the presence of a stereochemically active lone pair. The compound can be viewed as a bis-donor stabilized silylene.

[1] Interestingly, when the protonation was carried out with HBF_4, a dimer $[Cp^*SiF]_2$ was isolated.[43]

N-heterocyclic silylenes

Electronic stabilization of silylenes can be achieved by analogous methods as in the case of carbenes. After the isolation of the first N-heterocyclic carbene (NHC) by Arduengo et al.,[53] several stable N-heterocyclic silylenes (NHSi) were reported.

The first bis(amino) silylene $Me_2Si(NtBu)_2Si$: (**2**) was prepared upon irradiation of the corresponding bis(azide) $Me_2Si(NtBu)_2Si(N_3)_2$ in argon matrix by Veith et al. in 1992 (Scheme 8).[54] The silylene was characterized by IR spectroscopy; it is stable at 77 K but decomposes at higher temperatures.

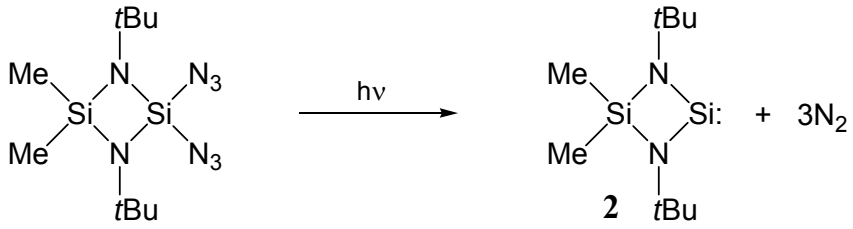

Scheme 8: Synthesis of the first bisaminosilylene **2** by Veith et al.[54]

Later, in 1994 two similar N-heterocyclic silylenes were prepared by Denk et al.[55] and Green et al.[56] Both silylenes were synthesized upon reduction of corresponding silicon(IV) dihalo-precursors with metals (Scheme 9). Compound **3** is remarkably stable and can be distilled at 85 °C (0.1 Torr); its solution in toluene showed no sign of decomposition after heating at 150 °C for 4 months. The silylene **4** slowly undergoes intermolecular insertion into the Si–N bond at ambient temperature. [57] The thermal stability of **3** and **4** contrasts with that of the acyclic silylene **2** , which is stable only below 77 K.[54]

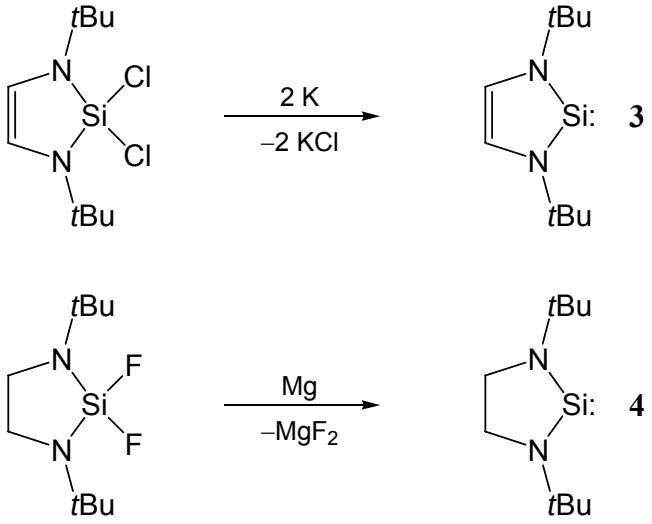

Scheme 9: Synthesis of the first stable N-heterocyclic silylenes.[55, 56]

Several substituted N-heterocyclic silylenes were prepared by analogous methods, including benzo- and pyridino-annelated systems (Scheme 10).[58] Interestingly, silylene **5** forms a stable adduct with an NHC, despite of the fact, that the *p*-orbital of silicon is involved to significant extend in the 6π-electron aromatic system.[59, 60] The adduct **6** features a trigonal pyramidal silicon center and a rather long Si–C bond (2.162(5) Å). The geometry of **6** suggests the presence of a stereochemically active lone pair at the Si atom.

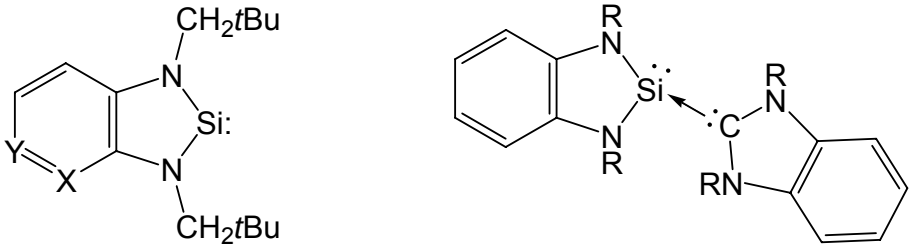

5 X = Y = CH; X = N; Y = CH; X = CH; Y = N

6 R = CH_2tBu

Scheme 10: Bicyclic N-heterocyclic silylenes (left) and a silylene-carbene adduct **6** (right).

An interesting example of a six-membered bis(amino) silylene **7** with ambivalent reactivity was reported by Driess et al. (Scheme 11).[61] The compound forms a stable Lewis adduct with 1,3,4,5-tetramethylimidazol-2-ilydene (**8**) and reacts with electrophiles.[62] Treatment of **7** with trimethylsilyl triflate leads to formation of the donor-stabilized silylene **9**, bearing a reactive OTf substituent (Scheme 11).

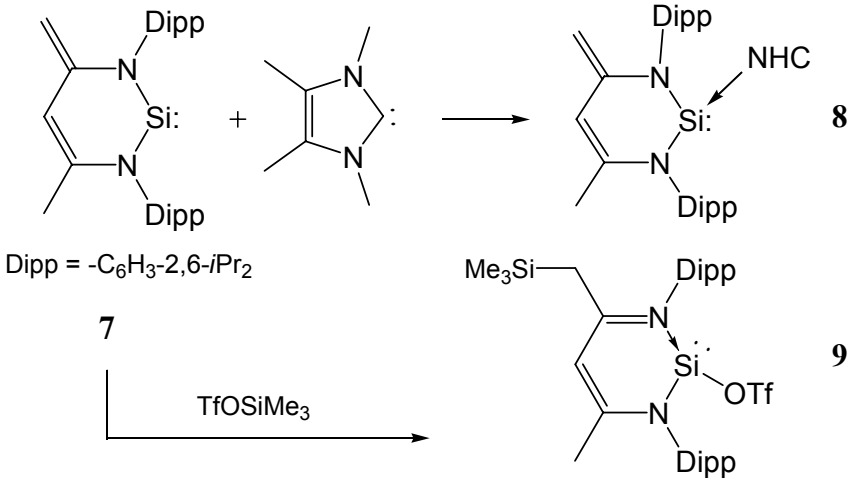

Scheme 11: Reactivity of β-diketiminato substituted silylene **7**. OTf = $-OSO_2CF_3$.

The first stable chlorosilylene was reported in 2006 by Roesky et al. [63-65] The compound was synthesized from the corresponding trichlorosilane upon reduction with potassium. The electronic stabilization is provided by the chelating amidinato ligand. The presence of the

chloro-substituent opens access to various substituted silylenes by treatment of **10** with nucleophiles.

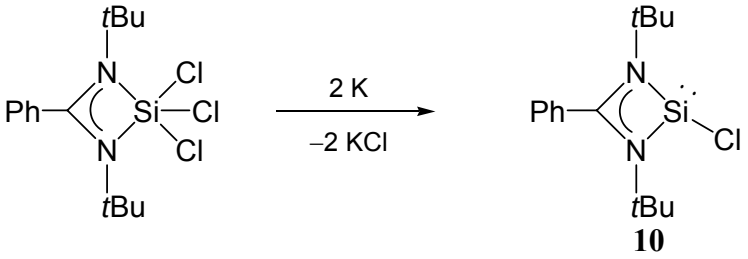

Scheme 12: Synthesis of the first stable chlorosilylene.

Notable silylenes

The first stable bis(alkyl) silylene was reported in 1999 by Kira et al.[66] The stability of the compound is attributed to the steric protection and to a minor part to the electronic effect of the $SiMe_3$ groups. However, the silylene decomposes slowly at room temperature upon 1,2-shift of the $SiMe_3$ group, thus forming a silaethene (Scheme 13):

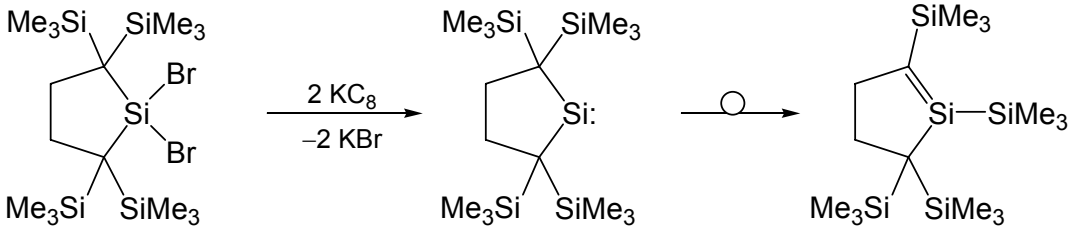

Scheme 13: Synthesis and isomerization of the first bisalkylsilylene.

The silylenes presented above have a singlet ground state. The first transient triplet silylene $Si(tBu_3Si)_2$ was generated upon decomposition of the silylenoids $(tBu_3Si)_2SiLiX$ (X = F, Cl, Br) and characterized by trapping reactions.[34] However, the intermediacy of the triplet silylene had not been directly proven. Later $Si(tBu_3Si)_2$ was synthesized upon photolysis of the corresponding silacyclopropenes at 77 K (Scheme 14) and was unambiguously shown by EPR spectroscopy to have a triplet ground state in agreement with theoretical predictions.[2,67]

[2] The silylene $tBu_3Si–Si–Si(iPr)_3$ was also suggested to have a triplet ground state on the basis of its reactivity, however the hypothesis was not confirmed by EPR studies: P. P. Gaspar, M. Xiao, D. H. Pae, D. J. Berger, T. Haile, T. Chen, D. Lei, W. R. Winchester, P. Jiang, *J. Organomet. Chem.* **2002**, *646*, 68.

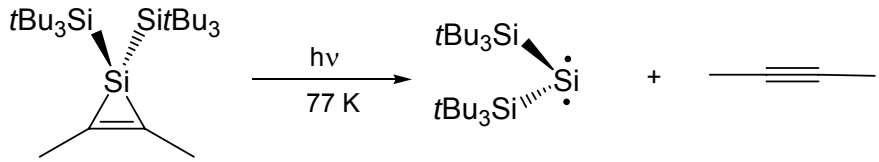

Scheme 14: The triplet ground state silylene.

Carbene-stabilized and amine-stabilized silylenes

In the previously mentioned NHC adducts of silylenes **6** and **8** the carbene does not play an important role in stabilization, since the free silylenes **5** and **7** are already stable at room temperature. The first silylenes, stabilized solely by NHCs were reported by Robinson et al. in 2008 (Scheme 15).[68]

The reduction of the NHC adduct of $SiCl_4$ with potassium graphite in THF afforded the bis(carbene)-stabilized disilene **12**, whereas the reduction in hexane afforded the bis(carbene)-stabilized dichlorodisilylene **11**. Both compounds were isolated as room temperature stable solids. The Si center in disilylene **11** exhibits a trigonal pyramidal geometry, similar to that of other NHC-adducts of silylenes **6** and **8**, suggesting the presence of a lone pair of electrons at the Si center. The Si–C bonds in **11** and **12** are rather short, suggesting rather strong donor-acceptor C–Si bonds.

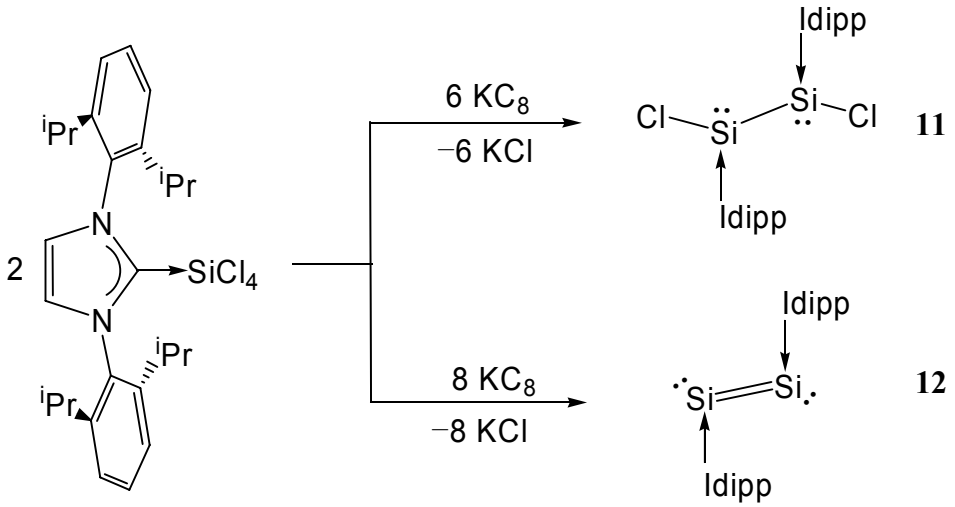

Scheme 15: Synthesis of NHC-stabilized dichlorodisilyne and Si_2 molecules, Robinson *et al.*
IDipp = 1,3-bis(2,6-diisopropylphenyl)-imidazol-2-ylidene.

Only recently, a pyridine-stabilized silylene was reported. The synthesis of the compound includes the reduction of an aryltribromosilane with lithium naphtalenide to give the *trans*-diaryldibromodisilene **13**, which exists in equilibrium with the corresponding

arylbromosilylene.[69] Addition of an amine shifted the equilibrium to the formation of the amine-stabilized arylbromosilylene **14**, which was isolated and structurally characterized. Notably, the ^{29}Si NMR shift of **14** (59.3 ppm) compares well with that, observed for the putative complex $SiCl_2(NMe_2Et)$ (42.7 ppm, –10 °C).[26]

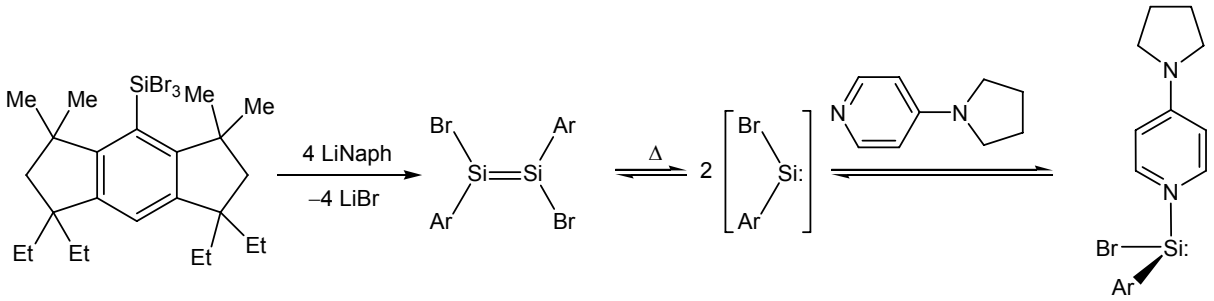

13 **14**

Scheme 16: The synthesis of the first amine-stabilized silylene.

1.2 Silylidene complexes [$L_nM{=}SiR_2$]

The first transition metals carbene complex $[(CO)_5W{=}CMe(OMe)]$ was discovered by E. O. Fisher et al. in 1964.[70] It was followed by the complex $(t\text{BuCH}_2)_3\text{Ta}{=}\text{CH}(t\text{Bu})$, prepared by R.R. Schrock in 1974.[71] Perhaps the most well-known applications of carbene complexes are the metathesis of alkenes and cross coupling reactions.[72, 73]

The close relationship of carbon and silicon inspired the research of heavier analogues of carbene complexes. Currently the research is ongoing in exploration of the chemistry of transition-metal silylidene complexes. The complexes are considered to be intermediates in several metal-catalyzed reactions, involving organosilicon compounds.[74] Recently, the ruthenium complex $[\text{Cp}^*(i\text{Pr}_3\text{P})\text{Ru}(\text{H})_2{=}\text{SiHPh}{\cdot}\text{Et}_2\text{O}][\text{B}(\text{C}_6\text{F}_5)_4]$ was shown to catalyze the hydrosilylation of alkenes.[75]

The silylidene complexes may be defined as complexes bearing a silylene as a ligand: $L_nM{=}SiR_2$. The silicon center in silylidene complexes is planar and the TM–Si bond possesses multiple bond character, and can be reasonably described by the Dewar-Chatt-Duncanson model. The overlap of the lone pair of the silicon fragment with an empty orbital of the metal fragment forms a σ-bond. The backdonation from a filled *d*-orbital of the metal to the empty *p*-orbital corresponds to a π-bond (d_π-p_π donation) (Figure 2).[76] The common feature of the silylidene complexes is the electrophilic silicon center, which can coordinate a Lewis base to form a base-stabilized silylidene complex. In such cases the TM–Si bond is elongated, as the result of the reduced backbonding from the metal to the silicon center.

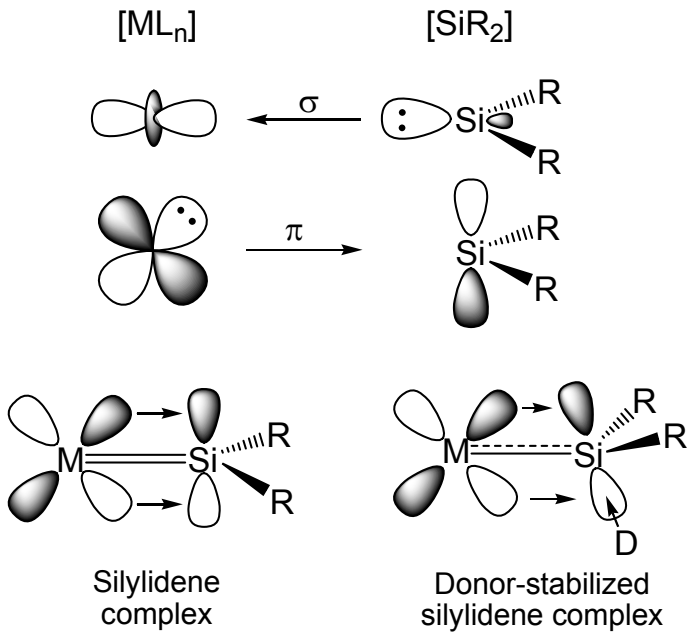

Figure 2: Bonding description of a transition-metal silylidene complex and a donor stabilized silylidene complex by the Dewar-Chatt-Duncanson model.

Transition-metal silylidene complexes were isolated relatively recently, despite the ongoing efforts from the 1960s.[77] The silicon center in silylidene complexes is electrophilic, and the first isolated complexes were base-stabilized: $[(CO)_4FeSi(O\textit{t}Bu)_2(OP(NMe_2)_3)]$[78] and $Cp^*(PMe_3)_2RuSiPh_2(NCMe)][BPh_4]$[79] reported in 1987, followed by $[Cp^*(CO)Fe\{(SiMe_2)_2OMe\}$ in 1988.[80] Whereas these complexes may be considered as silylidene complexes, the long M–Si bond length and the distorted tetrahedral geometry of the silicon center resemble those of silyl complexes.[77]

The first base-free silylidene complexes $[Cp^*(PMe_3)_2Ru{=}Si(SR)_2][BPh_4]$ (R = Et, -C_6H_3-4-Me) were prepared from the corresponding triflate-derivatives $[Cp^*(PMe_3)_2Ru–Si(SR)_2OTf]$ by reaction with $Na[BPh_4]$.[81] Several base-free silylidene complexes were reported since then. There are three general synthetic approaches to these complexes (Scheme 17).

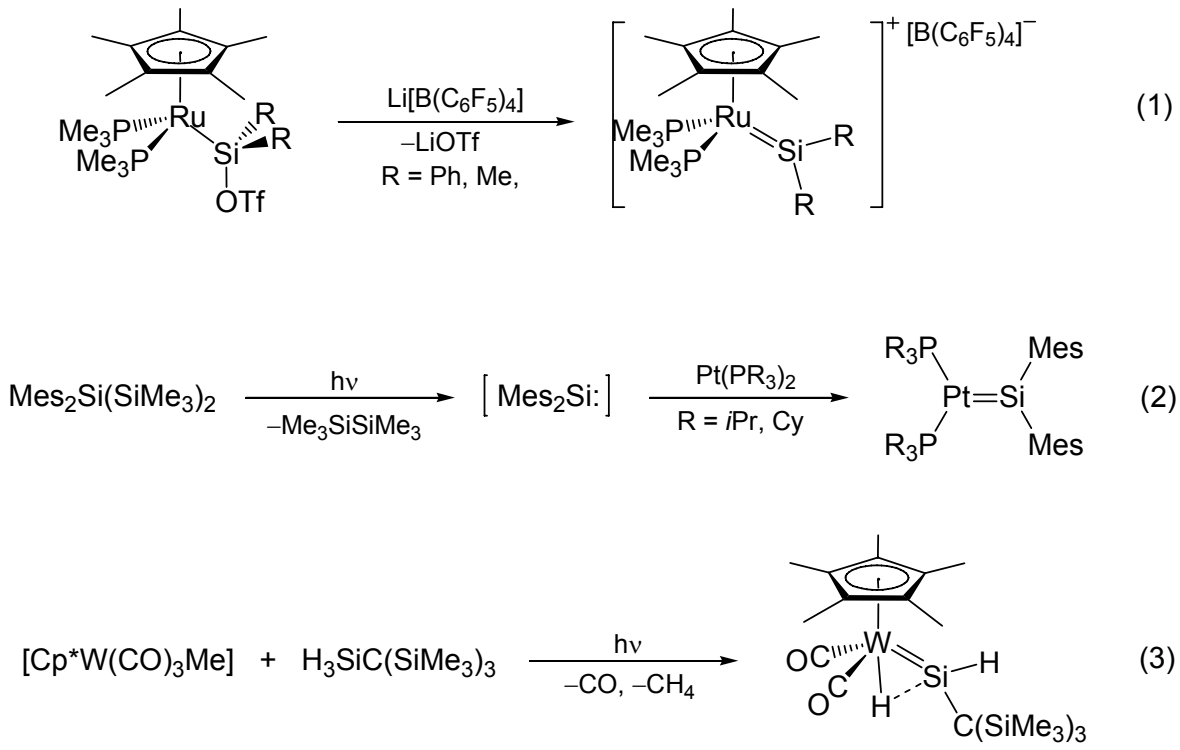

Scheme 17: Synthesis of silylidene complexes by ligand abstraction (1), coordination of a silylene to a TM (2), and migration of an α-substituent (3).

Abstraction of an anionic group from a transition-metal silyl complex, leading to a cationic silylidene complex. The approach was used for the preparation of complexes of Group 8, 9 and 10 metals.[82, 83] Because of the positive charge, these complexes feature a very electrophilic silicon center.

The isolation of N-heterocyclic silylenes opened access to NHSi complexes of transition metals via ligand substitution by NHSi.[47, 84] These complexes resemble the base-stabilized silylidene complexes, because the silicon center is stabilized by p_π-p_π donation from two nitrogen substituents. As the result of the stabilization, the complexes are only weak Lewis-acids and resemble the donor stabilized silylidene complexes. The ^{29}Si NMR resonances of NHSi-complexes (97.5–146.9 ppm) appear at similar positions to those of base-stabilized complexes.[77] However, coordination of a transient silylene $SiMes_2$ was utilized to prepare a base-free complex.[85]

The migration of an α-substituent of a silyl substituent to a vacant coordination site of a metal (typically 16 VE) affords silylidene complexes. The 1,2-migration of hydrogen afforded silylidene complexes of Mo,[86-88] W,[89-91] Ru,[92, 93] Os,[94] Ir[95] and Pt.[96] The 1,2-migration of SiR_3 group afforded silylidene complexes of Fe[97] and Ru;[98] 1,2-migration of alkyl/aryl group afforded base-stabilized complexes of W.[99, 100]

The silylidene complex $[(\eta^5\text{-}C_5H_4Et)_2(PMe_3)Hf{=}Si(Si\textit{t}Bu_2Me)_2]$ was obtained by treatment of $(\eta^5\text{-}C_5H_4Et)_2HfCl_2$ with $Li_2Si(Si\textit{t}Bu_2Me)_2$ in the presence of PMe_3.[101]

The synthesis of silylidene complexes is based on Si(IV) precursors, except of the syntheses of transition-metal N-heterocyclic silylene complexes. Also, the specificity of the existing methods lays restrictions upon the substituents at the silicon center. A possible general strategy to various silylidene complexes could be based on silylidene complexes, bearing reactive substituents, e.g. halide or OTf^- ($CF_3SO_3^-$). Nucleophilic substitution of the halide can be a rational approach to a variety of compounds.

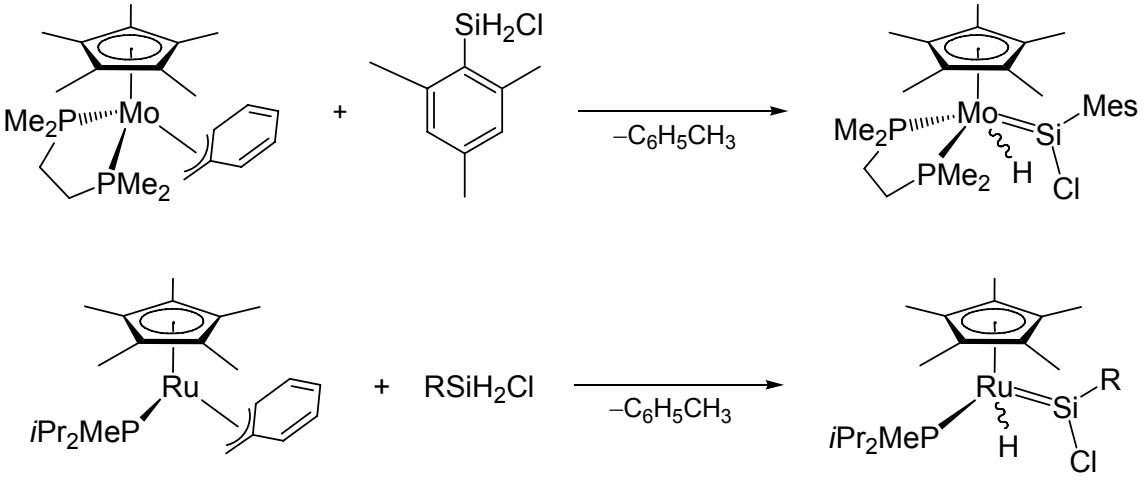

Scheme 18: Synthesis of halosilylidene complexes.

The halosilylidene complexes were reported only recently and are rare, a molybdenum and a ruthenium complex have been reported (Scheme 18). The research in this field is currently underway.[87, 92]

1.3 Group 14 ylidyne complexes $[L_nM{\equiv}E{-}R]$ (E = Ge–Pb)

After the discovery of transition-metal carbene complexes, E. O. Fischer et al. reported the first carbyne complex $[Br(CO)_4W{\equiv}C{-}CH_3]$.[102] Several years later Schrock et al. synthesized the alkylidyne complex $[Cp^*Cl(PMe_3)_2Ta{\equiv}C{-}Ph]$. Subsequently, alkylidyne complexes were developed, which efficiently catalyze the metathesis of alkynes, e.g. $[(\textit{t}BuO)_3W{\equiv}C{-}Ph]$.[103]

The bonding in ylidyne complexes $L_nM{\equiv}E{-}R$ (E = C–Pb) can be described reasonably by the Dewar-Chatt-Duncanson model (Figure 3).[76] The positively charged $[ER]^+$ fragment bears a lone pair of electrons and two empty orbitals. The donation from the lone pair to an empty orbital of the metal fragment ML_n forms the σ-component of the bond. Backdonations

from appropriately filled orbitals of the metal fragment to the two empty p-orbitals of $[ER]^+$ form two orthogonal π-bonds.

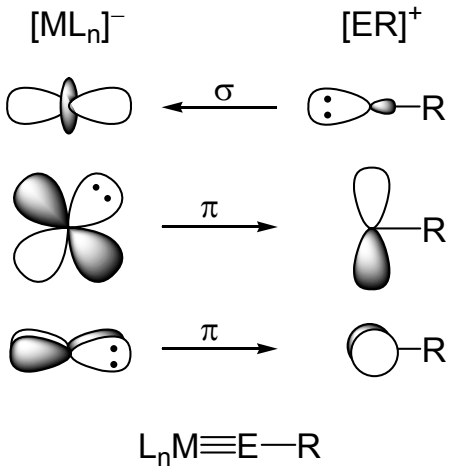

Figure 3: Bonding description of a transition-metal ylidyne complex by the Dewar-Chatt-Duncanson model; E = C–Pb.

As in the case of alkylidene complexes, the heavier analogues of alkylidyne complexes are inherently less stable than the alkylidyne complexes itself. The first germylidyne complex was synthesized only in 1996 by Power et al. upon treatment of the molybdenum carbonyl metallate $Na[CpMo(CO)_3]$ with $Ge(C_6H_3\text{-}2,6\text{-}Mes_2)Cl$ according to equation (1), Scheme 19.[104] The approach was extended to chromium and tungsten, as well as to the bulkier germylene $Ge(C_6H_3\text{-}2,6\text{-}Trip_2)Cl$.[105] Later, a principally new approach to the germylidyne complexes has been developed by Filippou et al., taking advantage of the Ge–halogen bond activation by electron rich dinitrogen complexes of molybdenum and tungsten (Scheme 19, equation (2).[106, 107]

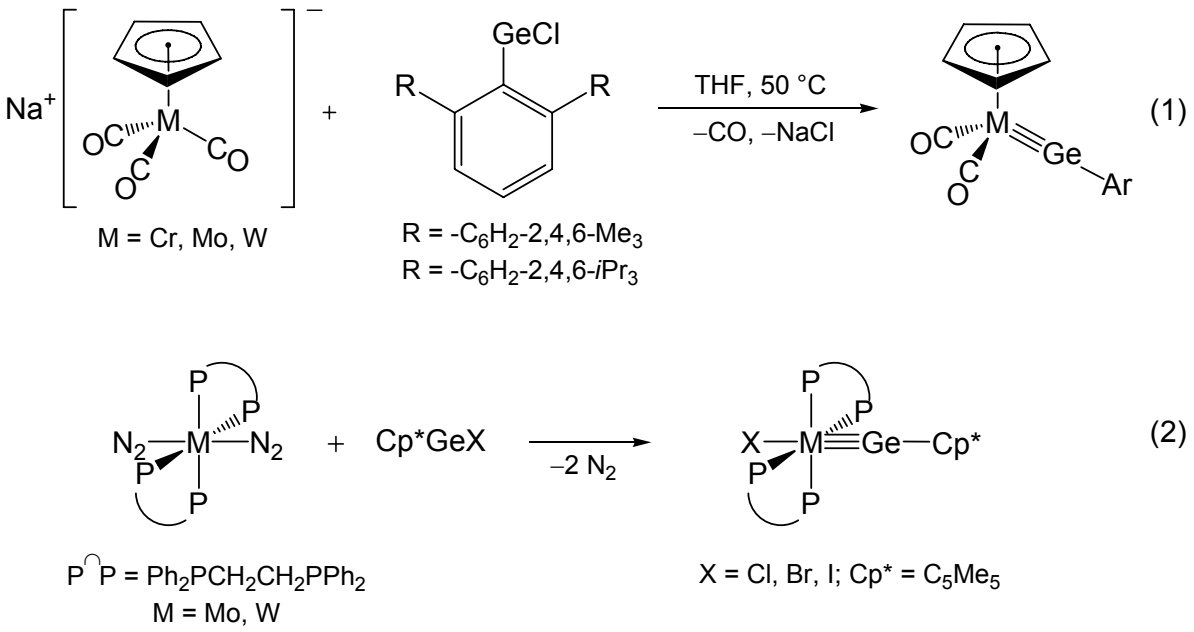

Scheme 19: Synthesis of the first germylidyne complexes by Power et al.[104, 105] and Filippou et al.[106, 107]

The synthesis of the germylidyne complexes was followed by the isolation of phosphane-substituted stannylidyne and plumbylidyne complexes (Figure 4, A).[106-109] Very recently, ylidyne complexes of Group 7 (manganese, renium) and group 8 (iron, ruthenium) metals were prepared (Figure 4, B,[110] C[3] and D[111, 112]).

Metallaylenes are in close relation to ylidyne complexes. The first ferriogermylene was reported in 1994 by Jutzi et al. (Figure 5, complexes A).[113] Later, in the synthesis of germylidyne complexes from carbonyl metallates (Scheme 19, equation 1) metallagermylenes were found to be intermediates, which upon decarbonylation lead to the final products. In several cases metallagermylenes were isolated and structurally characterized (Figure 5, complexes B).[105] In the cases of tin and lead, decarbonylation of complexes B does not occur. Base-stabilized ferrioylenes have been prepared, but no decarbonylation reactions were reported (Figure 5, complexes C).[114, 115] Notably, ferriogermylenes $[Cp(CO)_2Fe–Ge–CH(SiMe_3)_2]$, $[Cp(CO)_2Fe–Ge–Mes^*]$, and $[Cp^*(CO)_2Fe–Ge–Mes^*]$, (Mes* = -C_6H_2-2,4,6-tBu$_3$)$_2$ could not be decarbonylated to the iron germylidyne complexes.[50]

[3] U. Chakraborty, *unpublished results*, University of Bonn, **2011**.

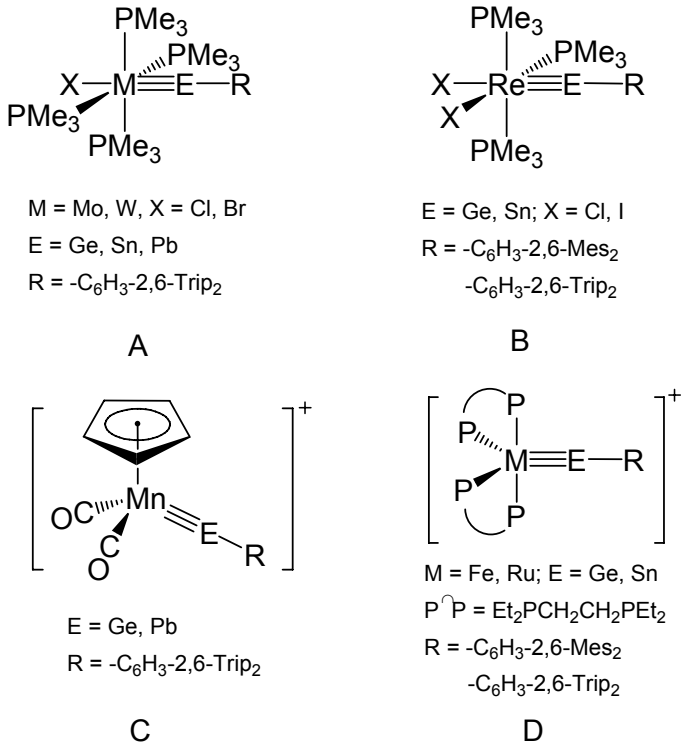

Figure 4: Types of ylidyne complexes of Group 6, 7, 8 transition metals.

Recently, decarbonylation of ferriostannylenes (Figure 5, complexes D) leading to formally dimer of stannylidyne complexes $\{Cp(CO)FeSnR\}_2$, featuring a planar Fe_2Sn_2, core was reported.[116]

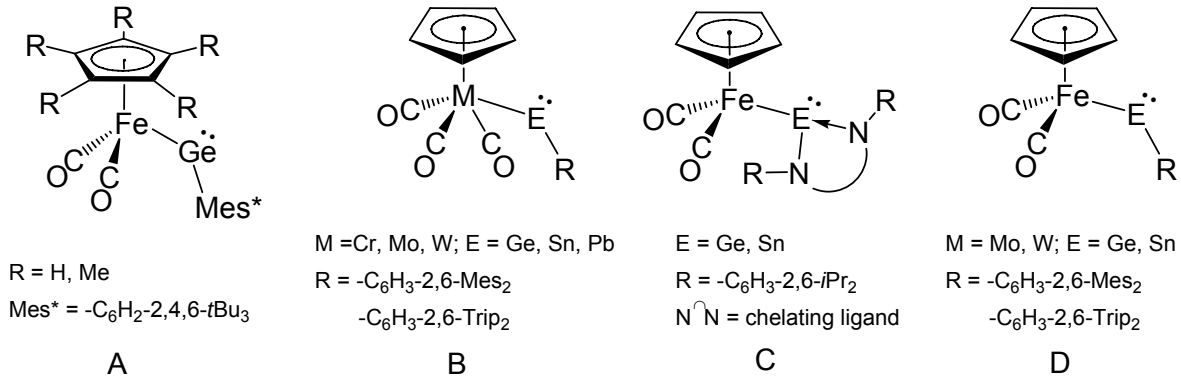

Figure 5: Stable metallagermylenes and stannylenes.

The silylidyne complexes are to the best of our knowledge presently unknown. A base-stabilized silylidyne complex $[Cp^*(Me_3P)_2RuSi\{(bipy)(SC_6H_4\text{-}4\text{-}Me)\}][OSO_2CF_3]_2$ was reported, however it features a four-coordinate silicon center and resembles more a silyl complex (Figure 6).[117] Jutzi et al. reported recently a ferriosilylene $[Cp^*(CO)_2Fe\text{–}Si(\eta^3\text{-}Cp^*)]$, a possible precursor for the silylidyne complex $[Cp^*(CO)Fe{\equiv}Si(Cp^*)]$.[50]

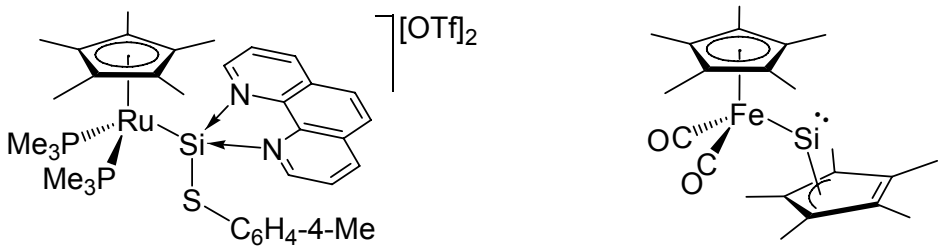

Figure 6: The bis-donor stabilized silylidyne complex and a ferriosilylene, OTf = -OSO_2CF_3.[50, 117]

Tilley et al. reported in 2003 a cationic molybdenum complex with considerable silylidyne character.[87] The complex was prepared upon abstraction of chloride from the corresponding chlorosilylidene complex. The position of the hydrogen atom was not precisely determined, however it was suggested to be in a bridging position between the molybdenum and the silicon atom in agreement with DFT calculations.[87]

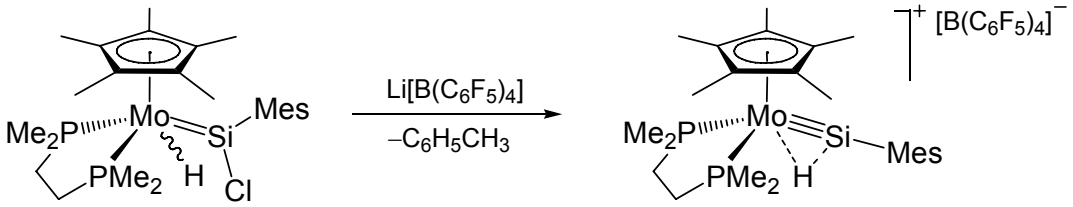

Scheme 20: Synthesis of a molybdenum complex with considerable silylidyne character.

The Mo–Si bond is very short and the Mo-Si-C angle is almost 180°, suggesting the silylidyne character of the complex, despite of the Si–H interaction.[87, 118, 119]

Synthesis of genuine silylidyne complexes remains a challenging task in coordination chemistry of silicon compounds.

1.4 Goals and objectives of the work

In the last years, complexes, featuring triple bonds between heavier analogues of carbon and transition metals have been isolated. The syntheses of these complexes relies solely on the E(II) precursors, ERX, where E = Ge, Sn, Pb, X = Cl, Br, NMe_2 and R = 2,6-Mes_2-C_6H_3-, 2,6-$Trip_2$-C_6H_3-. The synthesis of silylidyne complexes by this approach was hampered due to the lack of suitable Si(II) compounds.

The heavier Group 14 element homologues of alkylidyne complexes are a relatively new class of compounds and very little is known about their reactivity. The marked difference between carbon and its heavier Group 14 analogues presumes a quite different chemistry of the ylidyne complexes in comparison to alkylidyne complexes. Proceeding from this, the objectives of this work were:

- to develop access to synthetic equivalents of silylenes SiRX, where X = halogen.
- to synthesize silylidyne complexes based on these precursors.
- to investigate the reactivity of silylidyne complexes.

2 Results and discussion

2.1 Carbene-stabilized silylenes SiX_2(NHC) and SiArCl(NHC) (NHC = N-heterocyclic carbene; X = halogen; Ar = aryl group)

N-heterocyclic carbenes (NHCs) are well known two electron σ-donors. In this work N-heterocyclic carbenes were employed to stabilize silylenes of the type SiX_2 and SiArX (Ar = aryl group, X = halogen). The NHCs are advantageous over chelating donors, previously used for the stabilization of silylenes.[61, 64] The monodentate NHC ligand can be abstracted from the silicon center, in contrast, abstraction of the chelating ligand (e.g. N,N-tethered group) in donor stabilized silylenes is not feasible. In addition, stabilization by NHCs allows functionalization of the silylene on both substituents X and Y, whereas in the case of chelating ligand only one X can be replaced e.g. by a nucleophile. In other words, carbene-stabilized halosilylenes can provide access to a wider variety of substituted silylenes.

General consideration on bonding of carbenes to silylenes

NHCs are room temperature stable compounds. The presence of a lone pair on the carbon atom accounts for the strong σ-donor properties of NHCs. The electronic stabilization of the carbene carbon atom arises from the interaction of the nitrogen lone pairs with the empty *p*-orbital of the carbon atom. This interaction dramatically decreases the electrophilicity of the carbon atom, rendering the NHCs weak π-acceptors. As the result, metal-NHC complexes feature almost no backbonding from the metal center.

However, in 1,1,2,2-tetraaminoalkenes (carbene dimers) the central bond is a distinct double bond.[4] In these cases the nitrogen atoms are pyramidal, suggesting that the interaction between the nitrogen lone pairs and the empty *p*-orbital of carbon atom is diminished.

[4] According to a CSD survey from 07.2011 of 30 structurally characterized 1,1,2,2-tetraaminoalkenes the mean C=C bond length is 1.34(1) Å. Median *d*(C–C) = 1.345 Å, LQ = 1.329 Å, HQ = 1.354 Å. Here and later the following abbreviations are used: LQ – the highest value in the lower quarter, HQ – the lowest value in the higher quarter.

Consequently, the C=C double bond length is nearly the same as in normal alkenes. Two structurally very close examples are presented in Figure 7, featuring essentially the same bond length, emphasizing the fact, that carbenes can participate in double bonding.[120]

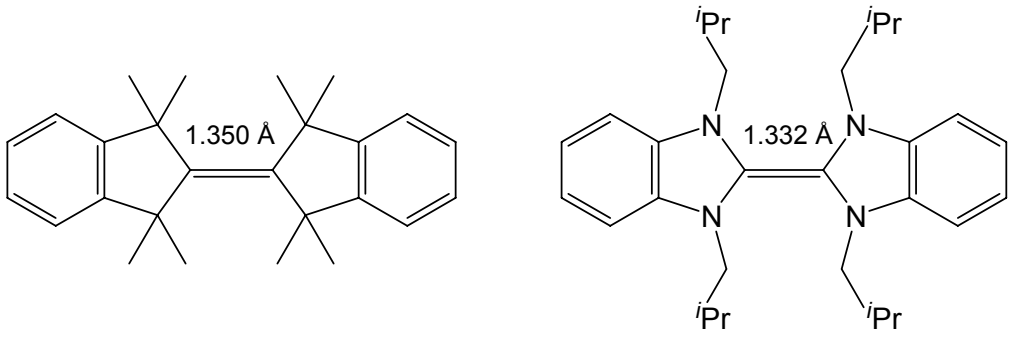

Figure 7: Comparison of alkenes and 1,1,2,2-tetraaminoalkenes.

The heavier analogues of carbon are reluctant to form π-bonds. The decreased Si–C π-bond strength, in comparison to the C–C π-bond can not compensate the loss of energy of π-conjugation of the nitrogen lone pair with the vacant *p*-orbital of carbon. Therefore, NHC adducts of silylenes feature a single C–Si bond, the carbene acts as two-electron σ-donor and the Si atom has a stereochemically active lone pair. The C–Si bond in these compounds can be considered as a donor-acceptor single bond. Two possible representations of the structure can be conceived (Scheme 21).

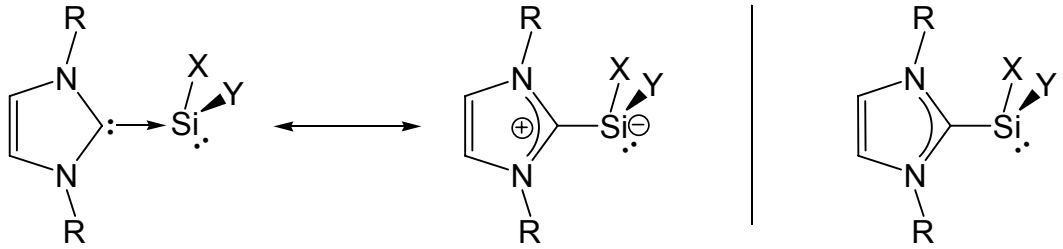

Scheme 21: Possible representations of carbene adducts of silylenes; X, Y = halogen or aryl group.

The formula on the left emphasizes the fact that the carbene is a two electron donor and donates electron density to an empty *p*-orbital of silicon. Depending on the substituents, the shift of electrons can be so strong that the structure is better described as a zwitter-ionic imidazolium salt (formula in middle).[5] For simplicity reasons I will use the formula presented on the right side. The formal charges will be omitted for clarity (Scheme 21).

[5] This situation can be found e.g. in the NHC-adduct of BBr_3. Wang, B. Quillian, P. Wei, C. S. Wannere, Y. Xie, R. B. King, H. F. Schaefer, P. R. Schleyer, G. H. Robinson, *J. Am. Chem. Soc.* **2007**, *129*, 12412.

2.1.1 NHC-stabilized silylenes, SiX_2(NHC) (X = Cl, Br, I; NHC = N-heterocyclic carbene).

In 2008 it was shown by Robinson et al. that NHC can be used to stabilize silicon compounds in low oxidation states.[68] However, the yields reported for $Si_2(IDipp)_2$ and $Si_2Cl_2(IDipp)_2$ were low, 23% and 6% respectively. We attempted to improve the yield of $Si_2(IDipp)_2$ by using silicon tetrabromide instead of silicon tetrachloride.[6]

Treatment of $SiBr_4$ with one equivalent of 1,3-bis(2,6-diisopropylphenyl)-imidazol-2-ylidene (IDipp) in hexane at ambient temperature afforded the ionic product $[SiBr_3(IDipp)]Br$ (**15**) which was isolated as a white solid in 95% yield (Scheme 22). The compound is insoluble in hexane, sparingly soluble in aromatic solvents and well soluble in polar solvents like THF or CH_2Cl_2.

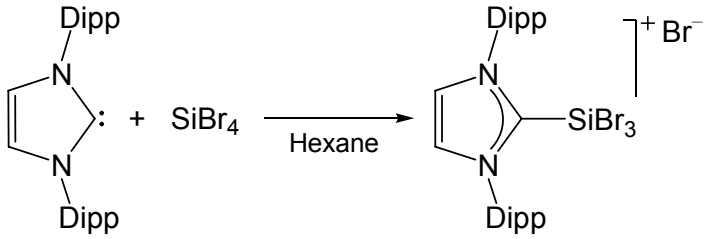

Scheme 22: Synthesis of the NHC adduct of $SiBr_4$ (**15**); Dipp = 2,6-diisopropylphenyl.

As was shown by ^{1}H NMR spectroscopy, the product always contains 10–20% of an impurity of unknown composition. Our attempts to isolate the byproduct by fractional crystallization were not successful. According to ^{1}H NMR spectrum it is likely the product of functionalization of the backbone of the carbene. The assumption is in agreement with preciously observed chlorination of IDipp, when treated with carbon tetrachloride, (Scheme 23).[121]

[6] For example, the disilyne $(TMS_2CH)_2$*i*PrSi–Si≡Si–Si*i*Pr$(CHTMS_2)_2$ was prepared by reduction of the tetrabromodisilane $(TMS_2CH)_2$*i*PrSi–$SiBr_2$–$SiBr_2$–Si*i*Pr$(CHTMS_2)_2$ but not the corresponding chloro derivative. A. Sekiguchi, R. Kinjo, M. Ichinohe, *Science* **2004**, *305*, 1755.

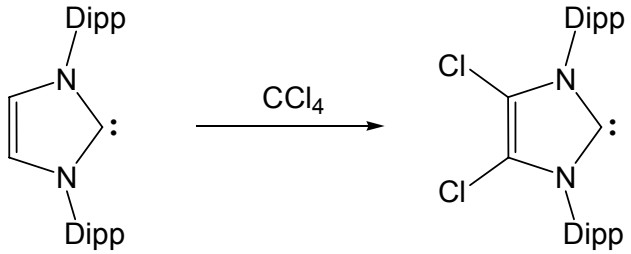

Scheme 23: Chlorination of the backbone of the IDipp. Dipp = 2,6-diisopropylphenyl.

An analytically pure sample **15** of was obtained upon recrystallization from dichloromethane. The structure of the dichloromethane solvate **15**·3CH_2Cl_2 was determined by X-ray crystallography and is shown in Figure 8. The compound **15** is ionic and composed of well separated tribromosilyl imidazolium cations and bromide anions. The shortest intermolecular Si···Br contact of 4.68 Å is longer than the sum of van der Waals radii of Si and Br thus ruling out any interactions between these atoms. The silicon atom adopts a distorted tetrahedral geometry with the bond angles in the range of 106–112°. The Si–C bond length of 1.880(9) Å lies within the range of the Si–C(sp^2) bond lengths in Ar–SiX_3 (1.845–1.907 Å, X= halogen) and compares well with the mean value of 1.87(2) Å.[7] The mean Si–Br bond length of 2.175(3) Å is slightly shorter than the average Si–Br distance in bromosilanes (2.26(6) Å)[8] and compares well with that of $SiBr_4$ obtained by gas phase electron diffraction (2.183(4) Å).[122]

Thus, according to the solid state structure, the compound is best described as an imidazolium salt, bearing a tribromosilyl group in C^2-position. Further information about the behavior of **15** is provided by NMR spectroscopy. The most distinctive features of the spectra are the ^{1}H shift of the $C^{4,5}$-*H* protons and the ^{13}C shift of the silicon-bonded atom C^2 of the N-heterocycle. Thus the ^{1}H NMR spectrum of **15** in CD_2Cl_2 shows a singlet resonance at 8.79 ppm for the $C^{4,5}$-. The shift compares more with the shift of the backbone protons in the imidazolium salt (IDippH)Br (7.86 ppm in CD_2Cl_2) than with the shift in the free carbene (6.62 ppm in C_6D_6). The shift of C^2 signal in **15** appears at δ = 136.3 ppm (CD_2Cl_2), at a very close position of that in (IDipp)Br (140.3 ppm in CD_2Cl_2) but strongly high-field shifted in comparison with that of the free IDipp (220.6 ppm in C_6D_6). In contrast, the ^{1}H NMR

[7] According to a CSD survey from 10.2011 of 7 structurally characterized compounds of the type Ar–SiX_3 (X = any halogen). Median *d*(Si–C) = 1.872 Å, LQ = 1.844 Å, HQ = 1.907 Å.

[8] According to a CSD survey from 11.2011 of 48 structurally characterized compounds of the formula $^{T4}SiX_3$–Br, where X is a non-metal bonded group. Median d(Si–Br) = 2.251 Å, LQ = 2.199, HQ = 2.326 Å.

resonance of $C^{4,5}$-*H* of **11** in C_6D_6 appears at 6.46 ppm, nearly 2 ppm high-field-shifted in comparison to that of **11** in CD_2Cl_2, suggesting the presence of a neutral NHC-adduct of $SiBr_4$ in non-polar solvents (Scheme 24).

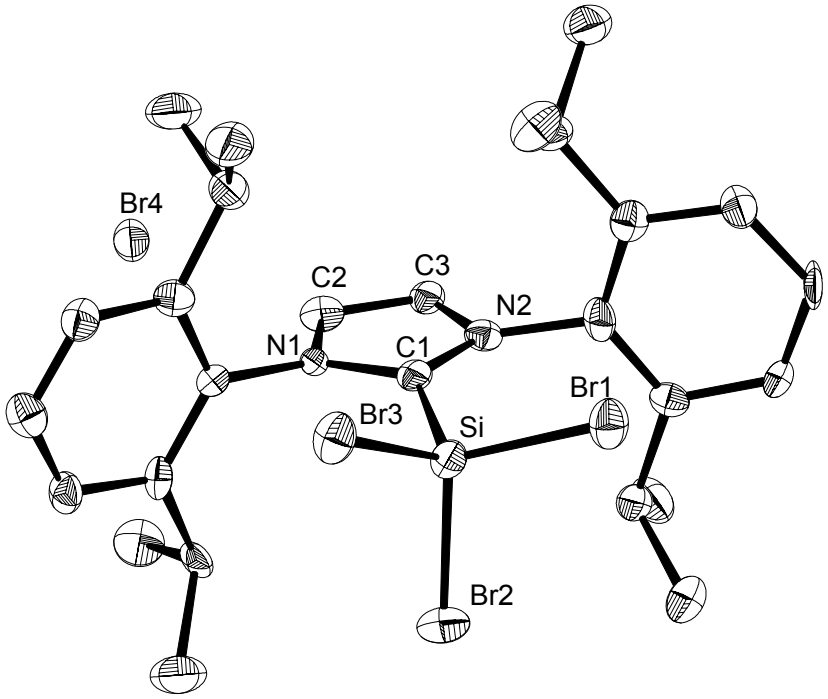

Figure 8: DIAMOND plot of the cation of **15**·$3CH_2Cl_2$ in the solid state. Ellipsoids are set at 50% probability; hydrogen atoms and solvent molecules are omitted for clarity. Selected bond lengths [Å] and angles [°]: Si–Br1 2.171(3), Si–Br2 2.180(2), Si–Br3 2.175(3), Si–C1 1.880(9), C1–N1 1.38(1), C1–N2 1.36(1), N1–C2 1.36(1), N2–C3 1.38(1), C2–C3 1.35(2); Br1-Si-Br2 109.0(1), Br1-Si-Br3 108.9(1), Br2-Si-Br3 109.0(1), C1-Si-Br1 111.4(3), C1-Si-Br2 106.2(2), C1-Si-Br3 112.3(3), N1-C1-N2 104.8(7).

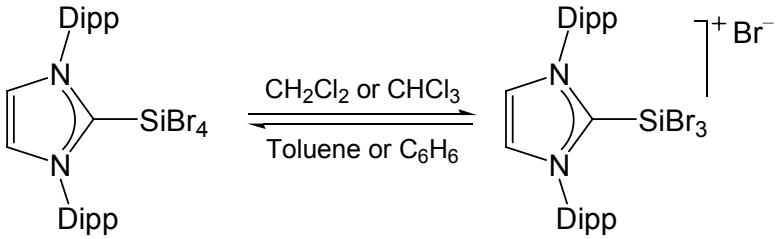

Scheme 24: Equilibrium in solution between the ionic and covalent form of **15**. Dipp = 2,6-diisopropylphenyl

Polar solvents such as dichloromethane or trichloromethane favor the ionic form, whereas in less polar solvents such as toluene or benzene the covalent form predominates. In fact, the covalent form of $SiBr_4$(IDipp) was recently characterized by X-ray crystallography, the crystals were obtained upon crystallization of compound **15** from toluene.[123]

We attempted to reduce the crude tribromosilylimidazolium salt **15** with KC_8 in THF. Surprisingly, it was found that besides the expected $Si_2(IDipp)_2$ (**12**) and free carbene, a new product was formed in the reaction. The product was found to be the carbene adduct of dibromosilylene (Scheme 25).[124]

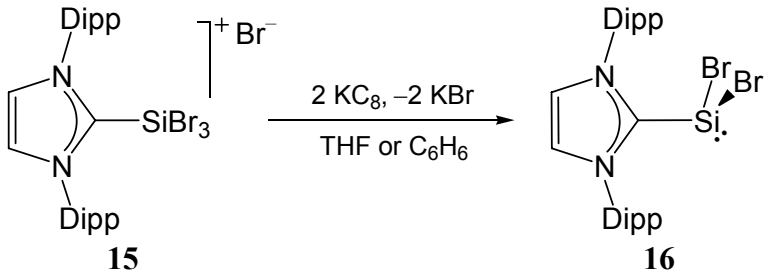

15 **16**

Scheme 25: Synthesis of the first NHC adduct of dibromosilylene. Dipp = 2,6-diisopropylphenyl

The reduction of **15** with 2.3 equivalents of KC_8 in THF afforded the carbene-stabilized dibromosilylene $SiBr_2$(IDipp) (**16**), which was isolated in 48% yield (Scheme 25). The compound was isolated as a yellow powder, soluble in THF, toluene and benzene and insoluble in hexane or pentane. The solution in C_6D_6 was monitored by ^{1}H NMR and showed no signs of decomposition of **16** after standing for one week at room temperature. The compound rapidly turns white upon exposure to air.

In the solid state the compound exhibits a monomeric structure with a trigonal pyramidal silicon center, suggesting the presence of a stereochemically active lone pair (sum of angles at Si is 293°, Figure 9) and a planar carbene ring. The Si–C bond length of 1.989(3) Å is considerably longer than that in **15** (1.880(9) Å) and in trihalo(aryl)silanes Ar–SiX_3 (1.87(2) Å),[7] but close to those in $Si_2(IDipp)_2$ and $Si_2Cl_2(IDipp)_2$ (1.927(2) Å and 1.934(7) Å respectively).[68]

The Si–C bond length reflects the donor acceptor character of the bond and a high *p*-character of the Si atomic orbital used for bonding (*vide infra*). The other examples, featuring somewhat longer Si–$C_{carbene}$ bonds, are the NHC-adducts of N-heterocyclic silylenes (NN)Si–C(NN) (2.162(5) Å, (NN) = 1,2-(Bu*t*$CH_2N)_2C_6H_4$) and {DippNC(CH_3)=CH–C(=CH_2)NDipp}Si–IMe_4 (2.016(3) Å, Dipp = 2,6-diisopropylphenyl, IMe_4 = 1,3,4,5-tetramethylimidazol-2-ylidene) (see p. 20).[60, 62, 125] The Si–C bond length excludes any strong π-interaction between the Si and C atoms; for comparison, the mean Si–C double bond length in silaethenes, featuring a Si–C *π*-bond and trigonal planar coordinated Si and C atoms,

is 1.75(2) Å.[9,[126]] The Si–Br bonds of 2.3379(8) Å and 2.3607(8) Å are longer than those in the [$SiBr_3$(IDipp)]Br (2.175(3) Å). This suggests that the silicon atom uses mainly *p*-orbitals for bonding, and the lone pair has high *s*-character.

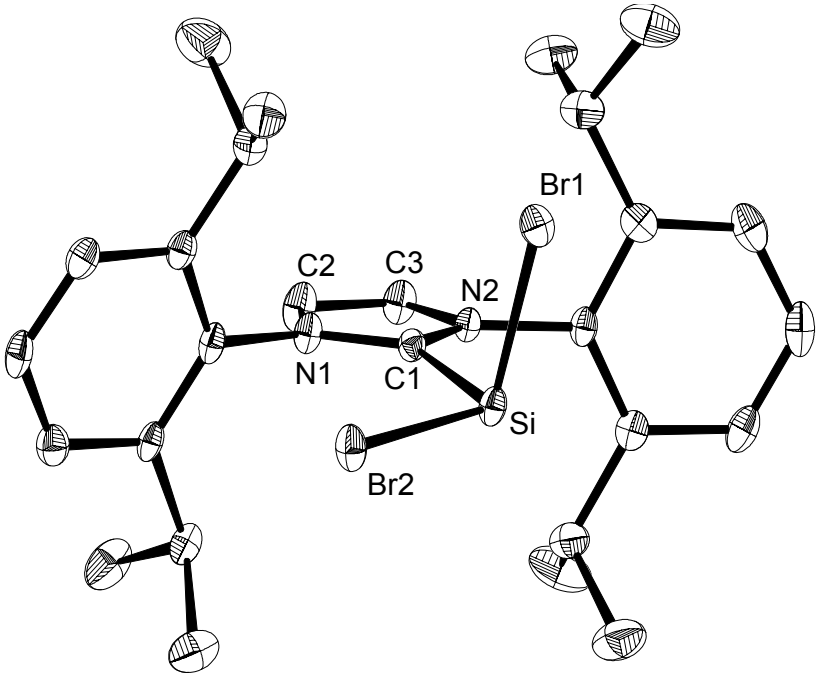

Figure 9: DIAMOND plot of the molecular structure of **16**. Thermal ellipsoids are set at 50% probability. Hydrogen atoms are omitted for clarity. Selected bond lengths [Å] and bond angles [°]: Si–Br1 2.3607(8), Si–Br2 2.3379(8), Si–C1 1.989(3), C1–N1 1.358(4), C1–N2 1.363(3), N1–C2 1.388(3) N1–C2 1.388(3), N2–C3 1.378(4), C2–C3 1.346(4); Br1-Si-Br2 97.94(3), C1-Si-Br1 94.86(8), C1-Si-Br2 99.93(8), N1-C1-N2 104.7(2).

Further information about the bonding is provided by the solution NMR spectra. The ^{1}H NMR spectrum of **16** in C_6D_6 shows a single set of resonance signals of the IDipp moiety. The diastereotopic methyl groups of the isopropyl substituents are not equivalent (Figure 10). The $C^{4,5}$-*H* protons of the carbene backbone display a signal at 6.41 ppm, close to that in free IDipp (6.62 ppm in C_6D_6). The signal of N_2C^2 at 164.5 ppm in C_6D_6 lies in-between the signals of the free IDipp (220.6 ppm in C_6D_6) and the imidazolium salt (IDippH)Br (140.3 ppm in CD_2Cl_2), reflecting the donor-acceptor character of the Si–C bond. The ^{29}Si NMR shift of **16** in C_6D_6 (10.9 ppm) is close to that in the solid state (15.8 ppm, $\Delta\nu_{1/2}$ (full width at half maximum) = 120 Hz) suggesting, that the solid state structure is retained also in solution.

[9] According to a CSD survey from 11.2011 of 11 structurally characterized compounds of the type ^{T3}Si=^{T3}C. Median *d*(Si–C) = 1.746 Å, LQ = 1.703 Å, HQ = 1.773 Å.

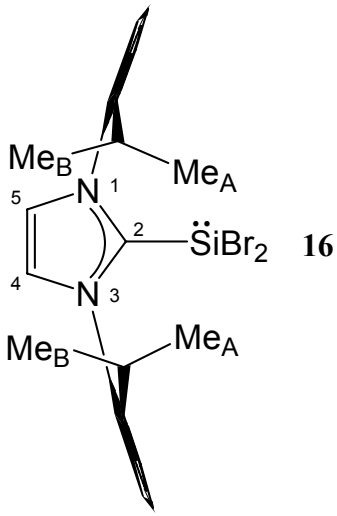

16

Figure 10: Diasteretopic methyl groups in 2,6- diisopropylphenyl substituent in **16**.

The structural parameters computed by DFT methods are also in good agreement with the experimental data.[124] Natural bond analysis (NBO) has shown that the Si–C natural bond orbital is occupied with 1.96e$^-$. The bond is strongly polarized towards the carbon center (%C = 79.9%). The Si–C bond results from the overlap of the filled $sp^{1.36}$ orbital of carbon with an empty *p*-orbital of the silicon atom. The silicon utilizes nearly unhybridized *p*-orbitals for the bonding and a high *s*-character orbital for the lone pair ($sp^{0.27}$). The high *p*-character of the orbitals used for bonding, also accounts for the elongated Si–C bond (*vide supra*).[10] The bond dissociation energy (BDE) was calculated to be 123.7 kJ·mol^{-1}, the value compares well with that of the ammonia-borane adduct (118.4 kJ·mol^{-1}), suggesting the presence of a strong donor-acceptor bond in $SiBr_2$(IDipp).[127]

The reduction of carbene adducts of tetrahalosilanes is a general way to synthesize NHC-stabilized dihalosilylenes, as is shown here by several examples (Scheme 26):

[10] The increase in bond length with the increase of the *p*-character of the carbony hybrid orbital is demonstrated for example by C–H bond lengths in the series acetylene–ethylene–ethane (106.0 pm–108.7 pm–109.4 pm).

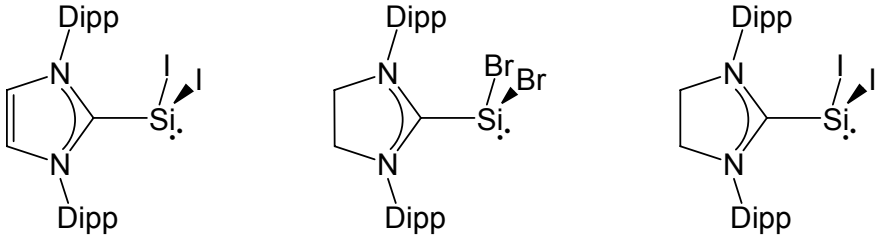

18 **20** **22**

Scheme 26: New NHC-stabilized dihalosilylenes.

The compounds were prepared by a two-step procedure that was also applied for preparation of $SiBr_2$(IDipp) (**16**). First, $SiBr_4$ or SiI_4 was treated with one equivalent of the carbene, leading to the corresponding $[SiX_3(NHC)]X$[11] adducts, which were then reduced with slightly more than two equivalents of KC_8 (NHC: IDipp = 1,3-bis(2,6-diisopropylphenyl)imidazol-2-ylidene; ISdipp = 1,3-bis(2,6-diisopropylphenyl)imidazolidin-2-ylidene). Initially the reduction was carried out in THF, but later it was shown that SiI_2(IDipp) is unstable in THF at ambient temperature.[12] This may account for the moderate yields of SiX_2(IDipp) of about 50%. The reduction in benzene afforded the compounds selectively and in higher yields, typically about 70%.[13] All compounds are air sensitive, thermally stable yellow solids, soluble in toluene and benzene, insoluble in hexane and pentane. The two-step one-pot synthesis in benzene affords SiI_2(IDipp) in one day on a multi-gram scale. The synthesis of $SiBr_2$(ISdipp) was also reproduced several times with yields of about 70%, the yield dropped to 37% on 20 g reaction scale without an apparent reason.

[11] The salts $[SiBr_3(ISdipp)]Br$ (**19**) and $[SiI_3(IDipp)]I$ (**17**) were isolated and fully characterized. The salt $[SiI_3(ISdipp)]I$ was used for the reduction without isolation; see the experimental section, p. 179.

[12] The decomposition of SiI_2(IDipp) was monitored by ^{1}H NMR spectroscopy. Substantial degree of decomposition was observed already after several hours.

[13] M. Arz, personal communication.

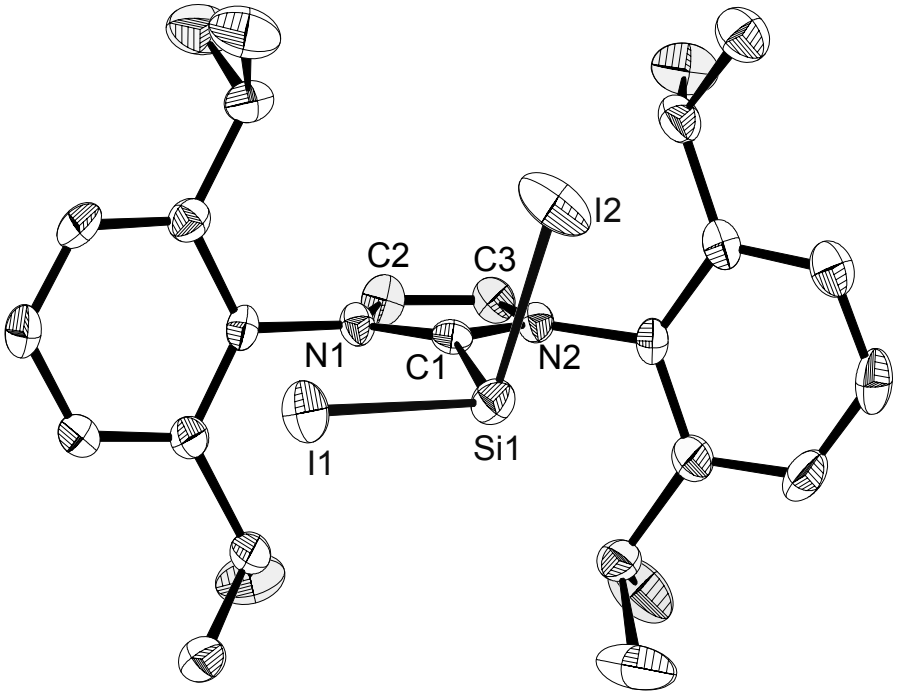

Figure 11: DIAMOND plot of one independent molecule of **18** found in the asymmetric unit. Thermal ellipsoids are set at 50% probability. Hydrogen atoms are omitted for clarity. Three independent molecules are found in the asymmetric unit. Selected bond lengths [Å] and bond angles [°] (values in brackets correspond to the second and third independent molecule): C1–Si1 1.997(4) [1.975(4), 1.980(4)], Si1–I1 2.567(1) [2.585(1), 2.563(1)], Si1–I2 2.576(1) [2.578(2), 2.5769(12)], C1–N1 1.362(5) [1.371(5), 1.362(5)], C1–N2 1.363(5) [1.369(5), 1.377(5)], C2–N1 1.388(5) [1.377(5), 1.383(5)], C3–N2 1.373(5) [1.378(5), 1.364(5)], C2–C3 1.339(6) [1.344(6), 1.338(6)]; C1-Si1-I1 103.1(1) [104.91(13), 102.8(1)], C1-Si1-I2 96.5(1) [97.5(1), 95.6(1)], I1-Si1-I2 95.63(4) [96.72(4), 97.16(4)], N1-C1-N2 104.7(3) [103.2(3), 103.7(3)].

The compounds were characterized by combination of NMR spectroscopy, elemental analyses and X-ray diffraction. The molecular structure of SiI_2(IDipp) (**18**) is depicted in Figure 11. Three very similar independent molecules were found in the asymmetric unit. The silicon center exhibits a trigonal pyramidal geometry, suggesting the presence of a stereochemically active lone pair as evidenced by the sum of bond angles between the substituents at the silicon atom of 297° (293° in $SiBr_2$(IDipp)). The Si–C bond length of 1.984(7) Å[14] compares well with that in $SiBr_2$(IDipp) (1.989(3) Å) and is considerably longer than that in [SiI_3(IDipp)]I

[14] The unweighted mean value x_u of bond lengths and angles are given, the standard deviation σ of x_u was calculated using the equation $\sigma^2 = \Sigma(x_i - x_u)^2/(n^2 - n)$, where x_i is the individual value and n – number of elements.

(1.911(3) Å).[15] The average Si–I bond length of 2.575(3) Å is longer than that in the Si(IV) precursor [SiI_3(IDipp)]I (2.420(9) Å).[14] The lengthening of the Si–C and Si–halogen bond is similar to that observed for $SiBr_2$(IDipp) (see p. 38).

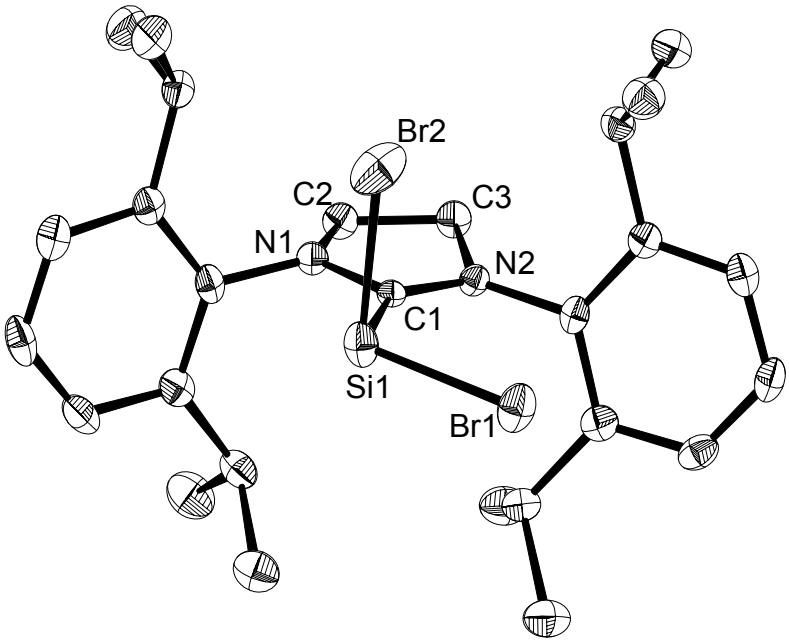

Figure 12: DIAMOND plot of the molecular structure of **20**. Thermal ellipsoids are set at 50% probability. Hydrogen atoms are omitted for clarity. Two independent molecules are found in the asymmetric unit. Selected bond lengths [Å] and bond angles [°] (values in brackets correspond to the second independent molecule): C1–Si1 2.012(2) [2.002(2)], Si1–Br1 2.3481(7) [2.3201(7)], Si1–Br2 2.3303(7) [2.3432(7)], C1–N1 1.337(2) [1.330(3)], C1–N2 1.331(2) [1.343(2)], C2–N1 1.478(2) [1.483(2)], C3–N2 1.493(2) [1.482(2)], C2–C3 1.524(3) [1.521(3)]; C1-Si1-Br1 102.53(7) [101.58(7)], C1-Si1-Br2 88.39(6) [91.06(6)], Br1-Si1-Br2 97.68(3) [98.15(3)], N1-C1-N2 110.3(2) [109.6(2)].

The ^{29}Si NMR spectrum of SiI_2(IDipp) (**18**) in C_6D_6 features a singlet resonance signal at –9.7 ppm at a position close to that of $SiBr_2$(IDipp) (10.9 ppm). The ^{29}Si{^{1}H} MAS-NMR spectrum of powder of **18** exhibits two signals with integral intensity ratio of 1:2 at –5.1 ppm ($\Delta\nu_{1/2}$ = 211 Hz) and –9.2 ppm ($\Delta\nu_{1/2}$ = 162 Hz) in agreement with the solid state structure featuring three independent molecules (from the expected three signals, two appear at close position around –9.2 ppm and are not resolved due to the broadness). The close positioning of the signals suggests, that the compound retains the molecular structure in solution.

[15] The structure of solvate [SiI_3(IDipp)]I·3($CHCl_3$) was determined by X-ray diffraction analysis. The structural features of the compound are very close to those of [$SiBr_3$(IDipp)]Br·3(CH_2Cl_2) (**15**). The mean value of the Si–I bond length is given.

Compounds **20** and **22** bear a carbene with a saturated backbone ISdipp (1,3-bis(2,6-diisopropylphenyl)imidazolidin-2-ylidene, ″*S*″ stands for ″saturated″). This carbene is advantageous to IDipp, because its saturated backbone is less susceptible for chemical transformations. Thus, the reaction of $SiBr_4$ with ISdipp is very selective, in contrast to its unsaturated analogue (Scheme 23). Additionally, compounds of the type SiX_2(ISdipp) are more reactive towards nucleophiles (see section 2.2.2).

The exchange of IDipp towards ISdipp does not have a dramatic effect on the structure and properties, as is expected **(**Figure 12). However, the dihalogenides, bearing the saturated carbene, were found more reactive towards carbonyl metallates (see section 2.2.2). The structural parameters in pairs $SiBr_2$(IDipp)–$SiBr_2$(ISdipp) and SiI_2(IDipp)–SiI_2(ISdipp) are very close and do not need to be discussed.[16] The ^{29}Si NMR shifts of $SiBr_2$(IDipp) and $SiBr_2$(ISdipp) are almost identical (10.9 and 10.8 ppm in C_6D_6; –9.7 and –11.2 for the iodo-derivative). The ^{13}C NMR signal of C^2 of the carbene moiety in $SiBr_2$(ISdipp) appears at 188.7 ppm, at a position between those of [$SiBr_3$(ISdipp)]Br (161.3 ppm) and of the free ISdipp (244.1 ppm). The signal of C^2 of SiI_2(ISdipp) was not observed in the spectrum due to unknown reasons. The important properties of SiX_2(NHC) are summarized in Table 1.

Compound	Yield, %	m.p., °C	^{13}C NMR sift of C^2, ppm	^{29}Si NMR shift, ppm	d(Si–C^2), Å[a)]
$SiBr_2$(IDipp) (**16**)	48	–	164 .5	10.9	1.989(3)
SiI_2(IDipp) (**18**)	76	dec. >160	158.4	–9.7	1.984(7)[a]
$SiBr_2$(ISdipp) (**20**)	77	191–192 (dec.)	188.7	10.8	2.007(5)[a]
SiI_2(ISdipp) (**22**)	78	–	not detected	–11.2	2.022(5)[a]

Table 1: Selected properties of carbene-stabilized halosilylenes. [a] Mean value of the bond lengths of several independent molecules found in the asymmetric unit.

The isolation of carbene stabilized dihalosilylenes shows, how an appropriate two-electron donor can make the reactive SiX_2 (X = Cl, Br, I) species stable at ambient temperature. The synthetic advantage of NHC-stabilized silylenes is that they have no chelating ligands. Even so the carbene is strongly bonded; it will be shown later that this bond can be cleaved. Thus, NHC-stabilized silylenes may become valuable silylene transfer reagents. The halogen atoms may be substituted with a variety of nucleophiles, providing access to new silylenes.

[16] Notably, the number of independent molecules in the asymmetric units doubled in each pair. Thus there are two molecules of $SiBr_2$(ISdipp) and six molecules of SiI_2(ISdipp).

2.1.2 NHC-stabilized organochlorosilylenes, SiClAr(NHC) (Ar = *m*-terphenyl; NHC = N-heterocyclic carbene)

We have shown how N-heterocyclic carbenes can be used to stabilize dihalosilylenes (Section 2.1.1). The next goal was to prepare other NHC-stabilized silylenes, for example NHC-adducts of SiClR. Alkylhalosilylenes are compounds of academic and industrial interest, e.g. SiMeCl is a reactive intermediate in the industrial Rochow-Müller synthesis of chloromethylsilanes $SiCl_n(CH_3)_{4-n}$.[128] To the best of our knowledge there are no isolated organohalosilylenes stable at ambient temperatures. In contrast to silicon, germanium, tin and lead form stable compounds of the formula EXR, where E = Ge, Sn, Pb; X = Cl or Br, R = bulky aryl group.[113, 129] Attempts to synthesize the corresponding silicon analogues were so far unsuccessful.[130]

At the same time, when $SiBr_2$(IDipp) was reported[124] the research group of Prof. H. W. Roesky gained access to $SiCl_2$(IDipp) upon reduction of $SiCl_4$(IDipp) with KC_8 or upon elimination of HCl from $SiHCl_3$ with two equivalents of the carbene (Scheme 27).[45] An analogous dehydrochlorination of cyclic silanes affording silylenes was reported by Cui et al. [131, 132]

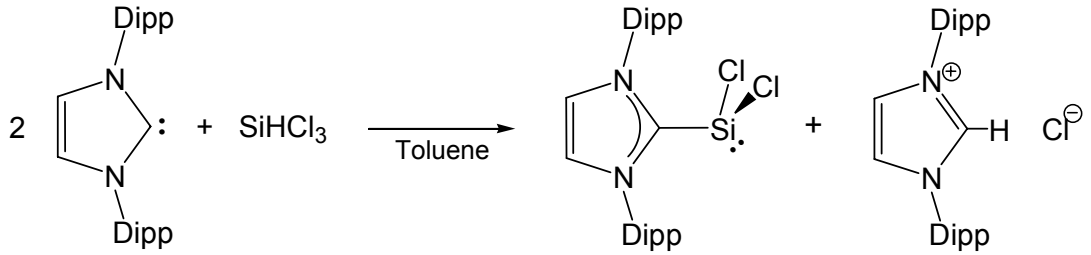

Scheme 27: Synthesis of NHC-stabilized dichlorosilylene by Roesky *et al.,* 2009.[45]

Taking advantage of the reported dehydrochlorination of trichlorosilane, the first NHC-stabilized arylchlorosilylenes were synthesized (Scheme 28).

For the synthesis the sterically demanding *m*-terphenyl substituents -C_6H_3-2,6-Mes_2,-C_6H_3-2,6-$Trip_2$ and -C_6H_3-2,6-$Dipp_2$ (Mes = 2,4,6-trimethylphenyl, Dipp = 2,6-diisopropylphenyl, Trip = 2,4,6-triisopropylphenyl) were chosen for several reasons. First, the starting aryldichlorosilanes $SiArHCl_2$ can be selectively prepared from $SiHCl_3$ and LiAr.[133] Secondly, the NHC-stabilized arylchlorosilylenes were considered as $[SiAr]^+$ synthones for the synthesis of silylidyne complexes, and it was advantageous to use a bulky group for kinetic stabilization. Due to the steric demand of the aryl groups, the aryldichlorosilanes $SiArHCl_2$ did not react with bulky carbenes, such as IMes, IS*t*Bu (1,3-bis(*tert*-

butyl)imidazolin-2-ylidene) and IMe_2iPr_2 (1,3-diisopropyl-4,5-dimethylimidazol-2-ilydene) but only with the small and more reactive 1,3,4,5-tetramethylimidazol-2-ylidene (IMe_4) (Scheme 28).

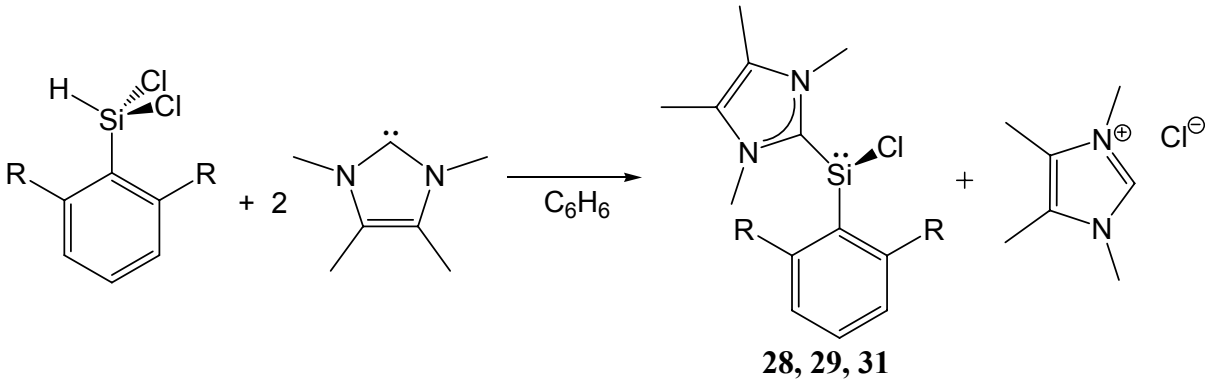

28, 29, 31

Scheme 28: Synthesis of NHC-stabilized arylchlorosilylenes. R = Mes (**28**); Trip (**29**); Dipp (**31**).

The appropriate conditions for the synthesis were optimized on the system $Si(C_6H_3\text{-}2,6\text{-}Trip_2)HCl_2$ (**29**) / 1,3,4,5-tetramethylimidazol-2-ylidene (IMe_4). In the preliminary experiments the pure $Si(C_6H_3\text{-}2,6\text{-}Trip_2)Cl(IMe_4)$ (**29**) was isolated and identified. However, the reaction was not selective and besides the formation of the compound **29,** an impurity was always formed. Depending on the conditions, its amount exceeded 50%. We did not succeed in determining the structure of the impurity; however an efficient approach was developed to minimize its formation in the reaction. After a number of trials, it was evident, that at higher temperatures and in the presence of an excess of aryldichlorosilane in the reaction mixture, the selectivity increases. In fact, addition of carbene to a solution of $SiArHCl_2$ in benzene at 80 °C leads to the selective formation of $Si(C_6H_3\text{-}2,6\text{-}Trip_2)Cl(IMe_4)$ (**29**), which was isolated with yields of up to 90%. The methodology was extended to the other aryldichlorosilanes $Si(C_6H_3\text{-}2,6\text{-}Mes_2)HCl_2$ and $Si(C_6H_3\text{-}2,6\text{-}Dipp_2)HCl_2$ (**30**) yielding the NHC-stabilized arylchlorosilylenes $Si(C_6H_3\text{-}2,6\text{-}Mes_2)Cl(IMe_4)$ (**28**)[17] and $Si(C_6H_3\text{-}2,6\text{-}Dipp_2)Cl(IMe_4)$ (**31**) in 48% and 82% yields respectively. The compounds are yellow solids, stable at ambient temperature in the solid state, soluble in toluene, benzene, diethyl ether, THF, fluorobenzene etc., and insoluble in hexane and pentane. The solution of **29** in C_6D_6 is stable at least for a week at room temperature.

[17] A significant amount of an orange impurity was formed during the reaction.

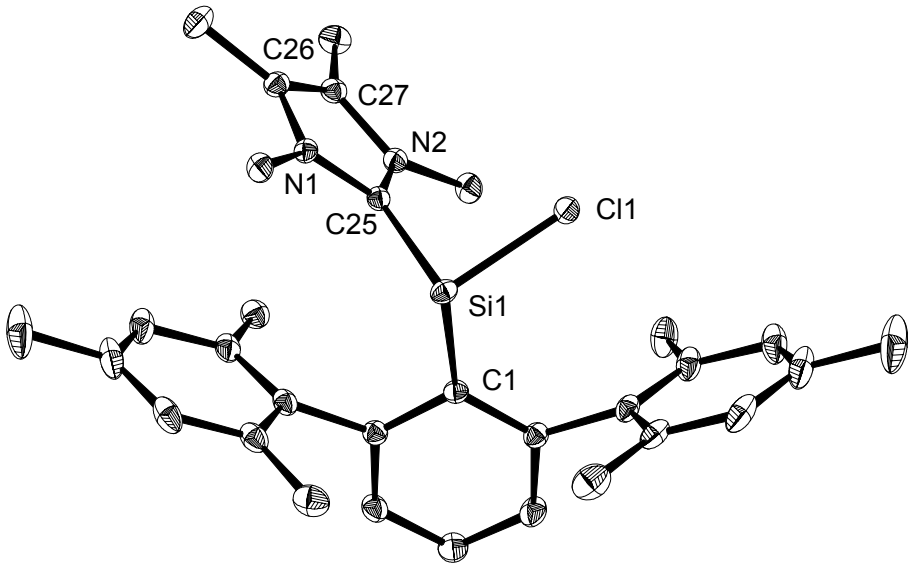

Figure 13: DIAMOND plot of the molecular structure of **28**. Thermal ellipsoids are set at 50% probability. Hydrogen atoms are omitted for clarity. Two independent molecules are found in the asymmetric unit. Selected bond lengths [Å] and bond angles [°] (values in brackets correspond to the second independent molecule): C1–Si1 1.941(1) [1.953(1)], Cl1–Si1 2.1747(6) [2.1933(6)], C25–Si1 1.968(2) [1.978(2)], C25–N1 1.356(2) [1.353(2)], C25–N2 1.348(2) [1.348(2)], C26–N1 1.388(2) [1.386(2)], C27–N2 1.388(2) [1.390(2)], C26–C27 1.358(2) [1.357(2)]; C1-Si1-Cl1 104.61(5) [105.04(5)], C25-Si1-Cl1 91.77(5) [90.89(5)], C1-Si-C25 98.80(6) [98.59(6)], N1-C25-N2 104.61(12) [104.8(1)].

Two of the compounds were structurally characterized, $Si(C_6H_3\text{-}2,6\text{-}Mes_2)Cl(IMe_4)$ (**28**, Figure 13) and $Si(C_6H_3\text{-}2,6\text{-}Trip_2)Cl(IMe_4)$ (**29**, Figure 14).[18] The compounds feature a trigonal pyramidal silicon center with sums of angles of 294.9° and 299.2° respectively, suggesting the presence of a stereochemically active lone pair. The values compare well with that for $SiBr_2$(IDipp) (293°). The Si–$C_{carbene}$ bond lengths (1.973(5) Å in **28**[18]; 1.963(2) Å in **29**) are only slightly longer than the corresponding Si–C_{Ar} bond lengths of (1.947(6) Å in **28**[18]; 1.937(2) Å in **29**), demonstrating a strong donor-acceptor Si–$C_{carbene}$ bond. The Si–$C_{carbene}$ bond lengths compare well with those in $SiCl_2$(IDipp) (1.985(4) Å) and in $SiBr_2$(IDipp) (1.989(3) Å), suggesting a similar bond strength.[19] The other examples, featuring somewhat longer Si–$C_{carbene}$ bonds, are the NHC-adducts of N-heterocyclic silylenes

[18] Two independent molecules of $[Si(C_6H_3\text{-}2,6\text{-}Mes_2)Cl(IMe_4)]$ (**28**) were found in the asymmetric unit. The unweighted mean value x_u of bond lengths and angles are given, the standard deviation σ of x_u was calculated using the equation $\sigma^2 = \Sigma(x_i - x_u)^2/(n^2 - n)$, where x_i is the individual value and n – number of elements.

[19] Here and later I will refer to $C_{carbene}$ as to the C^2 of the carbene N-heterocyle. The C_{Ar} corresponds to the C^1 of the central ring of the *m*-terphenyl substituent.

(NN)Si–C(NN) (2.162(5) Å, (NN) = 1,2-(Bu*t*$CH_2N)_2C_6H_4$) and {DippNC(CH_3)=CH–C(=CH_2)NDipp}Si–IMe_4 (2.016(3) Å, Dipp = 2,6-diisopropylphenyl, IMe_4 = 1,3,4,5-tetramethylimidazol-2-ylidene).[60, 62, 125]

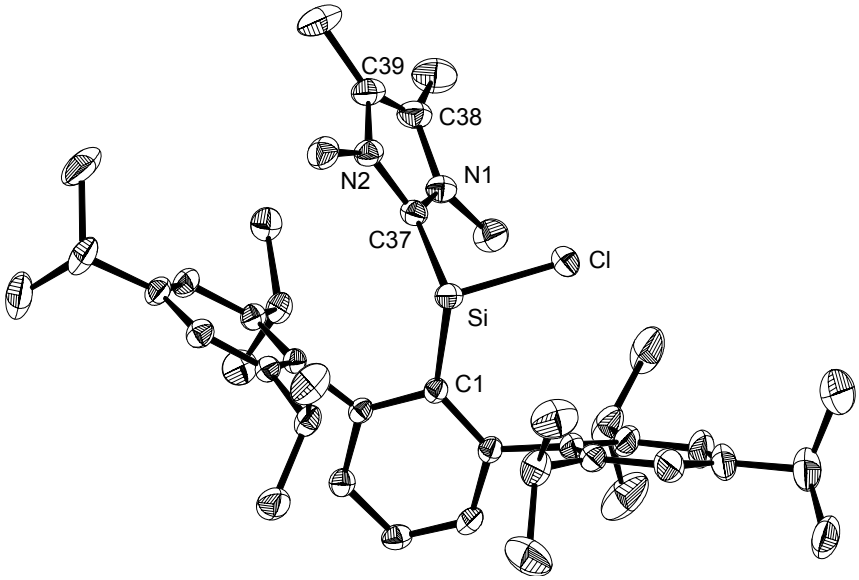

Figure 14: DIAMOND plot of the molecular structure of **29**. Thermal ellipsoids are set at 50% probability. Hydrogen atoms are omitted for clarity. Selected bond lengths [Å] and bond angles [°]:Si–C1 1.937(2), Si–C37 1.963(2), Si–Cl 2.1836(8), N1–C37 1.355(2), N2–C37 1.352(2), N1–C38 1.386(3), N2–C39 1.389(3), C38–C39 1.348(3); C1-Si-Cl 105.23(7), C1-Si-C37 102.18(8), C37-Si-Cl 91.78(7).

The Si–C_{Ar} bond lengths of 1.947(6) Å (**28**)[18] and 1.937(2) Å (**29**) are considerably longer than Si–C_{Ar} bond lengths in Si(C_6H_3-2,6-Mes_2)Cl_3 (1.872(3) Å), Si(C_6H_3-2,6-$Trip_2$)Cl_3 (1.906(6) Å) and in Si(C_6H_3-2,6-$Trip_2$)H_2Cl (1.859(4) Å).[133, 134] The same trend is observed for the Si–Cl bond lengths. They are longer in the Si(II) compounds: 2.184(9) Å (**28**), 2.1836(8) Å (**29**) in comparison to the Si(IV) compounds Si(C_6H_3-2,6-Mes_2)Cl_3 (2.031(1) Å), Si(C_6H_3-2,6-$Trip_2$)Cl_3 (2.091(3) Å) and Si(C_6H_3-2,6-$Trip_2$)H_2Cl (2.032(8) Å). The Si–Cl bond lengths of **28** and **29** (2.184(9) Å[18] and 2.1836(8) Å) compares well with those of $SiCl_2$(IDipp) (2.166(8) Å, mean value) and the chelating donor-stabilized aminochlorosilylene {PhC(*t*$BuN)_2$}SiCl (2.156(1) Å).[45, 63, 64] The long Si–C_{Ar} and Si–Cl bonds in **28** and **29** suggest that the silicon atom uses mainly *p*-orbitals for bonding to the substituents, and the lone pair orbital has high *s*-character.

This hypothesis is supported by DFT calculations of the compound **29**.[135] According to the NBO analysis, the lone pair occupies an $sp^{0.55}$ hybridized orbital. The silicon atom utilizes an $sp^{5.04}$ hybrid orbital for the Si–C_{Ar} bond, an $sp^{7.99}$ hybrid orbital for the Si–$C_{carbene}$ bond and an $sp^{10.78}$ hybrid orbital for the Si–Cl bond.[135]

The solution NMR spectra in C_6D_6 corroborate the solid state molecular structures of the NHC-stabilized silylenes. The trigonal pyramidal silicon atom has three different substituents and therefore is a chiral center in the molecule. No stereochemical inversion of the NHC-stabilized silylenes was observed in solution or in the solid state. The configurational stability was supported by computations, the inversion barrier was calculated to be 109.2 $kJ \cdot mol^{-1}$ for $Si(C_6H_3\text{-}2,6\text{-}Trip_2)Cl(IMe_4)$.[135] The inversion barrier compares with those of alkyl/aryl substituted chiral phosphanes (122–149 $kJ \cdot mol^{-1}$).[136] Due to the presence of the chirality center the $C^{2,6}$-*R* and $C^{3,5}$-*H* positions of the Mes, Dipp and Trip substituents are not equivalent, and are not equilibrated, since rotation of the Mes, Dipp and Trip substituents about the C_{ring}–C_{ring} bond is frozen out on the NMR timescale. In comparison, the rotation about the Si–C_{Ar} bond and the Si–$C_{carbene}$ bond is rapid on the NMR timescale, as indicated by the equivalency of the 2- and 6-positioned aryl groups of the *m*-terphenyl substituent and the N^1-*CH*$_3$ and the N^3-*CH*$_3$ groups of IMe_4. The NMR spectra of the compounds **28**, **29** and **31** present typical sets of resonance signals, characteristic for chiral compounds bearing a *m*-terphenyl group. The ^1H NMR spectrum of $Si(C_6H_3\text{-}2,6\text{-}Trip_2)Cl(IMe_4)$, for example displays 6 doublets for the 2-, 4- and 6-positioned isopropyl groups of the Trip substituent, each isopropyl group bearing two diastereotopic methyl groups -$CHMe_AMe_B$. It also displays 3 septets for the C*H*Me_AMe_B protons, 2 singlets for the $N^{1,3}$-*Me* and $C^{4,5}$-*Me* groups of IMe_4; 2 doublets with a ^4J coupling for the C^3-*H* and C^5-*H* of the Trip groups and a doublet and a triplet for the $C^{3,5}$-*H* and C^4-*H* protons of the central C_6H_3 ring (Figure 15).

The hybridization change of the silicon center from $SiArHCl_2$ to $SiArCl(IMe_4)$ is indicated by the ^{13}C NMR spectra. The ^{13}C NMR signal of the Si-bonded C_{Ar} atoms appear at 150.6 ppm (**28**), 156.0 ppm (**29**) and 150.2 ppm (**31**), and are about 25 ppm shifted to lower field in comparison to those of the silanes $SiArHCl_2$ (128.8, 130.3 and 129.9 ppm, respectively). This low-field shift of the C_{ipso} atom seems to be a common feature of aryl substituted Si(II) compounds.[20] The hybridization changes are also reflected in the Si–C coupling constants. From the $^{13}C\{^1H\}$ spectrum of $Si(C_6H_3\text{-}2,6\text{-}Mes_2)Cl(IMe_4)$ (**28**) in C_6D_6 the $^1J(Si,C_{Ar})$ coupling constant was found to be 48 Hz. Both coupling constants are significantly smaller than in phenyl substituted Si(IV) compounds (97 Hz in $Si(C_6H_3\text{-}2,6\text{-}Mes_2)HCl_2$ and 67 Hz in

[20] A similar trend is observed for Ge–Pb compounds.

PhSiMe$_3$).[137] In agreement with the data presented in the ref. 137, the ^1J(Si,C) is proportional to the *s*-character of the orbitals involved in bonding.[21]

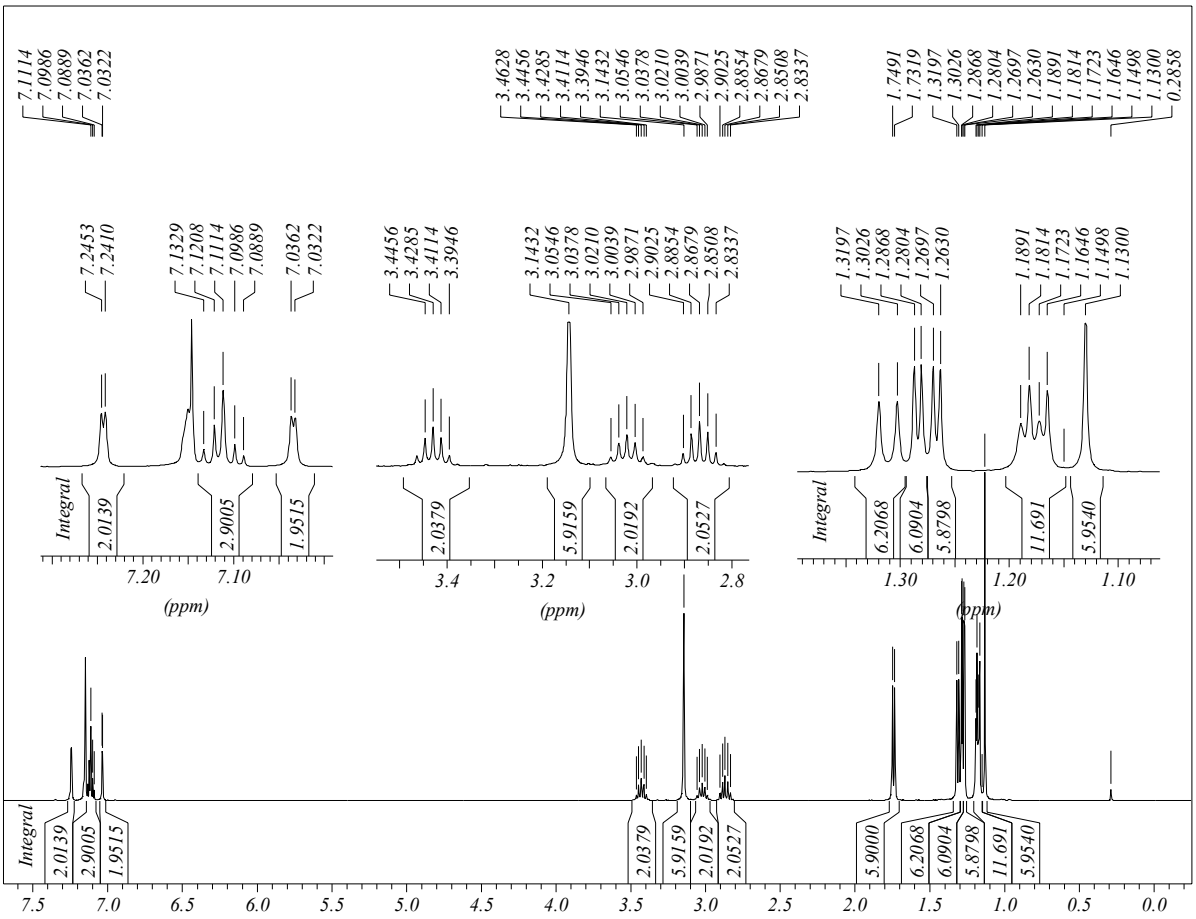

Figure 15: 400.1 MHz ^{1}H NMR spectrum of Si(C_6H_3-2,6-Trip$_2$)Cl(IMe$_4$) (**29**) in C_6D_6 at 298 K.

The ^{29}Si NMR signals of the arylsilicon(II) chlorides **28–31** appear as expected at slightly higher field than those of SiCl$_2$(IDipp) and [PhC(NtBu)$_2$]SiCl (see Table 2). It is important to note, that the structural and spectroscopic features of SiArCl(IMe$_4$) are similar to those of GeArCl(IMe$_4$) (Ar = -C_6H_3-2,6-Mes$_2$, -C_6H_3-2,6-Trip$_2$), which were also prepared in the research group of Filippou.[135]

[21] On the basis of the hybridization of the Si atom (derived from the DFT calculations) and the ^{13}C{^{1}H} NMR spectra an empirical linear law approximating the $^1J_{Si,C}$ was found: $^1J_{Si,C}$ = 250x + 10y, where s^xp^y is the hybridization of the Si orbital involved in the Si–C bonding bonding.

Compound	Yield, %	m.p, °C	^{29}Si NMR, ppm (C_6D_6)	Si–$C_{carbene}$, Å	Si–Cl, Å
Si(C_6H_3-2,6-Mes_2)Cl(IMe_4) (**28**)	48	120(dec)	1.34	1.973(5)	2.184(9)[18]
Si(C_6H_3-2,6-$Trip_2$)Cl(IMe_4) (**29**)	88	172(dec)	0.77	1.963(2)	2.1836(8)
Si(C_6H_3-2,6-$Dipp_2$)Cl(IMe_4) (**31**)	82	n/a	0.04	n/a	n/a
[PhC($NtBu)_2$]SiCl[64, 65]	90	178	14.6	–	2.156(1)
$SiCl_2$(IDipp)[45]	79	n/a	19.1	1.985(4)	2.166(8) (mean)

Table 2: Summary of the properties of SiArCl(IMe_4) and comparison with [PhC($N^tBu)_2$]SiCl and $SiCl_2$(IDipp); n/a = information is not available.

2.1.3 Preliminary reactivity studies of NHC-stabilized silylenes SiX_2(NHC) and SiArCl(NHC)

NHC-stabilized silylenes are very suitable precursors for low-valent silicon compounds. Their isolation led to the synthesis of a number of unprecedented compounds. The major part of this work, devoted to the synthesis and reactivity studies of silylidene and silylidyne complexes, will be presented in Chapters 2.2 and 2.3. In this section only preliminary reactivity studies are discussed.

Reaction of SiI_2(IDipp) (18) with $Et_2N–C≡C–NEt_2$. IDipp = 1,3-bis(2,6-diisopropyl-phenyl)-imidazol-2-ylidene

The reaction of transient silylenes with acetylenes is known to produce substituted 1,4-disilacyclohexa-2,5-dienes. The reaction mechanism includes formation of the silirene (silacyclopropene) intermediate, which dimerizes to give the 1,4-disilacyclohexa-2,5-diene (Scheme 29).[9, 11] We investigated the reaction of SiI_2(IDipp) (**16**) with bis(diethylamino)acetylene. The reaction proceeds fast already at ambient temperature to give the substituted silacyclopentadiene **24** (Scheme 29). The carbene formed in the reaction does not coordinate to the silicon center probably because of steric hindrance. The reaction presents a convenient route to substituted silacyclopentadienes (siloles) in one step under mild conditions.

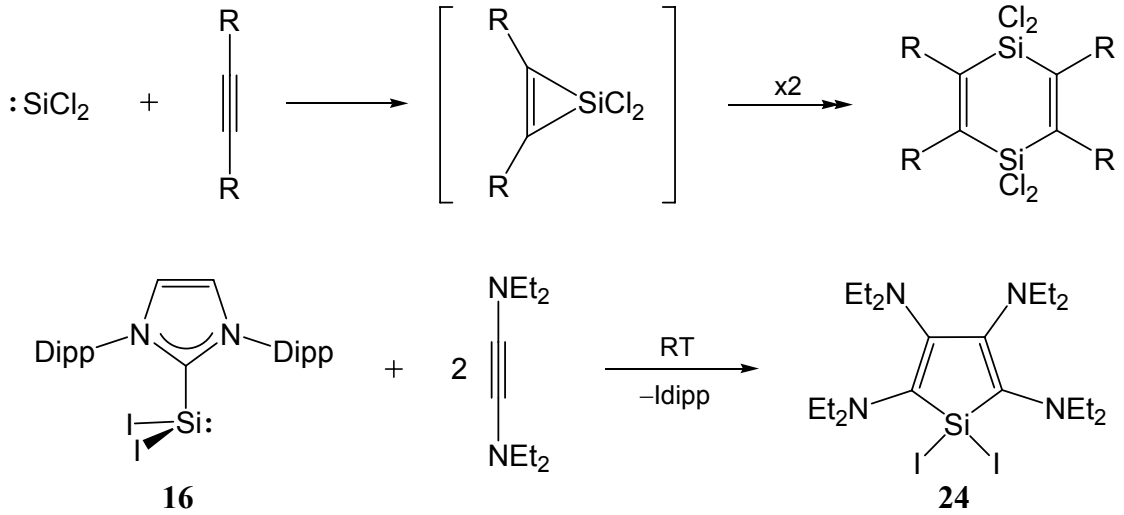

16 **24**

Scheme 29: Reactivity of $SiCl_2$ and SiI_2(IDipp) (**16**) towards acetylenes.

The product was isolated as orange air sensitive crystals soluble in common organic solvents in 42% yield. The compound was fully characterized and the solid-state structure was determined by X-ray crystallography (Figure 16).

The compound features an almost planar silacyclopentadiene ring with isolated single and and double carbon–carbon bonds (1.524(2) Å and 1.370(2) Å respectively). The silicon center exhibits a distorted tetrahedral geometry with the C1-Si-C4 angle of 96.58(7)° and angles between other substituents in the range of 105–119°. The smaller endocyclic C1-Si-C4 is the result of the constraints imposed by the 5-membered ring and is typical for this type of compounds.[138] The Si–C bond length of 1.852(3) Å (mean value) compares well with the that in the previously reported 1,1-dibromo-2,5-bis(trimethylsilyl)-3,4-diphenylsilole (1.850(1) Å).[138] The mean Si–I bond length of 2.466(1) Å is shorter than that in SiI_2(Idipp) (2.575(3) Å) and compares well with that in 2,3,5,6-tetraphenyl-1,4-diiodo-1,4-disilacyclohexa-2,5-diene (2.436(2) Å).[139],22 Overall, the structure of **24** is similar to the previously reported siloles. The ^{29}Si NMR spectrum of **24** displays a singlet resonance signal at –83.5 ppm shifted strongly in higher field in comparison to that of 1,1-dibromo-2,5-bis(trimethylsilyl)-3,4-diphenylsilole (4.9 ppm in $CDCl_3$). The strong high-field shift of iodosilanes in ^{29}Si NMR spectra is a common phenomenon, thus for example Si(C_6H_3-2,6-

22 The unweighted mean value x_u of bond lengths and angles are given, the standard deviation σ of x_u was calculated using the equation $\sigma^2 = \Sigma(x_i - x_u)^2/(n^2 - n)$, where x_i is the individual value and n – number of elements.

Trip$_2$)HI$_2$, MesSiI$_3$ and SiI$_4$ feature resonance signals at –92.2, –175.3[134] and -346.6 ppm[23] respectively.

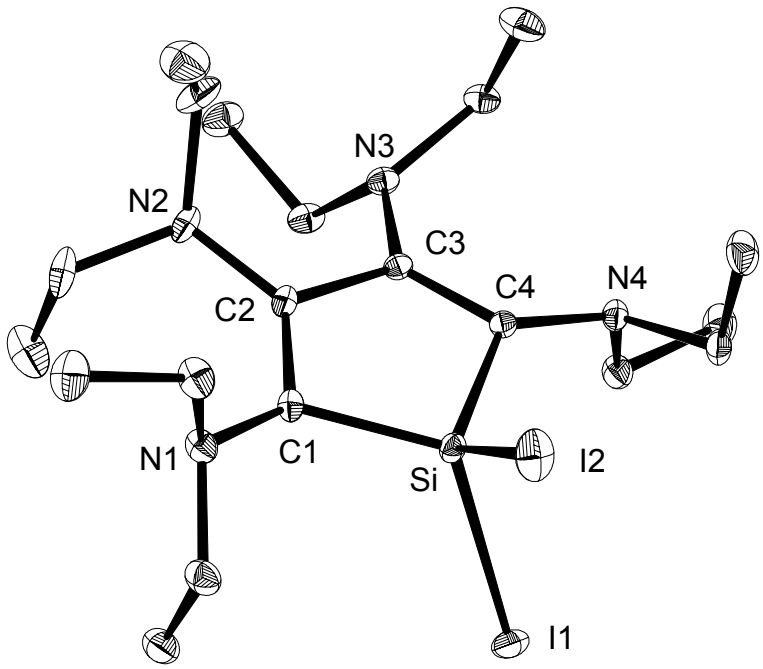

Figure 16: DIAMOND plot of the molecular structure of **24** . Thermal ellipsoids are set at 30% probability. Hydrogen atoms are omitted for clarity. Selected bond lengths [Å] and bond angles [°]: Si–C1 1.849(2), C1–C2 1.370(2), C2–C3 1.524(2), C3–C4 1.370(2), C4–Si 1.854(2), Si–I1 2.4654(5), Si–I2 2.4672(5), C1–N1 1.426(2), C2–N2 1.392(2), C3–N3 1.402(2), C4–N4 1.420(2); C1-Si-C4 96.58(7), C1-Si-I1 118.54(6), C1-Si-I2 110.38(5), C4-Si-I1 108.94(5), C4-Si-I2 118.51(5), I1-Si-I2 104.57(2).

SiI$_2$(Idipp) reacts also with Ph–C≡C–NMe$_2$, however the product was not isolated due to its instability at room temperature. Interestingly, the recently reported reaction of an analogous compound SiCl$_2$(IDipp) with diphenylacetylene afforded the carbene adduct of 1,1,2,2,3,3-hexachloro-4,5-diphenyl-1,2,3-trisilacyclopent-4-ene.[45]

Reduction of SiBr$_2$(ISdipp); ISdipp = 1,3-bis-(2,6-diisopropylphenyl)imidazolin-2-ylidene

The compounds SiX$_2$(IDipp) (X = Cl, Br, I) are intermediate products in the reduction of SiX$_4$(IDipp) to Si$_2$(IDipp)$_2$. For example, reduction of SiI$_2$(IDipp) affords Si$_2$(IDipp)$_2$ in a

[23] M. Arz, *Diploma thesis*, **2010**, Universilty of Bonn.

good yield as was shown recently.[24] In this work the reduction of $SiBr_2$(ISdipp) (**20**) with potassium graphite was shortly investigated.

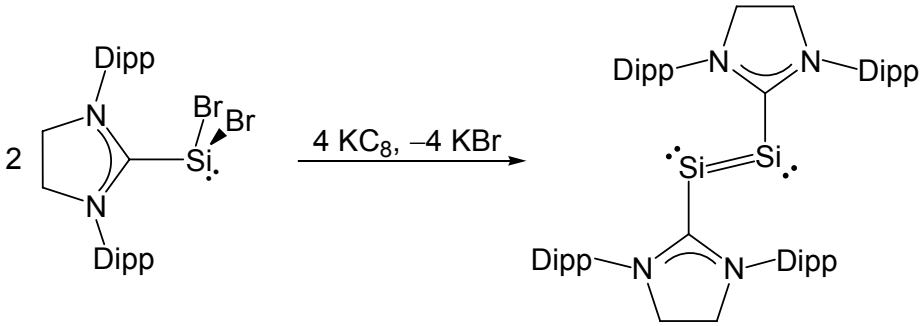

Scheme 30: Synthesis of the carbene stabilized disilene Si_2(ISdipp)$_2$ (**21**). Dipp = 2,6-diisopropylphenyl.

The reduction with 2.0 equivalents of KC_8 afforded the Si(0) compound Si_2(ISdipp)$_2$ **(21)** in 45% yield as a dark red crystalline powder (Scheme 30). The product is almost insoluble in diethyl ether and hexane, is moderately soluble in toluene and THF and is relatively good soluble in hot toluene. In contrast to the reduction of SiI_2(IDipp), the intermediate Si(I) bromide was not observed in the ^{1}H NMR spectra.[25] The molecular structure of **21** was determined by the X-ray diffraction and is depicted in Figure 17.

The bonding parameters of **21** are similar to those of the unsaturated analogue Si_2(IDipp)$_2$ (**12)**. The molecule features a coplanar C–Si–Si–C array atoms as indicated by the torsion angle C1-Si-Si#-C1# of 180.0°. The silicon adopts a bent geometry with a C–Si–Si# angle of 93.07(5)°. The Si–C bond length of 1.924(2) Å is shorter than in the parent compound $SiBr_2$(ISdipp) (2.007(5) Å).[26] The same bond shortening was already observed in the series $SiCl_2$(IDipp)–Si_2Cl_2(IDipp)$_2$–Si_2(IDipp)$_2$ (1.985(4) Å–1.934(5) Å[27]–1.9271(15) Å)[45, 68] and in the series $SiBr_2$(IDipp)–Si_2Br_2(IDipp)$_2$–Si_2(IDipp)$_2$ (1.989(3) Å–1.938(3) Å[27,28]–1.9271(15) Å). Steric effects may not account for this trend, since upon going from Si(II) to Si(I) the coordination number of the Si atoms does not change.

---

[24] M. Arz, *personal communication*, University of Bonn, **2011**.

[25] Also, the reduction is accompanied by formation of a larger amount of the carbene ISdipp, than in the case of IDipp. M. Arz, *personal communication*, University of Bonn, **2011**.

[26] The mean value of the Si–C bond lengths of the two independent molecules found in the asymmetric unit is given.

[27] The unweighted mean value of the Si–$C_{carbene}$ bond length found in the molecule is given, the standard deviation was calculated using the equation $\sigma^2 = \Sigma(x_i - x_u)^2/(n^2 - n)$, where x_i is the individual value and n – number of elements.

[28] M. Arz, *personal communication*, University of Bonn, **2011**.

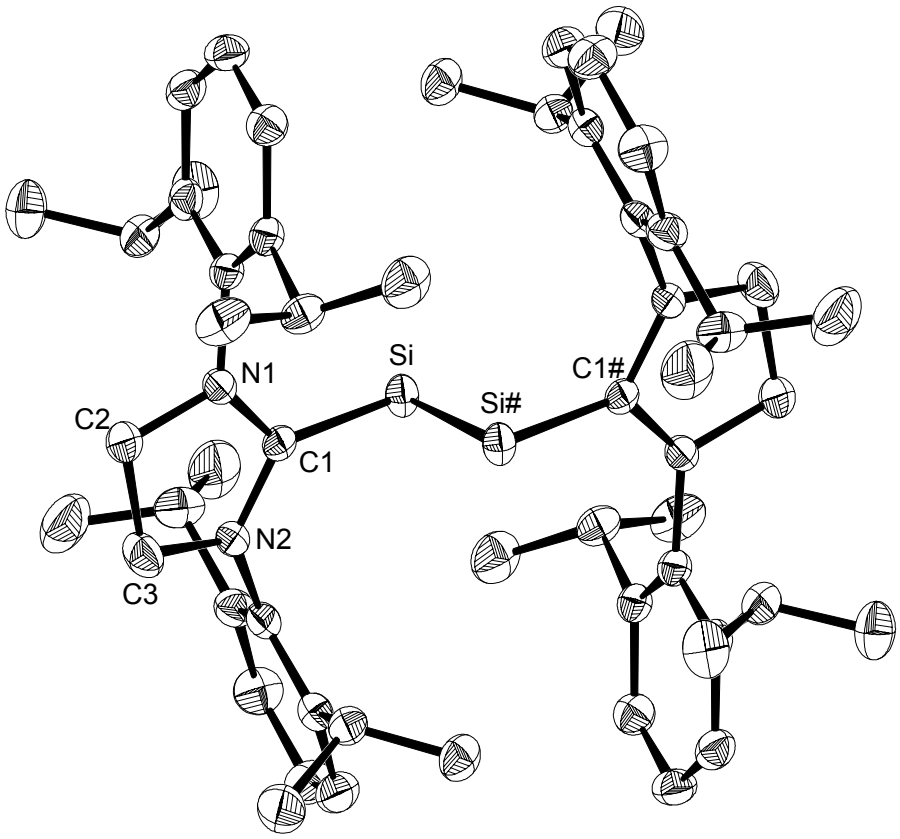

Figure 17: DIAMOND plot of the molecular structure of **21**. Thermal ellipsoids are set at 50% probability. Hydrogen atoms are omitted for clarity. Selected bond lengths [Å] and bond angles [°]: Si–Si# 2.2323(8), Si–C1 1.924(2), C1–N1 1.359(2), C1–N2 1.353(2), N1–C2 1.469(2), C2–C3 1.512(2), N2–C3 1.378(4); C1-Si-Si# 93.07(5), N1-C1-Si 127.3(1), N2-C1-Si 125.4(1), N1-C1-N2 107.2(1), C1-Si-Si#-C1# 180.0.

Analysis of results of DFT calculations reveals, that the Si hybrid orbital involved in Si–C bonding acquires higher *p*-character along the series $SiBr_2$(IDipp) ($s^{0.4}p^{0.6}$) – Si_2Cl_2(IDipp)$_2$ ($s^{0.1}p^{0.9}$) – Si_2(IDipp)$_2$ ($s^{0.1}p^{0.9}$).[68, 135] This hybridization change would suggest that the Si–C bond length should increase along the series, in contradiction to the experimental data. A plausible explanation may be, that in Si_2X_2(IDipp)$_2$ and Si_2(IDipp)$_2$ there is a weak π-interaction between the lone pair of the silicon atom and the *p*-orbital of the carbene carbon atom, leading to the shortening of the Si–C bond (backbonding).

Halide substitution in SiX_2(IDipp) (X =Br, I; IDipp = 1,3-bis(2,6-diisopropylphenyl)-imidazol-2-ylidene)

We attempted to substitute one iodide in SiI_2(IDipp) (**18**) with nucleophiles e.g. Li(C_6H_3-2,6-Mes_2). The reaction resulted in the formation of a large amount of 2,6-$Mes_2C_6H_3I$ together

with other unidentified products. The reason for this may be the stronger tendency of SiI_2(IDipp) to reduction than e.g. $SiBr_2$(IDipp) (**16**) or $SiCl_2$(IDipp) in analogy to Si(IV) compounds. For example, treatment of $SiHCl_3$ with Li(C_6H_3-2,6-Mes_2) affords $SiHCl_2$(C_6H_3-2,6-Mes_2).[133] In contrast, reaction of Li(C_6H_3-2,6-$Trip_2$) with $SiHI_3$ leads to the quantitative formation of 2,6-$Trip_2C_6H_3I$. We believe, that the right choice of a nucleophile and silicon(II) halide is crucial for the preparation of the compounds [SiRX(NHC)] (X = Cl, Br, I; NHC = IDipp, ISdipp).

The reaction of $SiBr_2$(IDipp) (**16**) with two equivalents of KCp* (Cp* = η^5-C_5Me_5) in diethyl ether afforded selectively decamethylsilicocene (Scheme 31). Notably, the carbene does not coordinated to the Si center in Cp^*_2Si. This synthesis is shorter than the originally published by Jutzi et al. in 1989 (four steps from LiC_5HMe_4 and $SiCl_4$).[48, 140] A possible drawback of the approach is that the carbene released in the reaction needs to be separated from Cp^*_2Si. Sublimation, fractional crystallization or carbene ″trapping″ agents such as $FeCl_2$, $SiBr_4$, and BR_3 etc. can be suggested for removal of the carbene.[29]

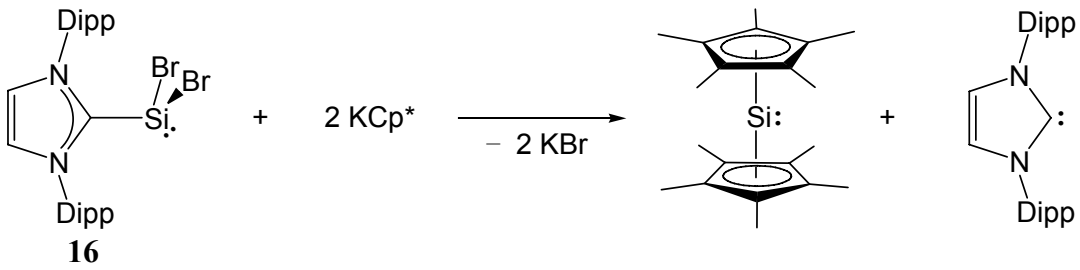

Scheme 31: Reaction of $SiBr_2$(IDipp) (**16**) with KCp*. Synthesis of decamethylsilicocene.

Already on the early stage of the studies relative the lability of the Si–$C_{carbene}$ bond in NHC-stabilized silylenes was observed. The sterically demanding 1,3-bis(2,6-diisopropylphenyl)-imidazol-2-ylidene in SiI_2(IDipp) can be substituted by the smaller and more reactive 1,3,4,5-tetramethyimidazol-2-ylidene (IMe_4). The substitution proceeds smoothly at ambient temperature in fluorobenzene or in toluene, leading to a precipitation of the unprecedented ionic compound **23** (Scheme 32). The substitution reaction probably follows an addition-elimination mechanism, because of the high bond dissociation energy of Si–$C_{carbene}$ bond in SiI_2(IDipp), e.g. the Si–$C_{carbene}$ bond dissociation energy in $SiBr_2$(IDipp) was calculated to be 123.7 kJmol^{-1}.[124]

[29] Only a small scale reaction was carried out. No attempts were made to separate the products.

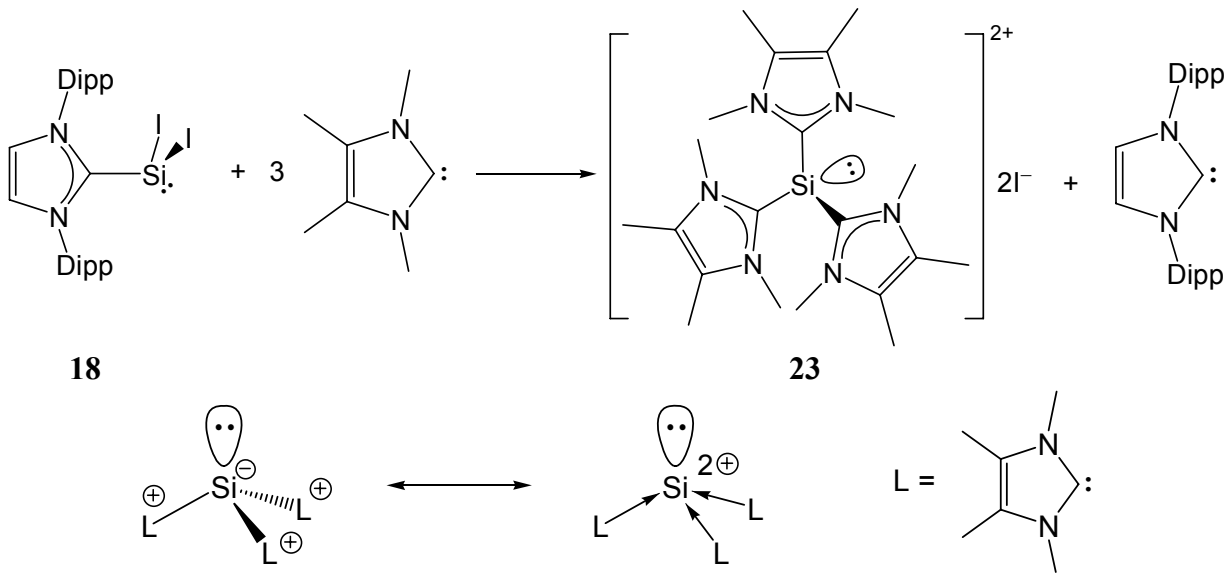

Scheme 32: Substitution of carbene in SiI_2(IDipp) (**18**). Mesomeric formulas of $[Si(IMe_4)_3]I_2$ (**23**).

P-block element-centered dications attracted considerable attention recently.[141, 142] The NHC-stabilized dications of P(III) and Ge(II) were isolated, but Si(II) analogues were inaccessible due to the lack of suitable precursors.[142, 143] Compound **23** features, among few other examples, a formally positively charged Si atom bearing a lone pair.[49, 144] Si(II) centered cations are interesting species, because they can exhibit unusual reactivity and provide access to new types of compounds.[50, 51]

The salt **23** was isolated as a light yellow solid in almost quantitative yield. It is insoluble in common organic solvents, such as hexane, toluene, diethyl ether, THF and fluorobenzene. A dichloromethane solution of **23** is stable at –30 °C for at least several hours, but decomposes slowly at ambient temperature. The crystals suitable for X-ray structure determination were grown from a concentrated dichloromethane solution, upon slow cooling from ambient temperature to –5 °C. The molecular structure of the cation in **23** is depicted in Figure 18.

The solid state structure of **23** features well separated cations and anions. The shortest Si···I distance of 5.88 Å is longer than the sum of Van der Waals radii of Si and I (4.08 Å), excluding any directional interaction.[145] The silicon centered dication **23** has a propeller-like structure. The silicon center is slightly distorted trigonal pyramidal-coordinated, suggesting the presence of a stereochemically active lone pair. The C-Si-C angles are very similar, the mean ∠C-Si-C = 104.0(4)°. The degree of pyramidalization in the cation **23** ($\Sigma^{\circ}_{at\ Si}$ = 312°) is smaller than that in the parent SiI_2(IDipp) (**18**, $\Sigma^{\circ}_{at\ Si}$ = 297°). This can be explained by increasing of the steric demand and/or by rehybridization. In SiI_2(IDipp), the Si atom utilizes orbitals of high *p*-character for the bonding with electron withdrawing iodine substituents. In

23 the Si–C bonds are less polar, therefore the *s*-character of the Si hybrid orbitals is higher, increasing the angles between the carbene substituents. A similar phenomenon was observed in the pair $GeI_2(IMe_2iPr_2)$ – $[Ge(IMe_2iPr_2)_3]I_2$ (287° to 312°).[142, 146]

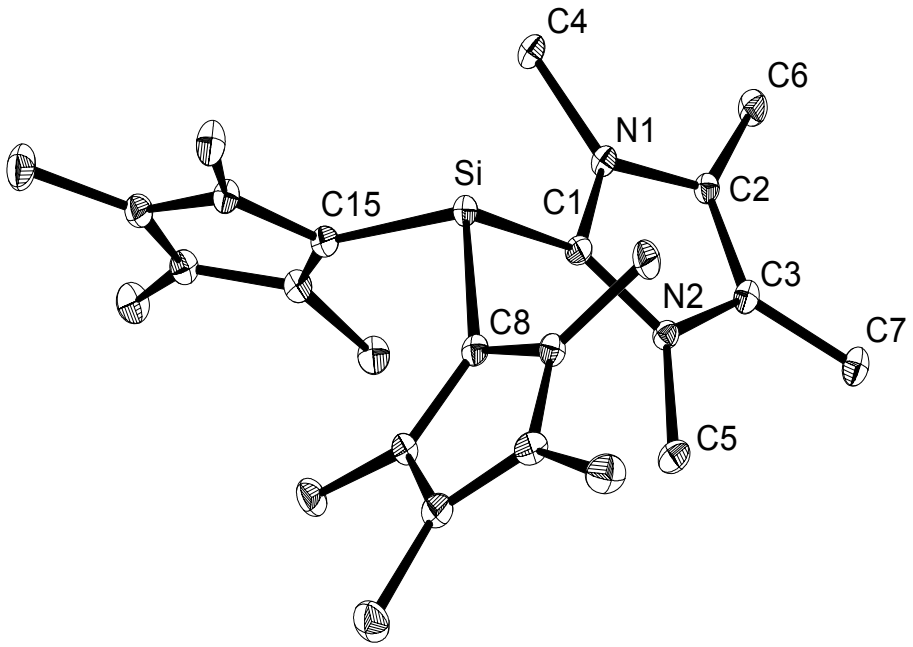

Figure 18: DIAMOND plot of the molecular structure of the cation **23**. Thermal ellipsoids are set at 30% probability. Hydrogen atoms are omitted for clarity. Selected bond lengths [Å], bond angles [°]: C1–Si 1.918(3), C8–Si 1.909(3), C15–Si 1.917(3), C1–N1 1.359(3), C1–N2 1.357(3), C2–N1 1.389(3), C3–N2 1.402(3), C2–C3 1.354(4); C1-Si-C8 103.8(1), C1-Si-C15 104.7(1), C8-Si-C15 103.4(1), N1-C1-N2 105.1(2).

The Si–C bonds are short (mean *d*(Si–C) = 1.915(3) Å) and compare well with those in the tribromosilylimidazolium salt $[SiBr_3(IDipp)]Br$ (**15,** 1.880(9) Å) and $Si(C_6H_3\text{-}2,6\text{-}Trip_2)H_2Cl$ (1.906(6) Å).[134] The bond lengths are somewhat shorter than those in the analogous germanium compound $[Ge(IMe_2iPr_2)_3]I_2$ (2.070(6) Å), if one takes into consideration the difference between single bond covalent radii of Si and Ge atoms of 0.05 Å.[142, 147]

NMR spectroscopy corroborates the structure of **23**. The ^1H and $^{13}C\{^1H\}$ NMR spectra display a single set of resonances of the carbene ligands, suggesting a fast rotation around the Si–C bonds. The ^{29}Si NMR signal of **23** (–89.9 ppm in CD_2Cl_2) appears at higher field than that of the $SiI_2(IDipp)$ (–9.7 ppm in C_6D_6), reflecting the higher donor ability of an NHC ligand in comparison to an iodide.

Reduction of SiArCl(IMe$_4$) (Ar = -C$_6$H$_3$-2,6-Mes$_2$, C$_6$H$_3$-2,6-Trip$_2$; IMe$_4$ = 1,3,4,5-tetramethyimidazol-2-ylidene)

The arylchlorosilylene-NHC adducts SiArCl(NHC) feature a silicon center in the oxidation state of +2. In analogy to the reduction of $SiCl_2$(IDipp)[68] one could expect that upon reduction of Si(C$_6$H$_3$-2,6-Mes$_2$)Cl(IMe$_4$) (**28**) or Si(C$_6$H$_3$-2,6-Trip$_2$)Cl(IMe$_4$) (**29**) biscarbene adducts of disilynes (bis(carbene)-stabilized disilylenes) will be formed. In fact, reduction of Si(C$_6$H$_3$-2,6-Mes$_2$)Cl(IMe$_4$) with KC_8 in THF or dioxane afforded a mixture of products, from which the silicon(I) compound (Si(C$_6$H$_3$-2,6-Mes$_2$)(IMe$_4$))$_2$ (**32**) was isolated in about 25% yield. The low yield of the product can be explained by concomitant further reduction of **32**, which occurs in the presence of unreacted Si(C$_6$H$_3$-2,6-Mes$_2$)Cl(IMe$_4$) (Scheme 33).

The compound **32** is a dark violet-blue (nearly black) very air sensitive solid.[30] It was characterized by X-ray crystallography and elemental analysis. The C_2 symmetric molecule features trigonal pyramidal Si centers with the sum of angles at Si of 313°. The value is larger than that in the parent Si(C$_6$H$_3$-2,6-Mes$_2$)Cl(IMe$_4$) (**28**) (295°) and compares well with that of Si_2Cl_2(IDipp)$_2$ (308.0°) and of [Si(IMe$_4$)$_3$]I$_2$ (**23**, 312°).[68] The change in the sum of bond angles can be attributed to the increased steric repulsion between the substituents and to changes in hybridization of the Si atom upon going from Si(C$_6$H$_3$-2,6-Mes$_2$)Cl(IMe$_4$) (**28**) to (Si(C$_6$H$_3$-2,6-Mes$_2$)(IMe$_4$))$_2$ (**32**).[31]

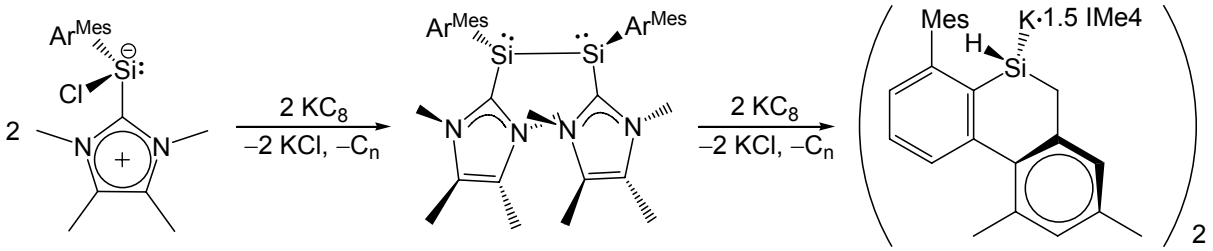

28 **32** **34**

Scheme 33: Stepwise reduction of Si(C$_6$H$_3$-2,6-Mes$_2$)Cl(IMe$_4$) (**28**) with KC_8.

[30] Interestingly, the analogous compound Si_2Cl_2(IDipp)$_2$ (**11**) is orange-red.

[31] The non-polar Si–Si bond has a higher *s*-character (or lower *p*-character) in comparison to the polar Si–Cl bond, therefore the angles between the substituents are higher in (Si(C$_6$H$_3$-2,6-Mes$_2$)(IMe$_4$))$_2$ (**32**). See also p. 56.

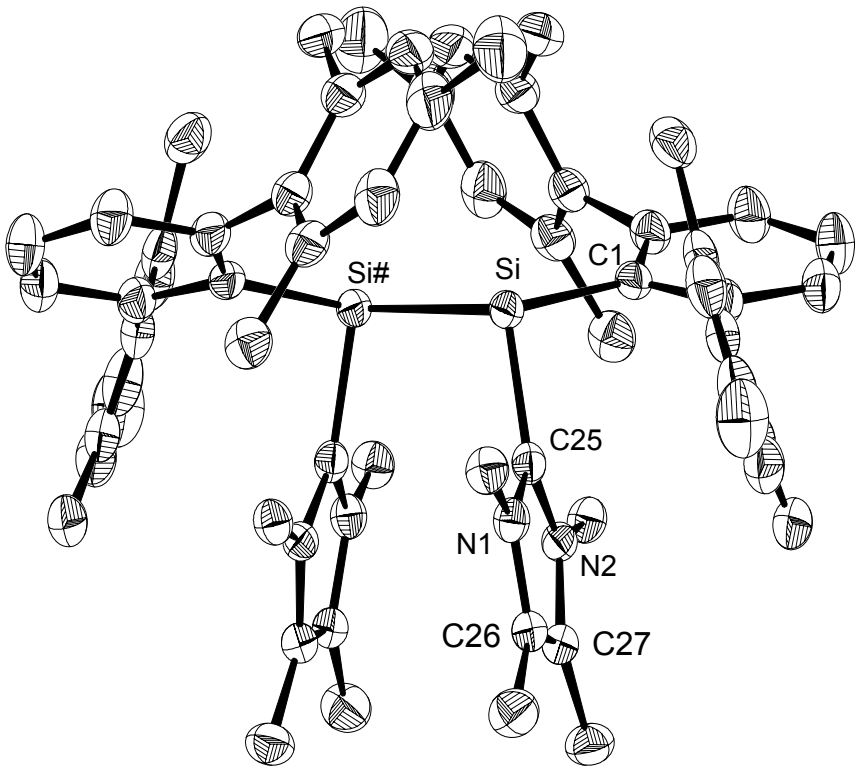

Figure 19: DIAMOND plot of the molecular structure of **32**. Thermal ellipsoids are set at 50% probability. Hydrogen atoms are omitted for clarity. Selected bond lengths [Å], bond angles and torsion angles [°]: Si–Si# 2.391(2), Si–C1 1.962(4), Si–C25 1.923(4), C25–N1 1.357(5), C25–N2 1.372(4), N1–C26 1.394(5), N2–C27 1.383(5), C26–C27 1.347(5); C1-Si-Si# 115.7(1), C1-Si-C25 96.3(2), C25-Si-Si# 101.5(1), C1-Si-Si#-C1# 157.2 (2), C25-Si-Si#-C25# 2.8(2).

The sterically demanding *m*-terphenyl substituents are arranged in an *anti*-conformation as indicated by the dihedral angle ∠C1-Si-Si#-C1# 157.2°, and the NHC-fragments in a *syn*-conformation (∠C25-Si-Si#-C25# 2.9°). It is interesting to note, that **32** is formed as a racemic mixture of S,S- and R,R-stereoisomers, but the *meso*-form (R,S-isomer) was not observed. The X-ray diffraction analysis revealed the presence of both enantiomers (R,R- and S,S-isomers) in the unit cell.[32] Therefore, the carbene fragments and the lone pairs of electrons are forced to be in a *syn*-conformation, despite of the steric repulsion of the carbenes (Scheme 34).

[32] The reduction of SiI_2(IDipp) leads also exclusively to a racemic mixture of S,S- and R,R-isomers of Si_2I_2(IDipp)$_2$, as evidenced by NMR spectroscopy. M. Arz, *personal communication*, University of Bonn, **2011**.

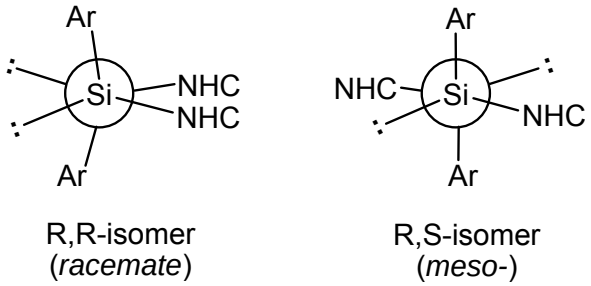

Scheme 34: Newman projections of the R,R-isomer of **32** found in the solid state (left) and the possible R,S-isomer (right).

Compound **32** can be viewed as a biscarbene adduct of the unknown disilyne Ar^{Mes}–Si≡Si–Ar^{Mes} (Ar^{Mes} = -C_6H_3-2,6-Mes_2), therefore it was reasonable to assume, that abstraction of the carbenes from **32** might lead to the disilyne. We attempted to abstract the carbenes with tris(aryl)borane B(C_6H_4-4-CH_3)$_3$ as a Lewis-acid. The ^{1}H NMR spectrum of the reaction mixture revealed the selective formation of the carbene-borane adduct IMe_4·B(Tol)$_3$ (Tol = -C_6H_4-4-Me) along with a number of other signals attributed to new products containing Mes groups. We were not able to isolate any of these products. The outcome of the reaction can be explained as follows: the abstraction of carbene with B(Tol)$_3$ occurs, but the formed disilyne (or monocarbene adduct of disilyne)[148] is not stable under the experimental conditions (heating at 110 °C in toluene (Scheme 35).

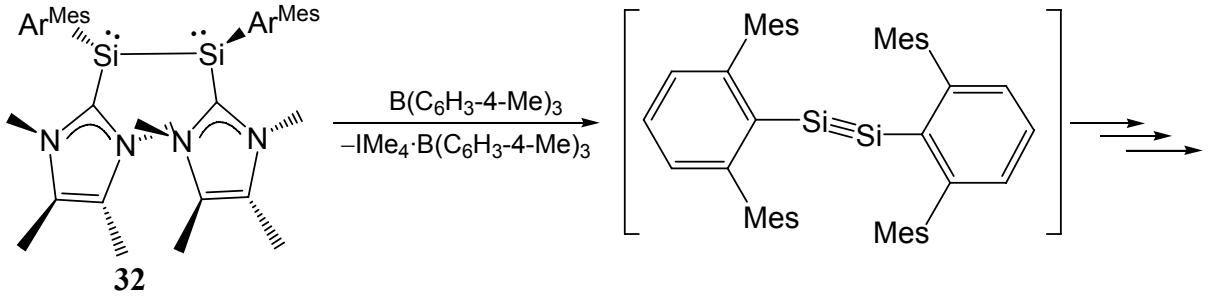

Scheme 35: The abstraction of carbene from **32** with tris(p-tolyl)borane (Ar^{Mes} = -C_6H_3-2,6-Mes_2).

As was mentioned earlier, the reduction of Si(C_6H_3-2,6-Mes_2)Cl(IMe_4) (**28**) even with one equivalent of KC_8 afforded a mixture of products. The mixture was composed of the starting material, the one-electron reduction product **32** and other products. The presence of the starting material suggested to, that further reduction of **32** might occur. Therefore, the reduction was repeated using 2.5 equivalents of KC_8 for a prolonged period of time. The originally developed dark violet-blue color (attributed to the presence of **32**) subsequently changed to brown. After work-up, the product of reduction **34** was isolated (Scheme 33). The reaction presumably proceeds via the intermediate formation of "K[Si-(C_6H_3-2,6-Mes_2)]"

which is unstable and undergoes a C–H activation of one C^2-*CH_3* group of the mesityl groups. Complex **34** is composed of dimers in the solid state (Figure 21). The immediate coordination environment of each silicon atom is depicted in Figure 20.

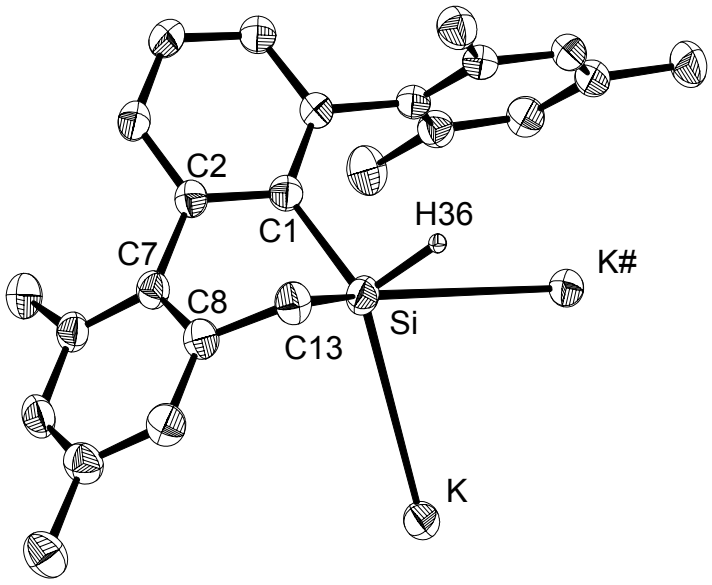

Figure 20: DIAMOND plot of a fragment of the molecular structure of **34**. Thermal ellipsoids are set at 50% probability. Hydrogen atoms are omitted for clarity. Selected bond lengths [Å], bond angles and torsion angles [°]: Si–C1 1.925(2), Si–C13 1.951(2), Si–H36 1.38(2), Si–K 3.4509(6), Si–K# 3.3370(5); C1-Si-C13 91.02(7), C1-Si-H36 101.1(9), C13-Si-H36 100.4(9), K-Si-K# 69.172(12), C1-C2-C7-C8 41.9(2).

The ^{1}H NMR spectroscopy corroborates the X-ray structure. The presence of a hydrogen atom at Si was confirmed by a resonance in ^{1}H NMR spectrum at 1.38 ppm in THF-d_8. The Si center is a chirality center and exhibits a distorted square pyramidal geometry in the solid state. The central C_6H_3-ring and the C–H activated mesityl ring are twisted against each other, as indicated by the torsion angle C1-C2-C7-C8 of 41.9(2)°. In the solid state the dimer **34** is bridged by the two potassium cations. Coordination of three 1,3,4,5-tetramethyimidazol-2-ylidene (IMe_4) molecules to the potassium ions complements the structure (Figure 21). The Si–K distances of 3.4509(6) and 3.3370(5) Å compare well with that, found in the dipotassium salt of a 9,9′-disila-9,9′-bifluorenyl dianion (3.456(1) Å)[149] and with the mean Si–K distance of 3.5(1) Å in potassium silanides[33]. Coordination of carbenes to potassium ions has been rarely observed. The K–C bond lengths in **34** (2.935(2) and 3.146(2) Å) are similar to those, found in other NHC-complexes of potassium (2.896(5)–2.954 Å).[150]

[33] According to a CSD survey from 8.2011 of 30 structurally characterized compounds of the type K–^{T4}Si. Median *d*(K–Si) = 3.441 Å, LQ = 3.321 Å, HQ = 3.584 Å.

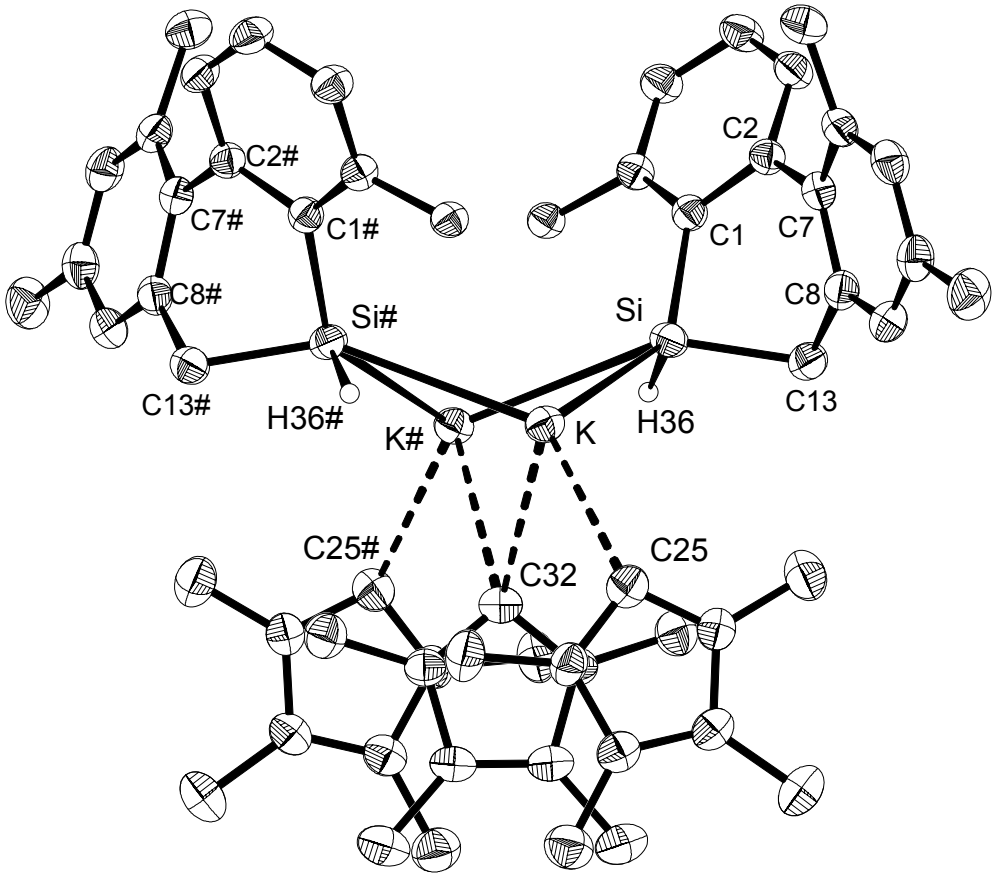

Figure 21: DIAMOND plot of the molecular structure of the dimer **34**. Thermal ellipsoids are set at 50% probability. Hydrogen atoms and one Mes group in each silafluorenyl anion Trip groups are omitted for clarity. Selected bond lengths [Å] and bond angles [°]: C25–K 2.935(2), C32–K 3.146(2); C25-K-C32 76.34(4); K-C32-K# 75.54(5).

The reduction of $Si(C_6H_3\text{-}2,6\text{-}Trip_2)Cl(IMe_4)$ (**29**) with KC_8 was also investigated (Scheme 36). The reduction proceeds stepwise, as in the case of $Si(C_6H_3\text{-}2,6\text{-}Mes_2)Cl(IMe_4)$ (**25**). Treatment of **29** with one equivalent of potassium graphite in THF at ambient temperature resulted in rapid development of an intense violet color. The new compound was found to be extremely sensitive towards moisture and oxygen. Its solutions rapidly decolorized even in contact with the nitrile gloves. All attempts to isolate the compound were unsuccessful, due to combination of factors: high sensitivity, instability in non-etheral solvents and low selectivity of the reduction. The compound decomposed also in the solid state fast, but a purple THF solution retained its color for at least one day. The EPR spectrum of the reaction mixture is presented in Figure 22, suggesting that the purple product of the reduction is a radical **33** (Scheme 36). The formation of the radical **33** and not the carbene-stabilized disilylene $(Si(C_6H_3\text{-}2,6\text{-}Trip_2)(IMe_4))_2$, analogues to $(Si(C_6H_3\text{-}2,6\text{-}Mes_2)(IMe_4))_2$ (**32**), can be explained by the higher steric hindrance of the Trip groups in comparison to the Mes groups. However,

the radical **33** is considered only as a possible intermediate product, further investigations of the reaction are necessary to confirm this hypothesis.

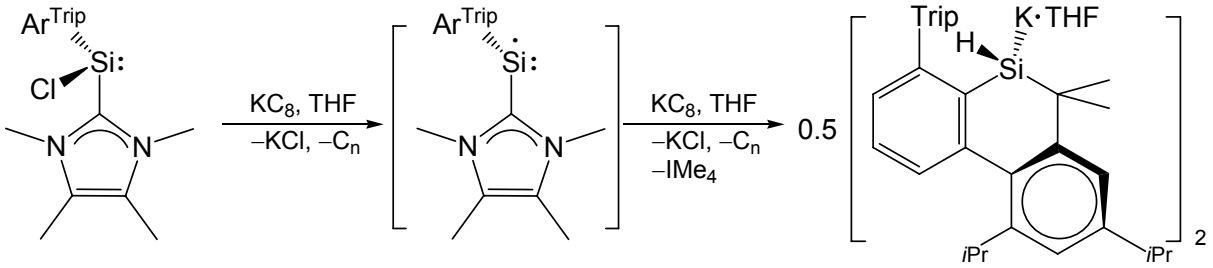

29, **33** **35**

Scheme 36: Stepwise reduction of $Si(C_6H_3\text{-}2,6\text{-}Trip_2)Cl(IMe_4)$ (**29**) with KC_8 (Ar^{Trip} = -C_6H_3-2,6-$Trip_2$).

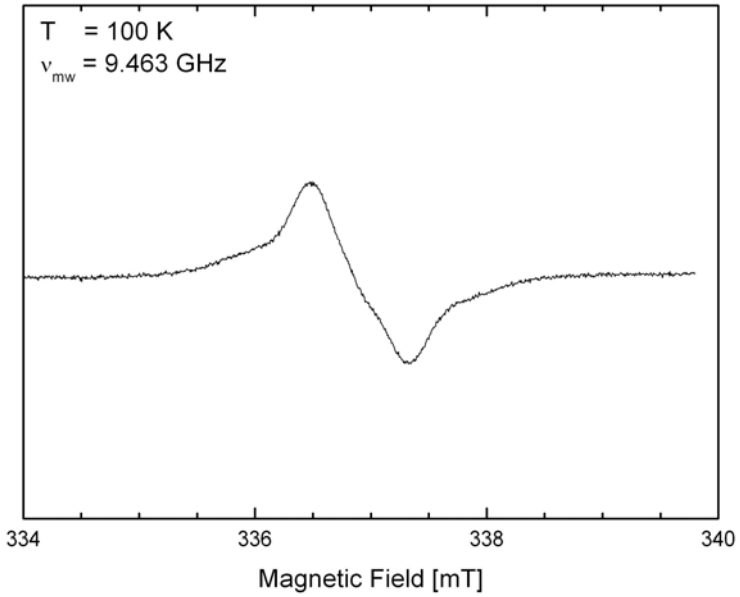

Figure 22: The EPR spectrum of the putative intermediate **33**.

Further reduction of $Si(C_6H_3\text{-}2,6\text{-}Trip_2)Cl(IMe_4)$ (**29**) with two equivalents of potassium graphite led to a C–H activated product, with structural motive similar to **34** (Scheme 36). The Si center has a distorted square pyramidal geometry. The central C_6H_3-ring and C–H activated Trip-ring are twisted against each other, as indicated by the torsion angle C1-C2-C7-C8 of 41.0(4)°.

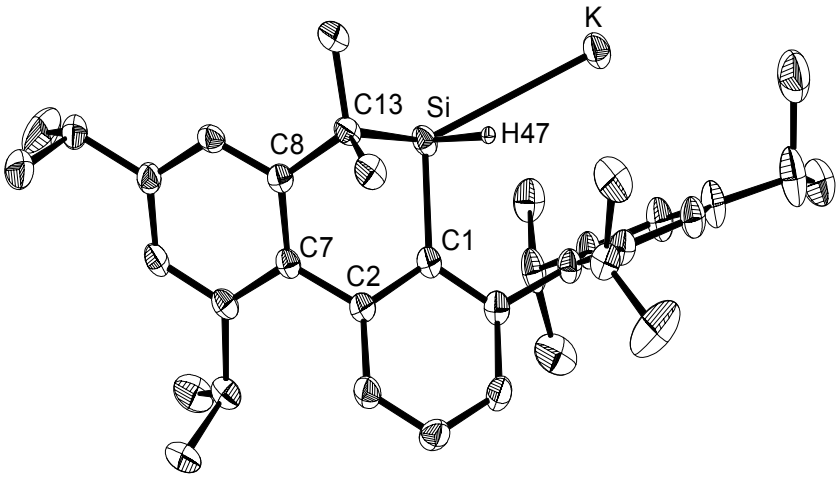

Figure 23: DIAMOND plot of the immediate Si coordination environment in **35**. Thermal ellipsoids are set at 50% probability. Hydrogen atoms are omitted for clarity. Selected bond lengths [Å], bond angles and torsion angles [°]: Si–C1 1.916(3), Si–C13 1.956(3), Si–H47 1.48(5), Si–K 3.425(1); C1-Si-C13 93.7(1), C1-Si-H47 89(2), C13-Si-H47 96 (2), C1-C2-C7-C8 41.0(4).

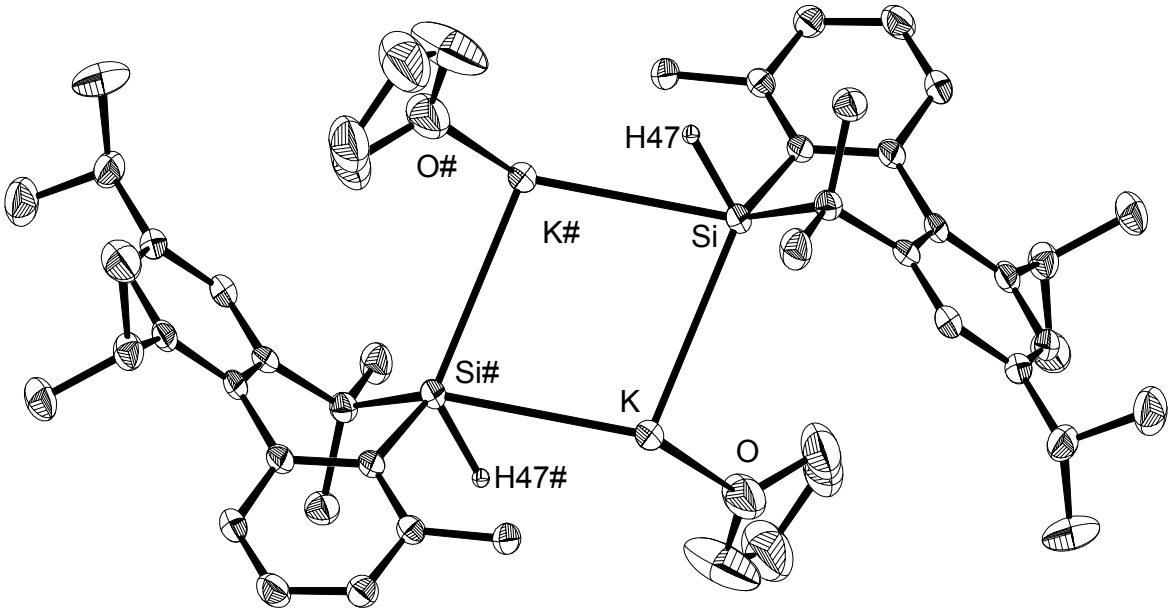

Figure 24: DIAMOND plot of the molecular structure of the dimmer **35**. Thermal ellipsoids are set at 50% probability. Hydrogen atoms and Trip groups are omitted for clarity. Selected bond lengths [Å] and bond angles [°]: O–K 2.637(3), Si–K 3.425(1), Si–K# 3.451(1); Si-K-Si# 103.64(2); K-Si-K# 76.36(2).

Compound **35** has a dimeric structure in the solid state. The two silyl anions are bridged by potassium cations, the Si–K bond lengths are almost equal (3.425(1) and 3.451(1) Å) and compare well with those in **34**. Due to the steric demand of the *m*-terphenyl substituent, the potassium centers are three-coordinated. This coordination number is quite unusual for

potassium. The K–O distance of 2.637(3) Å compares well with those found in other THF solvates of K^+, e.g. 2.666(2) Å in $[(THF)K\{\mu\text{-}NTMS_2\}_2Ca(NTMS)]_n$ and 2.709(2)–2.726(2) Å in $(THF)_3K\{\mu\text{-}NTMS_2\}_2K(THF)_3$ (TMS = $-SiMe_3$).[151]

The reduction of carbene-stabilized silylenes **28** and **29** leads to different products than the reduction of aryltrifluorosilanes bearing similar substituents, demonstrating the impact of a carbene on the reactivity of silicon in low oxidation states. Thus, treatment of $SiF_3(C_6H_3\text{-}2,6\text{-}Mes_2)$ and $SiF_3(C_6H_3\text{-}2,6\text{-}Trip_2)$ with sodium metal in THF leads to products of insertion into C–C bonds, according to Scheme 37.[130] The proposed mechanism for this transformation suggested the intermediate formation of Ar–Si≡Si–Ar and SiArF. We also observed the insertion of a silicon center in low-oxidation state into a C–C bonds (see p. 126). In contrast, in the cases where the silicon center was coordinated to a carbene, only insertion into C–H bonds was observed (pp. 58, 63, 66, 70, 77).

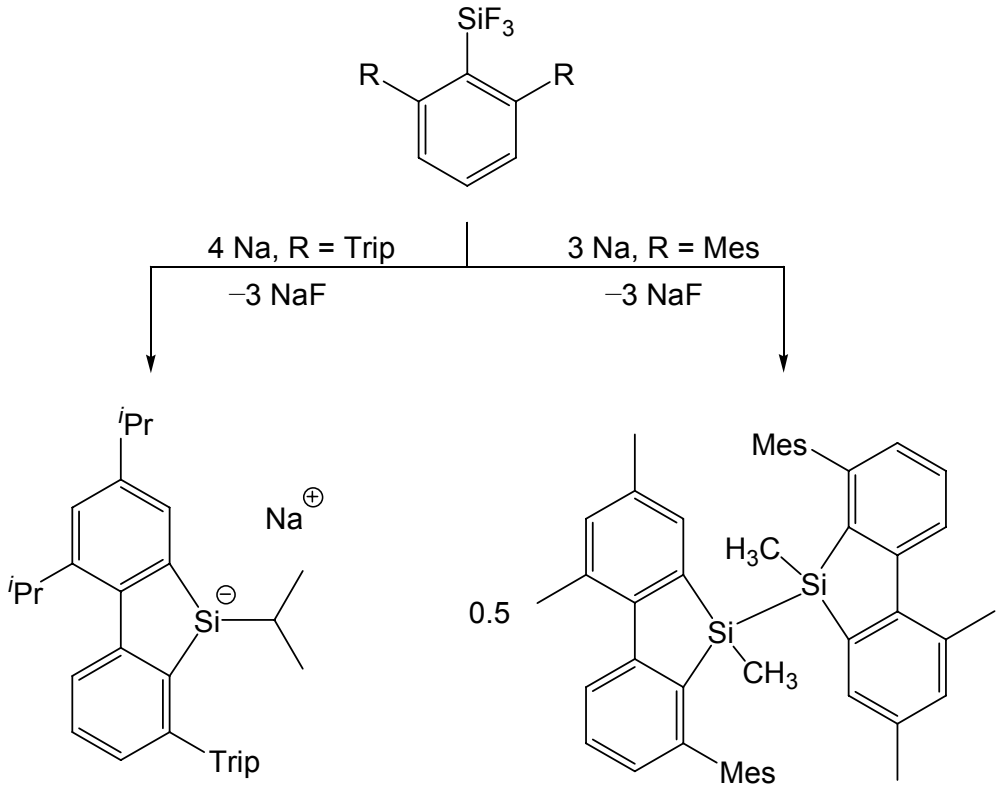

Scheme 37: Reduction of $SiF_3(C_6H_3\text{-}2,6\text{-}R_2)$ with Na (R = Mes or Trip).

Various reactions of the NHC-stabilized arylchlorosilylenes

We investigated the reactivity of NHC-stabilized arylchlorosilylenes towards various reagents. The reaction of Si(C_6H_3-2,6-$Trip_2$)Cl(IMe_4) (**29**) with KPF_6 leads to a mixture of two products, one of which was identified by X-ray crystallography to be the product of C–H activation of the carbene (Scheme 38). The oxidation of Si(C_6H_3-2,6-Mes_2)Cl(IMe_4) (**28**) with white phosphorous afforded the Si(IV) cluster compound **37**, and treatment of Si(C_6H_3-2,6-$Trip_2$)Cl(IMe_4) with $CpCo(C_2H_4)_2$ gave upon elimination of ethylene complex **38** (Scheme 38).

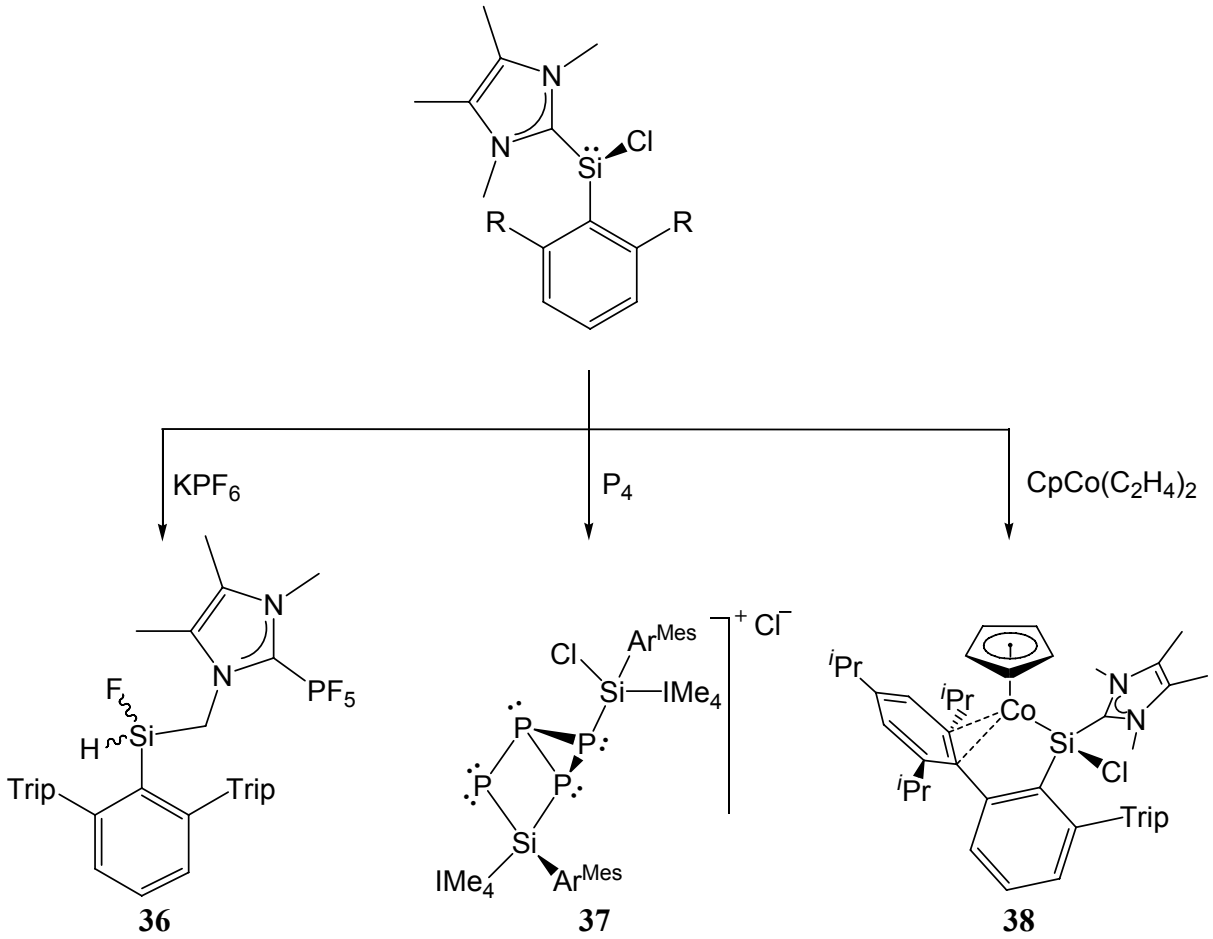

Scheme 38: Reactivity of the NHC-stabilized arylchlorosilylene towards KPF_6, P_4 and $CpCo(C_2H_4)_2$ (Trip = 2,4,6-*i*Pr_3-C_6H_2-; Ar^{Mes} = 2,6-Mes_2-C_6H_3-; IMe_4 = 1,3,4,5-tetramethyimidazol-2-ylidene).

The abstraction of chloride, leading to **36** proceeds only at elevated temperatures (110 °C). We suppose, that the intermediately formed cationic species $[Si(C_6H_3\text{-}2,6\text{-}Trip_2)(IMe_4)]^+$ undergoes fast C–H activation of one of the N-*CH_3* groups of the carbene ligand leading after

abstraction of a fluorine atom to **36**.[34]. The structure of **36** was determined by X-ray diffraction analysis, Figure 25.

The silicon center exhibits a distorted tetrahedral geometry. The presence of the Si–*H* functionality was confirmed by NMR studies. The carbene fragment is coordinated to the Lewis acidic PF_5 fragment. The C–P bond length of 1.880(3) Å compares well with that of the PF_5 adduct of 1,3-dimesityl-4,5-dichloroimidazol-2-ylidene (1.898(3) Å).[152]

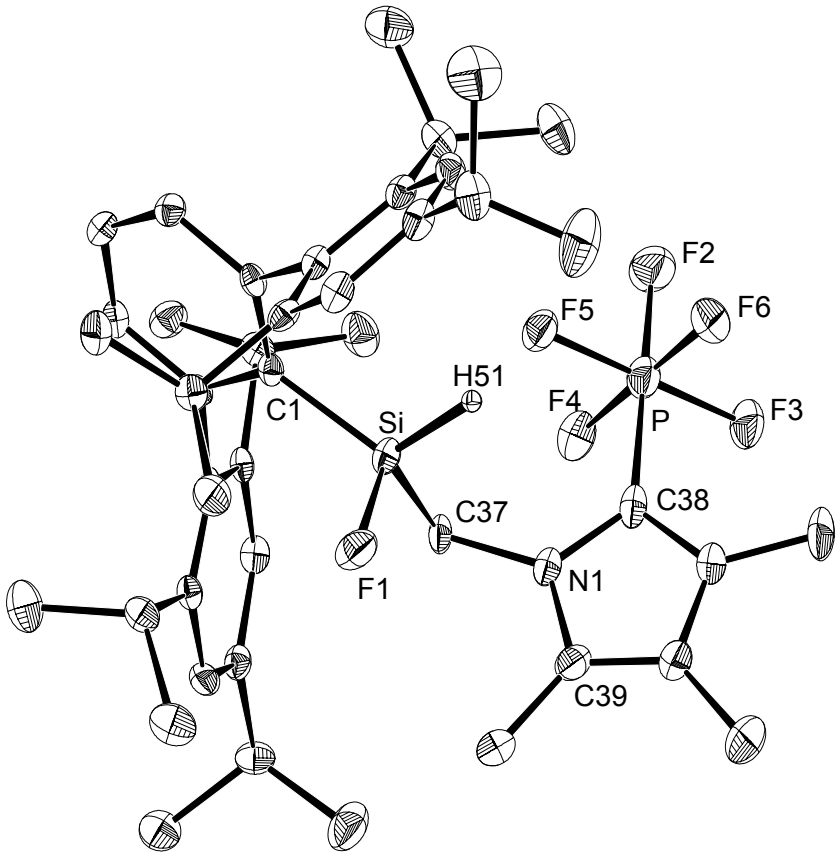

Figure 25: DIAMOND plot of the molecular structure of **36**. Thermal ellipsoids are set at 50% probability. Hydrogen atoms are omitted for clarity. Selected bond lengths [Å] and bond angles [°]: C1–Si 1.868(2), Si–H 1.45(3), C37–Si 1.889(3), C37–N1 1.474(3), C38–P 1.880(3), F1–Si 1.636(2); C1-Si-C37 117.0(1), C1-Si-F1 108.02(9), F1-Si-C37 105.9(1).

The Si atom in the NHC-stabilized silylenes has a formal oxidation state of +2 and can be oxidized to Si (+4). The addition of P_4 to $Si(C_6H_3\text{-}2,6\text{-}Mes_2)Cl(IMe_4)$ (**28**) with white phoshporus in benzene resulted in the precipitation of the ionic product **37**, featuring a SiP_4

[34] A similar C–H activation reaction was observed upon treatment of $Si(C_6H_3\text{-}2,6\text{-}Trip_2)Cl(IMe_4)$ with carbonyl metallates $Li[CpM(CO)_3]$, M = Cr, Mo, W, see Section 2.2.2.

core (Figure 26). An analogues reaction with $Si(C_6H_3\text{-}2,6\text{-}Trip_2)Cl(IMe_4)$ was less selective and identification of any products was impossible.

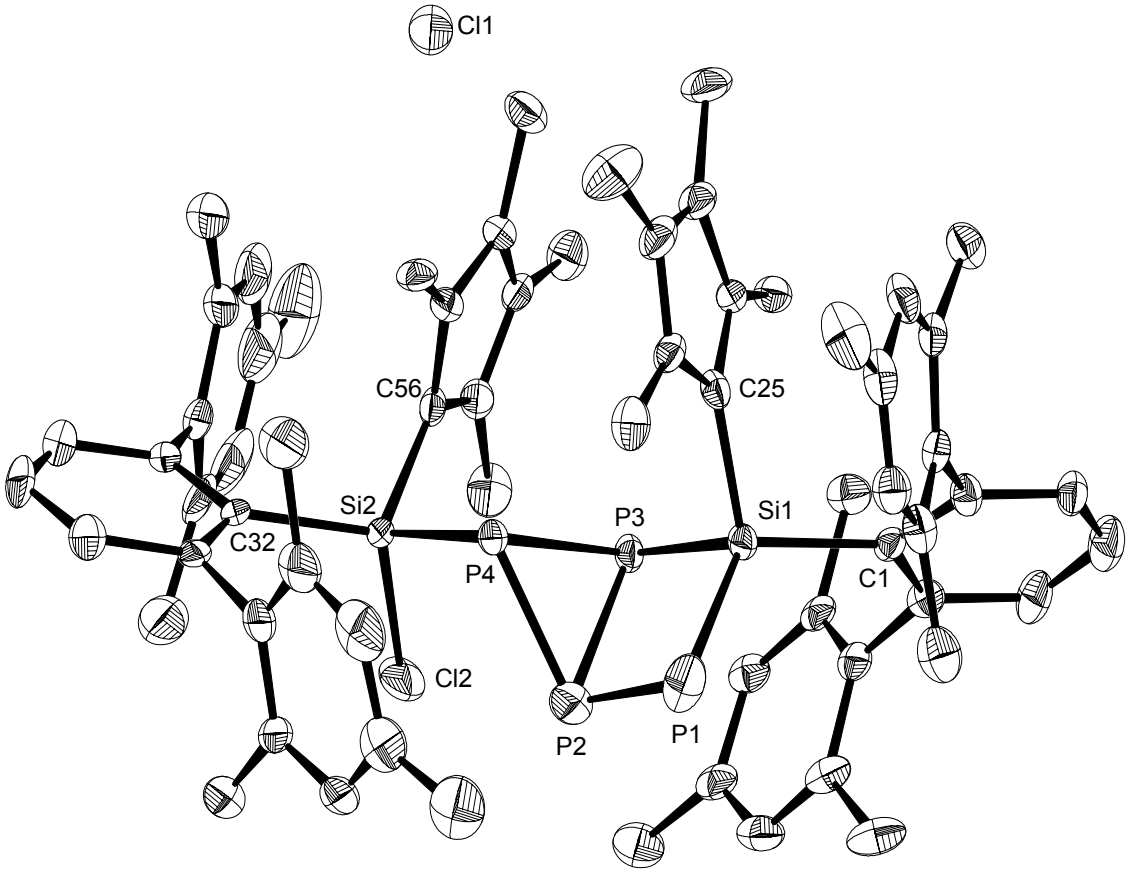

Figure 26: DIAMOND plot of the molecular structure of **37**. Thermal ellipsoids are set at 50% probability. Hydrogen atoms are omitted for clarity. Selected bond lengths [Å], bond angles and torsion angles [°]: C1–Si1 1.909(3), C32–Si2 1.899(4), C25–Si1 1.934(4), C56–Si2 1.922(4), Cl2–Si2 2.1699(14), P1–Si1 2.107(1), P1–P2 2.272(2), P2–P4 2.207(2), P2–P3 2.259(1), P3–P4 2.242(1), P3–Si1 2.275(1), P4–Si2 2.265(1); Si1-P1-P2 83.25(5), P4-P2-P3 60.25(4), P4-P2-P1 96.55(7), P3-P2-P1 96.50(6), P4-P3-P2 58.73(5), P4-P3-Si1 89.74(5), P2-P3-Si1 81.22(5), P2-P4-P3 61.02(5), P2-P4-Si2 102.92(6), P3-P4-Si2 89.75(5); P1-P2-P3-P4 93.84(7), P4-P2-P3-Si1 95.08(5).

In the salt **37** the silicon atoms exhibit a distorted tetrahedral geometry. The Si–P bond lengths of 2.17–2.27 Å are in the range observed for compounds featuring Si–P bonds.[35] Similar cluster compounds have been synthesized by the reactions of white phosphorous with N-heterocyclic carbenes, silylenes and Al(I) compounds.[153] Compound **37** features a complicated $^{31}P\{^1H\}$ NMR spectrum due to the presence of four inequivalent phosphorous

[35] According to a CSD survey from 11.2011 of 639 structurally characterized compouds, featuring P–^{T4}Si fragment. Mean *d*(P–Si) = 2.25(4) Å; median *d*(P–Si) = 2.253 Å, LQ = 2.209 Å, HQ = 2.289 Å, min *d*(P–Si) = 2.067 Å, max *d*(P–Si) = 2.608 Å.

nuclei. Coupling was observed between each pair of phosphorous atoms with coupling constants in the range of 7–290 Hz.

$Si(C_6H_3\text{-}2,6\text{-}Trip_2)Cl(IMe_4)$ (**29**) reacts smoothly with $[CpCo(C_2H_4)_2]$ at ambient temperature under elimination of two molecules of ethylene, leading to complex **38** (Scheme 37). The reaction demonstrates the donor properties of the lone pair at the Si atom. The $Si(C_6H_3\text{-}2,6\text{-}Trip_2)Cl(IMe_4)$ serves as 4-electron ligand, with the lone pair and the $C^1{=}C^2$ bond of one of the Trip substituents coordinated to the cobalt center (Figure 27). The $Si–C_{carbene}$ bond length (1.961 Å) is slightly shorter than that in $Si(C_6H_3\text{-}2,6\text{-}Trip_2)Cl(IMe_4)$ (1.963(2) Å). Also the $Si–C_{Ar}$ (1.883 Å) and Si–Cl (2.120 Å) bond lengths are shorter in comparison to those in $Si(C_6H_3\text{-}2,6\text{-}Trip_2)Cl(IMe_4)$ (1.937(2) Å and 2.1836(8) Å respectively). The ^{13}C NMR shift of $C_{carbene}$ appears at higher field than that of **29 (**157.2 ppm and 166.7 ppm respectively). These data suggest, that complex **38** is better described as a silyl complex (see also the discussion on p. 45).

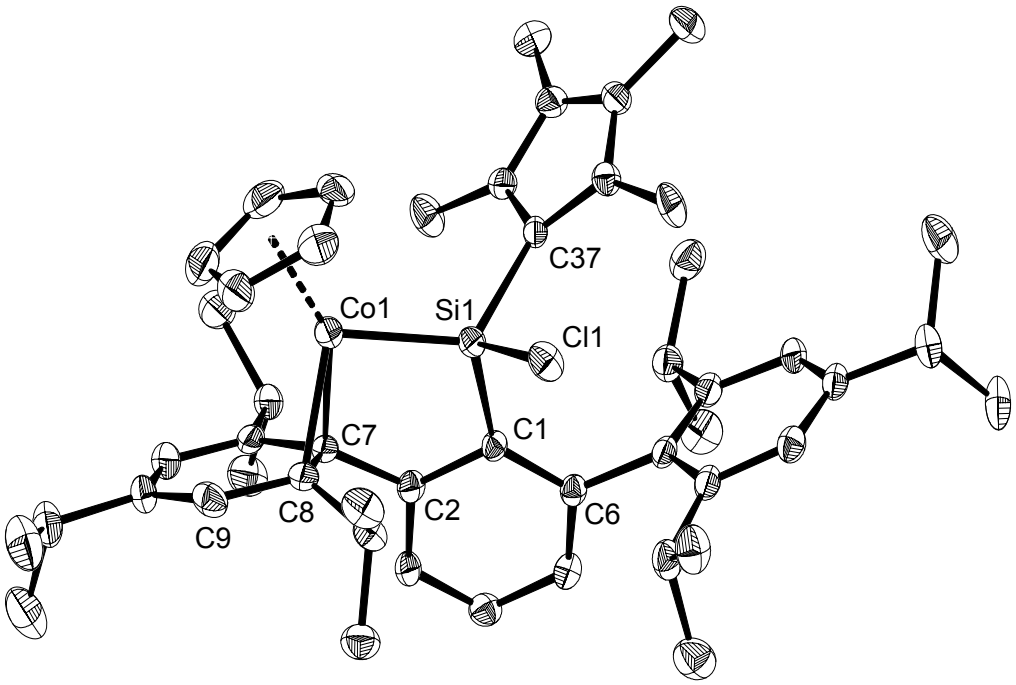

Figure 27: DIAMOND plot of the molecular structure of **38**. Thermal ellipsoids are set at 50% probability. Hydrogen atoms are omitted for clarity. Two independent molecules were found in the asymmetric unit. Selected bond lengths [Å], bond angles and torsion angles [°] (values in brackets correspond to the second independent molecule): C1–Si1 1.885(3) [1.881(3)], Cl1–Si1 2.122(1) [2.119(1)], Si1–C37 1.963(3) [1.959(3)], Co1–Si1 2.169 (1) [2.165(1)], C7–Co1 2.042(3) [2.055(3)], C8–Co1 2.050(3) [2.053(3)]; C2-C1-Si1 107.6(2) [108.3(2)], C6-C1-Si1 133.4(2) [132.1(2)], C2-C7-Co1 119.2(2) [117.6(2)], C1-Si1-Co1 108.2(1) [107.64(2)]; C2-C7-C8-C9 139.7(3) [142.8(3)].

Due to the fixed orientation of the *m*-terphenyl group, the hindered rotation about the Si–$C_{carbene}$ bond and the presence of a chiral Si center (overall C_1 symmetry), all atoms in **38** are rendered not equivalent (excluding only the C_5H_5 ligand). This leads, for example, to the rise of 12 doublets (12 × CH*Me*), 6 septets (6 × C*H*Me_AMe_B), 4 singlets (2 × N-*Me*, 2 × C-*Me*, IMe_4), 4 doublets (4 × C_{meta}-*H*, Trip) and a multiplet corresponding to the 3 signals of the central C_6H_3 ring in the ^{1}H NMR spectrum. This pattern is typical for chiral compounds bearing the -C_6H_3-2,6-$Trip_2$ group, if a rotation about the C^1-X bond does not occur on the NMR timescale. Analysis and assignment of the signals in NMR spectra of these compounds was a challenging task, which was fulfilled by a thorough analysis of HMBC, HMQC andH,H-COSY NMR spectra.

Complex **38** is thermally unstable and slowly undergoes a C–H activation of one of the N-CH_3 group of the carbene fragment (Scheme 39). The reaction is slow at ambient temperature, however it occurs rapidly at 50 °C in benzene solution is ($\tau_{1/2} \approx 1$ h). The structure of the compound was verified by X-ray crystallography.[36] The characteristic Co-*H* resonance appears in the ^{1}H NMR spectrum at −17.26 ppm.

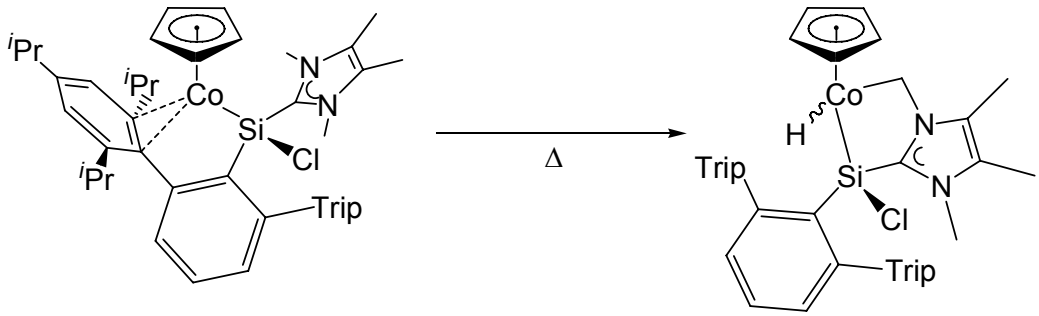

38 **39**

Scheme 39: Intramolecular insertion of Si center into the C–H bond in **38**.

Another reaction demonstrating the basic properties of SiArCl(IMe_4) is presented in Scheme 40. Treatment of Si(C_6H_3-2,6-$Trip_2$)Cl(IMe_4) (**29**) in THF at –70 °C with HCl resulted in fast discoloration. However, upon warming up, a white solid precipitated from the clear reaction solution. We assumed the solid to be the imidazolium salt [IMe_4H]Cl. The formation of [IMe_4H]Cl is probably the result of decomposition of the intermediately formed salt [Si(C_6H_3-2,6-$Trip_2$)Cl(IMe_4)H]Cl. When **29** was treated with HCl at –70 °C and subsequently with Li[CpMo$(CO)_3$], a stable complex **40** was isolated, probably due to the fact that the complex anion [CpMo$(CO)_3$]$^-$ is a rather large weak nucleophile and can not attack the Si center because of steric reasons. Complex **40** is best described as an imidazolium salt, bearing an

[36] The quality of the structure was very low with $wR_2 = 0.5120$, and will not be discussed.

arylchlorosilyl substituent in C^2 position. Thus, the ^{13}C NMR spectrum displays a signal at 139.2 ppm corresponding to the N-C^2-N atom. The position of the signal compares well with that of $[IMe_4H]Cl$. The structure was confirmed by X-ray diffraction analysis.

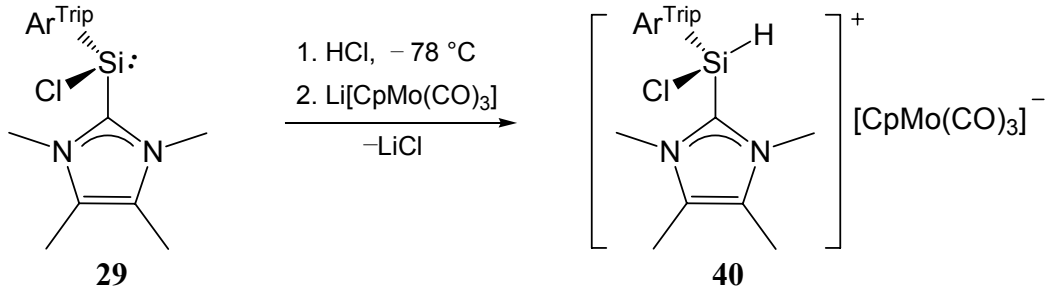

29 **40**

Scheme 40: Basic properties of $Si(C_6H_3\text{-}2,6\text{-}Trip_2)Cl(IMe_4)$ (**29**); IMe_4 = 1,3,4,5-tetramethyimidazol-2-ylidene. Ar^{Trip} = -C_6H_3-2,6-$Trip_2$.

We attempted to substitute chloride in $Si(C_6H_3\text{-}2,6\text{-}Trip_2)Cl(IMe_4)$ (**29**) with several nucleophiles. When **29** was reacted with MeLi in benzene/Et_2O mixture 3:4 no reaction was observed even with excess of MeLi. The reaction with LiI in benzene resulted in fast discoloration of the yellow solution; the ^1H NMR spectrum revealed unselective transformation. **29** did not react with NaN_3 at ambient temperature, however in boiling toluene the reaction proceeded and resulted in formation of the product of insertion of the Si center in C–H bond of one N–CH_3 group of the carbene ligand (Scheme 41). The compound **41** was isolated as a white microcrystalline solid in 47% yield; it is soluble in common organic solvents, including hexane and pentane.

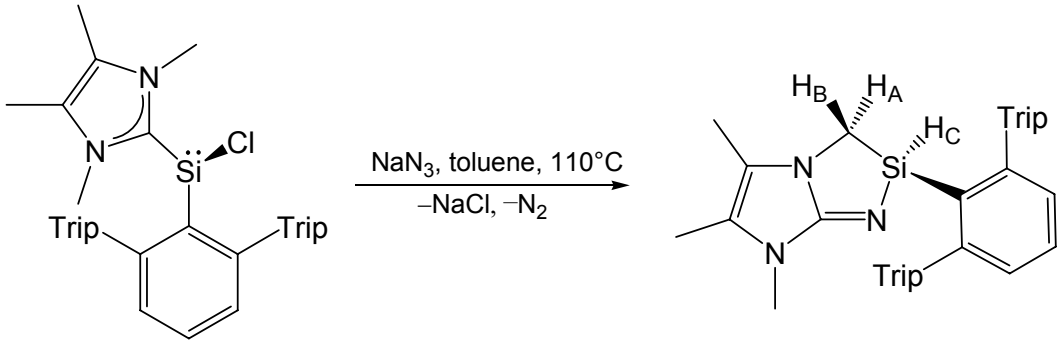

29 **41**

Scheme 41: Reaction of $Si(C_6H_3\text{-}2,6\text{-}Trip_2)Cl(IMe_4)$ (**29**) with NaN_3 (Trip = - C_6H_2-2,4,6-iPr$_3$).

The structure of the product was identified by X-ray diffraction analysis and confirmed by the NMR, IR spectroscopy and elemental analysis.[37] The compound features two fused N-heterocycles, presumably resulted from substitution of the Cl atom in **29** with an azido group and subsequent decomposition and rearrangements. The silicon atom features distorted

[37] The quality of the X-ray structure was rather low with wR_2 = 0.2564 and will not be discussed.

tetrahedral coordination geometry with four different substituents and therefore is a chiral center. The rotation about Si–C_{Ar} bond is fast on the NMR timescale, as indicated by the multiplicity of the signals in the spectra, e.g. the presence of 6 doublets and 3 septets for the isopropyl groups of the Trip substituents in the ^{1}H NMR spectrum (Figure 28). The signal of the Si–H proton appears at 5.33 ppm and shows coupling to the neighboring H_A and H_B protons, as well as to the Si nucleus with ^1J(Si,H) = 216.5 Hz. The ^{29}Si NMR spectrum of **41** displays a singlet resonance at 3.9 ppm in the usual region for silanes. The presence of the Si–H moiety was also confirmed by the solid state IR absorption band at 2139 cm^{-1}.

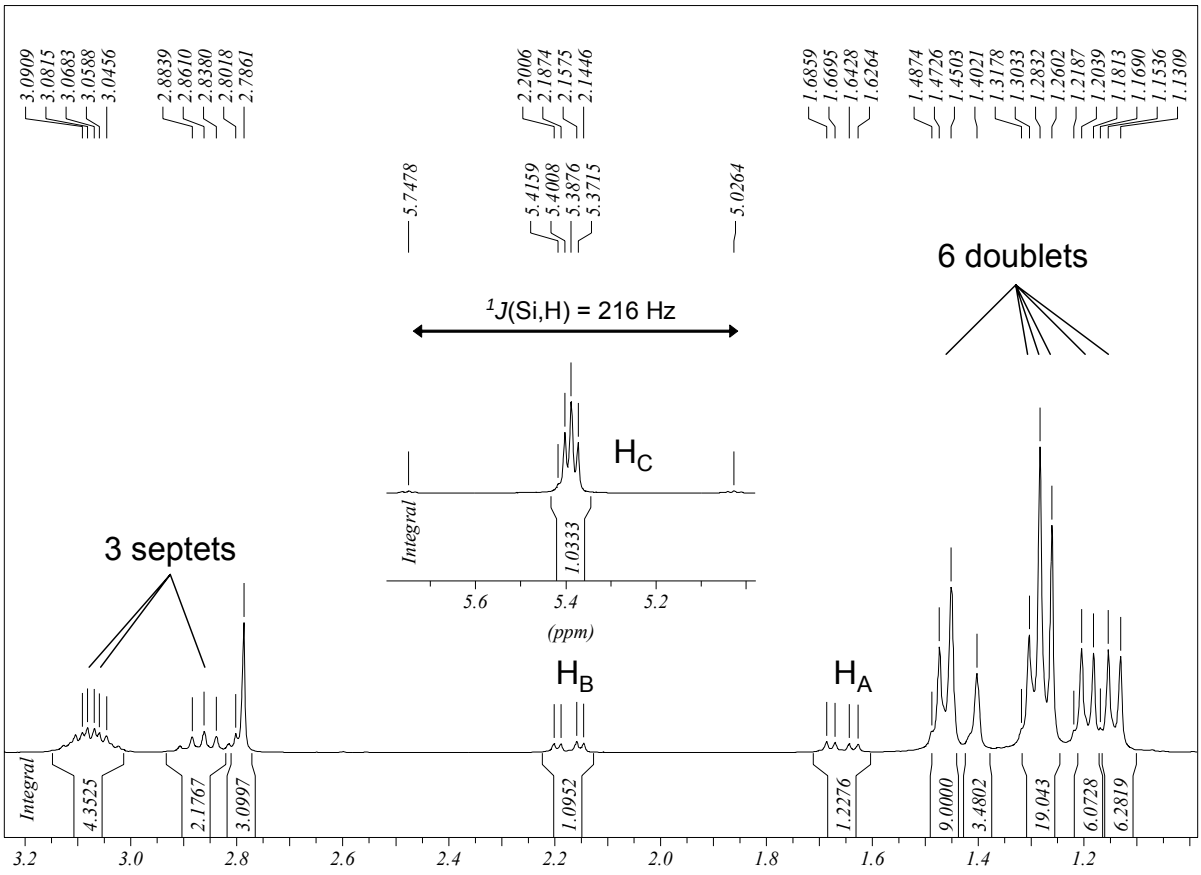

Figure 28: Fragment of the ^{1}H NMR spectrum of **41** (300.1 MHz, C_6D_6, 298 K).

2.2 Access to the first silylidyne complexes

In the previous chapter the stabilization of dihalo- and arylchlorosilylenes with N-heterocyclic carbenes was reported. In this chapter the reactivity of NHC-stabilized silylenes towards carbonyl metallates of Group VI transition metals will be presented, which provided access to a series of unprecedented complexes, featuring metal-silicon multiple bonds.

2.2.1 Synthesis of zwitterionic silylidene complexes of Mo and W

There are essentially two synthetic routes to ylidyne complexes. The first approach was reported by P. P. Power et al. [104, 105] and the second approach reported by A. C. Filippou et al. (Scheme 42).[106, 108, 110, 111, 154, 155] The synthesis of silylidyne complexes has been hindered so far because of the lack of suitable Si(II) precursors, e.g. SiRCl.

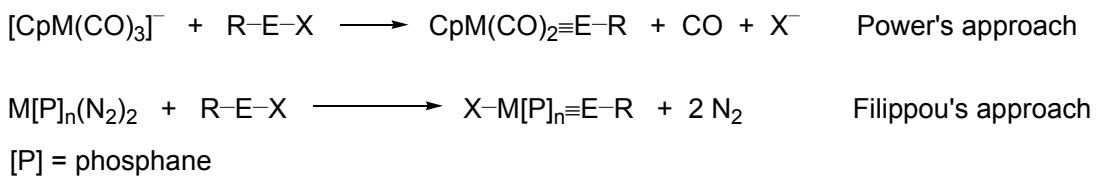

Scheme 42: The approaches to Group 14 ylidyne complexes (X = halogen, E = Ge–Pb).

Having in hands the carbene stabilized arylchlorosilylenes, the reactions of Si(C_6H_3-2,6-$Trip_2$)Cl(IMe_4) (**29**) with *cis*-[$Mo(N_2)_2(PMe_3)_4$] and [$W(\eta^2$-$CH_2PMe_2)H(PMe_3)_4$] were investigated in order to synthesize silylidyne complexes (Filippou's approach, Scheme 42). Both reactions were found to be unselective.[38] Therefore it was decided to investigate the reactivity of SiArCl(IMe_4) towards carbonyl metallates (Power's approach, Scheme 42). The reaction of Li[$CpMo(CO)_3$] with Si(C_6H_3-2,6-$Trip_2$)Cl(IMe_4) (**29**) in hot toluene was quite selective and afforded under elimination of CO and LiCl the zwitterionic silylidene complex **42** (Scheme 43).

[38] The reaction conditions were 5 min at 110 °C in toluene for *cis*-[$Mo(N_2)_2(PMe_3)_4$]; 20 h at 80 °C in benzene for [$W(\eta^2$-$CH_2PMe_2)H(PMe_3)_4$]. The reactions were monitored by ^1H and $^{31}P\{^1H\}$ NMR spectroscopy.

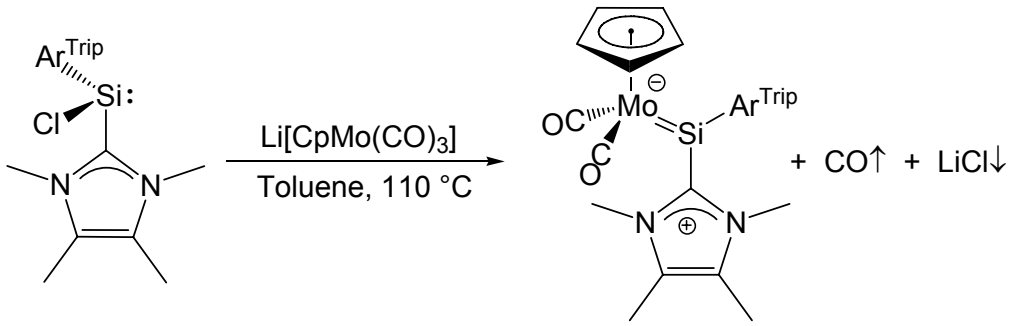

29 **42**

Scheme 43: Synthesis of silylidene complex **42**.

The complex was isolated in 51% yield as a brown thermally stable solid, which melts without decomposition at 125–130 °C and is soluble in common organic solvents, such as toluene, benzene and THF, slightly soluble in diethyl ether, and is insoluble in hexane or pentane. The compound was fully characterized and the structure was determined by X-ray crystallography (Figure 29).

The complex features a trigonal planar coordinated Si center as shown by the sum of bond angles of 357° and a short Mo–Si bond length of 2.345 Å.[39] The bond length is in the range previously reported for silylidene complexes of molybdenum (2.288–2.387 Å).[86, 87, 156] The shorter Mo–Si bond in **42** in comparison with the previously reported metal complexes of N-heterocyclic silylenes (2.413–2.480 Å) can be explained by the stronger Mo→Si backbonding in **42**.[84, 157, 158] The Si–$C_{carbene}$ bond length of 1.944 Å compares well with that in Si(C_6H_3-2,6-$Trip_2$)Cl(IMe_4) (**29**, 1.963(2) Å) and is only slightly longer than the Si–C_{Ar} bond length (1.920 Å in **42**, 1.937(2) Å in **29**). The silylidene ligand plane defined by the atoms Si, C_{Ar} and $C_{carbene}$ adopts an upright orientation with the aryl group pointing towards the C_5H_5 ring. The upright orientation is demonstrated by the dihedral angle of 10.8° between the silylidene ligand plane and the plane passing through the atoms Si, Mo and the center of gravity of the C_5H_5 ring (C_g). This conformation was also found in the isolobal carbene complex of chromium.[159]

For a sp^2 hybridized silicon atom one would expect the angles between its substituents to be close to 120°. In **42** and other silylidene complexes, the angles deviate from this value. The wide Mo-Si-C_{Ar} angle of 145.3° reflects the steric demand posed by the *m*-terphenyl substituent. The smaller C_{Ar}-Si-$C_{carbene}$ angle of 100.4° suggests that the Si atom utilizes mainly *p*-orbitals for the bonding to the aryl group and the carbene (the theoretical value would be 90°if silicon employ pure *p*-orbitals).

[39] The mean values of the bonding parameters of the two independent molecules are given.

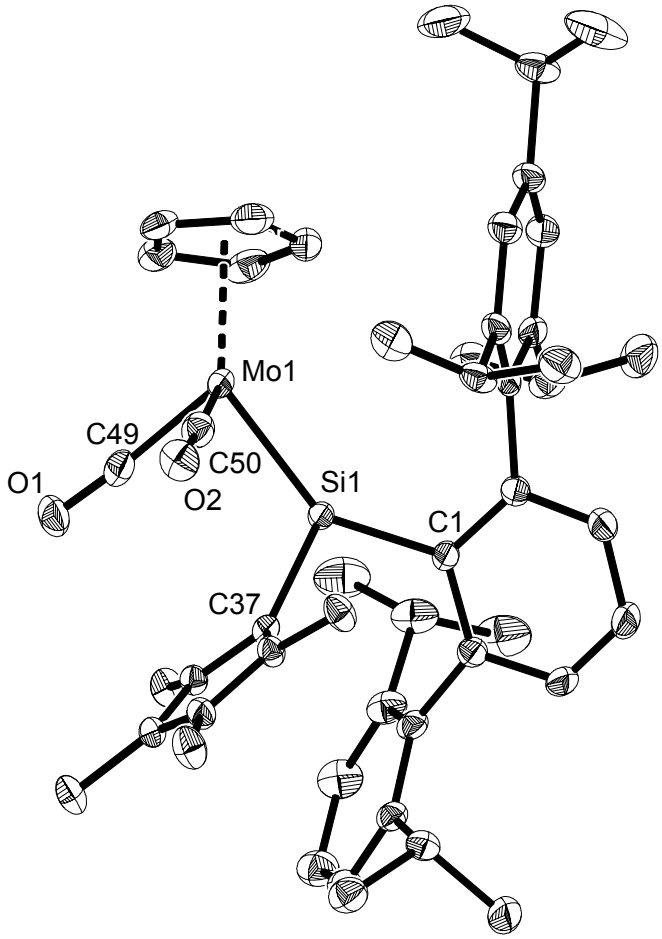

Figure 29: DIAMOND plot of the molecular structure of **42**. Thermal ellipsoids are set at 50% probability. Hydrogen atoms are omitted for clarity. Two independent molecules were found in the asymmetric unit. Selected bond lengths [Å] and bond angles [°] (values in brackets correspond to the second independent molecule): Mo1–Si1 2.3474(6) [2.3430(6)], Mo1–C49 1.917(2) [1.906(2)], Mo1–C50 1.936(2) [1.938(3)], Si1–C1 1.918(2) [1.922(2)], Si1–C37 1.943(2) [1.945(2)]; Mo1-Si1-C1 145.71(6), [144.92(6)], Mo-Si1-C37 111.08(6) [111.58(6)], C1-Si-C37 99.64(8) [101.12(8)], Si1-Mo1-C49 90.67(6) [91.36(7)], Si1-Mo1-C50 82.43(7) [82.53(8)], C49-Mo1-C50 78.80(9) [80.2(1)].

NMR and IR spectroscopy provided important information about the electronic structure of the complex. The IR spectrum of **42** in toluene shows two absorptions of approximately equal intensities at rather low wavenumbers (1859 and 1785 cm^{-1}). The IR absorption bands are at close positions to those of the isolobal complex $[Cp(CO)_2Cr{=}CPh(PMe_3)]$ (1894 and 1795 cm^{-1}).[159] The signals of $C_{carbene}$ and C_{Ar} nuclei appear in the ^{13}C NMR spectrum at 165.3 ppm and 150.3 ppm, respectively, i.e. close to those of **29** (166.7 and 150.6 ppm). All these data imply, that **42** is best described as a zwitterionic silylidene complex (see formula with formal

charges in Scheme 43). The ^{29}Si NMR spectrum shows a singlet resonance at 201.8 ppm (C_6D_6). The low-field shift is characteristic for silylidene complexes of transition metals and compares well with those of other molybdenum silylidene complexes (182–414 ppm)[86, 87, 156]

Formally, complex **42** can be also regarded as an NHC-adduct of the silylidyne complex [Cp(CO)$_2$Mo≡Si(C$_6$H$_3$-2,6-Trip$_2$)]. It is isolobal to the complex [Cp(CO)$_2$Cr=CPh(PMe$_3$)], which was obtained upon treatment of the chromium carbyne complex [Cp(CO)$_2$Cr≡C–Ph] with PMe$_3$.[159] Therefore it was assumed, that abstraction of the carbene from **42** would lead to the targeted silylidyne complex. DFT calculations were performed on the complex **42** to assess the Si–C$_{carbene}$ bond strength.[160] The bond dissociation enthalpy $D^o(0)$ and Gibbs free dissociation energy $\Delta G_D^\circ(298)$ of the Si–C$_{carbene}$ bond in **42** were calculated to be 61.2 and 1.2 kJ/mol respectively. The values were substantially lower than those calculated for Si(C$_6$H$_3$-2,6-Trip$_2$)Cl(IMe$_4$) (94.3 and 28.1 kJ·mol^{-1} respectively),[135] suggesting that dissociation of carbene may occur to some extent at elevated temperatures, leading to the silylidyne complex.

We tried to develop access to silylidene complexes analogous to **42** bearing other substituents. However, the reaction of Si(C$_6$H$_3$-2,6-Mes$_2$)Cl(IMe$_4$) (**28**) with Li[CpMo(CO)$_3$] was not selective and afforded the silylidene complex [Cp(CO)$_2$Mo=Si(C$_6$H$_3$-2,6-Mes$_2$)(IMe$_4$)] in only very low yield. We assumed, that the phosphane-substituted carbonyl metallates, such as Li[CpM(CO)$_2$(PMe$_3$)] (M = Cr, Mo, W) would improve the yields of the targeted products due to the combination of two factors: a) the anions [CpM(CO)$_2$(PMe$_3$)]$^-$ are more nucleophilic and hence more reactive than [CpM(CO)$_3$]$^-$; b) elimination of PMe$_3$ might be easier than elimination of CO. This assumption was verified and the silylidene complexes of molybdenum (**43**) and tungsten (**44**) bearing a -C$_6$H$_3$-2,6-Mes$_2$ substituent could be prepared under mild conditions (Scheme 44).

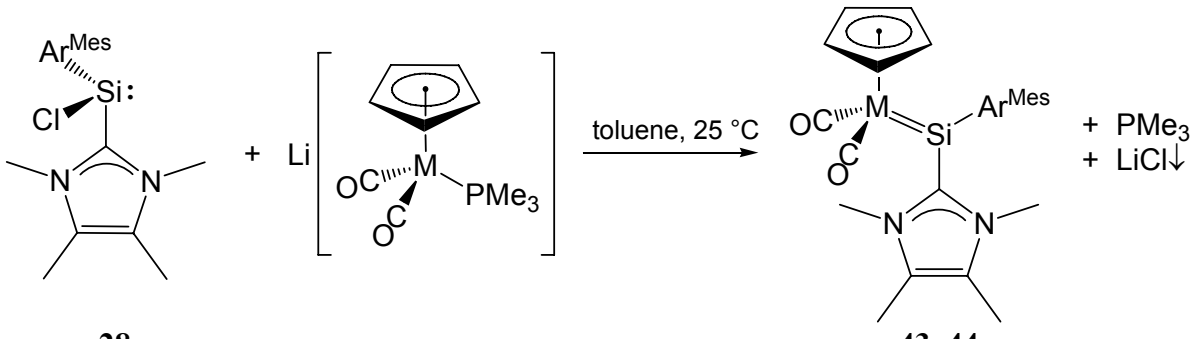

28 **43, 44**

Scheme 44: Synthesis of silylidene complexes **43** (M = Mo) and **44** (M = W) (Ar^{Mes} = -C$_6$H$_3$-2,6-Mes$_2$).

The complexes **43** and **44** were isolated as dark green air-sensitive solids in 56 and 48% yields respectively. The complexes are soluble in toluene benzene and other polar solvents,

but insoluble in hexane and pentane. The *in situ* IR spectra of the reaction solutions revealed the selective formation of **43** and **44**, however the medium product yields suggest that some of the starting materials were remained unreacted. The structural and spectroscopic features of **43** and **44** are similar to those of **42** and are summarized in Table 3.

	Yield, %	^{13}C NMR sift of the $C_{carbene}$, ppm	^{29}Si NMR shift, ppm	IR, cm^{-1}, toluene	M=Si, Å	Si–$C_{carbene}$, Å
$Cp(CO)_2Mo{=}Si(C_6H_3\text{-}2,6\text{-}Trip_2)(IMe_4)$ (**42**)	51	165.3	201.8	1859 (vs), 1785 (vs)	2.345 (mean)	1.944 (mean)
$Cp(CO)_2Mo{=}Si(C_6H_3\text{-}2,6\text{-}Mes_2)(IMe_4)$ (**43**)	56	162.9	200.5	1854 (vs), 1779 (vs)	2.3160(6)	1.936 (2)
$Cp(CO)_2W{=}Si(C_6H_3\text{-}2,6\text{-}Mes_2)(IMe_4)$ (**44**)	48	168.4	180.0	1849 (vs), 1775 (vs)	n/a	n/a

Table 3: Selected properties of the silylidene complexes **42–44.**

We also attempted to synthesize the chromium and tungsten analogues of **42**. Surprisingly, heating of $Si(C_6H_3\text{-}2,6\text{-}Trip_2)Cl(IMe_4)$ with the carbonyl metallates $K[CpW(CO)_3]\cdot 0.05DME$ and $Na[CpCr(CO)_3]\cdot 2DME$ (xylene, 140 °C, 15 min) afforded selectively the products of C–H activation of the N-*CH*$_3$ groups, instead of the expected silylidene complexes (Scheme 45).[40]

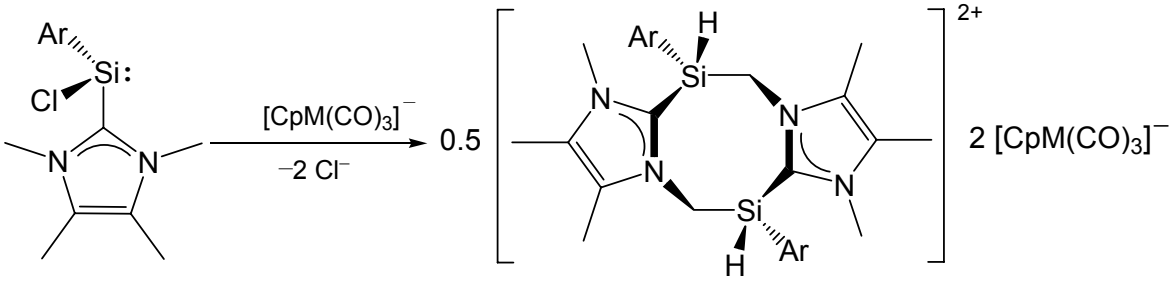

Scheme 45: Unexpected C–H activation NHC ligand. M = Cr (**45**), Mo (**46**), W (**47**).

In fact, in the reaction of $Li[CpMo(CO)_3]$ with $Si(C_6H_3\text{-}2,6\text{-}Trip_2)Cl(IMe_4)$ the product of C–H activation **46** is also formed in quantities of about 20%, besides the silylidene complex $[Cp(CO)_2Mo{=}Si(C_6H_3\text{-}2,6\text{-}Trip_2)(IMe_4)]$ (Scheme 45). Complex **46** was isolated in one experiment, when $Li[CpMo(CO)_3]\cdot THF$ was employed, since the presence of THF increased the yield of **46**.[40]

[40] The reaction of the solvent free complex $Li[CpCr(CO)_3]$ with $Si(C_6H_3\text{-}2,6\text{-}Trip_2)Cl(IMe_4)$ afforded according to IR spectroscopy a mixture of the C–H activated complex **45** (ca 80%) and $[Cp(CO)_2Cr{=}Si(C_6H_3\text{-}2,6\text{-}Trip_2)(IMe_4)]$ (ca 15%; ν(CO) at 1852 (vs), 1782 (vs)). In contrast, in the reaction with $Na[CpCr(CO)_3]\cdot 2DME$ the formation of the silylidene complex was not observed at all, therefore in the next experiments only solvent-free lithium salts were used.

The complexes were isolated by crystallization from toluene/hexane mixtures as yellow air-sensitive solids in low yields. They are insoluble in hexane or pentane, slightly soluble in toluene, benzene, and are good soluble in THF. Notably, the metastable toluene reaction solutions contained these complexes in large quantities; the solubility of the isolated products is significantly lower.

Complexes **45** and **47** were investigated by X-ray diffraction analysis, their structures are very similar. The structure of the chromium complex **45** is shown in Figure 30. Two independent complex cations were found in the asymmetric unit together with disordered solvent molecules and the complex anions accounting for over 250 heavy atoms, a challenging problem to solve for a crystallographer.

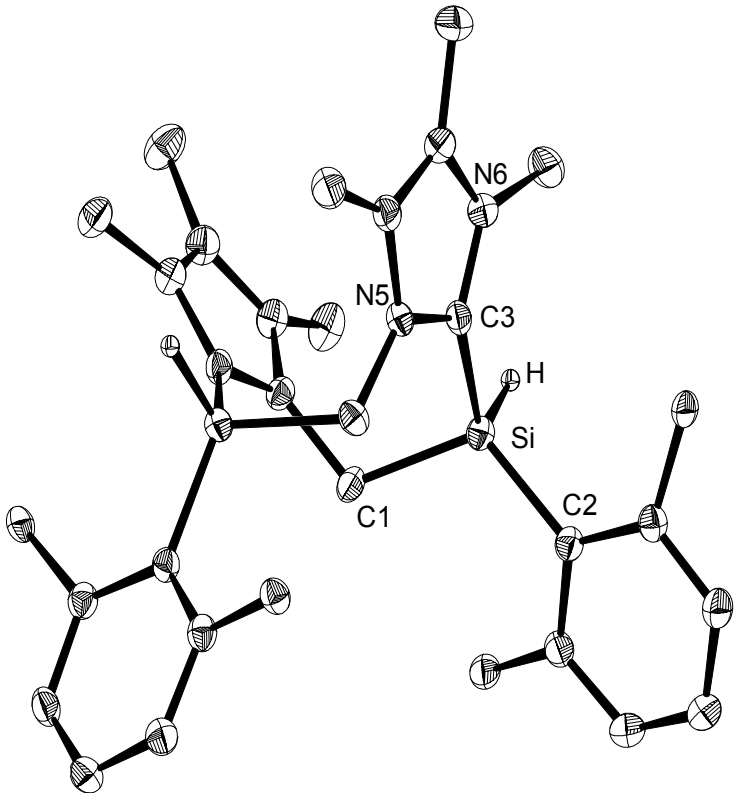

Figure 30: DIAMOND plot of the structure of the complex cation in **45**. Thermal ellipsoids are set at 50% probability. Hydrogen atoms, Trip groups and complex anions are omitted for clarity. Two independent complex cations are found in the asymmetric unit. Selected bond lengths [Å] and bond angles, mean values,[41] [°]:C1–Si 1.914(2), C2–Si 1.873(4), C3–Si 1.898(2), Si–H 1.34(2); C1-Si-C2 113.6(5), C1-Si-C3 101.9(5), C2-Si-C3 117.5(7).

[41] The unweighted mean value x_u of bond lengths and angles are given, the standard deviation σ of x_u was calculated using the equation $\sigma^2 = \Sigma(x_i - x_u)^2/(n^2 - n)$, where x_i is the individual value and n – number of elements.

The complex cations are well separated from the complex anions; the silicon centers exhibit a distorted tetrahedral geometry. The 8-membered ring adopts a twisted boat conformation.[42] The complex cation in **45** is best described as a bis-imidazolium salt, bearing silyl substituents in C^2-positions, as indicated by the short Si–$C_{carbene}$ bond lengths (1.898(3) Å), which compare well with the Si–C_{Ar} bond lengths (1.873(4) Å).[41] This is further confirmed by the ^{13}C NMR shift of the $C_{carbene}$ nucleus of **45** (125.3 ppm in THF-d_8), which compares with those of the imidazolium salts [IMe_4H]Cl[105] (136.9 ppm in CD_2Cl_2) or 1,3-diethyl-4,5-dimethyl-2-(trimethylsilyl)imidazolium iodide (145.4 ppm in $CDCl_3$).[161] The ν(CO) absorption bands of the complex anion of **45** in THF (1892 (s), 1779 (vs), 1753 (s) cm^{-1}) compares well e.g. with those of Na[$CpCr(CO)_3$] (1881, 1775 and 1734 cm^{-1} in DME), suggesting weak interactions between cations and anions in solution. Solution NMR spectra corroborate the structures of **45**–**47**. The complex dications have an overall C_2 symmetry (racemic mixture of R,R- and S,S-isomers).

Attempt to prepare a pentamethylcyclopentadienyl complex [$Cp^*(CO)_2Mo$=Si(C_6H_3-2,6-$Trip_2$)(IMe_4)] in analogy to the complex **42** was unsuccessful. Reaction of Li[$Cp^*Mo(CO)_3$] ($Cp = \eta^5$-C_5Me_5) with Si(C_6H_3-2,6-$Trip_2$)Cl(IMe_4) in toluene was unselective leading to an untractable complex mixture of products as indicated by the ^1H NMR and IR spectra.

2.2.2 Synthesis of zwitterionic halosilylidene complexes of Cr, Mo and W

As has been shown, SiArCl(IMe_4) can be used to transfer formally a [SiAr(IMe_4)]$^+$ group to a metal center. The approach was demonstrated by the preparation of the complexes [$Cp(CO)_2M$=Si(IMe_4)Ar] (M = Mo, W; IMe_4 = 1,3,4,5-tetramethyimidazol-2-ylidene, Ar = -C_6H_3-2,6-Mes_2, -C_6H_3-2,6-$Trip_2$, Section 2.2.1). Analogous reaction of the carbene-stabilized dihalosilylenes with carbonyl metallates would be expected to lead to NHC-stabilized halosilylidyne complexes of the general formula [$Cp(CO)_2M$=SiX(NHC)] upon transfer of the [SiX(NHC)] fragment (X = halogen, Scheme 46). These complexes bear a big synthetic potential, since the halogen atom could be substituted by a variety of nucleophiles.

[42] Conformations of related systems, e.g. 1,5-dibenzocyclooctane, were previously investigated. The twisted boat conformation was found to be higher in energy that the minimum chair conformation by only ca.4 kJ/mol, see I. Alkorta, J. Elguero, *Struct. Chem.* **2010**, *21*, 885.

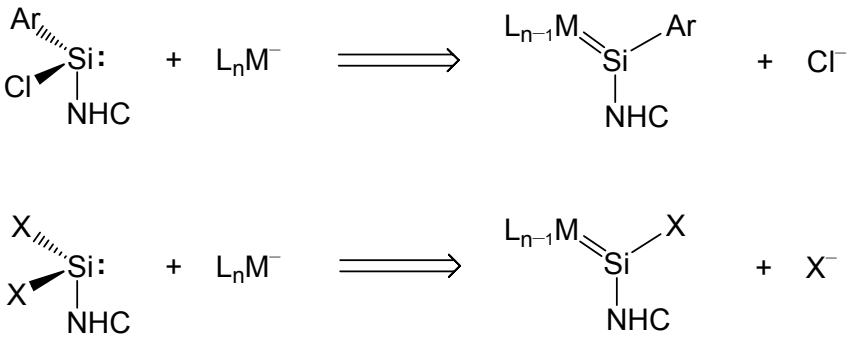

Scheme 46: Analogous reactions of $SiArCl(NHC)$ and $SiX_2(NHC)$ with metallates (NHC = N-heterocyclic carbene, X = halogen).

We investigated the reactions of $SiX_2(IDipp)$[45, 124] with $Li[CpM(CO)_3]$ (X = Cl, I; M =Cr, Mo). All reactions were very slow at RT and required heating in toluene or benzene. Generally, the reactions led to mixtures of the expected products, along with the starting Si(II) dihalides and non-coordinated carbene IDipp, as was evidenced by ^{1}H NMR spectroscopy of the reaction mixtures. The Si(II) dihalides were present, even when an excess of the metallate was used. The formation of the imidazolium salts $[IDippH][CpM(CO)_3]$ M = Cr, Mo, was also suggested by *in situ* IR spectra (*vide infra*). The reaction of $Li[CpCr(CO)_3]$ with $SiI_2(IDipp)$ proceeded most selective, and the complex $[Cp(CO)_2Cr{=}SiI(IDipp)]$ was formed in 64% yield according to ^{1}H NMR spectroscopy. However, I could not separate the complex from the impurities due to their similar solubility. The experimental data of the reactions are summarized in Table 4.

Complex	Reaction conditions	IR, cm^{-1}, toluene	Estimated yield, %[43]	Amount of IDipp, %[43]	Amount of $SiX_2(IDipp)$, %[43]
$[Cp(CO)_2Cr{=}SiCl(IDipp)]$	25 min, 100 °C, toluene	1891vs, 1807vs	41	22	32
$[Cp(CO)_2Mo{=}SiCl(IDipp)]$	30 min 55 °C, 60 min 70 °C, toluene	1895vs, 1810vs	27	44	4
$[Cp(CO)_2Cr{=}SiI(IDipp)]$	30 min, 110 °C, toluene	1898vs, 1814vs	64	7	17
$[Cp(CO)_2Mo{=}SiI(IDipp)]$	30 min, 100 °C, toluene	1901vs, 1815vs	n/a	n/a	n/a

Table 4: Summary of experimental details and IR spectra of the complexes $[Cp(CO)_2M{=}SiX(IDipp)]$, M = Cr, Mo; X = Cl, Br; IDipp = 1,3-bis(2,6-diisopropylphenyl)-imidazol-2-ylidene. n/a – not available.

[43] According to ^{1}H NMR spectroscopy of the crude reaction mixtures, as determined by the relative intensities of $C^{4,5}$-*H* of the carbene backbone. The putative imidazolium salts $[IDippH][CpM(CO)_3]$ (M = Cr, Mo) present in the mixtures, were excluded from the analysis, because their quantities could not be precisely determined due to limited solubility in C_6D_6.

The IR absorptions of the complexes, as expected, are shifted to slightly higher wavenumbers in comparison to the analogoues aryl-substituted complexes [$Cp(CO)_2M$=SiAr(IMe_4)] (M = Mo, W, see Table 3).

The important conclusion drawn from these first trials was, that the zwitterionic halosilylidene complexes [$Cp(CO)_2M$=SiX(IDipp)] were formed in the reactions and they appeared to be stable even at elevated temperatures. The NHC-adduct $SiBr_2$(ISdipp) (**20**), bearing the carbene ISdipp (1,3-bis(2,6-diisopropylphenyl)imidazolidin-2-ylidene with a saturated backbone was more reactive towards carbonyl metallates. Although the reaction of $SiBr_2$(ISdipp) with Li[$CpCr(CO)_3$] in benzene at 80 °C was not very selective, complex [$Cp(CO)_2$Cr=SiBr(ISdipp)] (**49**) could be isolated (Scheme 47). The analogous chloro-derivative [$Cp(CO)_2$Cr=SiCl(ISdipp)] was prepared similarly.[44]

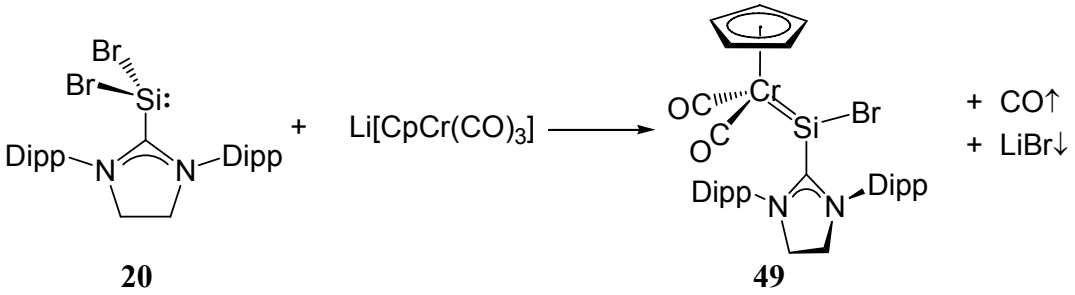

20 **49**

Scheme 47: Synthesis of zwitterionic complex **49** (formal charges are not depicted).

Complex **49** was isolated in 53% yield as a dark brown, air sensitive, thermally stable solid, which decomposes upon heating above 140 °C. It is soluble in common organic solvents, but insoluble in hexane or pentane. The moderate yield of the complex is a result of a side-reaction, leading to the formation of the imidazolinium salt [ISdippH][$CpCr(CO)_3$] (**51**) in quantities of up to 40%.[45] The source of the hydrogen atom remains unknown, but it certainly does not originate from traces of water in the solvents. Complex **49** was separated from the byproduct by taking advantage of their different solubility in benzene-hexane mixtures. The formation of [ISdippH][$CpCr(CO)_3$] resembles the formation of the C–H activated products **45**–**47** in the reactions of SiArCl(IMe_4) with carbonyl metallates (Section 2.2.1, p. 73).

[44] M. Speer, *Bachelor thesis*, University of Bonn, **2011**.

[45] The salt [ISdippH][$CpCr(CO)_3$] was characterized by NMR and IR spectroscopy, see the experimental section for details, p. 200. The structure of the salt was verified by X-ray diffraction analysis.

Complex **49** is isolobal to the previously described silylidene complexes [Cp(CO)$_2$M=SiAr(IMe$_4$)] (**42**–**44**; M = Mo, W; Ar = -C$_6$H$_3$-2,6-Mes$_2$, -C$_6$H$_3$-2,6-Trip$_2$), and has a similar structure. It features a trigonal planar coordinated silicon center with a sum of angles at the Si atom of 359.9° (Figure 31). The silylidene ligand adopts an upright conformation, with the bromine atom pointing towards the Cp ring (a similar geometry was found also in the complexes **42**–**44**). The Cr–Si bond length of 2.1618(9) Å is the shortest reported up to date. The value compares well with the calculated Cr=Si double bond length of 2.18 Å on the basis of the sum of double-bond covalent radii of Si (1.07 Å) and Cr (1.11 Å).[162]

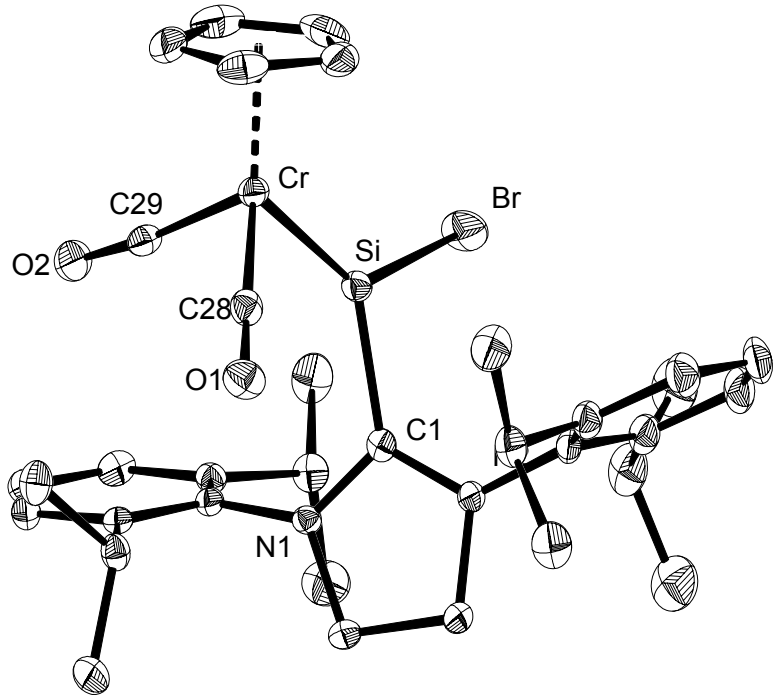

Figure 31: DIAMOND plot of the molecular structure of **49**. Thermal ellipsoids are set at 50% probability. Hydrogen atoms are omitted for clarity. Selected bond lengths [Å] and bond angles [°]: Cr–Si 2.1618(9), C1–Si 1.957(3), Br–Si 2.2728(8), C28–Cr 1.827(3), C29–Cr 1.833(3); C1-Si-Cr 131.27(8), C1-Si-Br 98.16(8), Cr-Si-Br 130.51(4), C28-Cr-C29 93.9(1), N1-C1-N2 109.8(2).

Only two chromium silylidene complexes featuring a trigonal planar coordinated Si atom were reported so far in the literature. These are complexes of N-heterocyclic silylenes and feature Si–Cr bond lengths of 2.326 Å in [Cr(CO)$_4${Si(^{t}BuNCH=CHN^{t}Bu)}$_2$] and 2.329 Å in [Cr(CO)$_4${Si(^{t}BuNCH$_2$-CH$_2$N^{t}Bu)}$_2$].[163] The other few examples are donor stabilized silylidene complexes of the general formula Cr(CO)$_5$SiR$_2$(L), where L is a Lewis base, and display even longer bonds of 2.335(2)–2.526(3) Å. These bond lengths are close to those of Cr–Si single bonds, as for example found in the chromium silyl complex

((η^6-Mes)Cr($SiCl_3$)$_2$(CO)$_2$] (2.380(3) Å),[164] and compare well with the sum of single-bond covalent radii of Si and Cr (2.38 Å).[147] The findings suggest that in the previously reported silylidene and base-stabilized silylidene complexes the degree of Cr–Si d_π–p_π backbonding is very small. In contrast, complex **49** features a strong Cr–Si π-bond.

The Si–Br and Si–$C_{carbene}$ bond lengths (2.2728(8) Å and 1.957(3) Å) in **49** are slightly shorter than those in $SiBr_2$(ISdipp) (**20**) (2.335(6) Å and 2.007(5) Å)) due to absence of repulsion from the lone pair of electrons at the Si atom. The shortening of the bond is somewhat more pronounced than in the pair SiArCl(IMe_4)–[Cp(CO)$_2$M=SiAr(IMe_4)] (IMe_4 = 1,3,4,5-tetramethylimidazol-2-ylidene) (see Section 2.2.1).

Complex **49** displays two *ν*(CO) absorption bands of almost equal intensities at low wavenumbers (1898, 1809 cm^{-1} in toluene; 1894, 1809 cm^{-1} in fluorobenzene) indicating a rather strong metal-carbonyl backbonding. As the result of backbonding, the mean Cr–C bond length in **49** (1.830 Å) is shorter than that e.g. in Cr(CO)$_6$ (1.914 Å).[165] The *ν*(CO) absorption bands appear at higher wavenumbers than those of [CpMo(CO)$_2$=Si(C_6H_3-2,6-Trip$_2$)(IMe_4)] (**42**: 1859, 1785 cm^{-1} in toluene) due to the presence of a more electron withdrawing Br substituent in comparison to the aryl-group. The ^{29}Si NMR spectrum of **49** displays a singlet resonance at 95.1 ppm, at lower field in comparison to that of $SiBr_2$(ISdipp) (**20**; 10.9 ppm).

DFT calculations were performed on complex **49** to assess the $C_{carbene}$–Si bond strength. The bond dissociation energy of the bond was calculated to be 110.1 kJ·mol^{-1} and the free Gibbs dissociation energy in the gas phase at 298 K to be 38.9 kJ·mol^{-1}.[166] The values are higher than those calculated for [CpMo(CO)$_2$=Si(C_6H_3-2,6-Trip$_2$)(IMe_4)] (62.1 kJ·mol^{-1} and 1.2 kJ·mol^{-1}, respectively).[160] The data suggest that carbene abstraction from complex **49** to give the hypothetical complex [Cp(CO)$_2$Mo≡SiBr] will be a more energy requiring process than abstraction from [CpMo(CO)$_2$=Si(C_6H_3-2,6-Trip$_2$)(IMe_4)].

The reaction of $SiBr_2$(ISdipp) with Li[CpMo(CO)$_3$] was less selective than with Li[CpCr(CO)$_3$]. Among the formation of the target complex [Cp(CO)$_2$Mo=SiBr(ISdipp)] and [ISdippH][CpMo(CO)$_3$] the presence of several other byproducts was evidenced by ^{1}H NMR and IR spectroscopy.[46] No attempts were made to isolate the complex [Cp(CO)$_2$Mo=SiBr(ISdipp)].

---

[46] A mixture of $SiBr_2$(ISdipp) and Li[CpMo(CO)$_3$] was heated in benzene at 80 °C for 15 min. After removal of the solvent the residue was analyzed. The following *ν*(CO) absorption bands were observed: 1993(w), 1945(m), 1929(m), 1900(vs), 1893(s sh), 1861(s) 1809(s), 1782(m), 1754(m) cm^-

As next, the reactivity of the more nucleophilic pentamethylcyclopentadienyl substituted metallates Li[Cp*M(CO)$_3$] (M = Cr, Mo, W) was studied. The metallates were proved to be more reactive towards SiX$_2$(NHC). In fact, treatment of SiBr$_2$(ISdipp) with Li[Cp*M(CO)$_3$] afforded the zwitterionic bromosilylidene complexes **52-Cr**, **52-Mo** and **52-W** under mild conditions, (Figure 32). The reactions were faster than in the case of Li[CpCr(CO)$_3$] and proceeded at temperatures of 25–50 °C, instead of 80 °C for Li[CpCr(CO)$_3$]. By using Cp*-substituted metallates it was also possible to obtain the complexes **53-Cr, 53-Mo**, containing the unsaturated carbene Idipp as a ligand, though in low yields (Figure 32; see also p. 80). The key properties of the prepared halosilylidene complexes are summarized in Table 5.

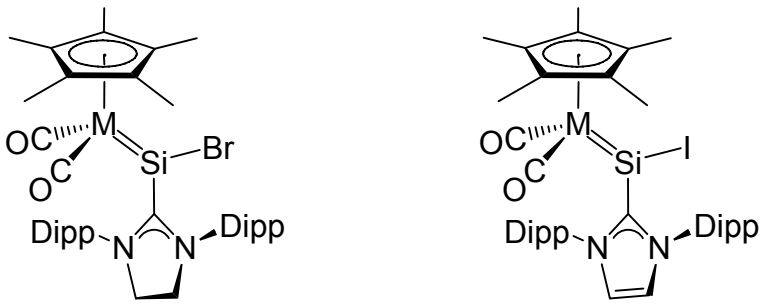

52-Cr, 52-Mo, 52-W **53-Cr, 53-Mo**

Figure 32: Halosilylidene complexes obtained upon reactions of Li[Cp*M(CO)$_3$] with SiX$_2$(NHC). M = Cr, Mo, W; NHC = IDipp, ISdipp; X = Br, I.

Structural and spectroscopic parameters of the complexes are similar. The three-legged piano stool complexes feature trigonal planar coordinated silicon centers, with sum of angles at Si of nearly 360°. The silylidene ligands adopt in all cases an upright conformation, with the halogen atoms pointing towards the Cp* rings (Figure 33). The M–Si double bonds in the complexes are among the shortest reported up to date. The Cr–Si bond length in **52-Cr** is only marginally longer than in **49** (2.1716(7) vs 2.1618(9) Å). The Mo–Si bond lengths in **52-Mo** and **53-Mo** are shorter than those in [Cp(CO)$_2$Mo=Si(C$_6$H$_3$-2,6-Trip$_2$)(IMe$_4$)] (2.2838(13) Å, 2.2853(8) Å and 2.345(2) Å respectively) and compare well with that of the only structurally characterized halosilylidene complex [Cp*(Me$_2$PCH$_2$CH$_2$PMe$_2$)Mo(H)=SiCl(Mes)] (2.288(2) Å).[87] The W–Si double bond length in **52-W** (2.2884(10) Å) is also shorter than those in the previously reported tungsten silylidene complexes (2.359–2.420 Å).[89, 167, 168] The

---

1. ^{1}H NMR data of [Cp(CO)$_2$Mo=SiBr(ISdipp)] are as follows (300.1 MHz, C$_6$D$_6$, 298 K): δ 1.13 (d, ^3J(H,H) = 6.8 Hz, 12H, 2 × C^{2,6}-CH*Me$_A$*Me$_B$, Dipp), 1.61 (d, ^3J(H,H) = 6.6 Hz, 12H, 2 × C^{2,6}-CHMe$_A$*Me$_B$*, Dipp), 3.51 (s, 4H, 2 × NC*H$_2$*), 3.46–3.59 (sept, ^3J(H,H) = 6.8 Hz, 4H, 2 × C^{2,6}-C*H*Me$_A$Me$_B$, Dipp); the position of the remaining signals is ambiguous.

findings support the formulation of strong π-bonds between the Si and the metal centers in these compounds.

Complex	Color	Yield, %	IR, toluene, cm^{-1}	^{13}C NMR of $C_{carbene,}$ ppm	^{29}Si NMR, ppm	*d*(M−Si), Å
$[Cp(CO)_2Cr{=}SiBr(ISdipp)]$ (**49**)	Brown	53	1898, 1809	177.4	95.1	2.1618(9)
$[Cp^*(CO)_2Cr{=}SiBr(ISdipp)]$ (**52-Cr**)	Red-brown	60	1886, 1804	178.7	74.8	2.1716(7)
$[Cp^*(CO)_2Mo{=}SiBr(ISdipp)]$ (**52-Mo**)[44]	Brown	52	1890, 1805	181.4	80.1	2.284(1)
$[Cp^*(CO)_2W{=}SiBr(ISdipp)]$ (**52-W**)	Brown	7	1883, 1799	185.6	71.2	2.288(1)
$[Cp^*(CO)_2Cr{=}SiI(IDipp)]$ (**53-Cr**)	Brown	9.5	1887, 1806	157.1	39.0	2.1791(7)
$[Cp^*(CO)_2Mo{=}SiI(IDipp)]$ (**53-Mo**)	Brown	18	1890, 1808	159.3	48.1	2.2853(8)

Table 5: Summary of properties of complexes $R(CO)_2M{=}SiX(L)$ (**49–53)**. R = η^5-C_5H_5, η^5-C_5Me_5; M = Cr, Mo, W; X = Cl, Br, I; L = IDipp = 1,3-bis(2,6-diisopropylphenyl)-imidazol-2-ylidene, L = ISdipp = 1,3-bis(2,6-diisopropylphenyl)imidazolidin-2-ylidene.

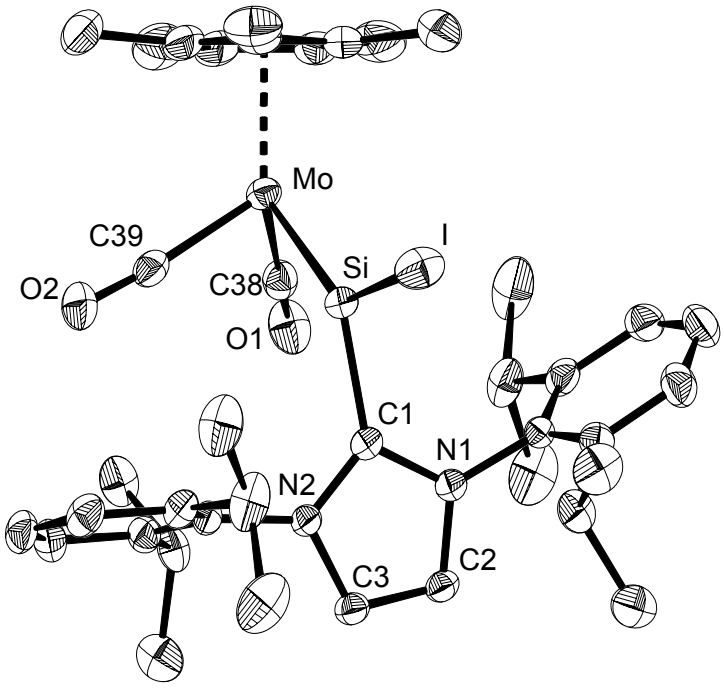

Figure 33: DIAMOND plot of the molecular structure of **53-Mo**. Thermal ellipsoids are set at 50% probability. Hydrogen atoms are omitted for clarity. Selected bond lengths [Å] and bond angles [°]: Mo–Si 2.2853(8), C1–Si 1.939(3), I–Si 2.5283(8), C38–Mo 1.935(3), C39–Mo 1.949(3), C2–C3 1.344(4); C1-Si-Mo 134.29(8), C1-Si-I 97.59(8), Mo-Si-I 128.10(3), C38-Cr-C39 87.3(1), N1-C1-N2 105.1(2).

The IR spectra of the zwitterionic halosilylidene complexes are similar and feature two *ν*(CO) absorption bands of almost equal intensities at ca. 1890 and 1805 cm^{-1} (Table 5). The

complex **52-Cr** displays ν(CO) absorption bands at slightly lower energy than those of [Cp(CO)$_2$Cr=SiBr(ISdipp)], as is consistent with Cp*/Cp substituents. The ^{29}Si NMR spectra of complexes **52–53** display singlet resonances in the range of 39–80 ppm (Table 5). The signals are significantly high-field shifted in comparison to the aryl-substituted zwitterionic silylidene complexes [Cp(CO)$_2$M=SiAr(IMe$_4$)] (**42–44,** M = Mo, W; δ = 180–200 ppm; Table 3) and also in comparison to other reported base-free silylidene complexes of molybdenum and tungsten (98–414 ppm).[86, 87, 89, 90, 156, 167]

We have demonstrated earlier, that the reaction of Li[CpMo(CO)$_2$(PMe$_3$)] with SiCl(C$_6$H$_3$-2,6-Mes$_2$)(IMe$_4$) leads selectively to the zwitterionic silylidene complexes **[**Cp(CO)$_2$M=Si(C$_6$H$_3$-2,6-Mes$_2$)(IMe$_4$)] (**43**, **44**; M = Mo, W, Scheme 44). We attempted to extend this approach to halosilylidene complexes of molybdenum (Scheme 48). Surprisingly, treatment of SiI$_2$(IDipp) with Li[CpMo(CO)$_2$(PMe$_3$)] afforded complex **48**, which was isolated as an orange solid in low yield (Scheme 48, reaction on the bottom). The structure of the complex was determined by X-ray crystallography and is presented in Figure 34.

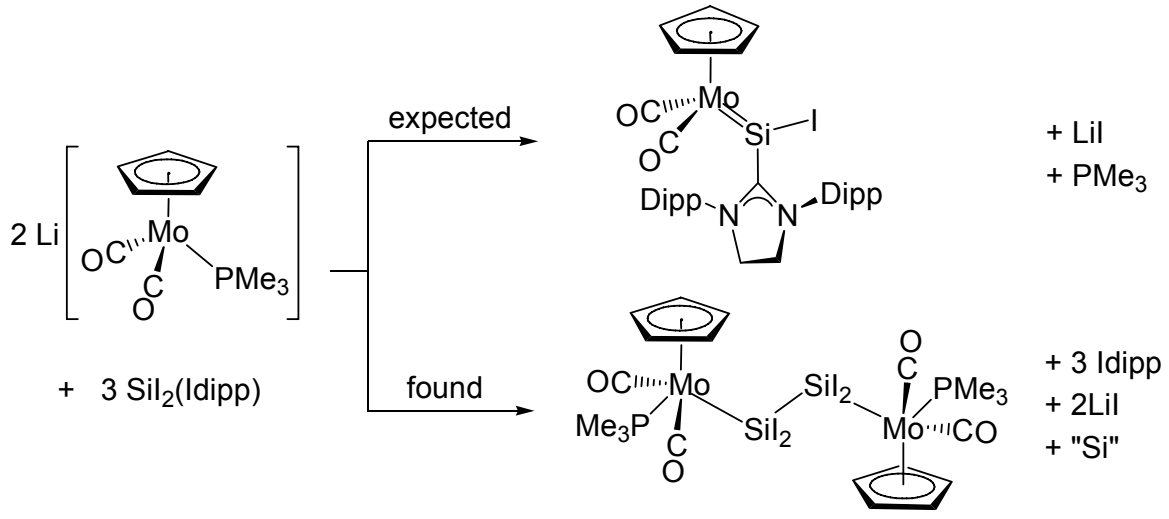

48

Scheme 48: SiI$_2$(IDipp) as oxidizing agent. Synthesis of complex **48**.

The four-legged piano stool silyl complex **48** features the PMe$_3$ and the silyl groups in *trans*-positions. The Si centers exhibit a distorted tetrahedral geometry with bond angles in the range of 98.0–126.4°. The average Mo–Si bond length of 2.515(5) Å compares well with bond lengths in other molybdenum halosilyl complexes Cp$_2$Mo(Cl)–SiCl$_3$ (2.492 Å) and

$Cp_2Mo(H)–SiClMe_2$ (2.513(1) Å).[47, [169]] The Si–Si bond length of 2.416(2) Å corresponds to a single bond and compares well with that in $(Me_3Si)_2CH\text{-}SiI_2\text{-}SiI_2\text{-}CH(SiMe_3)_2$ (2.423(2) Å).[170] It is, however, slightly longer in comparison to the average Si–Si bonds found in 1,1,2,2-dihalosilanes (2.34(3) Å),[48] due to steric bulk and/or the hyperconjugation of the molybdenum *d*-orbitals of with the σ* orbital of the Si–Si bond.

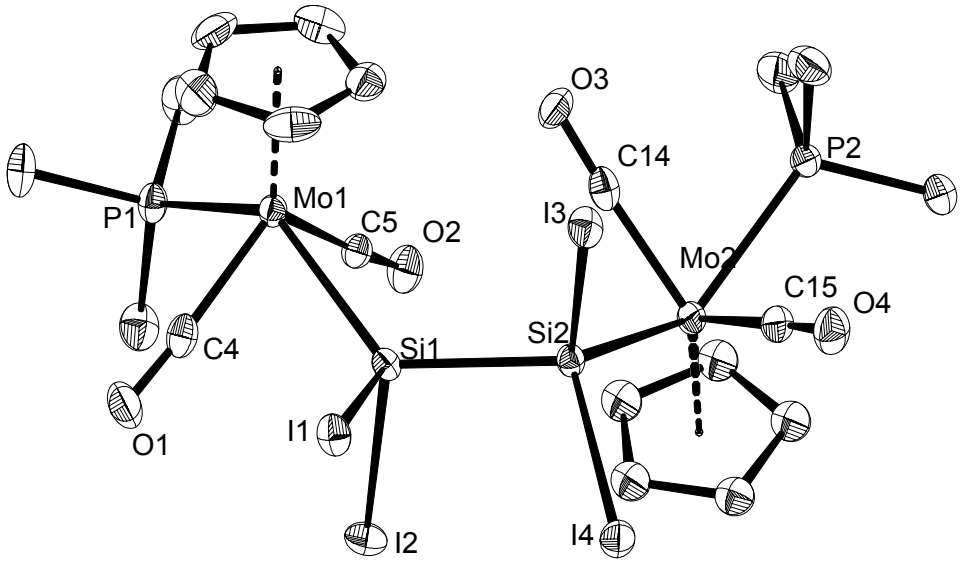

Figure 34: DIAMOND plot of the molecular structure of **48**. Thermal ellipsoids are set at 50% probability. Hydrogen atoms are omitted for clarity. Selected bond lengths [Å] and bond angles [°]: Mo1–Si1 2.520(1), Mo2–Si2 2.510(1), Mo1–P1 2.453(1), Mo2–P2 2.444(1), Si1–Si2 2.416(2); Si2-Si1-Mo1 126.39(6), Si1-Si2-Mo2 125.36(5).

The reaction provides access to 1,1,2,2-dihalosilyl derivatives. Reduction of 1,1,2,2-dihalosilanes, bearing very sterically demanding substituents, afforded several unprecedented low-valent silicon compounds.[171] The synthetic potential of **48** could not be explored due to its low yield and time restrains.

2.2.3 Reactions of the NHC-stabilized halosilylidyne complexes

In Chapter 2.1.3 the substitution of 1,3-bis(2,6-diisopropylphenyl)-imidazol-2-ylidene in SiI_2(IDipp) by the more reactive 1,3,4,5-tetramethylimidazol-2-ylidene (IMe_4) was reported

[47] The unweighted mean value x_u of the bond length is given, the standard deviation σ of x_u was calculated using the equation $\sigma^2 = \Sigma(x_i - x_u)^2/(n^2 - n)$, where x_i is the individual value and n – number of elements.

[48] According to a CSD survey from 11.2011 of 24 structurally characterized compounds ($^{T4}SiX_2$–$^{T4}SiX_2$, where X = any halogen). The median d(Si–Si) = 2.336 Å, LQ = 2.316 Å, HQ = 2.379 Å.

(Scheme 32). The Si–$C_{carbene}$ bond dissociation energy in $SiBr_2$(IDipp) was calculated to be 123.7 kJ·mol^{-1}.[124] The Si–$C_{carbene}$ bond dissociation energy in [Cp(CO)$_2$=SiBr(ISdipp)] (**49**, 110.1 kJ·mol^{-1})[166] is similar, suggesting that ISdipp could also be displaced. Therefore, the reaction of **49** with 1,3,4,5-tetramethylimidazol-2-ylidene (IMe_4) was investigated.

Addition of IMe_4 to a solution of [Cp(CO)$_2$=SiBr(ISdipp)] (**49**) in toluene resulted in an immediate precipitation of a red-brown solid. The low solubility of the product in diethyl ether, THF or PhF rendered the characterization difficult. The IR spectrum of the solid product displayed two CO-absorption bands of equal intensities at 1772 and 1700 cm^{-1}. The *v*(CO) absorption bands of the product are shifted by roughly 110 cm^{-1} to lower wavenumbers in comparison to those of the starting material (1893, 1805 cm^{-1} in the solid state). The shift was consistent with the coordination of an additional carbene to the Si center to give either the complex [Cp(CO)$_2$CrSi(IMe_4)(ISdipp) Br] or the complex [Cp(CO)$_2$CrSi(IMe_4)$_2$Br].

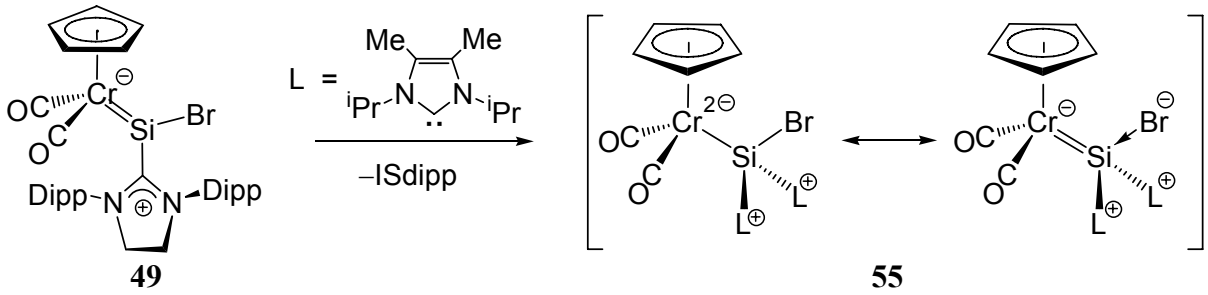

Scheme 49: Synthesis of **55**. Carbene-exchange reaction.

The low solubility of the product prevented characterization and so the more lipophilic carbene 1,3-diisopropyl-2,4-dimethylimidazol-2-ilydene (IMe_2iPr_2) was employed in the substitution reaction in the hope, that the resulting product would be more soluble. In fact, the reaction of [Cp(CO)$_2$Cr=SiBr(ISdipp)] (**49**) with IMe_2iPr_2 proceeded smoothly at ambient temperature in benzene solution leading after substitution of ISdipp and coordination of a second carbene to the Si center to complex **55** (Scheme 49). Red-brown crystals of the benzene solvate [Cp(CO)$_2$CrSi(IMe_2iPr_2)$_2$Br]·C_6H_6 (**55**) started to grow from the solution soon after the reaction was complete. The compound was isolated in 88% yield after filtration.

The mild reaction conditions for the formation of **55** and the high bond dissociation energy of the Si–$C_{carbene}$ bond in **49** (110.1 kJ·mol^{-1}) suggests, that **55** is probably formed by the addition-elimination mechanism, via the intermediate complex [Cp(CO)$_2$Cr-Si(ISdipp)(IMe_2iPr_2)Br]. However, no such intermediate was observed. In fact, monitoring of the reaction of **49** with only one equivalent of IMe_2iPr_2 by IR spectroscopy showed the direct formation of the complex **55** along with unreacted [Cp(CO)$_2$=SiBr(ISdipp)] (**49**).

The three-legged piano stool complex **55** displays a distorted tetrahedral geometry of the Si center. The complex exhibits several interesting bonding parameters (Figure 35).

- The Cr–Si bond length (2.2515(7) Å) is longer than the double bond length in [Cp(CO)$_2$=SiBr(ISdipp)] (**49**, 2.1618(9) Å), but considerably shorter than the calculated Cr–Si single bond (2.38 Å).[147] It is also shorter than the Cr–Si single bond lengths of chromium silyl complexes (2.376–2.660 Å).[172]

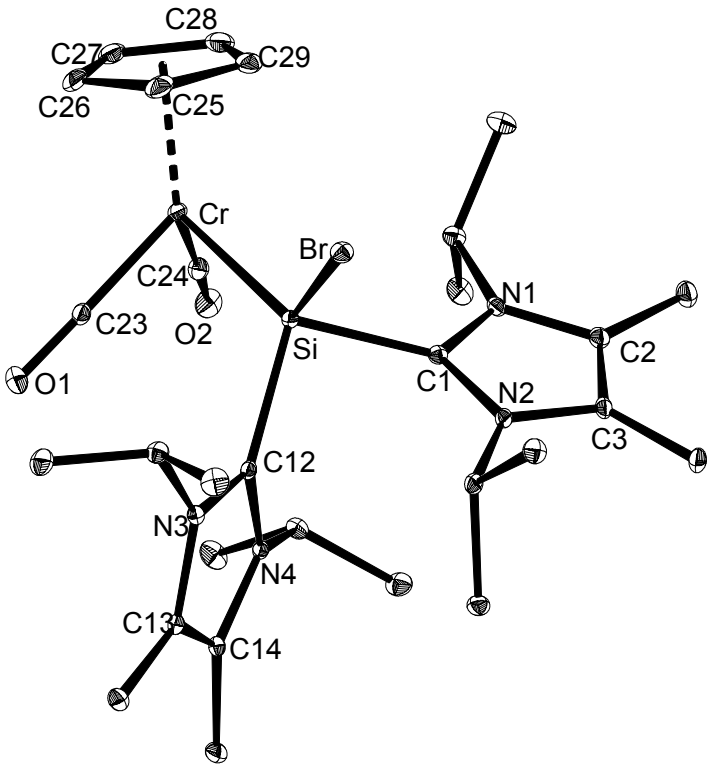

Figure 35: DIAMOND plot of the molecular structure of **55**. Thermal ellipsoids are set at 30% probability. Hydrogen atoms are omitted for clarity. Selected bond lengths [Å] and bond angles [°]: Cr–Si 2.2515(7), Cr–C23 1.796(2), Cr–C24 1.803(3), Si–Br 2.4340(6), Si–C1 2.007(2), Si–C12 1.964(2), O1–C23 1.185(3), O2–C24 1.189(3); Cr-Si-Br 114.45(3), Cr-Si-C1 132.56(7), Cr-Si-C12 116.86(7), Br-Si-C1 87.47(6), Br-Si-C12 104.67(7), C1-Si-C12 94.92(9).

- In contrast, the Si–Br distance is unusually long (2.4340(6) Å) in comparison to the mean Si–Br bond lengths in structurally characterized bromosilanes (2.26(6) Å)[49] and bromosilyl complexes (2.28–2.38 Å).[173]

[49] According to a CSD survey from 11.2011 of 48 structurally characterized compounds $^{T4}SiX_3$–Br, where X is any non-metal substituent. Median *d*(Si–Br) = 2.251 Å, LQ = 2.199 Å, HQ = 2.326 Å.

- The sum of angles around Si atom, excluding bromine amounts to 344°, and lies in-between the sum of angles expected for a tetrahedral (328.5°) and a planar geometry (360°).
- All these bonding parameters suggest a strong polarization of the Si–Br bond in **55**, due to d_π(Cr)–σ*(Si–Br) hyperconjugation, which can be expressed by the ionic canonical resonance formula $[Cp(CO)_2Cr{=}Si(IMe_2iPr_2)_2]^+Br^-$.

The IR spectrum of **55** in fluorobenzene displays two *ν*(CO) absorption bands of almost equal intensities at 1794 and 1726 cm^{-1} (1776 and 1707 cm^{-1} in the solid state).[50] The considerable shift to lower frequencies in the IR spectra of **55** in comparison to **49** is consistent with the increase of electron density on the chromium center due to the coordination of the second carbene. Strengthening of the backbonding to the CO-groups is also reflected in Cr–C bond length, thus the mean Cr–C distance in **55** (1.800(4) Å) is shorter than that in **49** (1.830(3) Å).

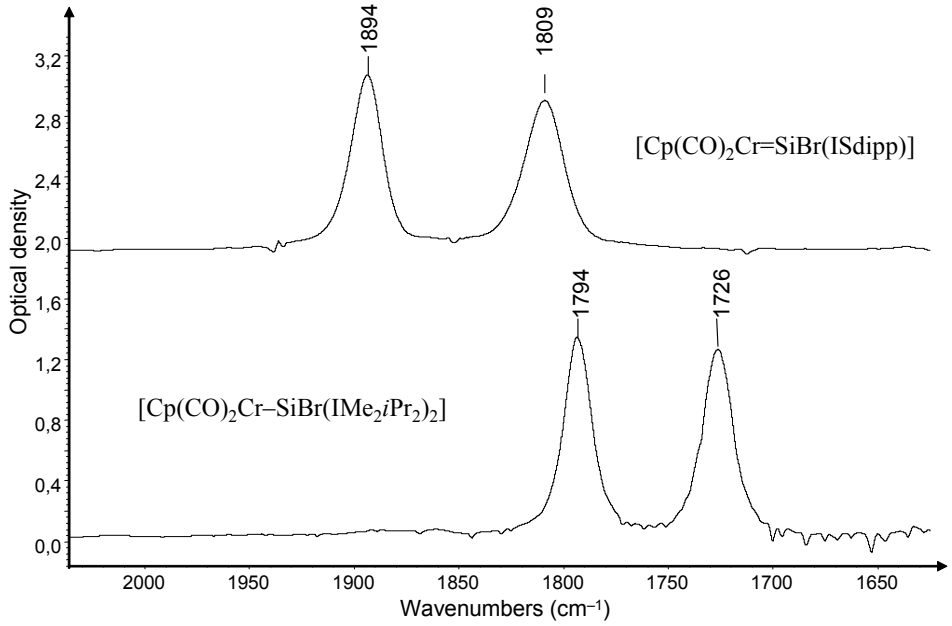

Figure 36: IR spectra of complexes **49** and **55** in fluorobenzene solution (cell with NaCl windows).

The NMR spectra of **55** in THF-d_8 at 298 K display a dynamic behavior of the compound, due to hindered rotation around the Si–$C_{carbene}$ bonds. The rotation is frozen out at 213 K, leading to an overall C_1 symmetric structure with two not equivalent carbene ligands, as was found in the solid state (Figure 37). The ^{29}Si NMR spectrum of **55** shows a singlet resonance at

[50] The IR *ν*(CO) absorption bands of **55** are similar to those observed for the putative product of the reaction $[Cp(CO)_2{=}SiBr(ISdipp)] + 2IMe_4 \rightarrow [Cp(CO)_2CrSi(IMe_4)_2Br] + ISdipp$; at 1772 and 1700 cm^{-1} (in the solid state).

17.3 ppm, at considerably higher field than that of **49** (95.1 ppm) as expected for a silyl complex.

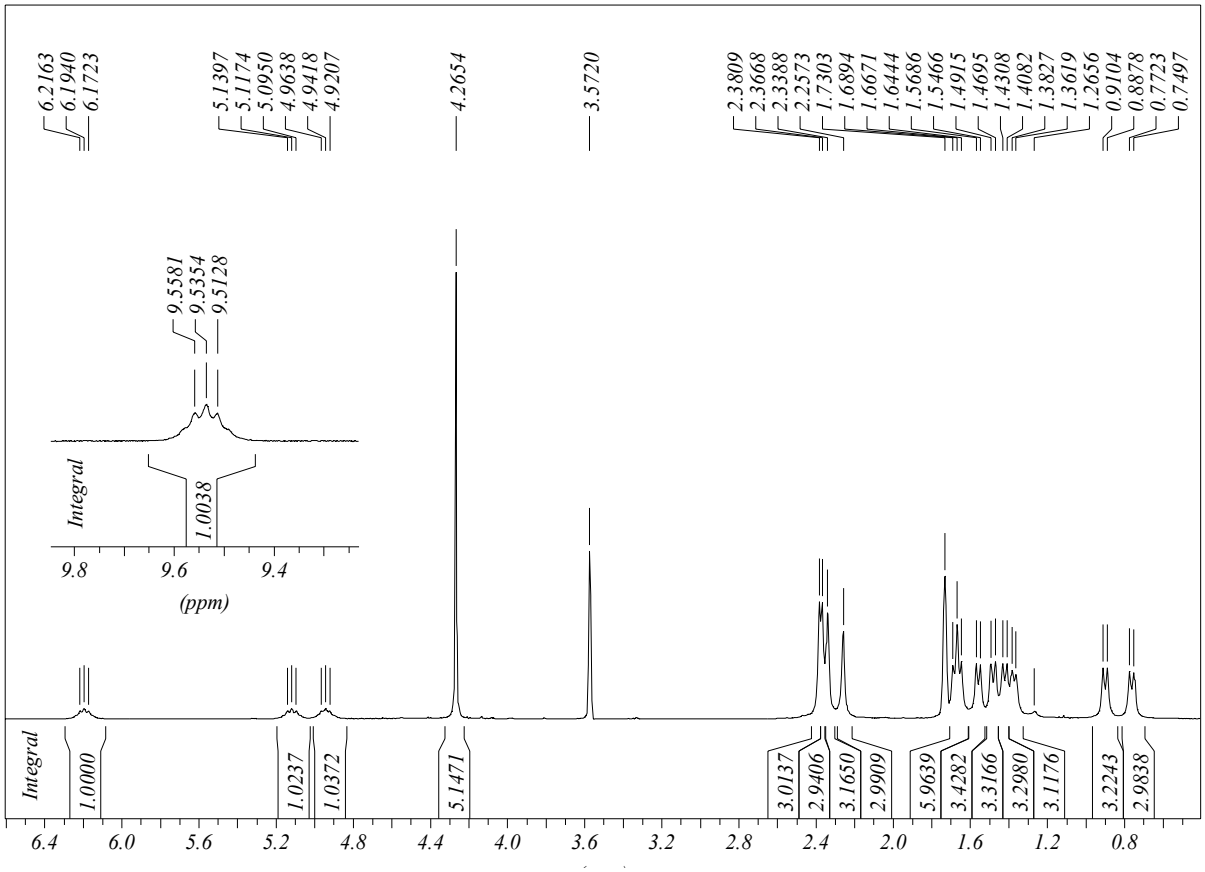

Figure 37: ^{1}H NMR spectrum of the complex [Cp(CO)$_2$CrSi(IMe$_2$*i*Pr$_2$)$_2$Br] (**55**) at 213 K (300 MHz, THF-d_8). The signals marked with an asterisk correspond to THF-d_8.

The polarization of the Si–Br bond implied, that abstraction of bromide with an electrophilic reagent might be possible. Indeed, treatment of **55** with Li[B(C$_6$F$_5$)$_4$] in fluorobenzene led to a color change from red-brown to green. An *in situ* IR spectrum revealed the selective formation of a new product with two ν(CO) absorptions bands of equal intensities at 1895 and 1821 cm^{-1}. The bands appear at significantly higher wavenumbers than those in **55** (1794 and 1726 cm^{-1} in fluorobenzene) but compare well with those of [Cp(CO)$_2$Cr=SiBr(ISdipp)] (1894 and 1809 cm^{-1} in PhF). The relative position of the ν(CO) absorptions bands of the product to those of **55** led us to assume, that the intermediate product is the cationic silylidene complex **56** (Scheme 50).

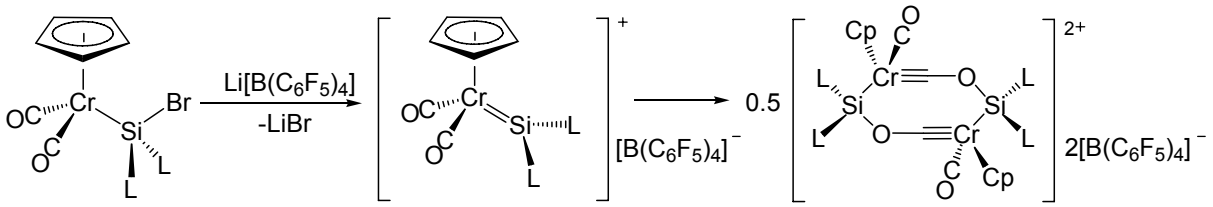

Scheme 50: Stepwise formation of the siloxycarbyne complex **57** (L = 1,3-diisopropyl-2,4-dimethylimidazol-2-ilydene (IMe_2iPr_2)).

However, all attempts to isolate **56** were not successful due to its unstability. In fact, complex **56** irreversibly dimerizes either upon concentration or storage of a fluorobenzene solution at –16 °C to yield the yellow siloxycarbyne complex **57** (Scheme 50). Complex **57** was found to be insoluble in common organic solvents, including dichloromethane and acetonitrile. The solid state IR spectrum of **57** shows only one ν(CO) absorption band at 1860 cm^{-1} indicating the presence of only one terminal carbonyl ligand.

Complex **57** is the first example of a chromium siloxycarbyne complex. It features a short Cr–C distance of 1.717(2) Å, comparable with those in $[Cp(CO)_2Cr{\equiv}CPh]$ (1.705(2) Å) and in $[Cp(CO)_2Cr{\equiv}CNiPr_2]$ (1.728(8) Å).[159, 174] The C24–O2 bond length compares well with the C_{sp}–O distance in *t*BuO–$(C{\equiv}C)_2$–O*t*Bu (1.303(1) Å).[175] The Cr-C-O angle of 172.4(2)° shows the almost linear arrangement of these atoms, as expected for a carbyne complex. However, the Cr–Si bond length of 2.2847(6) Å lies in-between that in the silylidene complexes $[Cp(CO)_2Cr{=}SiBr(ISdipp)]$ (2.1618(9) Å), and **55** ((2.2515(7) Å); and the Cr–Si single bond length in chromium silyl complexes, e.g. $[(\eta^6\text{-Mes})Cr(SiCl_3)_2(CO)_2]$ (2.380(3) Å).[164] The Si–O distance in **57** (1.749(1) Å)) is longer than the mean Si–O bond length in alkoxysilanes (1.66(3) Å).[51] This suggests, that d_π(Cr)-σ*(Si–O) hyperconjugation contributes to the bonding (see discussion above for complex **55**).

[51] According to a CSD survey from 11.2011 of 2102 structurally characterized alkoxysilanes of the formula ($RO–^{T4}SiR_3$, where R = carbon-bonded substituent). Median *d*(Mo–Si) = 1.654 Å, LQ = 1.632 Å, HQ = 1.680 Å.

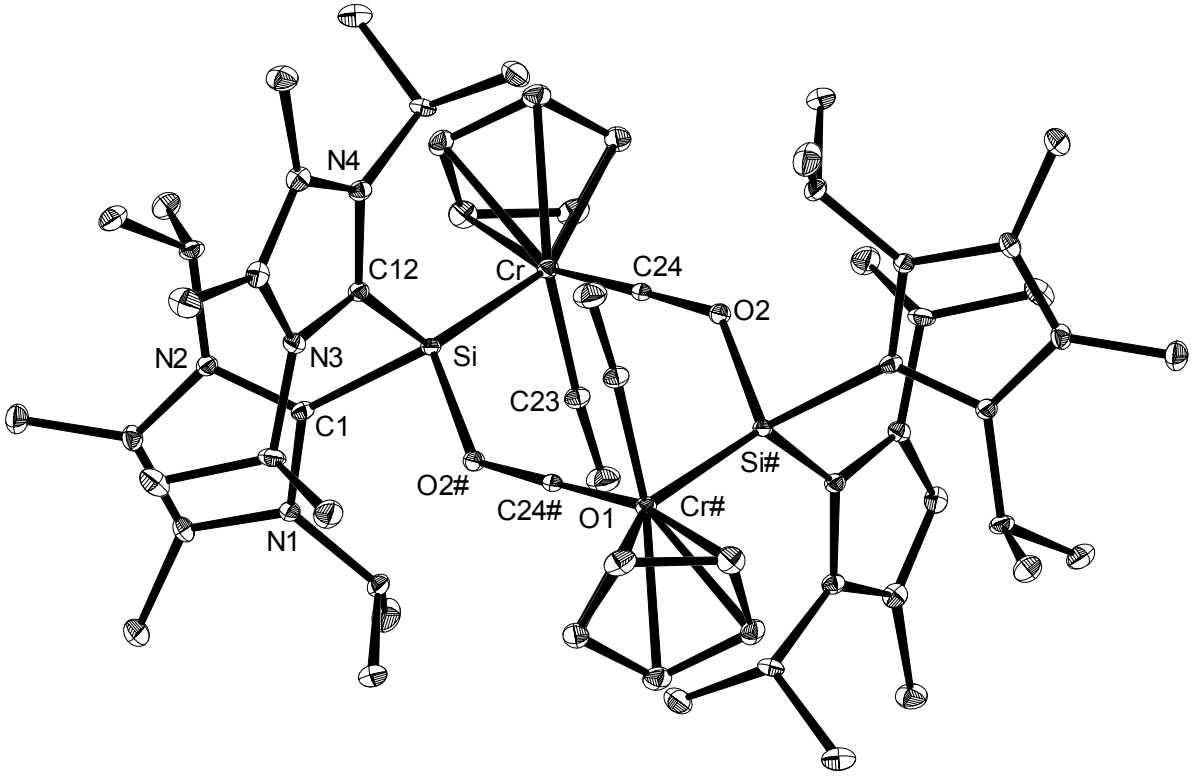

Figure 38: DIAMOND plot of the molecular structure of the complex cation of **57**. Thermal ellipsoids are set at 30% probability. Hydrogen atoms are omitted for clarity. Selected bond lengths [Å] and bond angles [°]: Cr–Si 2.2847(6), Cr–C23 1.803(2), Cr–C24 1.717(2), Si–C1 1.965(2), Si–C12 1.993(2), Si–O2# 1.749(1), O1–C23 1.178(2), O2–C24 1.291(2); Cr-Si-C1 119.76(6), Cr-Si-C12 130.53(6), Cr-Si-O2# 115.94(5), C1-Si-C12 93.84(8), C1-Si-O2# 94.37(7), C12-Si-O2# 94.33(7), C1-Si-C12 93.84(8), Cr-C23-O1 175.2(2), Cr-C24-O2 172.4(2), C24-O2-Si# 133.8(1).

Formation of **57** can be explained by the insufficient steric protection of the highly electrophilic Si center in **56** from the nucleophilic attack of a CO-group. One possible way to stabilize the intermediate complex might be to increase the steric bulk at the metal center using a Cp*ligand. Attempts in this direction were not undertaken.

Halide substitution of the halosilylidene complex [Cp*(CO)$_2$Cr=SiBr(ISdipp)]

The halosilylidene complexes [(η^5-C_5R_5)(CO)$_2$M=SiX(NHC)] (**49–53**, R=H, CH_3) possess the synthetic potential for the synthesis of substituted silylidene complexes. Halide substitution by nucleophiles can be a general approach to novel zwitterionic silylidene complexes. These carbene stabilized silylidyne complexes can provide access to free silylidyne complexes upon elimination of the carbene.

The choice of nucleophiles can be very broad, since the Si–X bonds are quite reactive. In fact, the reaction of [Cp*(CO)$_2$Cr=SiBr(ISdipp)] with trityllithium ([Li(THF)$_4$][CPh$_3$]) selectively afforded the product of substitution of bromine. Interestingly, the substitution afforded not the expected complex [Cp*(CO)$_2$Cr=Si(CPh$_3$)(ISdipp)], but its isomer, resulting from the attack of the [CPh$_3$]$^-$ anion in *para*-position, probably because of steric reasons (Scheme 51).

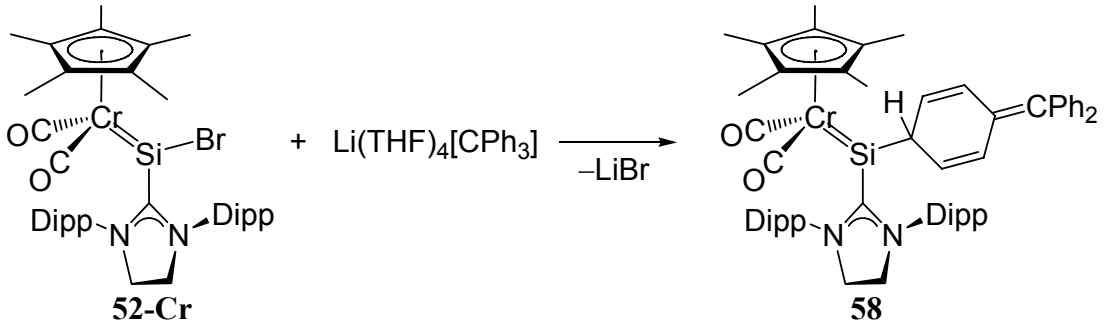

Scheme 51: Bromide substitution of the bromosilylidene complex.

Complex **58** was isolated as a brown crystalline solid in 71% yield. Unfortunately, the complex did not crystallize well, and only the structural motive was obtained by X-ray diffraction. The complex is unstable at ambient temperature, the decomposition leads to formation of the free carbene among with other unidentified products, as evidenced by ^{1}H NMR spectroscopy. The IR spectrum of **58** displays two ν(CO) absorption bands of equal intensities at 1875 and 1785 cm^{-1} in toluene. As expected, the ν(CO) absorptions are slightly shifted to lower wavenumbers in comparison to those of the starting material (1886, 1804 cm^{-1}) and compare well with those of the isolobal complex [Cp(CO)$_2$Mo=Si(C$_6$H$_3$-2,6-Trip$_2$)(IMe$_4$)] (**42**; 1859, 1785 cm^{-1}).

An analogous reaction was carried out with the complex [Cp*(CO)$_2$Mo=SiBr(ISdipp)], leading to the same type of the product.[52] However, several attempts to substitute the bromide with other bulky nucleophiles, such as LiMes or Li[SiMe(SiMe$_3$)$_2$] were not selective. A reaction with a very bulky nucleophile Li(C$_6$H$_3$-2,6-Mes$_2$) did not occur. We believe that substitution of the halogen atom requires specific nucleophiles. One has to consider the following possibilities: a) the substitution will not occur with very bulky nucleophiles; b) the carbene (ISdipp) can dissociate after the substitution, leading to possibly unstable silylidyne complexes; c) the substitution products can react with a second equivalent of the nucleophile;

[52] M. Speer, *Bachelorarbeit*, University of Bonn, **2011**.

d) simple addition to the halosilylidene complex can occur, without elimination of the bromide atom.

2.2.4 Synthesis of the first silylidyne complexes

The isolation of the zwitter-ionic silylidene complex $[Cp(CO)_2Mo{=}Si(C_6H_3\text{-}2,6\text{-}Trip_2)(IMe_4)]$ (Section 2.2.1) was the crucial step in the synthesis of the first silylidyne complex. The calculations have shown, that the bond dissociation energy and the Gibbs free dissociation energy of the $Si–C_{carbene}$ bond in $[Cp(CO)_2Mo{=}Si(C_6H_3\text{-}2,6\text{-}Trip_2)(IMe_4)]$ (**42**) are 61.2 and 1.2 kJ/mol correspondingly. The rather low dissociation energies suggested, that dissociation of the carbene might occur to some extent at elevated temperatures. It was assumed, that in the presence of a strong Lewis acid, the equilibrium would be shifted towards the silylidyne complex $[Cp(CO)_2Mo{\equiv}Si(C_6H_3\text{-}2,6\text{-}Trip_2)]$ and the carbene adduct of the Lewis acid employed.

Treatment of $[Cp(CO)_2Mo{=}Si(C_6H_3\text{-}2,6\text{-}Trip_2)(IMe_4)]$ (**42**) with tris(perfluorophenyl)-borane already at ambient temperature led to a rapid color change from dark brown to brown-orange.[53] Addition of hexane afforded large violet-red crystals of a new silylidene complex **59** in 58% yield (Scheme 52). The complex is insoluble in hexane or toluene, is soluble but unstable in THF at ambient temperature. A solution of **59** in THF-d_8 prepared in the cold was stable for at least several hours at –60 °C.

Formation of **59** can be explained by the electrophilic attack of the Lewis acid $B(C_6F_5)_3$ on the electron rich Cp ring, leading to the intermediate 16 VE molybdenum η^4-cyclopentadiene complex, which undergoes hydrogen migration to the metal center to give the **59** (Scheme 53). A similar reaction was reported earlier.[176]

[53] An *in situ* IR spectrum, in toluene displayed ν(CO) absorption bands at 1875(vs) and 1785(vs) cm^{-1}, which probably corresponds to the 16VE intermediate.

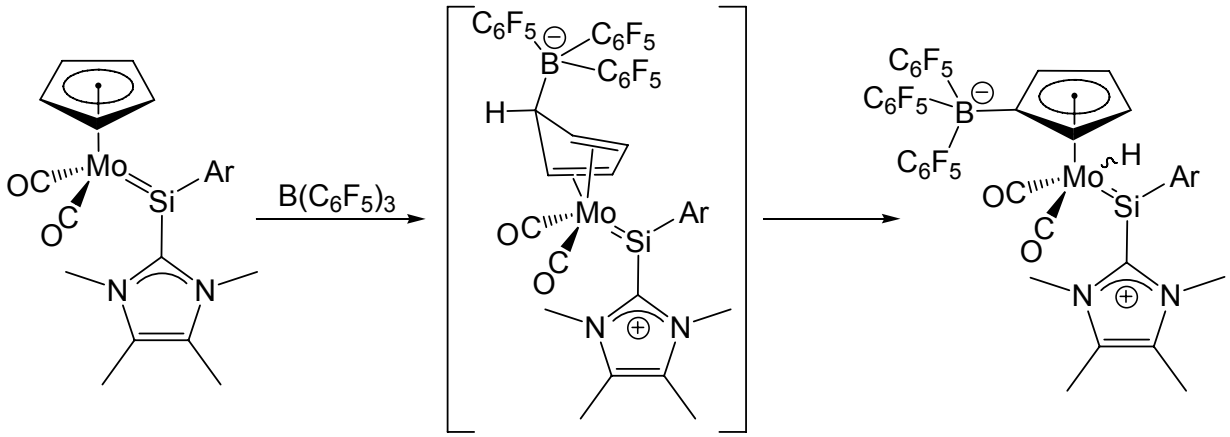

42 **59**

Scheme 52: Reaction of **42** with $B(C_6F_5)_3$.

The four-legged piano stool complex **59** features a Mo–Si double bond of 2.3741(7) Å, slightly longer than that in $[Cp(CO)_2Mo{=}Si(C_6H_3\text{-}2,6\text{-}Trip_2)(IMe_4)]$ (**42**; 2.3474(6) Å) and in the bromosilylidene complexes **52-Mo** and **53-Mo** (2.2838(13) Å and 2.2853(8) Å, Table 5). The bond length lies on the outer border of bond lengths in previously reported silylidene complexes of molybdenum (2.228–2.387 Å).[86, 87, 156] The coordination of the Si center is planar, if one excludes the hydrogen atom (sum of angles at Si 360.0°). The hydrogen atom was localized by the difference in the Fourier synthesis map in a bridging position between the molybdenum and silicon centers. The *cis*-orientation of the silylidene ligand and the hydrogen atom is also indicated by a large C68-Mo-Si and a small C67-Mo-Si angles (79.34(8)° and 102.37(8)° respectively). As has been observed earlier, a Si···H interaction does not affect the planarity of the silylidene ligand.[87] However, the X-ray crystallography is not very reliable in determination of position of hydrogen atoms in close proximity to a heavy metal. The ^{1}H NMR spectrum displays a singlet resonance for the bridging hydride at –9.95 ppm, with a J(Si,H) coupling constant of 60.1 Hz consistent with a Si···H interaction.[177] The ^{1}H NMR signal of the bridging proton compares with that in the similar complex $[Cp^*(dmpe)Mo(H)SiCl(Mes)]$[54] ($\delta$ = –12.50 ppm, J(Si,H) = 38Hz).[87]

[54] dmpe = 1,2-bis(dimethylphosphino)ethane

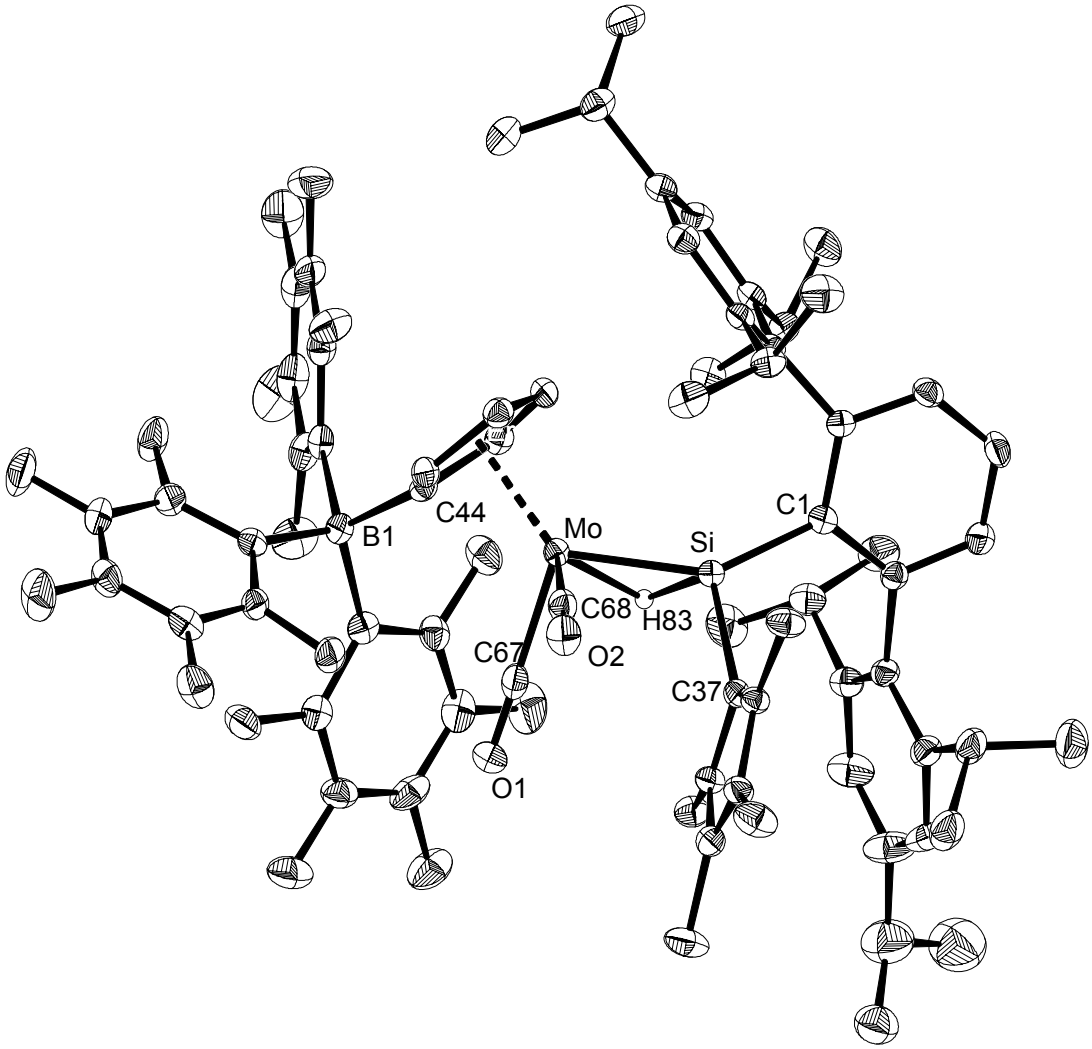

Figure 39: DIAMOND plot of the molecular structure of **59**. Thermal ellipsoids are set at 50% probability. Hydrogen atoms except H83 are omitted for clarity. Selected bond lengths [Å] and bond angles [°]: Mo–Si 2.3741(7), C1–Si 1.890(2), C37–Si 1.935(2), H83–Si 1.62(3), H83–Mo 1.79(3), B1–C44 1.663(4), C68–Mo 1.945(3), C67–Mo 1.975(3); C1-Si-Mo 144.34(8), C37-Si-Mo 110.60(8), C1-Si-C37 105.1(1), C68-Mo-Si 79.34(8), C67-Mo-Si 102.37(8), C67-Mo-C68 80.1(1).

The reaction with $B(C_6F_5)$ demonstrated, that a weaker Lewis base was necessary to prevent an attack on the Cp ring. Trisarylboranes were considered to be a good alternative. For example, the Lewis acidity of tris(*p*-Tol)borane (*p*-Tol = -C_6H_3-4-Me) is significantly weaker, but it forms a stable adduct with 1,3,4,5-tetramethylimidazol-2-ylidene (IMe_4). The *p*-tolyl substituent was used to simplify the ^1H and ^{13}C NMR spectra of the products.[55]

In fact, heating of a mixture of complex $[Cp(CO)_2Mo{=}Si(C_6H_3\text{-}2,6\text{-}Trip_2)(IMe_4)]$ (**42**) and $B(p\text{-Tol})_3$ in xylene under reflux (144 °C) was accompanied by a color change from yellow-

[55] K. Stumpf, *Diploma thesis*, University of Bonn, **2009**.

brown to red-brown. An *in situ* IR spectrum of the reaction mixture revealed a selective formation of the silylidyne complex **60** (Scheme 53).

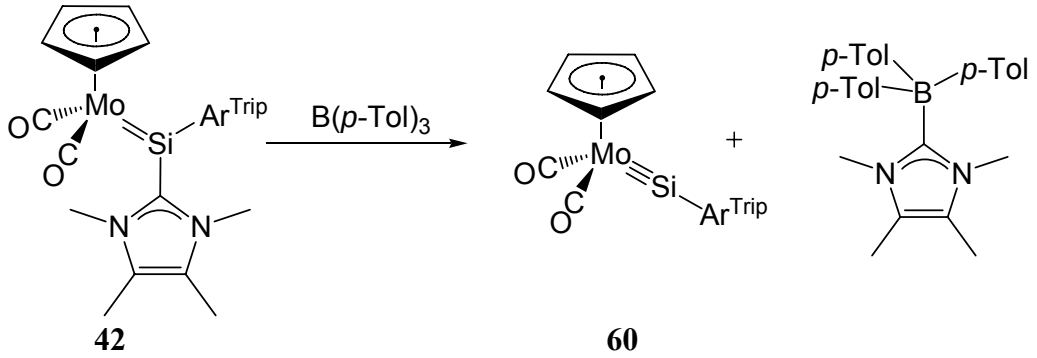

42 **60**

Scheme 53: Preparation of the first silylidyne complex **60**.

Complex **60** was isolated in 53% yield as a brick-red crystalline solid, after crystallization from pentane. The two-step synthesis with intermediate isolation of **42** afforded the silylidyne complex **60** in 27% overall yield. Synthesis of **60** was also performed without intermediate isolation of the carbene-adduct **42** and afforded the product in 39% yield from $SiCl(C_6H_3$-2,6-$Trip_2)(IMe_4)$.

The three-legged piano stool complex features a very short Mo–Si bond length of 2.2241(7) Å and an almost linear coordination of the Si center (Mo-Si-C1 = 173.49(8)°). The Mo–Si bond length in **60** is 0.12 Å shorter than the Mo–Si double bond length in the NHC-adduct **42** (2.345(2) Å) and compares well with the Mo–Si bond lengths calculated for the hypothetical complexes $[Cp(CO)_2Mo{\equiv}SiR]$ (R = H: 2.213 Å; R = Me: 2.229 Å).[118, 119] Complex **60** is isostructural with its germanium analogue $[Cp(CO)_2Mo{\equiv}Ge(C_6H_3$-2,6-$Trip_2)]$. Interestingly, the Mo–Si distance in **60** is nearly the same, as that found in the previously reported complex $[Cp^*(dmpe)Mo(H)SiMes)][B(C_6F_5)_4]$ (dmpe = 1,2-bis(dimethylphosphino)ethane), in which a hydride bridges the Mo–Si triple bond (2.219(2) Å).[87]

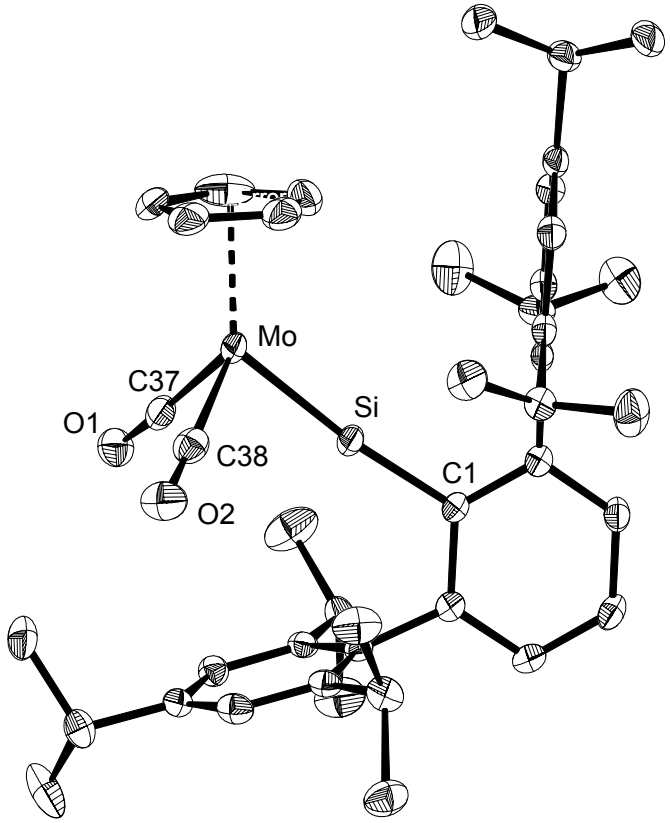

Figure 40: DIAMOND plot of the molecular structure of **60**. Thermal ellipsoids are set at 50% probability. Hydrogen atoms are omitted for clarity. Selected bond lengths [Å] and bond angles [°]: Mo–Si 2.2241(7), Si–C1 1.859(2), Mo–C37 1.968(3), Mo–C38 1.973(3); C1-Si-Mo 173.49(8), Si-Mo-C37 90.56(7), Si-Mo-C38 89.63(8), C37-Mo-C38 87.0(1).

The spectroscopic data corroborate the structure of complex **60**. The carbene abstraction is accompanied by a shift of the *ν*(CO) absorption bands in the IR spectra in toluene from 1859, 1785 cm^{-1} in **42** to 1937, 1875 cm^{-1} in **60 (**Figure 41**)**. The positions of the *ν*(CO) absorption bands compare well with those of [$Cp(CO)_2Mo{\equiv}Ge(C_6H_3$-2,6-$Trip_2)$] (1930, 1875 cm^{-1} in Nujol).[104] However, they appear at lower wavenumbers than those in [$Cp(CO)_2Mo{\equiv}C(C_6H_3$-2,6-$Me_2)$] (1992 and 1919 cm^{-1} in CH_2Cl_2), indicating the higher σ-donor/π-acceptor ratio of the silylidyne ligand. The ^{29}Si NMR spectrum displays a singlet resonance at 320 ppm, which is shifted by 120 ppm to lower field in comparison to [$Cp(CO)_2Mo{=}Si(C_6H_3$-2,6-$Trip_2)(IMe_4)$] (**42**). The low-field shift of the signal in the ^{29}Si NMR spectrum is characteristic for a multiply bonded silicon center. The shift in **60** can be compared with that of [Cp*(dmpe)Mo(H)SiMes)][$B(C_6F_5)_4$] (289 ppm).[87] The ^{1}H and $^{13}C\{^{1}H\}$ NMR spectra of **60** corroborate the structure of the complex (Figure 42).

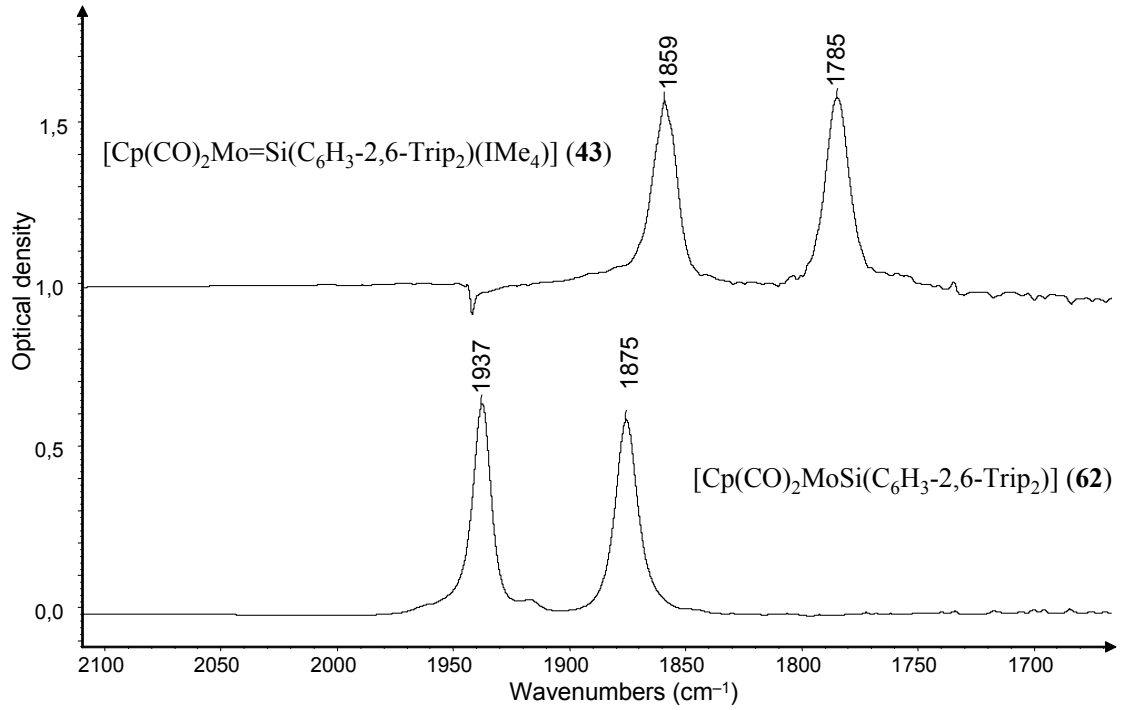

Figure 41: The IR spectra of complexes **42** and **60** in toluene.

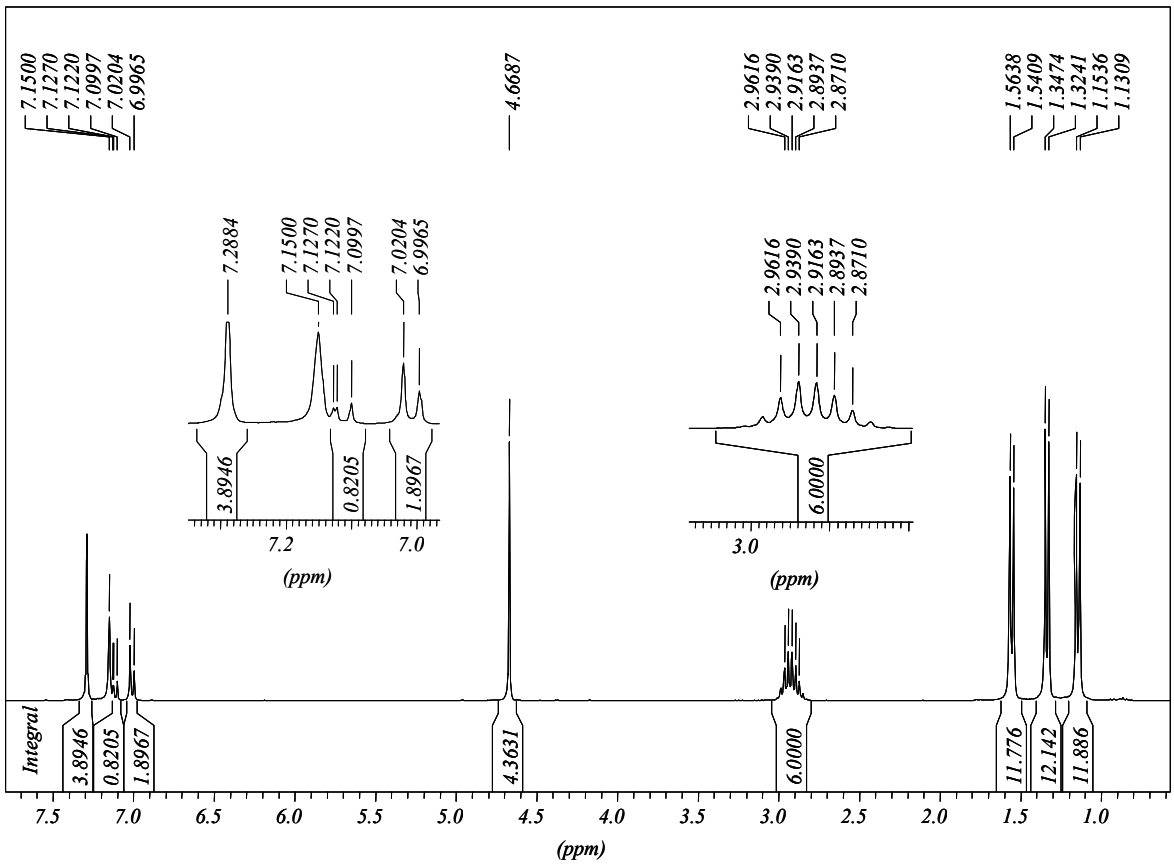

Figure 42: ^{1}H NMR spectrum of the silylidyne complex **60** (C_6D_6, 300.1 MHz).

The analogous silylidene complex [Cp(CO)$_2$Mo=Si(C$_6$H$_3$-2,6-Mes$_2$)(IMe$_4$)] (**43**) also reacts with B(*p*-Tol)$_3$ in boiling xylene. Analysis of the reaction mixture revealed the formation of

the carbene-borane adduct among several other products, which probably results from the decomposition of the putative intermediate [Cp(CO)$_2$Mo≡Si(C$_6$H$_3$-2,6-Mes$_2$)]. This suggests, that the decrease of the steric bulk of the *m*-terphenyl substituent (Mes *vs* Trip group) might slightly increase the Si–C$_{carbene}$ dissociation energy and at the same time lower the stability of the silylidyne complex [Cp(CO)$_2$Mo≡Si(C$_6$H$_3$-2,6-Mes$_2$)] hindering thereby its isolation.

Cationic silylidyne complexes

The halosilylidene complexes [(η^5-C$_5$R$_5$)(CO)$_2$M=SiX(NHC)] (R = H, CH$_3$; M = Cr, Mo, W; X = Br, I; NHC = IDipp, ISdipp; **49, 52, 53**; Table 5) are isolobal to the complexes [Cp(CO)$_2$M=SiAr(IMe$_4$)] (M = Mo, W; Ar = C$_6$H$_3$-2,6-Trip$_2$, C$_6$H$_3$-2,6-Mes$_2$; **42–44**, Table 3). Therefore, in analogy to the abstraction of the carbene from **42**, abstraction of X$^-$ from the halosilylidene complex should lead to the formation of cationic silylidyne complexes (Scheme 54).

Scheme 54: Possible ways to silylidyne complexes.

In fact, bromide abstraction from the complexes **52-Cr**, **52-Mo** and **52-W** with Li[Al(OR^F)$_4$] (OR^F = -OC(CF$_3$)$_3$) or Na[B(C$_6$H$_3$-3,5-(CF$_3$)$_2$)$_4$] in fluorobenzene led to the formation of unprecedented cationic silylidyne complexes of chromium, molybdenum and tungsten (Scheme 55).

Complexes **61-Cr** and **61-Mo**[56] were isolated as very dark-brown, thermally stable crystalline solids in 81 and 67% yields. The complexes were fully characterized. Complex **61-W** was prepared on a small scale and was characterized by IR and NMR spectroscopy. The complexes are very sensitive towards oxygen and moisture; they are soluble and stable in fluorobenzene, chlorobenzene and diethyl ether, insoluble in hexane and pentane. Complex **61-Cr** decomposes in THF at room temperature. A dichloromethane solution of complex **61-Mo** showed no signs of decomposition 5 minuts after preparation as was shown by ^{1}H NMR,

[56] M. Speer, *Bachelor thesis*, University of Bonn, **2011**.

however it decomposed within hours. In contrast, decomposition of the chromium analogue in dichloromethane was evident already after 5 min.

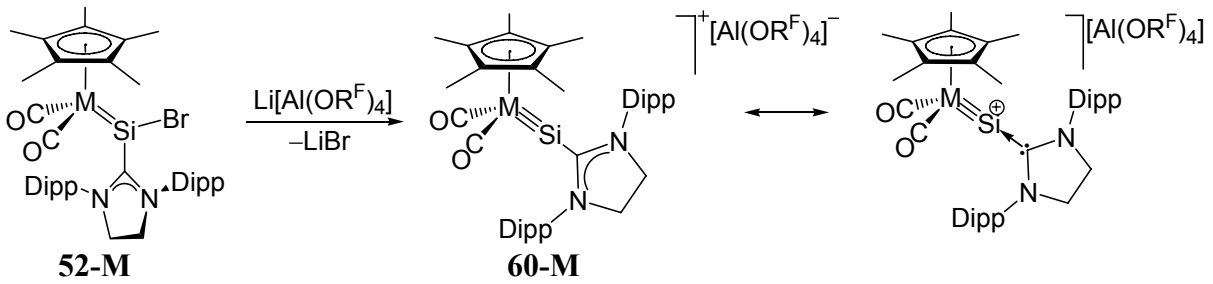

Scheme 55: Synthesis of cationic silylidyne complexes **60-M** (M = Cr, Mo, W; OR^F = -$OC(CF_3)_3$).

Complexes **61-Cr** and **61-Mo** crystallized as stacks of thin plates from a fluorobenzene/hexane mixtures; therefore a selection of a single crystal of high quality for the X-ray diffraction analysis was not possible and only a low quality structure of **61-Cr** was resolved from the diffraction pattern. Therefore also the complexes $[Cp^*(CO)_2M{\equiv}Si(ISdipp)][B(C_6H_3\text{-}3,5\text{-}(CF_3)_2)_4]$ (**62-Cr, 62-Mo**) were prepared, which crystallized to give good quality crystals, suitable for X-ray diffraction analyses. The IR spectra of the complexes with different complex anions were identical, suggesting only weak interactions between the anions and cations in solutions in all cases. The bonding parameters of complexes **61-Cr** and **62-Cr** are very close. Unfortunately, it was not possible to obtain single crystals of the tungsten silylidyne complexes **61-W** or **62-W** due to the tendency of the compounds to precipitate as oils. The spectroscopic features of **61-W** are virtually identical to those of **61-Cr** and **61-Mo**, suggesting than **61-W** is in fact a silylidyne complex.

Complex **62-Cr** (Figure 43) features the shortest chromium–silicon bond reported up to date of (2.1219(9) Å). The bond length is slightly longer than that, predicted by theory for the putative complexes $[Cp(CO)_2Cr{\equiv}SiH]$ (2.080 Å) and $[Cp(CO)_2Cr{\equiv}SiMe]$ (2.128 Å).[118, 119] The Cr–Si bond length can be compared with the Cr–Ge bond length in $[CpCr(CO)_2{\equiv}Ge(C_6H_3\text{-}2,6\text{-}Trip_2)]$ of 2.1666(4) Å, taking into account that the covalent radius of the germanium atom is ca. 0.05 Å smaller than that of silicon.[105, 160] The Mo–Si bond length of 2.2212(9) Å in **62-Mo** compares well with that in $[Cp(CO)_2Mo{\equiv}Si(C_6H_3\text{-}2,6\text{-}Trip_2)]$ (2.2241(7) Å) and $[Cp^*(dmpe)Mo(H)SiMes)][B(C_6F_5)_4]$ (2.219(2) Å).[87, 160] The Si center is almost linearly coordinated as demonstrated by the M-Si-$C_{carbene}$ angle of 169.75(9)° (**62-Cr**) and 174.17(11)°(**62-Mo**). The deviation from linearity can be attributed to the steric demand imposed by the η^5-C_5Me_5 ligand and/or crystal packing forces.

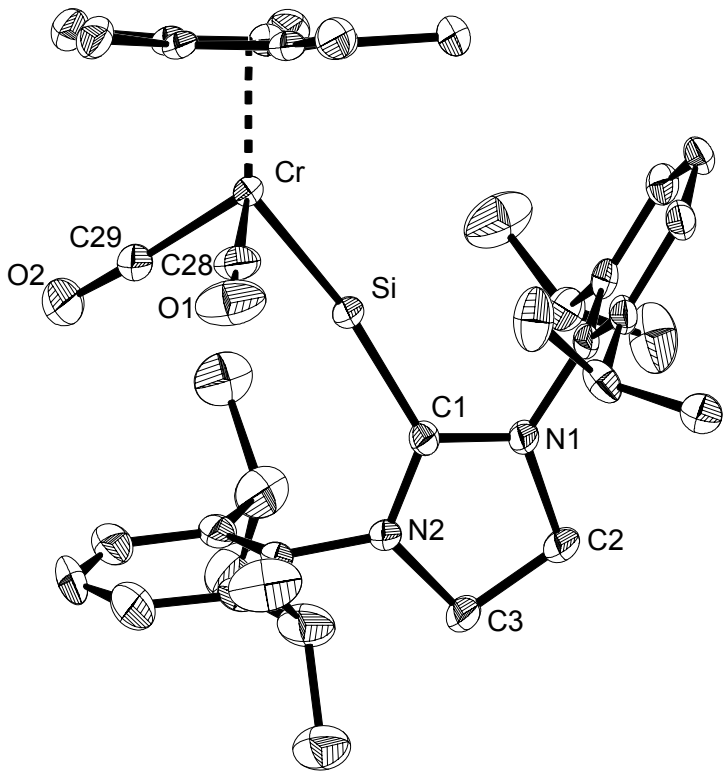

Figure 43: DIAMOND plot of the molecular structure of the complex cation in **62-Cr**. Thermal ellipsoids are set at 50% probability. Hydrogen atoms are omitted for clarity. Selected bond lengths [Å] and bond angles [°], values in square brackets correspond to the molybdenum analogue **62-Mo**: Cr–Si 2.1219(9) [2.2212(9)], Si–C1 1.906(3) [1.898(3)], Cr–C28 1.844(3) [1.967(4)], Cr–C29 1.860(3) [1.978(4)], C1–N1 1.323(4) [1.320(4)], C1–N2 1.317(4) [1.319(4)], C2–N1 1.484(4) [1.484(4)], C3–N2 1.485(4) [1.484(4)], C2–C3 1.544(4) [1.543(5)]; C1-Si-Cr 169.75(9) [174.2(1)], N1-C1-N2 111.9(3) [112.3(3)], C28-Cr-Si 90.4(1) [90.1(1)], C29-Cr-Si 92.3(1) [91.1(1)], C28-Cr-C29 91.50(16) [90.0(2)].

The Si–$C_{carbene}$ bonds are further shortened to 1.906(3) Å (**62-Cr**) and 1.898(3) Å (**62-Mo**) in comparison to the parent halosilylidene complexes (1.957(2) Å in **52-Cr**; 1.959(4) Å in **52-Mo**).[119] The Si–C bonds are only slightly longer than those in [$CpMo(CO)_2{\equiv}Si(C_6H_3$-2,6-$Trip_2)$] (1.859(2) Å) reflecting the strong covalent character of the bond. Further evidence of strengthening of the Si–C bond is provided by the ^{13}C NMR shifts of $C_{carbene}$ nuclei, δ ppm: 244.1 (ISdipp); 188.7 (**20**); 178.7 (**52-Cr**) and 181.4 (**52-Mo**); 172.7 (**61-Cr**); and 160.0 [ISdippH]Cl. The shifts indicate that in the series $SiBr_2$(ISdipp) – $L_nM{=}SiBr$(ISdipp) − $L_nM{\equiv}Si$(ISdipp) the carbene ligand acquires more and more dihydroimidazolium salt character with a covalent Si–$C_{carbene}$ bond. According to the experimental and computational data the compounds **61-Cr** and **61-Mo** are best described as silylidyne complexes, bearing an imidazolinium substituent that is bonded to the Si center via a covalent single bond, that is strongly polarized towards the $C_{carbene}$ atom. A small contribution of the resonance structure featuring a formal positive charge on the silicon atom can be rationalized by the higher

reactivity of **61-M**. For example, **61-Cr** is unstable in THF solution and reacts with ethylene[57] in contrast to [CpMo(CO)$_2$≡Si(C$_6$H$_3$-2,6-Trip$_2$)] (**60**); **61-Cr** and **61-Mo** also react much faster with alkynes than **60** (see p. 129).

Bromide abstraction from the complexes **52-M** was accompanied by a substantial shift of the *ν*(CO) absorption bands in the IR spectra in all cases by roughly 100 cm^{-1} (e.g. from 1882, 1802 cm^{-1} for **52-Cr** to 1966, 1912 cm^{-1} for **61-Cr** in fluorobenzene). The shifts compare well with those, observed upon carbene abstraction from the carbene-stabilized silylidyne complex [Cp(CO)$_2$Mo=Si(C$_6$H$_3$-2,6-Trip$_2$)(IMe$_4$)] (**42**) (Figure 44). The *ν*(CO) absorption bands appear at higher wavenumbers than those of the silylidyne complex [CpMo(CO)$_2$≡Si(C$_6$H$_3$-2,6-Trip$_2$)] (**60**: 1936, 1872 cm^{-1} in fluorobenzene), reflecting the lower σ-donor/π-acceptor ratio of the [Si(NHC)]$^+$ ligand in comparison to [SiAr]. However, the average Mo–C distance in **61-Mo** of 1.973(6) Å is similar to that in the neutral silylidyne complex [CpMo(CO)$_2$≡SiAr] (1.971(3) Å).

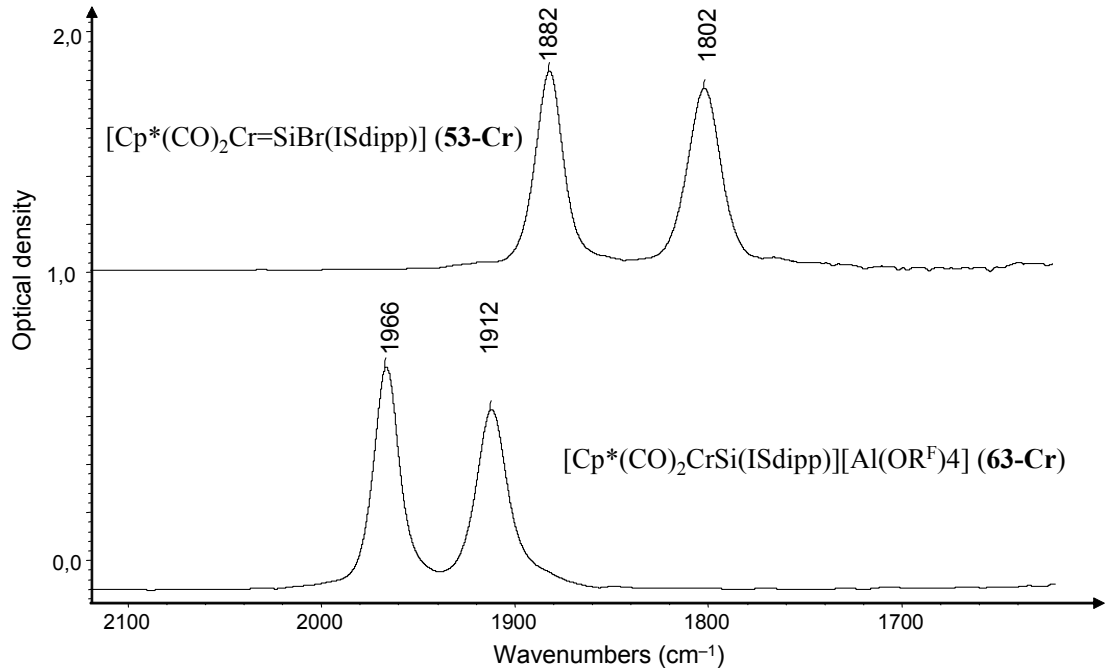

Figure 44: The IR spectra of complexes **52-Cr** and **61-Cr** in fluorobenzene (OR^F = -OC(CF$_3$)$_3$).

[57] As indicated by the ν(CO) absorption bands of the green reaction mixture at 1960(vs) and 1870(vs) cm^{-1} in fluorobenzene. The product was not isolated.

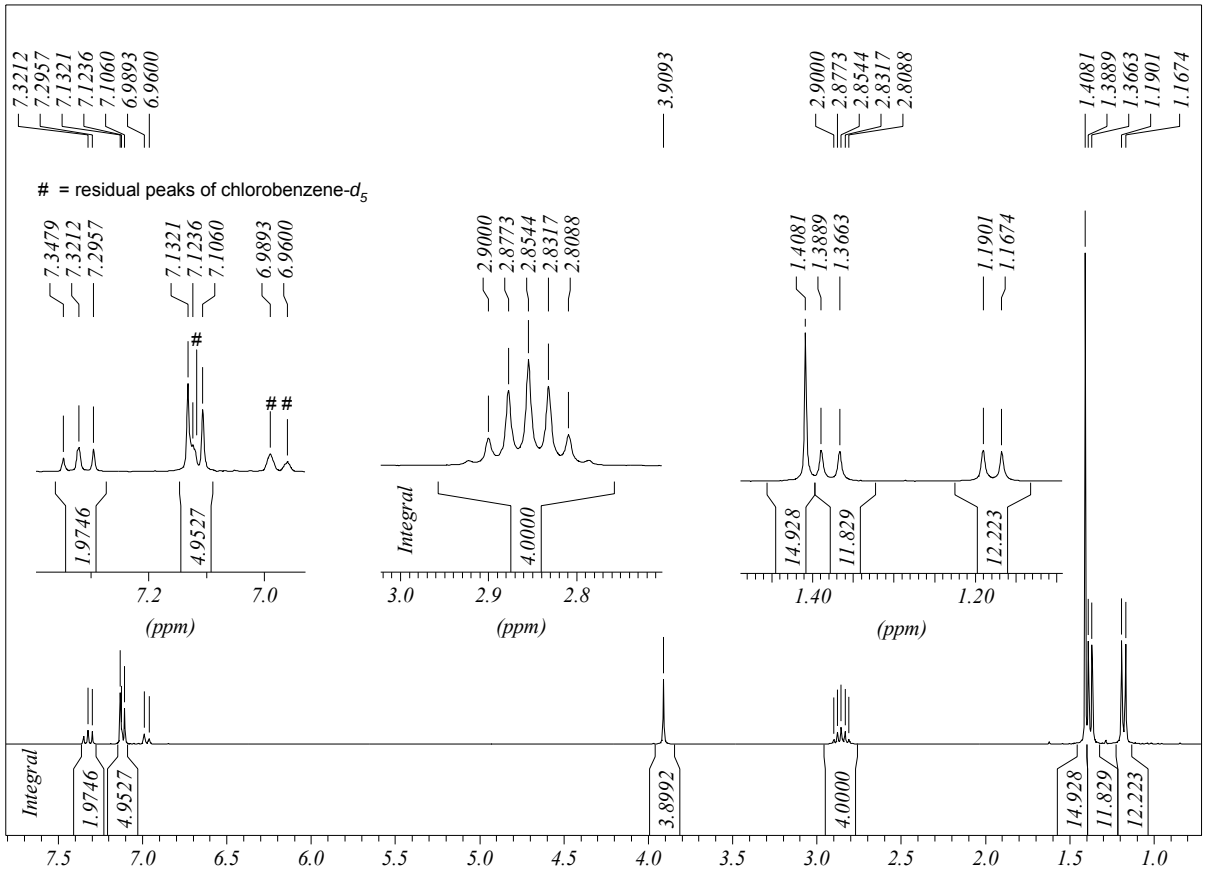

Figure 45: ^{1}H NMR spectrum of the silylidyne complex **61-Cr** (C_6D_5Cl, 300.1 MHz).

The ^{1}H and $^{13}C\{^{1}H\}$ NMR spectra of **61-Cr** corroborate the structure of the complex (Figure 45). The ^{29}Si NMR spectra show singlet resonances at 129.0 ppm (**61-Cr**), 149.1 ppm (**61-Mo**) and 178.5 ppm (**61-W**; ^{1}J(W,Si) = 420.5 Hz), which are all shifted to the lower field in comparison to those of the starting materials (74.8, 80.1 and 71.2 ppm respectively). The ^{29}Si NMR signals appear at considerably higher field than that of [CpMo(CO)$_2$≡Si(C$_6$H$_3$-2,6-Trip$_2$)] (**60**: 320.1 ppm), which cannot be explained presently (Table 6).

Complex	Color	Yield, %	IR, PhF, cm^{-1}	^{13}C NMR of $C_{carbene}$, ppm	^{29}Si NMR, ppm	d(M−Si), Å (in)
[Cp(CO)$_2$Mo≡Si(C$_6$H$_3$-2,6-Trip$_2$)] (**60**)	Brick-red	53	1936, 1872	177.4	320.1	2.2241(7)
[Cp*(CO)$_2$Cr≡Si(ISdipp)][Al(OR^F)$_4$] (**61-Cr**)	Dark brown	81	1966, 1912	172.7	129.0	2.1219(9)[a]
[Cp*(CO)$_2$Mo≡Si(ISdipp)][Al(OR^F)$_4$] (**61-Mo**)[56]	Dark brown	52	1973, 1914	176.6	149.9	2.2212(9)[a]
[Cp*(CO)$_2$W≡Si(ISdipp)][Al(OR^F)$_4$] (**61-W**)	Dark brown	–	1967, 1905	184.7	178.5	–

Table 6: Summary of properties of the silylidyne complexes **60** and **61-Cr**, **61-Mo**, **61-W** (OR^F = -OC(CF$_3$)$_3$).
[a] The values found in complexes **62-Cr** and **62-Mo**.

An interesting product was isolated in an attempts to crystallize the silylidyne complex **62-W** [Cp*(CO)$_2$M≡Si(ISdipp)][B(C$_6$H$_3$-3,5-(CF$_3$)$_2$)$_4$]. Thus, diffusion of hexane in fluorobenzene solution of **62-W** at –16 °C resulted in precipitation of a brown oil, however upon standing at ambient temperature for about 1 month a small amount of orange crystals of complex **63** were formed in the mixture. The crystals were separated and analyzed by IR spectroscopy and X-ray diffraction. The later method has shown that **63** is a product of C-H activation of hexane, with concomitant dehydrogenation (Scheme 56).

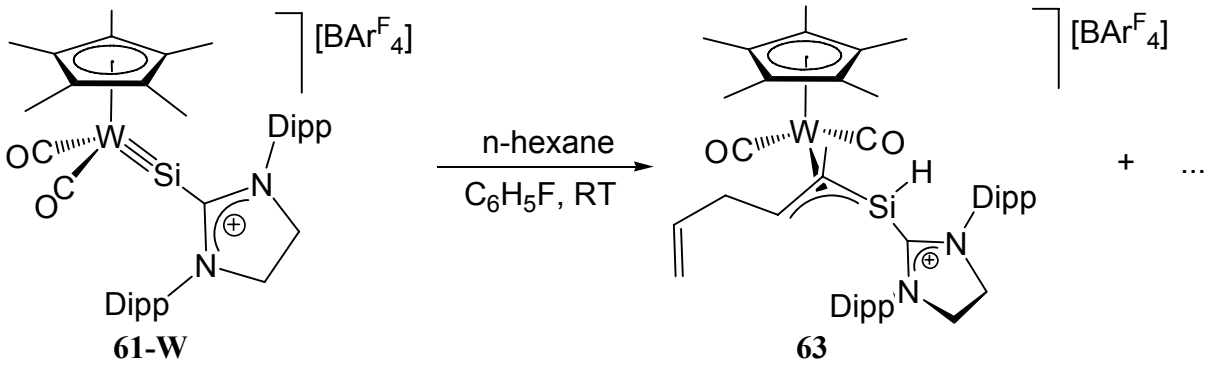

61-W **63**

Scheme 56: C-H activation of hexane by complex **62-W** at 25 °C (only one stereoisomer is depicted).

Because of the marginal yield of the complex **63** and the lack of information about the byproducts it is not clear how the reaction proceded. Further investigation of this interesting process is certainly necessary.[58]

The *cis*-dicarbonyl complex cation features a η^3-1-silaallyl ligand coordinated in *exo*-fashion (Figure 46**)**. Silaallyl complexes are rare. To the best of our knowledge only one η^3-1-silaallyl complex [Cp*(CO)$_2$W(η^3-Me$_2$SiCHCMe$_2$)] has been structurally characterized[178] and a few of related "hydrogen-bridged" complexes have been reported.[179] Complex **63** features short Si–C28 and C28–C29 bonds of 1.798(3) Å and 1.439(4) Å respectively, which lie in-between those of typical double and single bonds (Si=C 1.702–1.775 Å,[126] Si–C 1.91 Å, C=C 1.34 Å, C–C 1.50 Å[147]). The structural parameters of **63** compare well with those in [Cp*(CO)$_2$W(η^3-Me$_2$SiCHCMe$_2$)], namely with the Si–C$_\alpha$ and C$_\alpha$–C$_\beta$ bond lengths of 1.800(4) Å and 1.411(5) Å of the η^3-1-silaallyl moiety respectively. The W–C bond lengths (2.352(2) Å and 2.423(2) Å) can be compared with the mean W–C bond length in tungsten ethylene complexes of 2.30(9) Å.[59]

---

[58] The origin of the 1,4-hexadiene chain from the *n*-hexane needs to be confirmed.

[59] According to a CSD survey from 04.2012 of 164 structurally characterized compounds W(R$_2$C=CR$_2$), where R = H or C. The median *d*(W–C) = 2.285 Å, LQ = 2.197 Å, HQ = 2.431 Å.

The IR spectra corroborate the solid state structure. In fluorobenzene solution the cis-dicarbonyl complex exhibits two *ν*(CO) absorption bands of almost equal intensity at 1936 and 1838 cm^{-1} (1950, 1840 cm^{-1} in the solid state). The presence of the Si–H moiety is confirmed by a weak absorption band at 2147 cm^{-1}, which compares, for example, with that of similar compounds $(CO)_5W$–SiHI–Idipp[60] (2113 cm^{-1}, solid; Idipp – 1,3-bis(2,6-diisopropylphenyl)imidazol-2-ylidene) and $(CO)_5W$–SiH_2–Idipp (2107, 2086 cm^{-1}).[180]

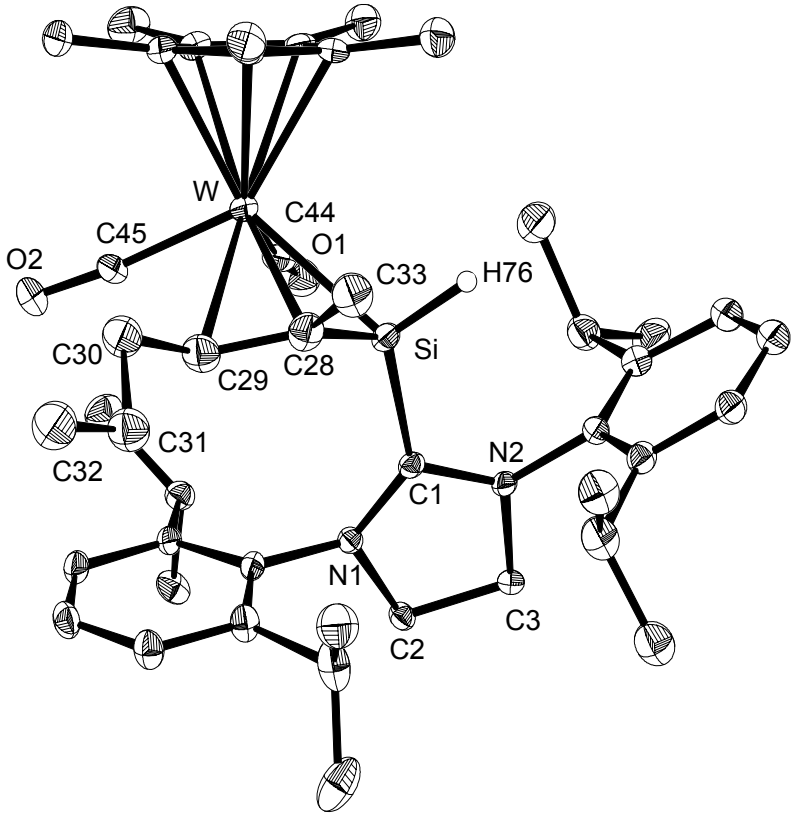

Figure 46: DIAMOND plot of the molecular structure of the complex cation in **63**. Thermal ellipsoids are set at 20% probability. Hydrogen atoms are omitted for clarity. Selected bond lengths [Å] and bond angles [°]: W–Si 2.5153(6), Si–C1 1.944(2), Si–H76 1.354(9), W–C28 2.352(2), W–C29 2.423(2), C33–C28 1.534(4), Si–C28 1.798(3), C28–C29 1.439(4), C29–C30 1.505(4), C30–C31 1.541(4), C31–C32 1.394(5); W-Si-C1 130.63(6), C1-Si-C28 123.8(1), Si-C28-C29 122.7(2), C28-C29-C30 128.9(3), C29-C30-C31 107.2(3), C30-C31-C32 112.2(3).

[60] Y. Lebedev, *unpublished results*, University of Bonn, **2012**.

2.3 Chemistry of the silylidyne complexes

The electron deficiency of the Si center in silylidyne complexes accounts for the major part of their reactivity. Here mostly the chemistry of the neutral complex [Cp(CO)$_2$Mo≡Si(C$_6$H$_3$-2,6-Trip$_2$)] (**60**) will be presented, but few reactions of the cationic silylidyne complexes [Cp(CO)$_2$M≡Si(ISdipp)][Al(OC(CF$_3$)$_3$)$_4$] (**61**, M = Cr, Mo) will also be discussed.

2.3.1 Addition of polar reagents

The silylidyne complex [Cp(CO)$_2$Mo≡Si(C$_6$H$_3$-2,6-Trip$_2$)] (**60**) reacts with compounds bearing polar X–H bonds. Water and ammonia add over the triple bond, leading to the unprecedented hydroxyl- and aminosilylidene complexes **64** and **66**. Addition of HCl affords the chlorosilylidene complex **67** (Scheme 57).

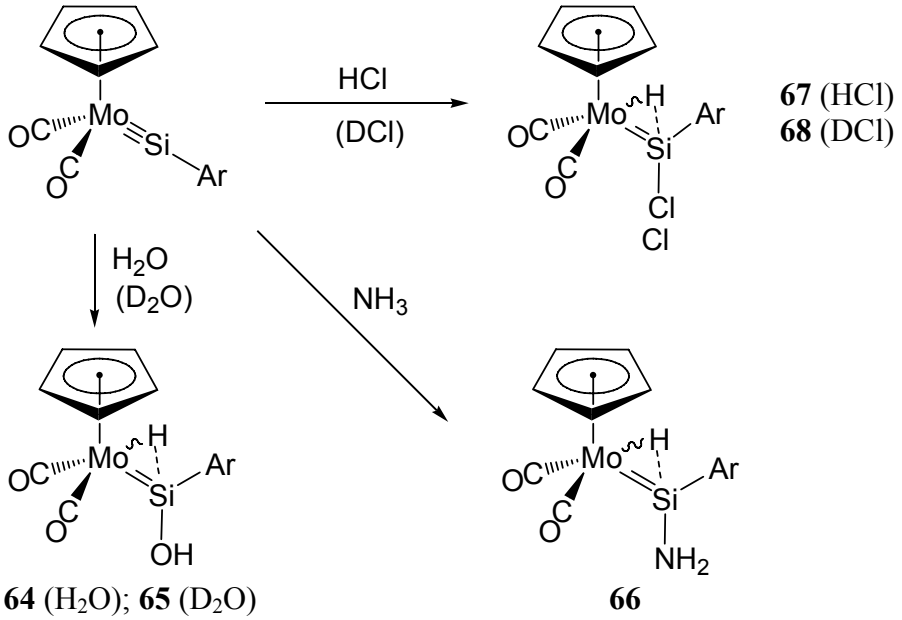

Scheme 57: Addition of HCl, DCl, H_2O, D_2O and NH_3 to the silylidyne complex [Cp(CO)$_2$Mo≡Si(C$_6$H$_3$-2,6-Trip$_2$)] (**60**).

Treatment of the complex [Cp(CO)$_2$Mo≡Si(C$_6$H$_3$-2,6-Trip$_2$)] (**60**) with a solution of H_2O in dioxane led to a rapid color change from red-brown to yellow at even –70 °C. The hydroxysilylidene complex **64** was isolated in 66% yield as a yellow air sensitive crystals, soluble in toluene and diethyl ether, sparingly soluble in hexane or pentane.

Complex **64** was characterized by NMR, IR spectroscopy and elemental analysis. The key features of the complex are: a) a low-field shifted signal in the ^{29}Si NMR spectrum at 213.4 ppm, which is comparable to that of [Cp(CO)$_2$Mo=Si(C$_6$H$_3$-2,6-Trip$_2$)(IMe$_4$)] (**42,**

201.8 ppm) and is characteristic for silylidene complexes; b) a high-field shifted resonance of the Mo-*H* functionality in the ^{1}H NMR spectrum at –10.26 with ^{1}J(Si,H) = 40.0 Hz, suggesting rather strong Si···H interaction;[177] c) a sharp resonance of the OH group in the ^{1}H NMR spectrum at 3.86 ppm.

The structure of the complex could not be solved by X-ray diffraction analysis. In analogy to the germanium analogue [Cp(CO)$_2$MoH=GeOH(C$_6$H$_3$-2,6-Trip$_2$)], a planar geometry of the Si center is expected, with the hydrogen atom in a bridging position over the Mo–Si double bond.[181]

In order to localize the absorption band of the moiety Mo–H···Si in the IR spectrum, the deuterated complex [Cp(CO)$_2$MoD=SiOD(C$_6$H$_3$-2,6-Trip$_2$)] was prepared (**65**) from [Cp(CO)$_2$Mo≡Si(C$_6$H$_3$-2,6-Trip$_2$)] (**60**) and D$_2$O. The ^{1}H NMR spectrum of **65** is very similar to that of **64**, except that the signals corresponding to the MoD and OD moieties are absent. ^{2}D NMR clearly shows two singlet resonances at –10.38 ppm (Mo–D) and 3.83 ppm (OD). We analyzed the IR spectra of **64** and **65** recorded in KBr matrix. The differences in spectra that are related to Mo–H (Mo–D) and OH (OD) vibrations can be conveniently seen after susbtraction of the spectrum of **65** from the spectrum of **64** (Figure 47).

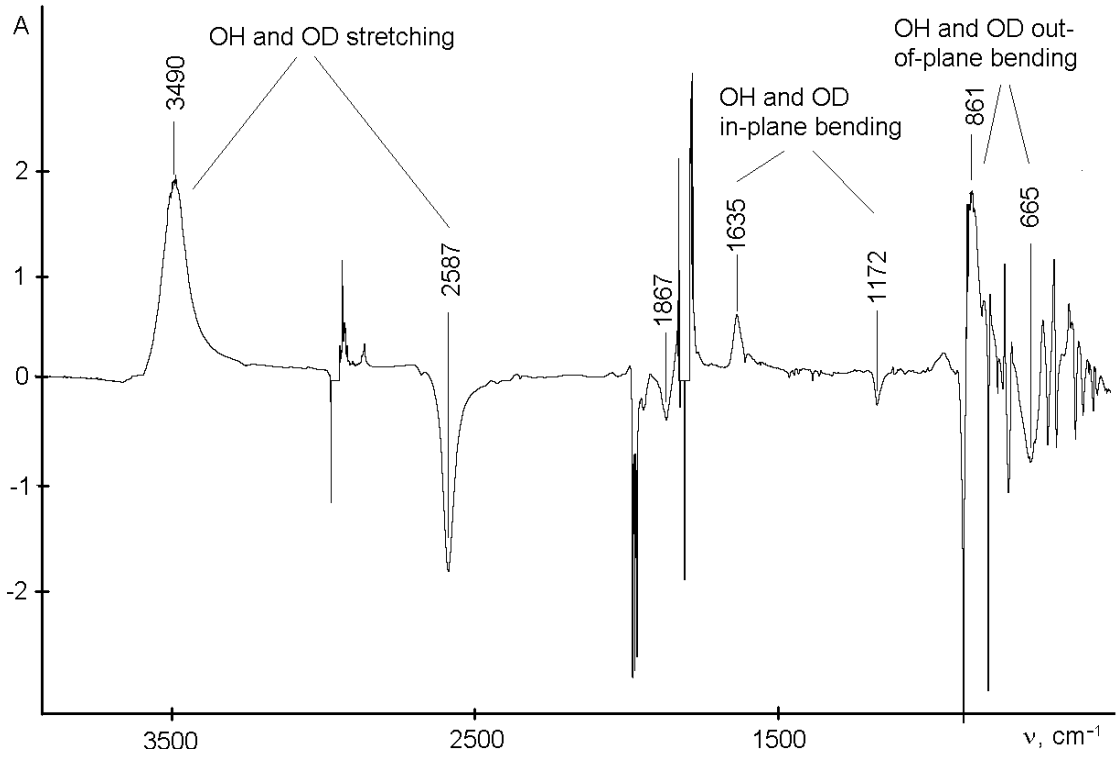

Figure 47: The result of subtraction of the IR spectrum of **65** from the IR spectrum of **64**; both spectra were recorded in KBr pellets.

The absorption bands in the IR spectra that correspond to OH and OD vibrations were assigned in accordance with the previously reported IR spectra of CH_3OH, CH_3OD, CD_3OH and CD_3OD (Table 7).[182] The negative absorption at 1867 cm^{-1} arises presumably from the small difference in the IR spectra of the compounds in the range of the very intense *ν*(CO) absorption bands of carbonyl groups and is not related to H/D vibrations.[61] Several peaks below 1000 cm^{-1} could not be unambiguously interpreted.

	″MoH=SiOH″ (**64**), cm^{-1}	″MoD=SiOD″ (), cm^{-1}	ν(**64**)/ν(**65**)	ν(CH_3OH)/ ν(CH_3OD)[62]
OH and OD stretching	3490	2587	1.349	1.343
OH and OD bending in-plane	1635	1172	1.395	1.507
OH and OD bending out-of-plane	861	665	1.295	1.379

Table 7: Assignment of OH and OD absorption bands in **64** and **65** and comparison to the pair CH_3OH/CH_3OD.

As one can see from the IR spectra, the expected Mo–H absorption band is missing. The free Mo–H vibration in [$CpMo(CO)_3H$] gives rise to an absorption at 1790 cm^{-1} in hexane, one could expect the corresponding Mo–D absorption at ca. 1300 cm^{-1}.[183] However, only the OD bending absorption was identified in the range of 1000–1700 cm^{-1}. The absence of the Mo–H and a Mo–D stretching vibrations in the expected ranges confirms the presence of a Si···H interaction in **64** (and Mo–D interaction in **65**) as suggested by the *J*(Si,H) coupling constant of 40.0 Hz.[63] The Si–H interaction is expected to decrease the intensity of the Mo–H (or Mo–D) absorption band and shift its position to lower frequency, where observation is hindered by other bands. The solution IR spectra of **64** in diethyl ether and toluene display two CO-absorption bands of almost equal intensities at 1845, 1872 and 1943, 1871 cm^{-1} respectively.

Treatment of the complex [$Cp(CO)_2Mo{\equiv}Si(C_6H_3$-2,6-$Trip_2)$] (**60**) with one equivalent of HCl in diethyl ether at –70 °C afforded selectively the chlorosilylidene complex **67** (Scheme 57). In contrast, addition of HCl to the carbyne complex [$Cp^*(CO)_2W{\equiv}CNEt_2$], affords the aminomethylene complex [$Cp^*(CO)_2W(Cl){=}CHNEt_2$].[184] The "reversed" regioselectivity of addition to the silylidyne complex reflects the higher electrophilicity of the silicon center in comparison to that of carbon in the alkylidyne complex [$Cp^*(CO)_2W{\equiv}CNEt_2$]. Complex **67** was isolated in nearly quantitative yield as a thermally labile orange solid that slowly turns to

[61] This conclusion is based on the fact, that there is no expected complementary absorption in the expected range of 2400–2600 cm^{-1} in the spectrum of H_2O-adduct **64**.

[62] For liquid films at ambient temperature.

[63] The *J*(Si,D) coupling constant was not observed, probably due to the low signal intensity.

brown at ambient temperature. Due to its extremely good solubility in hexane or pentane even at –60 °C single crystals of the compound suitable for X-ray diffraction analysis were not obtained.

The ^{1}H NMR spectrum of the complex displays a singlet resonance at −9.03 ppm corresponding to the Mo−*H* functionality with a *J*(Si,H) coupling constant of 27.9 Hz.[63] The ^{29}Si NMR spectrum displays a low-field shifted resonance at 236.8 ppm, which is characteristic for silylidene complexes. According to the ^{1}H NMR spectrum, a dynamic process occurs at ambient temperature in C_6D_6 solution of the complex. The IR spectrum of **67** in hexane displays four sharp CO-absorption bands at 1977, 1972, 1911 and 1890 cm^{-1}, at slightly higher wavenumbers than those observed for the H_2O- and NH_3-adducts. The IR and NMR spectra suggest the presence of two isomers that interconvert slowly on the NMR timescale (vide infra).

Complex [Cp(CO)$_2$MoD=SiCl(C$_6$H$_3$-2,6-Trip$_2$)] (**68**) was synthesized in an attempt to localize the Mo–H absorption in the IR spectra by comparison to **67**. A thorough analysis of the solid state IR spectra of **67** and **68** was hampered by the presence of decomposition products of the complexes. We were not able to localize any Mo–H and Mo–D absorption bands. We suppose that as the H(D) atom is localized in a bridging position between Si and Mo atoms in the solid state on the basis of *J*(Si,H) coupling constant and quantum chemical calsulations.

The geometry of the minimum structures of the model complex [Cp(CO)$_2$MoH=SiCl(C$_6$H$_3$-2,6-Mes$_2$)] (**67-model**) were calculated.[64] Two minimum structures were found corresponding to the cis- and trans-isomers. The cis-complex represents the global minimum and features a cis-orientation of the H atom and the silylidene ligand. The hydrogen atom occupies the bridging position between the Mo and Si centers (Figure 48). The trans-isomer features an isolated Mo–H functionality and is by 19 kJ·mol^{-1} less favourable than the cis-isomer. The transition between the isomers involves the "rotation" of the hydrogen atom around the Mo–Si bond to the position opposite to the Cp-ligand and subsequent migration of the hydrogen atom to the trans-position to the silylidene ligand. The transition state (Figure 48, in the center) corresponds to a saddle point on the potential energy surface and lies just 59 kJ·mol^{-1} above the global minimum structure. The potential energy surface of **67-model** was calculated as a function of the Mo–H and Si-H bond lengths (Figure 49). It is evident, that at ambient temperature (298 K) corresponding to an energy of roughly 75 kJ·mol^{-1}, the hydrogen atom moves around the complex, in agreement with the experimental results.

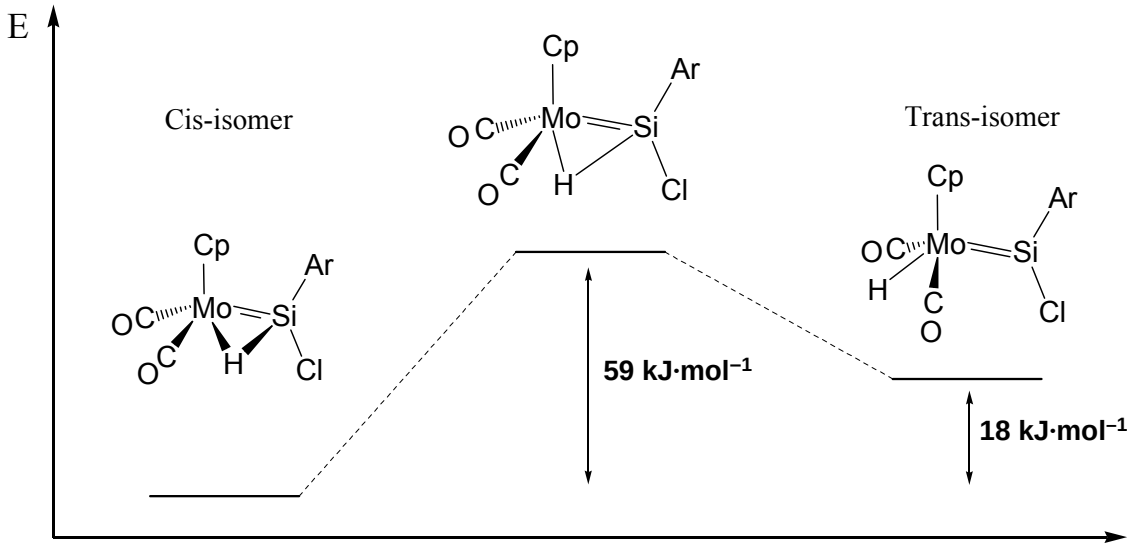

Figure 48: The equilibrium between the cis- and trans-isomers of complex **67-model** $[Cp(CO)_2MoH{=}SiCl(C_6H_3\text{-}2,6\text{-}Mes_2)]$ according to the DFT calculations.[64]

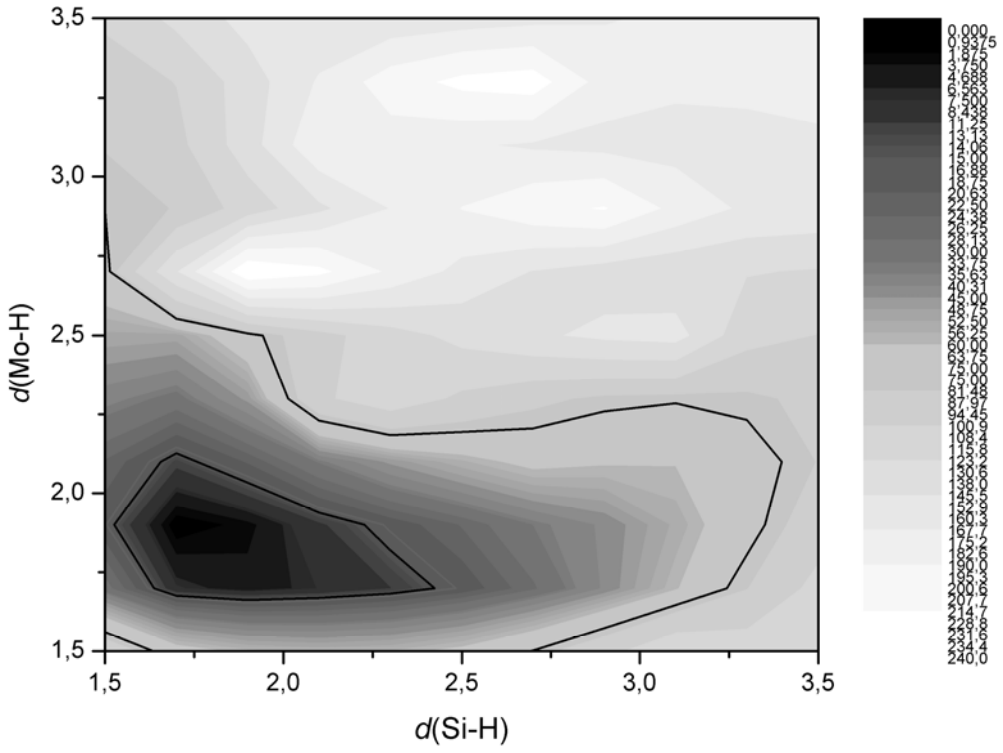

Figure 49: Potential energy of the complex **67-model** as a function of Mo–H and Si–H bond lengths according to DFT calculations. The encircled areas correspond to energies of 15 and 75 $kJ \cdot mol^{-1}$.[64]

The IR spectrum of cis- and trans-complexes **67-model** have been calculated. The Mo–H and Si–H stretching absorptions of the cis-complex are expected at 1514(w) and 803(vw) cm^{-1}, in

[64] The calculations were performed by Dr. G. Schnakenburg at the BP86/LANL2DZ level of theory, University of Bonn, **2011**.

the region where observation is hampered by other signals. The Mo–H stretching vibrations in the trans-complex are expected at 1854(m) and 1846(vw) cm^{-1}, where observation is disturbed by the very strong *ν*(CO) absorptions. The findings explain, why the Mo–H and Si–H absorptions were not observed in the IR spectrum. The results are also in agreement with the presence of the four (CO) absorption bands, observen in a hexane solution, which correspond to the cis- and trans-isomers of **67**.

Addition of ammonia to the silylidyne complex $[Cp(CO)_2Mo{\equiv}Si(C_6H_3\text{-}2,6\text{-}Trip_2)]$ (**60**) at −78 °C led to the formation of the unprecedented aminosilylidene complex $[Cp(CO)_2MoH{=}Si(NH_2)(C_6H_3\text{-}2,6\text{-}Trip_2)]$ (**66**) (Scheme 57). The complex was isolated as a yellow solid in 87% yield. The spectroscopic fetures of the complex are: a) a low-field shifted ^{29}Si NMR signal at 207.4 ppm; b) a high-field shifted ^{1}H NMR signal of the Mo–H functionality at –9.56 ppm with a *J*(Si,H) coupling constant of 29.5 Hz; c) a singlet NH_2 resonance at 2.96 ppm. The key spectroscopic features compare well with those of **64**. Interestingly, the germanium analogue $[Cp(CO)_2Mo{\equiv}Ge(C_6H_3\text{-}2,6\text{-}Trip_2)]$ does not react with ammonia to give an analogous product.[65]

The structure of the four-legged piano-stool complex **66** was determined by X-ray diffraction analysis (Figure 50). In the solid state, the carbonyl groups are located in *cis*-positions, the other "legs" are occupied by the aminosilylidene ligand and a bridging hydrogen atom. The position of the hydrogen atom was deduced from the difference in the Fourier synthesis map, and its position is supported by the small C42-Mo-Si angle of 77.41(5)° and the large C43-Mo-Si angle of 105.31(5)°. The angle between the *cis*-CO groups C42-Mo-C43 of 82.61(3)° is smaller than that in the starting material (**60**; 87.0(1)°) and compares well with that in complex **59** $[((C_6F_5)_3B\text{-}\eta^5\text{-}C_5H_4)Mo(H){=}Si(IMe_4)(C_6H_3\text{-}2,6\text{-}Trip_2)]$ (80.11(11)°). The Si–Mo bond length of 2.3796(5) Å is comparable with that in the complex $[Cp(CO)_2Mo{=}Si(C_6H_3\text{-}2,6\text{-}Trip_2)(IMe_4)]$ (**42**, 2.345(3) Å) and in complex **59** (2.3741(7) Å) but is shorter than those in the halosilylidene complexes **52-Mo** (2.284(1) Å) and **53-Mo** (2.2853(8) Å). The lengthening of the Mo–Si bond can be attributed to decreased Mo–Si d_π–p_π backbonding.

[65] K. W. Stumpf, *unpublished results*, university of Bonn, **2010**.

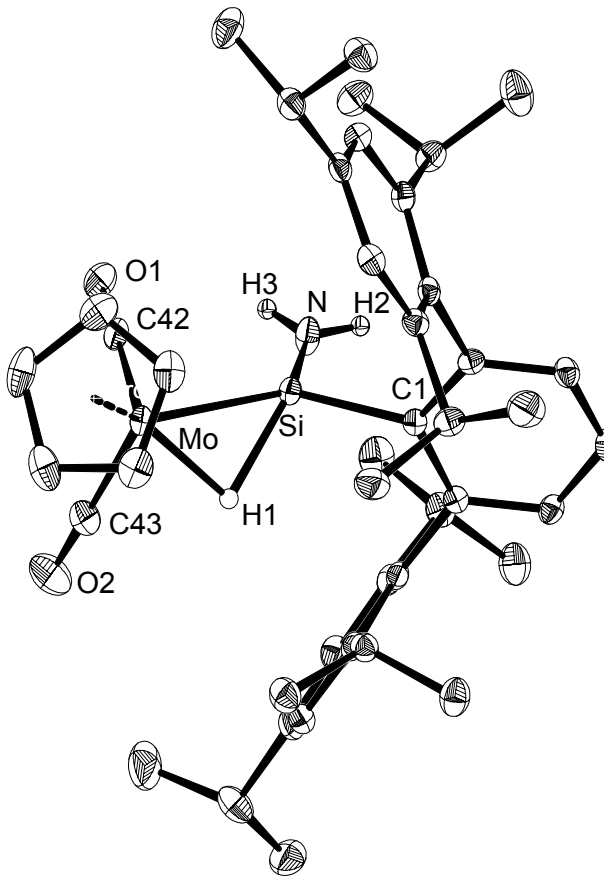

Figure 50: DIAMOND plot of the molecular structure of complex **66**. Thermal ellipsoids are set at 50% probability. Hydrogen atoms are omitted for clarity. Selected bond lengths [Å], bond angles and torsion angles [°]: Mo–Si 2.3796(5), Si-C1 1.907(2), N–Si 1.679(1), Mo–H1 1.75(2), Si–H1 1.77(2), Mo–C42 1.921(2), Mo–C43 1.979(2); C1-Si-Mo 139.31(4), C1-Si-N 97.52(7), N-Si-Mo 122.88(5), C42-Mo-C43 82.61(3), C42-Mo-Si 77.41(5), C43-Mo-Si 105.31(5), Si-Mo-H1 47.7(6), Si-N-H2 122.8(13), Si-N-H3 124.0(14); C1-Si-Mo-H1 56.9(9).

The Si center exhibits a planar geometry (without considering the hydrogen atom), as indicated by the sum of bond angles between the substituents of 359.7°. It was already observed earlier that Si···H interaction does not affect the planarity of the silylidene ligand in similar type of complexes.[87] The nitrogen atom was found to be planar, reflecting the conjugation of the lone pair with the electrophilic Si center. The Si–N bond length of 1.679(1) Å is shorter than that in the molybdenum NHSi complex [$Cp_2MoSi(NtBuCH)_2$] (1.748(5) Å)[157] and in the free silylene $Si(NtBuCH)_2$ (1.753(5) Å).[55] The Si–N bond length lies in-between the values observed for a Si–N double and single bonds (1.567(2) Å and 1.75(3) Å respectively),[66] also suggesting Si–N conjugation. However, the ^{1}H NMR spectrum

[66] According to a CSD surveys from 02.2012 on 9 structurally characterized componds featuring Si–N double bond (median *d*(Si–N) = 1.569 Å, LQ = 1.533 Å, HQ = 1.582 Å); and 1782 compounds of

at 298 K displays only a singlet resonance of the NH_2 group, indicating that the barrier of rotation about the Si–N bond is rather low.

In summary, the synthesis of the neutral silylidene complexes **64–68** demonstrate the synthetic potential of the silylidyne complex [$Cp(CO)_2Mo{\equiv}Si(C_6H_3$-2,6-$Trip_2)$] (**60**). The key properties of the complexes **64–68** are summarized in Table 8.

Complex	Color	Yield, %	IR, ν(CO), $cm^{-1,}$	^{29}Si NMR, ppm	d(Mo−Si), Å
[$Cp(CO)_2MoH{=}SiOH(C_6H_3$-2,6-$Trip_2)$] (**64**)	Yellow-brown	66	1954 (sh), 1943 (vs), 1871 (vs) (toluene)	213.4	n/a
[$Cp(CO)_2MoH{=}Si(NH_2)(C_6H_3$-2,6-$Trip_2)$] (**66**)	Yellow	87	1954 (s), 1945 (s), 1883 (s sh), 1875 (vs) (toluene)	207.4	2.3796(5)
[$Cp(CO)_2MoH{=}SiCl(C_6H_3$-2,6-$Trip_2)$] (**67**)	Orange-brown	Quantitative	1977 (vs), 1972 (vs), 1911 (s), 1890 (s) (hexane)	236.8	n/a
[$Cp(CO)_2Mo\{\eta^2$-$SiH(C_6H_3$-2,6-$Trip_2)$–PHMes$\}$] (**69**)	Yellow	85	1942 (vs), 1877 (vs) (hexane)	−47.2	2.511(2)

Table 8: Selected properties of the silylidene complexes **64–69**. n/a – not available.

Surprisingly, the reaction of [$Cp(CO)_2Mo{\equiv}Si(C_6H_3$-2,6-$Trip_2)$] (**60**) with mesityl phosphane led to a different type of product than in the previous cases (Scheme 57) and followed the same pathway as in the case of the carbyne complex [$Cp(CO)_2W{\equiv}C(p$-Tol)].[185]

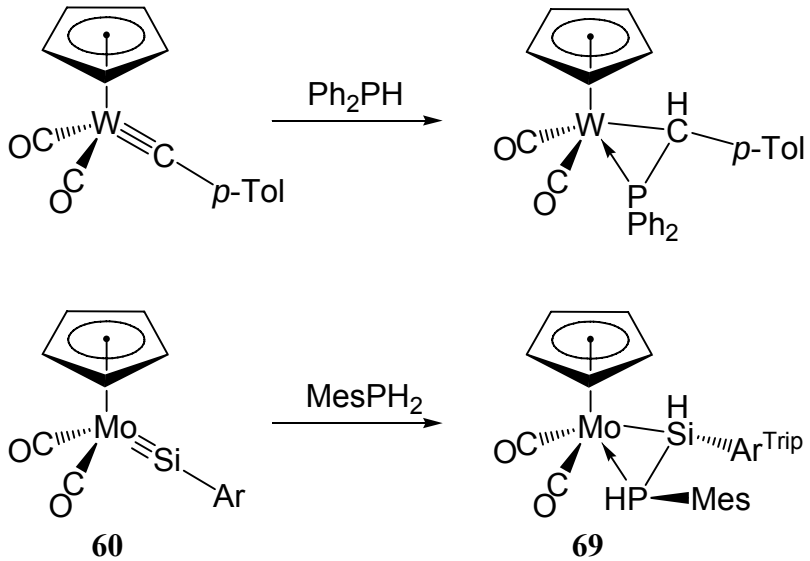

60 **69**

Scheme 58: Addition of Ph_2PH to a carbyne complex and addition of $MesPH_2$ to the silylidyne complex **60** (p-Tol = -C_6H_3-4-CH_3, Mes = -C_6H_2-2,4,6-Me_3).

the type $NM_3Si^{T4}–N^{T3}NM_2$ featuring Si–N single bonds (NM is any non metal substituent, median d(Si–N) = 1.745 Å, LQ = 1.708 Å, HQ = 1.783 Å).

The reaction with the silylidyne complex proceeded fast already at ambient temperature, whereas the reaction of $[Cp(CO)_2W{\equiv}C(p\text{-Tol})]$ with PPh_2H required refluxing in toluene (Scheme 58). The four-legged yellow piano-stool complex **69** was isolated as a bright yellow microcrystalline solid in 85% yield and was fully characterized. The structure of **69** was determined by X-ray diffraction analysis (Figure 51).

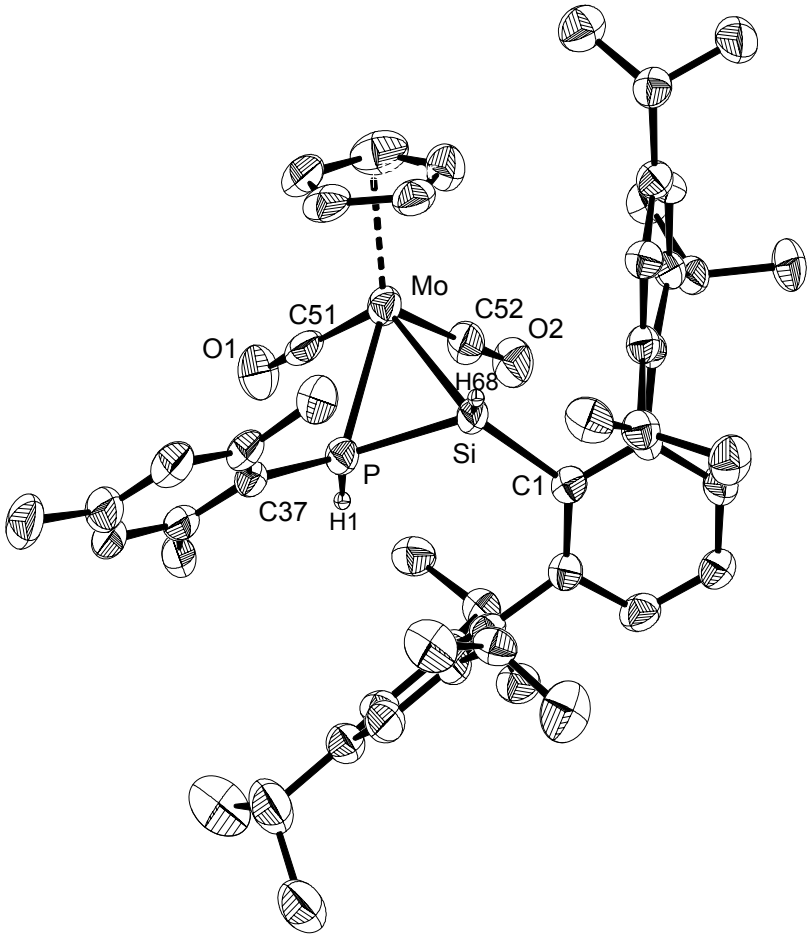

Figure 51: DIAMOND plot of the molecular structure of **69**. Thermal ellipsoids are set at 50% probability. Hydrogen atoms are omitted for clarity. Selected bond lengths [Å], bond angles and torsion angles [°]: Mo–Si 2.511(2), Mo–P 2.482(2), Si–P 2.207(3), Si–H68 1.24(6), P–H1 1.00, C1–Si 1.930(7), C37–P 1.822(7), C51-1.961(9), C52–P 1.960(8); P-Mo-Si 52.47(6), Mo-Si-P 63.09(7), Si-P-Mo 64.44(7), C51-Mo-C52 82.3(3), C1-Si-Mo 129.8(2); C1-Si-P-C37 121.9(4).

The Mo–Si distance of 2.511(2) Å clearly indicates the presence of a single bond. The bond length is comparable with that in the complex $[Cp^*(CO)_2Mo(PMe_3){-}SiCH_3(OH)_2]_2$

(2.571(1) Å)[186] and the mean value of Mo–Si single bond lengths of 2.55(5) Å.[67] The Mo–P bond length of 2.482(2) Å compares well with that in the complex [Cp*(CO)$_2$Mo(PMe$_3$)–SiCH$_3$(OH)$_2$]$_2$ (2.433(1) Å) and the mean Mo–P single bond lengths of phosphane complexes (2.50(6) Å).[68] The Si–P distance of 2.207(3) is close to the value, calculated for a single Si–P bond on the basis of the single-bond covalent radii of Si and P (2.27 Å).[147]

Further information about the complex was provided by the NMR and IR spectroscopy. The chirality of the complex renders the C^2/C^6 and C^3/C^5 positions of the Trip substituent non-equivalent, giving rise to three septets and six doublets corresponding to three not equivalent isopropyl groups in the ^{1}H NMR spectrum. The rotation of the -C$_6$H$_3$-2,6-Trip substituent about the Si–C bond is slightly hindered as evidenced by the broadened doublets of the methyl groups of the C^{2,6} bonded isopropyl substituents. The Si–*H* resonance is observed as doublet of doublets at 4.85 ppm with Si satellites (^2J(P,H) = 20.7 Hz, ^4J(H,H) = 2.3 Hz, ^1J(Si,H) = 230 Hz). The ^{29}Si{^{1}H} NMR spectrum displays a doublet resonance at −47.2 ppm (^2J(P,Si) = 97.6 Hz) in the range expected for silyl complexes.[169] The IR spectrum of the *cis*-dicarbonyl complex shows two CO-absorption bands of equal intensities at 1942 and 1877 cm^{-1} (in hexane) close to the bands of the complex [Cp(CO)$_2$W{η^2-CH(*p*-Tol)PPh$_2$}] (1930, 1845 cm^{-1} in CH$_2$Cl$_2$).[185]

2.3.2 Addition of nucleophiles

The electrophilic character of the Si atom in the silylidyne complexes is best demonstrated by the reactions with nucleophiles. The complex [Cp(CO)$_2$Mo≡Si(C$_6$H$_3$-2,6-Trip$_2$)] (**60**) reacts smoothly with various nucleophiles leading to unprecedented anionic silylidene complexes (Scheme 59).

Treatment of **60** with (NMe$_4$)Cl in 1,2-dimethoxyethane afforded selectively the chlorosilylidene complex **70-Cl**, which was isolated as a bright orange solid in 72% yield. Reaction of **60** with (NEt$_4$)N$_3$ afforded the orange thermolabile azidosilylidene complex **71-**

---

[67] According to a CSD survey from 11.2011 of 37 structurally characterized molybdenum silyl complexes (Mo–^{T4}SiX$_3$, where X = any non-metal) leading to a median value *d*(Mo–Si) = 2.549 Å, LQ = 2.487 Å, HQ = 2.629 Å.

[68] According to a CSD survey from 11.2011 of 2026 structurally characterized phosphane complexes of molybdenum (Mo–^{T4}PX$_3$, where X = any non-metal) leading to a median value *d*(Mo–P) = 2.507 Å, LQ = 2.424 Å, HQ = 2.579 Å.

N₃ in nearly quantitative yield. Similarly, addition of methyllithium to the silylidyne complex led to formation of the methylsilylidene complex **72-CH₃** which was isolated as a yellow thermolabile diethyl ether solvate in 76% yield. The azidosilylidene complexes are unprecedented up to date, and chlorosilylidene complexes are very rare.[87, 92, 154]

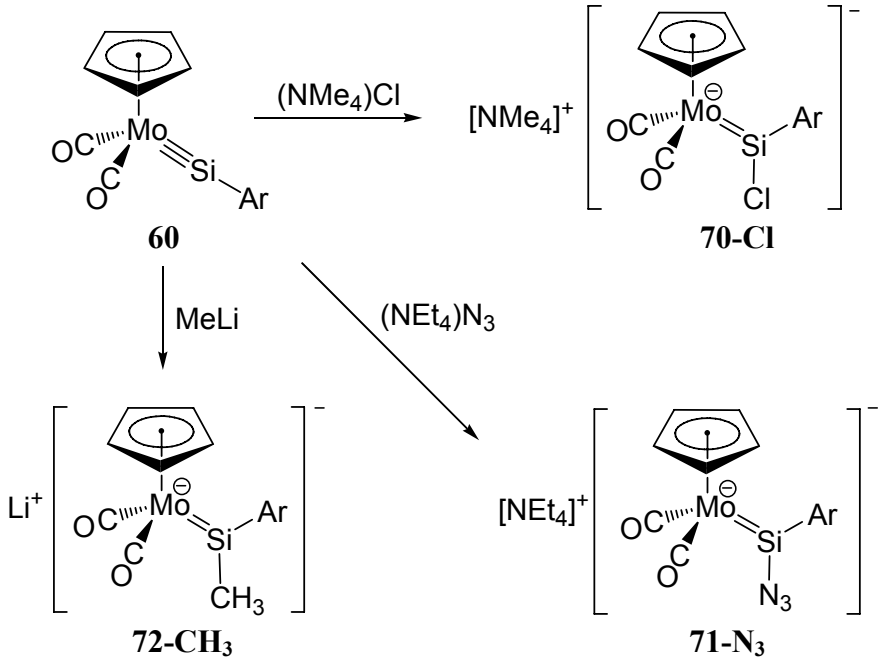

Scheme 59: Addition of nucleophiles to the complex [Cp(CO)₂Mo≡SiAr] (**60**) (Ar = -C₆H₃-2,6-Trip₂).

The structures of the complexes were determined by X-ray diffraction analyses (Figures 52, 53 and 55). The structures of the complexes are similar to those of the NHC-stabilized silylidene complexes **42**–**44** (Table 3), and halosilylidene complexes **49, 52, 53** (Table 5). The key structural features are:

- The short Mo–Si distances of 2.300(1) Å (**70-Cl**), 2.287(1) Å (**71-N₃**), 2.3403(6) Å (**72-CH₃**) indicating the presence of Mo=Si double bonds;
- The trigonal planar coordination of the Si center, as indicated by the sum of angles of 359.4° (**70-Cl**), 359.6° (**71-N₃**), 359.9° (**72-CH₃**), characteristic for base-free silylidene complexes;
- The upright conformation of the silylidene ligands, as indicated by the torsion angles C_g-Mo-Si-C_{Ar} of 28.9° (**70-Cl**), 23.0° (**71-N₃**), 4.6 (**72-CH₃**), where C_g is the center of gravity of the Cp-ring.
- The obtuse Mo-Si-C_{Ar} angles of 145.0(1)° (**70-Cl**), 142.2(1)° (**71-N₃**), 139.12(6)° (**72-CH₃**) reflecting the steric demand of the -C₆H₃-2,6-Trip₂ group.

- The smaller C_{Ar}-Si-X angles of 93.58(10)° (X = Cl, **70-Cl**), 91.1(2)° (X = N, **71-N_3**), 98.48(10)° (X = CH_3, **72-CH_3**) reflecting the low tendency of multiply-bonded Si atoms for hybridization.

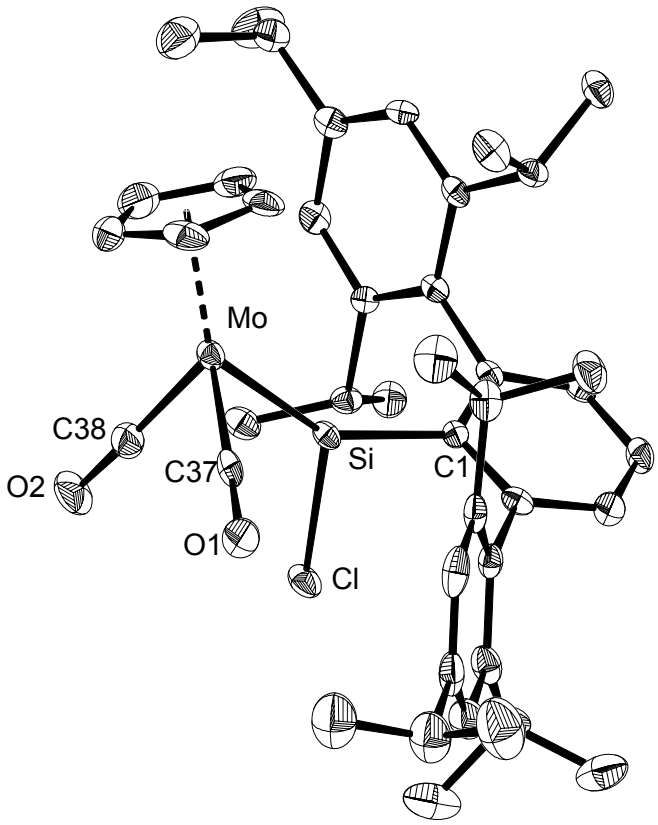

Figure 52: DIAMOND plot of the molecular structure of the complex anion in **70-Cl**. Thermal ellipsoids are set at 50% probability. Hydrogen atoms and complex cation are omitted for clarity. Selected bond lengths [Å] and bond angles [°]: Mo–Si 2.300(1), Cl–Si 2.145(1), C1–Si 1.909(4), C37–Mo 1.930(4), C38–Mo 1.900(4); C1-Si-Mo 145.0(1), C1-Si-Cl 93.6(1), Cl-Si-Mo 120.81(5), C37-Si-Mo 79.5(1), C38-Si-Mo 85.8(1), C37-Mo-C38 83.8(2).

The Si–Cl bond length in **70-Cl** of 2.145(1) Å is slightly shorter than that in SiCl(C_6H_3-2,6-$Trip_2$)(IMe_4) (**29**, (2.1836(8) Å) which can be attributed to the rehybridization of the Si atom, with a higher s-character of the orbital involved in bonding to Cl in **70-Cl** and/or decreased steric repulsion of the silicon-bonded substituents in comparison to **29**. The bond length compares well with that in [Cp*(dmpe)MoH=SiCl(Mes)] of 2.162 Å.[87] However, the Si–Cl bond length is considerably longer than those of Si(IV) compounds $SiH_2Cl(C_6H_3$-2,6-$Trip_2)$ (2.032(8) Å)[134] and in $SiCl_3(C_6H_3$-2,6-$Trip_2)$ (2.091(3) Å, see also p. 47).[133]

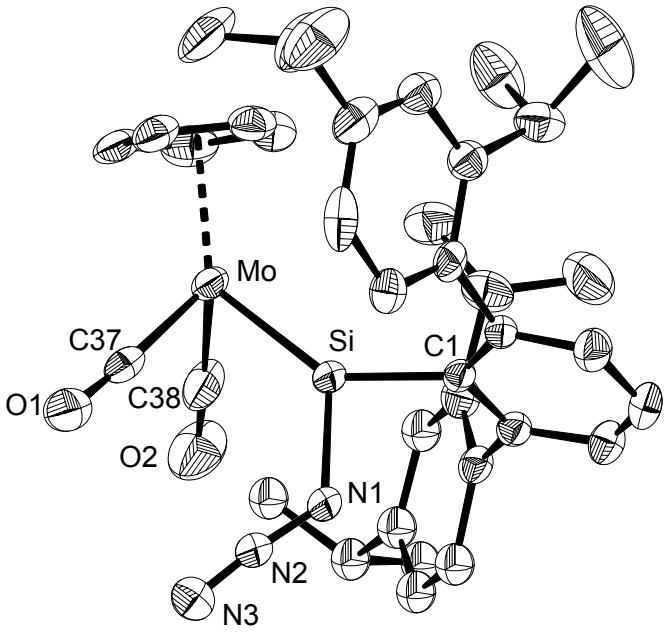

Figure 53: DIAMOND plot of the molecular structure of the complex anion in **71-N_3**. Thermal ellipsoids are set at 50% probability. Hydrogen atoms and the complex cation are omitted for clarity. Selected bond lengths [Å] and bond angles [°]: Mo–Si 2.287(1), C37–Mo 1.922(5), Mo–C38 1.929(5), Si–N1 1.801(4), Si–C1 1.919(4), N1–N2 1.217(5), N2–N3 1.124(6); Mo-Si-C1 142.2(1), Mo-Si-N1 126.3(1), N1-Si-C1 91.1(2), Si-Mo-C37 90.9(1), Si-Mo-C38 81.4(1), C37-Mo-C38 83.3(2).

The strong polarization of the Si–Cl bond is demonstrated by the reversible dissociation of the chlorosilylidene complex **70-Cl**, verified by IR and NMR spectroscopy. Thus, solutions of **70-Cl** in toluene or C_6D_6 display among the signals of **70-Cl** also the signals of the silylidyne complex **60**. In polar solvents like DME or THF the equilibrium is fully shifted to the anionic complex:

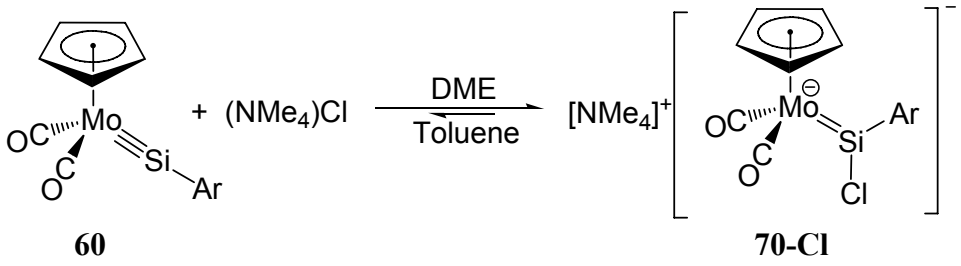

60 **70-Cl**

Scheme 60: The equilibrium between **60** and **70-Cl**.

In contrast, the Si–N1 bond length in **71-N_3** of 1.801(4) Å compares with those found in azidosilanes 1.760(3)–1.814(2) Å[187] or the mean Si–N bond length (1.73(4) Å)[69] found in

[69] According to a CSD survey from 11.2011 of 315 structurally characterized amino(phenyl)silanes ($Ph^{T4}SiX_2$–N where X = any non-metal) with a median *d*(Si–N) = 1.725Å, LQ = 1.683 Å, HQ = 1.769 Å.

amino(phenyl)silanes. The IR and NMR spectra of solutions of **71-N_3** display no signs of dissociation of the compound to the silylidyne complex **60** and $(NEt_4)N_3$.

The methylsilylidene complex **72-CH_3** has a dimeric structure in the solid state, in which two complex anions are complexed to the lithium cations via the carbonyl groups to form a 12-membered ring, Figure 54.

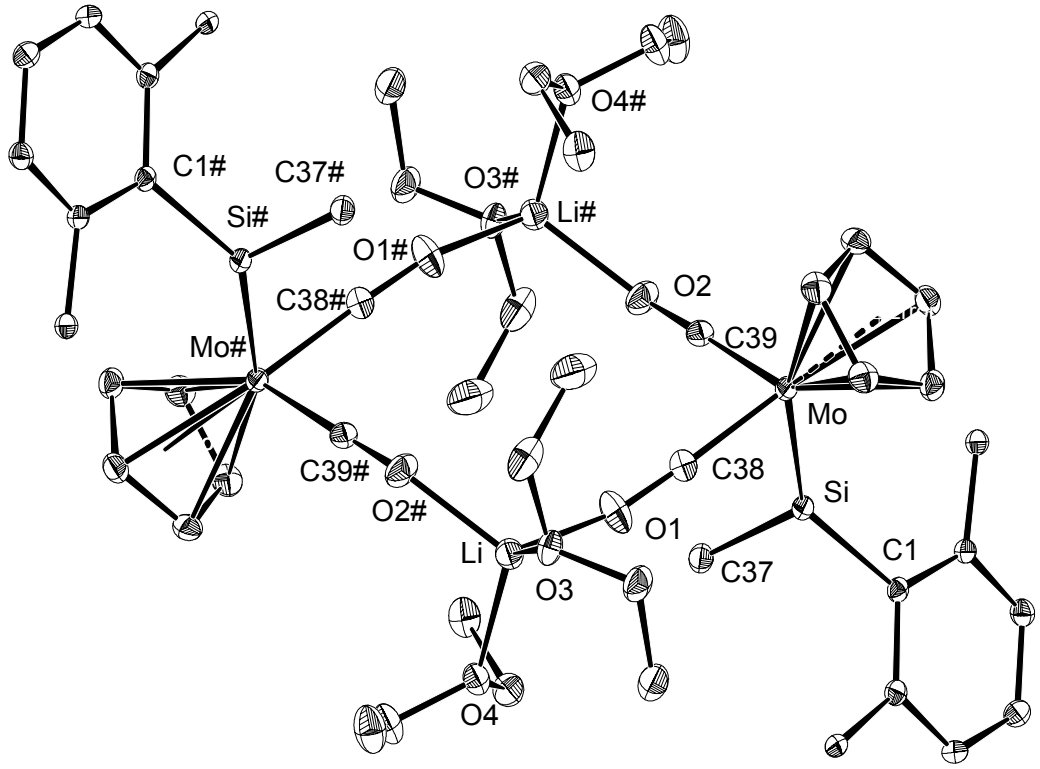

Figure 54: DIAMOND plot of the dimer of complex **72**. Thermal ellipsoids are set at 30% probability. Hydrogen atoms and the Trip groups are omitted for clarity. Selected bond lengths [Å] and angles [°]: Mo–Si 2.3403(6), C1–Si 1.933(2), C37–Si 1.891(2), C38–Mo 1.886(2), C39–Mo 1.898(2); C1-Si-Mo 139.12(6), C37-Si-Mo 122.25(7), C1-Si-C37 98.5(1), C38-Mo-Si 81.88(7), C39-Mo-Si 84.05(7), C38-Mo-C39 81.34(9).

In the centrosymmetric dimer each of the Li cation is bonded to two carbonyl groups of the two complex anions and two molecules of diethyl ether. The structure of the complex anion is depicted in Figure 55. In solution the complex dissociates, as indicated by NMR spectroscopy. The ^{1}H NMR spectrum of **72-CH_3** in THF-d_8 displays a signal set of resonances corresponding to *m*-terphenyl substituent, consistent with a C_s symmetric structure and fast rotation of the *m*-terphenyl substituent about the Si–C_{Ar} bond. In addition, the signals of diethyl ether (from the solvate) appear at almost the same positions as in the spectrum of pure Et_2O recorded in THF-d_8, indicating that Li^+ ions are solvated by THF molecules.[188] The ^{13}C NMR spectra of the complex displays a singlet resonance signal of the carbonyl

group at 243.2 ppm at a position, close to that of **71-N_3** (240.2 ppm) and **70-Cl** (240.6 ppm), suggesting that the CO-groups are not coordinated to the Li^+ ions.

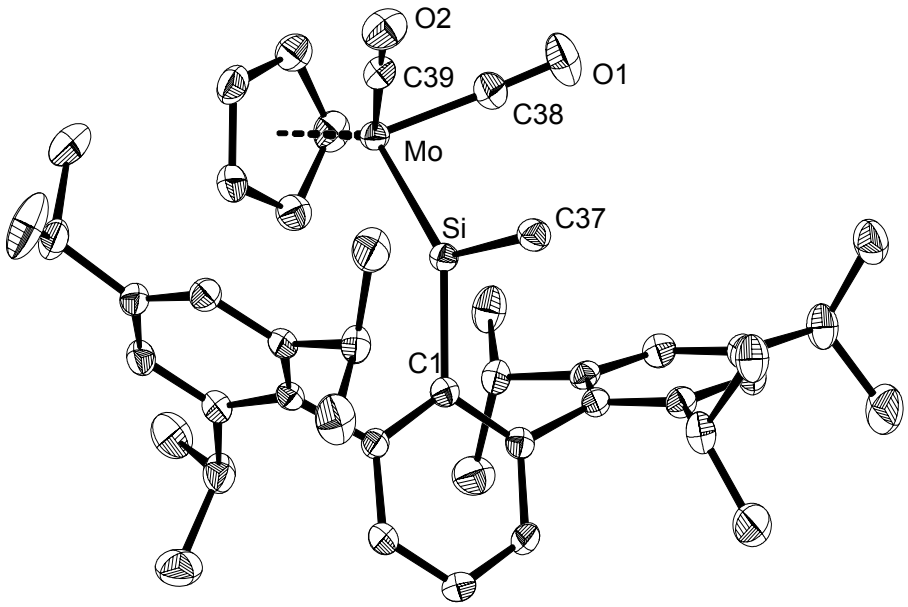

Figure 55: DIAMOND plot of a fragment of the molecular structure **72**. Thermal ellipsoids are set at 50% probability. Hydrogen atoms, lithium atoms and coordinated solvents are omitted for clarity. Selected bond lengths [Å] and angles [°]: Mo–Si 2.3403(6), C1–Si 1.933(2), C37–Si 1.891(2), C38–Mo 1.886(2), C39–Mo 1.898(2); C1-Si-Mo 139.12(6), C37-Si-Mo 122.25(7), C1-Si-C37 98.48(10), C38-Mo-Si 81.88(7), C39-Mo-Si 84.05(7), C38-Mo-C39 81.34(9).

Complexes **70–72** display low-field shifted signals in the ^{29}Si NMR spectra, which are characteristic for silylidene complexes (*vide supra*). The IR spectra of the complexes display two CO-absorption bands at rather low wavenumbers, reflecting the strong M–CO backbonding in these compounds (Table 9). Complex **71-N_3** features also a broad absorption of the azido group at 2109 cm^{-1} in DME. According to the positions of the ν(CO) absorption bands, the σ-donor/π-acceptor ratio of the following ligands increases in the series (Ar = -C_6H_3-2,6-$Trip_2$):

$$Si(ISdipp)^{2+} < SiAr^+ < SiAr(IMe_4)^+ < SiClAr < Si(N_3)Ar < Si(CH_3)Ar$$

	Color	Yield, %	IR, ν(CO), DME, $cm^{-1,}$	^{29}Si NMR, ppm	d(Mo−Si), Å
$[NMe_4][Cp(CO)_2Mo{=}SiCl(C_6H_3\text{-}2,6\text{-}Trip_2)]$ (**70**)	Orange	72	1840 (vs), 1762 (vs)	228.2	2.300(1)
$[NEt_4][Cp(CO)_2Mo{=}Si(N_3)(C_6H_3\text{-}2,6\text{-}Trip_2)]$ (**71**)	Orange	Quantitative	1826 (vs), 1756 (vs)	228.5	2.287(1)
$Li[Cp(CO)_2Mo{=}Si(CH_3)(C_6H_3\text{-}2,6\text{-}Trip_2)]$ (**72**)	Orange-yellow	76	1824 (vs), 1695 (vs)	138.0	2.3403(6)
$Li_2[Cp(CO)_2Mo{-}Si(CH_3)_2(C_6H_3\text{-}2,6\text{-}Trip_2)]$ (**73**)	Yellow	88	1677 (vs), 1589 (vs)	27.4	2.5153(7)
$K_2[Cp(CO)_2Mo{-}Si(i\text{Pr})(C_{33}H_{39})]$ (**74**)	Orange	90	1685 (vs), 1593 (vs)	50.8	2.486(6)[a]

Table 9: Selected properties of complexes **70**−**74**. [a] Mean value.

It is well established, that the silicon center in silylidene complexes is electrophilic.[83, 100, 189] Thus, the silylidene complex **72**-CH_3 reacts with a second equivalent of MeLi, leading to the dianionic silyl complex **73**, whereas complexes **70-Cl** and **71-N_3** do not react with an excess of $(NMe_4)Cl$ and $(NEt_4)N_3$ respectively (Scheme 61).

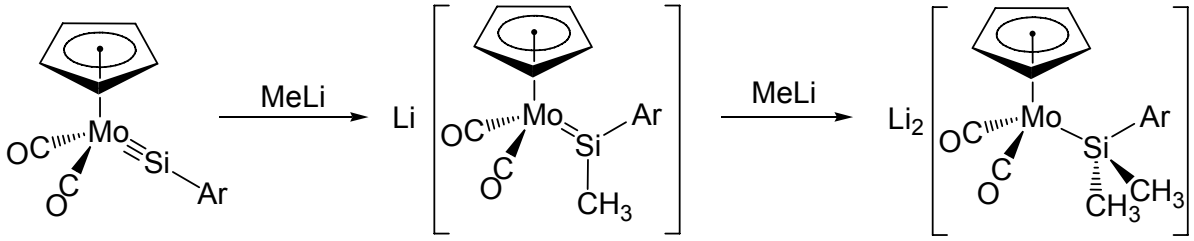

Scheme 61: Addition of methyllithium to $[Cp(CO)_2Mo{\equiv}Si(C_6H_3\text{-}2,6\text{-}Trip_2)]$.

The structure of **73** was determined by X-ray diffraction analysis, the complex has a dimeric structure with bridging lithium cations, coordinated to solvent molecules (DME) and carbonyl groups, Figure 56. The structure of the complex anion is depicted in Figure 57. The silicon center is tetrahedral, and the Mo–Si bond length of 2.5153(7) Å lies within the range observed for other molybdenum silyl complexes (2.474–2.669 Å)[169] and compares well with the mean value of Mo–Si single bond lengths of 2.55(3) Å.[67] The Si–Mo bond length is ca. 0.2 Å longer than in the silylidene complexes **70**–**72**.

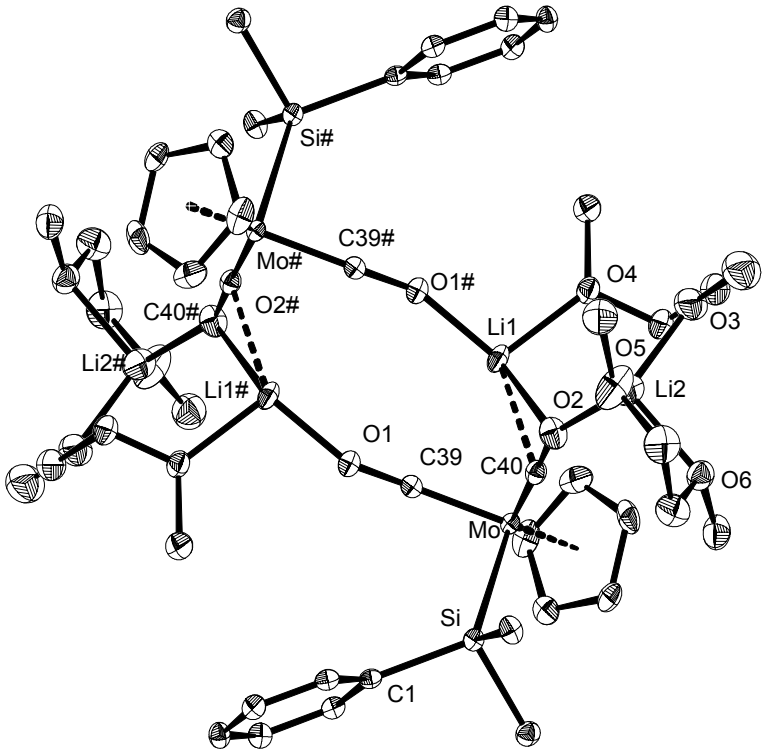

Figure 56: DIAMOND plot of a fragment of the dimer of **73**. Thermal ellipsoids are set at 50% probability. Hydrogen atoms and -C_6H_2-2,4,6-*i*Pr_3 groups are omitted for clarity. Selected bond lengths [Å] and angles [°]: Mo–Si 2.5153(7), Mo–C39 1.902(2), Mo–C40 1.868(2), C39–O1 1.208(3), C40–O2 1.231(2), C39–Li1 2.713(5), C40–Li 2.223(5), O1–Li1# 1.856(5), O2–Li2 1.832(5), O2–Li1 2.452(5), O3–Li2 1.965(6), O4–Li1 1.994(5), O5–Li2 1.969(6), O6–Li2 1.996(5), Li1–O1# 1.856(5); C39-Mo-C40 87.7(1), Mo-C40-O2 174.9(2), Mo-C39-O1 178.8(2).

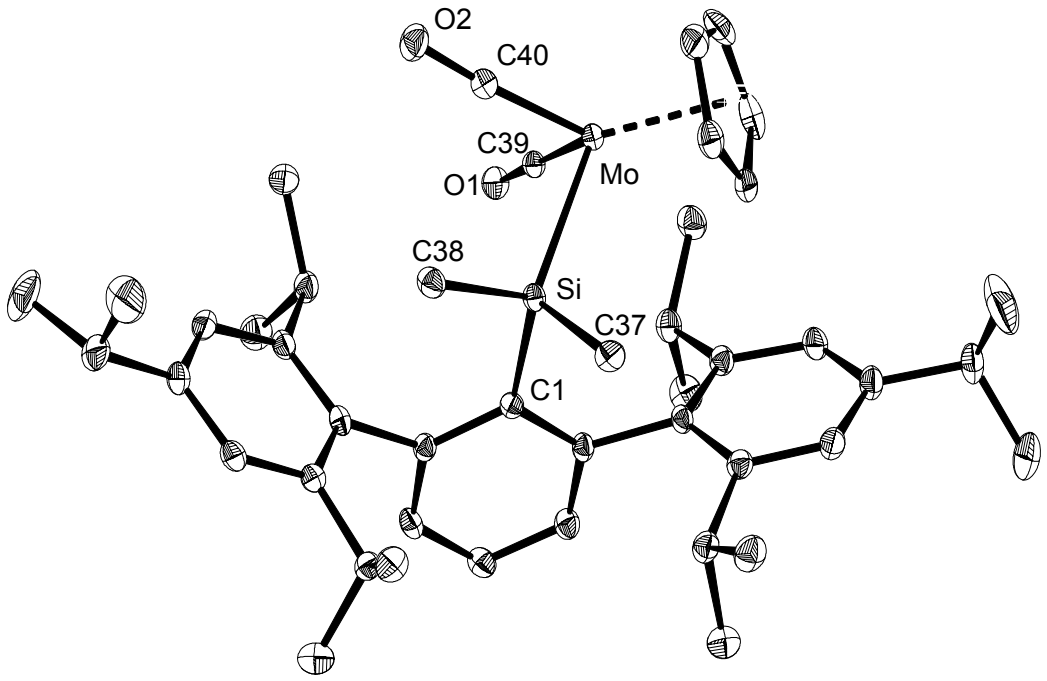

Figure 57: DIAMOND plot of a fragment of the molecular structure of **73**. Thermal ellipsoids are set at 50% probability. Hydrogen atoms, lithium atoms and coordinated solvents are omitted for clarity. Selected bond lengths [Å] and angles [°]: Mo–Si 2.5153(7), C1–Si 1.979(2), C37–Si 1.917(3), C38–Si 1.911(2), C39–Mo 1.902(2), C40–Mo 1.868(2); C1-Si-Mo 121.98(7), C37-Si-Mo 112.94(8), C38-Si-Mo 111.53(8), C37-Si-C1 102.3(1), C38-Si-C1 108.9(1), C38-Si-C37 95.8(1), C39-Mo-C40 87.7(1).

Reduction of $[Cp(CO)_2Mo{\equiv}Si(C_6H_3\text{-}2,6\text{-}Trip_2)]$ with KC_8.

A complex similar to **73** was obtained upon reduction of the silylidyne complex **60** with 2.2 equivalents of potassium graphite in dimethoxyethane (DME) at ambient temperature (Scheme 62). The complex was isolated after crystallization as an orange DME-Et_2O solvate in 90% yield. The reduction was accompanied by insertion of the silicon center into the C–*i*Pr bond of the -C_6H_2-2,4,6-*i*Pr_3 (Trip) substituent, leading to a silafluorenyl complex. According to cyclic voltammetry, the first irreversible one-electron transfer to silylidyne complex occurs at a potential of –2060 mV, leading probably to a silafluorenyl radical anion. The radical anion is further reduced at –2270 mV to give the final dianionic silafluorenyl complex **74**.[70, 154]

[70] The redox potential is given vs. the redox couple $[Fe(C_5Me_5)_2]/[Fe(C_5Me_5)_2]^+$; electrolyte 0.1M $(NBu_4)PF_6$ in THF; scan rate = 100 mVs^{-1}.

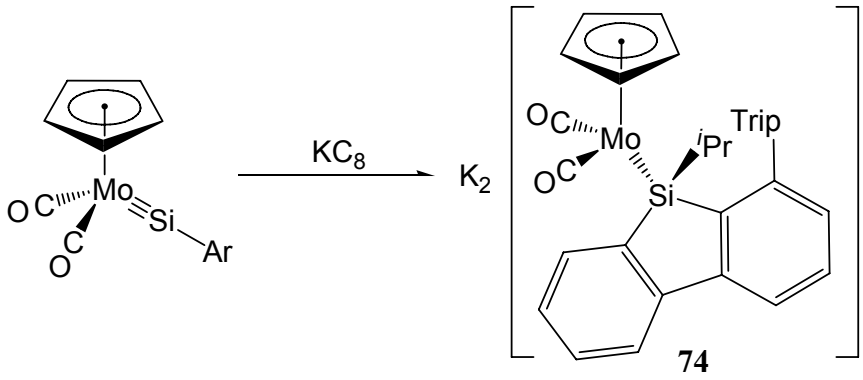

Scheme 62: Reduction of complex $[Cp(CO)_2Mo{\equiv}Si(C_6H_3\text{-}2,6\text{-}Trip_2)]$ with KC_8.

Complexes **73** and **74** have similar spectroscopic features. The CO-absorption bands appear at very low wavenumbers (in DME): 1677 and 1589 cm^{-1} (**73**); 1685 and 1593 cm^{-1} (**74**) as the result of the strong Mo–CO backbonding from a very electron rich metal center. The position of the absorption bands compares with those of highly reduced carbonyl metallates, e.g. $[Mn(CO)_4]^{3-}$ ($[Re(CO)_4]^{3-}$) at 1805, 1670 cm^{-1}, (1825, 1690 cm^{-1}) and $[M(CO)_3]^{3-}$ (M = Rh, Ir) at 1664, 1666 cm^{-1}.[190]

The ^{29}Si NMR spectrum of **74** in THF-d_8 displays signals at 27.4 ppm (**73**) and 50.8 ppm (**74**) in the range expected for silyl complexes.[169] The $^{13}C\{^1H\}$ NMR signals of the carbonyl groups appear at 248.8 ppm (**73**) and 245.7, 248.3 ppm (**74**) in lower field than that in the silylidene complexes **70–72** (240.6, 240.4 and 243.2 ppm) and in **60** (231.1 ppm). The trend was already earlier observed for a series of carbonyl complexes, in which the increase in electron density on a metal center (evaluated by ν(CO) absorptions) correlates with the increase of the $^{13}C\{^1H\}$ NMR shift of the carbonyl carbon atom.[191]

The structure of complex **74** was determined by X-ray crystallography. The complex has a dimeric structure, in which two molecules of the complex anions are held together by the potassium anions, coordinated to carbonyl groups and solvent molecules, Figure 58. Two independent centrosymmetric dimers were found in the asymmetric unit, the molecular structure of one complex anion is depicted in Figure 59.

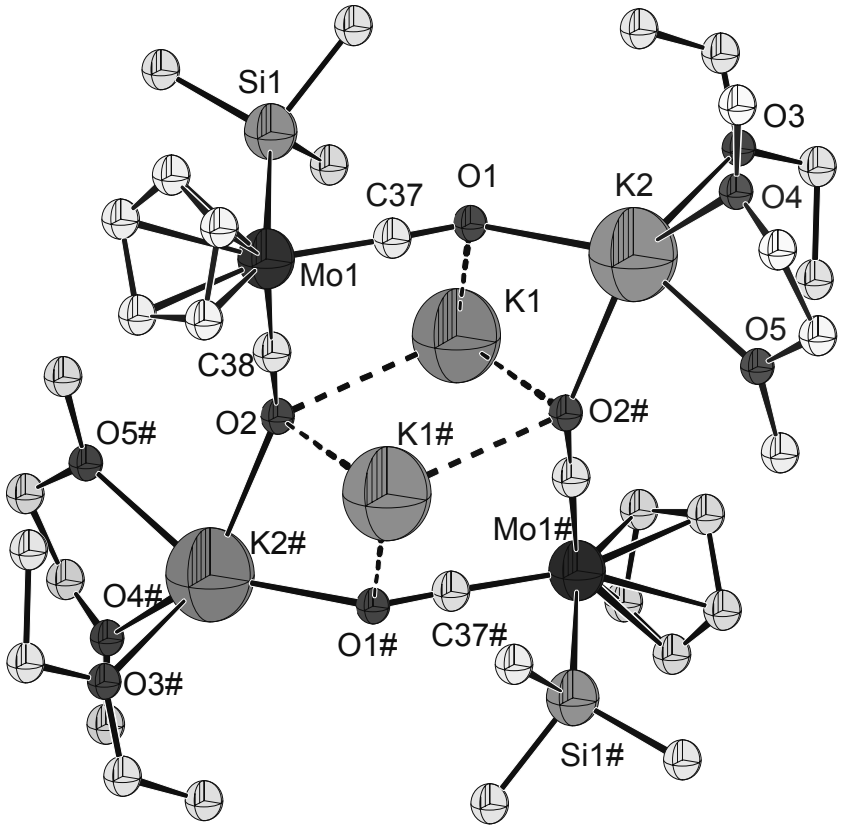

Figure 58: DIAMOND plot of a fragment of the molecular structure of the dimer of **74**.[71] Hydrogen atoms and substituents at the silicon atoms are omitted for clarity. Two independent dimer molecules are found in the asymmetric unit. Selected bond lengths [Å] and angles [°]: Mo1–Si1 2.480(2), C37–Mo1 1.910(9), C38-Mo1 1.89(1), O1–K2 2.627(6), O1–K1 2.806(7), O2–K2# 2.652(7), O2–K1# 2.913(6), O2–K1 2.950(7), O3–K2 2.72(1), O4–K2 2.827(9), O5–K2 2.639(9); C37-Mo1-C38 90.9(4), Mo1-C37-O1 174.9(8), Mo1-C38-=2 175.4(7), C37-O1-K2 146.0(4), C38-O2-K2# 149.2(6), O1-K2-O2# 69.8(2).

The three legged piano-stool complex features a chiral silafluorenyl substituent, the Mo–Si single bond length is 2.486 Å.[72] The bond length compares well with that in complex **73** (2.5153(7) Å) and other silyl complexes of molybdenum.[73] The silicon center has a distorted

[71] The dimer, presented on the Figure 58 has one Et_2O and one DME molecules, coordinated to the potassium atom K2. The second independent dimer features two DME molecules, coordinated to the potassium atom, however the other structural parameters are very similar.

[72] Two independent molecules were found in the asymmetric unit. The mean value of the parameter is given.

[73] According to a CSD survey from 11.2011 of 37 structurally characterized complexes of the type Mo–$^{T4}Si(NM)_3$, where NM = any nonmetal. Median *d*(Mo–Si) = 2.549 Å, LQ = 2.487 Å, HQ = 2.629 Å, range 2.474–2.669 Å.

tetrahedral environment. The two phenyl rings composing the silafluorenyl group are twisted in relation to each other, as indicated by the torsion angle C1-C2-C7-C8 of 15.3°.[72]

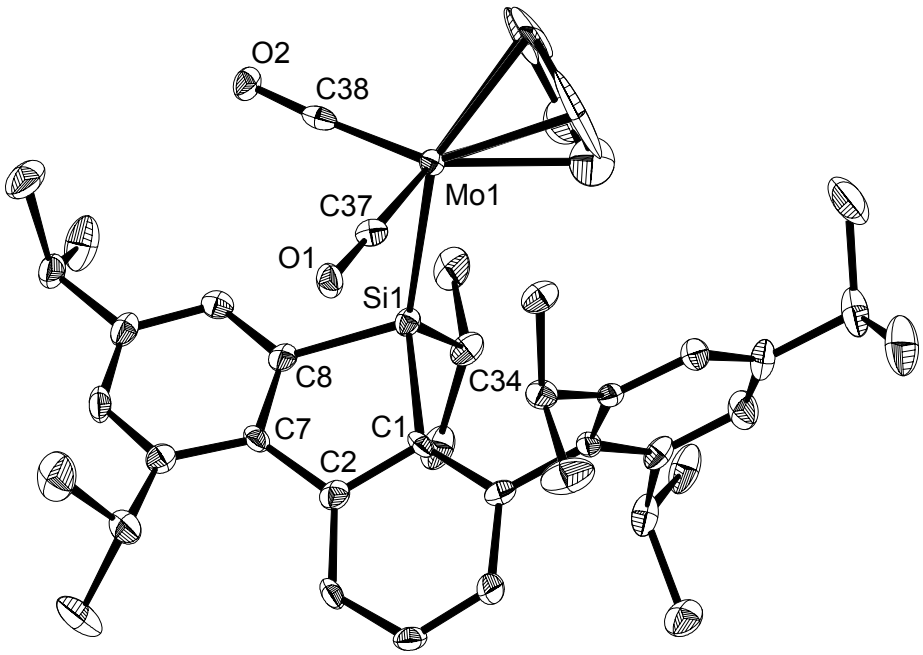

Figure 59: DIAMOND plot of a fragment of the molecular structure of **74**. Thermal ellipsoids are set at 30% probability. Hydrogen atoms, potassium atoms and coordinated solvent molecules are omitted for clarity. Two independent molecules are found in the asymmetric unit. Selected bond lengths [Å] bond angles and torsion angles[°] (values in brackets correspond to the second independent molecule): Mo1–Si1 2.480(2) [2.491(2)], Si1–C1 1.934(9) [1.915(8)], Si1–C8 1.920(9) [1.915(9)], Si1–C34 1.944(9) [1.939(9)], C37–Mo1 1.910(9) [1.91(1)], C38-Mo 1.89(1) [1.89(1)], C37–O1 1.20(1) [1.19(1)], C38–O2 1.22(1) [1.21(1)]; Mo1-Si1-C1 121.8(3) [121.8(3)], Mo1-Si1-C8 115.6(3) [115.8(3)], Mo1-Si1-C34 119.9(3) [119.0(3)], C1-Si1-C8 87.2(4) [86.4(4)], C1-Si1-C34 102.4(4) [104.8(4)], C8-Si1-C34 104.3(4) [103.2(4)]; C1-C2-C7-C8 14 (1) [17(1)].

The presence of the electron rich metal center is reflected also in the Mo–CO bond lengths. Thus, the mean Mo–C bond lengths in **74 (**1.901(5) Å)[74] are shorter than those in the silylidyne complex **60** (1.971(3) Å) as a result of the stronger Mo–CO backbonding (*vide supra*). In contrast, the C–O bond lengths in **74** (1.208(6) Å) are longer than those in **60** (1.157(3) Å) due to the same reason.[74]

As have been shown on several examples, addition of nucleophiles to the silylidyne complex **60** leads to the formation of silylidene complexes in high yields. We assume, that the cationic silylidyne complexes $[Cp^*(CO)_2M{\equiv}Si(ISdipp)][Al(OC(CF_3)_3)_4]$ **(61-M)** will also

[74] The unweighted mean value x_u of the Mo–C bond lengths and are given, the standard deviation σ of x_u was calculated using the equation $\sigma^2 = \Sigma(x_i - x_u)^2/(n^2 - n)$, where x_i is the individual value and n – number of elements.

react with nucleophiles, leading to silylidene complexes of the general formula [Cp*(CO)$_2$M=Si(Nu)(ISdipp)] (Nu = nucleophile, M = Cr, Mo, W). These reactions provide access to a variety of new compounds, thus rendering the silylidyne complexes as valuable starting materials in the coordination chemistry of silicon.

2.3.3 Reactivity towards acetylenes

Metathesis of alkenes and alkynes is now a well established and important reaction in organic synthesis. The importance of the reaction was acknowledged by awarding the Nobel Prize in Chemistry to Yves Chauvin, Robert H. Grubbs and Richard R. Schrock in 2005.[72] Metathesis of alkynes by metal alkylidyne complexes was investigated; the reaction involves formation of metallacyclobutadiene intermediates according to the mechanism proposed by T. Katz (Scheme 63, on the top).[192] Metallacyclobutadiene complexes of tungsten were isolated in several cases upon addition of alkynes to alkylidyne complexes, and some of them were shown to catalyze the alkyne metathesis.[193, 194]

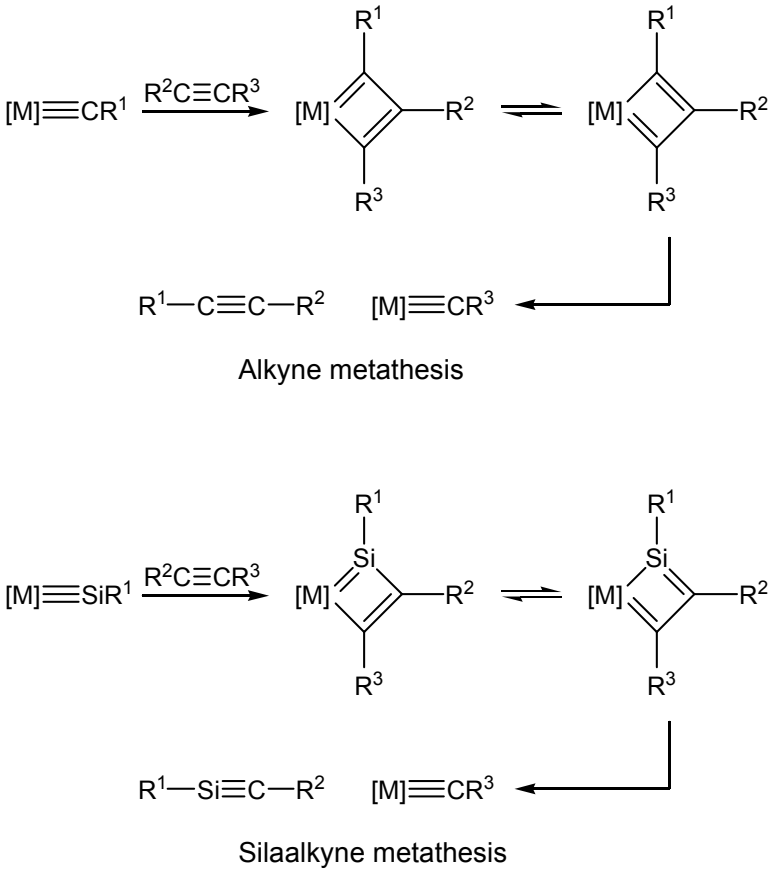

Scheme 63: Alkyne metathesis on alkylidyne complexes. Prospective mechanism for silyne metathesis.

Since silylidyne complexes were previously unknown, no studies were undertaken to investigate the possibility of "silyne metathesis". The prospective reaction mechanism can include formation of a metallasilacyclobutadiene intermediate followed by rearrangement and ring opening which would lead to a silyne and an alkylidyne complex, as depicted in Scheme 63 on the bottom. It was interesting to investigate if such a transformation was possible.

The silylidyne complex $[Cp(CO)_2Mo{\equiv}Si(C_6H_3\text{-}2,6\text{-}Trip_2)]$ reacts smoothly with various alkynes (Scheme 64). The reactivity of an alkyne is roughly proportional to its electron richness and steric accessibility. The reaction rates increase in the row:[75]

$$EtC{\equiv}CEt < MeC{\equiv}CMe \approx HC{\equiv}CH < Et_2NC{\equiv}CNEt_2 < Me_2NC{\equiv}CNMe_2 \approx PhC{\equiv}CNMe_2$$

Thus, the reaction with 3-hexyne required heating at 50 °C for 30 min, whereas reaction with bis(dimethylamino)acetylene or phenyl(dimethylamino)acetylene is fast already at ambient temperature.

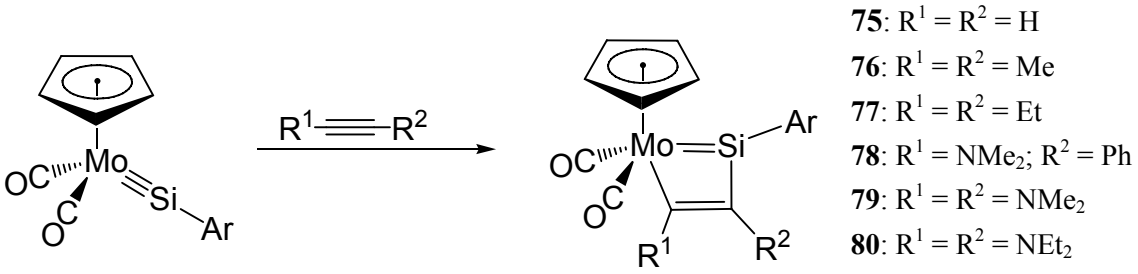

75: $R^1 = R^2 = H$
76: $R^1 = R^2 = Me$
77: $R^1 = R^2 = Et$
78: $R^1 = NMe_2$; $R^2 = Ph$
79: $R^1 = R^2 = NMe_2$
80: $R^1 = R^2 = NEt_2$

Scheme 64: Addition of acetylenes to the silylidyne complex $[Cp(CO)_2Mo{\equiv}Si(C_6H_3\text{-}2,6\text{-}Trip_2)]$.

Complexes **75–77** were isolated upon crystallization from hexane as orange crystalline solids. The reaction with C_2H_2 is not very selective, due to a combination of two factors: a) complex **75** reacts further with acetylene and b) is thermally unstable. Formation of a black insoluble solid with metallic glitter was observed even when the starting material was still present in the solution. Complex **75** was isolated as an orange solid after crystallization from hexane in 20% yield. Addition of 2-butyne proceeded selectively according to IR spectroscopy, however upon crystallization a small amount of colorless crystals of a byproduct were observed among the orange crystals of complex **76**. The orange crystals were separated manually on the basis of color. Addition of 3-hexyne and $PhC{\equiv}CNMe_2$ to the silylidyne complex in hexane resulted in the clean formation of complexes **77** and **78**, which were isolated as orange and red solids in nearly quantitative yields, respectively. Complexes **79** and **80** were isolated as brown solids upon crystallization from hexane in 65% yields.

[75] As suggested by reaction conditions and rate of colour change.

The solid-state structures of **75**–**78** were determined by X-ray diffraction analysis. The structural features of the complexes are similar, thus only two examples will be discussed here. The structure of the complex **76** is depicted in Figure 60:

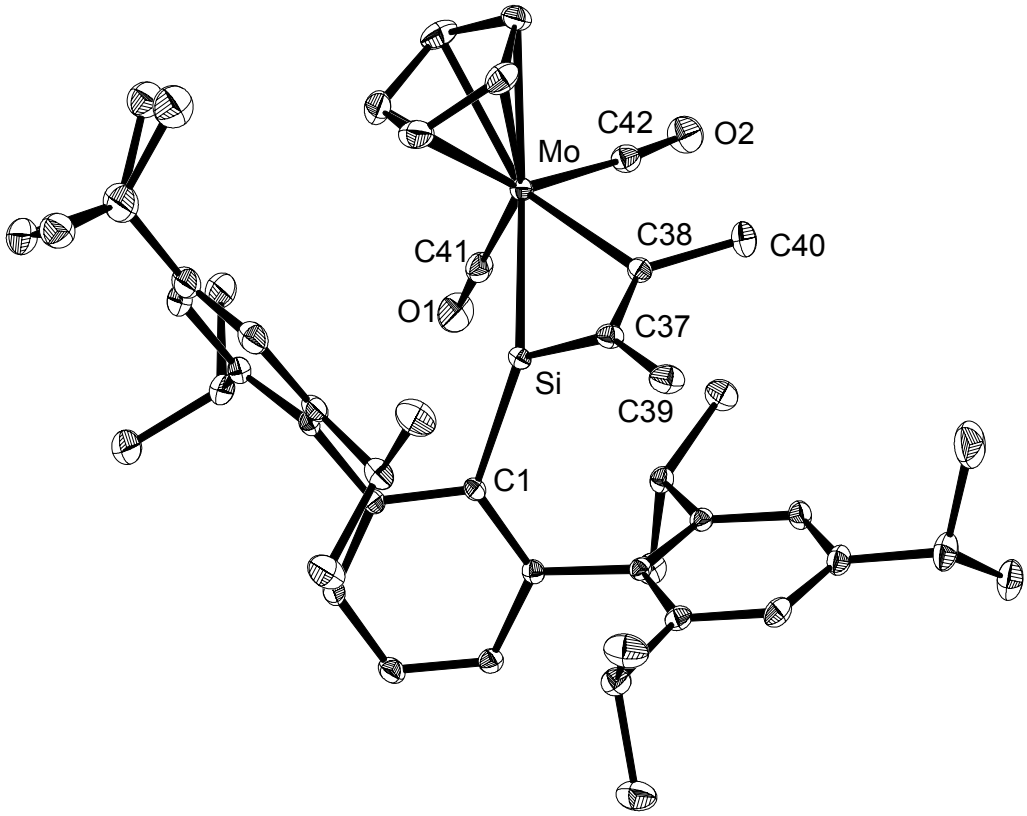

Figure 60: DIAMOND plot of the molecular structure of **76**. Thermal ellipsoids are set at 50% probability. Hydrogen atoms are omitted for clarity. Selected bond lengths [Å] and bond angles [°]: Mo–Si 2.3907(6), C1–Si 1.889(2), C38–Si 2.039(2), C37–Si 1.783(2), C38–Mo 2.290(2), C41–Mo 1.954(2), C42–Mo 1.961(2), C37–C38 1.368(3); C1-Si-Mo 137.21(6), C1-Si-C37 123.9(1), C38-C37-Si 79.4(1), C37-Si-Mo 96.96(7), C38-Mo-Si 51.58(6), C37-C38-Mo 116.7(2), C41-Mo-C42 79.4(1).

The four-legged piano stool complex **76** features a puckered four-membered metallasilacyclobutadiene ring as indicated by the dihedral angle of 34.6° between the planes defined by the atoms (Si, Mo, C38) and (Si, C38, C37).[76] The Mo–Si bond length of 2.3907(6) Å is significantly longer in comparison to that of the starting material (2.2241(7) Å) and compares with those of the silylidene complexes Li[$Cp(CO)_2Mo{=}Si(CH_3)(C_6H_3$-2,6-$Trip_2)$] (**72**, 2.3403(6) Å) and [$Cp(CO)_2Mo{=}Si(C_6H_3$-2,6-$Trip_2)(IMe_4)$] (**42**, 2.345 Å).

[76] Different types of metallacyclobutadienes were reported in the literature. The puckered, localized type of structure was observed among planar and tetrahedrane-like systems. See for an example M. R. Churchill, J. W. Ziller, L. McCullough, S. F. Pedersen, R. R. Schrock, *Organometallics* **1983**, *2*, 1046.

However, the bond is about 10 pm longer than those in halosilylidene complexes, e.g. in [Cp*(CO)$_2$Mo=SiI(IDipp)] (**53-Mo**, 2.2853(8) Å, Table 5) and [NMe$_4$]$^+$-[Cp(CO)$_2$Mo=SiCl(C$_6$H$_3$-2,6-Trip$_2$)]$^-$ (**70**, 2.300(1) Å, Table 9), suggesting a weaker Mo–Si backbonding (*vide supra*). The silicon center is essentially planar as indicated by the sum of bond angles between the substituents of 358.0°. The Mo–C38 bond length of 2.290(2) Å is in the range observed for alkyl complexes of molybdenum.[77] The C37–C38 double bond length (1.368(3) Å) is just slightly longer than the normal value of 1.34 Å and compares well to that of the tungstacyclobutadiene [CpW(C(Ph)C(^{t}Bu)C(Ph))Cl$_2$] (1.372(8) Å).[194]. The structure reveals several peculiarities, e.g. the Si–C38 bond length of 1.776(3) Å is about 10 pm shorter than the Si–C(sp^2) mean bond length found in silacyclobutenes (1.87(2) Å).[78] Surprisingly, the Si···C37 separation of 2.005(3) Å is very small, even compares well with a silicon-carbon single bond length calculated on the basis of the single-bond covalent radii (1.91 Å).[147] This and the acute C38-C37-Si angle of 79.4(1)° suggest that bonding interaction may be present.

Further information about complex **76** was provided by IR and NMR spectroscopy. According to the ^{1}H NMR spectrum in C$_6$D$_6$ at ambient temperature the complex displays fluxional behavior. Notably, the resonances of the methyl groups of the metallosilacyclobutadiene C(Me$_A$)=C(Me$_B$) appear as a broadened singlet at 1.85 ppm, indicating that a dynamic process equilibrating the substituents occurs in the four-membered ring.[79] Further information was provided by variable temperature NMR studies, Figure 61. In the NMR spectra, the dynamic process equilibrating the Me$_A$ and Me$_B$ groups is evident above –40 °C. However the complex remains chiral, as is suggested by the spectrum at 0 °C, where six broadened septets are still observed for the *i*Pr groups of the *m*-terphenyl substituent, whereas C-*Me$_A$* and C-*Me$_B$* are already collapsed. At higher temperatures (60 °C) the rotation of the *m*-terphenyl substituent about the Si–C$_{Ar}$ bond occurs, as indicated by the

[77] According to a CSD survey from 11.2011 of 323 structurally characterized compounds of the type L$_n$Mo–CX$_3$, where X = any non-metal. Mean *d*(Mo–C) = 2.2(1) Å, median *d*(Mo–C) = 2.203 Å, LQ = 2.111 Å, HQ = 2.339 Å.

[78] According to a CSD survey from 11.2011 of 48 structurally characterized compounds. Median *d*(Si–C(sp^2) = 1.858 Å, LQ = 1.845 Å, HQ =1.897 Å.

[79] A similar process accurs also in complex **75**, featuring two broad resonances of C*H*=C*H* moiety. Fluxional behaviour of the WC$_3$ ring, equilibrating C$_\alpha$ and C$_\beta$ atoms was also observed in metallacyclobutadiene complexes CpW(C(R)C(CMe$_3$)C(R))Cl$_2$, see M. R. Churchill, J. W. Ziller, L. McCullough, S. F. Pedersen, R. R. Schrock, *Organometallics* **1983**, *2*, 1046.

presence of six signals of the methyl groups of the *i*Pr groups of the *m*-terphenyl substituent in the ^{13}C NMR spectrum.[80]

The IR spectrum of **76** in hexane features two absorption bands at 1936 (vs) and 1856 (s) cm^{-1}, a shoulder is present at ca. 1862 cm^{-1}, suggesting the presence of more than one conformer in solution, in agreement with the NMR spectroscopy, which revealed fluxional behaviour of the tungstacyclobutadiene ring. The ^{29}Si NMR spectrum displays a singlet resonance at low field (135.5 ppm) in the range expected for silylidene complexes.

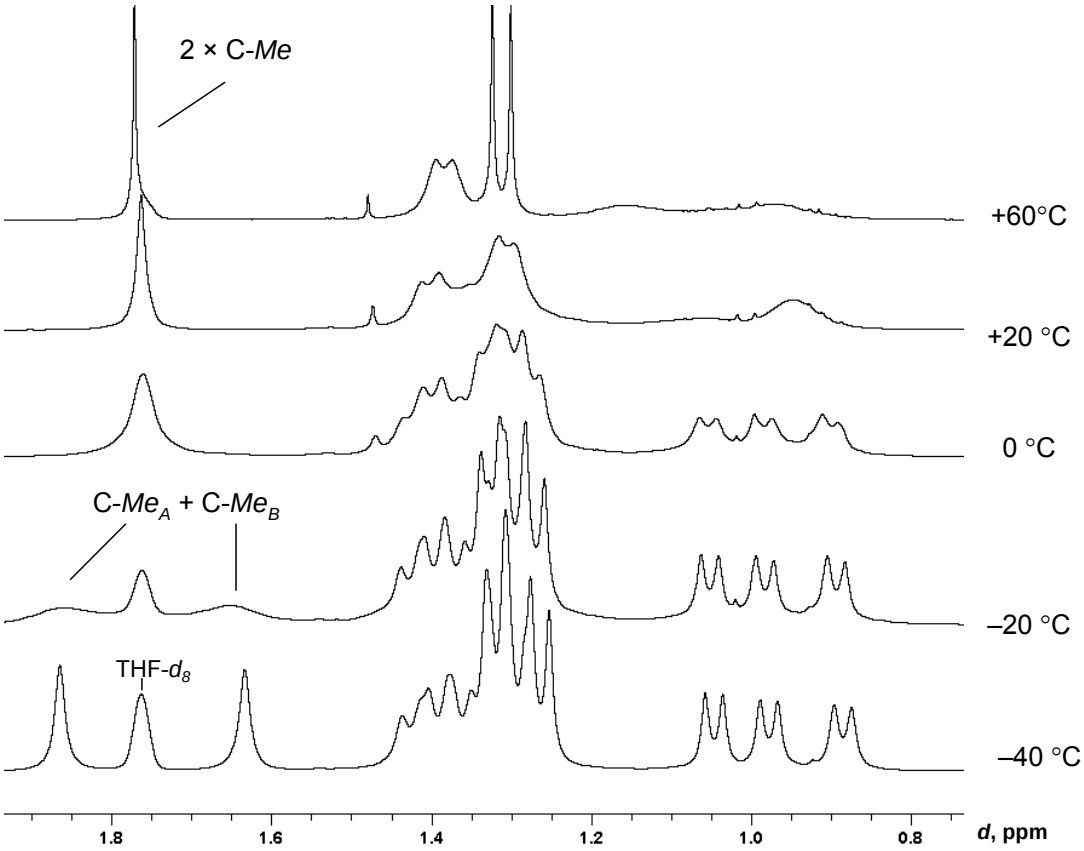

Figure 61: Fragment of variable temperature ^1H NMR spectra of complex **76** (THF-d_8, 300 MHz)

It was already mentioned, that electron rich alkynes react faster with the silylidyne complex than alkyl-substituted alkynes. Addition of the alkyne Ph–C≡C–NMe_2 to complex [$Cp(CO)_2Mo{\equiv}Si(C_6H_3$-2,6-$Trip_2)$] provides an insight into the mechanism of the reaction. One can imagine the formation of two regioisomers i.e. adducts **78-A** and **78-B**. However, only the isomer **78-A** was observed (Scheme 65).

[80] In the ^{13}C NMR spectrum the methyl groups of the butyne moiety appear as one sharp signal, as expected. However several signals in the aromatic region, including those of the *C*-Me moieties were not observed.

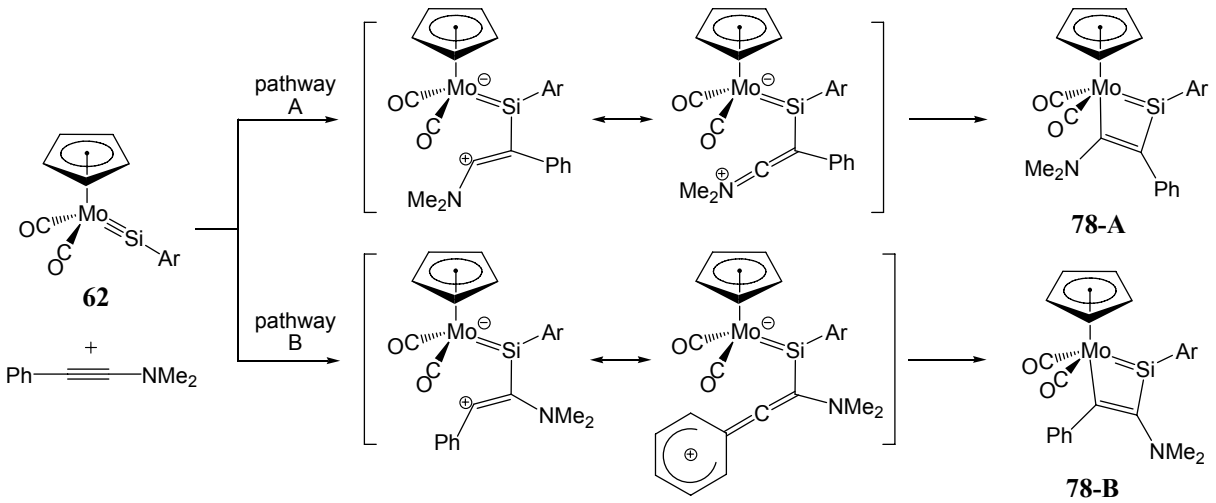

Scheme 65: Proposed mechanism of the reaction of the silylidyne complex **60** with Ph–C≡C–NMe_2.

We suppose, that the reaction proceeds in two steps. First, the alkyne is attacked by the electrophilic silicon center to form a zwitter-ionic intermediate, which then ring-closes and forms the metallasilacyclobutadiene. In the case of Ph–C≡C–NMe_2, the intermediate formed by pathway **A** is more favorable than that of **B**, therefore only complex **78-A** is formed.

The structure of complex **78** in the solid state is depicted in Figure 62. The key features of this compound are similar to those of **76**:

- a puckered $MoSiC_2$-ring, with the angle between the planes (Si-Mo-C37)/(Si-C37-C38) of 25.3°;[81]
- a Mo=Si double bond length of 2.424 Å[81] and a planar Si center (Σ° at Si = 359.7°);[81]
- a short Si–C_α bond length of 1.774 Å, suggesting some bonding interaction.[81]
- The C_α–C_β bond length of 1.424 Å[81] lies in-between the accepted value for a double bond (1.34 Å) and a single bond length (1.54 Å). The nitrogen center is planar, Σ° at N = 359.5°.[81] The C_β–N bond length of 1.347 Å[81] lies in-between the values for a double bond (1.28 Å) and for a single bond length (1.47 Å) and compares well with the mean value of the C–N bond length in compounds featuring a C=C–NR_2 moiety, where nitrogen is planar (1.36 Å).[195] The C_β–N bond length suggests conjugation of the lone pair of the nitrogen atom with the four-membered ring as also evidenced by NMR spectroscopy.

[81] Mean value of two independent molecules found in the asymmetric unit.

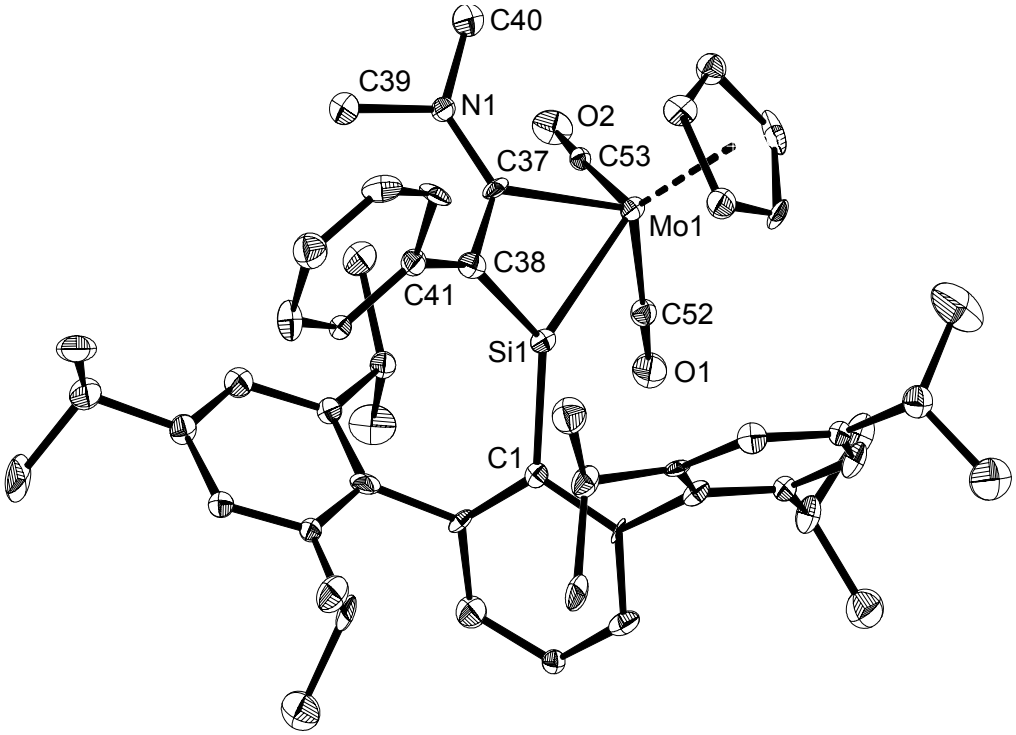

Figure 62: DIAMOND plot of the molecular structure of **78**. Thermal ellipsoids are set at 50% probability. Hydrogen atoms are omitted for clarity. Two independent molecules are found in the asymmetric unit. Selected bond lengths [Å] and bond angles [°] (values in brackets correspond to the second independent molecule): Mo1–Si1 2.424(4) [2.423(4)], C1-Si1 1.89(1) [1.87(1)], C38–Si1 1.79(1) [1.76(1)], C37–Si1 2.23(1) [2.25(1)], C37-C38 1.41(2) [1.44(2)], C37–Mo1 2.29(1) [2.30(1)], C37–N1 1.35(1) [1.35(2)], C38–C41 1.48(2) [1.46(2)]; C1-Si1-Mo1 134.8(4) [133.8(4)], C1-Si-C38 129.8(6) [130.4(6)], C38-Si1-Mo1 95.0(4) [95.5(4)], C37-C38-Si1 87.3(8) [88.9(8)], C38-C37-Mo1 113.6(8) [111.8(8)], C37-Mo1-Si1 56.3(3) [56.8(3)].

The ^{1}H NMR spectrum at 298 K in C_6D_6 displays a broad signal corresponding to the C_β–N*Me*$_2$ group, however, at –40 °C in toluene-d_8 the signal splits into two, with the rest of the signals practically unchanged. The IR spectrum of **78** in hexane reveals the presence of two conformers of the complex in solution. It is likely, that the conformers exhibit *exo*- and *endo*-orientation of the puckered C_2SiMo ring and interconvert fast on the NMR timescale.[82]

We were not able to obtain crystals of the complexes **79** and **80** suitable for the X-ray diffraction analysis, however their spectroscopic features are similar to those of complexes **75**–**78**, suggesting a similar structure. The key spectroscopic and bonding parameters of the complexes **75**–**80** are summarized in Table 10.

[82] A possible explanation, than the two regioisomers **78-A** and **78-B** co-exist in solution is excluded on the basis of the low-temperature NMR studies, which showed the presence of the single isomer according to the C,H-correlation spectra.

	Yield, %	^{29}Si NMR, δ, ppm	IR, cm^{-1}, hexane	d(Mo–Si), Å	d(Si–C$_\alpha$), Å	Puckering angle, [°]
[Cp(CO)$_2$Mo=Si(Ar)-C(H)C(H))] (**75**)	20	123.8	1949 (vs), 1869 (s)	2.3887(8)	1.776(3)	34.3
[Cp(CO)$_2$Mo=Si(Ar)-C(Me)C(Me))] (**76**)	54	135.5	1936 (vs), 1862 (sh), 1856 (s)	2.3907(6)	1.783(2)	34.6
[Cp(CO)$_2$Mo=Si(Ar)-C(Et)C(Et))] (**77**)	quant.	119.7	1935 (vs), 1856 (s)	2.394(2)	1.84(1)	37.9
[Cp(CO)$_2$Mo=Si(Ar)-C(Ph)C(NMe$_2$))] (**78**)	94	206.1	1938 (vs), 1925 (s), 1867 (s), 1854 (m)	2.424(4)*	1.77(2)*	25.3*
[Cp(CO)$_2$Mo=Si(Ar)-C(NMe$_2$)C(NMe$_2$))] (**79**)	65	134.2	1930 (vs), 1921 (m), 1851 (s), 1842 (m)	–	–	–
[Cp(CO)$_2$Mo=Si(Ar)-C(NEt$_2$)C(NEt$_2$))] (**80**)	65	155.5	1931 (vs), 1919 (s), 1855 (s), 1841 (m)	–	–	–

Table 10: Selected spectroscopic and bonding parameters of complexes **75**–**80**. *Average value of the two independent molecules found in the asymmetric unit is given.

The reaction of *p*-methoxyphenylacetylene with the silylidyne complex **60** afforded a 2:1 addition product (Scheme 66).

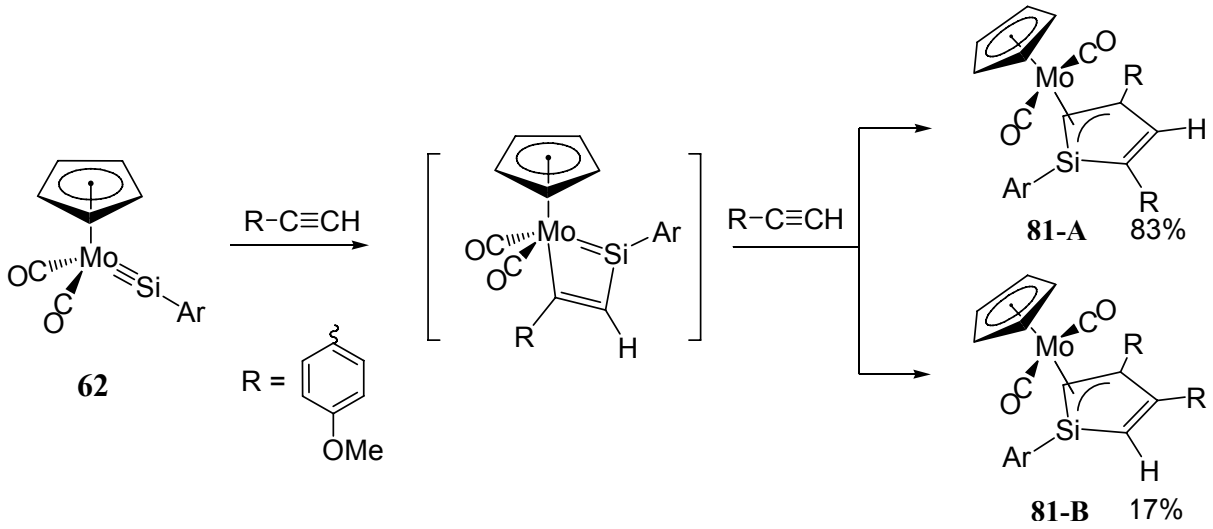

Scheme 66: The reaction of complex [Cp(CO)$_2$Mo≡Si(C$_6$H$_3$-2,6-Trip$_2$)] with a terminal alkyne.

We suppose that the product of the 1:1 addition is unstable under the experimental conditions and reacts fast with another equivalent of the alkyne to give a mixture of complexes **81-A** and **81-B**. Complexes **81-A** and **81-B** have similar solubility, and after crystallization a mixture of both regioisomers in a ratio of 5:1 in total yield of 81% was obtained. Complex **81-A** was identified by X-ray diffraction analysis (Figure 63), complex **81-B** was identified on the basis of NMR spectroscopy.

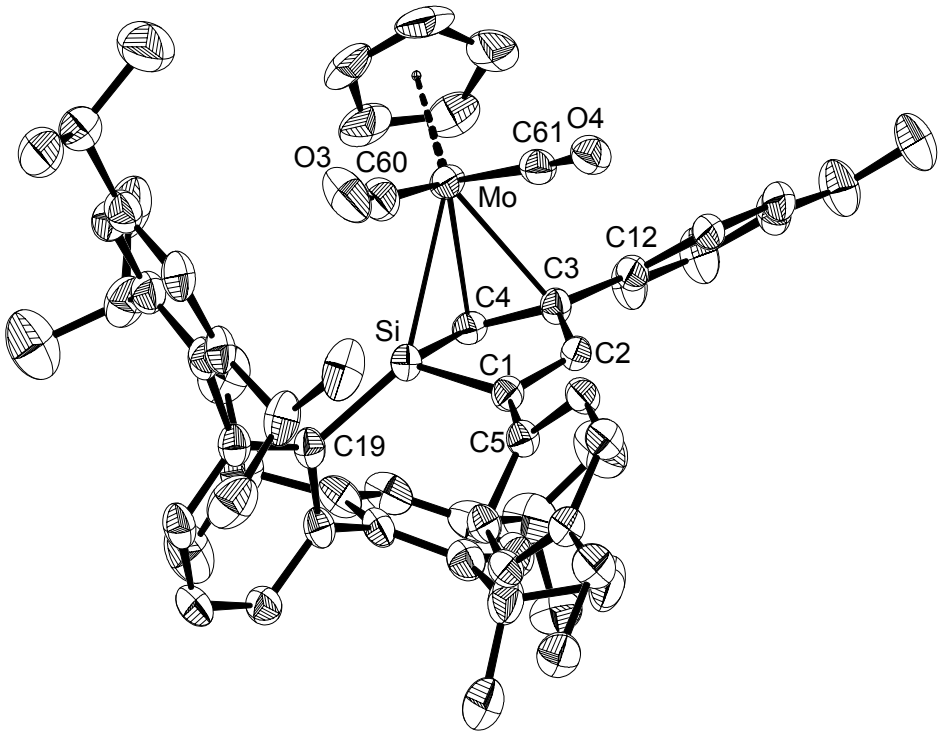

Figure 63: DIAMOND plot of the molecular structure of **81-A**. Thermal ellipsoids are set at 30% probability. Hydrogen atoms are omitted for clarity. Selected bond lengths [Å] and bond angles [°]: Mo–Si 2.6635(11), C4–Mo 2.269(4), C3–Mo 2.418(4), C19–Si 1.884(4), C1–Si 1.893(4), C1–C2 1.356(6), C2–C3 1.493(6), C3–C4 1.414(6), C4–Si 1.805(4), C60–Mo 1.953(5), C61–Mo 1.917(5); C19-Si-C1 119.6(2), C19-Si-C4 123.2(2), C1-Si-C4 94.5(2), C3-C4-Si 104.8(3), C2-C3-C4 113.3(3), C60-Mo-C61 77.7(2).

Complex **81-A** features an η^3-coordinated silacyclopentadienyl (silolyl) ligand. This type of coordination is unprecedented so far for silolyl complexes, which have been so far observed to contain either an η^1-[196] or an η^5-[197] coordinated silacyclopentadienyl ligand. The Mo–Si, Mo–C4 and Mo–C3 bonds are slightly elongated in comparison to those in alkyl and silyl complexes of molybdenum, as one can expect for a η^3-silolyl complex.[67, 77] Complex **81-A** is isolobal to complex [(η^5-Ind)Mo(CO)$_2$(η^3-Ind)], (Ind = indenyl), and its structural parameters are similar to those of the indenyl complex. The IR spectrum of **81-A** features two ν(CO)-absorption bands at 1919 (vs), 1850 (s) cm^{-1} in toluene, which appear at slightly lower wavenumbers than those of [(η^5-Ind)Mo(CO)$_2$(η^3-Ind)] 1944 (vs), 1851 (vs) in KBr.[198]

Reactions of cationic silylidyne complexes [Cp*(CO)$_2$M≡Si(ISdipp)][Al(OC(CF$_3$)$_3$)$_4$], (M = Cr, W) with alkynes.

Similarly to the neutral complex [Cp(CO)$_2$Mo≡Si(C$_6$H$_3$-2,6-Trip$_2$)], the cationic silylidyne complexes [Cp*(CO)$_2$M≡Si(ISdipp)][Al(OC(CF$_3$)$_3$)$_4$], (**61-Cr, W**) react with alkynes. In fact,

due to the increased electrophilicity of the silicon center in the cationic complexes, the reactions with unsaturated systems proceeds significantly faster. Thus, while the reaction of $[Cp(CO)_2Mo{\equiv}Si(C_6H_3\text{-}2,6\text{-}Trip_2)]$ with 3-hexyne was slow at ambient temperature, the reaction with $[Cp^*(CO)_2M{\equiv}Si(ISdipp)][Al(OC(CF_3)_3)_4]$ proceeded immediately. Moreover, the cationic complex **61-Cr** even reacts with ethylene, whereas the neutral complex $[Cp(CO)_2Mo{\equiv}Si(C_6H_3\text{-}2,6\text{-}Trip_2)]$ does not.[83]

Complexes $[Cp^*(CO)_2M{\equiv}Si(ISdipp)][Al(OC(CF_3)_3)_4]$ (**61-Cr** and **61-Mo**) react with 2-butyne, to give the metallasilacyclobutadienes **83-Cr** and **83-Mo** (Scheme 67).

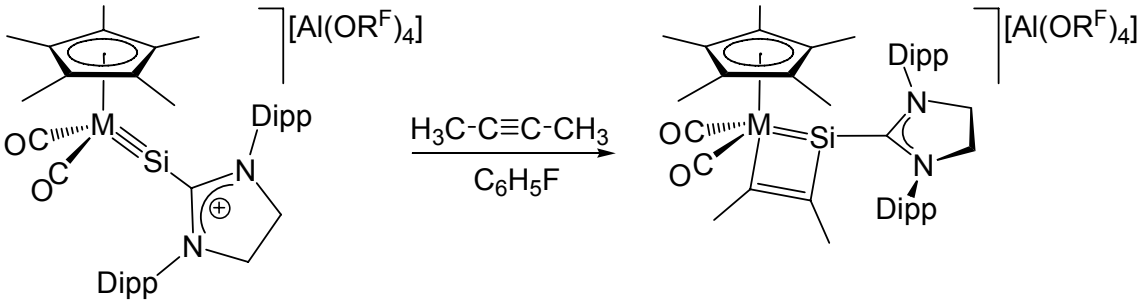

61-Cr, Mo **83-Cr, Mo**

Scheme 67: Reaction of cationic silylidyne complexes with 2-butyne, M = Cr, Mo.

Complex **83-Cr** was isolated as a dark green-black crystalline solid in 62% yield upon crystallization from a fluorobenzene-hexane mixture. The complex is air sensitive, soluble in fluorobenzene, insoluble in hexane or pentane, unstable in diethyl ether. The structure of complex **83-Cr** was determined by X-ray diffraction analysis (Figure 64); attempts to crystallize complex **83-Mo** were unsuccessful so far.[84]. The complexes have similar structures, as is evidenced by their similar IR and NMR spectra. The four-legged piano-stool complex **83-Cr** features a puckered $CrSiC_2$-ring as demonstrated by the dihedral angle between the planes (Si, Cr, C28) and (Si, C29, C28) of 35.6(2)°.

[83] As evidences by IR spectrum of the product: 1960 (vs), 1870 (vs) cm^{-1} (fluorobenzene). The product was not isolated.

[84] Complex **83-Cr** also have tendency to form oils. For the details about complex **83-Mo** see M. Speer, *Bachelor thesis*, University of Bonn, **2011**.

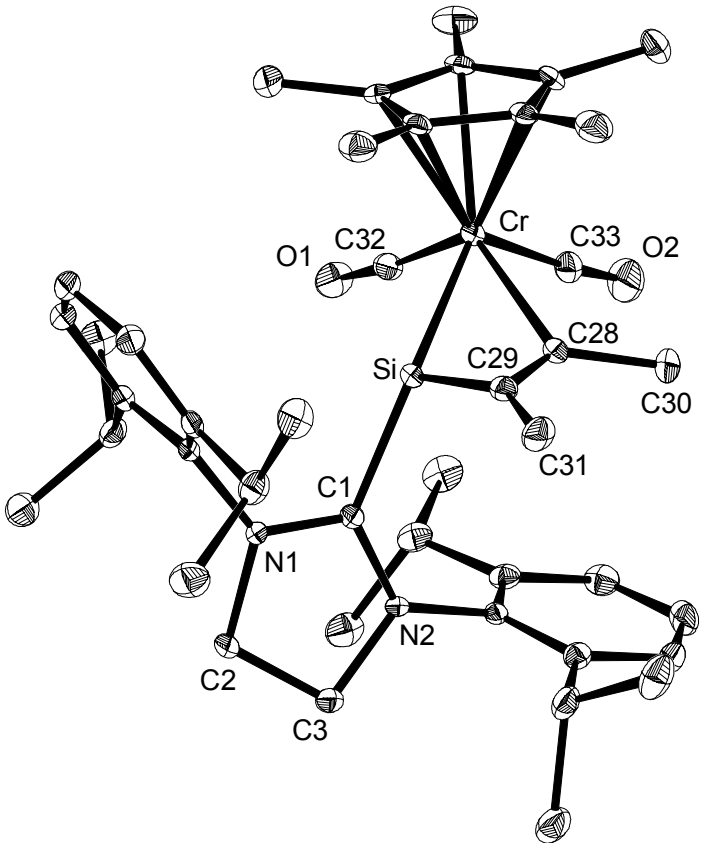

Figure 64: DIAMOND plot of the molecular structure of the complex cation of **83-Cr** . Thermal ellipsoids are set at 30% probability, and hydrogen atoms are omitted for clarity. Selected bond lengths [Å] and angles [°]: Cr–Si 2.2323(8), Si–C1 1.949(2), Si–C29 1.799(3), Si–C28 1.939(3), C28–C29 1.360(4), Cr–C28 2.270(3), Cr-Si-C1 140.84(8), Cr-Si-C29 101.17(9), Si-C29-C28 74.28(17), C29-C28-Cr 116.7(2), C28-Cr-Si 51.02(7).

The silicon center is nearly planar as indicated by the sum of the bond angles between the substituents of 350.4°. The Cr–Si bond length of 2.2323(8) Å compares with that of the halosilylidene complex **52-Cr** (2.1716(7) Å) and the Mo–Si bond length in complex [Cp(CO)$_2$Mo=Si(Ar)C(Me)C(Me))] (**76-Mo**, 2.3907(6) Å), taking into account the difference between the Cr and Mo double-bond covalent radii of ca. 0.10 Å.[162] The C28–C29 bond length of 1.360(4) Å compares well with the C=C bond length of 1.372(8) Å found in the tungstocyclobutadiene complex [CpW(C(Ph)C(^{t}Bu)C(Ph))Cl$_2$].[194]

The structure displays several peculiarities. Thus, the Cr–C bond length of 2.270(3) Å is considerably longer than the mean value for chromium alkyl complexes of 2.10(7) Å.[85] The Si–C29 bond length of 1.799(3) Å is short and can be compared with those in silaethenes (1.702–1.775 Å).[126] The Si···C28 distance is also short (1.939(3) Å) and compares well with

[85] According to a CSD survey from 11.2011 of 90 structurally characterized chromium alkyl complexes (Cr–^{T4}CR$_3$, where R = C or H). Median *d*(Cr–C) = 2.089 Å, LQ = 2.041 Å, HQ = 2.178 Å.

Si–C single bond length predicted on the basis of the single-bond covalent radii (1.91 Å) suggesting an interaction.[147] Overall, the structure of **83-Cr** resembles that of **76**, but is more distorted, as evidenced e.g. by the even shorter Si–C28 bond length (1.939(3) vs 2.005(3) Å), and longer Si–C29 bond length (1.799(3) vs 1.776(3) Å), see p. 131.

On the basis of the solid state structure, several possible resonance structures can be suggested, which help to understand the geometry of the complex (Scheme 68). In comparison to complex [Cp(CO)$_2$Mo=Si(Ar)C(Me)C(Me))] (**76**), the Si–C$_\beta$ bond is shortened and the Cr–C bond is relatively elongated in **83-Cr** (2.270(3) Å vs 2.290(2) Å in **76**) as depicted by the resonance structure in the middle. It would be interesting, if one can find a system, where the distortion is more pronounced, ultimately leading to a silacyclopropenyl complex **A** or a metallasilatetrahedrane **B** (Scheme 68, on the bottom).

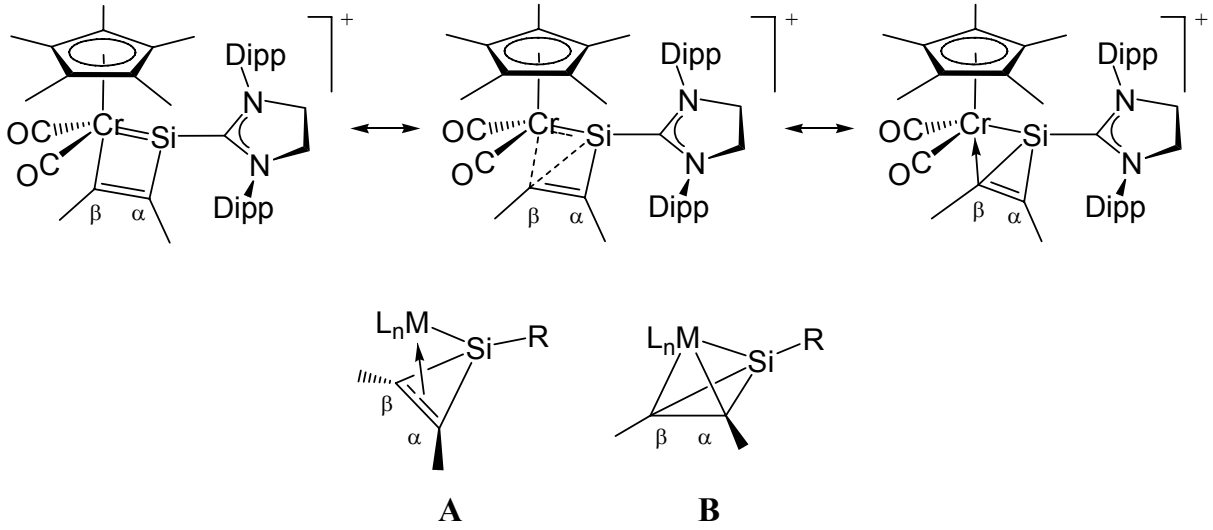

Scheme 68: Resonance structures of complex **83-Cr**. Hypothetical cyclopropenyl (**A**) and tetrahedrane (**B**) structures.

2.4 Metallagermylenes

The synthesis of the heavier analogues of alkylidyne complexes is an important contribution to the chemistry of the elements Si–Pb. The majority of ylidyne complexes incorporate Group 6 metals (Cr, Mo, W), but there are also examples of Group 7 and 8 complexes (chapter 1.3, p. 26). It was shown, how NHC-stabilized silylenes can be used for the preparation of silylidyne complexes of Cr, Mo and W (Chapter 2.2, p. 73). It was interesting to extend this methodology to Group 8 transition-metals.

First, the synthesis of ferrio- and ruthenogermylenes [$Cp(CO)_2M$–Ge–Ar] was investigated. These compounds could provide access to germylidyne complexes of the type [Cp(CO)M≡Ge–Ar] *via* elimination of CO under irradiation as a possibility (see also p. 29); however the resulting ylidyne complexes could have unstable nature. Another possible approach to ylidyne complexes could be to use bulky phosphanes as ligands, thus increasing the steric shielding and the electron density on the metal, leading to more stable complexes [$Cp(R_3P)M$≡Ge–R]. Furthermore, having in hands arylsilicon(II)chlorides it was intriguing to investigate their reactivity towards iron and ruthenium carbonyl metallates. The ideas are summarized in Scheme 69.

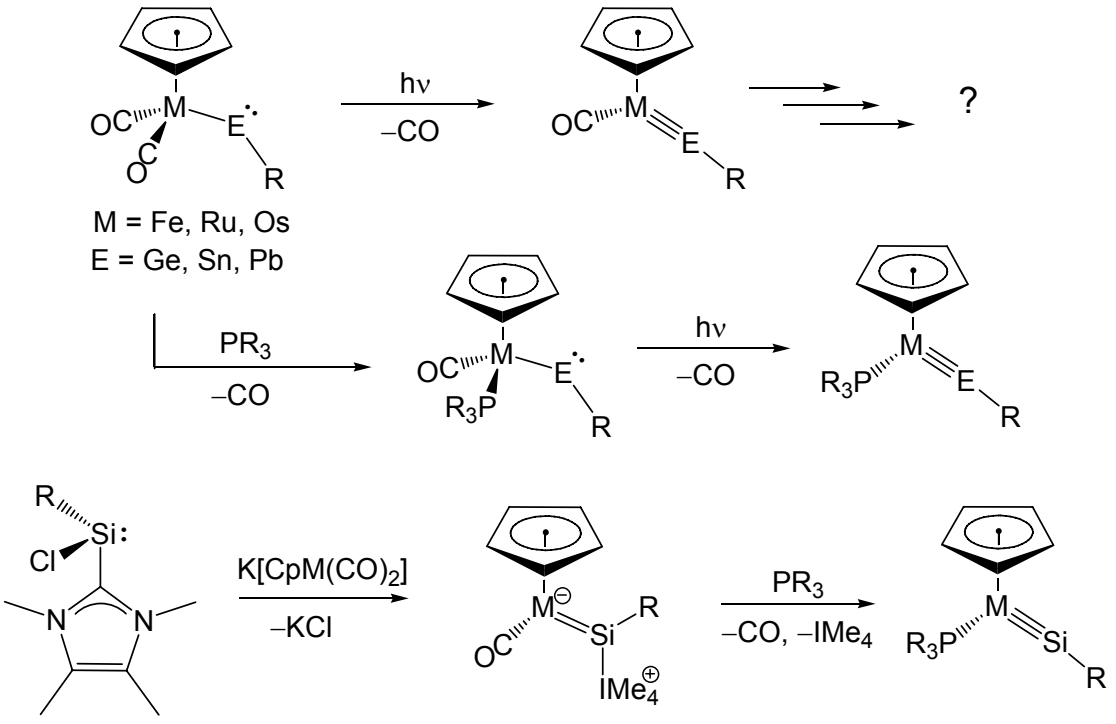

Scheme 69: Strategy to Group 8 ylidyne complexes.

In fact, treatment of the carbonyl metallates K[CpFe(CO)$_2$] and K[Cp*Ru(CO)$_2$] with Ge(C$_6$H$_3$-2,6-Trip$_2$)Cl at ambient temperature led to an immediate color change from brown to deep green. *In situ* IR spectra the revealed the selective formation of the dicarbonyl complexes [Cp(CO)$_2$Fe–Ge(C$_6$H$_3$-2,6-Trip$_2$)] (**84**) and [Cp*(CO)$_2$Ru–Ge(C$_6$H$_3$-2,6-Trip$_2$)] (**86**). The complexes were isolated after crystallization from pentane as dark green solids in 68% and 30% yields respectively. Both complexes were crystallographically characterized; the molecular structures are presented in Figure 65 and Figure 66.

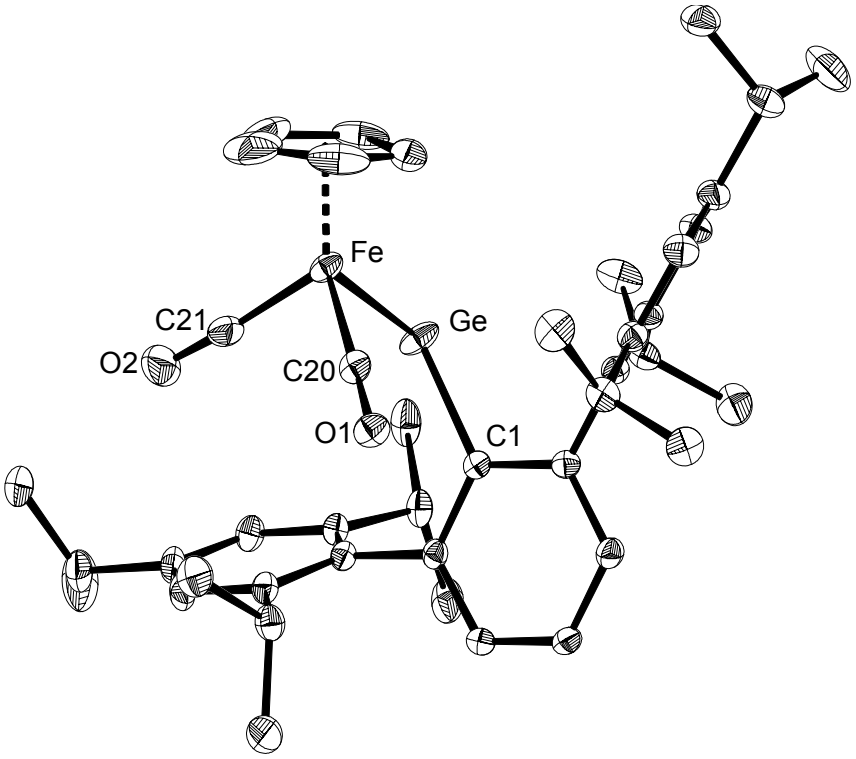

Figure 65: DIAMOND plot of the molecular structure of **84**. Thermal ellipsoids are set at 30% probability. Hydrogen atoms are omitted for clarity. Selected bond lengths [Å] and bond angles [°]: Fe–Ge 2.3793(5), C1–Ge 2.015(3), C20–Fe 1.752(3), C21–Fe 1.875(9); C1-Ge-Fe 112.54(7), C20-Fe-Ge 87.68(10), C21-Fe-Ge 88.3(2), C20-Fe-C21 93.6(2).

Both three-legged piano-stool complexes feature M–Ge single bonds. The germylenes exhibit a bent structure with C1-Ge-M angles of 112.54(7)° (M = Fe, **84**) and 114.44(9)° (M = Ru, **86**). The Fe–Ge bond length of 2.3793(5) Å corresponds to a single bond[86] and compares well e.g. with that in Cp*Fe(CO)$_2$–GeCl(CH$_3$)$_2$ (2.349(2) Å) or with that calculated on the basis of the single-bond covalent radii of Fe and Ge (1.16 Å + 1.21 Å = 2.37 Å).[147] Interestingly, the

[86] According to a CSD survey from 11.2011 of 24 structurally characterized iron germyl complexes (Fe–GeX$_3$, where X = any non-metal) the mean Fe–Ge bond length is 2.37(6) Å. Median *d*(Fe–Ge) = 2.375 Å, LQ = 2.269 Å, HQ = 2.406 Å.

bond is substantially shorter than those in the donor-stabilized ferriogermylenes $CpFe(CO)_2$–E(N⁀N) (2.4961(17) Å; N⁀N = $CH\{CMe(NDipp)\}_2$)[114] and $CpFe(CO)_2$–$Ge\{(NDipp)_2C\textit{t}Bu\}$ (2.4415(11) Å).[115] The Ru–Ge bond length of 2.4555(5) Å compares well with the values found in ruthenium germyl complexes and with the predicted value on the basis of single-bond covalent radii (2.46 Å).[147]

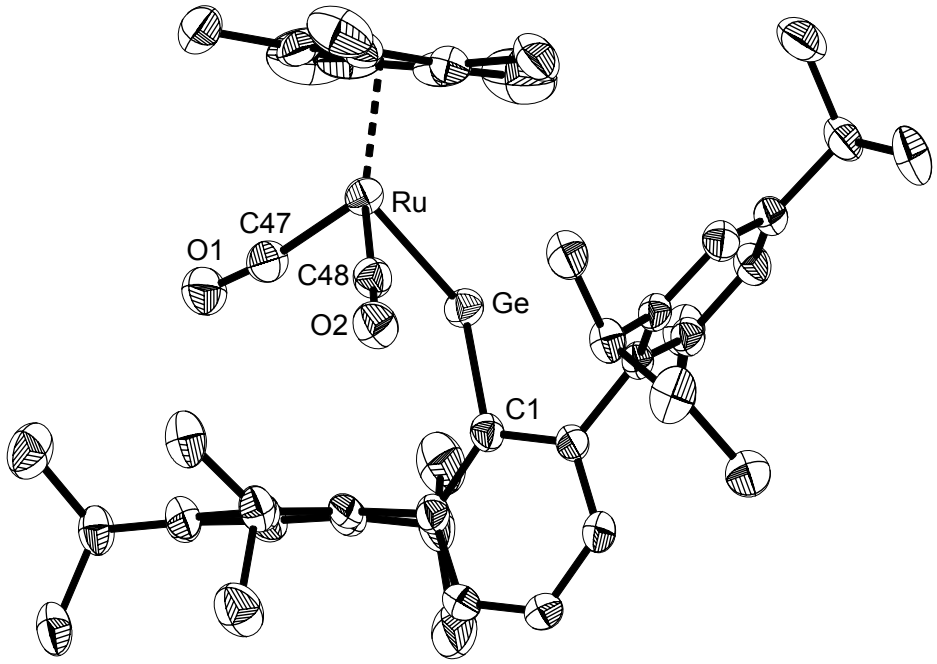

Figure 66: DIAMOND plot of the molecular structure of **86**. Thermal ellipsoids are set at 50% probability. Hydrogen atoms are omitted for clarity. Selected bond lengths [Å] and bond angles [°]: Ru–Ge 2.4555(5), C1–Ge 2.020(3), C47–Ru 1.869(4), C48–Ru 1.850(4); C1-Ge-Ru 114.44(9), C47-Ru-Ge 87.2(1), C48-Ru-Ge 87.5(1), C47-Ru-C48 94.8(2).

In the solid state structure of **84** the two carbonyl groups are distinctly not equivalent, as indicated by the distances *d*(Fe–C21) = 1.875(9) Å and *d*(Fe–C20) = 1.752(3) Å, however the C–O bond lengths are essentially the same (1.148(3) Å and 1.149(3) Å). Furthermore, the plane of the bent germylyne ligand defined by the atoms (C1, Ge, Fe) is nearly orthogonal to the (Ge, Fe, C21) plane, as indicated by the dihedral angle of 86.3(2)°. A plausible explanation of such an orientation in complex **84** can be a bonding interaction between the empty p_z orbital of Ge and the filled d_{xz} orbital of Fe (Scheme 70). Consequently, the Fe→CO π-backdonation is reduced, thus elongating the Fe–C21 bond. The d_{xy} orbital, involved in the backbonding to the other CO group does not overlap with the p_z orbital of Ge atom, therefore

the Fe–C20 bond length remains normal (1.752 Å).[87] The conjugation explains also the shorter Fe–Ge bond length in comparison to those in the base stabilized complexes $CpFe(CO)_2$–E(N⁀N) (N⁀N = CH{CMe(NDipp)}$_2$)[114] and $CpFe(CO)_2$–Ge{(NDipp)$_2$C*t*Bu}.[115]

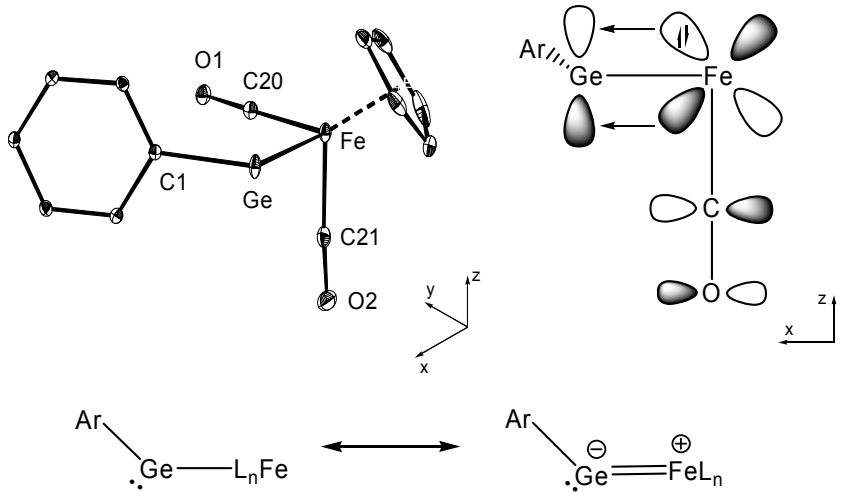

Scheme 70: Conjugation between the empty p_z orbital of Ge and the filled d_{xz} orbital of Fe. The reduced Fe–CO backbonding leads to elongation of the Fe–C21 bond but not of the Fe–C20 bond.

In the case of the ruthenium complex **86** the interaction is also observed, however it is less pronounced. The dihedral angle between the bent germylyne ligand plane (C1, Ge, Ru) and (Ge, Ru, C47) plane is 86.0(2)°, close to than in the iron analogue. However, the Ru–C47 bond length is only slightly longer than the Ru–C48 bond length (1.869(4) Å and 1.850(4) Å respectively).

Further evidence of a M–Ge conjugation is provided by NMR spectroscopy. In C_6D_6 solution, the *m*-terphenyl group of complex [$Cp(CO)_2Fe$–$Ge(C_6H_3$-2,6-$Trip_2)$] (**84**) displays a set of signals, which is consistent with the presence of a chiral group in C^1 position and a fast rotation about the Ge–C1 bond (Figure 67), in agreement with the X-ray diffraction studies. However, only one sharp signal corresponding to the CO groups was observed in ^{13}C NMR spectrum at 25 °C (212.3 ppm). At -10 °C a broad signal at 212.3 was observed, which splits into two signals at 207.4 and 217.3 ppm at –50 °C (all spectra in toluene-d_8). The chirality of compound is retained in all three cases.[88] The data suggest, that in solution "flipping" of $CpFe(CO)_2$ fragment occurs, alternating the d_{xz} and d_{xy} orbitals utilized for the Fe–Ge

[87] For example the mean Fe–CO bond length in complex [$CpFe(CO)_2$-$(CH_2)_4$-$Fe(CO)_2Cp$] is 1.74 Å. L. Pope, P. Sommerville, M. Laing, K. J.Hindson, J. R.Moss, *J.Organomet.Chem.* **1976**, *112*, 309.

[88] The chirality is evidenced by the signal pattern of the *m*-terphenyl substituent.

conjugation (Scheme 70), but the $CpFe(CO)_2$ fragment does not make a full turn about Fe–Ge bond, therefore the overall chirality of the complex is retained.

In agreement with the weaker π-interaction in complex [Cp*(CO)$_2$Ru–Ge(C$_6$H$_3$-2,6-Trip$_2$)] (**86**) according to the Ru–CO bond lengths, the complex displays dynamic behavior in solution, as evidenced by the broadening of the signals, corresponding to the C^{2,6}-*i*Pr and C^{3,5}-H positions of the Trip groups. The dynamic process is suggested to involve a rotation of the bent germylyne ligand about the Ru–Ge bond, also equilibrating the CO-ligands.

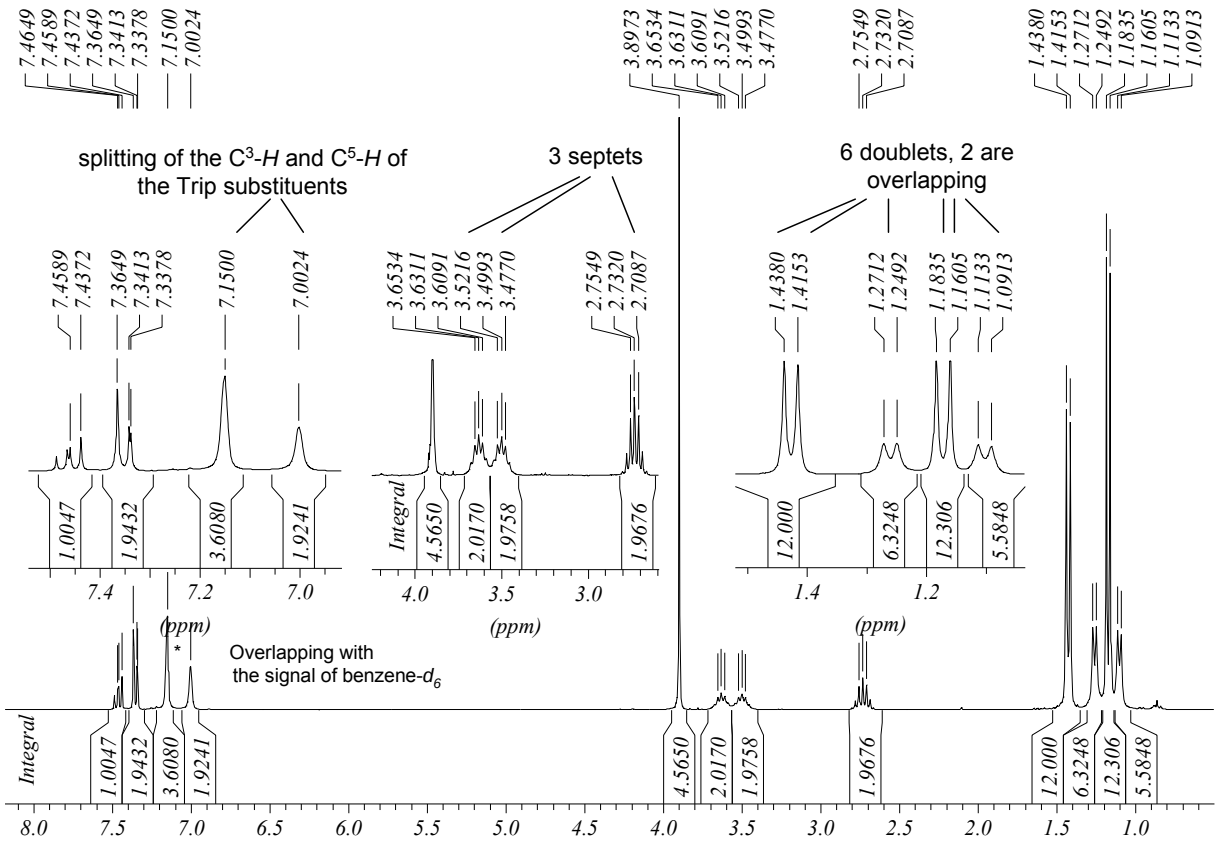

Figure 67: 300.1 MHz ^{1}H NMR spectrum of the complex [Cp(CO)$_2$Fe–Ge(C$_6$H$_3$-2,6-Trip$_2$)] (**84**) in C$_6$D$_6$.

The IR spectra of the complexes display two bands of slightly different intensities at 1989 (s), 1943 (vs) cm^{-1} (**84**; in pentane) and 1996, 1944 cm^{-1} (**86**; in hexane). The spectra are comparable with those of the complexes [Cp(CO)$_2$Fe–Ge–Mes*] (2004, 1950 cm^{-1} in THF) and [Cp*(CO)$_2$Fe–Ge–Mes*] (1969, 1920 cm^{-1} in hexane).[89] Due to the presence of Fe→Ge

[89] For comparison: IR spectrum of Cp*(CO)$_2$Fe-CH$_2$Bu (hexane, cm^{-1}): 1987 (vs), 1933 (vs) [ν(CO)]; IR spectrum of Cp*(CO)$_2$Ru-CH$_3$ (pentane, cm^{-1}): 2005 (vs), 1946 (vs) [ν(CO)]. R. O. Hill, C. F. Marais, J. R. Moss, K. J. Naidoo, *J. Organomet. Chem*. **1999**, *587*, 28; J. R. Moss, S. Ngubane,

π-donation the *ν*(CO) IR absorptions appear at higher energy than those of the donor-stabilized ferriogermylenes (*vide infra*).

The conjugation with the metal center reduces to some extent the electrophilicity of the germanium center. However, complexes **84** and **86** readily react with the strong σ-donor 1,3,4,5-tetramethylimidazol-2-ilydene (IMe_4) at ambient temperature (Scheme 71).

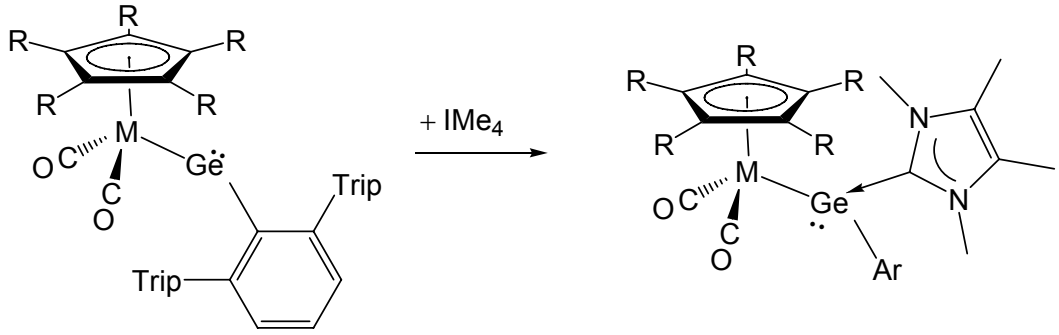

84
86

85: R = H, M = Fe
87: R = CH_3, M = Ru

Scheme 71: Addition of NHC to metallagermylenes.

Complex **85** was isolated as a dark brown-purple crystalline thermolabile solid in 55% yield upon crystallization from hexane at –30°C and was characterized by NMR and IR spectroscopy. Addition of the carbene to the complex **84** is accompanied by a substantial shift of the *ν*(CO) absorption bands in the IR spectrum to lower wavenumbers, 1989, 1943 cm^{-1} in **84** to 1943, 1890 cm^{-1} in **85**. The shift in the IR spectrum is consistent with the electronic changes caused by the coordination of carbene. The carbene donates electron density into the empty *p*-orbital of the Ge atom, which breaks down the π-backdonation from the Fe to the Ge center (see Scheme 70). The IR spectrum of complex **85** compares well with those of other donor-stabilized ferriogermylenes (1966, 1910 cm^{-1} in $CpFe(CO)_2$–E(N⁀N) (N⁀N = $CH\{CMe(NDipp)\}_2$; 1964, 1921 cm^{-1} in $CpFe(CO)_2$–$Ge\{(NDipp)_2C$*t*$Bu\}$.[114, 115])

Addition of the carbene to the NMR sample of complex **86** was accompanied by a color change from green to red. The ^1H NMR spectroscopy revealed the selective formation of a new complex, presumably the carbene adduct (complex **87**). The red solution of complex **87** gradually turned yellow upon standing at ambient temperature for one week. A selective formation of a new complex (**88**) was observed by NMR spectroscopy.

A. Sivaramakrishna, B. C. E. Makhubela, J. E. Bercaw, J. A. Labinger, M. W. Day, L. M. Henling, H. Su, *J. Organomet. Chem*. **2008**, *693*, 2700.

Complex **88** was isolated from the NMR sample in form of yellow crystals. The structure of the complex was determined by X-ray diffraction analysis (Figure 68).

The three-legged piano stool ruthenium germyl complex **88** features a C–H activated Cp* group. The Ru–Ge bond length of 2.4853(3) Å compares well with that of the germyl complex $[(Me_2Ge)(\eta^5\text{-}C_5H_4)Ru(CO)_2]_2$ (2.4623(7) Å)[199] and that in the ruthenogermylene **86** **(**2.4555(5) Å). The germanium center exhibits a distorted tetrahedral geometry. The Ru-Ge-C1 angle of 125.99(7)° is slightly widened probably due to the steric demand of the *m*-terphenyl substituent. It interesting to note, than in the solid state the carbonyl groups are equivalent as is expected, unlike in the parent complex **86 (***vide supra***)**. The C37–C49 distance of 1.355(3) Å unambiguously corresponds to a double bond.[147]

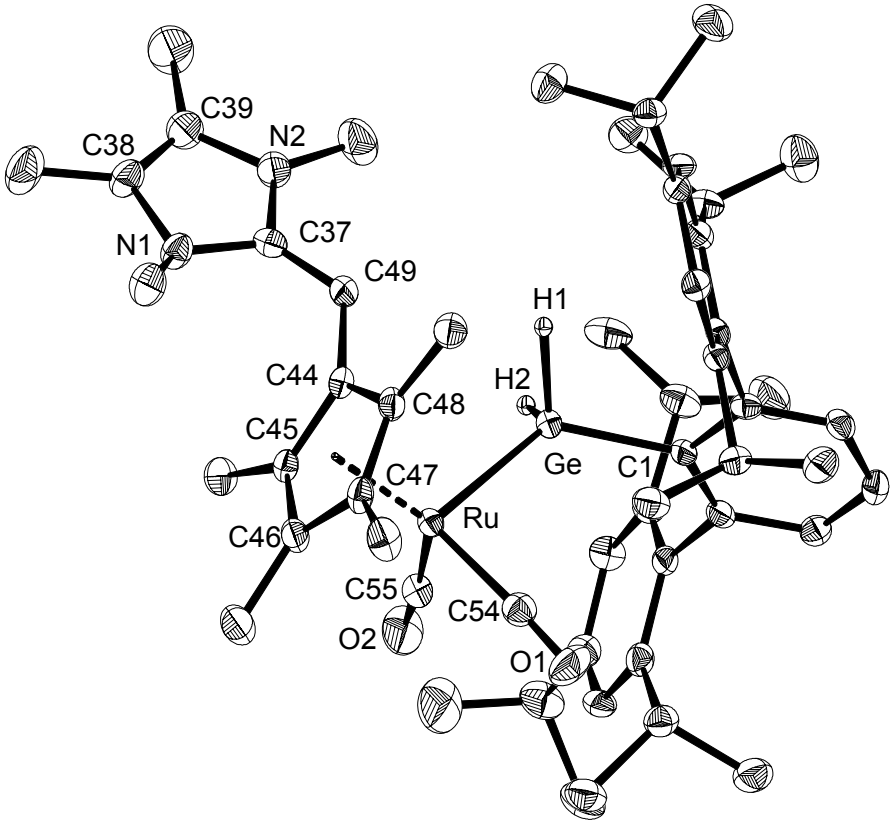

Figure 68: DIAMOND plot of the molecular structure of **88**. Thermal ellipsoids are set at 50% probability. Hydrogen atoms are omitted for clarity. Selected bond lengths [Å] and bond angles and [°]: Ru–Ge 2.4853(3), C1–Ge 1.994(2), C54–Ru 1.868(3), C55–Ru 1.870(3), C44–C49 1.451(3), C37–C49 1.355(3), C37–N1 1.398(3), C38–N2 1.377(3), C38–N1 1.419(3), C39–N2 1.419(3), C38–C39 1.324(4), Ge–H1 1.48(2), Ge–H2 1.42(2); C1-Ge-Ru 125.99(7), C54-Ru-C55 93.12(12), C44-C49-C37 126.2(3), N1-C37-N2 105.0(2).

It can be hypothesized, that the mechanism for the formation of complex **88** involves the insertion of the germanium center into the C–H bond of one CH_3 group of the Cp* group (Scheme 72). The hypothesis is supported by the fact, that the ferriogermylene $[Cp(CO)_2Fe$–

GeMes*] undergoes an intramolecular oxidative addition of the germanium center into the C–H bond of a *t*Bu group of the Mes* substituent (-C_6H_2-2,4,6-*t*Bu_3) just above 80°C, and that the related germylene GeMes*$_2$ undergoes an intramolecular C–H activation already at ambient temperature.[113, 200]

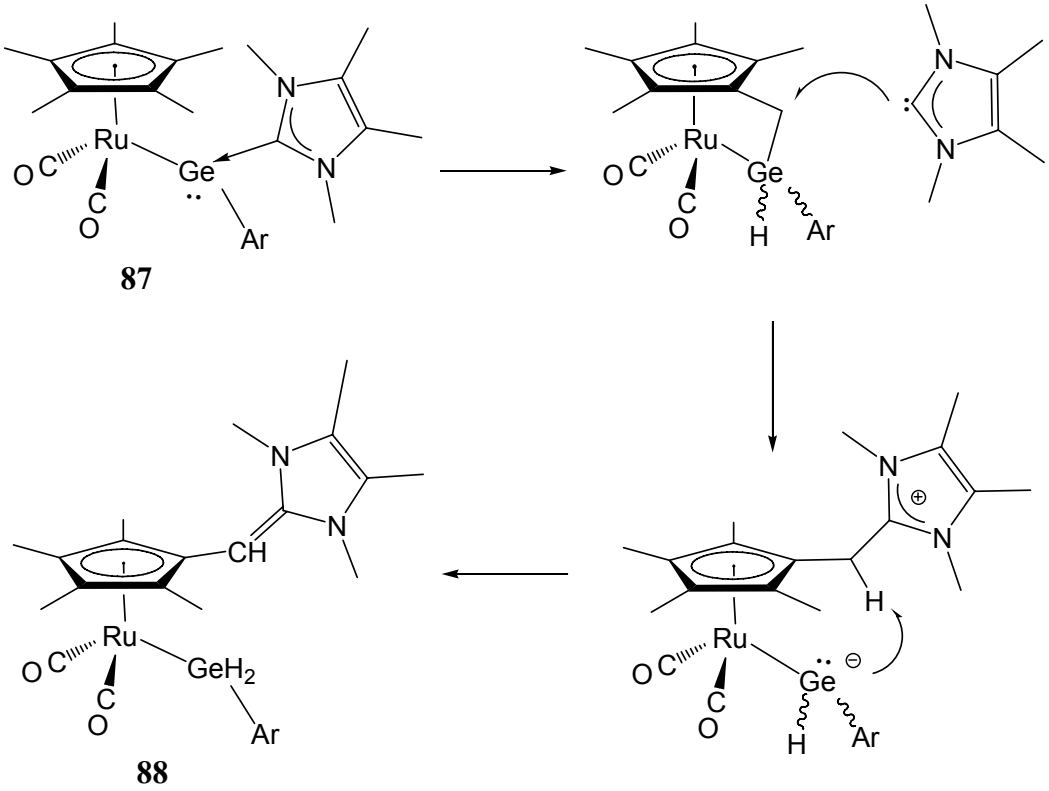

Scheme 72: The proposed mechanism for the formation of complex **88**. Ar = C_6H_3-2,6-$Trip_2$.

NMR spectra corroborate the solid state structure of the complex. At ambient temperature in C_6D_6 the rotation of the N-heterocycle around the Cp′–CH bond is hindered. The set of signals of the *m*-terphenyl group corresponds to an overall C_s symmetry of the complex, suggesting that rotation around the Ru–Ge bond is fast.[90] The IR spectrum of the complex features three *ν*(CO) absorption bands at 1998 (s), 1990 (s), 1939 (vs) cm^{-1} (in toluene), probably corresponding to two conformers, in agreement with the NMR spectra.[91] The key properties of the complexes **84**–**88** are summarized in Table **11**.

[90] This observation provided additional support for the presence of M→Ge backbonding in the structurally related complexes **84** and **86**. Thus, hindered rotation around the M–Ge in **84** and **86** is not accounted for by steric effects.

[91] It is suggested, that the two isomers intercorvert on the NMR timescale upon rotation of the 1,3,4,5-tetrametylimidazol-2-yl fragment about the Cp′–CH bond.

	Yield, %	IR, cm^{-1}	*d*(M–Ge), Å	*d*(Ge–C_{Ar}), Å	M-Ge-C_{Ar} angle, [°]
$[Cp(CO)_2Fe–Ge(C_6H_3\text{-}2,6\text{-}Trip_2)]$ (**84**)	68	1989 (s), 1943 (vs) (pentane)	2.3793(5)	2.015(3)	112.54(7)
$[Cp(CO)_2Fe–Ge(IMe_4)(C_6H_3\text{-}2,6\text{-}Trip_2)]$ (**85**)	55	1943 (s), 1890 (vs) (hexane)	–	–	–
$[Cp^*(CO)_2Ru–Ge(C_6H_3\text{-}2,6\text{-}Trip_2)]$ (**86**)	30	1996 (s), 1944 (vs) (hexane)	2.4555(5)	2.020(3)	114.44(9)
$[Cp'(CO)_2Ru–GeH_2(C_6H_3\text{-}2,6\text{-}Trip_2)]$ (**88**)	n/a	1998 (s), 1990 (s), 1939 (vs) (toluene)	2.4853(3)	1.994(2)	125.99(7)

Table 11: Selected spectroscopic and bonding parameters of the complexes **84**–**88**.

$Cp' = \eta^5\text{-}C_5(CH=(2\text{-}IMe_4)Me_4$.

We attempted to decarbonylate the metallagermylenes **84** and **86** in two test experiments. To the NMR sample of the complex **84** 50 mg of pyridine were added. The mixture was degassed and then irradiated for 30 min at ca. 40 °C with a 125W high-pressure mercury UV lamp from ca. 5 cm distance. The target complex [CpFe(CO)(Py)–Ge–Ar] was thought to be a good precursor for the germylidyne complex [CpFe(CO)≡Ge–Ar], since a coordinated pyridine (Py) can be abstracted under mild conditions with tris(aryl)borane.[93] However the ^{1}H NMR spectrum showed no apparent reaction. Irradiation of a hexane solution of the complex **86** was also not successful, as shown by IR spectroscopy. A more detailed investigation of the decarbonylation of the metallagermylenes was not conducted.

During writing of this thesis, complexes $[Cp(CO)_2Fe–E(C_6H_3\text{-}2,6\text{-}R_2)]$ have been reported (E = Ge, Sn; R = $\text{-}C_6H_3\text{-}2,6\text{-}i\text{Pr}_2$, $\text{-}C_6H_2\text{-}2,4,6\text{-}i\text{Pr}_3$) by Power et al.[116] The ferriostannylenes were decarbonylated to form the μ-stannylidyne complexes $[\{Cp(CO)_2FeSn(C_6H_3\text{-}2,6\text{-}R_2)\}_2]$, whereas the ferriogermylenes did not decarbonylate, supporting our observations.

2.5 Open-shell carbene complexes of iron

There are essentially two approaches to the ylidyne complexes (see section 1.3, p. 26). One of them utilizes electron rich phosphane complexes of Group 6 transition-metals.[106-111] B. Blom investigated the reactions of Fe(0) polyphosphane complexes with ERCl (E = Ge Sn), which led to the isolation of iron ylidyne complexes.[111] At the time attempts were undertaken to synthesize Fe(0) carbene complexes, which could also be used as starting materials for the synthesis of Fe–Ge and Fe–Sn triple bonds. This project resulted in the isolation of several interesting low-coordinated carbene complexes of iron, described below.

The strategy implied the synthesis of iron(II) carbene complexes and their reduction to iron(0) complexes. Treatment of iron(0) complexes with EArX (X = halogen, E = Ge–Pb) or

SiArCl(NHC) was thought to lead to iron ylidyne complexes (Scheme 73). The key compounds $Fe^{(0)}(NHC)_n$ were required to have not more than 14VE to be able to form complexes of the type $[ClFe(NHC)_n{\equiv}EAr]$ ($n \leq 3$), therefore bulky carbenes were utilized.

$$FeX_2 + n\ NHC \longrightarrow FeX_2(NHC)_n$$

$$FeX_2(NHC)_n + 2\ M \longrightarrow Fe(NHC)_n + 2\ MX$$

$$Fe(NHC)_n + EArCl \longrightarrow Cl{-}Fe(NHC)_n{\equiv}E{-}Ar$$

X = halogen, M = alkali metal, NHC = N-heterocyclic carbene, E = Si–Pb

Scheme 73: Carbene complexes of iron. The strategy to iron ylidyne complexes.

Starting from iron dichloride and iron dibromide several new iron carbene complexes were prepared. Stirring of a mixture of iron dihalide and 1,3-bis(2,4,6-trimethylphenyl)imidazol-2-ylidene (IMes) in toluene at ambient temperature resulted in the clean formation of the iron(II) biscarbene complexes **89-Cl** and **89-Br** (Scheme 74).

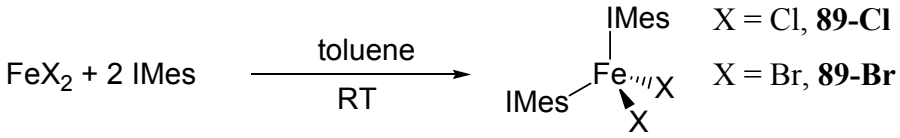

Scheme 74: Synthesis of iron(II) carbene complexes. IMes = 1,3-bis(2,4,6-trimethylphenyl)imidazol-2-ylidene.

The complexes were isolated as colorless solids after crystallization from toluene in 75 and 85% yields, respectively. The complexes are insoluble in hexane, soluble in toluene and THF, and slightly soluble in Et_2O. The compounds were fully characterized and the solid state structures were determined by X-ray crystallography. The structure of complex **89-Cl** is depicted in Figure 69, complex **89-Br** is isostructural.

Complex **89-Cl** features a distorted tetrahedral geometry at the iron center. The C1-Fe-C22 angle (125.23(5)°) is larger than the Cl1-Fe-Cl2 angle (106.79(2)°), probably as the result of the steric repulsion between the sterically demanding carbene ligands. The $Fe{-}C_{carbene}$ bond lengths are essentially identical (2.144(3) Å)[92] and compare well with those in similar carbene complexes of iron: $[FeCl_2(IPr)_2]$ (2.133(3) Å,[92] IPr = 1,3-diisopropyl-4,5-dimethylimidazol-2-ylidene) and $[Fe(O\text{^}NHC)_2]$ (2.085(3) Å, O^NHC = -O-4,6-tBu$_2$C$_6$H$_2$-2-CH_2{C(NCHCHNCH$_2$Ph)}}).[201, 202]

[92] The unweighted mean value x_u of the Fe–X bond lengths is given, the standard deviation σ of x_u was calculated using the equation $\sigma^2 = \Sigma(x_i - x_u)^2/(n^2 - n)$, where x_i is the individual value and n – number of elements.

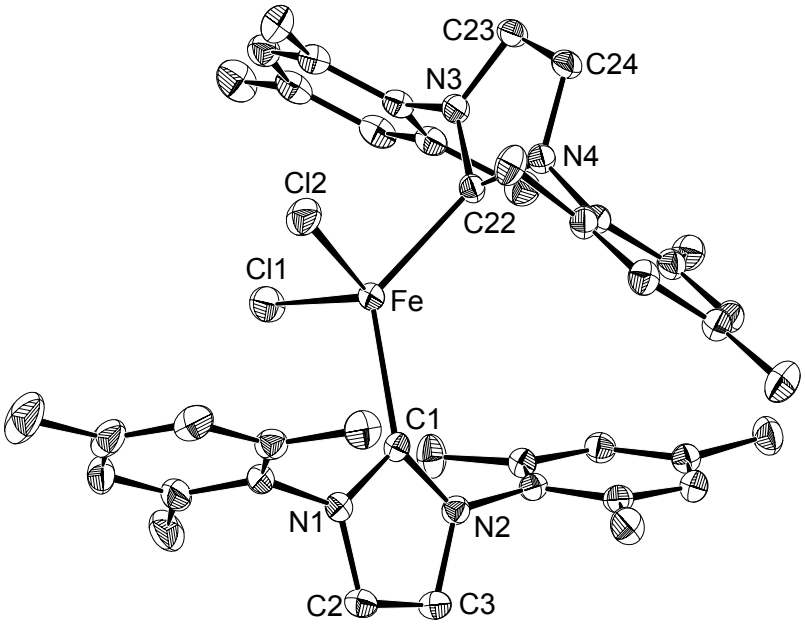

Figure 69: DIAMOND plot of the molecular structure of **89-Cl**. Thermal ellipsoids are set at 50% probability. Hydrogen atoms are omitted for clarity. Selected bond lengths [Å] and bond angles [°]: C1–Fe 2.141(1), C22–Fe 2.146(2), Cl1–Fe 2.2858(5), Cl2–Fe 2.3032(4), C1–N1 1.364(2), C1–N2 1.367(2), C22–N3 1.370(2), C22–N4 1.366(2), C2–C3 1.345(2), C23–C24 1.342(2); C1-Fe-C22 125.23(5), C1-Fe-Cl1 99.68(4), C22-Fe-Cl1 113.35(4), C1-Fe-Cl2 116.64(4), C22-Fe-Cl2 94.70(4), Cl1-Fe-Cl2 106.79(2).

The mean Fe–Cl bond length (2.295(9) Å)[92] compares well with those in $[FeCl_2(IPr)_2]$ (2.301(3) Å),[92,[202]] and in [CpFeCl(IMes)] (2.2715(7) Å).[[203]] The bonding parameters of **89-Br** are quite similar, the mean *d*(Fe–Br) is 2.453(15) Å.[92]

Complexes **89-Cl** and **89-Br** are paramagnetic compounds, as is evident from their ^{1}H NMR spectra that display broad resonances in the range of 0–30 ppm. The strongest effect on the chemical shift experience the protons of the carbene backbone in close proximity to the iron center ($C^{4,5}$-*H* positions) in comparison to the free carbene (≈27 ppm and 6.62 ppm correspondingly). Despite of the fact that the compounds are paramagnetic and chemical shifts are unpredictable, ^{1}H NMR spectroscopy was helpful to verify the purity of the complexes.[93]

When 1,3-bis(2,6-diisopropylphenyl)imidazol-2-ylidene (IDipp) was employed for the reaction, only the monocarbene complex $[FeCl_2(IDipp)]$ (**90)** was isolated, as result of the

[93] The integral intensity of the signals corresponding to these paramagnetic compounds is about 50% lower, than the actual "content" of the complexes in solution, as was once checked by a measurement of a mixture of complex $FeCl_2(IMes)_2$ and carbene IMes.

increased steric demand of the carbene. The reaction required heating to reach completion (Scheme 75).

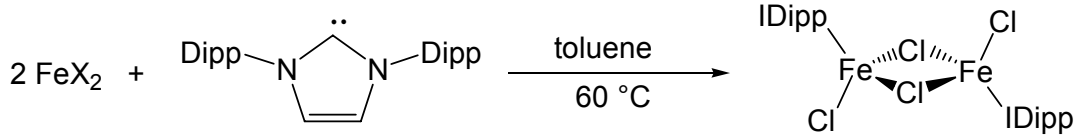

Scheme 75: Synthesis of complex **90**. IDipp = 1,3-bis(2,6-diisopropylphenyl)imidazol-2-ylidene.

The complex was isolated as brown crystals in 46% yield and characterized by ^{1}H NMR spectroscopy and elemental analysis. The structure was determined by X-ray crystallography (Figure 70).

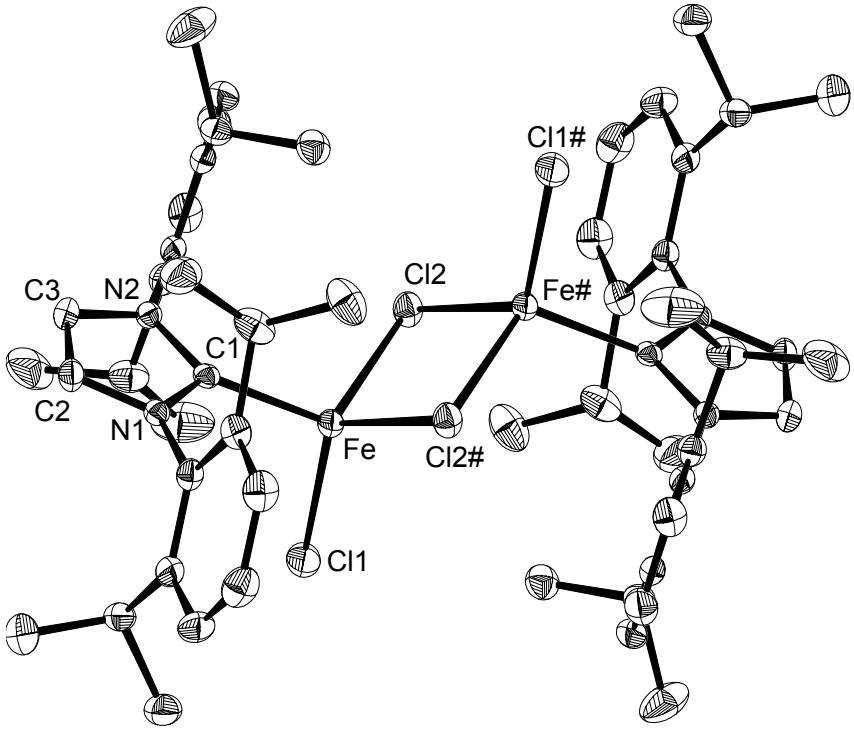

Figure 70: DIAMOND plot of the molecular structure of **90**. Thermal ellipsoids are set at 50% probability. Hydrogen atoms are omitted for clarity. Selected bond lengths [Å] and bond angles [°]: C1–Fe 2.104(1), Cl1–Fe 902.2421(4), Cl2–Fe 2.3639(4), Fe–Cl2# 2.4006(4), C1–N1 1.364(2), C1–N2 1.362(2), C2–C3 1.348(2); Fe-Cl2 Fe# 89.42(1), C1-Fe-Cl1 106.22(3), C1-Fe-Cl2 114.65(3), Cl1-Fe-Cl2 118.48(2), C1-Fe-Cl2# 114.07(3), Cl1-Fe-Cl2# 112.60(2), Cl2-Fe-Cl2# 90.58(1), N1-C1-N2 103.2(1).

Complex **90** features a dimeric structure in the solid state with bridging chlorine atoms. A crystallographic inversion center is located in the midpoint of the planar Fe_2Cl_2 ring. The iron center exhibit a distorted tetrahedral geometry with the bond angles ranging from 106–118° except of the Cl2-Fe-Cl2# angle (90.6°). There are three types of Fe–Cl bonds in the molecule. The distances between the iron center and the terminal and the two bridging atoms

are 2.2421(4) Å, 2.3639(4) Å, and 2.4006(4) Å respectively. The Fe–C bond length of 2.104(1) Å compares well with that in **89-Cl** (2.144(2) Å, mean value). The structure of the complex is similar to that of the iron dichloride-imine complex [(*i*Pr_3PNCH_2SPh)FeCl(μ-Cl)$_2$FeCl(*i*Pr_3PNCH_2SPh)].[204]

In the course of the studies complex **89-Cl** was treated with two equivalents of MeLi in diethyl ether at –78 °C (Scheme 76). The reaction afforded selectively the orange dimethyl derivative **91** which was isolated in 77% yield after crystallization from toluene. The reduction of complex **89-Cl** with sodium amalgam in toluene at room temperature lead to the formation of the biscarbene iron(I) chloride **92,** which was isolated in form of very dark purple-brown crystals in 66% yield, starting from $FeCl_2$. The coordinatevely unsaturated complex **92** reacted with two equivalents of isonitrile 2,6-$Mes_2C_6H_3NC$ to form bis-isonitrile complex **93** upon elimination of one carbene ligand (Scheme 76). The complex was isolated in 78% yield as brown-purple powder after crystallization from hexane. The compounds were characterized by X-ray crystallography, elemental analysis, ^{1}H NMR, EPR and Mössbauer spectroscopy.

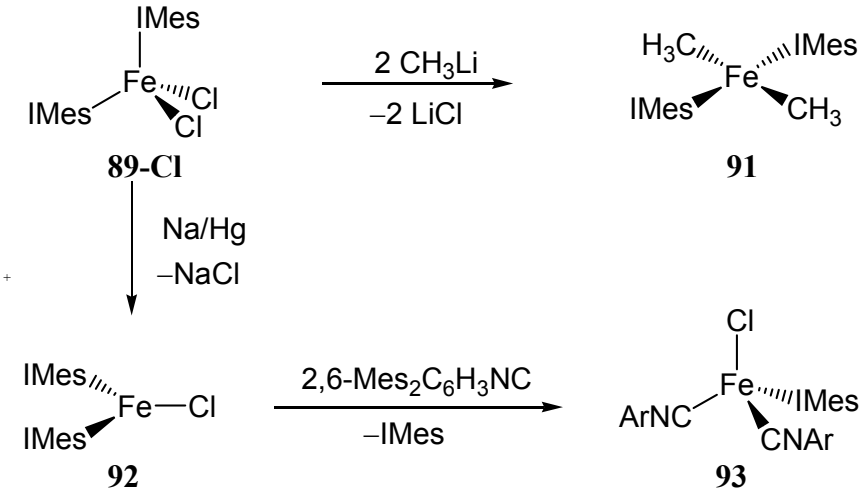

Scheme 76: Synthesis of carbene complexes **91**–**93**. IMes = 1,3-bis(2,4,6-trimethylphenyl)imidazol-2-ylidene. Ar = -C_6H_3-2,6-Mes_2.

The structure of the complex *trans*-[Fe$(CH_3)_2$(IMes)$_2$] (**91**) is depicted in Figure 71. The complex exhibits a square planar geometry of the iron center. The carbenes are twisted in relation to each other to minimize steric repulsion.[94] The Fe–CH_3 bond lengths are very similar (mean value 2.070(3) Å) and compare well with those, found in other iron methyl complexes, e.g. [Cp(CO)Fe(IMes)CH_3] (2.034(4) Å),[205] [Cp*($Ph_2PCH_2CH_2PPh_2$)FeCH_3]-

[94] As indicated by dihedral angles between the N-heterocycles of about 60°.

[BF_4] (2.109(7) Å)[206] and with the mean Fe–CH_3 bond length found in iron methyl complexes (2.08(6) Å).[95]

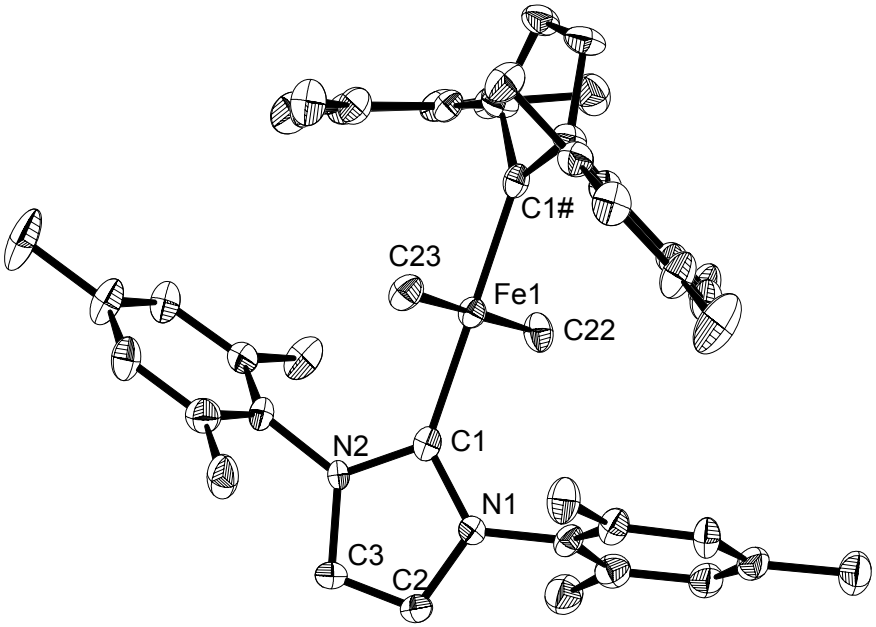

Figure 71: DIAMOND plot of the molecular structure of **91**. Thermal ellipsoids are set at 50% probability. Hydrogen atoms are omitted for clarity. Two independent molecules are found in the asymmetric unit. Selected bond lengths [Å] and bond angles [°] (values in brackets correspond to the second independent molecule): C1–Fe1, 1.948(3) [1.949(3)], C22–Fe1 2.072(5) [2.075(3)], C23–Fe 2.062(5) [2.072(3)], C2–C3 1.353(5) [1.334(5)], C1–N1 1.381(4) [1.386(4)], C1–N2 1.390(4) [1.377(4)]; C1-Fe-C2 179.3(2) [179.6(2)], C1-Fe1-C22 90.4(1) [90.6(1)], C1-Fe1-C23 89.6(1) [89.4(1)], N1-C1-N2 101.0(3) [101.4(2)].

It is interesting to compare the tetrahedral complex [$FeCl_2(IMes)_2$] (**89-Cl**) with the square planar complex [$Fe(CH_3)_2(IMes)_2$] (**91**). The Fe–$C_{carbene}$ bonds in **91** of 1.949(3) Å are significantly shorter than those in the tetrahedral complex **89-Cl** (2.144(2) Å) and **89-Br** (2.142(3) Å).[92] A similar phenomenon was observed earlier for the Fe–P bond lengths of the square planar complex [$Fe(PMe_3)_2Mes_2$] and tetrahedral [Fe(depe)Mes_2] complexes (depe = 1,2-bis(diethylamino)ethane.[207] The lengthening of the Fe–$C_{carbene}$ bond can be attributed to the population of antibonding orbitals in the high-spin complex **89-Cl** (*vide infra*).

The complexes **89-Cl** and **91** were investigated by Mössbauer spectroscopy (Figure 72). The isomer shifts of the complexes (0.81 and 0.27 mm/s respectively) compare well with those in previously reported iron (II) compounds.[208] The quadrupole splitting differ dramatically and is 1.97 mm/s for the tetrahedral complex **89-Cl** and 4.75 mm/s for the square

[95] According to a CSD survey from 10.2011 of 42 structurally characterized compounds of the type $L_nFe–CH_3$. Median *d*(Fe–C) = 2.085 Å, LQ = 2.008 Å, HQ = 2.179 Å.

planar complex **91**. The large quadrupole splitting was also observed earlier for the square planar complexes [Fe(PR_3)$_2$$Mes_2$] (4.63 mm/s, PR_3 = PEt_2Ph; 4.53 mm/s (PR_3)$_2$ = 1,2-bis(diphenylphosphino)ethane) and is consistent with the intermediate spin state (S = 1).[207] The geometry and spin changes are in agreement with the substitution of weak-field ligands (Cl) by strong-field ligands (CH_3), which increases the quadrupole splitting (Scheme 77).

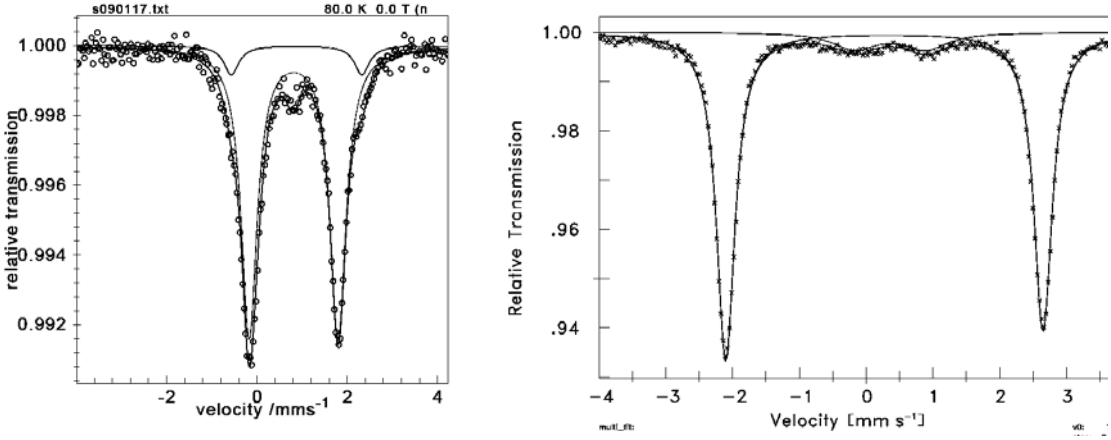

Figure 72: Mössbauer spectra of $FeCl_2(IMes)_2$ (**89-Cl**, left, I.S 0.81 mm/s, Q.S 1.97 mm/s) and $Fe(CH_3)_2(IMes)_2$ (**91**, right, I.S 0.27 mm/s, Q.S 4.75 mm/s).

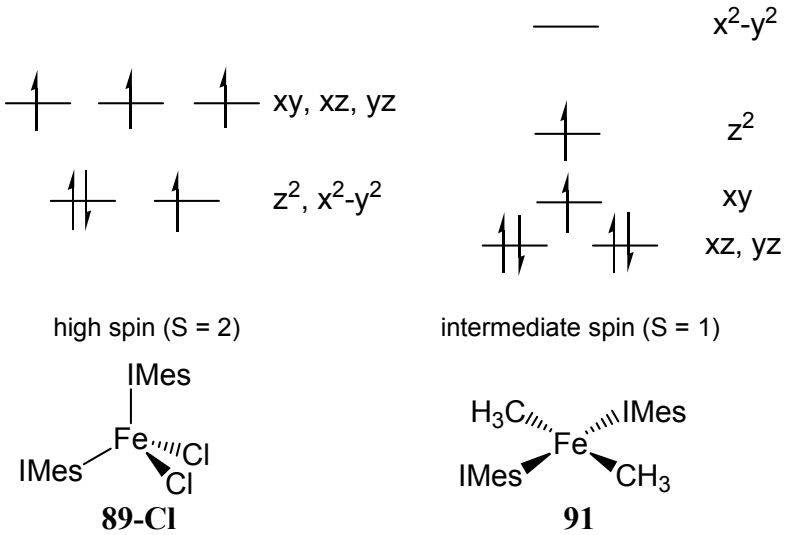

Scheme 77: Crystal field splitting diagram of tetrahedral and square planar complexes. IMes = 1,3-bis(2,4,6-trimethylphenyl)imidazol-2-ylidene. Adopted from ref. [207]

The reduction of **89-Cl** with sodium amalgam in toluene afforded the purple-brown iron (I) complex [Fe(IMes)$_2$Cl] (**92**, Scheme 76). The complex was isolated in 66% yield, starting from $FeCl_2$. The complex is soluble in aromatic hydrocarbons, insoluble in hexane or pentane and reacts with etheral solvents. Reduction of [Fe(IMes)$_2$$Br_2$] with Na/Hg was also attempted, but was unsuccessful. The structure of **92** was determined by X-ray diffraction analysis (Figure 73).

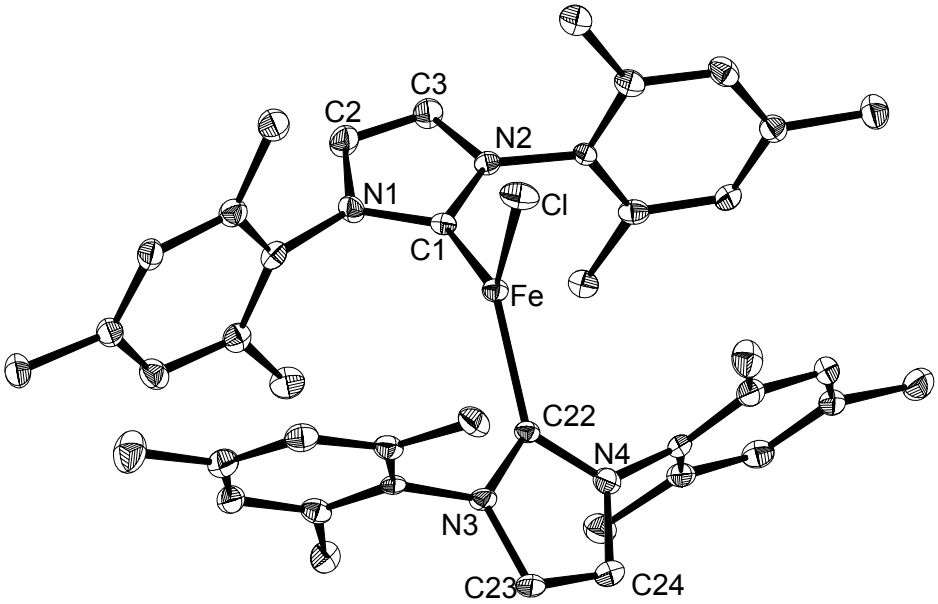

Figure 73: DIAMOND plot of the molecular structure of **92**. Thermal ellipsoids are set at 50% probability. Hydrogen atoms are omitted for clarity. Selected bond lengths [Å] and bond angles [°]: C1–Fe 2.009(3), C22–Fe 2.005(3), Cl–Fe 2.2554(8), C1–N1 1.399(4), C1–N2 1.359(4), C22–N3 1.365(4), C22–N4 1.381(4), C2–C3 1.323(5), C23–C24 1.341(5); C1-Fe-C22 126.56(12), C22-Fe-Cl 116.56(9), C1-Fe-Cl 116.88(9), N1-C1-N2 102.0(3), N3-C22-N4 101.7(3).

Complex **92** is a rare example of trigonal planar (Σ° = 360.0°) iron (I) complexes.[209-211] The mean Fe–C bond length of 2.007(3) Å, compares with that in the square planar complex **91 (**1.949(3) Å**)** and is significantly shorter than that in **89-Cl** (2.144(2) Å). The Fe–Cl bond of 2.2554(8) Å compares well with those in **89-Cl** (2.295(9) Å)[92] and **90** (2.2421(4) Å, terminal).

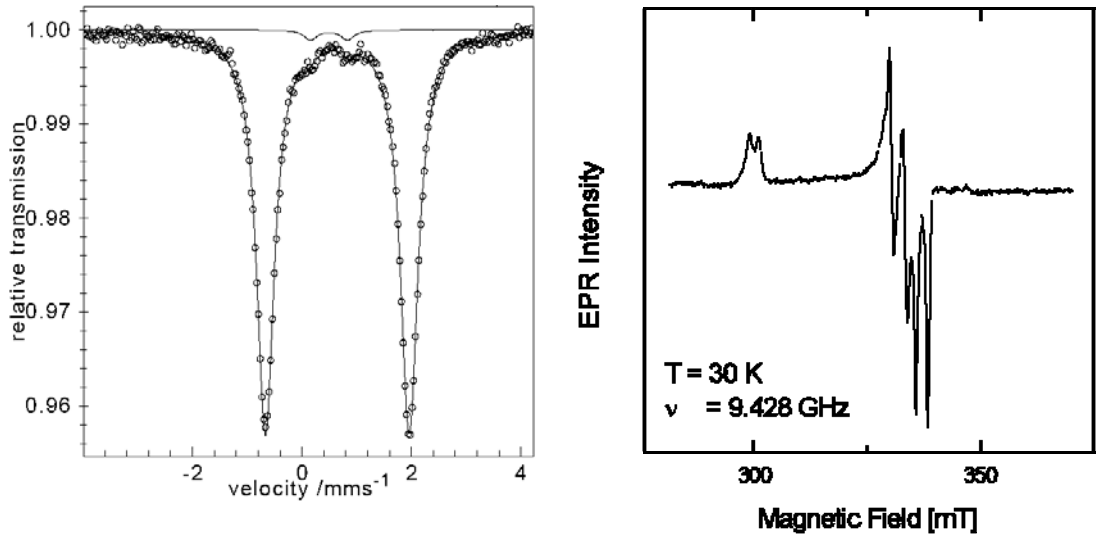

Figure 74: Mossbauer spectrum (I.S 0.65 mm/s, Q.S 2.63 mm/s) and EPR spectrum of $FeCl(IMes)_2$ (**92**).

The Mössbauer spectrum of complex **92** is depicted in Figure 74. The isomer shift (0.65 mm/s) and quadrupole splitting (2.63 mm/s) compares well with those of the formally Fe(I) dinitrogen complex [(N⌒N)Fe–N2–Fe(N⌒N)] (N⌒N = CH{C(Me)N(Dipp)}$_2$), reported by Holland et al. (0.62 mm/s and 1.41 mm/s respectively).[210] The isomeric shift also compares well with that of the pentacoordinate [(depe)$_2$FeCl] (0.29 mm/s; depe = 1,2-bis(diethylphosphino)ethane) and to those of four-coordinate Fe(I) complexes (0.41–0.59 mm/s).[111, 211, 212]

The reaction with the sterically demanding isonitrile (C_6H_3-2,6-Mes_2)NC afforded the product of substitution of one of the carbenes with additional coordination of one isonitrile ligand (**93**, Scheme 76). The brown-purple thermolabile complex was isolated in 78% yield and characterized by elemental analysis and NMR spectra. The structure of the tetrahedral complex was determined by X-ray diffraction analysis, however the crystals were of rather low quality. Attempts to reduce [Fe(IMes)$_2$Cl] (**92)** to Fe(0) products or substitute Cl by a CH_3 group were unsuccessful.

2.6 Other reactions

The discovery of reductive dehydrochlorination of chlorosilanes with N-heterocyclic carbenes suggested that the synthesis of silylidyne complexes might be possible from corresponding metallachlorosilanes (Scheme 78).[45, 131, 135]

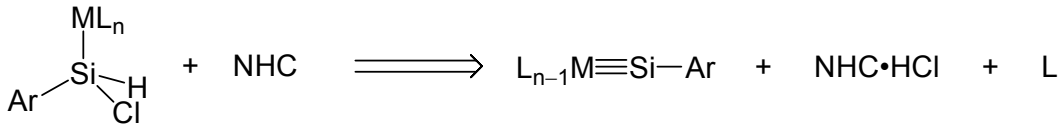

Scheme 78: A possible approach to silylidyne complexes.

To check this hypothesis the molybdenum silyl complexes **94**–**97** were prepared, starting from aryldichlorosilanes and carbonyl metallates according to Scheme 79.

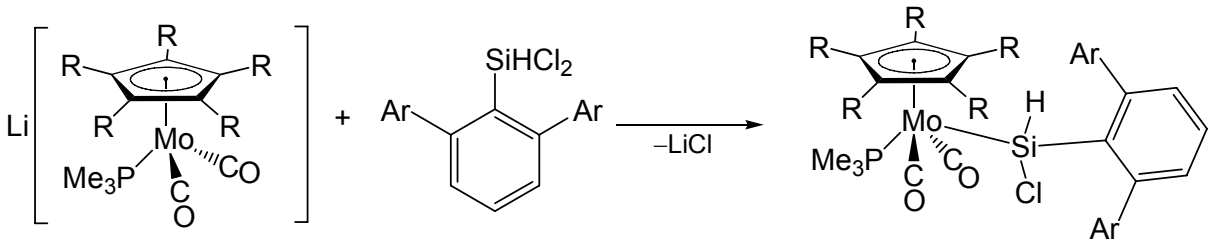

Scheme 79: Synthesis of molybdenum silyl complexes **94–97**. R = H, Ar = Mes (**94**), R = H, Ar = Trip (**95**), R = CH_3, Ar = Mes (**96**), R = CH_3, Ar = Trip (**97**).

The solid state structure of complex **95** was determined by X-ray diffraction analysis (Figure 75). On the basis of the NMR and IR spectra the structure of complexes **94**, **96**, **97** were found to be similar to that of **95**. The four-legged piano-stool complex **95** features a diagonal orientation of the carbonyl ligands. The Si center exhibits a distorted tetrahedral geometry with the bond angles lying in the range of 100–130°. The Mo–Si single bond length of 2.536(1) Å compares well with the previously reported silyl complexes (mean *d*(Mo–Si) = 2.55(5) Å).[73] The NMR and IR spectra of the complexes **94–97** are consistent with the structures. The complexes **94–97** feature two *ν*(CO) absorption bands of different intensities, e.g. for [Cp*Mo(CO)$_2$(PMe$_3$)–SiHCl(C$_6$H$_3$-2,6-Trip$_2$)] (**97**) at 1927 (s), 1853 (vs) cm^{-1} in hexane (1923 (s), 1848 (vs) cm^{-1} in toluene). For example, the IR spectra of **97** compares well with that of *trans*-[Cp*Mo(CO)$_2$(PMe$_3$)SiHCl$_2$] at 1930 (s), 1855 (vs) cm^{-1} in toluene.[213] The ^{29}Si NMR spectra display a doublet resonance signal due to the coupling to phosphorus nuclei, in the region, common for silyl complexes of molybdenum, e.g. 55.4 ppm for **97** (^2J(P,Si) = 13 Hz).[169]

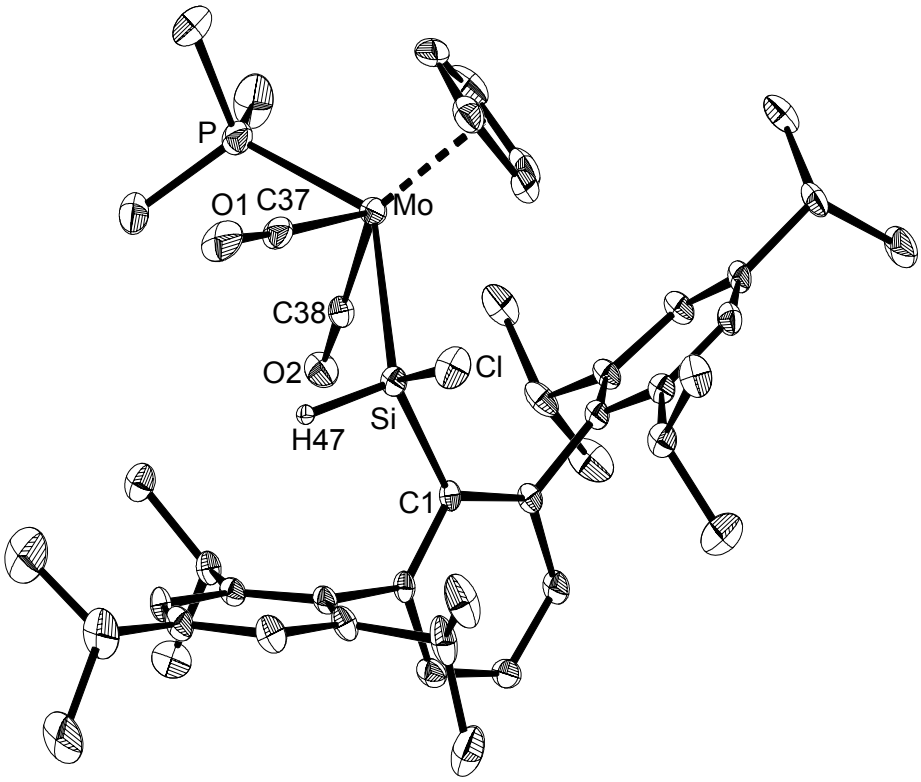

Figure 75: DIAMOND plot of the molecular structure of **95**. Thermal ellipsoids are set at 50% probability. Hydrogen atoms are omitted for clarity. Selected bond lengths [Å] and bond angles [°]: Mo–Si 2.536(1), C1–Si 1.928(3), Cl–Si 2.128(1), Mo–P 2.441(1), Si–H 1.40(4); C1-Si-H47 102(2), C1-Si-Mo 128(1), Cl-Si-H47 100(2), Cl-Si-Mo 109.67(5), H-Si-Mo 107(2), C38-Mo-C37 101.5(2), Si-Mo-P 129.78(3).

Attempts to eliminate HCl from the complex [$CpMo(CO)_2(PMe_3)$–$SiHCl(C_6H_3$-2,6-$Trip_2)$] (**95**) with several bases were made. The complex **95** was found to be stable towards heating with two equivalents of 1,3,4,5-tetramethylimidazol-2-ylidene in toluene for 24 h. The reaction was monitored by IR spectroscopy. Similarly, there was no reaction with *t*BuLi (Et_2O, –90 °C to RT); MeLi (Et_2O, 34 °C, several hours) and $NaN(SiMe_3)_2$ (Et_2O, RT, 15 min). We assume that complex **95** is unreactive due to steric reasons.

3 Summary and Outlook

3.1 Summary

Just like carbenes, elementary silylenes SiX_2 are reactive species. Their chemistry has been investigated in the past and typically relied on high temperature gas phase preparation *in situ*. Very little was known about the ways to stabilize elementary silylenes until recently (Chapter 1.1).

However in 2006 stabilization of a chlorosilylenes was achieved by using a suitable chelating two-electron donor ligand, blocking the empty *p*-orbital of the silicon center.[61, 64] In 2008 the Si(0) compound $Si_2(NHC)_2$ was reported.[68] That spurred my interest to investigate NHC-stabilized silylenes and how these compounds can be used in the chemistry of low-valent silicon compounds. The idea was to use *monodentate* donors, because like vices they could "grasp" the silylenes on the empty orbital, provide stability and allow derivatization. The key point is that they could also be removed later, much easier than a chelating ligand, thus enabling to study template chemistry of silylenes.

In the present work it was shown N-heterocyclic carbenes (NHC) are very suitable donors for this purpose. Following this approach several NHC-adducts of reactive silylenes were isolated as crystalline thermally stable solids. The NHC-adducts of $SiBr_2$ and SiI_2 were prepared upon reduction of the corresponding NHC adducts of silicon tetrahalides (Scheme 80).

The carbene-stabilized silylenes feature trigonal coordinated silicon center, suggesting the presence of a lone pair of eletrons. The structural and spectroscopic data indicate a rather strong Si–carbene donor acceptor bond, between the silylene fragment as the Lewis acid and the carbene as the Lewis base. The Si–carbene bond is therefore stable towards dissociation, as indicated by the stability of compounds themselves and also by the quantum chemical calculations. Thus, for example, the Si–carbene bond disscociation energy and Gibbs free dissociation energy in $SiBr_2$(IDipp) was calculated to be 123.7 $kJ \cdot mol^{-1}$ and +57.3 $kJ \cdot mol^{-1}$, respectively.

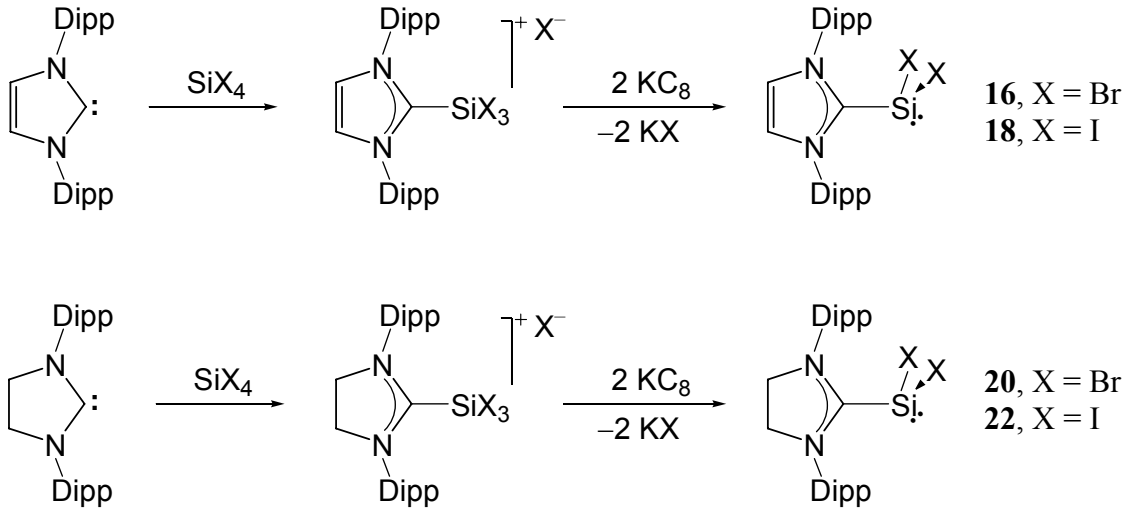

Scheme 80: Synthesis of NHC-stabilized dihalosilylenes upon reduction of Si(IV) precursors.

For studying the coordination chemistry of silylenes on transition metals, the first NHC-adducts of arylchlorosilylenes were also prepared upon dehydrochlorination of the corresponding aryldichlorosilanes with two equivalents of N-heterocyclic carbene (Scheme 81**)**. The compounds feature very bulky *m*-terphenyl substitunts that have been very useful in the chemistry of low-valent germanium tin and lead.

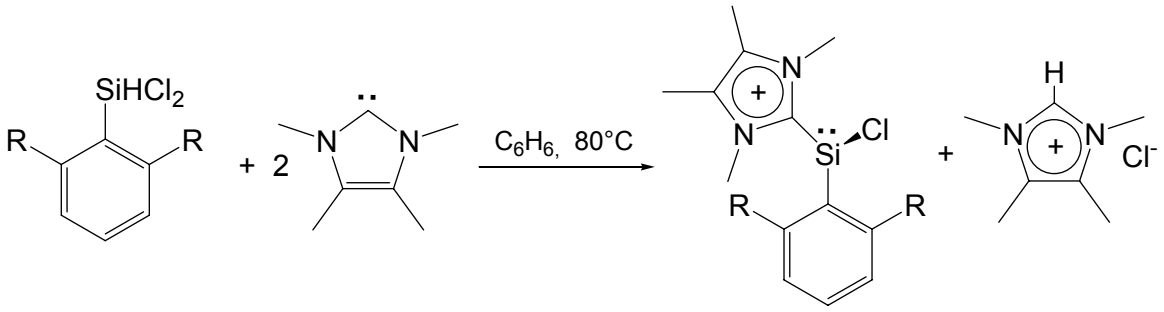

Scheme 81: Dehydrochlorination of aryldichlorosilanes with NHC.

The reactivity of SiX_2(NHC) and SiArCl(NHC) has been investigated in more detail. Thus, for example, the reduction of $SiBr_2$(ISdipp) afforded the corresponding Si(0) compound $Si_2(NHC)_2$ (**21**), and the reduction of $Si(C_6H_3\text{-}2,6\text{-}Mes_2)Cl(IMe_4)$ the Si(I) compound $\{Si(C_6H_3\text{-}2,6\text{-}Mes_2)(IMe_4)\}_2$ (**32**, Scheme 82**)**.

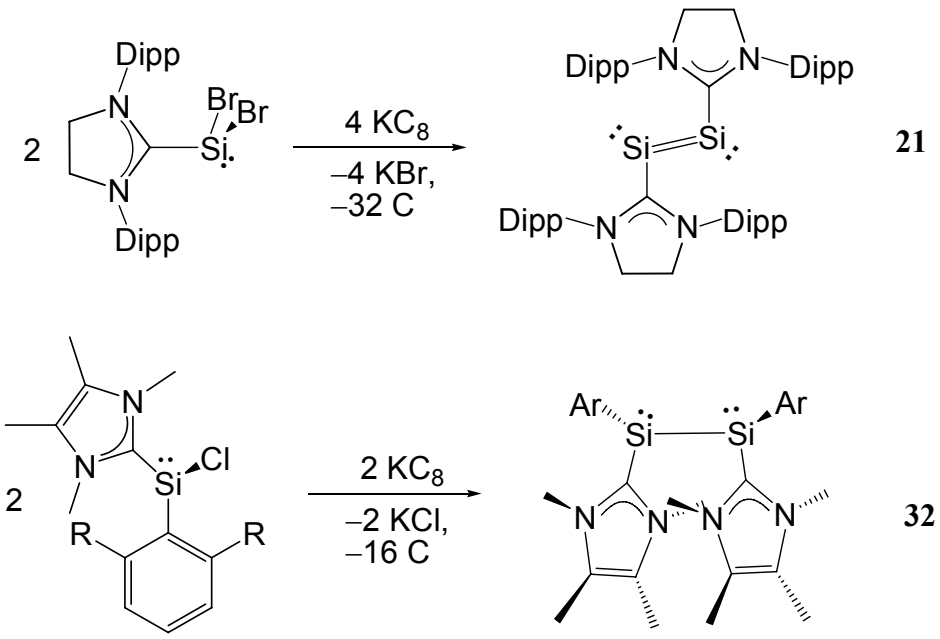

Scheme 82: Reduction of $SiBr_2$(ISdipp) and Si(C_6H_3-2,6-Mes_2)Cl(IMe_4).

The NHC-stabilized silylenes were found to be compounds of high synthetic potential. Starting from these Si(II) compounds, a unique approach to silylidene complexes of Group 6 transition-metals was achieved by metathetical exchange with carbonyl metallates was developed (Scheme 83**)**. Thereby, a series of zwitterionic silylidene complexes unprecedented up to date was obtained. The complexes were isolated as crystalline thermally stable solids and were fully characterized, also by X-ray diffraction analysis. The key features of the complexes are:

- The short and strong Si=M double bonds; *d*(Cr=Si) = 2.16–2.18 Å, *d*(Mo=Si) = 2.28–2.35 Å, *d*(W=Si) = 2.29 Å;
- The presence of trigonal planar coordinated silicon centers; sum of bond angles at the Si center is 360°;
- The ^{29}Si NMR resonances of the compounds, which apperar at low field (δ = 39–202 ppm).

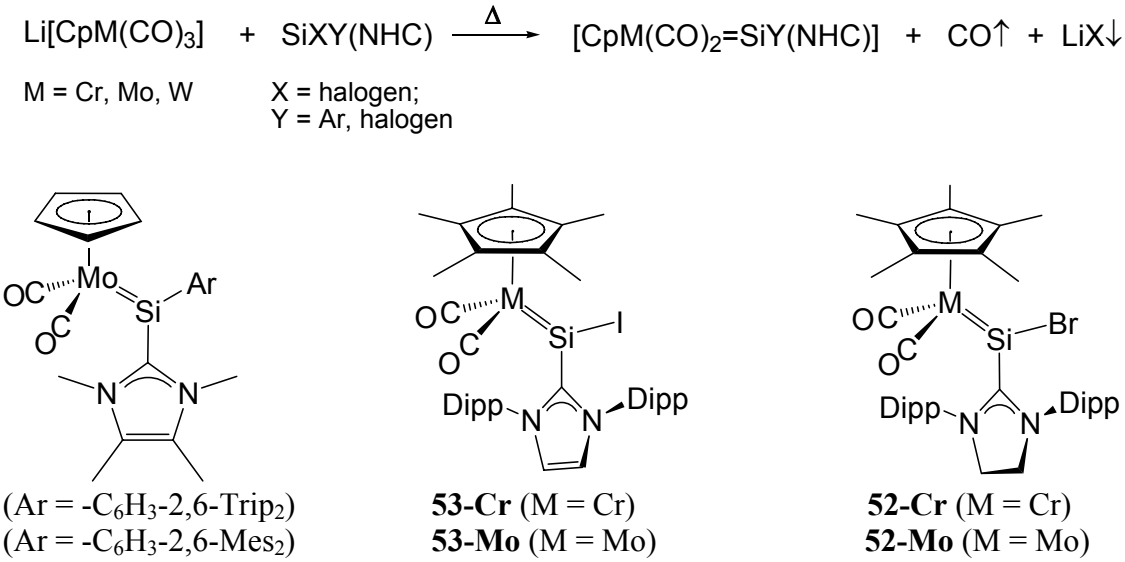

42 (Ar = -C_6H_3-2,6-$Trip_2$) **53-Cr** (M = Cr) **52-Cr** (M = Cr)
43 (Ar = -C_6H_3-2,6-Mes_2) **53-Mo** (M = Mo) **52-Mo** (M = Mo)

Scheme 83: NHC-stabilized silylenes as sources of new types of silylidene complexes.

The halosilylidene complexes are particularly interesting in the light of a possible halide substitution by nucleophiles, providing a general access to various silylidene complexes. This approach was exemplified by exchange of halogen towards carbon-centered nucleophile (Scheme 84**)**.

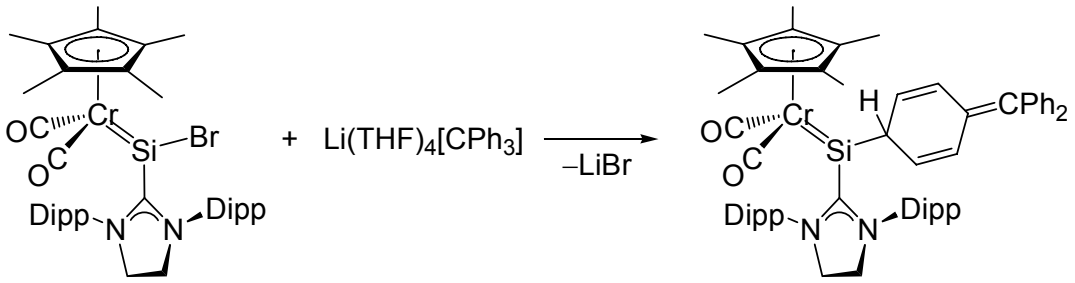

52-Cr **58**

Scheme 84: Halide substitution as a generic approach to silylidene complexes.

The zwitterionic silylidene complexes can be formally viewed as NHC-stabilized silylidyne complexes. In fact, NHC abstraction from the complex [$Cp(CO)_2Mo$=SiAr(NHC)] (**42**, Ar = -C_6H_3-2,6-$Trip_2$) by an appropriate Lewis acid, such as a tris(aryl)borane, afforded the first silylidyne complex **60**. Furthemore, halide abstraction from halosilylidene complexes afforded unprecedented cationic silylidyne complexes of Cr, Mo and W (Scheme 85**)**. The complexes were isolated as thermally stable solids and were fully characterized.

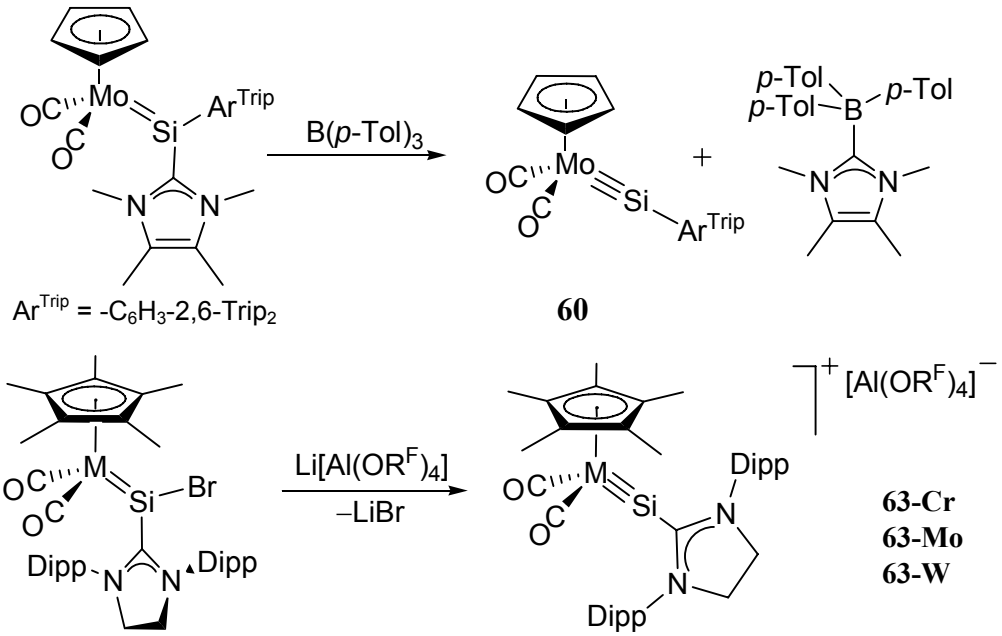

Scheme 85: Sythesis of the first silylidyne complexes (Dipp = -C_6H_3-2,6-*i*Pr_2).

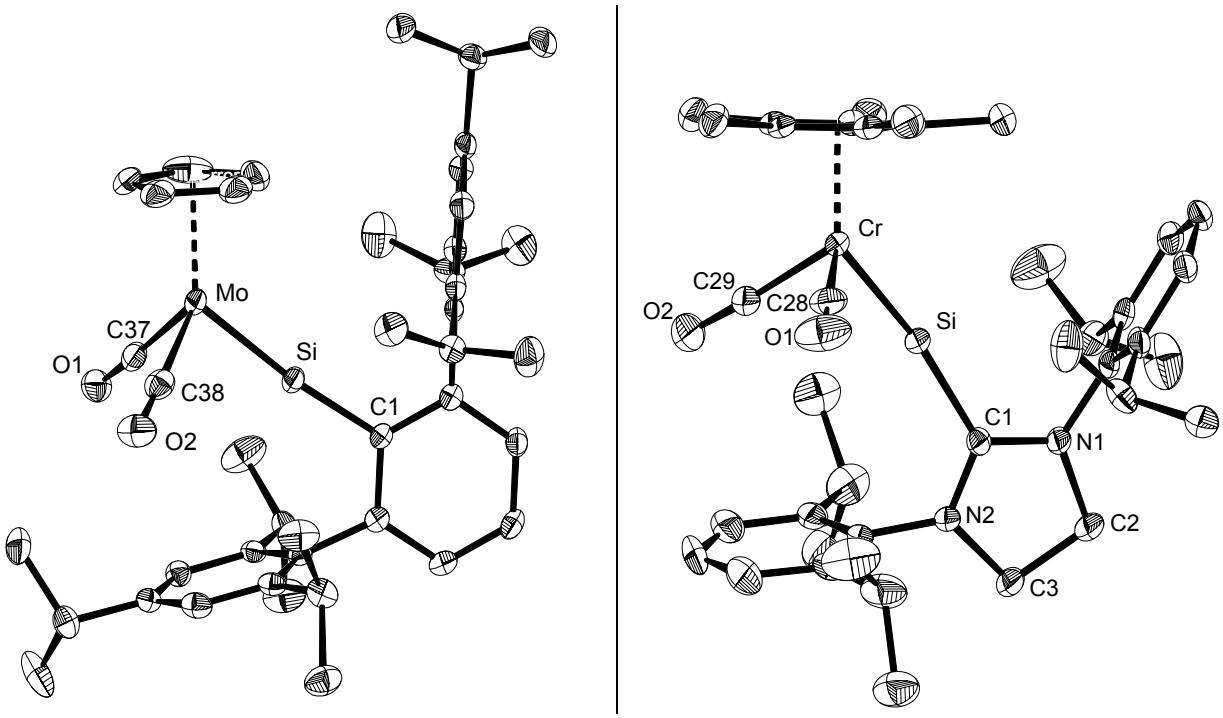

Figure 76: DIAMOND plot of the molecular structure of **60** (left) and complex cation in **62-Cr** (right).

The silylidyne complexes have several distinctive features:

- The M≡Si bonds are even shorter than the M=Si double bonds; *d*(Cr≡Si) = 2.12 Å, *d*(Mo≡Si) = 2.22 Å;
- The silicon center is linearly coordinated; ∠M-Si-C = 170–174°;

- The ^{29}Si NMR resonances of the compounds apperar at lower field (δ = 129–320 ppm), than those of the parent silylidene complexes.

Metal ylidyne complexes of Ge, Sn and Pb have been known for more than 15 years, however reactivity studies are still at their infancy. Therefore, I decided to investigate the chemistry of the prepared silylidyne complexes. The compouds have a very electrophilic silicon center. It was found, that the complexes react with almost every nucleophile. First reactions of the silylidyne complexes with polar reagents, such as HCl, H_2O, NH_3, $MesPH_2$, and anionic nucleophiles: Cl^-, N_3^-, CH_3^- are reported in the present work, providing access to a series of unprecedented silylidene complexes.

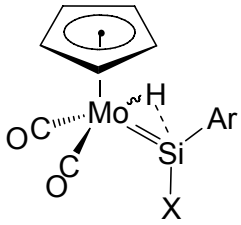

64 (X = OH),
66 (X = NH_2),
67 (X = Cl)

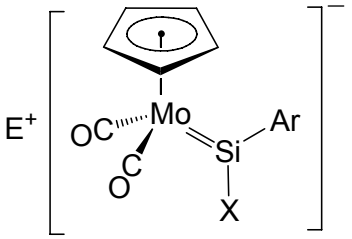

70 (E = NMe_4, X = Cl)
71 (E = NEt_4, X = N_3)
72 (E = Li, X = CH_3)

Figure 77: Silylidene complexes synthesized from [Cp(CO)$_2$Mo≡Si(C$_6$H$_3$-2,6-Trip$_2$) upon additrion of polar reagents (left) and nucleophiles (right).

The marked difference between carbon and silicon is reflected in the reactions of the silylidyne complexes with alkynes, which proceed smoothly already at ambient temperatures, leading to first metallasilacyclobutadienes. The isolation of these compounds raises the question about heteroalkyne metathesis.

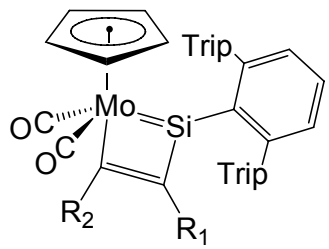

75–77 (R_1, R_2 = H, Me, Et),
78 (R_1 = Ph, R_2 = NMe_2),
79, 80 (R_1, R_2 = NMe_2, NEt_2)

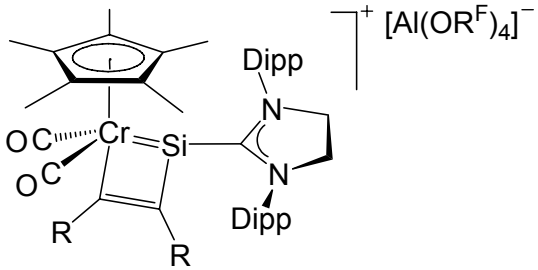

82 (R = Et)
83 (R = Me)

After the development of Group 6 silylidene complexes, an attempt was made to access group 8 transition-metals ylidyne complexes. Althogh, the silylidyne complexes were not synthesized, the project resulted in the isolation of ferrio- and ruthenogermylenes (Scheme 86**)**.

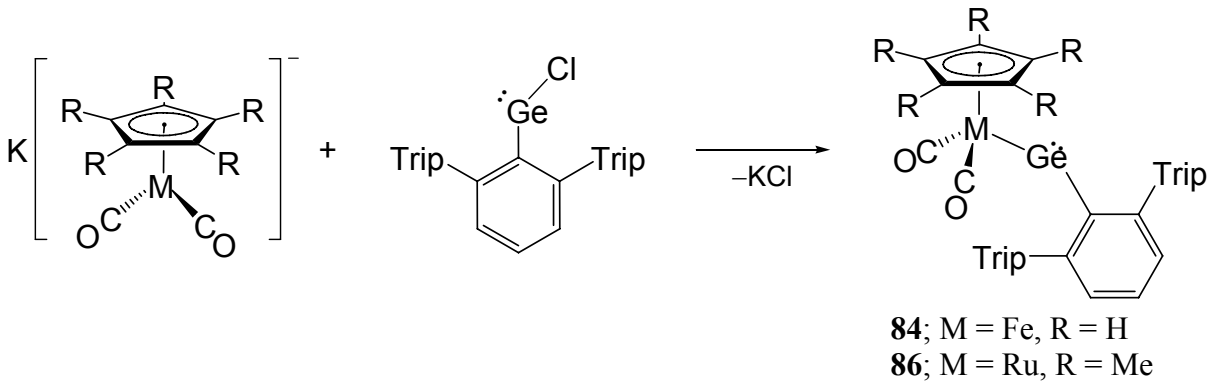

Scheme 86: Preparation of ferrio- and ruthenogermylenes.

In attempt to develop low oxidation state iron complexes, several novel open shell compounds have been made. The most interesting examples are very rare iron (I) chlorides: a trigonal planar 13VE complex **93** and a 15VE tetrahedral complex **94** (Scheme 87**)**. The complexes were isolated in a crystalline form and were fully characterized (p. 149).

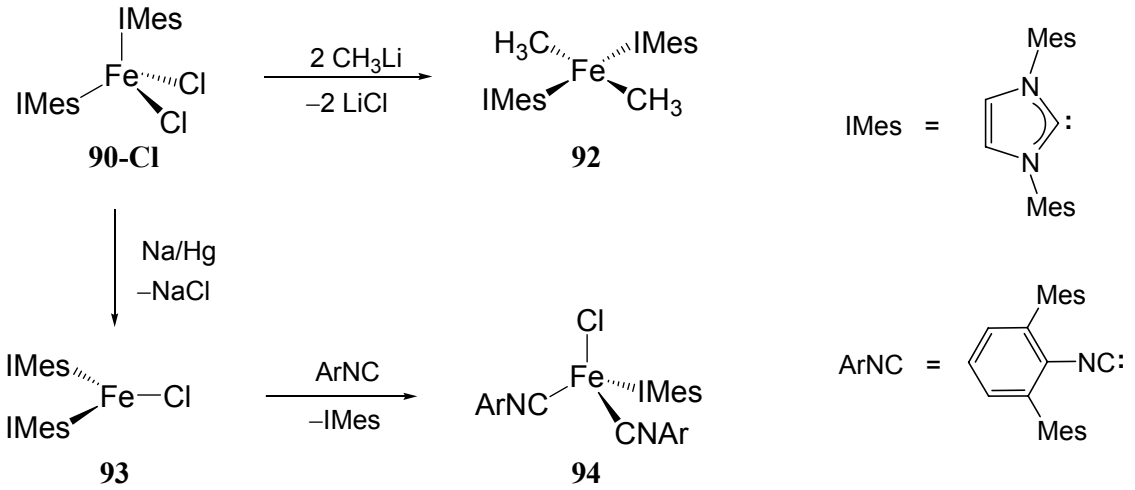

Scheme 87: Synthesis of carbene complexes **90–94**. IMes = 1,3-bis(2,4,6-trimethylphenyl)imidazol-2-ylidene.

3.2 Outlook

The high Si–$C_{carbene}$ bond strength in the NHC-adducts of silylenes is the key factor for the stabilization of the silylenes. However, in order to develop more reactive Si(II) synthons, a stabilization of the Si(II) center by weaker donors, such as amines or phosphanes, should be

advantageous (Figure 78). This approach was employed recently leading to the isolation of an amino-stabilized arylbromosilylene by Tamao et al.[69]

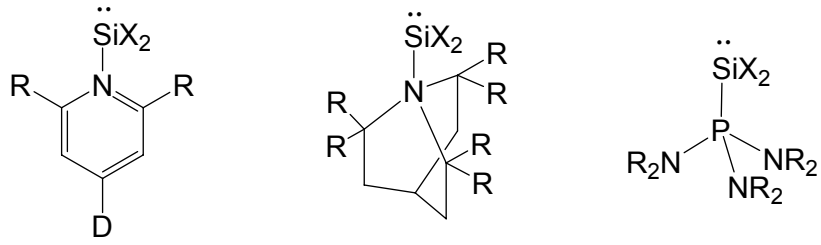

X = halogen, alkyl, aryl; R = bulky groups; D = H, R', NR'$_2$

Figure 78: Plausible donor-stabilized silylenes.

Both, the reduction of SiX_4 (X = Cl–I) and dehydrochlorination of silanes $SiRHCl_2$ in the presence of NHCs proceeds probably *via* the silylenoid intermediates $[SiX_3]^-$ and $[SiRCl_2]^-$. So far, very little is known about these possible intermediates. Therefore it would be very interesting to isolate such species, stabilized by bulky cations (e.g. $[PPh_4]^+$, $[PPN]^+$, Figure 79). For comparison, $[GeCl_3]^-$ and $[GeRCl_2]^-$ anions were reported.[111, 214] The synthesis of the corresponding silicon analogues may be achieved starting from SiX_2(NHC), SiRX(NHC) or better from $SiX_2(NR_3)$, $SiRX(NR_3)$, upon treatment with [cation]X, or upon deprotonation of the corresponding silanes ($SiHX_3$ and $SiRHX_2$) with a suitable bulky base, e.g. $[PPN][NR_2]$[96] or Schwesinger *t*Bu-P_4.[215]

Figure 79: Feasible silyl and organosilyl anions (X = F–I, N_3 etc.).

Substitution of halogen atoms in donor-stabilized silylenes can afford various Si(II) compounds, such as halosilylenes, substituted silylenes (donor-stabilized or not) and disilenes (Figure 80).

[96] It is not clear if such bases could be obtained. However other bases featuring bulky cations and anions should be considered.

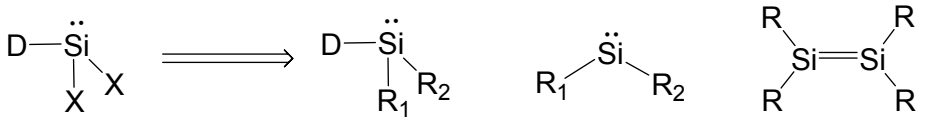

Figure 80: Synthesis of low-valent silicon compounds starting from silicon(II) halides.

By using donor-stabilized silylenes, the synthesis of metallasilylenes, silylidene and silylidyne complexes of other transition metals can be investigated. The synthetic approaches could be similar to those, which were proven successful for the syntheses of germylidyne complexes. However, using NHC- or other donor-stabilized silylenes implicates difficulties associated with the presence of the donor at the silicon center. In this respect amine- or phosphane-stabilized stabilized silylenes are potentially more attractive reagents, because in these compounds the Si–donor bond dissociation energy should be lower.

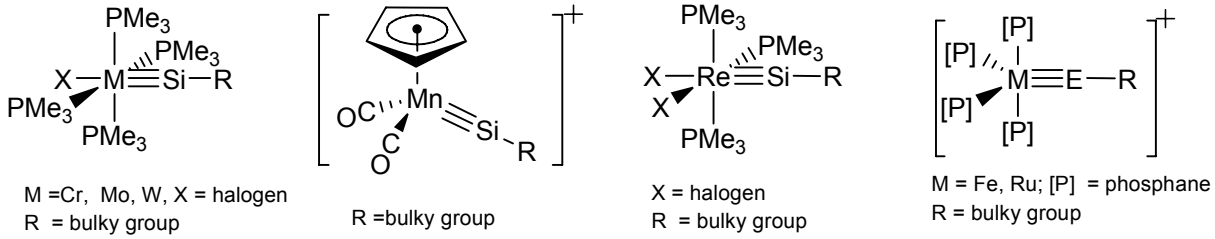

Figure 81: Feasible silylidyne complexes.

The reactions of silylidyne complexes with alkynes afforded metallasilacyclobutadienes. This type of compounds can be intermediates in silyne metathesis. As was found in the case of the alkyne metathesis, only metallacyclobutadiens featuring metals in high oxidation state undergo ring opening (metathesis). In this respect, the synthesis of high oxidation state silylidyne complexes should be investigated (Scheme 88).

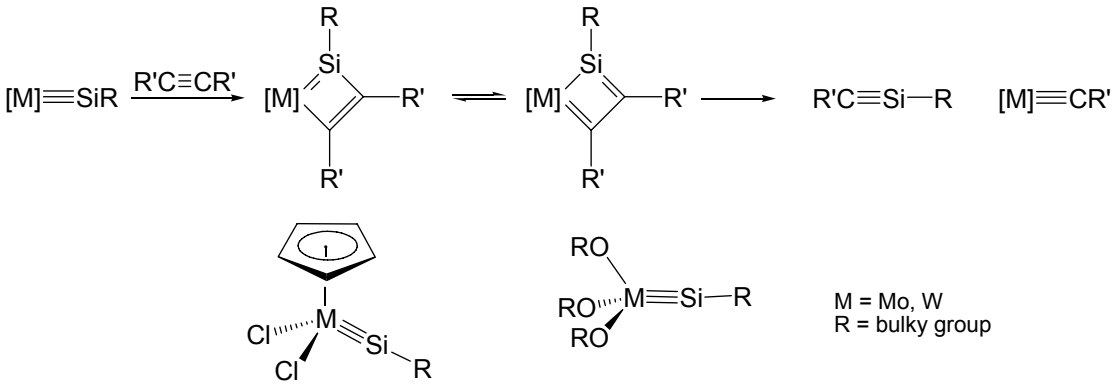

Scheme 88: Silyne metathesis. High oxidation state silylidyne complexes.

4 Experimental Section

4.1 General part

All experiments, if not otherwise mentioned, were carried out under an atmosphere of argon or nitrogen using Schlenk or glovebox techniques. Argon (99.996%) was used for glove boxes (MBraun). Argon (99.996%) was further purified by passing the gas through a column of 4 Å molecular sieves and Chromatography Research Supplies Model 1000 Oxygen trap before admission to the Schlenk lines, nitrogen (99.998%) was used without further purification. The glassware was kept in an isopropanol/KOH bath (typically overnight), washed with tap water, 5% HCl (for 1 h), then rinsed with water, deionised water and finally with acetone. The glassware was dried in the oven at approximately 110 °C and baked *in vacuo* (ca. 10^{-2} mbar) prior to use.

The solvents were refluxed over the corresponding drying agent, flushed several times with argon during reflux and distilled under argon. Solvents stored in the gloveboxes were additionally degassed. If not otherwise mentioned, for large scale experiments solvents stored over 4 Å molecular sieves were used.

Solvent	Predrying agent	Drying agent
Pentane, C_6H_5F, C_6H_5Cl, CH_3CN	–	CaH_2
Hexane	Na	Na/benzophenone/tetraglyme
Toluene, Xylene	–	Na
Benzol Et_2O, THF, DME	Na	Na/benzophenone
CH_2Cl_2	Sicapent	Na/Pb alloy

Table 12: Agents used for drying solvents.

For very sensitive compounds the solvents were recondenced from the corresponding drying agent: pentane, hexane from KC_8, diethyl ether, THF from K/benzophenone, DME from Na/K alloy. For air-stable compounds commercially available solvents were used without purification.

Whatman glass microfibre filters (GF/B, d = 25 mm) were used for filtrations. Cannulas with the filter attached to the one end with Teflon band were used for filtrations with pressure gradient of the inert gas. Syringes embedded with the filters were used in the gloveboxes.

Hydrocarbon Glisseal HV grease was routinely used. In the cases, when prolonged stirring or refluxing was required Roth PTFE paste was used. When working under inert gas conditions, the solvents were transferred via cannula from a Shlenk tube or with help of a syringe, sealed with a piece of rubber. Heating was carried out in an oil bath or in a heating mantle. Isopropanol, dry ice or liquid nitrogen were used for cooling to low temperatures. Cryostate Thermo Haake C50P was employed for circulation of cooling agent at low temperatures when nesseccary(sublimations, reflux condencers).

4.1.1 IR spectroscopy

IR spectra of solutions were recorded on a Nicolet 380 FT-IR spectrometer in the range of 2200−1500 cm^{-1} using a cell of NaCl or KBr windows. IR spectra of the pure solids were recorded on a Bruker Alpha FT-IR spectrometer in the range of 4000−400 cm^{-1} in the glove box using the platinum single reflection diamond ATR module or in a KBr pellet on a Nicolet 380 FT-IR spectrometer. IR spectra of solids in Nujol were recorded between a pair of NaCl plates. The following abbreviations were used for the intensities of the absorption bands: vs − very strong, s − strong, m − medium, w − weak, vw − very weak.

4.1.2 NMR spectroscopy

NMR spectra were recorded on a Bruker Avance DMX-300, DPX-300, DPX-400, DMX-500 or DRX-500 NMR spectrometer. The solvents for samples were dried over the corresponding drying agent, degassed and trap-to-trap recondenced; they were kept over 4 Å molecular sieves.

The ^{1}H and ^{13}C NMR spectra were calibrated against the residual proton and natural abundance ^{13}C resonances of the deuterated solvent relative to tetramethylsilane.[188] The ^{19}F, ^{29}Si, ^{31}P NMR spectra were calibrated against external pure $CFCl_3$, $SiMe_4$ and 85% H_3PO_4 respectively. The standard was filled in a capillary, which was sealed-off and introduced in a 5 mm NMR tube containing the corresponding deuterated solvent. The NMR tube was finally vacuum-sealed and used for the calibration. The ^{19}F NMR spectra recorded in fluorobenzene were calibrated against the solvent signal, set at δ_F = −113.1 ppm. The ^{29}Si NMR spectra recorded in C_5D_5Cl were calibrated against internal pure $SiMe_4$. The following abbreviations were used for the forms and multiplicities of the NMR signals: s − singlet, d − doublet, t − triplet, sept − septet, m − multiplet, br − broad. The ^{1}H and ^{13}C NMR signals were routinely

assigned by a combination of H,H-COSY, HMQC, HMBC and DEPT experiments. Indexes (‘) and (‘‘) were used to designate pair of diastereotopic groups in chiral compounds, e.g. the Trip substituents in 2,6-$Trip_2$-C_6H_3-X (**28**, **29**, **38**, **41** etc.). Indexes (A) and (B) were used to designate diastereotopic methyl groups of the isopropyl substituents, typically in Trip.

Solvent	Drying agent	^{1}H NMR, δ, ppm	^{13}C NMR, δ, ppm
C_6D_6	Na	7.15 (br)	128.0 (3)
Toluene-d_8	Na	2.09 (5)	20.4 (7)
THF-d_8	Na	1.73 (br)	25.3 (5)
CD_3CN	CaH_2	1.93 (5)	1.3 (7)
CD_2Cl_2	CaH_2	5.32 (3)	53.8 (5)
$CDCl_3$	CaH_2	7.24 (1)	77.0 (3)
C_6D_5Cl	CaH_2	6.96 (br)	125.96 (3)[97]
DMSO-d_6	none	2.49 (5)	39.5 (7)

Table 13: Preparation of deuterated solvents and calibration (multiplicity of the signals in brackets).

4.1.3 X-ray crystallography

Typically, crystals for the X-ray diffraction analysis were collected from a supernatant solution at the temperature of crystallization, washed if necessary, and covered with Fomblin Y® lubricant. A crystal suitable for the measurement was selected on a microscope and transferred to the y diffractometer. The data were collected on a OE IPDS IIT equipped with an Oxford Cryostream 700er series low-temperature cooling device; on a Bruker X8-KappaApexII equipped with a KRYOFLEX, Bruker AXS low-temperature cooling device; or on a Nonius Kappa CCD equipped with an Oxford Cryostream 600er series low-temperature cooling device. In all diffractometers Mo-K_α graphite-monochromated radiation (λ = 0.71073 Å) was used. The sample handling, measurement, structure solution and full refinement was done by the central X-ray facility of the Institute.

[97] G. R. Fulmer, A. J. M. Miller, N. H. Sherden, H. E. Gottlieb, A. Nudelman, B. M. Stoltz, J. E. Bercaw, K. I. Goldberg, *Organometallics* **2010**, *29*, 2176.

4.1.4 Elemental analysis

The Elemental analysis samples were prepared in a glovebox under argon. The measurements were conducted on an Elementar Vario Micro elemental analyzer or a Leco CHNS-932 analyzer. The samples were measured in triplicate; the individual C, H, N values did not differ by more than 0.3% (absolute). The mean values of the measurements are given. The sample handling and measurement was done by the central EA facility of the Institute.

4.1.5 Melting points determination

The melting points were measured on a Büchi apparatus (patent №320388). The apparatus was calibrated against pure samples of vanillin (m.p. 83 °C), phenancilin (136 °C) and caffeine (237 °C). The measurements were done in duplicate. The s samples were ealed under vacuum and heated fast to a temperature of ca 20 K below the melting (decomposition) point, and then heated slowly (2–3 K/min) until they melted or decomposed.

4.1.6 Mössbauer and EPR spectroscopy

The samples for the Mössbauer measurements were placed in airtight aluminum sample holders in the glovebox under argon and stored in a Schlenk-tube prior to measurement. The samples for EPR measurements (about 1 mM solutions) were degassed and sealed in quartz tubes under vacuum. All samples were measured at the Max Planck Institute for Bioinorganic Chemistry in Mülheim, Germany.

4.1.7 Cyclic voltammetry

All cyclic voltammetric studies were performed with an Autolab Eco electrochemical workstation composed of an Autolab PGSTAT 20 potentiostat/galvanostat. The results were analyzed with the Autolab software version 4.9. The experiments were carried out in a glovebox under argon in a gas-tight specially designed full-glass three-electrode cell. A glass-carbon disk electrode (d = 2 mm) was used as working electrode, a Pt wire of 1 mm diameter as counter electrode and a $Fe(C_5Me_5)_2/Fe(C_5Me_5)_2^+$ solution (4 mM in THF/0.1 M $(NBu_4)PF_6$) as reference electrode, which was separated from the substrate/electrolyte solution by a Luggin capillary fitted with a Vycor Diaphragm (4 mm). THF was used as solvent and 0.1 M tetra-*n*-butylammonium hexafluorophosphate, as supporting electrolyte.

THF was dried upon refluxing over sodium-wire, purged several times during reflux with argon and distilled under argon. *iR*-drop compensation was used for all experiments.[154]

4.2 Syntheses

4.2.1 [SiBr$_3$(IDipp)]Br (15)

Silicon tetrabromide (2.79 g, 8.02 mmol) was added to a stirred suspension of IDipp (3.12 g, 8.03 mmol) in 25 mL of hexane at ambient temperature within 2 min. The formation of a voluminous, white precipitate was observed. The mixture was stirred for 3 h, the precipitate was filtered off and then dried *in vacuo* to give 5.62 g (7.63 mmol, 95%) of the crude product as a white powder. The crude product can be directly used for the synthesis SiBr$_2$(IDipp). It was found by ^{1}H NMR spectroscopy to contain 10% of an impurity of unknown structure. Crystallization of the crude product from CH_2Cl_2 at –60 °C afforded large, colorless crystals of the solvate **15**·3(CH_2Cl_2), which were separated from the mother liquor and dried for 12 h at ambient temperature and to give **15** as a white solid. Elemental analysis calcd (%) for $C_{27}H_{36}Br_4N_2Si$ (736.27): C 44.04, H 4.93, N 3.81; found: C 44.07, H 4.99, N 3.64%.

^{1}H NMR (300.1 MHz, C_6D_6, 298 K, ppm): δ = 0.92 (d, ^3J(H,H) = 6.8 Hz, 12H, 4 × CH*Me$_A$*Me$_B$), 1.48 (d, ^3J(H,H) = 6.8 Hz, 12H, 4 × CHMe$_A$*Me$_B$*), 3.30 (sept, ^3J(H,H) = 6.8 Hz, 4H, 4 × C*H*Me$_A$Me$_B$), 6.46 (s, 2H, C^{4,5}-*H*), 7.12 (d, ^3J(H,H) = 7.8 Hz, 4H, 2 × C^{3,5}-*H*, Dipp), 7.23 (t, ^3J(H,H) = 7.8 Hz, 2H, 2 × C^4-*H*, Dipp).

^{1}H NMR (300.1 MHz, CD_2Cl_2, 298 K, ppm): δ = 1.23 (d, ^3J(H,H) = 6.8 Hz, 12H, 4 × CH*Me$_A$*Me$_B$), 1.34 (d, ^3J(H,H) = 6.8 Hz, 12H, 4 × CHMe$_A$*Me$_B$*), 2.34 (sept, ^3J(H,H) = 6.8 Hz, 4H, 4 × C*H*Me$_A$Me$_B$), 7.39 (d, ^3J(H,H) = 7.8 Hz, 4H, 2 × C^{3,5}-*H*, Dipp), 7.65 (t, ^3J(H,H) = 7.8 Hz, 2H, 2 × C^4-H, Dipp), 8.79 (s, 2H, C^{4,5}-*H*).

^{13}C{^{1}H} NMR (75.47 MHz, CD_2Cl_2, 298 K, ppm): δ = 22.5 (s, 4C, 4 × CHMe$_A$*Me$_B$*), 26.2 (s, 4C, 4 × CH*Me$_A$*Me$_B$), 29.8 (s, 4C, 4 × C*H*Me$_A$Me$_B$), 125.4 (s, 4C, 2 × *C^{3,5}*-H, Dipp), 131.1 (s, 2C, 2 × *C^1*, Dipp), 132.6 (s, 2C, *C^{4,5}*-H), 133.4 (s, 2C, 2 × *C^4*-H, Dipp), 136.3 (s, 1C, Si-*C*N$_2$), 145.7 (s, 4C, 2 × *C^{2,6}*, Dipp).

^{29}Si NMR (99.36 MHz, CD_2Cl_2, 298 K, ppm): δ = –63.9 (s).

4.2.2 SiBr$_2$(IDipp) (16)

20 mL of precooled THF (–60 °C) was added to a Schlenk tube containing a mixture of **15** (1.00 g, 1.36 mmol) and KC_8 (459 mg, 3.40 mmol, 2.50 eq). The reaction mixture was stirred

for 30 min at −35 °C, and then for 2 h at ambient temperature to give a yellow to orange solution and a black precipitate (carbon). The suspension was filtered, and the filtrate was evaporated to dryness in vacuo. The residue was dried for 30 min *in vacuo* and treated with 20 mL of benzene. The suspension was filtered from a small amount of insoluble material, the filtrate was concentrated *in vacuo* to ca. 3 mL (incipient crystallization) and stored for 12 h at +5 °C to complete crystallization of the product. The obtained crystals were separated by filtration from the mother liquor and dried under vacuum (30 min, 25 °C) to give **2** as a yellow powder. Yield: 380 mg (0.66 mmol, 48%). Elemental analysis calcd (%) for $C_{27}H_{36}Br_2N_2Si$ (576.47): C 56.25, H 6.29, N 4.86; found: C 57.78, H 6.44, N 4.82%.

^{1}H NMR (400.1 MHz, C_6D_6, 298 K, ppm): δ = 0.98 (d, ^3J(H,H) = 6.8 Hz, 12H, 4 × CHMe_AMe$_B$), 1.43 (d, ^3J(H,H) = 6.8 Hz, 12H, 4 × CHMe$_A$$Me_B$), 2.81 (sept, ^3J(H,H) = 6.8 Hz, 4H, 4 × C*H*Me$_A$Me$_B$), 6.41 (s, 2H, C^{4,5}-*H*), 7.06 (d, ^3J(H,H) = 7.8 Hz, 4H, 2 × C^{3,5}-*H*, Dipp), 7.21 (t, ^3J(H,H) = 7.8 Hz, 2H, 2 × C^4-*H*, Dipp).

^{13}C{^{1}H} NMR (125.8 MHz, C_6D_6, 298 K, ppm): δ = 22.9 (s, 4C, 4 × CHMe$_A$$Me_B$), 25.7 (s, 4C, 4 × CH$Me_AMe_B$), 29.4 (s, 4C, 4 × *C*HMe$_A$Me$_B$), 124.5 (s, 4C, 2 × $C^{3,5}$-H, Dipp), 124.8 (s, 2C, $C^{4,5}$-H), 131.3 (s, 2C, 2 × C^4-H, Dipp), 133.4 (s, 2C, 2 × C^1, Dipp), 145.7 (s, 4C, 2 × $C^{2,6}$, Dipp), 164.5 (s, 1C, Si-*C*N$_2$).

^{29}Si NMR (99.36 MHz, C_6D_6, 298K, ppm): δ = 10.9 (s). ^{29}Si{^{1}H} MAS-NMR (79.77 MHz, 298 K, ppm): δ = 15.8 ppm (s, $\Delta\nu_{1/2}$ (full width at half maximum) = 120 Hz).

4.2.3 [SiI$_3$(IDipp)]I (17)

A solution of IDipp (3.81 g, 9.80 mmol) in 50 mL of toluene was added to a stirred suspension of SiI_4 (5.35 g, 10.0 mmol) in 20 mL of toluene at ambient temperature within 10 min. A voluminous, yellow precipitate was rapidly formed. The mixture was stirred for 14 h, the precipitate was filtered off, washed with 30 mL of toluene and then dried *in vacuo* for 30 min at room temperature to give **17** as a yellow powder. Yield: 8.71 g (9.42 mmol, 96% based on IDipp). Crystallization of the product from $CHCl_3$ at –60 °C afforded large, yellow crystals of the solvate **17**·3($CHCl_3$), which were suitable for a single-crystal X-ray diffraction study. M.p. = 197 °C (dec.). Elemental analysis calcd (%) for $C_{27}H_{36}I_4N_2Si$ (924.27): C 35.08, H 3.93, N 3.03; found: C 35.19, H 3.96, N 2.97%.

^{1}H NMR (300.1 MHz, $CDCl_3$, 298 K, ppm): δ = 1.23 (d, ^3J(H,H) = 6.9 Hz, 12H, 4 × CHMe_AMe$_B$), 1.37 (d, ^3J(H,H) = 6.9 Hz, 12H, 4 × CHMe$_A$$Me_B$), 2.41 (sept, ^3J(H,H) = 6.7 Hz,

4H, 4 × C*H*Me$_A$Me$_B$), 7.34 (d, ^3J(H,H) = 7.8 Hz, 4H, 2 × $C^{3,5}$-*H*, Dipp), 7.60 (t, ^3J(H,H) = 7.8 Hz, 2H, 2 × C^{4}-*H*, Dipp), 8.54 (s, 2H, C^{4,5}-*H*).

^{13}C{^{1}H} NMR (125.8 MHz, $CDCl_3$, 298 K, ppm): δ = 22.9 (s, 4C, 4 × CHMe$_A$*Me$_B$*), 26.5 (s, 4C, 4 × CH*Me$_A$*Me$_B$), 29.6 (s, 4C, 4 × *C*HMe$_A$Me$_B$), 125.3 (s, 4C, 2 × $C^{3,5}$-H, Dipp), 125.5 (s, 1C, Si-*C*N$_2$), 131.6 (s, 2C, 2 × C^{1}, Dipp), 132.5 (s, 2C, $C^{4,5}$-H), 133.2 (s, 2C, 2 × C^{4}-H, Dipp), 145.8 (s, 4C, 2 × $C^{2,6}$, Dipp).

^{29}Si NMR (59.63 MHz, $CDCl_3$, 298 K, ppm): δ = –225.8 (s).

4.2.4 SiI_2(IDipp) (18)

100 mL of precooled THF (−100 °C) was added to a Schlenk tube containing a mixture of **17** (8.71 g, 9.42 mmol) and KC_8 (2.94 g, 21.7 mmol, 2.31 eq). The stirred reaction mixture was allowed to warm up slowly to –15 °C. In the temperature range of –30 °C to –15 °C a gradual color change of the reaction mixture from red-brown over brown and to green was observed. The reaction mixture was then allowed to warm within 1 h to ambient temperature to give an orange-brown solution and a green precipitate. The suspension was filtered, and the filtrate was evaporated to dryness in vacuo. The residue was dried for 15 min *in vacuo* and treated with a mixture of 60 mL of benzene and 2 mL of hexane. The yellow-brown extract was filtered from an insoluble brown-red material, and the filtrate was concentrated in *vacuo* to ca. 10 mL (incipient crystallization). 10 mL of hexane were added and the mixture was stored for 12 h at +5 °C to complete crystallization of the product. The obtained microcrystalline product was separated by filtration from the mother liquor, washed with 8 mL of a hexane-toluene mixture (3:1) and dried at 0.05 mbar for 90 min at ambient temperature to give **18** as a yellow powder. Yield: 3.98 g (5.94 mmol, 63%). The compound starts to decompose above 160 °C turning brown. Elemental analysis calcd (%) for $C_{27}H_{36}I_2N_2Si$ (670.48): C 48.37, H 5.41, N 4.18; found: C 49.31, H 5.41, N 4.13%.

^{1}H NMR (300.1 MHz, C_6D_6, 298 K, ppm): δ = 0.97 (d, ^3J(H,H) = 6.8 Hz, 12H, 4 × CH*Me$_A$*Me$_B$), 1.45 (d, ^3J(H,H) = 6.8 Hz, 12H, 4 × CHMe$_A$*Me$_B$*), 2.83 (sept, ^3J(H,H) = 6.8 Hz, 4H, 4 × C*H*Me$_A$Me$_B$), 6.42 (s, 2H, C^{4,5}-*H*), 7.05 (d, ^3J(H,H) = 7.8 Hz, 4H, 2 × C^{3,5}-*H*, Dipp), 7.22 (t, ^3J(H,H) = 7.8 Hz, 2H, 2 × C^{4}-*H*, Dipp).

^{13}C{^{1}H} NMR (125.8 MHz, C_6D_6, 298 K, ppm): δ = 23.1 (s, 4C, 4 × CHMe$_A$*Me$_B$*), 25.9 (s, 4C, 4 × CH*Me$_A$*Me$_B$), 29.4 (s, 4C, 4 × *C*HMe$_A$Me$_B$), 124.8 (s, 4C, 2 × $C^{3,5}$-H, Dipp), 125.4 (s,

2C, $C^{4,5}$-H), 131.5 (s, 2 × C^4-H, Dipp), 133.8 (s, 2 × C^1, Dipp), 145.8 (s, 2 × $C^{2,6}$, Dipp), 158.4 (s, ^1J(Si,C) = 77.6 Hz, Si-CN$_2$).

^{29}Si NMR (59.63 MHz, C_6D_6, 298K, ppm): δ = –9.7 (s). ^{29}Si{^{1}H} MAS-NMR (79.77 MHz, 298 K, ppm): δ = −5.1 (s, $\Delta\nu_{1/2}$(full width at half maximum) = 211 Hz, 1Si, Si_A), −9.2 (s, $\Delta\nu_{1/2}$ = 162 Hz, 2Si, Si_B + Si_C). The ^{29}Si{^{1}H} MAS-NMR is in accordance to the crystal structure of **18** with three symmetrically independent molecules in elementary cell (the integral intensity of signals in solid state NMR is 1:2).

One-pot two-step synthesis, without isolation of the intermediate [SiI$_3$(IDipp)]I.[98]

To a well stirred solution of IDipp (3.89 g, 10.0 mmol) in 60 mL of benzene a solution of SiI_4 (5.36 g, 10.0 mmol) in 40 mL of benzene was added dropwise. The mixture turned immediately yellow and a yellow precipitate was observed. After 1 h of stirring KC_8 (3.04 g, 22.5 mmol, 2.25 eq) was added and stirring continued at ambient temperature for 24 h. The suspension was filtered and the brown filtrate was concentrated *in vacuo* to ca. 10 mL. A part of the product precipitated out as a yellow solid. Hexane (20 mL) was added and the suspension was stirred at 0 °C for 30 min to complete precipitation of the product. The brown-yellow precipitate was filtered off, washed with a toluene/hexane mixture (2 × 10 mL, 1:5) and dried *in vacuo* (1 h, RT) to afford **18** as a fine yellow powder. Yield: 5.08 g (7.58 mmol, 76%). The sample was shown by ^{1}H NMR spectroscopy to be pure.

4.2.5 [SiBr$_3$(ISdipp)]Br (19)

Silicon tetrabromide (1.25 mL, 3.48 g, 10.0 mmol) was added to a stirred suspension of ISdipp (3.91 g, 10.0 mmol) in 80 mL of petrol ether at ambient temperature within 5 min. Formation of a voluminous, white precipitate was observed. The reaction mixture was stirred for 20 min, the precipitate was filtered off and then dried *in vacuo* to give **19** as a white powder. Yield: 7.16 g (9.70 mmol, 97%) The compound decomposes at 171−172 °C turning into a yellow liquid with gas evolution. Elemental analysis calcd (%) for $C_{27}H_{38}Br_4N_2Si$ (738.31): C 43.92, H 5.19, N 3.79; found: C 44.09, H 5.23, N 3.70.

^{1}H NMR (300.1 MHz, CD_2Cl_2, 298 K, ppm):[99] δ = 1.38 (d, ^3J(H,H) = 6.8 Hz, 12H, 2 × C^{2,6}-CHMe_AMe$_B$, Dipp), 1.43 (d, ^3J(H,H) = 6.8 Hz, 12H, 2 × C^{2,6}-CHMe$_A$$Me_B$, Dipp), 3.16 (sept,

[98] Y. Lebedev, personal communication.

^{3}J(H,H) = 6.8 Hz, 4H, 2 × C^{2,6}-C*H*Me$_A$Me$_B$, Dipp), 4.83 (s, 4H, 2 × NC*H*$_2$), 7.34 (d, ^{3}J(H,H) = 7.8 Hz, 4H, 2 × C^{3,5}-*H*, Dipp), 7.54 (t, ^{3}J(H,H) = 7.8 Hz, 2H, 2 × C^{4}-*H*, Dipp).

^{13}C{^{1}H} NMR (75.47 MHz, CD_2Cl_2, 298 K, ppm): δ = 23.7 (s, 4C, 2 × C^{2,6}-CHMe$_A$*Me$_B$*, Dipp), 26.8 (s, 4C, 2 × C^{2,6}-CH*Me$_A$*Me$_B$, Dipp), 29.7 (s, 4C, 2 × C^{2,6}-*C*HMe$_A$Me$_B$, Dipp), 57.0 (s, 2C, 2 × N*C*H$_2$), 125.9 (s, 4C, 2 × *C^{3,5}*-H, Dipp), 131.2 (s, 2C, 2 × *C^{1}*, Dipp), 132.5 (s, 2C, 2 × *C^{4}*-H, Dipp), 147.1 (s, 4C, 2 × *C2,6*, Dipp), 161.3 (s, 1C, Si-*C*N$_2$).

^{29}Si NMR (59.63 MHz, CD_2Cl_2, 298K, ppm): δ = −73.0 (s).

4.2.6 $SiBr_2$(ISdipp) (20)

A mixture of [$SiBr_3$(ISdipp)]Br (**19**) (7.16 g, 9.70 mmol) and KC_8 (3.08 g, 22.8 mmol, 2.35 eq.) was treated with 100 mL of benzene and the suspension was stirred at ambient temperature for 16 h. The suspension was filtered from the black residue (carbon) and the red-brown filtrate was concentrated *in vacuo* to ca. 20 mL. A part of the product precipitated out as a yellow solid. Hexane (30 mL) was added and the suspension was stirred at 0 °C for 10 min to complete precipitation of the product. The yellow precipitate was filtered off, washed first with a benzene/hexane mixture (2 × 12 mL, 1:5) then with hexane (10 mL) and finally dried *in vacuo* (10 min, 40 °C) to afford **20** as a fine yellow powder. Yield: 4.30 g (7.43 mmol, 77%). The compound decomposes at 191−192 °C turning into a brown liquid. Elemental analysis calcd (%) for $C_{27}H_{38}Br_2N_2Si$ (578.50): C 56.06, H 6.62, N 4.84; found: C 56.27, H 6.47, N 4.78%.

IR (solid, cm^{-1}): δ = 3065 (vw), 2961 (s), 2926 (m), 2867 (m), 1589 (w), 1488 (s), 1476 (s), 1453 (s), 1446 (s), 1419 (m), 1384 (m), 1363 (m), 1344 (vw), 1321 (m), 1302 (w), 1269 (s), 1245 (m), 1182 (m), 1163 (vw), 1150 (vw), 1102 (m), 1056 (m), 1047 (m), 1018 (w), 987 (vw), 956 (vw), 933 (w), 916 (m), 801 (s), 754 (s), 709 (vw), 677 (vw), 633 (vw), 619 (m), 611 (w, sh), 581 (vw), 572 (vw), 546 (w), 530 (vw), 457 (m), 423 (m).

^{1}H NMR (300.1 MHz, C_6D_6, 298 K, ppm): δ = 1.10 (d, ^{3}J(H,H) = 6.8 Hz, 12H, 2 × C^{2,6}-CH*Me$_A$*Me$_B$, Dipp), 1.51 (d, ^{3}J(H,H) = 6.8 Hz, 12H, 2 × C^{2,6}-CHMe$_A$*Me$_B$*, Dipp), 3.29 (sept,

---

[99] ^{1}H NMR spectroscopy revealed that compound **19** decomposes slowly in CD_2Cl_2. Therefore, the ^{13}C{^{1}H} NMR spectrum of **19** displayed also the signals of the decomposition products, which could be, however, easily distinguished from those of **19** using also correlation spectroscopy.

^{3}J(H,H) = 6.8 Hz, 4H, 2 × C^{2,6}-C*H*Me$_A$Me$_B$, Dipp), 3.47 (s, 4H, 2 × NC*H*$_2$), 7.03 (d, ^{3}J(H,H) = 7.7 Hz, 4H, 2 × C^{3,5}-*H*, Dipp), 7.17 (t, ^{3}J(H,H) = 7.7 Hz, 2H, 2 × C^{4}-*H*, Dipp).

^{13}C{^{1}H} NMR (75.47 MHz, C_6D_6, 298 K, ppm): δ = 23.8 (s, 4C, 2 × C^{2,6}-CHMe$_A$*Me$_B$*, Dipp), 26.1 (s, 4C, 2 × C^{2,6}-CH*Me$_A$*Me$_B$, Dipp), 29.4 (s, 4C, 2 × C^{2,6}-*C*HMe$_A$Me$_B$, Dipp), 54.1 (s, 2C, 2 × N*C*H$_2$), 124.9 (s, 4C, 2 × *C*^{3,5}-H, Dipp), 130.5 (s, 2C, 2 × *C*^{4}-H, Dipp), 133.7 (s, 2C, 2 × *C*^{1}, Dipp), 146.6 (s, 4C, 2 × *C*^{2,6}, Dipp), 188.7 (s, 1C, Si-*C*N$_2$).

^{29}Si NMR (59.63 MHz, C_6D_6, 298K, ppm): δ = 10.8 (s).

4.2.7 Si_2(ISdipp)$_2$ (21)

To a mixture of $SiBr_2$(ISdipp) (**20**) (578 mg, 1.00 mmol) and KC_8 (270 mg, 2.00 mmol) 20 mL of precooled THF were added at –78 °C. The mixture was allowed to warm up slowly under stirring to –10 °C overnight (in a cooling bath) and then further stirred for 20 min at room temperature. The red-brown suspension was filtered from a black solid, the red-brown filtrate was concentrated *in vacuo* to about 1 mL and 3 mL of diethyl ether were added. The mixture was stirred for 5 min at 0 °C to complete the crystallization. The red product was filtered off, washed with diethyl ether (4 × 3 mL, 0 °C) until the washings were just light red and dried *in vacuo* (1 h, RT) to give 240 mg of crude material, containing about 10% of ISdipp.[100] The product was recrystallized from 5 mL of hot toluene (to 0 °C), isolated by filtration, washed with hexane (3 × 2 mL) and dried under vacuum to give an analytically pure sample. Yield: 190 mg (0.227 mmol, 45%), dark red powder. Diffusion of heptane in a THF solution afforded small red plate-like crystals of **21**, suitable for X-ray diffraction analysis.

Elemental analysis calcd (%) for $C_{54}H_{76}N_4Si_2$ (837.38): C 77.45, H 9.15, N 6.69; found: C 76.88, H 8.76, N 6.40%.

^{1}H NMR (300.1 MHz, C_6D_6, 298 K, ppm): δ = 1.15 (d, ^{3}J(H,H) = 6.9 Hz, 12H, 2 × C^{2,6}-CH*Me$_A$*Me$_B$, Dipp), 1.18 (d, ^{3}J(H,H) = 6.9 Hz, 12H, 2 × C^{2,6}-CHMe$_A$*Me$_B$*, Dipp), 3.45 (sept, ^{3}J(H,H) = 6.9 Hz, 4H, 2 × C^{2,6}-C*H*Me$_A$Me$_B$, Dipp), 3.57 (s, 4H, 2 × NC*H*$_2$), 6.97 (d, ^{3}J(H,H) = 7.6 Hz, 4H, 2 × C^{3,5}-*H*, Dipp), 7.18 (t, ^{3}J(H,H) = 7.6 Hz, 2H, 2 × C^{4}-*H*, Dipp).

[100] According to the ^{1}H NMR spectrocopy.

^{1}H NMR (300.1 MHz, C_6D_6, 348 K, ppm): δ = 1.15 (d, ^{3}J(H,H) = 6.9 Hz, 12H, 2 × $C^{2,6}$-CHMe_AMe$_B$, Dipp), 1.20 (d, ^{3}J(H,H) = 6.9 Hz, 12H, 2 × $C^{2,6}$-CHMe$_A$$Me_B$, Dipp), 3.38 (sept, ^{3}J(H,H) = 6.9 Hz, 4H, 2 × $C^{2,6}$-CHMe$_A$Me$_B$, Dipp), 3.64 (s, 4H, 2 × NCH_2), 6.98 (d, ^{3}J(H,H) = 7.7 Hz, 4H, 2 × $C^{3,5}$-H, Dipp), 7.15 (t, ^{3}J(H,H) = 7.7 Hz, 2H, 2 × C^{4}-H, Dipp).

^{13}C{^{1}H} NMR (75.47 MHz, C_6D_6, 348 K, ppm): δ = 24.2 (s, 4C, 2 × $C^{2,6}$-CHMe$_A$$Me_B$, Dipp), 26.0 (s, 4C, 2 × $C^{2,6}$-CHMe_AMe$_B$, Dipp), 28.9 (s, 4C, 2 × $C^{2,6}$-CHMe$_A$Me$_B$, Dipp), 53.1 (s, 2C, 2 × NCH_2), 124.3 (s, 4C, 2 × $C^{3,5}$-H, Dipp), 128.6 (s, 2C, 2 × C^{4}-H, Dipp), 137.3 (s, 2C, 2 × C^{1}, Dipp), 147.5 (s, 4C, 2 × $C^{2,6}$, Dipp), 217.0 (s, 1C, Si-CN$_2$).

^{29}Si NMR (59.63 MHz, C_6D_6, 348K, ppm): δ = 215.2 (s).

4.2.8 SiI_2(ISdipp) (22)

To a stirred solution of IDipp (781 mg, 2.00 mmol) in 25 mL of benzene a solution of SiI_4 (1.07 mg, 2.00 mmol) in 15 mL of benzene was added dropwise in 2 min. The solution immediately turned orange and soon after a yellow precipitate was observed.[101] After 30 min of stirring KC_8 (594 mg, 4.40 mmol, 2.20 eq) was added and stirring was continued at ambient temperature for 20 h. The suspension was filtered, the black precipitate (carbon) was washed with 10 mL of benzene. The combined orange filtrate was concentrated under vacuum to about 3 mL (a yellow precipitate was observed) and then 10 mL of hexane were added. The suspension was stirred at 0 °C for 10 min, the product was filtered off, washed with hexane (2 × 5 mL) and dried *in vacuo* (30 min, RT) to afford **22** as a yellow powder. Yield: 1.05 g (1.56 mmol, 78%). Yellow single crystals of **22** were obtained upon diffusion of hexane in benzene solution at room temperature.

^{1}H NMR (300.1 MHz, C_6D_6, 298 K, ppm): δ = 1.08 (d, ^{3}J(H,H) = 6.8 Hz, 12H, 2 × $C^{2,6}$-CHMe_AMe$_B$, Dipp), 1.54 (d, ^{3}J(H,H) = 6.8 Hz, 12H, 2 × $C^{2,6}$-CHMe$_A$$Me_B$, Dipp), 3.29 (sept, ^{3}J(H,H) = 6.8 Hz, 4H, 2 × $C^{2,6}$-CHMe$_A$Me$_B$, Dipp), 3.48 (s, 4H, 2 × NCH_2), 7.03 (d, ^{3}J(H,H) = 7.8 Hz, 4H, 2 × $C^{3,5}$-H, Dipp), 7.18 (t, ^{3}J(H,H) = 7.8 Hz, 2H, 2 × C^{4}-H, Dipp).

^{13}C{^{1}H} NMR (75.47 MHz, C_6D_6, 298 K, ppm): δ = 23.8 (s, 4C, 2 × $C^{2,6}$-CHMe$_A$$Me_B$, Dipp), 26.3 (s, 4C, 2 × $C^{2,6}$-CHMe_AMe$_B$, Dipp), 29.3 (s, 4C, 2 × $C^{2,6}$-CHMe$_A$Me$_B$, Dipp), 54.1

[101] The yellow precipitate was assumed to be the imidazolinium salt [SiI_3(ISdipp)]I, see also p. 175.

(s, 2C, 2 × N*C*H$_2$), 125.2 (s, 4C, 2 × *C*^{3,5}-H, Dipp), 130.8 (s, 2C, 2 × *C*^{4}-H, Dipp), 134.1 (s, 2C, 2 × *C*^{1}, Dipp), 146.7 (s, 4C, 2 × *C*^{2,6}, Dipp).[102]

^{29}Si NMR (59.63 MHz, C_6D_6, 298K, ppm): δ = –11.2 (s).

4.2.9 [Si(IMe$_4$)$_3$]I$_2$ (23)

To a solution, containing SiI$_2$(IDipp) (**18**) (335 mg, 0.500 mmol) in 5 mL of fluorobenzene, a solution of IMe$_4$ (140 mg, 1.13 mmol, 2.25 eq) was added dropwise in 1 min. A voluminous yellow precipitate was immediately observed. The suspension was stirred for 15 min and then filtered. The yellow precipitate was washed with fluorobenzene (3 × 5 mL) and dried *in vacuo* (RT, 30 min). The yellow filtrate and light yellow washings were discarded. Yield 260 mg (0.49 mmol, 98%), light yellow powder. Compound **23** starts to decompose above 160 °C.

IR (solid, cm^{-1}): δ = 2971 (m), 2947 (m), 2922 (m), 2865 (w), 1640 (vs), 1590 (w), 1539 (vs), 1485 (m), 1435 (vs), 1384 (vs), 1372 (vs), 1340 (m), 1256 (vw), 1225 (m), 1210 (m), 1183 (vw), 1153 (w), 1129 (vw), 11 07 (vw), 1092 (vw), 1058 (m), 1037 (m), 910 (vw), 902 (vw), 847 (vs), 803 (m), 757 (vs), 688 (w), 676 (m), 652 (vw), 643 (vw), 596 (vw), 571 (m), 518 (w), 503 (w), 492 (w), 478 (w), 472 (w), 462 (w), 437 (vs), 404 (m), 386 (m).

Elemental analysis calcd (%) for $C_{21}H_{36}I_2N_6Si$ (654.45): C 38.54, H 5.54, N 12.84; found: C 38.05, H 5.39, N 10.82%. ^{1}H NMR (300.1 MHz, CD_2Cl_2, 298 K, ppm): δ = 2.34 (s, 12H, 2 × C^{4,5}-*Me*), 3.65 (s, 12H, 2 × N^{1,3}-*Me*). ^{13}C{^{1}H} NMR (75.47 MHz, CD_2Cl_2, 298 K, ppm): δ = 10.3 (s, 4C, 2 × C^{4,5}-*Me*), 36.1 (s, 4C, 2 × N^{1,3}-*Me*), 130.9 (s, 4C, 2 × *C*^{4,5}), 152.0 (s, 2C, 2 × *C*^{2}). ^{29}Si NMR (59.63 MHz, CD_2Cl_2, 298 K, ppm): δ = –89.9 (s).

4.2.10 1,1-diodo-2,3,4,5-tetra(diethylamino)silole (24)

Bis(diethylamino)acetylene (0.355 g, 2.00 mmol) was added within 1 min to a solution of SiI$_2$(IDipp) (671 mg, 1.00 mmol) in 4 mL of benzene. During the addition the solution gradually turned orange. The reaction was subsequently stirred for 10 min, and a solution of SiI$_4$ (0.536 g, 1.00 mmol) in 5 mL of benzene was added dropwise. A precipitate ([IDippSiI$_3$]I, **17**) was observed.[103] The resulting mixture was stirred for 5 min. 10 mL of

[102] The signal of C$_{carbene}$ (*C*N$_2$) expected at about 190 ppm was not observed.

[103] Two equivalents of FeCl$_2$ were also successfully used to eliminate the carbene. S. Reis, *Diploma thesis*, University of Bonn, **2012**.

hexane were added; the suspension was filtered from brown sticky material which was discarded. The filtrate was evaporated *in vacuo,* the residue was extracted with 10 mL of hexane and filtered, and the filtrate was concentrated in vacuo to ca 2 mL. Crystallization at 30 °C afforded the compound **24** as large orange crystals. Yield 0.26 g, 42%. M.p. = 85 °C. Elemental analysis calcd (%) for $C_{20}H_{40}I_2N_4Si$ (618.45): C 38.84; H 6.52; N 9.06; found: C 38.39; H 6.21; N 8.85.

^{1}H NMR (400.1 MHz, C_6D_6, 298 K, ppm): δ = 0.95 (t, ^3J(H,H) = 7.1 Hz, 12H, 4 × (CH_3)$_A$), 1.16 (t, ^3J(H,H) = 7.1 Hz, 12H, 4 × (CH_3)$_B$), 3.17 (q, ^3J(H,H) = 7.1 Hz, 4H, 4 × (CH_2)$_A$), 3.22 (q, ^3J(H,H) = 7.1 Hz, 4H, 4 × (CH_2)$_B$). ^{13}C{^{1}H} NMR (75.47 MHz, C_6D_6, 298 K, ppm): δ = 13.9 (s, 4 × (*C*H$_3$)$_A$), 15.5 (s, 4 × (*C*H$_3$)$_B$), 44.3 (s, 4 × (*C*H$_2$)$_A$), 49.7 (s, 4 × (*C*H$_3$)$_B$), 124.3 (s, 2 × C_B), 146.7 (s, 2 × C_A). ^{29}Si NMR (59.63 MHz, C_6D_6, 298K, ppm): δ = −83.5 (s).

EI-MS (70 eV): m/z (rel. intensity in %) = 618 (100, [M^+]), 589 (5, [$M^+ - C_2H_5$]), 560 (47, [$M^+ - 2\ C_2H_5$]), 545 (20, [$M^+ - 2\ C_2H_5 - CH_3$]), 534 (67, [$M^+ - 2\ C_2H_5 - CN$].

4.2.11 SiCl(C$_6$H$_3$-2,6-Mes$_2$)(IMe$_4$) (28)

Si(C$_6$H$_3$-2,6-Mes$_2$)HCl$_2$ (**26**) (6.06 g, 14.7 mmol) was dissolved in 100 mL of benzene and the colorless solution was heated to 70 °C. A solution of 1,3,4,5-tetramethylimidazol-2-ylidene (3.73 g, 30.0 mmol, 2.04 equiv.) in 50 mL of benzene was added dropwise to the solution of the silane within 10 min at 70 °C. During addition an orange solid precipitated, and the reaction solution turned yellow. After the addition was complete, the suspension was concentrated *in vacuo* to about 10 mL, and 20 mL of hexane were added. The orange precipitate was isolated by filtration and treated with 150 mL of benzene. The obtained suspension was filtered at 40 °C *via* cannula. The benzene insoluble, orange solid was dried *in vacuo* and was shown by NMR spectroscopy to contain mainly the imidazolium salt [IMe$_4$H]Cl.[105] The yellow filtrate was concentrated to about 10 mL and then 10 mL of hexane were added. A yellow precipitate was filtered, washed with 10 mL of hexane and dried *in vacuo* (30 min, RT) to afford the compound **28** as a yellow solid. Yield 3.50 g (6.98 mmol, 48%). The compound starts to decompose upon heating at 120 °C. Recrystallization of the solid from toluene afforded an analytically pure sample of the toluene-hemisolvate. Yellow single crystals of **28**·0.5toluene were suitable for X-Ray diffraction analysis. Elemental analysis calcd (%) for $C_{31}H_{37}ClN_2Si{\cdot}0.5C_7H_8$ (547.23): C 75.72, H 7.55, N 5.12; found: C 75.47, H 7.44, N 5.11%.

^{1}H NMR (C_6D_6, 300.1 MHz, 298 K, ppm): δ = 1.18 (s, 6H, $C^{4,5}$-*Me*, IMe_4), 2.11 (s, 6H, 2 × C^{2}-*Me*, Mes), 2.18 (s, 6H, 2 × C^{4}-*Me*, Mes), 2.57 (s, 6H, 2 × C^{6}-*Me*, Mes), 3.02 (s, 6H, $N^{1,3}$-*Me*, IMe_4), 6.63 (s, 2H, 2 × C^{3}-*H*, Mes), 6.88 (s, 2H, 2 × C^{5}-*H*, Mes), 6.93 (d, ^{3}J(H,H) = 7.5 Hz, 2H, $C^{3,5}$-*H*, C_6H_3), 7.19 (t, ^{3}J(H,H) = 7.5 Hz, 1H, C^{4}-*H*, C_6H_3).

^{13}C{^{1}H} (75.47 MHz, C_6D_6, 298 K, ppm): δ = 7.9 (s, 2C, $C^{4,5}$-*Me*, IMe_4), 21.13 and 21.17 (s each, 4C, 2 × C^{4}-*Me* + 2 × C^{2}-*Me*, Mes), 22.0 (s, 2C, 2 × C^{6}-*Me*, Mes), 34.0 (s, 2C, $N^{1,3}$-*Me*, IMe_4), 124.5 (s, 2C, *C*^{4,5}-Me, IMe_4), 126.1 (s, 1C, *C*^{4}-H, C_6H_3), 128.0 (s, 2C, 2 × *C*^{3}-H, Mes), 128.6 (s, 2C, 2 × *C*^{5}-H, Mes), 129.2 (s, 2C, *C*^{3,5}-H, C_6H_3), 135.1 (s, 2C, 2 × *C*^{4}, Mes), 135.8 (s, 2C, 2 × *C*^{2}, Mes), 136.7 (s, 2C, 2 × *C*^{6}, Mes), 141.8 (s, 2C, 2 × *C*^{1}, Mes), 146.2 (s, 2C, *C*^{2,6}, C_6H_3), 150.6 (s, ^{1}J(^{13}C,^{29}Si) = 48 Hz, 1C, Si-*C*^{1}, C_6H_3), 165.2 (s, ^{1}J(^{13}C,^{29}Si) = 33 Hz, 1C, Si-*C*^{2}, IMe_4).

^{29}Si NMR (C_6D_6, 59.63 MHz, 298 K, ppm): δ = 1.34 (s).

4.2.12 SiCl(C_6H_3-2,6-$Trip_2$)(IMe_4) (29)

Si(C_6H_3-2,6-$Trip_2$)HCl_2 (**27**) (7.93 g, 13.6 mmol) was dissolved in benzene (100 mL), and the colorless solution was heated to 75 °C. A solution of 1,3,4,5-tetramethylimidazol-2-ylidene (3.46 g, 27.9 mmol, 2.05 eq.) in benzene (70 mL) was added dropwise over 5 min.[104] During addition a precipitate formed, and the mixture turned orange. After the addition was complete, the mixture was concentrated *in vacuo* to about 10 mL and 30 mL of hexane were added. The mixture was stirred for a short time, then filtered, the orange-yellow precipitate was washed with hexane (2 × 20 mL). The washings were discarded and the solid dried under vacuum. The obtained yellow solid was extracted with hot benzene (200 mL, ca. 70 °C), and the extract was filtered to remove an insoluble, almost white solid, which was shown by NMR spectroscopy to be the imidazolium salt [IMe_4H]Cl (see below)[105]. The filtrate was evaporated

[104] It is important to keep the mixture nearly boiling during the addition. Lower temperatures as well as prolonged reaction time (more than about 30 min) will decrease the yield.

[105] Spectral data of [IMe_4H]Cl: ^{1}H NMR (CD_2Cl_2, 300.1 MHz, 298 K, ppm): δ =2.19 (s, 6H; $C^{4,5}$-*Me*), 3.86 (s, 6H; $N^{1,3}$-*Me*), 10.80 (s, 1H; C^{2}-*H*); ^{13}C{^{1}H} NMR (CD_2Cl_2, 75.47 MHz, 298 K, ppm): δ =8.4 (s, 2C, $C^{4,5}$-*Me*), 33.9 (s, 2C, $N^{1,3}$-*Me*), 126.9 (s, 2C, *C*^{4,5}), 137.9 (s, 1C, *C*^{2}-H); ^{1}H NMR ($CDCl_3$, 300.1 MHz, 298 K, ppm): δ =2.17 (s, 6H; $C^{4,5}$-*Me*), 3.82 (s, 6H; $N^{1,3}$-*Me*), 10.46 (s, 1H; C^{2}-*H*); ^{13}C{^{1}H} NMR (CD_2Cl_2, 75.47 MHz, 298 K, ppm): δ =8.3 (s, 2C, $C^{4,5}$-*Me*), 33.6 (s, 2C, $N^{1,3}$-*Me*), 126.6 (s, 2C, *C*^{4,5}), 136.9 (s, 1C, *C*^{2}-H).

to dryness, and the residue washed with 10 mL of hexane and dried *in vacuo* (1 h, RT) to afford **29** as a yellow microcrystalline powder. Yield: 8.03 g (12.0 mmol, 88%). The product contains small amount of benzene as the only impurity. An analytically pure sample was obtained after recrystallization from benzene-hexane mixture. Yellow single crystals of **29** were grown upon cooling of a concentrated toluene solution from ambient temperature to 4 °C. The compound starts to decompose on heating at 172 °C. Elemental analysis calcd (%) for $C_{43}H_{61}ClN_2Si$ (669.48): C 77.14, H 9.18, N 4.19; found: C 75.41, H 8.72, N 3.89.

^{1}H NMR (400.1 MHz, C_6D_6, 298 K, ppm): δ = 1.13 (s, 6H, $C^{4,5}$-*Me*, IMe_4), 1.173 (d, ^3J(H,H)=6.8 Hz, 6H, 2 × C^2-CH*Me*$_A$Me$_B$, Trip), 1.183 (d, ^3J(H,H)=6.8 Hz, 6H, 2 × C^2-CHMe$_A$*Me*$_B$, Trip), 1.271 (d, ^3J(H,H)=6.9 Hz, 6H, 2 × C^4-CH*Me*$_A$Me$_B$, Trip), 1.277 (d, ^3J(H,H)=6.9 Hz, 6H, 2 × C^4-CHMe$_A$*Me*$_B$, Trip) 1.31 (d, ^3J(H,H)=6.8 Hz, 6H, 2 × C^6-CH*Me*$_A$Me$_B$, Trip), 1.74 (d, ^3J(H,H)=6.8 Hz, 6H, 2 × C^6-CHMe$_A$*Me*$_B$, Trip), 2.87 (sept, ^3J(H,H)= 6.9 Hz, 2H, 2 × C^4-C*H*Me$_A$Me$_B$, Trip), 3.02 (sept, ^3J(H,H)=6.8 Hz, 2H, 2 × C^2-C*H*Me$_A$Me$_B$, Trip), 3.14 (s, 6H, $N^{1,3}$-*Me*, IMe_4), 3.43 (sept, ^3J(H,H)=6.8 Hz, 2H, 2 × C^6-C*H*Me$_A$Me$_B$, Trip), 7.03 (d, ^4J(H,H)=1.6 Hz, 2H, 2 × C^3-*H*, Trip), 7.10–7.13 (m, 3H, $C^{3,4,5}$-*H*, C_6H_3), 7.24 (d, ^4J(H,H)=1.6 Hz, 2H, 2 × C^5-*H*, Trip).

^{13}C{^{1}H} NMR (75.47 MHz, C_6D_6, 298 K, ppm): δ = 7.9 (s, 2C, $C^{4,5}$-*Me*, IMe_4), 23.0 (s, 2C, 2 × C^2-CHMe$_A$*Me*$_B$, Trip), 23.7 (s, 2C, 2 × C^6-CHMe$_A$*Me*$_B$, Trip), 24.4 (s, 2C, 2 × C^4-CH*Me*$_A$Me$_B$, Trip), 24.7 (s, 2C, 2 × C^4-CHMe$_A$*Me*$_B$, Trip), 26.5 (s, 2C, 2 × C^6-CH*Me*$_A$Me$_B$, Trip), 26.9 (s, 2C, 2 × C^2-CH*Me*$_A$Me$_B$, Trip), 31.0 (s, 2C, 2 × C^2-*C*HMe$_A$Me$_B$, Trip), 31.7 (s, 2C, 2 × C^6-*C*HMe$_A$Me$_B$, Trip), 33.8 (s, 2C, $N^{1,3}$-*Me*, IMe_4), 34.7 (s, 2C, 2 × C^4-*C*HMe$_A$Me$_B$, Trip), 120.1 (s, 2C, 2 × C^3-H, Trip), 121.0 (s, 2C, 2 × C^5-H, Trip), 124.4 (s, 1C, C^4-H, C_6H_3), 125.1 (s, 2C, $C^{4,5}$-Me, IMe_4), 130.8 (s, 2C, $C^{3,5}$-H, C_6H_3), 140.0 (s, 2C, 2 × C^1, Trip), 145.0 (s, 2C, $C^{2,6}$, C_6H_3), 147.3 (s, 2C, 2 × C^2, Trip), 147.4 (s, 2C, 2 × C^4, Trip), 147.5 (s, 2C, 2 × C^6, Trip), 150.6 (s, 1C, Si-C^1, C_6H_3), 166.7 (s, ^1J(^{13}C,^{29}Si) = 37 Hz, 1C, Si-C^2, IMe_4).

^{29}Si NMR (59.63 MHz, C_6D_6, 298 K, ppm): δ = 0.77 (s).

4.2.13 Si(C$_6$H$_3$-2,6-Dipp$_2$)HCl$_2$ (30)

To a solution of 2,6-Dipp$_2$-C_6H_3I (1.79 g, 3.41 mmol) in 15 mL of hexane a 2.5 M solution of *n*-BuLi (1.45 mL, 3.63 mmol, 1.06 eq.) was added at –30 °C. The reaction was allowed to warm to room temperature and soon after a white precipitate was observed. The suspension

was stirred for 1 h, heated to 30 °C for 15 min and cooled down to 0 °C in an ice bath. The white precipitate was filtered, washed with hexane at 0 °C (2 × 5 mL) and dried *in vacuo* (30 min, RT) to give 1.07 g (2.64 mmol, 78%) of Li(2,6-$Dipp_2$-C_6H_3).

A solution of Li(2,6-$Dipp_2$-C_6H_3) (500 mg, 1.24 mmol) in 10 mL of diethyl ether was added dropwise at –78 °C to $SiHCl_3$ (0.37 mL, 500 mg, 3.7 mmol, 3.0 eq.) within 2 min. A white precipitate was observed (LiCl). The mixture was allowed to warm to ambient temperature and stirred for 2 h. All volatilities were removed under vacuum and the white residue was extracted with 10 mL of hexane. The extract was filtered, the filtrate was concentrated to about 2 mL *in vacuo*, during this a white solid precipitated. The mixture was stored at –78 °C to complete the crystallization and then filtered. The product was dried *in vacuo* (15 min, RT) to give a white powder. Yield 460 mg (0.924 mmol, 75%).

^{1}H NMR (C_6D_6, 300.1 MHz, 298 K, ppm): δ = 1.01 (d, ^3J(H,H)=6.8 Hz, 12H, 4 × CH$Me_A$$Me_B$, Dipp), 1.29 (d, ^3J(H,H)=6.8 Hz, 6H, 4 × CH$Me_A$$Me_B$, Dipp), 2.78 (sept, ^3J(H,H)=6.8 Hz, 4H, 4 × C*H*$Me_A$$Me_B$, Dipp), 5.34 (s, 1H, ^2J(Si,H)=300.6 Hz, Si-*H*), 7.12–7.16 (m, 7H, 2 × $C^{3,5}$-*H*, Dipp + $C^{3,4,5}$-*H*, C_6H_3), 7.26–7.32 (m, 2H, 2 × C^4-*H*, Dipp);

^{13}C{^{1}H} NMR (75.47 MHz, C_6D_6, 298 K, ppm): δ = 22.6 (s, 4C, 4 × CH$Me_A$$Me_B$, Dipp), 25.8 (s, 4C, 4 × CH$Me_A$$Me_B$, Dipp), 31.2 (s, 4C, 4 × *C*H$Me_A$$Me_B$, Dipp), 123.1 (s, 4C, 4 × $C^{3,5}$-H, Dipp), 129.5 (s, 2C, 2 × C^4-H, Dipp), 129.9 (s, 1C, C^1, C_6H_3), 130.6 (s, 1C, C^4-H, C_6H_3), 130.7 (s, 2C, $C^{3,5}$-H, C_6H_3), 138.0 (s, 2C, 2 × C^1, Dipp), 147.2 (s, 4C, 2 × $C^{2,6}$, Dipp), 148.1 (s, 2C, $C^{2,6}$, C_6H_3).

4.2.14 SiCl(C_6H_3-2,6-$Dipp_2$)(IMe_4) (31)

Si(C_6H_3-2,6-$Dipp_2$)HCl_2 (**30**) (450 mg, 0.904 mmol) was dissolved in 7 mL of benzene and the colorless solution was heated to 70 °C. A solution of 1,3,4,5-tetramethylimidazol-2-ylidene (235 mg, 1.89 mmol, 2.09 equiv.) in 5 mL of benzene was added dropwise to the solution of the silane within 3 min at 70 °C. During addition a solid precipitated, and the reaction mixture turned orange. After the addition was complete, the suspension was stirred for 2 min and then filtered hot from the imidazolium salt [IMe_4H]Cl. The filtrate was evaporated *in vacuo* to give orange foam. The foam was treated with 5 mL of hexane leading to formation of an orange precipitate. The mixture was cooled to –30 °C, the precipitate was isolated by filtration and washed with hexane (3 × 4 mL) at –30 °C. Drying *in vacuo* (30 min, 30 °C) afforded the compound **31** as an orange powder. Yield 435 mg (0.743 mmol, 82%).

^{1}H NMR (400.1 MHz, C_6D_6, 298 K, ppm): δ = 1.11 (d, ^{3}J(H,H)=6.8 Hz, 12H, 2 × C^{2}-CHMe_AMe$_B$ + 2 × C^{2}-CHMe$_A$$Me_B$, Dipp), 1.14 (s, 6H, $C^{4,5}$-*Me*, IMe$_4$), 1.25 (d, ^{3}J(H,H)=6.8 Hz, 6H, 2 × C^{6}-CHMe_AMe$_B$, Dipp), 1.66 (d, ^{3}J(H,H)=6.8 Hz, 2 × C^{6}-CHMe$_A$$Me_B$, Dipp), 2.98 (sept, ^{3}J(H,H)= 6.8 Hz, 2H, 2 × C^{2}-C*H*Me$_A$Me$_B$, Dipp), 3.09 (s, 6H, $N^{1,3}$-*Me*, IMe$_4$), 3.35 (sept, ^{3}J(H,H)=6.8 Hz, 2H, 2 × C^{6}-C*H*Me$_A$Me$_B$, Trip), 7.04 (dd, ^{3}J(H,H)=6.0 Hz, ^{3}J(H,H)=2.9 Hz, 2H, 2 × C^{3}-*H*, Dipp), 7.10 (m, ^{3}J(H,H)=7.5 Hz, 2H, $C^{3,5}$-*H*, C_6H_3),[106] 7.16 (m, ^{3}J(H,H)=7.5 Hz, 1H, C^{4}-*H*, C_6H_3),[106] 7.25 (m, ^{3}J(H,H)=5.8 Hz, ^{3}J(H,H)=6.0 Hz, 2H, 2 × C^{4}-*H*, Dipp),[106] 7.26 (m, ^{3}J(H,H)=5.8 Hz, ^{4}J(H,H)=2.9 Hz, 2H, 2 × C^{5}-*H*, Dipp).[106]

^{13}C{^{1}H} NMR (100.6 MHz, C_6D_6, 298 K, ppm): δ = 8.0 (s, 2C, $C^{4,5}$-*Me*, IMe$_4$), 22.8 (s, 2C, 2 × C^{2}-CHMe_AMe$_B$, Dipp), 23.6 (s, 2C, 2 × C^{6}-CHMe$_A$$Me_B$, Dipp), 26.3 (s, 2C, 2 × C^{6}-CH*MeA*Me$_B$, Dipp), 26.7 (s, 2C, 2 × C^{2}-CHMe$_A$$Me_B$, Dipp), 30.9 (s, 2C, 2 × C^{2}-*C*HMe$_A$Me$_B$, Dipp), 31.6 (s, 2C, 2 × C^{6}-*C*HMe$_A$Me$_B$, Dipp), 33.8 (s, 2C, $N^{1,3}$-*Me*, IMe$_4$), 122.2 (s, 2C, 2 × C^{3}-H, Dipp), 123.1 (s, 2C, 2 × C^{5}-H, Dipp), 124.4 (s, 1C, C^{4}-H, C_6H_3), 125.3 (s, 2C, $C^{4,5}$-Me, IMe$_4$), 127.7 (s, 2C, 2 × C^{4}-H, Dipp), 130.6 (s, 2C, $C^{3,5}$-H, C_6H_3), 142.1 (s, 2C, 2 × C^{1}, Dipp), 144.8 (s, 2C, $C^{2,6}$, C_6H_3), 147.4 (s, 2C, 2 × C^{2}, Dipp), 147.7 (s, 2C, 2 × C^{6}, Dipp), 150.2 (s, 1C, Si-C^{1}, C_6H_3), 166.3 (s, 1C, Si-C^{2}, IMe$_4$).

^{29}Si NMR (C_6D_6, 59.63 MHz, 298 K, ppm): δ = 0.04 (s).

4.2.15 {Si(C_6H_3-2,6-Mes_2)(IMe$_4$)}$_2$ (32)

To a mixture of SiCl(C_6H_3-2,6-Mes_2)(IMe$_4$) (110 mg, 0.219 mmol) and KC_8 (33 mg, 0.24 mmol, 1.1 eq.) 3 mL of THF were added and the mixture was stirred 2 h at ambient temperature. The color changed to dark violet-blue. The reaction was filtered from black material; the filtrate was concentrated under reduced pressure to about 0.3 mL. Hexane (5 mL) was added to the filtrate and the mixture was stored at –16 °C overnight. The solvents were syringed off and the mixture of yellow (SiClAr(IMe$_4$)) and black-blue (the product) crystals was washed with benzene (3 × 0.5 mL). The yellow crystals of the starting material dissolved, leaving the pure dark crystals of the product. Drying *in vacuo* afforded **32** as small blue-black plates. Yield 25 mg (2.7 mmol, 24%). Elemental analysis calcd (%) for $C_{62}H_{74}N_4Si_2$ (931.45): C 79.95, H 8.01, N 6.02; found: C 79.75, H 8.04, N 5.38%. Crystals

[106] The coupling constant was obtained by analysis of the spectrum using Ivory Soft gNMR program.

suitable for X-ray analysis were obtained upon diffusion of diethyl ether into a concentrated THF solution of the compound at –16 °C.

4.2.16 Synthesis of 34; $K_2(IMe_4)_3[SiHR_2]_2$; "Mes"

To a mixture of $SiCl(C_6H_3\text{-}2,6\text{-}Mes_2)(IMe_4)$ (200 mg, 0.399 mmol) and KC_8 (135 mg, 1.00 mmol, 2.5 eq.) and 1,3,4,5-tetramethylimidazol-2-ylidene (25 mg, 0.20 mmol, 0.5 eq.) 5 mL of THF were added and the mixture was stirred 5 h at ambient temperature. The color changed to dark violet-blue and then to brown. The reaction was filtered from black material which was discarded; the filtrate was evaporated to dryness *in vacuo*. The residue was washed with hexane/benzene mixture (1:1, 3 × 3 mL). The resulting precipitate was dried *in vacuo* to give brown microcrystalline powder of **34**·1.5(IMe_4). Yield 110 mg (0.097 mmol, 49%). Crystals suitable for X-ray analysis were obtained upon diffusion of hexane into a concentrated THF solution of the compound at –16 °C.

^{1}H NMR (300.1 MHz, THF-d_8, 298 K, ppm): δ = 1.38 (d br, ^3J(H,H)=11.2 Hz, 1H, Si*H*), 2.02 (s, 9H, 3 × C-CH_3, IMe_4), 2.03 (s br, 6H, 2 × CH_3, Mes), 2.17 (s br, 3H, CH_3, Mes), 2.25 (s br, 3H, CH_3, Mes), 2.30 (s br, 3H, CH_3, Mes), 2.6 (s br, $\nu_{1/2}$ = ca. 80 Hz, 1H, Si-CH_AH$_B$), 3.20 (m br, 1H, Si-CH$_A$$H_B$), 3.49 (s, 9H, 3 × N-C$H_3$, IMe_4), 6.43 (d br, ^3J(H,H)=6.8 Hz, 1H, C$^{3\text{ or }5}$-*H*, C_6H_3), 6.59 (s br, 1H, C$^{3\text{ or }5}$-*H*, Mes), 6.64 (s br, 1H, C$^{3\text{ or }5}$-*H*, Mes), 6.70 (s br, 1H, C$^{3\text{ or }5}$-*H*, Mes), 6.77 (s br, 1H, C$^{3\text{ or }5}$-*H*, Mes), 6.91 (t br, ^3J(H,H)=7.2 Hz, 1H, C^4-*H*, C_6H_3), 7.07 (s br, 1H, C$^{3\text{ or }5}$-*H*, C_6H_3).

4.2.17 Synthesis of 35; $K_2(THF)_2[SiHR_2]_2$; "Trip"

To a mixture of $SiCl(C_6H_3\text{-}2,6\text{-}Trip_2)(IMe_4)$ (100 mg, 0.149 mmol) and KC_8 (100 mg, 0.740 mmol, 5.0 eq.) 4 mL of THF were added and the suspension was stirred for 1.5 h. The color of the reaction changed over deep purple to dark-brown. The reaction mixture was filtered; the filtrate was concentrated *in vacuo* and diluted with 2 mL of pentane. After standing for 30 min at ambient temperature brown crystals were formed, which were filtered, washed with hexane and dried *in vacuo*. Yield ca. 20 mg (18%). The crystals were suitable for X-ray diffraction analysis and were solely used for this purpose. No further characterisation was carried out.

4.2.18 SiFH(C_6H_3-2,6-$Trip_2$)(CH_2-$IMe_3(PF_5)$) (36)

A suspension of SiCl(C_6H_3-2,6-$Trip_2$)(IMe_4) (100 mg, 0.149 mmol) and KPF_6 (28 mg, 0.15 mmol) in 10 mL of toluene was refluxed overnight with stirring. The color of the mixture changed from yellow to very pale yellow. The suspension was filtered and the dark brown filtrate was evaporated to dryness *in vacuo*. The residue was extracted with 10 mL of hexane at room temperature and the extract was filtered from a tiny amount of an insoluble white solid. The filtrate was concentrated *in vacuo* to about 0.5 mL. Colorless solid started to crystallize soon after. The mixture was stored at –30 °C overnight to complete the crystallization, the crystals were separated by decantation at –30 °C and dried *in vacuo*. Yield: ca. 50 mg. The product was shown by NMR spectroscopy to to contain some impurities, the components have similar solubility and their separation by fractional crystallization failed. The crystals were suitable for X-ray diffraction analysis, the major product (**36**) was identified.

^{1}H NMR (300.1 MHz, C_6D_6, 298 K, ppm): δ = 0.75 (s, 3H, C-*Me*, IMe_3-CH_2), 1.09 (d, ^3J(H,H)=6.7 Hz, 6H, 2 × CH*Me*, Trip), 1.10 (d, ^3J(H,H)=6.7 Hz, 6H, 2 × CH*Me*, Trip), 1.182 (d, ^3J(H,H)=6.9 Hz, 6H, 2 × CH*Me*, Trip), 1.187 (d, ^3J(H,H)=6.9 Hz, 6H, 2 × CH*Me*, Trip), 1.39 (s, 3H, C-*Me*, IMe_3-CH_2), 1.49 (d, ^3J(H,H)=6.8 Hz, 6H, 2 × CH*Me*, Trip), 1.58 (d, ^3J(H,H)=6.7 Hz, 6H, 2 × CH*Me*, Trip), 2.34 (dd, *J*(H,H)= 16.3 Hz, *J*(H,H)= 4.1 Hz, 1H, N-C$H_A$$H_B$-, IMe_3-CH_2), 2.79 (sept, ^3J(H,H)= 6.9 Hz, 2H, 2 × C*H*Me_2, Trip), 2.89 (sept, ^3J(H,H)=6.9 Hz, 2H, 2 × C*H*Me_2, Trip), 2.92 (s, 6H, N-*Me*, IMe_3-CH_2), 3.06 (sept, ^3J(H,H)=6.8 Hz, 2H, 2 × C*H*Me_2, Trip), 4.32 (dd, *J*(H,H)= 16.3 Hz, *J*(H,H)= 17.9 Hz, 1H, N-C$H_A$$H_B$-, IMe_3-CH_2), 4.76 (d mult, *J*(F,H)= 57.7 Hz, 1H, SiF*H*), 7.2–7.3 (m, 7H, Ar-*H*).

^{19}F NMR (282.4 MHz, C_6D_6, 298 K, ppm): δ = –165.9 (s, 1F, ^1J(Si,F) = 296.2 Hz, Si–F), –73.1 (d quint, ^1J (P,F) = 771.1 Hz, ^2J(F,F) = 50.6 Hz, 1F, $C_{carbene}$–PF_4–*F*), –52.6 (dd, ^1J (P,F) = 781.0 Hz, ^2J(F,F) = 50.6 Hz, 4F, $C_{carbene}$–P*F*$_4$–F).

^{31}P NMR (121.5 MHz, C_6D_6, 298 K, ppm): δ = 1.98 (d quint, ^1J (P,F) = 771.3 Hz, ^1J (P,F) = 781.1 Hz, $C_{carbene}$–*P*F_4–F)

4.2.19 [Si(C_6H_3-2,6-Mes_2)(Cl)(IMe_4){P_4}Si(C_6H_3-2,6-Mes_2)(IMe_4)]Cl (37)

A solution of white phosphorus (25 mg, 0.20 mmol) in 10 mL of benzene was added dropwise to a solution of SiCl(C_6H_3-2,6-Mes_2)(IMe_4) (200 mg, 1.00 mmol) in 20 mL of benzene. The

color changed from yellow to orange-red, an orange-red precipitate was observed. The mixture was stirred for 45 min and filtered. The red precipitate was washed with benzene (2 × 10 mL) and dried *in vacuo*. The yield of the crude product was about 45%. To obtain an analytically pure sample, the product was dissolved in 15 mL of THF, the solution was concentrated to about 3 mL and stored at –60 °C for crystallization. The resulting precipitate was filtered off and dried in vacuo (30 min, RT). Yield: 70 mg (0.052 mmol, 10%), red powder. The crystals suitable for an X-ray diffraction study were obtained upon crystallization of the product (the first precipitate from benzene) from a THF-d_8 solution upon standing overnight. Elemental analysis calcd (%) for $C_{62}H_{74}Si_2Cl_2N_4P_4$ (1342.52): C 66.20, H 7.36, N 4.27; found: C 66.61, H 6.89, N 4.60.

^{1}H NMR (300.1 MHz,THF-d_8, 298 K, ppm):[107] δ = 1.98 (s, 6H, 2 × CH_3), 2.02 (s br, 6H, 2 × CH_3), 2.24 (s, 9H, 3 × CH_3), 2.36 (s, 6H 2 × CH_3), 2.54 (s, 6H, 2 × CH_3), 3.09 (s, 3H, N-CH_3), 3.27 (s br, 6H, 2 × N-CH_3), 3.47 (s, 3H, N-CH_3), 6.80 (s br, 4H, 2 × $C^{3,5}$-*H*, Mes), 6.89 (s br, 4H, 2 × $C^{3,5}$-*H*, Mes), 6.7–6.9 (br, 2H, $C^{3,5}$-*H*, C_6H_3), 7.04 (d, ^3J(H,H) = 7.5 Hz, 2H, $C^{3,5}$-*H*, C_6H_3), 7.35 (t, ^3J(H,H) = 7.5 Hz, 1H, C^4-*H*, C_6H_3), 7.56 (t, ^3J(H,H) = 7.6 Hz, 1H, C^4-*H*, C_6H_3).

^{31}P NMR (121.5 MHz,THF-d_8, 298 K, ppm):[108] δ = –214.9 (ddd, $^1J_{P,P}$ = 291.2, $^1J_{P,P}$ = 89.7 Hz, $^2J_{P,P}$ = 38.0 Hz, 1P), –181.6 (ddd, $^1J_{P,P}$ = 134.5 Hz, $^1J_{P,P}$ = 89.7 Hz, $^2J_{P,P}$ = 7.3 Hz, 1P), –144.4 (ddd, $^1J_{P,P}$ = 262.4 Hz, $^2J_{P,P}$ = 38.0 Hz, $^2J_{P,P}$ = 38.0 Hz, $^2J_{P,P}$ = 7.3 Hz, 1P), –67.9 (ddd, $^1J_{P,P}$ = 291.2 Hz, $^1J_{P,P}$ = 262.4 Hz, $^2J_{P,P}$ = 134.5 Hz, 1P).

4.2.20 [CpCo{SiCl(C_6H_3-2,6-$Trip_2$)(IMe_4)}] (38)

To a stirred suspension of SiCl(C_6H_3-2,6-$Trip_2$) (IMe_4) (740 mg, 1.105 mmol) in 10 mL of toluene, a solution of CpCo(C_2H_4)$_2$ (210 mg, 1.166 mmol, 1.06 eq) in 25 mL of pentane was added in 30 s. The mixture was stirred for 10 min. The color of the solution changed over red to deep brown and the yellow precipitate dissolved gradually. The reaction mixture was filtered from tiny amount of an insoluble material. The filtrate was stored at −60 °C overnight for crystallization. The precipitate was then filtered off at −60 °C, washed with 5 mL of

[107] Some signals were not observed due to the broadness. The ^{13}C{^{1}H}, ^{29}Si NMR and correlation spectra were not recorded because of the low solubility of the compound.

[108] Coupling constants in the ^{31}P NMR were obtained from analysis in gNMR Spectra Simulation program. We were not able to unambiguously assign signals in the ^{31}P {^{1}H} NMR spectrum.

pentane at −60 °C and dried *in vacuo* (30 min, RT). Yield: 710 mg (0.895 mmol), 81% of dark brown crystals.[109] Elemental analysis calcd (%) for $C_{48}H_{66}ClCoN_2Si$ (793.5): C 72.65, H 8.38, N 3.53; found: C 72.81, H 8.50, N 3.56%.

^{1}H NMR (300.1 MHz, C_6D_6, 298 K, ppm): δ = 0.31 (d, ^3J(H,H) = 6.8 Hz, 3H, C$^{2'}$-CH*Me$_A$*Me$_B$), 0.81 (d, ^3J(H,H) = 6.7 Hz, 3H, C$^{2''}$-CH*Me$_A$*Me$_B$, Trip), 1.03 (d, ^3J(H,H) = 6.8 Hz, 3H, C$^{2'}$-CHMe$_A$*Me$_B$*, Trip), 1.06 (d, ^3J(H,H) = 6.8 Hz, 3H, C$^{6'}$-CH*Me$_A$*Me$_B$, Trip), 1.13 (s, 3H, C^3-C*H$_3$*, IMe$_4$), 1.245 (s, 3H, C^4-C*H$_3$*, IMe$_4$) 1.245 (d, ^3J(H,H) = 6.9 Hz, 3H, C$^{4'}$-CH*Me$_A$*Me$_B$, Trip), 1.251 (d, ^3J(H,H) = 6.9 Hz, 3H, C$^{4'}$-CHMe$_A$*Me$_B$*, Trip), 1.403 (d, ^3J(H,H) = 6.8 Hz, 3H, C$^{4''}$-CH*Me$_A$*Me$_B$, Trip), 1.408 (d, ^3J(H,H) = 6.8 Hz, 3H, C$^{4''}$-CHMe$_A$*Me$_B$*, Trip), 1.49 (sept, ^3J(H,H) = 6.7 Hz, 1H, C$^{2''}$-C*H*Me$_A$Me$_B$, Trip), 1.54 (d, ^3J(H,H) = 6.8 Hz, 3H, C$^{6'}$-CHMe$_A$*Me$_B$*, Trip), 1.64 (d, ^3J(H,H) = 6.5 Hz, 3H, C$^{6''}$-CH*Me$_A$*Me$_B$, Trip), 1.74 (d, ^3J(H,H) = 6.7 Hz, 3H, C$^{6''}$-CHMe$_A$*Me$_B$*, Trip), 2.17 (d, ^3J(H,H) = 6.7 Hz, 3H, C$^{2''}$-CHMe$_A$*Me$_B$*, Trip), 2.27 (sept, ^3J(H,H) = 6.8 Hz, 1H, C$^{2'}$-C*H*Me$_A$Me$_B$, Trip), 2.52 (sept, ^3J(H,H) = 6.8 Hz, 1H, C$^{6'}$-C*H*Me$_A$Me$_B$, Trip), 2.74 (sept, ^3J(H,H) = 6.8 Hz, 1H, C$^{4''}$-C*H*Me$_A$Me$_B$, Trip), 2.84 (sept, ^3J(H,H) 6.5 Hz, 1H, C$^{4'}$-C*H*Me$_A$Me$_B$, Trip), 2.99 (sept, ^3J(H,H) = 6.4 Hz, 1H, C$^{6''}$-C*H*Me$_A$Me$_B$, Trip), 3.07 (s, 3H, N^2-C*H$_3$*, IMe$_4$), 4.02 (s, 5H, C$_5$*H$_5$*), 4.10 (s, 3H, N^5-C*H$_3$*, IMe$_4$), 6.44 (d, ^4J(H,H) = 1.5 Hz, 1H, C$^{5''}$-*H*, Trip), 6.84 (d, ^4J(H,H) = 1.9 Hz, 1H, C$^{3'}$-*H*, Trip), 6.93 (dd, ^4J(H,H) = 1.2 Hz, ^3J(H,H) = 7.4 Hz, 1H, C^3-*H*, C$_6$H$_3$), 7.01 (dd, ^3J(H,H) = 7.4 Hz, ^3J(H,H) = 7.6 Hz, 1H, C^4-*H*, C$_6$H$_3$), 7.18 (d, ^4J(H,H) = 1.9 Hz, 1H, C$^{5'}$-*H*, Trip), 7.21 (s br, 1H, C$^{3''}$-*H*, Trip), 7.27 (dd, ^4J(H,H) = 1.2 Hz, ^3J(H,H) = 7.6 Hz, 1H, C^5-*H*, C$_6$H$_3$).

---

[109] The compound is thermolabile in solution and therefore must be stored at low temperatures. It decomposes to a product of C–H activation of one of the N−CH$_3$ groups by the cobalt atom (weeks at rt, hours at 50 °C). The structure was verified by X-ray crystallography. The ^{1}H NMR spectrum recorded after preparation revealed already about 10% of decomposition. ^{1}H NMR of the decomposition product (300.1 MHz, C_6D_6, 298 K, ppm): δ = −17.26 (s br, 1H, Co-H), 1.07 (d, ^3J(H,H) = 6.6 Hz, 6H, 2×C$^{2\text{ or }6}$-CH*Me*, Trip), 1.12 (s, 3H, C^4-*Me*, CH$_2$-IMe$_3$), 1.15−1.30 (s br, 6H), 1.31 (d, ^3J(H,H) = 6.8 Hz, 12H, 2×C^4-CH*Me$_2$*, Trip), 1.40 (s, 3H, C^3-*Me*, CH$_2$-IMe$_3$), 1.61 (d, ^3J(H,H) = 6.8 Hz, 6H, 2×C$^{2\text{ or }6}$-CH*Me*, Trip), 2.84 (s, 3H, N^5-*Me*, CH$_2$-IMe$_3$), 2.91 (d, ^2J(H,H) = 9.8 Hz, 1H, Co-C*H$_A$*H$_B$-N, CH$_2$-IMe$_3$), 2.85−2.95 (br, 1H, C*H*Me$_2$), 3.15−3.32 (br, 2H, C*H*Me$_2$), 3.60 (d, ^2J(H,H) = 9.8 Hz, 1H, Co-CH$_A$*H$_B$*-N), 4.64 (s, 5H, C$_5$*H$_5$*), 7.06−7.30 (m br, 7H, Ar-*H*). Two methyl groups and three methyne groups of an isopropyl substituent could not be unambiguously detected due to the presence of impurities.

$^{13}C\{^1H\}$ NMR (75.47 MHz, toluene-d_8, 233 K, ppm): δ = 7.8 (s, 1C, C^4-CH_3, IMe_4), 8.2 (s, 1C, C^3-CH_3, IMe_4), 21.0 (s, 1C, $C^{2'}$-CH$Me_A$$Me_B$), 22.4 (s, 1C, $C^{6'}$-CH$Me_A$$Me_B$), 23.93 (s, 1C, $C^{2''}$-CH$Me_A$$Me_B$), 23.95 (s, 1C, $C^{4''}$-CH$Me_A$$Me_B$), 24.2 (s, 1C, $C^{2''}$-CH$Me_A$$Me_B$), 24.4 (s, 1C, $C^{4'}$-CH$Me_A$$Me_B$, Trip), 24.6 (s, 1C, $C^{4'}$-CH$Me_A$$Me_B$, Trip), 24.7 (s, 1C, $C^{4''}$-CH$Me_A$$Me_B$, Trip), 26.2 (s, 1C, $C^{6''}$-CH$Me_A$$Me_B$, Trip), 26.6 (s, 1C, $C^{6'}$-CH$Me_A$$Me_B$, Trip), 27.1 (s, 1C, $C^{2'}$-CH$Me_A$$Me_B$, Trip), 27.7 (s, 1C, $C^{6''}$-CH$Me_A$$Me_B$, Trip), 30.84 (s, 1C, $C^{2'}$-CH$Me_A$$Me_B$, Trip), 30.89 (s, 1C, $C^{6'}$-CH$Me_A$$Me_B$, Trip), 33.2 (s, 1C, $C^{6''}$-CH$Me_A$$Me_B$,Trip), 33.6 (s, 1C, N^5-CH_3, IMe_4), 35.1 (s, 1C, N^2-CH_3, IMe_4), 34.7 (s, 1C, $C^{4'}$-CH$Me_A$$Me_B$, Trip), 35.0 (s, 1C, $C^{4''}$-CH$Me_A$$Me_B$, Trip), 36.3 (s, 1C, $C^{2''}$-CH$Me_A$$Me_B$, Trip), 75.1 (s, 1C, $C^{1''}$, Trip), 76.6 (s, 1C, $C^{2''}$, Trip), 83.5 (s, 5C, C_5H_5), 114.6 (s, 1C, $C^{5''}$-H, Trip), 118.3 (s, 1C, $C^{3'}$-H, Trip), 120.9 (s, 1C, $C^{5'}$-H, Trip), 126.0 (s, 1C, C^4, IMe_4), 126.48 (s, 1C, C^3, IMe_4), 126.54 (s, 1C, C^4-H, C_6H_3) 128.8 (s, 1C, C^3-H, C_6H_3), 130.8 (s, 1C, C^5-H, C_6H_3), 132.0 (s, 1C, $C^{3''}$-H, Trip), 135.1 (s, 1C, $C^{4''}$, Trip), 138.7 (s, 1C, $C^{1'}$, Trip), 142.5 (s, 1C, C^2, C_6H_3), 142.7 (s, 1C, C^1, C_6H_3), 145.0 (s, 1C, $C^{2'}$, Trip), 147.5 (s, 1C, $C^{4'}$, Trip), 149.8 (s, 1C, $C^{6'}$, Trip), 153.6 (s, 1C, $C^{6''}$, Trip), 157.2 (s, 1C, C^1, IMe_4), 159.5 (s, 1C, C^6, C_6H_3).

^{29}Si NMR (59.63 MHz, C_6D_6, 298K, ppm): δ = 47.7 (s).

Numbering scheme

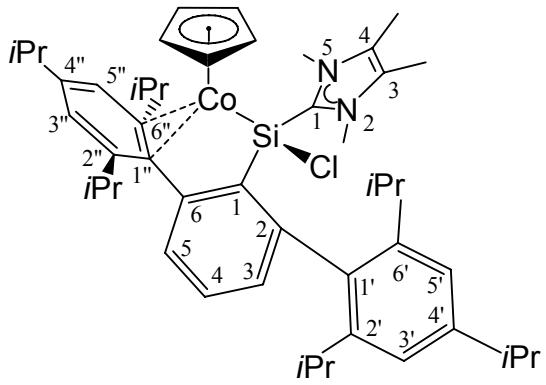

4.2.21 [SiCl(C_6H_3-2,6-$Trip_2$)H(IMe_4)][CpMo(CO)$_3$] (40)

To a precooled to –70 °C solution of SiCl(C_6H_3-2,6-$Trip_2$)(IMe_4) (135 mg, 0.20 mmol) in 5 mL of THF, a solution of HCl in dioxane (0.46 mL, 0.435 M, 0.20 mmol) was added dropwise. The mixture was stirred for several minutes, without the cooling bath, until the yellow color gradually disappeared. The formation of [SiCl(C_6H_3-2,6-$Trip_2$)H(IMe_4)]Cl was assumed and a solution of Li[CpMo(CO)$_3$] (55 mg, 0.22 mmol, 1.1 equiv.) in THF was added dropwise. The yellow mixture was allowed to warm up to room temperature under stirring and then all volatilities were removed under vacuum. The yellow residue was treated with

3 mL of hexane and then the mixture was dried under vacuum (10 min, RT). The resulting yellow solid was extracted with 2 mL of toluene, the extract was filtered. The filtrate was carefully layered with 2 mL of hexane. After 1 week of diffusion at room temperature yellow crystals were formed, which were separated by decantation, washed with hexane (3 × 1 mL) and dried in an atmosphere of the glovebox for 15 min. Yield: ca. 20 mg (0.022 mmol, 11%). The crystals were suitable for X-ray diffraction analysis. IR (THF, cm^{-1}): 1895 (vs), 1779 (vs), 1769(vs) [*ν*(CO)].

^{1}H NMR (300.1 MHz, C_6D_6, 298 K, ppm): δ = 0.95 (d, ^{3}J(H,H) = 6.6 Hz, 6H, 2 × CH*Me*, Trip), 1.01 (d, ^{3}J(H,H) = 6.6 Hz, 6H, 2 × CH*Me*, Trip), 1.08 (d, ^{3}J(H,H) = 6.8 Hz, 6H, 2 × CH*Me*, Trip), 1.24 (d, ^{3}J(H,H) = 6.9 Hz, 12H, 4 × CH*Me*, Trip), 1.26 (d, ^{3}J(H,H) = 6.6 Hz, 6H, 2 × CH*Me*, Trip), 2.03 (s, 6H, $C^{4,5}$-*Me*, IMe_4), 2.50 (sept, ^{3}J(H,H) = 6.7 Hz, 2H, 2 × C*H*Me_2, Trip), 2.63 (sept, ^{3}J(H,H) = 6.9 Hz, 2H, 2 × C*H*Me_2, Trip), 2.83 (sept, ^{3}J(H,H) = 6.9 Hz, 2H, 2 × C*H*Me_2, Trip), 3.06 (s, 6H, 2 × N-*Me*, IMe_4), 5.34 (s, 1H, Si–H, ^{1}J(Si,H) = 265 Hz), 5.40 (s, 5H, C_5H_5), 6.94 (m, 2H, $C^{3,5}$-*H*, C_6H_3), 7.00–7.07 (m, 3H, C_6H_3), 7.05 (d, ^{4}J(H,H) = 1.5 Hz, 2H, $C^{3\text{ or }5}$-*H*, Trip), 7.12 (d, ^{4}J(H,H) = 1.5 Hz, 2H, $C^{5\text{ or }3}$-*H*, Trip).

^{13}C{^{1}H} NMR (75.47 MHz, C_6D_6, 298 K, ppm): δ = 9.2 (s, 2C, $C^{4,5}$-*Me*, IMe_4), 22.0 (s, 2C, 2 × CH*Me*, Trip), 22.7 (s, 2C, 2 × CH*Me*, Trip), 24.27 (s, 2C, 2 × CH*Me*, Trip), 24.32 (s, 2C, 2 × CH*Me*, Trip), 26.25 (s, 2C, 2 × CH*Me*, Trip), 26.34 (s, 2C, 2 × CH*Me*, Trip), 31.4 (s, 4C, 2 × *C*HMe, Trip; $N^{1,3}$-*Me*, IMe_4), 34.2 (s, 2C, 2 × *C*HMe, Trip), 34.6 (s, 2C, 2 × *C*HMe, Trip), 87.0 (s, 5C, C_5H_5), 121.3 (s, 2C, 2 × $C^{3\text{ or }5}$-H, Trip), 121.6 (s, 2C, 2 × $C^{5\text{ or }3}$-H, Trip), 126.5 (s, 1C, C^{1}, C_6H_3), 131.2 (s, 1C, C^{4}-H, C_6H_3), 131.87 (s, 2C, $C^{4,5}$-Me, IMe_4), 131.91 (s, 2C, $C^{3,5}$-H, C_6H_3), 135.6 (s, 2C, 2 × C^{1}, Trip), 139.2 (s, 1C, Si-*C*N_2, IMe_4), 147.4 (s, 2C, 2 × $C^{2\text{ or }4\text{ or }6}$, Trip), 147.5 (s, 2C, 2 × $C^{2\text{ or }4\text{ or }6}$, Trip), 148.8 (s, 2C, $C^{2,6}$, C_6H_3), 150.6 (s, 2C, 2 × $C^{2\text{ or }4\text{ or }6}$, Trip), 237.1 (s, 3C, 3 × *C*O).

^{29}Si{^{1}H} NMR (59.63 MHz, C_6D_6, 298 K, ppm): δ = –31.0 (s).

4.2.22 3,7-dihydro–2-(2,6-bis(2,4,6-triisopropylphenyl)phenyl)-5,6,7-trimethyl–2H-imidazo[1,2-d][1,4,2]diazasilole (41) (NaN_3 + $SiCl(C_6H_3$-2,6-$Trip_2)(IMe_4)$)

A suspension of $SiCl(C_6H_3$-2,6-$Trip_2)(IMe_4)$ (370 mg, 0.553 mmol) and NaN_3 (270 mg, 4.15 mmol, 7.51 eq) in 15 mL of toluene was refluxed for 2 h with stirring. The yellow color of the mixture gradually faded. All volatilities were removed *in vacuo*, the residue was treated with 2 mL of hexane. After hexane was evaporated the residue was dried *in vacuo* at ambient

temperature and then extracted with 10 mL of hexane. The extract was filtered, concentrated under reduced pressure to about 2 mL and stored at –60 °C for one week for crystallization. Colorless crystals were filtered off, washed with hexane (2 × 1 mL) and dried *in vacuo* (–60 °C to RT). Yield 170 mg (0.262 mmol, 47%), white powder. Slow cooling of a hexane solution of **41** afforded colorless single crystals suitable for X-ray diffraction analysis. IR (benzene, cm^{-1}): ν = 2133 (w). IR (solid, cm^{-1}): 3045 (vw), 3034 (vw), 2956 (s), 2924 (m), 2866 (m), 2131 (m), 1584 (vs), 1459 (s), 1447 (m), 1425 (s), 1402 (m), 1381 (m), 1360 (m), 1444 (vw), 1316 (w), 1267 (vw), 1247 (vw), 1239 (vw), 1213 (vw), 1169 (w), 1143 (m), 1116 (w), 1103 (w), 1078 (w), 1071 (w), 1049 (w), 1018 (vw), 1006 (vw), 954 (vw), 940 (vw), 922 (s), 881 (vs), 849 (vw), 839 (vw), 823 (vw), 806 (vs), 779 (w), 744 (s), 730 (m), 717 (s), 662 (w), 651 (w), 6161 (vw), 584 (w), 564 (vw), 492 (vw), 456 (s), 420 (w), 399 (w), 389 (w).

^{1}H NMR (300.1 MHz, C_6D_6, 298 K, ppm): δ = 1.14 (d, ^{3}J(H,H) = 6.8 Hz, 6H, 2 × C^{2}-CH*Me$_A$*Me$_B$, Trip), 1.19 (d, ^{3}J(H,H) = 6.9 Hz, 6H, 2 × C^{6}-CH*Me$_A$*Me$_B$, Trip), 1.27 (d, ^{3}J(H,H) = 6.9 Hz, 12H, 2 × C^{4}-CH*Me$_A$Me$_B$*, Trip), 1.29 (d, ^{3}J(H,H) = 6.8 Hz, 6H, 2 × C^{2}-CHMe$_A$*Me$_B$*, Trip), 1.40 (s, 3H, C^{4}-C*H$_3$*, IMe$_3$CH$_2$), 1.45 (s, 3H, C^{5}-C*H$_3$*, IMe$_3$CH$_2$), 1.46 (d, ^{3}J(H,H) = 6.9 Hz, 6H, 2 × C^{6}-CH*Me$_A$*Me$_B$, Trip), 1.66 (dd, ^{3}J(H,H) = 12.8 Hz, ^{3}J(H,H) = 4.9 Hz, 1H, N-C*H$_A$*H$_B$), 2.17 (dd, ^{3}J(H,H) = 12.8 Hz, ^{3}J(H,H) = 3.9 Hz, 1H, N-CH$_A$*H$_B$*), 2.79 (s, 3H, N-C*H$_3$*), 2.86 (sept, ^{3}J(H,H) = 6.9 Hz, 2H, 2 × C^{4}-C*H*Me$_A$Me$_B$, Trip), 3.07 (sept, ^{3}J(H,H) = 6.8 Hz, 2H, 2 × C^{2}-C*H*Me$_A$Me$_B$, Trip), 3.08 (sept, ^{3}J(H,H) = 6.9 Hz, 2H, 2 × C^{6}-C*H*Me$_A$Me$_B$, Trip), 5.39 (dd, ^{3}J(H,H) = 4.9 Hz, ^{3}J(H,H) = 3.9 Hz, 1H, Si*H*, ^{1}J(Si,H) = 216.5 Hz), 7.14 (d, ^{4}J(H,H) ≈ 1.5 Hz, 2H, C^{5}-*H*, Trip), 7.17–7.28 (m, 3H, C^{3,4,5}-*H*, C_6H_3), 7.21 (d, 2H, C^{3}-*H*, Trip).[110]

^{13}C{^{1}H} NMR (75.47 MHz, C_6D_6, 298 K, ppm): δ = 8.4 (s, 2C, C^{4}-*Me*, IMe$_3$CH$_2$), 8.7 (s, 2C, C^{5}-*Me*, IMe$_3$CH$_2$), 22.6 (s, 2C, 2 × C^{2}-CHMe$_A$*Me$_B$*, Trip), 23.4 (s, 2C, 2 × C^{6}-CHMe$_A$*Me$_B$*, Trip), 24.4 (s, 2C, 2 × C^{4}-CH*Me$_A$*Me$_B$, Trip), 24.5 (s, 2C, 2 × C^{4}-CHMe$_A$*Me$_B$*, Trip), 25.7 (s, 2C, 2 × C^{6}-CH*Me$_A$*Me$_B$, Trip), 25.8 (s, 2C, 2 × C^{2}-CH*Me$_A$*Me$_B$, Trip), 28.2 (s, C, N^{3}-*Me*, IMe$_4$), 29.7 (s, 1C, N-*C*H$_A$H$_B$), 31.07 (s, 2C, 2 × C^{6}-*C*HMe$_A$Me$_B$, Trip), 31.12 (s, 2C, 2 × C^{2}-*C*HMe$_A$Me$_B$, Trip), 34.8 (s, 2C, 2 × C^{4}-*C*HMe$_A$Me$_B$, Trip), 113.0 (s, 1C, *C^{4}*-Me, IMe$_3$CH$_2$), 114.6 (s, 1C, *C^{5}*-Me, IMe$_3$CH$_2$), 120.3 (s, 2C, 2 × *C^{5}*-H, Trip), 120.5 (s, 2C, 2 × *C^{3}*-H, Trip), 128.6 (s, 1C, *C^{4}*-H, C_6H_3), 129.8 (s, 2C, *C^{3,5}*-H, C_6H_3), 136.0 (s, 1C, Si-*C^{1}*,

[110] The signal overlaps with the multiplet at 7.17–7.28 ppm. The chemical shift and coupling constant could not be directly measured. The value should be taken as approximate.

C_6H_3), 138.6 (s, 2C, 2 × C^1, Trip), 147.0 (s, 2C, 2 × C^2, Trip), 147.3 (s, 2C, 2 × C^6, Trip), 147.9 (s, 2C, $C^{2,6}$, C_6H_3), 148.3 (s, 2C, 2 × C^4, Trip), 160.8 (s, 1C, C^2N_3, IMe_3CH_2).

$^{29}Si\{^1H\}$ NMR (59.63 MHz, C_6D_6, 298 K, ppm): δ = 3.9 (s).

4.2.23 [Cp(CO)$_2$Mo=Si(C$_6$H$_3$-2,6-Trip$_2$)(IMe$_4$)] (42)

A mixture of SiCl(C_6H_3-2,6-$Trip_2$)(IMe_4) (670 mg, 1.00 mmol) and Li[$CpMo(CO)_3$] (260 mg, 1.03 mmol) was treated with 25 mL of toluene. The resulting suspension was immersed in an ultrasonic bath for 5 min and then heated at 100 °C for 25 min with stirring allowing for pressure release through a mercury bubbler. Evolution of carbon monoxide was observed and the color of the mixture changed from yellow over brown-green to brown, and most of the solid dissolved. The suspension was filtered and the dark brown filtrate was concentrated *in vacuo* to ca. 3 mL. 15 mL of hexane was added and the mixture was stored at −50 °C for 0.5 h. The crystalline precipitate was filtered, washed twice with 5 mL of a toluene/hexane mixture (1/5) and dried in vacuo at ambient temperature. Recrystallization of the solid from a toluene/hexane mixture (1/5) afforded the product as a dark-brown, crystalline powder, which was dried *in vacuo* at 50 °C. Yield: 430 mg (0.505 mmol, 51%). M.p. 125−130 °C. Elemental analysis calcd (%) for $C_{50}H_{66}MoN_2O_2Si$ (851.08): C 70.56, H 7.82, N 3.29; found: C 70.38, H 7.89, N 3.14%. IR (toluene, cm^{-1}): 1859 (vs), 1785 (vs) [ν(CO)].

^1H NMR (300.1 MHz, C_6D_6, 298 K, ppm): δ = 1.15 (d, ^3J(H,H) = 6.9 Hz, 12H, 2 × $C^{2,6}$-CH$Me_A$$Me_B$, Trip), 1.20–1.30 (br, 12H, 2 × $C^{2,6}$-CH$Me_A$$Me_B$, Trip), 1.27 (d, ^3J(H,H) = 6.9 Hz, 12H, 2 × C^4-CH*Me*, Trip), 1.36 (s, 6H, $C^{4,5}$-*Me*, IMe_4), 2.84 (sept, ^3J(H,H) = 6.9 Hz, 2H, 2 × C^4-C*H*Me_2, Trip), 3.03 (br, 4H, 2 × $C^{2,6}$-C*H*$Me_A$$Me_B$, Trip), 3.09 (s, 6H, 2 × N-*Me*, IMe_4), 5.03 (s, 5H, C_5H_5), 6.94 (m, 2H, $C^{3,5}$-*H*, C_6H_3), 7.02 (m, 1H, C^4-*H*, C_6H_3), 7.17 (s, 4H, $C^{3,5}$-*H*, Trip).

$^{13}C\{^1H\}$ NMR (75.47 MHz, C_6D_6, 298 K, ppm): δ = 8.0 (s, 2C, $C^{4,5}$-*Me*, IMe_4), 23.3 (s, 4C, 2 × $C^{2,6}$-CH$Me_A$$Me_B$, Trip), 24.3 (s, 4C, 2 × C^4-CHMe_2, Trip), 26.3 (s br, 4C, 2 × $C^{2,6}$-CH$Me_A$$Me_B$, Trip), 31.4 (s, 4C, 2 × $C^{2,6}$-*C*H$Me_A$$Me_B$, Trip), 32.6 (s, 2 × N-*Me*, IMe_4), 34.8 (s, 2C, 2 × C^4-*C*HMe_2, Trip), 89.2 (s, 5C, C_5H_5), 121.8 (s br, 4C, 2 × $C^{3,5}$-H, Trip), 124.8 (s, 2C, $C^{4,5}$-Me, IMe_4), 126.7 (s, 1C, C^4-H, C_6H_3), 131.8 (s, 2C, $C^{3,5}$-H, C_6H_3), 140.3 (s, 2C, 2 × C^1, Trip), 145.0 (s br, 2C, $C^{2,6}$, C_6H_3), 147.8 (s br, 4C, 2 × $C^{2,6}$, Trip), 148.4 (s, 2C, 2 × C^4, Trip), 151.6 (s, 1C, Si-C^1, C_6H_3), 165.3 (s, 1C, Si-C^2, IMe_4), 243.5 (s, 2C, 2 × *C*O).

^{29}Si NMR (59.63 MHz, C_6D_6, 298 K, ppm): δ = 201.8 (s).

4.2.24 [Cp(CO)$_2$Mo=Si(C$_6$H$_3$-2,6-Mes$_2$)(IMe$_4$)] (43)

15 mL of toluene were added to a mixture of Li[CpMo(CO)$_2$(PMe$_3$)], (177 mg, 0.597 mmol) and SiCl(C$_6$H$_3$-2,6-Mes$_2$)(IMe$_4$), (285 mg, 0.569 mmol). The mixture was stirred for 6 h at ambient temperature. The color gradually changed from yellow over brown to dark green and most of the solid dissolved, leaving some of a brown precipitate. The reaction mixture was filtered; the filtrate was concentrated to about 5 mL in *vacuo*. About 15 mL of hexane were added fast, in such a way that some amorphous brown material precipitated (estimated 50–100 mg, the composition is unknown, could be the starting SiCl(C$_6$H$_3$-2,6-Mes$_2$)(IMe$_4$)), whereas the green product remained in the oversaturated supernatant solution. After hexane addition the mixture was filtered, and the filtrate was placed at 0 °C for 30 min for crystallization. The obtained black-green crystals were filtered, washed with hexane (2 × 3 mL) and dried in *vacuo* (10 min, RT). Yield 220 mg (0.322 mmol, 56%). Elemental analysis calcd (%) for C$_{38}$H$_{42}$MoN$_2$O$_2$Si (682.78): C 66.84, H 6.20, N 4.10; found: C 66.63, H 6.43, N 4.10%. IR (toluene, cm^{-1}): 1854 (vs), 1779 (vs) [ν(CO)]. ^{1}H NMR (300.1 MHz, C$_6$D$_6$, 298 K, ppm): δ = 1.21 (s, 6H, C^{4,5}-*Me*, IMe$_4$), 2.14 (s, 12H, 2 × C^{2,6}-*Me*, Mes), 2.17 (s, 6H, 2 × C^4-*Me*, Mes), 3.10 (s, 6H, N^{1,3}-*Me*, IMe$_4$), 5.24 (s, 5H, C$_5$*H*$_5$), 6.77 (s, 4H, 2 × C^{3,5}-*H*, Mes), 7.78 (d, 2H, ^3J(H,H) = 7.5 Hz, C^{3,5}-*H*, C$_6$H$_3$), 7.13 (t, 1H, d, ^3J(H,H) = 7.5 Hz, C^4-*H*, C$_6$H$_3$). ^{13}C{^{1}H} NMR (125.8 MHz, C$_6$D$_6$, 298 K, ppm): δ = 7.7 (s, 2C, C^{4,5}-*Me*, IMe$_4$), 20.9 (s, 2C, C^4-*Me*, Mes), 21.8 (s, 4C, 2 × C^{2,6}-*Me*, Mes), 33.1 (s, 2C, N^{1,3}-*Me*, IMe$_4$), 88.8 (s, 5C, C$_5$H$_5$), 124.0 (s, 2C, *C*^{4,5}, IMe$_4$), 128.7 (s, *C*^{4}-H, C$_6$H$_3$), 129.0 (s, 4C, 2 × *C*^{3,5}-H, Mes), 130.0 (s, 2C, *C*^{3,5}-H, C$_6$H$_3$), 136.3 (s, 2C, 2 × *C*^{4}-H, Mes), 136.6 (s, 4C, 2 × *C*^{2,6}, Mes), 141.2 (s, 2C, 2 × *C*^{1}, Mes), 146.3 (s, 2C, *C*^{2,6}, C$_6$H$_3$), 150.3 (s, 1C, *C*^{1}, C$_6$H$_3$), 162.9 (s, 1C, *C*^{2}, IMe$_4$), 240.6 (s, 2C, *C*O). ^{29}Si NMR (59.63 MHz, C$_6$D$_6$, 298 K, ppm): δ = 200.5 (s).

4.2.25 [Cp(CO)$_2$W=Si(C$_6$H$_3$-2,6-Mes$_2$)(IMe$_4$)] (44)

15 mL of toluene were added to a mixture of Li[CpW(CO)$_2$(PMe$_3$)] (80 mg, 0.21 mmol) and SiCl(C$_6$H$_3$-2,6-Mes$_2$)(IMe$_4$) (100 mg, 0.20 mmol). The mixture was immersed in an ultrasonic bath for 10 min and subsequently stirred for 12 h at ambient temperature. The color gradually changed to dark green and most of the solid dissolved. The reaction mixture was filtered; the filtrate was concentrated to about 3 mL *in vacuo*. About 5 mL of hexane were added fast, in such a way that some amorphous brown material precipitated (estimated 20–40 mg, the composition is unknown, could be the starting SiCl(C$_6$H$_3$-2,6-Mes$_2$)(IMe$_4$)), whereas the green product remained in the oversaturated supernatant solution. After hexane addition the

mixture was filtered, and the filtrate was left for crystallization for 1 h at ambient temperature. The obtained black-green crystals were filtered, washed with hexane (3 × 2 mL) and dried *in vacuo* (30 min, RT). Yield 75 mg (0.097 mmol, 48%). Elemental analysis calcd (%) for $C_{38}H_{42}N_2O_2SiW$ (770.68): C 59.22, H 5.49, N 3.63; found: C 59.21, H 5.67, N 3.66%. IR (toluene, cm^{-1}): 1849 (vs), 1775 (vs) [ν(CO)]. ^{1}H NMR (300.1 MHz, C_6D_6, 298 K, ppm): δ = 1.23 (s, 6H, $C^{4,5}$-*Me*, IMe_4), 2.13 (s, 12H, 2 × $C^{2,6}$-*Me*, Mes), 2.16 (s, 6H, 2 × C^4-*Me*, Mes), 3.12 (s, 6H, $N^{1,3}$-*Me*, IMe_4), 5.15 (s, 5H, C_5H_5), 6.75 (s, 4H, 2 × $C^{3,5}$-*H*, Mes), 7.77 (d, 2H, ^3J(H,H) = 7.5 Hz, $C^{3,5}$-*H*, C_6H_3), 7.18 (t, 1H, ^3J(H,H) = 7.5 Hz, C^4-*H*, C_6H_3). $^{13}C\{^1H\}$ NMR (75.5 MHz, C_6D_6, 298 K, ppm): δ = 7.7 (s, 2C, $C^{4,5}$-*Me*, IMe_4), 20.9 (s, 2C, 2 × C^4-*Me*, Mes), 21.7 (s, 4C, 2 × $C^{2,6}$-*Me*, Mes), 32.5 (s, 2C, $N^{1,3}$-*Me*, IMe_4), 87.2 (s, 5C, C_5H_5), 124.0 (s, 2C, $C^{4,5}$, IMe_4), 128.3 (s, 1C, C^4, C_6H_3), 129.0 (s, 4C, 2 × $C^{3,5}$-H, Mes), 130.4 (s, 2C, $C^{3,5}$-H, C_6H_3), 136.3 (s, 2C, 2 × C^4-H, Mes), 136.5 (s, 4C, 2 × $C^{2,6}$, Mes), 141.4 (s, 2C, 2 × C^1, Mes), 145.5 (s, 2C, $C^{2,6}$, C_6H_3), 152.6 (s, 1C, C^1, C_6H_3), 168.4 (s, 1C, C^2, IMe_4), 232.0 (s, 2C, *C*O). ^{29}Si NMR (59.63 MHz, C_6D_6, 298 K, ppm): δ = 180.0 (s, ^1J(W,Si) = 302.3 Hz).

4.2.26 [(-Ar^{Trip}SiH-CH$_2$-IMe$_3$-)$_2$][CpCr(CO)$_3$]$_2$ (45)

A mixture of $SiCl(C_6H_3$-2,6-$Trip_2)(IMe_4)$ (200 mg, 0.299 mmol) and Na[CpCr(CO)$_3$] 2DME (140 mg, 0.347 mmol) was treated with 10 mL of xylene. The resulting suspension was immersed in an ultrasonic bath for 3 min and then heated at 140 °C for 15 min with stirring. IR spectroscopy revealed selective formation of the product. The color of the mixture changed from yellow to brown, and most of the solid dissolved. The suspension was filtered from a small amount of a black solid and the brown filtrate was concentrated *in vacuo* to ca 5 mL (incipient crystallization). The mixture was left at ambient temperature for crystallization; a yellow crystalline solid was filtered, washed with xylene and dried *in vacuo*. Yield: 75 mg (0.045 mmol, 30%), orange crystalline powder.[111] The filtrate was evaporated *in vacuo* and then 10 mL hexane and 10 mL of diethyl ether were added to the residue. The mixture was stirred for 10 min to give a yellow precipitate, which was filtered and dried *in vacuo* to give a second crop of the product (25 mg). Slow evaporation of a xylene-THF solution of **45** afforded large orange single crystals of **45**·2(xylene) suitable for the X-ray diffraction analysis. Elemental analysis calcd (%) for $C_{102}H_{132}Cr_2N_4O_6Si_2$ (1670.3): C 73.34, H 7.97, N

[111] The yield seems to be rather low given the high selectivity of the reaction.

3.35; found: C 73.76, H 8.06, N 2.84 %. IR (toluene, cm^{-1}): 1888 (vs), 1776 (vs), 1754 (s) [ν(CO)]. IR (THF, cm^{-1}): 1892 (vs), 1779 (vs), 1753 (s) [ν(CO)].

The NMR spectra are formally described for a half of the molecule. ^{1}H NMR (300.1 MHz, THF-d_8, 298 K, ppm): δ = 0.56 (d, ^{3}J(H,H) = 6.6 Hz, 3H, C$^{2'}$-CH*Me*$_A$Me$_B$), 0.71 (d, ^{3}J(H,H) = 6.8 Hz, 3H, C$^{2''}$-CH*Me*$_A$Me$_B$), 0.80 (d, ^{3}J(H,H) = 6.7 Hz, 3H, C$^{6'}$-CH*Me*$_A$Me$_B$), 0.84 (d, ^{3}J(H,H) = 6.9 Hz, 3H, C$^{6''}$-CH*Me*$_A$Me$_B$), 1.18 (d, ^{3}J(H,H) = 6.6 Hz, 3H, C$^{2'}$-CHMe$_A$*Me*$_B$), 1.25 (d, ^{3}J(H,H) = 6.9 Hz, 3H, C$^{4'}$-CH*Me*$_A$Me$_B$), 1.27 (d, ^{3}J(H,H) = 6.9 Hz, 3H, C$^{4'}$-CHMe$_A$*Me*$_B$), 1.35 (d, ^{3}J(H,H) = 6.9 Hz, 3H, C$^{4''}$-CH*Me*$_A$Me$_B$), 1.366 (d, ^{3}J(H,H) = 6.9 Hz, 3H, C$^{6''}$-CHMe$_A$*Me*$_B$), 1.372 (d, ^{3}J(H,H) = 6.7 Hz, 3H, C$^{6'}$-CHMe$_A$*Me*$_B$), 1.42 (d, ^{3}J(H,H) = 6.9 Hz, 3H, C$^{4''}$-CHMe$_A$*Me*$_B$), 1.50 (d, ^{3}J(H,H) = 6.8 Hz, 3H, C$^{2''}$-CHMe$_A$*Me*$_B$), 1.98 (s, 3H, C^{4}-*Me*, CH$_2$-IMe$_3$)[112], 2.03 (s, 3H, C^{5}-*Me*, CH$_2$-IMe$_3$), 2.188 (sept, ^{3}J(H,H) = 6.7 Hz, 1H, C$^{6'}$-C*H*Me$_A$Me$_B$), 2.195 (sept, ^{3}J(H,H) = 6.6 Hz, 1H, C$^{2'}$-C*H*Me$_A$Me$_B$), 2.82 (dd, ^{2}J(H,H) = 16.5 Hz, ^{3}J(H,H) = 1.5 Hz, 1H, N^{1}–C*H*$_A$H$_B$, CH$_2$-IMe$_3$), 2.90 (s, 3H, N^{3}-*Me*, CH$_2$-IMe$_3$), 2.91 (sept, ^{3}J(H,H) = 6.8 Hz, 1H, C$^{2''}$-C*H*Me$_A$Me$_B$), 2.93 (sept, ^{3}J(H,H) = 6.9 Hz, 1H, C$^{4'}$-C*H*Me$_A$Me$_B$), 3.02 (sept, ^{3}J(H,H) = 6.9 Hz, 1H, C$^{6''}$-C*H*Me$_A$Me$_B$), 3.09 (sept, ^{3}J(H,H) = 6.9 Hz, 1H, C$^{4''}$-C*H*Me$_A$Me$_B$), 3.54 (dd, ^{2}J(H,H) = 16.5 Hz, ^{3}J(H,H) = 8.5 Hz, 1H, N^{1}–CH$_A$*H*$_B$, CH$_2$-IMe$_3$), 4.25 (s, 5H, C$_5$*H*$_5$), 5.30 (d, ^{3}J(H,H) = 8.5 Hz, ^{1}J(Si,H) = 223 Hz, 1H, Si*H*), 6.74 (d, ^{4}J(H,H) = 1.7 Hz, 1H, C$^{3'}$-*H*, Trip), 7.19 (d, ^{4}J(H,H) = 1.7 Hz, 1H, C$^{5'}$-*H*, Trip), 7.31 (dd, ^{3}J(H,H) = 7.7 Hz, ^{4}J(H,H) = 1.1 Hz, 1H, C^{3}-*H*, C$_6$H$_3$), 7.32 (d, ^{4}J(H,H) = 1.7 Hz, 1H, C$^{5''}$-*H*, Trip), 7.47 (d, ^{4}J(H,H) = 1.7 Hz, 1H, C$^{5''}$-*H*, Trip). 7.49 (dd, ^{3}J(H,H) = 7.7 Hz, ^{4}J(H,H) = 1.1 Hz, 1H, C^{5}-*H*, C$_6$H$_3$), 7.74 (t, ^{3}J(H,H) = 7.7 Hz, 1H, C^{4}-*H*, C$_6$H$_3$). ^{13}C{^{1}H} NMR (75.47 MHz, THF-d_8, 298 K, ppm): δ = 9.91 (s, 1C, C^{5}-*Me*, CH$_2$-IMe$_3$), 10.3 (s, 1C, C^{4}-*Me*, CH$_2$-IMe$_3$), 22.4 (s, 1C, C$^{4''}$-CHMe$_A$*Me*$_B$), 22.5 (s, 1C, C$^{2''}$-CHMe$_A$*Me*$_B$), 23.1 (s, 1C, C$^{2'}$-CH*Me*$_A$Me$_B$), 23.3 (s, 1C, C$^{6''}$-CH*Me*$_A$Me$_B$), 23.4 (s, 1C, C$^{6'}$-CHMe$_A$*Me*$_B$), 24.1 (s, 1C, C$^{4'}$-CHMe$_A$*Me*$_B$), 24.7 (s, 1C, C$^{4'}$-CH*Me*$_A$Me$_B$), 25.6 (s, 1C, C$^{2''}$-CH*Me*$_A$Me$_B$), 25.8 (s, 1C, C$^{4''}$-CH*Me*$_A$Me$_B$), 26.0 (s, 1C, C$^{6'}$-CH*Me*$_A$Me$_B$), 27.2 (s, 1C, C$^{2'}$-CHMe$_A$*Me*$_B$), 27.3 (s, 1C, C$^{6''}$-CHMe$_A$*Me*$_B$), 31.5 (s, 1C, C$^{6'}$-*C*HMe$_A$Me$_B$), 31.8 (s, 1C, C$^{2''}$-*C*HMe$_A$Me$_B$), 31.9 (s, 1C, C$^{6''}$-*C*HMe$_A$Me$_B$), 32.1 (s, 1C, C$^{2'}$-*C*HMe$_A$Me$_B$), 35.0 (s, 1C, C$^{4'}$-*C*HMe$_A$Me$_B$), 35.3 (s, 1C, C$^{4''}$-*C*HMe$_A$Me$_B$), 35.8 (s, 1C, N^{3}-Me, CH$_2$-IMe$_3$), 36.9 (s, 1C, N^{1}-*C*H$_A$CH$_B$), 82.0 (s, 5C, *C*$_5$H$_5$), 121.6 (s, 1C, *C*$^{3'}$-H, Trip), 122.6 (s, 1C, *C*$^{3''}$-H, Trip), 123.6 (s, 1C, *C*$^{5'}$-H, Trip), 125.1 (s, 1C, *C*$^{5''}$-H, Trip), 125.3 (s, 1C, *C*^{2}, CH$_2$-IMe$_3$), 131.0 (s, 1C, *C*$^{4\ or\ 5}$, CH$_2$-IMe$_3$), 132.4 (s, 1C, *C*^{4}-H, C$_6$H$_3$),

[112] CH$_2$-IMe$_3$ represents the C–H activated imidazolium moiety: (3,4,5-trimethylimidazol-2-ilydenyl)-methyl.

134.0 (s, 1C, C^5-H, C_6H_3), 134.5 (s, 1C, C^3-H, C_6H_3), 136.2 (s, 1C, $C^{4\ or\ 5}$, CH_2-IMe_3), 137.0 (s, 1C, $C^{1'}$, Trip), 137.67 (s, 1C, C^1, C_6H_3),137.69 (s, 1C, $C^{1''}$, Trip), 146.8 (s, 1C, $C^{2'}$, Trip), , 147.3 (s, 1C, $C^{6''}$, Trip), 148.8 (s, 1C, $C^{2''}$, Trip), 149.1 (s, 1C, C^6, C_6H_3), 149.4 (s, 1C, $C^{6'}$, Trip), 150.2 (s, 1C, C^2, C_6H_3), 151.4 (s, 1C, $C^{4'}$, Trip), 152.2 (s, 1C, $C^{4''}$, Trip), 246.8 (s, 3C, *C*O). $^{29}Si\{^1H\}$ NMR (59.63 MHz, THF-d_8, 298K, ppm): $\delta = -41.5$ (s).

4.2.27 [(-Ar^{Trip}SiH-CH$_2$-IMe$_3$-)$_2$][CpMo(CO)$_3$]$_2$ (46)

A mixture of SiCl(C_6H_3-2,6-Trip$_2$)(IMe_4) (335 mg, 0.500 mmol) and Li[CpMo(CO)$_3$] THF[113] (140 mg, 0.586 mmol) was treated with 25 mL of toluene. The resulting suspension was heated at 110 °C for 2 h with stirring. The color of the mixture changed from yellow to brown, and most of the solid dissolved. IR spectroscopy revealed formation of the product together with the silylidene complex **42** (about 1:1). The suspension was filtered and the brown filtrate was concentrated *in vacuo* to ca 3 mL. Hexane (10 mL) was added to the mixture to precipitate the product. Two types of solids were observed: brown crystals and a yellow powder. The mixture was filtered and the solids were separated by repeated suspending of the yellow solid in hexane and decantation together with the solvent. The two batches were shown by IR spectroscopy to be the same product. Total yield: ca. 30 mg (0.017 mmol, 7%), brown crystals. IR (toluene, cm^{-1}): 1891 (vs), 1778 (vs), 1753 (vs) [ν(CO)]. IR (THF, cm^{-1}): 1896 (s), 1782 (vs), 1755 (s) [ν(CO)].

The NMR spectra are formally described for a half of the molecule. ^{1}H NMR (300.1 MHz, C_6D_6, 298 K, ppm): $\delta = 0.45$ (d, ^3J(H,H) = 6.8 Hz, 3H, CH*Me*), 0.65 (d, ^3J(H,H) = 6.8 Hz, 3H, CH*Me*), 0.70 (d, ^3J(H,H) = 6.7 Hz, 3H, CH*Me*), 0.74 (d, ^3J(H,H) = 6.6 Hz, 3H, CH*Me*), 1.03 (d, ^3J(H,H) = 6.4 Hz, 3H, CH*Me*), 1.17 (d, ^3J(H,H) = 7.0 Hz, 3H, CH*Me*), 1.19 (d br, 3H, CH*Me*), 1.20 (d, ^3J(H,H) = 7.0 Hz, 3H, CH*Me*), 1.34 (d, ^3J(H,H) = 6.9 Hz, 3H, CH*Me*), 1.40 (d, ^3J(H,H) = 7.0 Hz, 3H, CH*Me*), 1.44 (d, ^3J(H,H) = 6.9 Hz, 3H, CH*Me*), 1.67 (d, ^3J(H,H) = 6.8 Hz, 3H, CH*Me*), 2.04 (s, 3H, C-*Me*, CH_2-IMe_3)[112], 2.0–2.2 (sept, 2H, 2 × C*H*Me$_A$Me$_B$), 2.16 (s, 3H, C-*Me*, CH_2-IMe_3), 2.25 (s, 3H, C-*Me*, CH_2-IMe_3), 2.74 (sept, ^3J(H,H) = 6.8 Hz, 1H, C*H*Me$_A$Me$_B$), 2.81 (d br, ^2J(H,H) = 15.8 Hz, N^1–C*H*$_A$H$_B$, CH_2-IMe_3), 2.8–3.0 (m, 3H, 3 × C*H*Me$_A$Me$_B$), 2.95 (s, 3H, N-*Me*, CH_2-IMe_3), 3.47 (dd, ^2J(H,H) = 15.8 Hz, ^3J(H,H) = 8.8 Hz, N^1–CH$_A$*H*$_B$, CH_2-IMe_3), 5.43 (s, 5H, C_5H_5), 5.46 (d, ^3J(H,H) = 8.8 Hz, 1H, Si*H*), 6.61 (d, ^4J(H,H) = 1.6 Hz, 1H, C$^{3\ or\ 5}$-*H*, Trip), 6.88 (dd, ^3J(H,H) = 7.6 Hz, ^4J(H,H) = 1.3 Hz, 1H, C$^{3\ or}$

[113] Donated by Y. Lebedev, University of Bonn, **2010**.

^{5}-*H*, C_6H_3), 6.97 (t, 5H, ^{3}J(H,H) = 7.6 Hz, C^4-*H*, C_6H_3), 7.065 (d, ^{4}J(H,H) = 1.6 Hz, 1H, $C^{3\text{ or }5}$-*H*, Trip), 7.067 (dd, ^{3}J(H,H) = 7.6 Hz, ^{4}J(H,H) = 1.3 Hz, 1H, $C^{3\text{ or }5}$-*H*, C_6H_3), 7.10 (d, ^{4}J(H,H) = 1.6 Hz, 1H, $C^{3\text{ or }5}$-*H*, Trip), 7.50 (d, ^{4}J(H,H) = 1.5 Hz, 1H, $C^{3\text{ or }5}$-*H*, Trip).

4.2.28 [(-Ar^{Trip}SiH-CH$_2$-IMe$_3$-)$_2$][CpW(CO)$_3$]$_2$ (47)

A mixture of SiCl(C_6H_3-2,6-Trip$_2$)(IMe_4) (200 mg, 0.299 mmol) and K[CpW(CO)$_3$] 0.05DME (114 mg, 0.302 mmol) was treated with 15 mL of toluene. The resulting suspension was immersed in an ultrasonic bath for 2 min and then heated at 110 °C for 80 min with stirring. The color of the mixture changed from yellow to brown, and most of the solid dissolved. IR spectroscopy revealed the selective formation of the product. The suspension was filtered from a small amount of a brown solid and the brown filtrate was evaporated to dryness. The residue was treated with a mixture of 10 mL of hexane and 5 mL of toluene. A light yellow precipitate was observed, which was filtered, washed with hexane (2 × 2 mL) and dried *in vacuo*. Yield: 160 mg (0.164 mmol, 55%), light yellow powder. The product was shown to be essentially pure by ^{1}H NMR and IR spectroscopy; however it was recrystallized from a toluene/hexane mixture for elemental analysis. Elemental analysis calcd (%) for $C_{102}H_{132}N_4O_6Si_2W_2$ (1934.0): C 63.34, H 6.68, N 2.90; found: C 63.21, H 7.11, N 2.74 %. IR (toluene, cm^{-1}): 1886 (s), 1776 (vs), 1753 (vs) [ν(CO)].

The NMR spectra are formally described for a half of the molecule. ^{1}H NMR (300.1 MHz, C_6D_6, 298 K, ppm): δ = 0.45 (d, ^{3}J(H,H) = 6.7 Hz, 3H, CH*Me*), 0.65 (d, ^{3}J(H,H) = 6.6 Hz, 3H, CH*Me*), 0.70 (d, ^{3}J(H,H) = 6.7 Hz, 3H, CH*Me*), 0.74 (d, ^{3}J(H,H) = 6.7 Hz, 3H, CH*Me*), 1.04 (d, ^{3}J(H,H) = 6.3 Hz, 3H, CH*Me*), 1.15 (d, ^{3}J(H,H) = 6.9 Hz, 3H, CH*Me*), 1.18 (d, ^{3}J(H,H) = 7.0 Hz, 6H, 2 × CH*Me*), 1.33 (d, ^{3}J(H,H) = 6.9 Hz, 3H, CH*Me*), 1.44 (d, ^{3}J(H,H) = 6.7 Hz, 6H, 2 × CH*Me*), 1.72 (d, ^{3}J(H,H) = 6.7 Hz, 3H, CH*Me*), 2.09 (s, 3H, C-*Me*, CH_2-IMe_3)[112], 2.0–2.2 (sept, 2H, 2 × C*H*Me_AMe_B), 2.25 (s, 3H, C-*Me*, CH_2-IMe_3), 2.71 (sept, ^{3}J(H,H) = 6.9 Hz, 1H, C*H*Me_AMe_B), 2.82 (d br, ^{2}J(H,H) = 16 Hz, N^1–CH_AH_B, CH_2-IMe_3), 2.8–3.0 (m, 3H, 3 × C*H*Me_AMe_B), 3.13 (s, 3H, N-*Me*, CH_2-IMe_3), 3.47 (dd, ^{2}J(H,H) = 16.4 Hz, ^{3}J(H,H) = 8.3 Hz, N^1–CH_AH_B, CH_2-IMe_3), 5.32 (s, 5H, C_5H_5), 5.53 (d, ^{3}J(H,H) = 7.5 Hz, 1H, Si*H*), 6.59 (d, ^{4}J(H,H) = 1.3 Hz, 1H, $C^{3\text{ or }5}$-*H*, Trip), 7.0–7.1 (m, 5H, $C^{3,4,5}$-*H*, C_6H_3 + $C^{3,5}$-*H*, Trip), 7.53 (d, ^{4}J(H,H) = 1.2 Hz, 1H, $C^{3\text{ or }5}$-*H*, Trip). ^{1}H and ^{13}C{^{1}H} NMR spectra of the product in THF-d_8 are almost identical to those of **45** except for the cyclopentadienyl group and CO-resonances (C_5H_5: 4.92 ppm, C_5H_5: 85.6 ppm; *C*O 226.5 ppm, ^{1}J(W,C) = 199.5 Hz).

$^{29}Si\{^{1}H\}$ NMR (59.63 MHz, THF-d_8, 298K, ppm): $\delta = -41.5$ (s).

4.2.29 [(*trans*-CpMo(CO)$_2$(PMe$_3$)-SiI$_2$-)$_2$] (48)

To a mixture of SiI_2(IDipp) (**18**) (335 mg, 0.500 mmol) and Li[CpMo(CO)$_2$(PMe$_3$)] (150 mg, 0.500 mmol) 10 mL of toluene were added and the suspension was stirred at RT for 24 h. During stirring the mixture gradually developed brown color and a brown precipitate was observed. The precipitate was filtered off, washed with diethyl ether (2 × 2 mL) and extracted with 10 mL of warm THF (at about 50 °C). The brown extract was filtered, concentrated to 4 mL and then 8 mL of diethyl ether were added to precipitate some of amorphous brown material. The mixture was filtered and the filtrate was concentrated to about 0.5 mL. Yellow crystals were observed upon standing at room temperature for 30 min. The crystals were separated and washed by decantation with THF (3 × 0.1 mL), diethyl ether (2 × 0.2 mL) and finally with hexane (2 × 1 mL). The solid was dried *in vacuo* (0.5 h, RT) to give a yellow crystalline powder. Yield 70 mg (0.061 mmol, 24% based on SiI_2(IDipp)).

IR (DME, cm^{-1}): ν = 1945 (w), 1936 (m), 1868 (vs), 1848 (m) [ν(CO)]. IR (THF, cm^{-1}): ν = 1947 (w), 1938 (m), 1870 (vs), 1849 (m) [ν(CO)]. ^{1}H NMR (300.1 MHz, THF-d_8, 298 K, ppm):[114] δ = 1.69 (d, ^{2}J(P,H) = 9.8 Hz, 18H, 2 × P*Me$_3$*), 5.52 (d, ^{3}J(P,H) = 1.1 Hz, 10H, 2 × C_5H_5). ^{31}P NMR (121.5 MHz, THF-d_8, 298 K, ppm): δ = 26.4 (s, 2P, 2 × *P*Me$_3$).

4.2.30 [Cp(CO)$_2$Cr=SiBr(ISdipp)] (49-Cr)

A mixture of $SiBr_2$(ISdipp) (517 mg, 0.894 mmol) and Li[CpCr(CO)$_3$] (217 mg, 1.04 mmol, 1.12 eq) was treated with 10 mL of benzene. The resulting suspension was immersed in an ultrasonic bath for 5 min and then heated at 80 °C for 30 min allowing for pressure release through a mercury bubbler. Evolution of carbon monoxide was observed and the color of the reaction mixture changed from yellow to dark red-brown. The mixture was cooled to room temperature, filtered to a Schlenk tube containing a new portion of Li[CpCr(CO)$_3$] (50 mg, 0.24 mmol, 0.27 eq), and heating was repeated as described above to complete the conversion of $SiBr_2$(ISdipp). Then the reaction mixture was cooled to ambient temperature, concentrated to ca. 7 mL *in vacuo* and diluted with 7 mL of hexane. After storage at ambient temperature

[114] The complex slowly decomposes in THF as monitored by ^{1}H NMR.

for 10 min the reaction mixture was filtered.[115] The brown filtrate was treated with 10 mL of hexane to precipitate a brown less soluble component, and the mixture was filtered as fast as possible before the product started to crystallize. The filtrate was stored at −5 °C for 16 h to give dark brown (almost black) crystals of (**49-Cr**)·0.5C_6H_6 and some brownish powder of a contaminant. The supernatant solution was decanted, and the crystals were washed with hexane (2 × 3 mL) and dried *in vacuo* (15 min, RT). The crystals (**49-Cr**)·0.5C_6H_6 were easily separated from the contaminant upon shaking into another Schlenk tube. Yield: 340 mg (0.478 mmol, 53%). Cooling of a hexane/toluene solution of **49-Cr** to −30 °C afforded brown needles of (**49-Cr**)·0.5(hexane). The compound starts to decompose above 140 °C and turns until 160 °C into a brown liquid with gas evolution. Elemental analysis calcd (%) for $C_{34}H_{43}BrCrN_2O_2Si$·0.5C_6H_6 (710.76): C 62.52, H 6.52, N 3.94; found: C 62.34, H 6.65, N 3.75%. IR (toluene, cm^{-1}): ν = 1898 (vs), 1809 (vs) [ν(CO)]. IR (fluorobenzene, cm^{-1}): ν = 1894 (vs), 1809 (vs) [ν(CO)].

IR (solid, cm^{-1}): ν = 3066 (vw), 3034 (vw), 3015 (vw), 2963 (m), 2927 (w), 2868 (w), 1893 (vs) [ν(CO)], 1867 (m, sh), 1805 (vs) [ν(CO)], 1776 (s, sh), 1630 (vw), 1588 (w), 1478 (s), 1465 (m), 1453 (s), 1445 (s), 1421 (m), 1386 (m), 1366 (w), 1345 (vw), 1323 (m), 1314 (w), 1302 (m), 1288 (vw), 1272 (s), 1242 (m), 1231 (w, sh), 1217 (vw, sh), 1190 (w, sh), 1180 (m), 1150 (vw), 1111 (w, sh), 1106 (w), 1097 (w, sh), 1055 (w), 1037 (vw), 1017 (vw), 1007 (w), 990 (vw), 963 (vw), 934 (w), 924 (m), 894 (vw), 886 (vw), 840 (vw), 822 (w), 801 (s), 754 (m), 725 (vw), 702 (vw), 680 (s), 651 (s), 623 (m), 602 (s), 567 (s), 547 (m), 523 (m), 505 (s), 488 (m), 464 (m), 445 (m), 429 (m), 416 (vw), 408 (vw), 378 (s).

---

[115] When another run of the reaction was carried out in toluene at 110 °C in a similar fashion, the residue after filtration was shown to contain mainly the imidazolium salt [ISdippH][CpCr(CO)$_3$] (**51**). IR (THF, cm^{-1}): ν = 1892 (vs), 1782 (vs), 1759 (s), 1634 (m) [ν(CO)]. ^{1}H NMR (300.1 MHz, THF-d_8, 298 K, ppm): δ =1.24 (d br, ^3J(H,H) = 6.5 Hz, 12H, 4 × CHMe_AMe$_B$), 1.42 (d br, ^3J(H,H) = 6.2 Hz, 12H, 4 × CHMe$_A$$Me_B$), 3.19 (sept br, 4H, 4 × CHMe$_A$Me$_B$), 4.29 (s, 5H, C_5H_5), 4.73 (s br, 4H, 2 × NCH_2), 7.38 (d, ^3J(H,H) = 7.6 Hz, 4H, 2 × C^{3,5}-H, Dipp), 7.51 (t, ^3J(H,H) = 7.8 Hz, 2H, 2 × C^4-H, Dipp). ^{13}C{^{1}H} NMR (75.47 MHz, THF-d_8, 298 K, ppm): δ = 24.1 (s, 4C, 2 × C^{2,6}-CHMe$_A$$Me_B$, Dipp), 25.5 (s, 4C, 2 × C^{2,6}-CHMe_AMe$_B$, Dipp), 29.7 (s, 4C, 2 × C^{2,6}-CHMe$_A$Me$_B$, Dipp), 55.6 (s, 4C, 4 × NCH_2), 82.07 (s, 5C, C_5H_5), 125.7 (s, 4C, 2 × $C^{3,5}$-H, Dipp), 130.9 (s, 2C, 2 × C^1, Dipp), 132.1 (s, 2C, 2 × C^4-H, Dipp), 147.7 (s, 4C, 2 × $C^{2,6}$, Dipp), 161.0 (s, 1C, NCHN), 246.9 (s, 3C, CO). Crystals suitable for the X-ray diffractin analysis were grown upon slow evaporation of a THF/xylene solution of the compound at ambient temperature.

^{1}H NMR (300.1 MHz, C_6D_6, 298 K, ppm): δ = 1.13 (d, ^{3}J(H,H) = 6.8 Hz, 12H, 2 × $C^{2,6}$-CHMe_AMe$_B$, Dipp), 1.59 (d, ^{3}J(H,H) = 6.8 Hz, 12H, 2 × $C^{2,6}$-CHMe$_A$$Me_B$, Dipp), 3.51 (s, 4H, 2 × NCH_2), 3.52 (sept, ^{3}J(H,H) = 6.8 Hz, 4H, 2 × $C^{2,6}$-CHMe$_A$Me$_B$, Dipp), 4.64 (s, 5H, C_5H_5), 7.10−7.14 (m, 4H, 2 × $C^{3,5}$-*H*, Dipp), 7.17−7.22 (m, 2H, 2 × C^{4}-*H*, Dipp).

^{13}C{^{1}H} NMR (75.47 MHz, C_6D_6, 298 K, ppm): δ = 23.8 (s, 4C, 2 × $C^{2,6}$-CHMe$_A$$Me_B$, Dipp), 26.9 (s, 4C, 2 × $C^{2,6}$-CHMe_AMe$_B$, Dipp), 29.1 (s, 4C, 2 × $C^{2,6}$-*C*HMe$_A$Me$_B$, Dipp), 53.9 (s, 2C, 2 × N*C*H$_2$), 85.9 (s, 5C, C_5H_5), 125.5 (s, 4C, 2 × $C^{3,5}$-*H*, Dipp), 130.7 (s, 2C, 2 × C^{4}-*H*, Dipp), 133.5 (s, 2C, 2 × C^{1}, Dipp), 146.6 (s, 4C, 2 × $C^{2,6}$-CHMe$_A$Me$_B$, Dipp), 177.4 (s, 1C, N*C*N), 251.7 (s, 2C, 2 × *C*O).

^{29}Si NMR (59.63 MHz, C_6D_6, 298K, ppm): δ = 95.1 (s).

4.2.31 [Cp*(CO)$_2$Cr=SiBr(ISdipp)] (52-Cr)

A mixture of $SiBr_2$(ISdipp) (300 mg, 0.519 mmol) and Li[Cp*Cr(CO)$_3$] (159 mg, 0.572 mmol, 1.10 eq) was treated with 10 mL of toluene. The resulting suspension was immersed in an ultrasonic bath for 2 min and then heated at 50 °C for 9 h allowing for pressure to release through a mercury bubbler. Evolution of carbon monoxide was observed and the color of the reaction mixture changed from yellow to dark red-brown. Monitoring of the reaction by IR spectroscopy revealed the formation of **52-Cr** in addition to some [SIdippH][Cp*Cr(CO)$_3$] and another byproduct (1994(w), 1910(m) cm^{-1}).[116] The mixture was cooled to room temperature and filtered. The filtrate was evaporated to dryness *in vacuo*. The residue was dissolved in 1 mL of toluene, 10 mL of hexane were added and the solution was filtered from a small amount of an insoluble material.[117] The filtrate was stored at ambient temperature for 6 h and finally 10 h at −16 °C to give large dark brown (almost black) crystals of **52-Cr**. The supernatant was decanted, the crystals were washed with hexane (2 × 3 mL) and dried in the atmosphere of the glovebox (1 h, RT). Yield: 230 mg (0.310 mmol, 60%).

[116] The origin of [SIdippH][Cp*Cr(CO)$_3$] is presently unknown. A similar side reaction yielding [SIdippH][CpCr(CO)$_3$] was observed during the synthesis of [Cp(CO)$_2$Cr=SiBr(SIdipp)] (**49-Cr**). The complex [SIdippH][Cp*Cr(CO)$_3$] was identified by its characteristic ν(CO) absorption bands; IR (toluene, cm^{-1}): 1875 (vs), 1768 (vs), 1749 (s) [ν(CO)]. IR (THF, cm^{-1}): 1877 (vs), 1770 (vs), 1751 (s) [ν(CO)].

[117] Presumably [ISdippH][Cp*Cr(CO)$_3$].

The crystals were suitable for X-ray diffraction analysis. The compound decomposes upon melting at 204−205 °C turning into black liquid. Elemental analysis calcd (%) for $C_{39}H_{53}CrBrN_2O_2Si$ (741.83): C 63.14, H 7.20, N 3.78; found: C 63.31, H 7.18, N 3.66%. IR (toluene, cm^{-1}): ν = 1886 (vs), 1804 (vs) [ν(CO)]. IR (fluorobenzene, cm^{-1}): ν = 1882 (vs), 1802 (vs) [ν(CO)].

IR (solid, cm^{-1}): ν = 3065 (vw), 2958 (m), 2924 (m) 2898 (m), 2868 (m), 2719 (vw), 1869 (vs) [ν(CO)], 1787 (vs) [ν(CO)], 1589 (vw), 1475 (vs), 1452 (vs), 1421 (s), 1381 (s), 1364 (m), 1343 (w), 1323 (m), 1304 (w), 1299 (w), 1273 (vs), 1243 (m), 1191 (vw), 1179 (w), 1150 (vw), 1106 (w), 1099 (w), 1069 (vw), 1055 (m), 1048 (m, sh), 1030 (m), 1020 (m), 991 (w), 956 (vw), 925 (m), 897 (w), 883 (vw), 801 (s), 755 (s), 730 (vw), 702 (vw), 660 (s), 619 (m), 606 (vs), 585 (s), 547 (m), 532 (m), 513 (s), 495 (m), 464 (w, sh), 457 (m), 444 (w, sh), 429 (m), 396 (vw).

^{1}H NMR (300.1 MHz, C_6D_6, 298 K, ppm): δ = 1.13 (d, ^3J(H,H) = 6.8 Hz, 12H, 2 × $C^{2,6}$-CHMe_AMe$_B$, Dipp), 1.65 (d br, ^3J(H,H) = 6.8 Hz, 12H, 2 × $C^{2,6}$-CHMe$_A$$Me_B$, Dipp), 1.89 (s, 15H, C_5Me_5), 3.47 (s, 4H, 2 × NCH_2), 3.51 (sept br, 4H, 2 × $C^{2,6}$-CHMe$_A$Me$_B$, Dipp), 7.10−7.22 (m, 6H, 2 × $C^{3,4,5}$-H, Dipp).

^{13}C{^{1}H} NMR (75.47 MHz, C_6D_6, 298 K, ppm): δ = 11.6 (s, 5C, C_5Me_5), 24.0 (s br, 4C, 2 × $C^{2,6}$-CHMe$_A$$Me_B$, Dipp), 26.8 (s, 4C, 2 × $C^{2,6}$-CHMe_AMe$_B$, Dipp), 29.1 (s, 4C, 2 × $C^{2,6}$-CHMe$_A$Me$_B$, Dipp), 54.1 (s, 2C, 2 × NCH_2), 98.5 (s, 5C, C_5Me$_5$), 125.4 (s, 4C, 2 × $C^{3,5}$-H, Dipp), 130.5 (s, 2C, 2 × C^4-H, Dipp), 134.0 (s, 2C, 2 × C^1, Dipp), 146.6 (s, 4C, 2 × $C^{2,6}$-CHMe$_A$Me$_B$, Dipp), 178.7 (s, 1C, NCN), 253.0 (s, 2C, 2 × CO).

^{29}Si NMR (59.63 MHz, C_6D_6, 298K, ppm): δ = 74.8 (s).

4.2.32 [Cp*(CO)$_2$W=SiBr(ISdipp)] (52-W)

A mixture of $SiBr_2$(ISdipp) (587 mg, 1.015 mmol) and Li[Cp*W(CO)$_3$] (460 mg, 1.122 mmol, 1.10 eq) was treated with 10 mL of toluene. The resulting suspension was stirred for 18 h at RT. Monitoring of the reaction by IR spectroscopy revealed the formation of **52-W** in addition to some [SIdippH][Cp*W(CO)$_3$] and another byproduct (2012(m), 2005(m), 1943(m), 1918(m) cm^{-1}).[118] the solvent was removed *in vacuo*. The brown residue was

[118] The origin of [SIdippH][Cp*W(CO)$_3$] is presently unknown. A similar side reaction yielding [SIdippH][CpCr(CO)$_3$] was observed during the synthesis of [Cp(CO)$_2$Cr=SiBr(SIdipp)] (**49-Cr**). The

extracted with 10 mL of hexane and the extract was filtered from insoluble material. The filtrate was stored for 4 days at −16 °C to give a mixture of large dark brown (almost black) crystals of **52-W** among with some yellow and orange crystals (the composition of byproducts is unknown). The supernatant was decanted,[119] the brown crystals were separated with a spatula, washed with hexane (2 × 0.5 mL) and dried in atmosphere of the glovebox (1 h, RT). Yield: 60 mg (0.069 mmol, 7%). The crystals suitable for X-ray diffraction analysis were grown upon storage of a hexane solution of **52-W** at –16 °C in a separate experiment. Elemental analysis calcd (%) for $C_{39}H_{53}BrN_2O_2SiW$ (873.68): C 53.61, H 6.11, N 3.21; found: C 53.40, H 6.22, N 3.05%. IR (hexane, cm^{-1}): ν = 1890 (vs), 1807 (s) [ν(CO)]. IR (toluene, cm^{-1}): ν = 1883 (vs), 1799 (vs) [ν(CO)]. IR (fluorobenzene, cm^{-1}): ν = 1879 (vs), 1796 (vs) [ν(CO)].

^{1}H NMR (300.1 MHz, C_6D_6, 298 K, ppm): δ = 1.14 (d, ^3J(H,H) = 6.8 Hz, 12H, 2 × $C^{2,6}$-CHMe_AMe$_B$, Dipp), 1.68 (d br, ^3J(H,H) = 4.8 Hz, 12H, 2 × $C^{2,6}$-CHMe$_A$$Me_B$, Dipp), 1.89 (s, 15H, C_5Me_5), 3.42 (s br, 4H, 2 × NCH_2), 3.51 (s br, 4H, 2 × $C^{2,6}$-CHMe$_A$Me$_B$, Dipp), 7.12−7.24 (m, 6H, 2 × $C^{3,4,5}$-H, Dipp).

^{13}C{^{1}H} NMR (75.47 MHz, C_6D_6, 298 K, ppm): δ = 11.9 (s, 5C, C_5Me_5), 23.9 (s br, 4C, 2 × $C^{2,6}$-CHMe$_A$$Me_B$, Dipp), 26.9 (s, 4C, 2 × $C^{2,6}$-CHMe_AMe$_B$, Dipp), 29.0 (s, 4C, 2 × $C^{2,6}$-CHMe$_A$Me$_B$, Dipp), 54.0 (s, 2C, 2 × NCH_2), 101.0 (s, 5C, C_5Me$_5$), 125.4 (s br, 4C, 2 × $C^{3,5}$-H, Dipp), 130.4 (s, 2C, 2 × C^4-H, Dipp), 133.7 (s, 2C, 2 × C^1, Dipp), 146.5 (s, 4C, 2 × $C^{2,6}$-CHMe$_A$Me$_B$, Dipp), 185.6 (s, 1C, NCN), 232.3 (s, ^1J(W,C) = 183.3 Hz, 2C, 2 × CO).

^{29}Si NMR (59.63 MHz, C_6D_6, 298K, ppm): δ = 71.2 (s, ^1J(W,Si) = 412.2 Hz).

The experiment was repeated as follows:

A mixture of $SiBr_2$(ISdipp) (579 mg, 1.00 mmol) and Li[Cp*W(CO)$_3$] (490 mg, 1.20 mmol, 1.20 eq) was treated with 25 mL of toluene. The resulting suspension was stirred for 6 h at

---

complex [SIdippH][Cp*W(CO)$_3$] was identified by its characteristic ν(CO) absorption bands; IR (toluene, cm^{-1}): 1873(vs), 1762 (vs), 1745 (vs) [ν(CO)]. IR (THF, cm^{-1}): 1875 (vs), 1763 (vs), 1748 (vs) [ν(CO)].

[119] An interesting unknown byproduct was observed in this supernatant solution according to IR spectroscopy. IR(hexane, cm^{-1}): 2020 (s), 2008 (s), 1945 (vs), 1933 (vs) [ν(CO)]. Another byproduct was present IR(hexane, cm^{-1}): 1950 (vs), 1925 (vs) [ν(CO)].

0 °C and then allowed to slowly warm up to RT. The mixture was subsequently stirred for 2 days at RT. The mixture was concentrated *in vacuo* to about 1 mL and then 20 mL of hexane were added. The suspension was filtered from insoluble light brown material and the brown filtrate was stored for 3 days at −16 °C to give a mixture of large dark brown (almost black) crystals of **52-W** along with some yellow powder on the walls. The supernatant was decanted, the brown crystals were separated with a spatula, washed with hexane (3 × 2 mL) and dried in atmosphere of the glovebox (2 h, RT). Yield: 230 mg (0.263 mmol, 26%). The product was shown by IR and NMR spectroscopy to be pure.

4.2.33 [Cp*(CO)$_2$Cr=SiI(IDipp)] (53-Cr)

A mixture of SiI_2(IDipp) (1.34 g, 2.00 mmol) and Li[Cp*Cr(CO)$_3$] (725 mg, 2.61 mmol, 1.19 eq) was treated with 20 mL of toluene. The resulting suspension was heated at 50 °C for about 15 h allowing for pressure to release through a mercury bubbler. Evolution of carbon monoxide was observed and the color of the reaction mixture changed from yellow to brown. IR spectroscopy revealed the formation of **53-Cr** as a major product (1886 (vs), 1807 (vs) cm^{-1}); the imidazolium salt [IDippH][Cp*Cr(CO)$_3$] (1864 (m), 1764 (s), 1742(m) cm^{-1}) and unknown by-product/-s (2005 (w), 1995 (w), 1938 (w), 1724 (m) cm^{-1}). The mixture was cooled to room temperature was concentrated to about 10 mL and 30 mL of hexane were added. The resulting suspension was filtered from a brown insoluble material. The filtrate was stored at –30 °C for 4 days for crystallization. The precipitate was filtered at –30 °C and washed with hexane (2 × 5 mL). Two types of crystals were found in the precipitate, dark brown (the product) and yellow crystals of an unknown product. 5 mL of hexane were added and the Schlenk tube was immersed in an ultrasonic bath for about 20 s; during the sonification the yellow crystals were crushed to powder but the big brown crystals survived. The solids were suspended in hexane and then the solvent was syringed off together with the yellow powder. The procedure was repeated until all yellow material was removed. The product was dried in atmosphere of the glovebox for 1 h. Yield: 150 mg (0.191 mmol, 9.5%). In a separate experiment crystallization from a toluene/hexane (1:4) mixture at –30 °C afforded dark brown single crystals of **53-Cr** suitable for X-ray diffraction analysis. Elemental analysis calcd (%) for $C_{39}H_{51}CrIN_2O_2Si$ (786.82): C 59.53, H 6.53, N 3.56; found: C 59.23, H 6.61, N 3.38%. IR (toluene, cm^{-1}): ν = 1887 (vs), 1806 (vs) [ν(CO)]. IR (fluorobenzene, cm^{-1}): ν = 1883 (vs), 1804 (vs) [ν(CO)].

^{1}H NMR (300.1 MHz, C_6D_6, 298 K, ppm): δ = 1.00 (d, ^{3}J(H,H) = 6.8 Hz, 12H, 2 × $C^{2,6}$-CHMe_AMe$_B$, Dipp), 1.59 (d br, ^{3}J(H,H) = 6.3 Hz, 12H, 2 × $C^{2,6}$-CHMe$_A$$Me_B$, Dipp), 1.88 (s, 15H, C_5Me_5), 3.25 (s br, 4H, 2 × $C^{2,6}$-C*H*Me$_A$Me$_B$, Dipp), 6.33 (s, 2H, $C^{4,5}$-*H*), 7.15−7.26 (m, 6H, 2 × $C^{3,4,5}$-*H*, Dipp).

^{13}C{^{1}H} NMR (75.47 MHz, C_6D_6, 298 K, ppm): δ = 11.3 (s, 5C, C_5Me_5), 23.4 (s, 4C, 2 × $C^{2,6}$-CHMe$_A$$Me_B$, Dipp), 26.3 (s, 4C, 2 × $C^{2,6}$-CHMe_AMe$_B$, Dipp), 29.3 (s, 4C, 2 × $C^{2,6}$-*C*HMe$_A$Me$_B$, Dipp), 98.7 (s, 5C, C_5Me$_5$), 124.1 (s, 2C, $C^{4,5}$-H), 125.2 (s, 4C, 2 × $C^{3,5}$-*H*, Dipp), 131.4 (s, 2C, 2 × C^{4}-*H*, Dipp), 133.9 (s, 2C, 2 × C^{I}, Dipp), 145.7 (s, 4C, 2 × $C^{2,6}$-CHMe$_A$Me$_B$, Dipp), 157.1 (s, 1C, N*C*N), 252.6 (s, 2C, 2 × *C*O).

^{29}Si NMR (59.63 MHz, C_6D_6, 298K, ppm): δ = 39.0 (s).

4.2.34 [Cp*(CO)$_2$Mo=SiI(IDipp)] (53-Mo)

A mixture of SiI_2(IDipp) (670 mg, 1.00 mmol) and Li[Cp*Mo(CO)$_3$] (419 mg, 1.30 mmol, 1.30 eq) was treated with 10 mL of toluene. The resulting suspension was stirred at ambient temperature for 18 h allowing for pressure to release through a mercury bubbler. Evolution of carbon monoxide was observed and the color of the reaction mixture changed from yellow to brown. IR spectroscopy revealed formation of **53-Mo** as a major product (1890 (vs), 1808 (vs) cm^{-1}); [IDippH][Cp*Mo(CO)$_3$] (1872 (m), 1763 (s), 1744(m) cm^{-1}); and unknown by-product/-s (2022 (w), 2005 (w), 1933 (w), 1727 (m) cm^{-1}). The mixture was cooled to room temperature was concentrated to about 5 mL and 20 mL of hexane were added. The resulting suspension was filtered after 30 min of standing at ambient temperature from a brown insoluble powder.[120] The filtrate was stored at −16 °C overnight for crystallization. The supernatant solution was syringed off and the precipitate was washed with hexane (4 × 2 mL). Two types of crystals were found in the initial precipitate, dark brown (the product) and yellow (unknown by-product), the later ones were removed together with hexane. The product was dried in atmosphere of the glovebox for 1 h. Yield: 150 mg (0.181 mmol, 18%). The

[120] Small solid dark purple "drops" were wound in the residual powder, which were separated manually by repeated shaking of the residue with hexane and removal of the solvent together with suspended powder. Yield: 150 mg, purple-brown solid "drops". IR (toluene, cm^{-1}): ν = 2005 (s), 1932 (s), 1928 (vs) [ν(CO)]. IR (THF, cm^{-1}): ν = 2004 (s), 1932 (s), 1926 (vs sh) [ν(CO)]. ^{1}H NMR spectrum recorded in C_6D_6 showed that the material is impure. The structure of the compound is unknown.

crystals were suitable for the X-ray diffraction analysis. Elemental analysis calcd (%) for $C_{39}H_{51}IMoN_2O_2Si$ (830.76): C 56.38, H 6.19, N 3.37; found: C 56.51, H 6.32, N 3.23%. IR (toluene, cm^{-1}): ν = 1890 (vs), 1808 (vs) [ν(CO)]. IR (fluorobenzene, cm^{-1}): ν = 1887 (vs), 1806 (vs) [ν(CO)]. IR (THF, cm^{-1}): ν = 1891 (vs), 1809 (vs) [ν(CO)].

^{1}H NMR (300.1 MHz, C_6D_6, 298 K, ppm): δ = 1.00 (d, ^3J(H,H) = 6.8 Hz, 12H, 2 × $C^{2,6}$-CHMe_AMe$_B$, Dipp), 1.59 (d br, ^3J(H,H) = 6.3 Hz, 12H, 2 × $C^{2,6}$-CHMe$_A$$Me_B$, Dipp), 1.99 (s, 15H, C_5Me_5), 3.22 (s br, 4H, 2 × $C^{2,6}$-CHMe$_A$Me$_B$, Dipp), 6.33 (s, 2H, $C^{4,5}$-H), 7.15−7.26 (m, 6H, 2 × $C^{3,4,5}$-H, Dipp).

^{13}C{^{1}H} NMR (75.47 MHz, C_6D_6, 298 K, ppm): δ = 11.6 (s, 5C, C_5Me_5), 23.3 (s, 4C, 2 × $C^{2,6}$-CHMe$_A$$Me_B$, Dipp), 26.3 (s, 4C, 2 × $C^{2,6}$-CHMe_AMe$_B$, Dipp), 29.3 (s, 4C, 2 × $C^{2,6}$-CHMe$_A$Me$_B$, Dipp), 102.4 (s, 5C, C_5Me$_5$), 124.1 (s, 2C, $C^{4,5}$-H), 125.2 (s, 4C, 2 × $C^{3,5}$-H, Dipp), 131.4 (s, 2C, 2 × C^4-H, Dipp), 133.7 (s, 2C, 2 × C^1, Dipp), 145.6 (s, 4C, 2 × $C^{2,6}$-CHMe$_A$Me$_B$, Dipp), 159.3 (s, 1C, NCN), 241.9 (s, 2C, 2 × CO).

^{29}Si NMR (59.63 MHz, C_6D_6, 298K, ppm): δ = 48.1 (s).

4.2.35 [Cp(CO)$_2$CrSiBr(IMe$_2$*i*Pr$_2$)$_2$] (55)

1,3-diisopropyl-2,4-dimethylimidazol-2-ilydene (90 mg, 0.50 mmol, 2.64 eq) was added in portions to a stirred solution of **49-Cr**·0.5C_6H_6 (134 mg, 0.189 mmol) in 5 mL of benzene. The reaction mixture was stirred for 15 min, filtered from a tiny amount of a brown insoluble material and stored overnight at ambient temperature. The supernatant solution was removed with a syringe, and the dark red-brown crystals of **55**·C_6H_6 were washed with benzene (2 × 1 mL), hexane (2 mL) and dried for 1 h at ambient temperature in the glovebox in an open vial. Yield: 120 mg (0.167 mmol, 88%). The compound **55**·C_6H_6 desolvates upon heating and then decomposes at 166−168 °C to give a black liquid. Elemental analysis calcd (%) for $C_{29}H_{45}BrCrN_4O_2Si$·C_6H_6 (719.79): C 58.40, H 7.14, N 7.78; found: C 59.25, H 7.16, N 7.56%. IR (THF, cm^{-1}): ν = 1797 (vs), 1733 (vs) [ν(CO)]. IR (fluorobenzene, cm^{-1}): ν = 1794 (vs), 1726 (vs) [ν(CO)].

IR (solid, cm^{-1}): ν = 3088 (vw), 3032 (vw), 2991 (vw, sh), 2975 (w), 2937 (w), 2874 (vw), 2654 (vw), 1889 (vw), 1776 (vs) [ν(CO)], 1707 (vs) [ν(CO)], 1632 (m), 1476 (w), 1463 (w), 1441 (m), 1402 (vw), 1384 (m), 1369 (s), 1346 (m), 1336 (w), 1313 (vw), 1209 (m), 1183 (vw), 1168 (vw), 1148 (vw), 1134 (w), 1109 (m), 1078 (w), 1058 (vw), 1033 (w), 1006 (vw),

997 (w), 932 (vw), 903 (w), 883 (vw), 837 (vw), 794 (m), 779 (m), 767 (m), 754 (m), 691 (s), 671 (s), 652 (w), 623 (s), 604 (s), 547 (s), 531 (s), 490 (m), 474 (s), 458 (s), 437 (s), 412 (m). ^{1}H NMR (300.1 MHz, THF-d_8, 298 K, ppm): δ = 1.31 and 1.47 (br each, 12H each, 2 × N^{1,3}-CHMe_AMe_B, IMe$_2i$Pr$_2$), 2.31 (s, 12H, 2 × C^{4,5}-*Me*, IMe$_2i$Pr$_2$), 4.30 (s, 5H, C$_5H_5$), 6.1 (br, $\Delta\nu_{1/2}$ ≈ 300 Hz, 4H, 2 × N^{1,3}-C*H*Me$_A$Me$_B$, IMe$_2i$Pr$_2$), 7.30 (s, 6H, C$_6$H$_6$).

^{13}C{^{1}H} NMR (75.47 MHz, THF-d_8, 298 K, ppm): δ = 10.6 (s, 4C, 2 × C^{4,5}-*Me*, IMe$_2i$Pr$_2$), 21.1 and 22.4 (s br each, 4C each, 2 × N^{1,3}-CHMe_AMe_B, IMe$_2i$Pr$_2$), 52.4 (s br, 4C, 2 × N^{1,3}-*C*HMe$_A$Me$_B$, IMe$_2i$Pr$_2$), 81.5 (s, 5C, C_5H$_5$), 127.0 (s, 4C, 2 × $C^{4,5}$, -Me, IMe$_2i$Pr$_2$), 129.0 (s, 6C, C_6H$_6$), 157.4 (s, 2C, 2 × C^2, IMe$_2i$Pr$_2$), 250.6 (s, 2C, 2 × *C*O). ^{29}Si NMR (59.63 MHz, THF-d_8, 298K, ppm): δ = 17.3 (s). ^{1}H NMR (300.1 MHz, THF-d_8, 213 K, ppm): δ = 0.76 (d, ^{3}J(H,H) = 6.7 Hz, 3H, N^1-CHMe_AMe$_B$, (IMe$_2i$Pr$_2$)^X), 0.90 (d, ^{3}J(H,H) = 6.7 Hz, 3H, N^1-CHMe_AMe$_B$, (IMe$_2i$Pr$_2$)^Y), 1.37 (d, ^{3}J(H,H) = 6.7 Hz, 3H, N^1-CHMe$_A$$Me_B$, (IMe$_2iPr_2$)^X), 1.42 (d, ^{3}J(H,H) = 6.7 Hz, 3H, N^3-CHMe_AMe$_B$, (IMe$_2i$Pr$_2$)^Y), 1.48 (d, ^{3}J(H,H) = 6.7 Hz, 3H, N^1-CHMe$_A$$Me_B$, (IMe$_2iPr_2$)^Y), 1.56 (d, ^{3}J(H,H) = 6.7 Hz, 3H, N^3-CHMe_AMe$_B$, (IMe$_2i$Pr$_2$)^X), 1.66 (d, ^{3}J(H,H) = 6.7 Hz, 3H, N^3-CHMe$_A$$Me_B$, (IMe$_2iPr_2$)^Y), 1.68 (d, ^{3}J(H,H) = 6.7 Hz, 3H, N^3-CHMe$_A$$Me_B$, (IMe$_2iPr_2$)^X), 2.26 (s, 3H, C^4-*Me*, (IMe$_2i$Pr$_2$)^X), 2.34 (s, 3H, C^4-*Me*, (IMe$_2i$Pr$_2$)^Y), 2.37 (s, 3H, C^5-*Me*, (IMe$_2i$Pr$_2$)^X), 2.38 (s, 3H, C^5-*Me*, (IMe$_2i$Pr$_2$)^Y), 4.27 (s, 5H, C$_5H_5$), 4.94 (sept, ^{3}J(H,H) = 6.7 Hz, 1H, N^1-C*H*Me$_A$Me$_B$, (IMe$_2i$Pr$_2$)^X), 5.12 (sept, ^{3}J(H,H) = 6.7 Hz, 1H, N^1-C*H*Me$_A$Me$_B$, (IMe$_2i$Pr$_2$)^Y), 6.19 (sept, ^{3}J(H,H) = 6.7 Hz, 1H, N^3-C*H*Me$_A$Me$_B$, (IMe$_2i$Pr$_2$)^X), 7.34 (s, 6H, C$_6$H$_6$), 9.54 (sept, ^{3}J(H,H) = 6.7 Hz, 1H, N^3-C*H*Me$_A$Me$_B$, (IMe$_2i$Pr$_2$)^Y).

^{13}C{^{1}H} NMR (75.47 MHz, THF-d_8, 213 K, ppm): δ = 10.36 (s, 1C, C^4-*Me*, (IMe$_2i$Pr$_2$)^Y), 10.42 (s, 1C, C^4-*Me*, (IMe$_2i$Pr$_2$)^X), 10.54 (s, 2C, C^5-*Me*, (IMe$_2i$Pr$_2$)^X and (IMe$_2i$Pr$_2$)^Y), 19.0 (s, 1C, N^1-CHMe_AMe$_B$, (IMe$_2i$Pr$_2$)^Y), 19.3 (s, 1C, N^1-CHMe_AMe$_B$, (IMe$_2i$Pr$_2$)^X), 20.9 (s, 1C, N^3-CHMe$_A$$Me_B$, (IMe$_2iPr_2$)^X), 21.7 (s, 1C, N^3-CHMe_AMe$_B$, (IMe$_2i$Pr$_2$)^X), 22.0 (s, 1C, N^1-CHMe$_A$$Me_B$, (IMe$_2iPr_2$)^Y), 22.37 (s, 1C, N^3-CHMe_AMe$_B$, (IMe$_2i$Pr$_2$)^Y), 22.43 (s, 1C, N^3-CHMe$_A$$Me_B$, (IMe$_2iPr_2$)^Y), 23.9 (s, 1C, N^1-CHMe$_A$$Me_B$, (IMe$_2iPr_2$)^X), 50.3 (s, 1C, N^3-*C*HMe$_A$Me$_B$, (IMe$_2i$Pr$_2$)^Y), 52.2 (s, 1C, N^3-*C*HMe$_A$Me$_B$, (IMe$_2i$Pr$_2$)^X), 53.3 (s, 1C, N^1-*C*HMe$_A$Me$_B$, (IMe$_2i$Pr$_2$)^Y), 54.1 (s, 1C, N^1-*C*HMe$_A$Me$_B$, (IMe$_2i$Pr$_2$)^X), 81.3 (s, 5C, C_5H$_5$), 126.6 (s, 1C, C^5-Me, (IMe$_2i$Pr$_2$)^Y), 126.8 (s, 1C, C^5 -Me, (IMe$_2i$Pr$_2$)^X), 127.4 (s, 1C, C^4-Me, (IMe$_2i$Pr$_2$)^X), 127.9 (s, 1C, C^4-Me, (IMe$_2i$Pr$_2$)^Y), 129.1 (s, 6C, C_6H$_6$), 156.2 (s, 1C, C^2, (IMe$_2i$Pr$_2$)^X or (IMe$_2i$Pr$_2$)^Y), 156.3 (s, 1C, C^2, (IMe$_2i$Pr$_2$)^X or (IMe$_2i$Pr$_2$)^Y), 248.9 (s, 1C, *C*O), 251.8 (s, 1C, *C*O).

4.2.36 [Cp(CO)Cr({μ-CO}Si(IMe$_2$*i*Pr$_2$)$_2$)$_2$Cr(CO)Cp][B(C$_6$F$_5$)$_4$]$_2$ (57)

A solution of Li[B(C$_6$F$_5$)$_4$]·2.5Et$_2$O (87 mg, 0.10 mmol) in 2 mL of fluorobenzene was added to a stirred solution of **55**·C$_6$H$_6$ (72 mg, 0.10 mmol) in 5 mL of fluorobenzene. The color of the reaction solution changed rapidly from dark brown to green. The reaction mixture was stirred for 3 min and then filtered from some insoluble yellow solid. An IR spectrum of an aliquot of the green filtrate was recorded, which revealed that the starting material had been consumed and that a new dicarbonyl complex had formed displaying two *ν*(CO) absorption bands of almost equal intensity at 1895 and 1821 cm^{-1}.[121] The green filtrate was stored at −16 °C for 2 days. The resulting yellow crystals of **57** were separated from the yellow mother liquor by decantation, washed with fluorobenzene (2 × 1 mL) and hexane (2 mL), and then dried for 15 min at ambient temperature *in vacuo*. Yield: 70 mg (0.028 mmol, 56%). Elemental analysis calcd (%) for C$_{106}$H$_{90}$B$_2$Cr$_2$F$_{40}$N$_8$O$_4$Si$_2$ (2481.62): C 51.30, H 3.66, N 4.52; found: C 51.49, H 3.77, N 4.36%. Complex **57** is insoluble in common organic solvents including fluorobenzene, MeCN and CH$_2$Cl$_2$. It turns brown upon heating above 170 °C, and then liquefies at 191−192 °C.

IR (solid, cm^{-1}): *ν* = 2985 (w), 2945 (vw), 1860 (s) [*ν*(CO)], 1642 (m), 1630 (w,sh), 1596 (w), 1513 (s), 1497 (w), 1458 (vs), 1385 (m, sh), 1373 (s), 1318 (w), 1273 (m), 1214 (m), 1183 (vw), 1170 (vw), 1153 (vw), 1137 (vw), 1085 (s), 1034 (vw), 976 (vs), 933 (vw), 903 (m), 883 (vw), 843 (vw), 824 (vw), 806 (m), 773 (m), 754 (s), 719 (m), 684 (m), 661 (s), 609 (m), 572 (m), 564 (m), 547 (w), 520 (m), 501 (m), 477 (m), 468 (m ,sh), 449 (m), 436 (sh), 410 (w), 388 (m).

4.2.37 [(η^5-C$_5$Me$_5$)(CO)$_2$Cr=Si{4-(diphenylmethylene)cyclohexa-2,5-dienyl}(ISdipp)] (58)

A mixture of [(η^5-C$_5$Me$_5$)(CO)$_2$Cr=SiBr(ISdipp)] (148 mg, 0.202 mmol) and [Li(THF)$_4$][CPh$_3$][122] (118 mg, 0.219 mmol, 1.08 eq) was treated with 2 mL of fluorobenzene.

---

[121] The dicarbonyl complex is suggested to be the silylidene complex [Cp(CO)$_2$Cr=Si(IMe$_2$^{i}Pr$_2$)$_2$][B(C$_6$F$_5$)$_4$].

[122] [Li(THF)$_4$][CPh$_3$] was prepared upon treatment of Ph$_3$CH with 1.07 equiv. of *n*BuLi in a Et$_2$O/THF mixture (2:5) at 0 °C. The dark red crystalline product was isolated after crystallization at –30 °C overnight, see H. Gilman, B. J. Gaj, *J. Org. Chem.* **1963**, *28* (6), 1725-1727.

The dark brown reaction mixture was stirred at ambient temperature for 5 min. *In situ* IR spectrum revealed selective formation of a product (1871, 1783 cm^{-1}). All volatilities were removed and the residue was dried *in vacuo* for 30 min. The residue was extracted with 4 mL of toluene and filtered. The filtrate concentrated to about 0.5 mL and diluted with 0.5 mL of hexane. The solution was stored at 5 °C overnight for crystallization. Brown crystals were filtered off, washed with hexane (3 × 0.5 mL) and dried *in vacuo* for 20 min. Yield 129 mg (0.143 mmol, 71%), brown crystals. Elemental analysis calcd (%) for $C_{58}H_{68}CrN_2O_2Si$ (905.25): C 76.95, H 7.57, N 3.09; found: C 76.25, H 7.58, N 2.78%. IR (toluene, cm^{-1}): 1875 (vs), 1785 (vs) [ν(CO)]. IR (fluorobenzene, cm^{-1}): 1869 (vs), 1782 (vs) [ν(CO)].

^{1}H NMR (300.1 MHz, C_6D_6, 298 K, ppm): δ = 0.95 (d, ^3J(H,H) = 6.6 Hz, 6H, 2 × C^2-CH$Me_A$$Me_B$, Dipp), 1.21 (d, ^3J(H,H) = 6.7 Hz, 6H, 2 × C^6-CH$Me_A$$Me_B$, Dipp), 1.27 (d, ^3J(H,H) = 6.6 Hz, 12H, 2 × C^2-CH$Me_A$$Me_B$, Dipp), 1.72 (d, ^3J(H,H) = 6.7 Hz, 6H, 2 × C^6-CH$Me_A$$Me_B$, Dipp), 2.03 (s, 15H, C_5Me_5), 3.23 (sept, ^3J(H,H) = 6.6 Hz, 2H, 2 × C^2-C*H*$Me_A$$Me_B$, Dipp), 3.28–3.34 (m, 2H, 2 × N-C$H_A$$H_B$, ISdipp), 3.83–3.91 (m, 2H, 2 × N-C$H_A$$H_B$, ISdipp), 3.99 (sept, ^3J(H,H) = 6.7 Hz, 2H, 2 × C^6-C*H*$Me_A$$Me_B$, Dipp), 4.11–4.18 (m br, 1H, C*H*(CH=CH)$_2$C, "CPh_3"), 4.86–4.98 (m br, 2H, CH(C*H*=CH)$_2$C, "CPh_3"), 6.70 (dd, ^3J(H,H) = 10.4 Hz, ^4J(H,H) = 1.7 Hz, 2H, CH(CH=C*H*)$_2$C, "CPh_3"), 6.94–7.15 (m, 14H, H, Dipp-H and C_6H_5)7.30–7.35 (m, 4H, 2 × $C^{2,6}$-*H*, C_6H_5).[123]

4.2.38 [((C$_6$F$_5$)$_3$B-η^5-C$_5$H$_4$)(CO)$_2$Mo(H)Si(IMe$_4$)(C$_6$H$_3$-2,6-Trip$_2$)] (59)

To a solution of **42** (85 mg, 0.10 mmol) in 6 mL of toluene a solution of tris(perfluorophenyl)borane (51 mg, 0.10 mmol) in 2 mL of toluene was added dropwise. The color turned from dark brown to brown-orange. An IR spectrum revealed the selective formation of a product with absorptions at 1875 (vs) and 1785 (vs) cm^{-1}, [ν(CO)].[124] 2 mL of hexane were added and the mixture was allowed to stand for 16 h without stirring at ambient temperature for crystallization. The supernatant was removed using a syringe from large violet-red crystals; the crystals were washed with toluene (3 × 2 mL) and dried *in vacuo* (1 h,

[123] The compound is thermally labile. The spectrum was measured some time after the preparation of the complex and therefore displayed about 30% decomposition. ISdipp was identified as the only decomposition product, containing the "carbene" moiety.

[124] The absorptions correspond probably to the 16VE intermediate complex [(C$_6$F$_5$)$_3$B(η^4-C$_5$H$_5$)(CO)$_2$Mo=Si(IMe$_4$)(C$_6$H$_3$-2,6-Trip$_2$)], see p. 96.

30 °C). Yield: 90 mg (0.058 mmol, 58%). The crystals for the X-ray diffraction analysis were obtained directly from another small-scale experiment. The product is insoluble in hexane, toluene, and diethyl ether; soluble, but unstable in THF at ambient temperature.

^{1}H NMR (300.1 MHz, THF-d_8, 213 K, ppm): δ = –9.95 (s, J(Si,H) = 60.1 Hz, Mo-*H*-Si), 0.86 (s br, 12H, 4 × C-CH*Me*, Trip), 1.12 (d br, ^{3}J(H,H) = 5.8 Hz, 6H, 2 × C-CH*Me*, Trip), 1.28 (d br, ^{3}J(H,H) = 6.5 Hz, 18H, 6 × C-CH*Me*, Trip), 2.10 (s, 6H, N^{1,3}-*Me*, IMe$_4$), 2.5–3.3 (br, 10H, 4 × C*H*Me, Trip + C^{4,5}-*Me*, IMe$_4$), 2.95 (sept, ^{3}J(H,H) = 6.6 Hz, 2H, 2 × C^{4}-C*H*Me$_2$, Trip), 4.79 (s br, 2H, C*H*=CH, C_5H_4), 5.04 (s br, 2H, CH=C*H*, C_5H_4), 7.27 (d, ^{3}J(H,H) = 7.6 Hz, 2H, C^{3,5}-*H*, C_6H_3), 7.32 (s br, 4H, C^{3,5}-*H*, Trip), 7.64 (t, ^{3}J(H,H) = 7.6 Hz, 1H, C^{4}-*H*, C_6H_3).

^{11}B NMR (96.29 MHz, THF-d_8, 213 K, ppm): δ = –15.4 (s br).

4.2.39 [Cp(CO)$_2$Mo≡SiC$_6$H$_3$-2,6-Trip$_2$] (60)

*Synthesis from isolated [Cp(CO)$_2$Mo{Si(C$_6$H$_3$-2,6-Trip$_2$)(IMe$_4$)] (**42**).*

A mixture of **42** (220 mg, 0.259 mmol) and B(*p*-Tol)$_3$ (74 mg, 0.26 mmol) was dissolved in 25 mL of *o*-xylene and the solution heated to reflux for 10 min. Complete conversion of the starting material **42** into complex **60** was confirmed by IR spectroscopy. The solvent was evaporated to dryness *in vacuo* and the brown residue treated with 3 mL of pentane. All volatiles were removed *in vacuo* to give a brown powder, which was treated with 5 mL of pentane. The suspension was stored at −78 °C for 10 min. The beige fine precipitate was filtered off and after drying in vacuo at ambient temperature identified by NMR spectroscopy to be the borane-carbene adduct B(*p*-Tol)$_3$(IMe$_4$).[125] The filtrate was concentrated to about 2 mL and stored at −78 °C for 3 h. The resulting brown-red crystals of 3 were isolated by filtration at −78 °C, washed at −78 °C with pentane (3 × 0.5 mL) and dried *in vacuo* for 60 min at 40°C to give 70 mg of complex 3 as a brown-red, microcrystalline solid. The pentane mother liquor and wash solutions were combined, concentrated to about 1 mL and stored at −78 °C for 6 h to give a second crop of the product (30 mg). Combined yield: 100 mg (0.138 mmol, 53%). Complex **60** gradually turns brown above 120 °C. Elemental analysis calcd (%) for $C_{43}H_{54}MoO_2Si$ (726.89): C 71.05, H 7.49; found: C 70.74, H 7.59%. IR

[125] ^{1}H NMR (300.1 MHz, C_6D_6, 298 K, ppm): δ = 1.11 (s, 6H, 2 × C^{4,5}-*Me*, IMe$_4$), 2.30 (s, 9H, 3 × C_6H_4-4-*Me*), 2.73 (s, 6H, 2 × N-*Me*, IMe$_4$), 7.21 (d, ^{3}J(H,H) = 7.6 Hz, C^{3,5}-*H*, C_6H_4-4-Me), 7.64 (d, ^{3}J(H,H) = 7.6 Hz, C^{2,6}-*H*, C_6H_4-4-Me).

(toluene, cm^{-1}): 1937 (vs), 1875 (vs) [ν(CO)]. IR (pentane, cm^{-1}): 1945 (vs), 1886 (vs) [ν(CO)].

^{1}H NMR (300.1 MHz, C_6D_6, 298 K, ppm): δ = 1.14 (d, ^{3}J(H,H) = 6.9 Hz, 12H, 2 × $C^{2,6}$-CH$Me_A$$Me_B$, Trip), 1.33 (d, ^{3}J(H,H) = 6.9 Hz, 12H, 2 × C^{4}-CHMe_2, Trip), 1.55 (d, ^{3}J(H,H) = 6.9 Hz, 12H, 2 × $C^{2,6}$-CHMe$_A$$Me_B$, Trip), 2.89 (sept, ^{3}J(H,H) = 6.9 Hz, 2H, 2 × C^{4}-CHMe$_2$, Trip), 2.94 (sept, ^{3}J(H,H) = 6.9 Hz, 4H, 2 × $C^{2,6}$-CHMe$_A$Me$_B$, Trip), 4.67 (s, 5H, C_5H_5), 7.01 (m, 2H, $C^{3,5}$-H, C_6H_3), 7.12 (m, 1H, C^{4}-H, C_6H_3), 7.29 (s, 4H, 2 × $C^{3,5}$-H, Trip).

^{13}C{^{1}H} NMR (75.47 MHz, C_6D_6, 298 K, ppm): δ = 23.7 (s, 4C, 2 × $C^{2,6}$-CHMe$_A$$Me_B$, Trip), 24.1 (s, 4C, 2 × C^{4}-CHMe_2, Trip), 25.4 (s, 4C, 2 × $C^{2,6}$-CHMe_AMe$_B$, Trip), 31.5 (s, 4C, 2 × $C^{2,6}$-CHMe$_A$Me$_B$, Trip), 35.0 (s, 2C, 2 × C^{4}-CHMe$_2$, Trip), 86.6 (s, 5C, C_5H_5), 122.1 (s, 4C, 2 × $C^{3,5}$-H, Trip), 128.6 (s, 2C, $C^{3,5}$-H, C_6H_3), 131.2 (s, 1C, C^{4}-H, C_6H_3), 133.6 (s, 2C, 2 × C^{1}, Trip), 145.7 (s, 2C, $C^{2,6}$, C_6H_3), 148.3 (s, 4C, 2 × $C^{2,6}$, Trip), 150.3 (s, 2C, 2 × C^{4}, Trip), 153.4 (s, 1C, Si-C^{1}, C_6H_3), 231.1 (s, 2C, 2 × CO).

^{29}Si NMR (59.63 MHz, C_6D_6, 298 K, ppm): δ = 320.1 (s).

*Synthesis from SiCl(C_6H_3-2,6-Trip$_2$)(IMe$_4$) without intermediate isolation of [Cp(CO)$_2$Mo{Si(C_6H_3-2,6-Trip$_2$)(IMe$_4$)}] (**42**).*

A mixture of SiCl(C_6H_3-2,6-Trip$_2$)(IMe$_4$) (**28**) (4.30 g, 6.42 mmol) and Li[CpMo(CO)$_3$] (1.70 g, 6.74 mmol, 1.05 eq) was treated with 50 mL of toluene. The resulting suspension was immersed in an ultrasonic bath for 5 min and then heated at 110 °C for 20 min with stirring. The color of the mixture changed from yellow over brown-green to brown, and most of the solid dissolved. The mixture was evaporated *in vacuo*. The residue was treated with 50 mL of hexane, during the treatment the material crystallized. The solid was filtered off, washed with 30 mL of hexane and dried *in vacuo* (1 h, 40 °C) to give a brown-green powder. The powder consisted of **42**, the ionic complex **46** (roughly 20%), LiCl and an excess of Li[CpMo(CO)$_3$].[126]

The solid was treated with 50 mL of xylene and the suspension was filtered to a Schlenk tube containing B(p-Tol)$_3$ (1.55 g, 5.46 mmol, 0.85 eq). The solution was heated for 1 h at

[126] The isolated complex **46** is only slightly soluble in aromatic solvents, however it forms a metastable solution directly after reaction. This is one of the reasons why the mixture is treated with hexane to precipitate it.

120 °C.[127] The color changed from dark-brown to brown-red. The solvent was removed *in vacuo* and the red-brown residue was treated with 30 mL of pentane in an ultrasonic bath for 10 min. All volatiles were removed and the crystalline rest was dried *in vacuo* (1 h, RT). The mixture was extracted with 140 mL of pentane at –30 °C and filtered. The filtrate was stored at –78 °C for 30 min (B(*p*-Tol)$_3$ precipitates) and then filtered.[128] The filtrate was stored at -60 °C for 2 days, the resulting brown-red crystals were filtered, washed with pentane (2 × 5 mL) and dried *in vacuo* (1 h, –60 °C to +40 °C). Yield: 1.80 g (2.48 mmol, 39%, based on SiClAr(IMe$_4$)) of brick-red crystalline powder. The product was shown by ^{1}H NMR spectroscopy to be pure.

4.2.40 [(η^5-C_5Me_5)(CO)$_2$Cr≡Si(ISdipp)][Al(OC(CF$_3$)$_3$)$_4$] (61-Cr)

A mixture of **52-Cr** (150 mg, 0.205 mmol) and Li[Al(OC(CF$_3$)$_3$)$_4$] (216 mg, 0.222 mmol, 1.08 eq) was treated with 5 mL of fluorobenzene, no color change was observed. 1 mL of hexane was added to the mixture after 2 min. The stirring continued for 2 min more and then the suspension was filtered. Diffusion of hexane at −16 °C into the filtrate afforded dark brown (almost black) thin plates of **61-Cr**. The supernatant light brown solution was syringed off, the crystals were washed with hexane (3 × 1 mL) and dried *in vacuo* (10 min, RT, 0.05 mbar). Yield: 272 mg (0.167 mmol, 81%), dark brown crystals. The compound decomposes at 230–232 °C to a black liquid. Elemental analysis calcd (%) for $C_{55}H_{53}AlCrF_{36}N_2O_6Si$ (1629.02): C 40.55, H 3.28, N 1.72; found: C 40.59, H 3.52, N 1.64%.

IR (PhF, cm^{-1}): ν = 1966 (vs), 1912 (vs) [ν(CO)]. IR (solid, cm^{-1}): ν = 2970 (w), 2953 (w), 2930 (w, sh) ,2922 (w), 2880 (vw), 1953 (vs), 1899 (vs), 1591 (w), 1533 (s), 1489 (w), 1478 (w), 1466 (m), 1436 (w), 1591 (vw), 1533 (m), 1489 (vw), 1478 (vw), 1466 (w), 1436 (vw), 1388 (w), 1351 (m), 1297 (s), 1274(vs), 1237 (vs), 1212 (vs), 1167 (s), 1058 (vw), 1050 (vw), 1028 (vw), 1011 (vw), 970 (vs), 936 (m, sh), 830 (m), 806 (m), 754 (w), 726 (vs), 627 (m), 605 (w), 601 (w), 561 (m), 550 8m), 536 (m), 496 (m), 442 (s), 410 (m).

[127] The progress should be monitored by IR spectroscopy. It was shown on a small scale that the synthesis can be carried out in toluene at 110 °C; toluene may be a better alternative to xylene, because **60** decomposes on heating.

[128] To avoid crystallization of the product, three conventional filter-cannulas were used for filtration.

^{1}H NMR (300.1 MHz, CD_2Cl_2, 298 K, ppm)[129]: δ = 1.39 (d, ^{3}J(H,H) = 6.8 Hz, 12H, 2 × $C^{2,6}$-CHMe_AMe$_B$, Dipp), 1.50 (d, ^{3}J(H,H) = 6.8 Hz, 12H, 2 × $C^{2,6}$-CHMe$_A$$Me_B$, Dipp), 1.63 (s, 15H, C_5Me_5), 3.03 (sept, ^{3}J(H,H) = 6.8 Hz, 4H, 2 × $C^{2,6}$-CHMe$_A$Me$_B$, Dipp), 4.33 (s, 4H, 2 × NCH_2), 7.42 (d, ^{3}J(H,H) = 7.8 Hz, 4H, 2 × $C^{3,5}$-H, Dipp), 7.59 (t, ^{3}J(H,H) = 7.8 Hz, 2H, 2 × C^{4}-H, Dipp).

^{1}H NMR (300.1 MHz, C_6D_5Cl, 298 K, ppm): δ = 1.18 (d, ^{3}J(H,H) = 6.8 Hz, 12H, 2 × $C^{2,6}$-CHMe_AMe$_B$, Dipp), 1.38 (d, ^{3}J(H,H) = 6.8 Hz, 12H, 2 × $C^{2,6}$-CHMe$_A$$Me_B$, Dipp), 1.41 (s, 15H, C_5Me_5), 2.85 (sept, ^{3}J(H,H) = 6.8 Hz, 4H, 2 × $C^{2,6}$-CHMe$_A$Me$_B$, Dipp), 3.91 (s, 4H, 2 × NCH_2), 7.12 (d, ^{3}J(H,H) = 7.8 Hz, 4H, 2 × $C^{3,5}$-H, Dipp), 7.32 (t, ^{3}J(H,H) = 7.8 Hz, 2H, 2 × C^{4}-H, Dipp).

^{13}C{^{1}H} NMR (75.47 MHz, C_6D_5Cl, 298 K, ppm): δ = 11.5 (s, 5C, C_5Me_5), 24.1 (s, 4C, 2 × $C^{2,6}$-CHMe$_A$$Me_B$, Dipp), 24.6 (s, 4C, 2 × $C^{2,6}$-CHMe_AMe$_B$, Dipp), 29.7 (s, 4C, 2 × $C^{2,6}$-CHMe$_A$Me$_B$, Dipp), 54.0 (s, 2C, 2 × NCH$_2$), 79.7 (s br, 4C, OC(CF$_3$)$_4$), 104.9 (s, 5C, C_5Me$_5$), 121.9 (quartet of sextets, ^{1}J(F,C) = 293 Hz, ^{3}J(^{27}Al,C) = ca. 1.5 Hz, 12C, OC(CF$_3$)$_4$), 125.9 (s, 4C, 2 × $C^{3,5}$-H, Dipp), 128.1 (s, 2C, 2 × C^{1}, Dipp), 132.6 (s, 2C, 2 × C^{4}-H, Dipp), 147.1 (s, 4C, 2 × $C^{2,6}$-CHMe$_A$Me$_B$, Dipp), 172.7 (s, 1C, NCN), 241.7 (s, 2C, 2 × CO).

^{19}F{^{1}H} NMR (282.4 MHz, C_5H_5F, 298K, ppm): δ = −74.8 (s).

^{29}Si NMR (59.63 MHz, C_5H_5F, 298K, ppm): δ = 129.0 (s).

4.2.41 [(η^5-C_5Me_5)(CO)$_2$W≡Si(ISdipp)][Al(OC(CF$_3$)$_3$)$_4$] (61-W)

A C_6D_6 solution, containing approximately 25 mg (0.029 mmol) of **52-W** in a Young NMR tube was evaporated *in vacuo* (1 h, RT). The residue was dissolved in 0.6 mL of chlorobenzene-d_6 and 35 mg (0.036 mmol) of Li[Al(OC(CF$_3$)$_3$)$_4$] were added to the solution. The mixture was placed in an ultrasonic bath for 10 min and then filtered.[130] The product was directly characterized by NMR spectroscopy. In a separate experiment the IR spectrum was

[129] ^{1}H NMR spectrum of **61-Cr** measured directly after preparation showed already ca. 30% of decomposition. Complex **61-Mo** is stable enough to be measured without a sign of deterioration, however it decomposes within hours.

[130] The completion of the reaction was monitored by ^{1}H NMR spectroscopy. The sample was found to contain ca. 20% of impurities.

recorded IR (PhF, cm^{-1}): ν = 1967 (vs), 1905 (vs) [ν(CO)]. All attempts to crystallize the product failed.

^{1}H NMR (300.1 MHz, C_6D_5Cl, 298 K, ppm): δ = 1.18 (d, ^{3}J(H,H) = 6.8 Hz, 12H, 2 × $C^{2,6}$-CH$Me_A$$Me_B$, Dipp), 1.37 (d, ^{3}J(H,H) = 6.8 Hz, 12H, 2 × $C^{2,6}$-CH$Me_A$$Me_B$, Dipp), 1.73 (s, 15H, C_5Me_5), 2.84 (sept, ^{3}J(H,H) = 6.8 Hz, 4H, 2 × $C^{2,6}$-C$H$$Me_A$$Me_B$, Dipp), 3.81 (s, 4H, 2 × NCH_2), 7.12 (d, ^{3}J(H,H) = 7.8 Hz, 4H, 2 × $C^{3,5}$-H, Dipp), 7.32 (t, ^{3}J(H,H) = 7.8 Hz, 2H, 2 × C^{4}-H, Dipp).

^{13}C{^{1}H} NMR (75.47 MHz, C_6D_5Cl, 298 K, ppm): δ = 11.5 (s, 5C, C_5Me_5), 23.8 (s, 4C, 2 × $C^{2,6}$-CH$Me_A$$Me_B$, Dipp), 24.6 (s, 4C, 2 × $C^{2,6}$-CH$Me_A$$Me_B$, Dipp), 29.7 (s, 4C, 2 × $C^{2,6}$-CH$Me_A$$Me_B$, Dipp), 54.0 (s, 2C, 2 × NCH_2), 105.1 (s, 5C, C_5Me_5), 121.9 (q, ^{1}J(F,C) = 292 Hz, 12C, OC(CF_3)$_4$), 125.8 (s, 4C, 2 × $C^{3,5}$-H, Dipp), 132.7 (s, 2C, 2 × C^{1}, Dipp), 132.7 (s, 2C, 2 × C^{4}-H, Dipp), 147.0 (s, 4C, 2 × $C^{2,6}$-CH$Me_A$$Me_B$, Dipp), 184.7 (s, 1C, N$C$N), 218.9 (s, 2C, 2 × CO).

^{29}Si NMR (59.63 MHz, C_5H_5F, 298K, ppm): δ = 178.5 (s, ^{1}J(W,Si) = 420.5 Hz).

4.2.42 [(η^5-C_5Me_5)(CO)$_2$Cr≡Si(ISdipp)][B(C_6H_2-3,5-(CF_3)$_2$)$_4$] (62-Cr)

A mixture of **52-Cr** (73 mg, 0.098 mmol) and Na[B(C_6H_2-3,5-(CF_3)$_2$)$_4$] (93 mg, 0.105 mmol, 1.07 eq) was treated with 0.7 mL of fluorobenzene. The mixture was stirred for 3 min. The completion of the reaction was confirmed by IR spectroscopy (1967 (vs), 1912 (vs) cm^{-1} in fluorobenzene). Hexane (0.3 mL) was added and the brown suspension was filtered from a brown precipitate (NaBr). Diffusion of hexane at –16 °C into the filtrate afforded large dark red-brown prisms, which were filtered off, washed with fluorobenzene/hexane mixture (1:4) and dried shortly in atmosphere of the glovebox. The crystals were suitable for X-ray diffraction analysis. Yield: ca. 70 mg (0.046 mmol, 47%).

4.2.43 [(η^5-C_5Me_5)(CO)$_2$Mo≡Si(ISdipp)][B(C_6H_2-3,5-(CF_3)$_2$)$_4$] (62-Mo)

A mixture of **52-Mo** (79 mg, 0.101 mmol) and Na[B(C_6H_2-3,5-(CF_3)$_2$)$_4$] (91 mg, 0.103 mmol, 1.02 eq) was treated with 0.7 mL of fluorobenzene. The mixture was stirred for 2 min. The completion of the reaction was confirmed by IR spectroscopy (1974 (vs), 1915 (vs) cm^{-1} in fluorobenzene). Hexane (0.7 mL) was added and the brown suspension was filtered from a brown precipitate (NaBr). Diffusion of hexane at –16 °C into the filtrate afforded a mixture of

brown oil and dark brown crystals. The oil was partially removed together with the supernatant solution with help of a syringe. The crystals were suitable for X-ray diffraction analysis.

4.2.44 [(η^5-C_5Me_5)$(CO)_2$W≡Si(ISdipp)][B(C_6H_2-3,5-$(CF_3)_2)_4$] (62-Mo) and 63

A mixture of **52-W** (87 mg, 0.10 mmol) and Na[B(C_6H_2-3,5-$(CF_3)_2)_4$] (92 mg, 0.104 mmol, 1.04 eq) was treated with 1.5 mL of fluorobenzene. The mixture was stirred for 3 min, no significant colour change was observed. The completion of the reaction was confirmed by IR spectroscopy (1967 (vs), 1905 (vs) cm^{-1} in fluorobenzene). Hexane (1.0 mL) was added and the brown suspension was filtered from a brown precipitate (NaBr). Diffusion of hexane at –16 °C resulted in precipitation of a dark brown oil. All attempts to crystallize the product failed.

Upon standing for about 1 month at room temperature the oil partially crystallized to give orange crystals. The supernatant solution (hexane-fluorobenzene) and the brown oil were syringed off. The orange crystals were washed with fluorobenzene/hexane mixture 1:1 (3 × 0.3 mL) and finally with hexane. The product was dried in the atmosphere of the glovebox for 5 min. The crystals were suitable for the X-ray diffraction analysis. Due to the very low yield (ca. 5 mg) full characterization was not possible.[131]

IR (PhF, cm^{-1}): 1936 (vs), 1838 (vs) [ν(CO)]

4.2.45 [$Cp(CO)_2$Mo(H){Si(OH)(C_6H_3-2,6-$Trip_2$)}] (64)

A 0.56 M solution of water in dioxane (0.32 mL, 0.18 mmol) was added dropwise to a solution of **60** (130 mg, 0.179 mmol) at –70 °C. Upon addition the solution turned from red-brown to yellow. The reaction mixture was allowed to warm to ambient temperature, upon which the color of the solution changed gradually to brown. All volatiles were removed *in*

[131] An experiment was caried out to prepare the complex **63**. The insitu prepared cationic silylidyne complex **62-W** was refluxed in a fluorobenzene/hexane mixture 1:1 for 72 h. The crude reaction mixture was shown by IR spectroscopy to contain several products, ν(CO), PhF: 2027m, 2014m, 1980m, 1955s sh, 1938vs, 1915 s sh, 1851vs, 1772m, 1711w. Attempts to crystallize the product resulted in precipitation of a brown oil.

vacuo and the residue was subjected to a freeze-pump cycle. The crude product was dissolved in approximately 10 mL of boiling hexane and stored over night at –30 °C for crystallization. The mother liquor was separated by filtration at –30 °C and the yellow, crystalline precipitate dried *in vacuo* at ambient temperature. Yield: 88 mg (0.12 mmol, 66%). The compound turns gradually brown above 195 °C and liquefies at 219−220 °C. Elemental analysis calcd (%) for $C_{43}H_{56}MoO_3Si$ (744.91): C 69.33, H 7.58; found: C 69.33, H 7.54%. IR (diethyl ether, cm^{-1}): 1958 (sh), 1945 (vs), 1872 (vs) [*ν*(CO)]. IR (toluene, cm^{-1}): 1954 (sh), 1943 (vs), 1871 (vs) [*ν*(CO)].

IR (KBr pellet, cm^{-1}): 3490 (s br., OH), 3051 (w), 3038 (w), 2960 (vs), 2934 (m), 2866 (m), 2046 (w), 1971 (vs, CO), 1947 (sh, CO), 1867 (m), 1808 (vs, CO), 1635 (w, OH), 1606 (m), 1572 (w), 1562 (w), 1554 (w), 1458 (m), 1443 (m), 1427 (m), 1383 (m), 1361 (m), 1317 (w), 1305 (sh), 1249 (w), 1239 (w), 1188 (vw), 1166 (w), 1152 (vw), 1117 (w), 1104 (w), 1077 (w), 1069 (w), 1052 (w), 1013 (w), 1002 (w), 954 (vw), 937 (w), 920 (w), 875 (s), 870–810 (s br., OH), 803 (s), 772 (w), 751 (m), 728 (w), 650.3 (w), 624 (m), 611 (m), 587 (m), 529 (m), 504 (w), 472 (m), 453 (m), 423 (vw)

^{1}H NMR (300.1 MHz, C_6D_6, 298 K, ppm): δ = –10.26 (s, ^1J(Si,H) = 40.0 Hz, 1H, Si-*H*-Mo), 1.09 (d, ^3J(H,H) = 6.8 Hz, 12H, 2 × $C^{2,6}$-CH*Me*$_A$Me$_B$, Trip), 1.29 (d, ^3J(H,H) = 6.8 Hz, 12H, 2 × C^4-CH*Me*$_2$, Trip), 1.38 (d, ^3J(H,H) = 6.8 Hz, 12H, 2 × C^6-CHMe$_A$*Me*$_B$, Trip), 2.86 (sept, ^3J(H,H) = 6.8 Hz, 2H, 2 × C^4-C*H*Me$_2$, Trip), 3.06 (sept, ^3J(H,H) = 6.8 Hz, 4H, 2 × $C^{2,6}$-C*H*Me$_A$Me$_B$, Trip), 3.86 (s, 1H, OH), 4.69 (s, 5H, C_5H_5), 7.22 (s, 4H, 2 × $C^{3,5}$-*H*, Trip), 7.24−7.29 (m, 3H, $C^{3,4,5}$-*H*, C_6H_3).

^{13}C{^{1}H} NMR (75.47 MHz, C_6D_6, 298 K, ppm): δ = 22.5 (s, 4C, 2 × $C^{2,6}$-CHMe$_A$*Me*$_B$, Trip), 24.3 (s, 4C, 2 × C^4-CH*Me*$_2$, Trip), 26.7 (s, 4C, 2 × $C^{2,6}$-CH*Me*$_A$Me$_B$, Trip), 31.1 (s, 4C, 2 × $C^{2,6}$-*C*HMe$_A$Me$_B$, Trip), 34.9 (s, 2C, 2 × C^4-*C*HMe$_2$, Trip), 88.4 (s, 5C, C_5H_5), 121.2 (s, 4C, 2 × $C^{3,5}$-H, Trip), 128.5 (s, 1C, C^4-H, C_6H_3), 129.7 (s, 2C, $C^{3,5}$-H, C_6H_3), 136.6 (s, 2C, 2 × C^1, Trip), 144.1 (s, 2C, $C^{2,6}$, C_6H_3), 146.7 (s, 1C, Si-C^1, C_6H_3), 148.0 (s, 4C, 2 × $C^{2,6}$, Trip), 149.6 (s, 2C, 2 × C^4, Trip), 233.8 (s, 2C, 2 × *C*O).

^{29}Si NMR (59.63 MHz, C_6D_6, 298 K, ppm): δ = 213.4 (s).

4.2.46 [Cp(CO)$_2$Mo(D){Si(OD)(C$_6$H$_3$-2,6-Trip$_2$)}] (65)

A 0.75 M, solution of D_2O in dioxane (0.18 mL, 0.135 mmol) was added dropwise to a solution of **60** in 10 mL of diethyl ether (100 mg, 0.138 mmol) at –78 °C. Upon addition the

solution turned from red-brown to yellow. The reaction mixture was allowed to warm to ambient temperature and worked up as described above for **64** to afford complex **65** as a yellow crystalline solid. Yield: 65 mg (0.087 mmol, 63%). Elemental analysis calcd (%) for $C_{43}H_{54}D_2MoO_3Si$ (746.93): C 69.14, H 7.83; found: C 69.07, H 7.67%. IR (diethyl ether, cm^{-1}): 1958 (sh), 1945 (vs), 1872 (vs) [*v* (CO)].

IR (KBr pellet, cm^{-1}): 3051 (w), 3038 (w), 3000−2890 (vs), 2865 (s), 2587 (s, OD), 2046 (w), 1968 (vs, CO), 1870 (m), 1801 (vs, CO), , 1830−1750 (vs, CO), 1605 (m), 1572 (w), 1562 (w), 1554 (w), 1458 (m), 1443 (m),1427 (m),1383 (m), 1361 (m), 1317 (w), 1250 (vw), 1239 (vw), 1167 (w), 1117 (w), 1104 (w), 1078 (w), 1069 (w), 1052 (w), 1013 (vw), 1002 (vw), 954 (vw), 937 (w), 920 (vw), 886 (vs), 875 (s), 834 (vw), 823 (wv), 804 (s), 773 (w), 753 (vw), 737 (w), 665 (m br), 650 (m), 608 (m), 579 (m), 530 (w), 516 (m), 503 (vw), 492 (w), 472 (m), 453 (m), 419 (w).

^{1}H NMR (300.1 MHz, C_6D_6, 298 K, ppm): δ = 1.09 (d, ^3J(H,H) = 6.8 Hz, 12H, 2 × $C^{2,6}$-CH$Me_A$$Me_B$, Trip), 1.29 (d, ^3J(H,H) = 6.8 Hz, 12H, 2 × C^4-CHMe_2, Trip), 1.37 (d, ^3J(H,H) = 6.8 Hz, 12H, 2 × C^6-CHMe$_A$$Me_B$, Trip), 2.86 (sept, ^3J(H,H) = 6.8 Hz, 2H, 2 × C^4-C*H*Me_2, Trip), 3.06 (sept, 4H, 2 × $C^{2,6}$-C*H*Me$_A$$Me_B$, Trip), 4.69 (s, 5H, C_5H_5), 7.22 (s, 4H, 2 × $C^{3,5}$-*H*, Trip), 7.24-7.29 (m, 3H, $C^{3,4,5}$-*H*, C_6H_3).

^{2}D NMR (76.77 MHz, C_6H_6/C_6D_6, 298 K, ppm) δ = −10.38 (s, $v_{1/2}$ = 1.8 Hz, 1D, Mo-*D*), 3.83 (s br, $v_{1/2}$ = 23.7 Hz, 1D, Si-O*D*).

4.2.47 [Cp(CO)$_2$Mo(H){SiCl(C_6H_3-2,6-Trip$_2$)}] (67)

To a solution of 100 mg of **60** (0.138 mmol) in 5 mL of diethyl ether at –70 °C a solution of HCl (0.32 mL, 0.435 M in dioxane, 0.14 mmol) was added dropwise. During the addition the reaction mixture turned from red-brown to orange-yellow. The mixture was allowed to warm to –30 °C at which point all volatilities were removed *in vacuo*.. The residue was allowed to warm up to ambient temperature in dynamic vacuum (0.05 mbar, 1 h). Yield – nearly quantitative, orange-brown powder. Attempts to purify the material by crystallization failed due to its high solubility and thermal lability (presumable). IR (hexane, cm^{-1}): 1977 (vs), 1972 (vs), 1911 (s), 1890 (s), [*v*(CO)]. IR (diethyl ether, cm^{-1}): 1969 (vs), 1905 (s), 1886 (s), [*v*(CO)].

^{1}H NMR (300.1 MHz, C_6D_6, 298 K, ppm): δ = −9.03 (s, ^1J(Si,H) = 27.9 Hz, 1H, Si-*H*-Mo), 1.10 (d, ^3J(H,H) = 6.8 Hz, 12H, 2 × $C^{2,6}$-CHMe$_A$Me$_B$, Trip), 1.28 (d, ^3J(H,H) = 6.8 Hz, 12H, 2

× C^4-CHMe_2, Trip), 1.51 (d, ^3J(H,H) = 6.8 Hz, 12H, 2 × $C^{2,6}$-CHMe$_A$Me$_B$, Trip), 2.85 (sept, ^3J(H,H) = 6.8 Hz, 2H, 2 × C^4-C*H*Me$_2$, Trip), 3.15 (br, 4H, 4 × $C^{2,6}$-C*H*Me$_A$Me$_B$, Trip), 4.66 (s, 5H, C_5H_5), 7.20−7.25 (m, 1H, C^4-*H*, C_6H_3), 7.25 (s, 4H, 2 × $C^{3,5}$-*H*, Trip), 7.26−7.30 (m, 2H, $C^{3,5}$-*H*, C_6H_3). $^{13}C\{^1H\}$ NMR (75.47 MHz, C_6D_6, 298 K, ppm): δ = 22.6 (s br, 4C, 2 × $C^{2,6}$-CHMe$_A$*Me*$_B$, Trip), 24.2 (s, 4C, 2 × C^4-CH*Me*$_2$, Trip), 26.8 (s, 4C, 2 × $C^{2,6}$-CH*Me*$_A$Me$_B$, Trip), 31.3 (s, 4C, 2 × $C^{2,6}$-*C*HMe$_A$Me$_B$, Trip), 34.9 (s, 2C, 2 × C^4-*C*HMe$_2$, Trip), 89.7 (s, 5C, C_5H_5), 121.4 (s, 4C, 2 × $C^{3,5}$-H, Trip), 128.9 (s, 1C, C^4-H, C_6H_3), 130.5 (s, 2C, $C^{3,5}$-H, C_6H_3), 136.0 (s, 2C, 2 × C^1, Trip), 143.5 (s, 2C, $C^{2,6}$, C_6H_3), 147.8 (s, 1C, Si-C^1, C_6H_3)*, ca. 147 (s br, 4C, 2 × $C^{2,6}$, Trip, extremely broad)*, 149.9 (s, 2C, 2 × C^4, Trip), 232.5 (s, 2C, 2 × *C*O). ^{29}Si NMR (59.63 MHz, C_6D_6, 298 K, ppm): δ = 236.8 (s).

The signals marked with an asterisk are questionable. The signal at 147.8 ppm from Si-C^1, C_6H_3 fits with the expected trend for E-C^{ipso} chemical shifts.

4.2.48 [Cp(CO)$_2$Mo(D){SiCl(C_6H_3-2,6-Trip$_2$)}] (68)

A 1.0 M solution of DCl in diethyl ether (0.18 mL, 0.18 mmol) was added dropwise to a solution of **60** (130 mg, 0.179 mmol) in 10 mL of diethyl ether at –80 °C. Upon addition the solution turned from red-brown to orange-yellow. The mixture was allowed to warm to –30 °C and all volatiles were removed *in vacuo*. The yellow residue was dissolved in 2 mL of hexane at –30 °C and the solution was again evaporated to dryness at –30 °C. The residue was dried for 0.5 h at –30 °C, and then allowed to warm slowly *in vacuo* to ambient temperature to give a brown solid. Yield: quantitative. IR (hexane, cm^{-1}): 1977 (vs), 1972 (vs), 1911 (s), 1891 (s) [ν(CO)]. ^{1}H NMR (300.1 MHz, C_6D_6, 298 K, ppm): δ = 1.10 (d, ^3J(H,H) = 6.8 Hz, 12H, 2 × $C^{2,6}$- CHMe$_A$Me$_B$, Trip), 1.28 (d, ^3J(H,H) = 6.8 Hz, 12H, 2 × C^4-CH*Me*$_2$, Trip), 1.51 (d, ^3J(H,H) = 6.8 Hz, 12H, 2 × $C^{2,6}$-CHMe$_A$Me$_B$, Trip), 2.85 (sept, ^3J(H,H) = 6.8 Hz, 2H, 2 × C^4-C*H*Me$_2$, Trip), 3.15 (br, 4H, 4 × $C^{2,6}$-C*H*Me$_A$Me$_B$, Trip), 4.66 (s, 5H, C_5H_5), 7.21 (m, 1H, C^4-*H*, C_6H_3), 7.25 (s, 4H, 2 × $C^{3,5}$-*H*, Trip), 7.29 (m, 2H, $C^{3,5}$-*H*, C_6H_3). ^{2}D NMR (76.77 MHz, C_6H_6/C_6D_6, 298 K, ppm): δ = −9.18 (s, $\nu_{1/2}$ = 2.3 Hz, 1D, Mo-D).

4.2.49 [Cp(CO)$_2$Mo(H){Si(NH$_2$)(C_6H_3-2,6-Trip$_2$)}] (66)

A 0.5 M solution of ammonia in dioxane (0.4 mL, 0.2 mmol) was added dropwise to a solution of **60** (146 mg, 0.201 mmol) in 5 mL of hexane at –78 °C. Upon addition the solution turned from red-brown to yellow and at this point addition was stopped (the precipitate of

dioxane was observed). The reaction mixture was allowed to warm to −30 °C and all volatiles were removed *in vacuo,* the residue was dried at ambient temperature (0.05 mbar, 30 min). The crude product was dissolved in approximately 10 mL of hexane. The yellow solution was filtered from a tiny amount of an insoluble material and stored for 4 days at –30 °C for crystallization. The crystals were separated by filtration at ~30 °C, washed with hexane (3 × 0.5 mL) and dried *in vacuo* at room temperature (30 min). Yield: 130 mg (0.175 mmol, 87%). Elemental analysis calcd (%) for $C_{43}H_{57}MoNO_2Si$ (743.94): C 69.42, H 7.72, N 1.88; found: C 69.61, H 7.73, N 1.73%. IR (toluene, cm^{-1}): 1954 (s), 1945 (s), 1883 (s sh), 1875 (vs) [*ν*(CO)]. IR (KBr pellet, cm^{-1}): 3884 (vw), 3649 (vw), 3462 (m, NH_2), 3372 (m, NH_2), 3113 (w), 3038 (w), 2954 (vs), 2926 (s), 2865 (s), 1948 (vs, CO), 1839 (vs, CO), 1672 (br w), 1605 (m), 1564 (vw), 1549 (m), 1457 (m), 1445 (vw), 1426 (m), 1382 (m), 1362 (m), 1316 (w), 1248 (w), 1237 (w), 1188 (vw), 1169 (w), 1153 (vw), 1132 (vw), 1108 (w), 1100 (w), 1077 (w), 1070 (w), 1054 (w), 1011 (w), 1005 (w), 956 (vw), 941 (w), 886 (m), 874 (m), 837 (vw), 824 (vw), 800 (m), 775 (vw), 753 (w), 717 (w), 652 (vw), 630 (w), 598 (w), 531 (m), 495 (w), 475 (w), 452 (m), 430 (w), 427 (w), 423 (w). ^{1}H NMR (300.1 MHz, C_6D_6, 298 K, ppm): δ = –9.56 (s, *J*(Si,H) = 29.5 Hz, 1H, Mo-*H*), 1.08 (d, ^{3}*J*(H,H) = 6.7 Hz, 12H, 2 × C^{2,6}-CH*Me*$_A$Me$_B$, Trip), 1.29 (d, ^{3}*J*(H,H) = 7.0 Hz, 12H, 2 × C^4-CH*Me*$_2$, Trip), 1.36 (d, ^{3}*J*(H,H) = 6.7 Hz, 12H, 2 × C^6-CHMe$_A$*Me*$_B$, Trip), 2.86 (sept, ^{3}*J*(H,H) = 7.0 Hz, 2H, 2 × C^4-C*H*Me$_2$, Trip), 2.954 (sept, ^{3}*J*(H,H) = 6.7 Hz, 4H, 2 × C^{2,6}-C*H*Me$_A$Me$_B$, Trip), 2.958 (s, 2H, N*H*$_2$), 4.73 (s, 5H, C_5H_5), 7.20 (s, 4H, 2 × C^{3,5}-*H*, Trip), 7.17−7.25 (m, 3H, C^{3,4,5}-*H*, C_6H_3). ^{13}C{^{1}H} NMR (75.47 MHz, C_6D_6, 298 K, ppm): δ = 22.5 (s, 4C, 2 × C^{2,6}-CHMe$_A$*Me*$_B$, Trip), 24.3 (s, 4C, 2 C^4-CH*Me*$_2$, Trip), 26.6 (s, 4C, 2 × C^{2,6}-CH*Me*$_A$Me$_B$, Trip), 31.4 (s, 4C, 2 × C^{2,6}-*C*HMe$_A$Me$_B$, Trip), 34.9 (s, 2C, 2 × C^4-*C*HMe$_2$, Trip), 88.2 (s, 5C, *C*$_5$H$_5$), 121.2 (s, 4C, 2 × *C*^{3,5}-H, Trip), 128.1 (s, 1C, *C*^{4}-H, C_6H_3), 130.0 (s, 2C, *C*^{3,5}-H, C_6H_3), 136.9 (s, 2C, 2 × *C*^{1}, Trip), 144.5 (s, 2C, *C*^{2,6}, C_6H_3), 146.7 (s, 1C, Si-*C*^{1}, C_6H_3), 147.3 (s, 4C, 2 × *C*^{2,6}, Trip), 149.5 (s, 2C, 2 × *C*^{4}, Trip), 234.1 (s, 2C, 2 × *C*O). ^{29}Si NMR (59.63 MHz, C_6D_6, 298 K, ppm): δ = 207.4 (s).

4.2.50 [Cp(CO)$_2$Mo{η^2-Si(H)(C$_6$H$_3$-2,6-Trip$_2$)(PHMes)}] (69)

A 0.11 M solution of $MesPH_2$ in hexane (1.9 mL, 0.21 mmol) was added dropwise to a solution of **60** (146 mg, 0.201 mmol) in 5 mL of hexane at ca. −60 °C. The reaction mixture was allowed to warm to ambient temperature and subsequently stirred for 1 h until the color changed from red-brown to yellow. All volatiles were removed *in vacuo,* the yellow residue was dissolved in 1 mL of hexane. The solution was stored for 4 days at –60 °C for

crystallization. The yellow microcrystalline precipitate was collected by filtration at –30°C, washed with hexane at–30 °C (2 × 1 mL) and dried *in vacuo* at room temperature for 1 h. Yield: 120 mg (0.17 mmol, 85%). Elemental analysis calcd (%) for $C_{52}H_{67}MoO_2PSi$ (879.09): C 71.05, H 7.68; found: C 71.07, H 7.87%. IR (hexane, cm^{-1}): 1942 (vs), 1877 (vs) [ν(CO)].

IR (solid, cm^{-1}): 3050 (vw), 3022 (vw), 2959 (s), 2926 (m), 2866 (m), 1933 (vs, CO), 1870 (vs, CO), 1845 (w sh), 1604 (m), 1562 (w), 1556 (w), 1461 (s), 1445 (m), 1428 (m), 1381 (m), 1361 (m), 1334 (vw), 1314 (w), 1294 (vw), 1246 (w), 1187 (vw), 1169 (w), 1152 (vw), 1130 (vw), 1102 (w), 1077 (w), 1070 (vw), 1050 (vw), 1029 (vw), 1007 (w), 957 (w sh), 943 (w), 923 (w), 893 (m), 875 (s), 846 (s), 822 (w), 799 (s), 776 (w), 757 (vw), 746 (w), 725 (vw), 707 (vw), 677 (m), 651 (w), 626 (vw), 602 (m), 579 (m), 560 (s), 533 (w sh), 518 (s), 499 (m), 491 (m), 471 (s), 427 (vw), 405 (s), 386 (m).

^{1}H NMR (300.1 MHz, C_6D_6, 298 K, ppm): δ = 1.07 (d br, ^3J(H,H) = 6.5 Hz, 6H, 2 × C^2-CH*Me*$_A$Me$_B$, Trip), 1.14 (d, ^3J(H,H) = 6.8 Hz, 6H, 2 × C^6-CH*Me*$_A$Me$_B$, Trip), 1.26 (d, ^3J(H,H) = 6.9 Hz, 6H, 2 × C^4-CH*Me*$_A$Me$_B$, Trip), 1.28 (d, ^3J(H,H) = 6.9 Hz, 6H, 2 × C^4-CHMe$_A$*Me*$_B$, Trip), 1.38 (d br, 6H, 2 × C^2-CHMe$_A$*Me*$_B$, Trip), 1.59 (d, ^3J(H,H) = 6.8 Hz, 6H, 2 × C^6-CHMe$_A$*Me*$_B$, Trip), 1.92 (s, 3H, C^4-*Me*, Mes), 2.23 (s br, 6H, C^{2,6}-*Me*, Mes), 2.86 (d br, ^1J(P,H) = 454 Hz, 1H, P*H*), 2.87 (sept, ^3J(H,H) = 6.9 Hz, 2H, 2 × C^4-C*H*Me$_A$Me$_B$, Trip), 3.12 (sept, ^3J(H,H) = 6.8 Hz, 2H, 2 × C^6-C*H*Me$_A$Me$_B$, Trip), 3.29 (sept, ^3J(H,H) = 6.8 Hz, 4H, 2 × C^2-C*H*Me$_A$Me$_B$, Trip), 4.53 (s, 5H, C_5H_5), 4.92 (dd, ^2J(P,H) = 21.3 Hz, ^4J(H,H) = 2.3 Hz, ^1J(Si,H) = 230 Hz, 1H, Si-*H*), 6.57 (d, ^4J(P,H) = 3.5 Hz, 2H, C^{3,5}-*H*, Mes), 7.0−7.2 (m br, 5H, C^3-*H*, Trip and C^{3,4,5}-*H*, C_6H_3), 7.28 (d, ^4J(H,H) = 1.7 Hz, 2H, 2 × C^5-*H*, Trip).

^{13}C{^{1}H} NMR (75.47 MHz, C_6D_6, 298 K, ppm): δ = 20.7 (s, 1C, C^4-*Me*, Mes), 23.1 (s br, 2C, 2 × C^2-CHMe$_A$*Me*$_B$, Trip), 23.3 (s br, 2C, 2 × C^6-CHMe$_A$*Me*$_B$, Trip), 23.5 (d, ^3J(H,H) = 8.7 Hz, 2C, C^{2,6}-*Me*, Mes), 24.0 (s, 2C, 2 × C^4-CH*Me*$_A$Me$_B$, Trip), 24.6 (s, 2C, 2 × C^4-CHMe$_A$*Me*$_B$, Trip), 26.3 (s br, 4C, 2 × C^2-CH*Me*$_A$Me$_B$ and 2 × C^6-CH*Me*$_A$Me$_B$, Trip), 31.1 (s br, 4C, 2 × C^{2,6}-*C*HMe$_A$Me$_B$, Trip), 34.7 (s, 2C, 2 × C^4-*C*HMe$_A$Me$_B$, Trip), 88.4 (s, 5C, C_5H_5), 120.8 (2C, 2 × *C*^{3} -H, Trip), 121.2 (s, 2C, 2 × *C*^{5}-H, Trip), 126.8 (d br, ^1J(P,C) = 30.7 Hz, 1C, *C*^{1}, Mes), 127.8 (s, 1C, *C*^{4}-H, C_6H_3), 129.8 (d, ^3J(P,C) = 9.0 Hz, 2C, *C*^{3,5}-Me, Mes), 130.4 (s br, 2C, *C*^{3,5}-H, C_6H_3), 135.8 (d, ^2J(P,C) = 5.8 Hz, 1C, Si-*C*^{1}, C_6H_3), 138.1 (d, ^4J(P,C) = 2.6 Hz, 1C, *C*^{4}-Me, Mes), 142.1 (d br, 2C, *C*^{2,6}-Me, Mes), 147.6 (s, 4C, 2 × *C*^{2}, Trip), 148.0 (s, 4C, 2 × *C*^{6}, Trip), 148.9 (s, 2C, 2 × *C*^{4}, Trip), 232.1 (s br, 2C, 2 × *C*O). Signals of *C*^{1}(Trip) and *C*^{2,6}(C_6H_3) are missing due to the broadness.

^{29}Si{^{1}H} NMR (59.63 MHz, C_6D_6, 298 K, ppm): δ = −47.2 (d, ^{2}J(P,Si) = 97.6 Hz).

^{1}H NMR (300.1 MHz, toluene-d_8, 333 K, ppm): δ = 1.05 (d, ^{3}J(H,H) = 6.8 Hz, 6H, 2 × C^{2}-CH*Me*$_A$Me$_B$, Trip), 1.10 (d, ^{3}J(H,H) = 6.8 Hz, 6H, 2 × C^{6}-CH*Me*$_A$Me$_B$, Trip), 1.27 (d, ^{3}J(H,H) = 6.8 Hz, 6H, 2 × C^{4}-CH*Me*$_A$Me$_B$, Trip), 1.29 (d, ^{3}J(H,H) = 6.8 Hz, 6H, 2 × C^{4}-CHMe$_A$*Me*$_B$, Trip), 1.33 (d, 6H, ^{3}J(H,H) = 6.8 Hz, 2 × C^{2}-CHMe$_A$*Me*$_B$, Trip), 1.51 (d, ^{3}J(H,H) = 6.8 Hz, 6H, 2 × C^{6}-CHMe$_A$*Me*$_B$, Trip), 2.08 (s, 3H, C^{4}-*Me*, Mes), 2.18 (s, 6H, C^{2,6}-*Me*, Mes), 2.84 (d br, ^{1}J(P,H) = 451 Hz, 1H, P*H*), 2.88 (sept, ^{3}J(H,H) = 6.8 Hz, 2H, 2 × C^{4}-C*H*Me$_A$Me$_B$, Trip), 3.03 (sept, ^{3}J(H,H) = 6.8 Hz, 2H, 2 × C^{6}-C*H*Me$_A$Me$_B$, Trip), 3.20 (sept, ^{3}J(H,H) = 6.8 Hz, 4H, 2 × C^{2}-C*H*Me$_A$Me$_B$, Trip), 4.53 (s, 5H, C_5H_5), 4.85 (dd, ^{2}J(P,H) = 20.7 Hz, ^{4}J(H,H) = 2.3 Hz, ^{1}J(Si,H) = 230 Hz, 1H, Si-*H*), 6.56 (d, ^{4}J(P,H) = 3.4 Hz, 2H, C^{3,5}-*H*, Mes), 7.0−7.2 (m br, 5H, C^{3}-*H*, Trip and C^{3,4,5}-*H*, C_6H_3), 7.22 (d, ^{4}J(H,H) = 1.6 Hz, 2H, 2 × C^{5}-*H*, Trip). ^{1}H{^{31}P} NMR (300.1 MHz, toluene-d_8, 313 K) spectrum showed a doublet resonance signal for Si-*H* (4.86 ppm) and a broad singlet for P-*H* (2.82 ppm) protons.

^{13}C{^{1}H} NMR (75.47 MHz, toluene-d_8, 333 K, ppm): δ = 20.7 (s, 1C, C^{4}-*Me*, Mes), 23.2 (s, 2C, 2 × C^{2}-CHMe$_A$*Me*$_B$, Trip), 23.4 (s, 2C, 2 × C^{6}-CHMe$_A$*Me*$_B$, Trip), 23.6 (d, ^{3}J(H,H) = 9.0 Hz, 2C, C^{2,6}-*Me*, Mes), 24.1 (s, 2C, 2 × C^{4}-CH*Me*$_A$Me$_B$, Trip), 24.5 (s, 2C, 2 × C^{4}-CHMe$_A$*Me*$_B$, Trip), 26.24 and 26.32 (s, 4C, 2 × C^{2}-CH*Me*$_A$Me$_B$ and 2 × C^{6}-CH*Me*$_A$Me$_B$, Trip), 31.2 (s, 4C, 2 × C^{2,6}-*C*HMe$_A$Me$_B$, Trip), 34.8 (s, 2C, 2 × C^{4}-*C*HMe$_A$Me$_B$, Trip), 88.5 (s, 5C, C_5H_5), 121.0 (2C, 2 × *C*^{3} -H, Trip), 121.3 (s, 2C, 2 × *C*^{5}-H, Trip), 126.9 (d, ^{1}J(P,C) = 31.0 Hz, 1C, *C*^{1}, Mes), 127.7 (s, 1C, *C*^{4}-H, C_6H_3), 129.9 (d, ^{3}J(P,C) = 9.0 Hz, 2C, *C*^{3,5}-Me, Mes), 130.8 (s, 2C, *C*^{3,5}-H, C_6H_3), 136.1 (d, ^{2}J(P,C) = 6.1 Hz, 1C, Si-*C*^{1}, C_6H_3), 138.1 (d, ^{4}J(P,C) = 2.9 Hz, 1C, *C*^{4}-Me, Mes), 138.7 (s br, 2C, 2 × *C*^{1}, Trip), 142.2 (d, ^{2}J(P,C) = 8.7 Hz, 2C, *C*^{2,6}-Me, Mes), 147.7 (s, 4C, 2 × *C*^{2}, Trip), 148.1 (s, 4C, 2 × *C*^{6}, Trip), 148.4 (s br, *C*^{2,6}, C_6H_3), 149.0 (s, 2C, 2 × *C*^{4}, Trip), 232.2 (d, ^{3}J(P,C) = 5.8 Hz, 1C, *C*O), 239.1 (d, ^{3}J(P,C) = 19.0 Hz, 1C, *C*O).

^{29}Si{^{1}H} NMR (59.63 MHz, C_6D_6, 298 K, ppm): δ = −47.2 (d, ^{2}J(P,Si) = 97.6 Hz).

4.2.51 [NMe$_4$][Cp(CO)$_2$Mo=Si(C$_6$H$_3$-2,6-Trip$_2$)Cl] (70)

A mixture of **60** (146 mg, 0.201 mmol) and (NMe$_4$)Cl (35 mg, 0.32 mmol) was treated with 3 mL of DME and the red-brown mixture was stirred for 3 h at ambient temperature. The Schlenk tube was immersed from time to time in an ultrasonic bath to accelerate the reaction. The color of the solution changed from red-brown to orange-red. Completion of the reaction was confirmed by IR spectroscopy and then the solvent was removed *in vacuo*. The resulting

solid was extracted with approximately 2 mL of toluene and the extract was filtered. Pentane (ca. 4 mL) was added to the filtrate until the solution became slightly turbid. After storage overnight at ambient temperature orange-red crystals of **70** were grown, which were separated by decantation and washed with pentane (3 × 3 mL). The obtained bright orange, micro-crystalline powder was dried under vacuum (30 min, RT). Yield: 121 mg (0.145 mmol, 72%), bright orange, microcrystalline powder. Orange single crystals of **70**·toluene were grown upon diffusion of pentane into a toluene solution at room temperature. The compound decomposes at 122–126 °C to give a green-black mass. Elemental analysis calcd (%) for $C_{47}H_{66}ClMoNO_2Si$ (836.51): C 67.48, H 7.95, N 1.67; found: C 67.16, H 8.01, N 1.84%. IR (DME, cm^{-1}): 1840 (vs), 1762 (vs) [ν(CO)]. IR (toluene, cm^{-1}): 1831 (vs), 1749 (vs) [ν(CO)]. The IR spectrum of **70** in toluene shows also two ν(CO) absorption bands of lower intensity at 1937 and 1876 cm^{-1} originating from the silylidyne complex **60**. It suggests in agreement with the ^{1}H NMR spectrum in C_6D_6 that dissociation equilibrium exists between **70** and **60** + $(NMe_4)Cl$ in aromatic solvents, which lies on the site of **70**. ^{1}H NMR (300.1 MHz, C_6D_6, 298 K, ppm): δ = 1.26 (d, ^3J(H,H) = 6.8 Hz, 12H, 2 × CH*Me*$_2$, Trip), 1.33 (d, ^3J(H,H) = 6.8 Hz, 12H, 2 × CH*Me*$_2$, Trip), 1.62 (d, ^3J(H,H) = 6.8 Hz, 12H, 2 × CH*Me*$_2$, Trip), 2.04 (s, 12H, N*Me*$_4$), 2.91 (sept, ^3J(H,H) = 6.9 Hz, 2H, 2 × C^4-C*H*Me$_2$, Trip), 3.59 (sept, ^3J(H,H) = 6.7 Hz, 4H, 2 × C^{2,6}-C*H*Me$_A$Me$_B$, Trip), 5.17 (s, 5H, C$_5$*H*$_5$), 7.29 (s, 4H, 2 × C^{3,5}-*H*, Trip), 7.31−7.35 (m, 3H, C^{3,5}-*H* and C^4-*H*, C$_6$H$_3$). The ^{1}H NMR spectrum of pure **70** in C_6D_6 shows also the signals of the silylidyne complex **1** in lower intensity. Only the ^{1}H NMR signals of **70** are given above. The methine proton signal of **2** at δ = 2.91 ppm overlaps with the methine proton signals of **60** at 2.89 ppm (C^4-C*H*Me$_2$) and 2.94 ppm (C^{2,6}-C*H*Me$_A$Me$_B$).

^{1}H NMR (300.1 MHz, THF-*d*$_8$, 298 K, ppm): δ = 1.00 (d, ^3J(H,H) = 6.8 Hz, 12H, 2 × C^{2,6}-CH*Me*$_A$Me$_B$, Trip), 1.25 (d, ^3J(H,H) = 6.8 Hz, 12H, 2 × C^4-CH*Me*$_2$, Trip), 1.30 (d, ^3J(H,H) = 6.8 Hz, 12H, 2 × C^{2,6}-CHMe$_A$*Me*$_B$, Trip), 2.85 (sept, ^3J(H,H) = 6.8 Hz, 2H, 2 × C^4-C*H*Me$_2$, Trip), 3.11 (s, 12H, N*Me*$_4$), 3.16 (sept, ^3J(H,H) = 6.8 Hz, 4H, 2 × C^{2,6}-C*H*Me$_A$Me$_B$, Trip), 4.60 (s, 5H, C$_5$*H*$_5$), 6.99 (s, 4H, 2 × C^{3,5}-*H*, Trip), 7.03 (d, ^3J(H,H) = 7.5 Hz, 2H, C^{3,5}-*H*, C$_6$H$_3$), 7.21 (dd, ^3J(H,H) = 7.0 Hz, ^3J(H,H) = 8.0 Hz, 1H, C^4-*H*, C$_6$H$_3$).

^{13}C{^{1}H} NMR (75.47 MHz, THF-*d*$_8$, 298 K, ppm): δ = 23.3 (s, 4C, 2 × C^{2,6}-CHMe$_A$*Me*$_B$, Trip), 24.6 (s, 4C, 2 × C^4-CH*Me*$_2$, Trip), 26.6 (s, 4C, 2 × C^{2,6}-CH*Me*$_A$Me$_B$, Trip), 31.4 (s, 4C, 2 × C^{2,6}-*C*HMe$_A$Me$_B$, Trip), 35.5 (s, 2C, C × C^4-*C*HMe$_2$, Trip), 56.2 (t, ^1J(^{14}N,^{13}C) = 3.9 Hz, 4C, N*Me*$_4$), 85.9 (s, 5C, *C*$_5$H$_5$), 121.0 (s, 4C, 2 × C^{3,5}-H, Trip), 126.0 (s, 1C, *C*^{4}-H, C$_6$H$_3$),

130.3 (s, 2C, $C^{3,5}$-H, C_6H_3), 139.0 (s, 2C, 2 ×C^{1}, Trip), 142.6 (s, 2C, $C^{2,6}$, C_6H_3), 147.8 (s, 2C, 2 × C^{4}, Trip), 147.9 (s, 4C, 2 × $C^{2,6}$, Trip), 158.0 (s, 1C, C^{1}, C_6H_3), 240.6 (s, 2C, *C*O).

^{29}Si NMR (59.63 MHz, THF-d_8, 298 K, ppm): δ = 228.2 (s).

4.2.52 [NEt$_4$][Cp(CO)$_2$Mo=Si(C$_6$H$_3$-2,6-Trip$_2$)N$_3$] (71)

A mixture of **60** (73 mg, 0.10 mmol) and $(NEt_4)N_3$ (17 mg, 0.10 mmol) was suspended in 2 mL of DME and the brown mixture was stirred for 45 min at ambient temperature. The color of the solution slightly brightened during this time. The solvent was removed *in vacuo*, and the obtained solid was treated with 2 mL of hexane. The solvent was evaporated to dryness in vacuo, and the resulting orange solid was dried for 0.5 h at ambient temperature *in vacuo*. Yield: quantitative. Orange solid. Diffusion of pentane into a toluene solution at −16 °C afforded orange plate-like crystals of **71**·2(toluene)·pentane. Compound **71** decomposes upon melting at 143 °C to give a brown mass. Elemental analysis calcd (%) for $C_{51}H_{74}MoN_4O_2Si$ (899.2): C 68.12, H 8.30, N 6.23. IR (DME, cm^{-1}): 2109 (vs) [ν(N_3)]; 1826 (vs) [ν(CO)], 1756 (vs) [ν(CO)].

^{1}H NMR (300.1 MHz, C_6D_6, 298 K, ppm): δ = 0.46 (t, ^{3}J(H,H) = 7.1 Hz, 12H, N(CH_2CH_3)$_4$), 1.24 (d, ^{3}J(H,H) = 6.8 Hz, 12H, 2 × $C^{2,6}$-CHMe_AMe$_B$, Trip), 1.38 (d, ^{3}J(H,H) = 6.8 Hz, 12H, 2 × C^{4}-CHMe_2, Trip), 1.68 (d, ^{3}J(H,H) = 6.8 Hz, 12H, 2 × $C^{2,6}$-CHMe$_A$$Me_B$, Trip), 2.28 (q, ^{3}J(H,H) = 7.1 Hz, 8H, N(CH_2CH$_3$)$_4$), 2.96 (sept, ^{3}J(H,H) = 6.9 Hz, 2H, 2 × C^{4}-C*H*Me$_2$, Trip), 3.52 (sept, ^{3}J(H,H) = 6.8 Hz, 4H, 2 × $C^{2,6}$-C*H*Me$_A$Me$_B$, Trip), 5.15 (s, 5H, C_5H_5), 7.29−7.33 (m, 3H, $C^{3,5}$-*H* and C^{4}-*H*, C_6H_3), 7.34 (s, 4H, 2 × $C^{3,5}$-*H*, Trip).

^{13}C{^{1}H} NMR (75.47 MHz, C_6D_6, 298 K, ppm): δ = 7.1 (s, 4C, N(CH_2CH_3)$_4$), 23.1 (s, 4C, 2 × $C^{2,6}$-CHMe$_A$$Me_B$, Trip), 24.5 (s, 4C, 2 × C^{4}-CHMe_2, Trip), 26.6 (s, 4C, 2 × $C^{2,6}$-CHMe_AMe$_B$, Trip), 31.5 (s, 4C, 2 × $C^{2,6}$-*C*HMe$_A$Me$_B$, Trip), 35.1 (s, 2C, 2 × C^{4}-*C*HMe$_2$, Trip), 52.2 (s, 4C, N(CH_2CH_3)$_4$), 85.9 (s, 5C, C_5H_5), 120.8 (s, 4C, 2 × $C^{3,5}$-H, Trip), 126.4 (s, 1C, C^{4}-H, C_6H_3), 129.7 (s, 2C, $C^{3,5}$-H, C_6H_3), 138.6 (s, 2C, 2 × C^{1}, Trip), 143.8 (s, 2C, $C^{2,6}$, C_6H_3), 147.6 (s, 4C, 2 × $C^{2,6}$, Trip), 147.7 (s, 2C, 2 × C^{4}, Trip), 153.2 (s, 1C, C^{1}, C_6H_3), 240.4 (s, 2C, *C*O).

^{29}Si NMR (59.63 MHz, C_6D_6, 298 K, ppm): δ = 228.5 (s).

4.2.53 Li[Cp(CO)$_2$Mo=Si(C$_6$H$_3$-2,6-Trip$_2$)Me] (72)

A solution of methyl lithium in diethyl ether (0.32 M, 0.70 mL, 0.22 mmol) was added via a syringe to a solution of **60** (146 mg, 0.201 mmol) in 4 mL of diethyl ether at −60 °C. Upon addition the color of the solution changed from dark red-brown to orange. The reaction mixture was subsequently stirred for 10 min at −60 °C, and the solution was concentrated to about 1 mL in *vacuo* at −60 °C. The yellow crystalline solid, which precipitated out, was filtered, washed with Et_2O (2 × 0.5 mL) at –60 °C and dried *in vacuo* for 30 min at ambient temperature. Yield 127 mg (0.152 mmol, 76%). Yellow, crystalline solid. The solid slowly turns brown at ambient temperature and should be stored at −30 °C. Elemental analysis calcd (%) for $C_{44}H_{57}LiMoO_2Si{\cdot}1.2Et_2O$ (837.8)[132]: C 69.95, H 8.30; found: C 69.96, H 8.32%. IR (DME, cm^{-1}): ν = 1824 (vs), 1695 (vs) [ν(CO)].

^{1}H NMR (300.1 MHz, THF-d_8, 298 K, ppm): δ = 0.52 (s, 3H, SiCH_3), 1.01 (d, ^3J(H,H) = 6.8 Hz, 12H, 2 × C^{2,6}-CHMe_AMe$_B$, Trip), 1.12 (t, ^3J(H,H) = 7.0 Hz, 7.2H, CH_3, 1.2Et$_2$O), 1.24 (d, ^3J(H,H) = 6.8 Hz, 12H, 2 × C^4-CHMe_2, Trip), 1.27 (d, ^3J(H,H) = 6.8 Hz, 12H, 2 × C^{2,6}-CHMe$_A$$Me_B$, Trip), 2.84 (sept, ^3J(H,H) = 6.8 Hz, 2H, 2 × C^4-CHMe$_2$, Trip), 3.12 (sept, ^3J(H,H) = 6.8 Hz, 4H, 2 × C^{2,6}-CHMe$_A$Me$_B$, Trip), 3.38 (q, ^3J(H,H) = 7.0 Hz, 4.8H, CH_2, 1.2Et$_2$O), 4.62 (s, 5H, C$_5H_5$), 6.98 (s, 4H, 2 × C^{3,5}-H, Trip), 7.04 (d, ^3J(H,H) = 7.4 Hz, 2H, C^{3,5}-H, C$_6$H$_3$), 7.20 (dd, ^3J(H,H) = 7.0 Hz, ^3J(H,H) = 8.0 Hz, 1H, C^4-H, C$_6$H$_3$).

^{13}C{^{1}H} NMR (75.47 MHz, THF-d_8, 298 K, ppm): δ = 15.7 (s, CH$_3$, 1.2Et$_2$O), 19.4 (s, 1C, SiCH$_3$), 23.0 (s, 4C, 2 × C^{2,6}-CHMe$_A$$Me_B$, Trip), 24.6 (s, 4C, 2 × C^4-CHMe_2, Trip), 26.6 (s, 4C, 2 × C^{2,6}-CHMe_AMe$_B$, Trip), 31.3 (s, 4C, 2 × C^{2,6}-CHMe$_A$Me$_B$, Trip), 35.5 (s, 2C, 2 × C^4-CHMe$_2$, Trip), 66.3 (s, CH$_2$, 1.2Et$_2$O), 87.1 (s, 5C, C_5H$_5$), 121.1 (s, 4C, 2 × $C^{3,5}$-H, Trip), 125.3 (s, 1C, C^4-H, C$_6$H$_3$), 130.1 (s, 2C, $C^{3,5}$-H, C$_6$H$_3$), 139.9 (s, 2C, 2 × C^1, Trip), 142.6 (s, 2C, 2 × $C^{2,6}$, C$_6$H$_3$), 147.4 (s, 4C, 2 × $C^{2,6}$, Trip), 147.8 (s, 2C, 2 × C^4, Trip), 162.1 (s, 1C, C^1, C$_6$H$_3$), 243.2 (s, 2C, CO).

^{29}Si{^{1}H} NMR (59.63 MHz, THF-d_8, 298 K, ppm): δ = 138.0 (s).

[132] The composition of the diethyl ether solvate of **72** was determined by ^{1}H NMR spectroscopy and verified by elemental analysis.

4.2.54 $Li_2[Cp(CO)_2Mo–Si(C_6H_3\text{-}2,6\text{-}Trip_2)Me_2]$ (73)

A solution of methyl lithium in diethyl ether (1.6 M, 0.25 mL, 0.40 mmol) was added via a syringe to a solution of 60 (146 mg, 0.201 mmol) in a mixture of 1 mL of DME and 4 mL of hexane at −70 °C. Upon addition the color of the solution changed from dark red-brown to orange. The solution was subsequently stirred for 5 min at −70 °C and warmed up. Precipitation of a yellow solid was observed, which was filtered at 0 °C, washed with hexane (2 × 1 mL) and dried *in vacuo* for 15 min at ambient temperature to afford the product as a yellow, microcrystalline solid. Yield: 170 mg (0.176 mmol, 88%). The solvate decomposes slowly under vacuum at ambient temperature probably due to loss of solvent. Decomposition is accompanied by a discoloration of the solid to beige. The solvate decomposes upon melting at 116−120 °C to a brown mass. Elemental analysis calcd (%) for $C_{45}H_{60}Li_2MoO_2Si{\cdot}1.7DME{\cdot}0.5C_6H_{14}$ (967.2)[133]: C 68.05, H 8.75%. IR (DME, cm^{-1}): 1677 (vs) [ν(CO)], 1589 (vs) [ν(CO)].

^{1}H NMR (300.1 MHz, THF-d_8, 298 K, ppm): δ = −0.20 (s, 6H, Si(CH_3)$_2$), 0.89 (t, ^3J(H,H) = 6.8 Hz, 3H, CH_3, 0.5C_6H_{14}), 0.92 (d, ^3J(H,H) = 6.8 Hz, 12H, 2 × $C^{2,6}$-CHMe_AMe$_B$, Trip), 1.26 (d, ^3J(H,H) = 6.8 Hz, 12H, 2 × C^4-CHMe_2, Trip), 1.29 (m, 4H, CH_2, 0.5C_6H_{14}), 1.36 (d, ^3J(H,H) = 6.8 Hz, 12H, 2 × $C^{2,6}$-CHMe$_A$$Me_B$, Trip), 2.83 (sept, ^3J(H,H) = 6.8 Hz, 2H, 2 × C^4-CHMe$_2$, Trip), 3.22 (sept, ^3J(H,H) = 6.8 Hz, 4H, 2 × $C^{2,6}$-CHMe$_A$Me$_B$, Trip), 3.27 (s, 10.2H, CH_3, 1.7DME), 3.43 (s, 6.8H, CH_2, 1.7DME), 4.49 (s, 5H, C_5H_5), 6.61 (d, ^3J(H,H) = 7.4 Hz, 2H, $C^{3,5}$-H, C_6H_3), 6.78 (t, ^3J(H,H) = 7.4 Hz, 1H, C^4-H, C_6H_3), 6.91 (s, 4H, 2 × $C^{3,5}$-H, Trip).

^{13}C{^{1}H} NMR (75.47 MHz, THF-d_8, 298 K, ppm): δ = 14.4 (s, CH$_3$, 0.5C_6H_{14}), 14.5 (s br, 2C, Si(CH$_3$)$_2$), 23.5 (s, CH$_2$, 0.5C_6H_{14}), 24.1 (s, 4C, 2 × $C^{2,6}$-CHMe$_A$$Me_B$, Trip), 24.8 (s, 4C, 2 × C^4-CHMe_2, Trip), 26.8 (s, 4C, 2 × $C^{2,6}$-CHMe_AMe$_B$, Trip), 31.3 (s, 4C, 2 × $C^{2,6}$-CHMe$_A$Me$_B$, Trip), 32.5 (s, CH$_2$, 0.5C_6H_{14}), 35.3 (s, 2C, C^4-CHMe$_2$, Trip), 58.9 (s, CH$_3$, 1.7DME), 72.7 (s, CH$_2$, 1.7DME), 85.8 (s, 5C, C_5H_5), 119.9 (s, 4C, 2 × $C^{3,5}$-H, Trip), 121.3 (s, 1C, C^4-H, C_6H_3), 131.8 (s, 2C, $C^{3,5}$-H, C_6H_3), 145.47 (s, 2C, 2 × C^1, Trip), 145.50 (s, 2C, 2 × C^4, Trip), 146.3 (s, 2C, $C^{2,6}$, C_6H_3), 147.2 (s, 4C, 2 × $C^{2,6}$, Trip), 162.2 (s, 1C, C^1, C_6H_3), 248.9 (s br, 2C, CO).

^{29}Si NMR (59.63 MHz, THF-d_8, 298 K, ppm): δ = 27.4 (s br).

[133] The composition of the solvate of **73** was determined by ^{1}H NMR spectroscopy.

4.2.55 K_2[CpMo(CO)$_2$–Si(*i*Pr)C$_6$H$_3$-2-Trip-6-C$_6$H$_2$-4,6-*i*Pr$_2$] (74)

A mixture of **60** (146 mg, 0.201 mmol) and KC_8 (60 mg, 0.44 mmol) was suspended in 10 mL of a DME−pentane (1:1) mixture at ambient temperature, and the suspension was stirred for 1 h. Completion of the reaction was confirmed by IR spectroscopy. The reaction mixture was filtered from the black insoluble solid, and the red-orange filtrate was evaporated to dryness *in vacuo*. The residue was treated with 3 mL of diethyl ether to give a solution, from which the orange crystalline product precipitated out after a short time. The orange precipitate was isolated by filtration, washed with 1 mL of diethyl ether and dried in vacuum (30 min, RT). Yield 170 mg (0.180 mmol, 90%). Orange, crystalline solid. Orange, prismatic parallelepipeds of **74**·1.5DME·0.5Et_2O were obtained upon addition of diethyl ether to a solution of **74** in DME. The solid decomposes above 162 °C to a brown mass. Elemental analysis calcd (%) for $C_{43}H_{54}K_2MoO_2Si$·0.4Et_2O·1.2DME[134] (942.9): C 62.92, H 7.48; found: C 62.29, H 7.50%. IR (DME, cm^{-1}): = 1685 (vs), 1593 (vs) [*ν*(CO)].

^{1}H NMR (300.1 MHz, THF-d_8, 298 K, ppm): δ = 0.06 (d, ^3J(H,H) = 7.1 Hz, 3H, Si-CH*Me$_A$*Me$_B$), 0.75 (sept, ^3J(H,H) = 7.1 Hz, 1H, Si-C*H*Me$_A$Me$_B$), 0.82 (d, ^3J(H,H) = 6.8 Hz, 3H, C^2-CH*Me$_A$*Me$_B$, Trip), 0.94 (d, ^3J(H,H) = 6.8 Hz, 3H, C^6-CH*Me$_A$*Me$_B$, Trip), 1.00 (d, ^3J(H,H) = 7.1 Hz, 3H, Si-CHMe$_A$*Me$_B$*), 1.12 (t, ^3J(H,H) = 7.0 Hz, 2.4H, C*H$_3$*, 0.4Et_2O), 1.22 (d, ^3J(H,H) = 6.7 Hz, 3H, C^4-CH*Me$_A$*Me$_B$, C$_6$H$_2$-2-Si-4,6-*i*Pr$_2$), 1.24 (d, ^3J(H,H) = 6.7 Hz, 3H, C^4-CHMe$_A$*Me$_B$*, C$_6$H$_2$-2-Si-4,6-*i*Pr$_2$), 1.257 (d, ^3J(H,H) = 6.7 Hz, 3H, C^4-CH*Me$_A$*Me$_B$, Trip), 1.266 (d, ^3J(H,H) = 6.7 Hz, 6H, C^6-CHMe$_A$*Me$_B$*, C^2-CHMe$_A$*Me$_B$* or C^4-CHMe$_A$*Me$_B$*, Trip), 1.271 (d, ^3J(H,H) = 6.7 Hz, 3H, C^4-CHMe$_A$*Me$_B$* or C^2-CHMe$_A$*Me$_B$*, Trip), 1.40 (d, ^3J(H,H) = 6.7 Hz, 3H, C^6-CH*Me$_A$*Me$_B$, C$_6$H$_2$-2-Si-4,6-*i*Pr$_2$), 1.45 (d, ^3J(H,H) = 6.8 Hz, C^6-CHMe$_A$*Me$_B$*, C$_6$H$_2$-2-Si-4,6-*i*Pr$_2$), 2.81 (sept, ^3J(H,H) = 6.7 Hz, 1H, C^4-C*H*Me$_A$Me$_B$, C$_6$H$_2$-2-Si-4,6-*i*Pr$_2$), 2.85 (sept, ^3J(H,H) = 6.8 Hz, 1H, C^4-C*H*Me$_A$Me$_B$, Trip), 2.94 (sept, ^3J(H,H) = 6.7 Hz, 1H, C^6-C*H*Me$_A$Me$_B$), 2.98 (sept, ^3J(H,H) = 6.7 Hz, 1H, C^2-C*H*Me$_A$Me$_B$, Trip), 3.27 (s, 7.2 H, C*H$_3$*, 1.2DME), 3.43 (s, 4.8 H, C*H$_2$*, 1.2DME), 3.39 (q, ^3J(H,H) = 7.0 Hz, 1.6 H, C*H$_2$*, 0.4Et_2O), 4.09 (sept, ^3J(H,H) = 6.7 Hz, 1H, C^6-C*H*Me$_A$Me$_B$, C$_6$H$_2$-2-Si-4,6-*i*Pr$_2$), 4.25 (s, 5H, C$_5$*H$_5$*), 6.64 (d, ^3J(H,H) = 7.5 Hz, 1H, C^3-*H*, C$_6$H$_3$), 6.97 (d, ^4J(H,H) = 1.8 Hz, 1H, C^3-*H*, Trip), 6.99 (d, ^4J(H,H) = 1.8 Hz, 1H, C^5-*H*, Trip), 7.00 (t, ^3J(H,H) = 7.5 Hz, 1H, C^4-*H*, C$_6$H$_3$), 7.03 (d, ^4J(H,H) = 1.9 Hz, 1H, C^5-*H*, C$_6$H$_2$-2-Si-4,6-*i*Pr$_2$), 7.72 (d, ^4J(H,H) = 1.8 Hz, 1H, C^3-*H*, C$_6$H$_2$-2-Si-4,6-*i*Pr$_2$), 7.83 (d, ^3J(H,H) = 7.5 Hz, 1H, C^5-*H*, C$_6$H$_3$),

[134] The composition of the solvate of **74** was determined by ^{1}H NMR spectroscopy and verified by elemental analysis.

$^{13}C\{H\}$ NMR (75.47 MHz, THF-d_8, 298 K, ppm): δ = 15.7 (s, CH_3, Et_2O), 19.5 (s, 1C, Si-CHMe$_A$Me$_B$), 20.3 (s, 1C, Si-CHMe_AMe$_B$), 22.6 (s, 1C, Si-CHMe$_A$$Me_B$), 22.9 (s, 1C, C^6-CH$Me_AMe_B$, Trip), 24.23 (s, 1C, C^4-CHMe_AMe$_B$, C_6H_2-2-Si-4,6-iPr$_2$), 24.29 (s, 1C, C^2-CHMe$_A$$Me_B$ or C^4-CHMe$_A$$Me_B$, Trip), 24.6 (s, 1C, C^4-CHMe$_A$$Me_B$ or C^2-CHMe$_A$$Me_B$, Trip), 24.9 (s with a shoulder, 3C, C^4-CHMe$_A$$Me_B$ and C^6-CHMe_AMe$_B$, C_6H_2-2-Si-4,6-iPr$_2$; C^4-CHMe_AMe$_B$, Trip), 25.4 (s, 1C, C^6-CHMe$_A$$Me_B$, C_6H_2-2-Si-4,6-iPr$_2$), 27.0 (s, 1C, C^2-CHMe_AMe$_B$, Trip), 27.1 (s, 1C, C^6-CHMe_AMe$_B$, Trip), 30.38 (s, 1C, C^6-CHMe$_A$Me$_B$, C_6H_2-2-Si-4,6-iPr$_2$), 30.45 (s, 1C, C^6-CHMe$_A$Me$_B$, Trip), 30.7 (s, 1C, C^2-CHMe$_A$Me$_B$, Trip), 34.9 (s, 1C, C^4-CHMe$_A$Me$_B$, C_6H_2-2-Si-4,6-iPr$_2$), 35.6 (s, 1C, C^4-CHMe$_A$Me$_B$, Trip), 58.9 (s, CH_3, DME), 66.3 (s, CH_2, Et_2O), 72.7 (s, CH_2, DME), 84.9 (s, 5C, C_5H_5), 120.3 (s, 1C, C^5-H, Trip), 120.5 (s, 1C, C^3-H, Trip), 121.5 (s, 1C, C^5-H, C_6H_2-2-Si-4,6-iPr$_2$), 123.5 (s, 1C, C^5-H, C_6H_3), 123.7 (s, 1C, C^4-H, C_6H_3), 129.4 (s, 1C, C^3-H, C_6H_3), 131.7 (s, 1C, C^3-H, C_6H_2-2-Si-4,6-iPr$_2$), 142.2 (s, 1C, C^1, C_6H_2-2-Si-4,6-iPr$_2$), 143.02 (s, 1C, C^6, C_6H_2-2-Si-4,6-iPr$_2$), 143.06 (s, 1C, C^1, Trip), 144.0 (s, 1C, C^4, C_6H_2-2-Si-4,6-iPr$_2$), 145.8 (s, 1C, C^6, C_6H_3), 146.3 (s, 1C, C^4, Trip), 147.2 (s, 1C, C^6, Trip), 148.3 (s, 1C, C^2, Trip), 149.2 (s, 1C, C^2, C_6H_3), 161.1 (s, 1C, Si-C^1, C_6H_3), 161.3 (s, 1C, Si-C^2, C_6H_2-2-Si-4,6-iPr$_2$), 245.7 (s, 1C, CO), 248.3 (s, 1C, CO).

^{29}Si NMR (59.63 MHz, THF-d_8, 298K, ppm): δ = 50.8 (s).

The following atom numbering scheme has been used to designate the aryl carbon atoms of the silyl substituent in **74**:

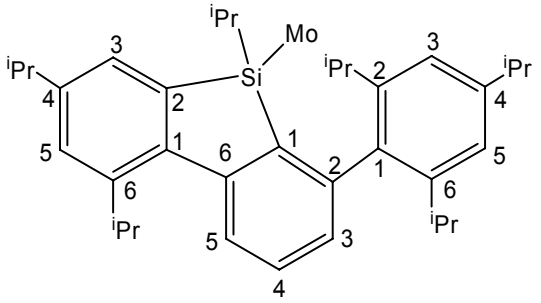

4.2.56 [Cp(CO)$_2$MoSi(C$_6$H$_3$-2,6-Trip$_2$)C(H)C(H)] (75)

To a Schlenk tube with a degassed frozen solution of **60** (146 mg, 0.20 mmol) in 5 mL of hexane, acetylene (ca. 75 mL gas, ca. 3.3 mmol) was introduced. The cooling bath was removed and the mixture was allowed to warm up to 0 °C and further stirred at this temperature for 30 min. The color of the solution changed from red-brown to brown and some

of black metallic solid precipitated. All volatiles were removed *in vacuo* to give a brown residue. IR spectroscopy confirmed formation of a new product with absorptions at 1948 and 1869 cm^{-1}; however ca. 7% of the starting material was present. The residue was treated with 1 mL of hexane, filtered, and the filtrate was stored at −30 °C for 2 months to give orange crystals. The crystals were separated by decantation with a cannula, washed with hexane (2 × 0.5 mL) and dried *in vacuo*. Yield: ca. 30 mg (0.04 mmol, 20%). The compound is unstable at ambient temperature and should be stored cold. Elemental analysis calcd (%) for $C_{45}H_{56}MoO_2Si$ (752.95): C 71.78, H 7.50; found: C 71.79, H 7.46%. IR (hexane, cm^{-1}): 1949 (vs), 1869 (s) [ν(CO)]. IR (Et_2O, cm^{-1}): 1944 (vs), 1864 (s) [ν(CO)].

^{1}H NMR (300.1 MHz, THF-d_8, 233 K, ppm): δ = 1.09 (d, ^3J(H,H) = 6.7 Hz, 12H, 2 × $C^{2,6}$-CH$Me_A$$Me_B$, Trip), 1.25 (d, ^3J(H,H) = 6.9 Hz, 12H, 2 × C^4-CHMe_2, Trip), 1.49 (d br, 12H, 2 × $C^{2,6}$-CH$Me_A$$Me_B$, Trip), 2.80 (sept, ^3J(H,H) = 6.9 Hz, 2H, 2 × C^4-C$H$$Me_A$$Me_B$, Trip), 3.13 (s br, 4H, 2 × $C^{2,6}$-C$H$$Me_A$$Me_B$, Trip), 4.49 (s, 5H, C_5H_5), 7.19 (s, 4H, 2 × $C^{3,5}$-*H*, Trip), 7.25–7.32 (m, 3H, $C^{3,4,5}$-*H*, C_6H_3), 8.47 (s br, CH_A=CH_B), 8.64 (s br, CH=CH_B).

^{13}C{^{1}H} NMR (75.47 MHz, C_6D_6, 298 K, ppm): δ = 22.6 (s br, 4C, 2 × $C^{2,6}$-CH$Me_A$$Me_B$, Trip), 24.2 (s, 4C, 2 × C^4-CHMe_2, Trip), 26.9 (s, 4C, 2 × $C^{2,6}$-CH$Me_A$$Me_B$, Trip), 31.0 (s, 4C, 2 × $C^{2,6}$-C$H$$Me_A$$Me_B$, Trip), 34.9 (s, 2C, 2 × C^4-C$H$$Me_2$, Trip), 89.5 (s, 5C, C_5H_5), 120.9 (s, 4C, 2 × $C^{3,5}$-H, Trip), 128.9 (s, 1C, C^4-H, C_6H_3), 129.6 (s, 2C, $C^{3,5}$-H, C_6H_3), 136.5 (s, 2C, 2 × C^1, Trip), 140.4 (s, 1C, Si-C^1, C_6H_3), 145.6 (s, 2C, $C^{2,6}$, C_6H_3), 148.4 (s br, 4C, 2 × $C^{2,6}$, Trip), 149.7 (s, 2C, 2 × C^4, Trip), 240.4 (s, 2C, 2 × *C*O).

^{29}Si NMR (59.63 MHz, C_6D_6, 298K, ppm): δ = 123.8 (s).

4.2.57 [Cp(CO)$_2$MoSi(C$_6$H$_3$-2,6-Trip$_2$)C(Me)C(Me)] (76)

To a suspension of **60** (146 mg, 0.20 mmol) in 5 mL of hexane 2-butyne was added in a single portion (ca 0.1 mL, excess) at –60 °C. The cooling bath was removed and the mixture was allowed to warm up to ambient temperature. The color of the solution changed from red-brown to orange. The reaction was further stirred for 5 min at ambient temperature and then all volatiles were removed *in vacuo* to give orange foam. Completion of the reaction was confirmed by IR spectroscopy and the resulting solid was dissolved in 2 mL of pentane. The solution was stored for 3 hours at ambient temperature leading to deposition of large orange and small colorless crystals, which were washed with hexane (3 × 0.5 mL) and dried *in vacuo*. The orange crystals were separated on the basis of color and dried *in vacuo* (30 min, ambient

temperature). Yield: 85 mg (0.109 mmol, 54%). M.p 203−204 °C. Elemental analysis calcd (%) for $C_{49}H_{64}MoO_2Si$ (809.06): C 72.28, H 7.74; found: C 72.09, H 7.78%. IR (hexane, cm^{-1}): 1936 (vs), 1862 (sh), 1856 (s) [*ν*(CO)]. IR (Et_2O, cm^{-1}): 1931 (vs), 1850 (s) [*ν*(CO)].

^{1}H NMR (300.1 MHz, THF-d_8, 233 K, ppm): δ = 0.85 (d, ^3J(H,H) = 6.9 Hz, 3H, C$^{2'}$-CH*Me$_A$*Me$_B$, Trip), 0.95 (d, ^3J(H,H) = 6.9 Hz, 3H, C$^{2''}$-CH*Me$_A$*Me$_B$, Trip), 1.01 (d, ^3J(H,H) = 6.7 Hz, 3H, C$^{6''}$-CH*Me$_A$*Me$_B$, Trip), 1.23* (d, ^3J(H,H) = 6.9 Hz, 6H, C$^{4''}$-CH*Me$_A$*Me$_B$ and C$^{4''}$-CHMe$_A$*Me$_B$*, Trip), 1.26 (d, ^3J(H,H) = 6.9 Hz, 3H, C$^{6'}$-CH*Me$_A$*Me$_B$, Trip), 1.28 (d, ^3J(H,H) = 6.7 Hz, 3H, C$^{6''}$-CHMe$_A$*Me$_B$*, Trip), 1.29* (d, ^3J(H,H) = 6.9 Hz, 6H, C$^{4'}$-CH*Me$_A$*Me$_B$ and C$^{4'}$-CHMe$_A$*Me$_B$*, Trip), 1.33 (d, ^3J(H,H) = 6.9 Hz, 3H, C$^{2''}$-CHMe$_A$*Me$_B$*, Trip), 1.36 (d, ^3J(H,H) = 6.9 Hz, 3H, C$^{6'}$-CHMe$_A$*Me$_B$*, Trip), 1.39 (d, ^3J(H,H) = 6.9 Hz, 3H, C$^{2'}$-CHMe$_A$*Me$_B$*, Trip), 1.60 (s, 3H, C-*Me$_A$*), 1.83 (s, 3H, C- *Me$_B$*), 2.40 (sept, ^3J(H,H) = 6.7 Hz, 1H, C$^{6''}$-C*H*Me$_A$Me$_B$, Trip), 2.86 (sept, ^3J(H,H) = 6.9 Hz, 1H, C$^{4''}$-C*H*Me$_A$Me$_B$, Trip), 2.96* (sept, ^3J(H,H) = 6.9 Hz, 1H, C$^{2''}$-C*H*Me$_A$Me$_B$, Trip), 2.97* (sept, ^3J(H,H) ≈ 7 Hz, 1H, C$^{4'}$-C*H*Me$_A$Me$_B$, Trip), 3.16 (sept, ^3J(H,H) 6.9 Hz, 1H, C$^{6'}$-C*H*Me$_A$Me$_B$, Trip), 3.23 (sept, ^3J(H,H) 6.9 Hz, 1H, C$^{2'}$-C*H*Me$_A$Me$_B$, Trip), 4.61 (s, 5H, C_5H_5), 7.02 (m, 2H, C$^{3''}$-*H* and C$^{5''}$-*H*, Trip), 7.25 (d, ^4J(H,H) = 1.4 Hz, 1H, C$^{3'}$-*H*, Trip), 7.32 (d, ^3J(H,H) = 7.6 Hz, 1H, C^3-*H*, C_6H_3), 7.35 (d, ^4J(H,H) = 1.4 Hz, 1H, C$^{5'}$-*H*, Trip), 7.38 (d, ^3J(H,H) = 7.6 Hz, 1H, C^5-*H*, C_6H_3), 7.58 (t, ^3J(H,H) = 7.6 Hz, C^4-*H*, C_6H_3).

^{13}C{H} NMR (75.47 MHz, THF-d_8, 233 K, ppm): δ = 20.7 (s, 1C, C-*Me$_A$*), 22.6 (s, 1C, C$^{2'}$-CHMe$_A$*Me$_B$*), 23.1 (s, 1C, C$^{2''}$-CHMe$_A$*Me$_B$*), 23.2 (s, 1C, C$^{6''}$-CHMe$_A$*Me$_B$*), 24.0 (s, 1C, C$^{6'}$-CHMe$_A$*Me$_B$*), 24.2 (s, 1C, C$^{4'}$-CHMe$_A$*Me$_B$*, Trip), 24.49 (s, 1C, C$^{4''}$-CH*Me$_A$*Me$_B$, Trip), 24.55 (s, 1C, C$^{4'}$-CH*Me$_A$*Me$_B$, Trip), 24.7 (s, 1C, C$^{4''}$-CHMe$_A$*Me$_B$*, Trip), 26.0 (s, 1C, C$^{2'}$-CH*Me$_A$*Me$_B$, Trip), 27.2 (s, 1C, C$^{2''}$-CH*Me$_A$*Me$_B$, Trip), 27.3 (s, 1C, C$^{6''}$-CH*Me$_A$*Me$_B$, Trip), 28.0 (s, 1C, C$^{6'}$-CH*Me$_A$*Me$_B$, Trip), 28.8 (s, 1C, C-*Me$_B$*), 31.1 (s, 1C, C$^{6''}$-*C*HMe$_A$Me$_B$, Trip), 31.31 (s, 1C, C$^{2''}$-*C*HMe$_A$Me$_B$, Trip), 31.37 (s, 1C, C$^{2'}$-*C*HMe$_A$Me$_B$,Trip), 31.5 (s, 1C, C$^{6'}$-*C*HMe$_A$Me$_B$, Trip), 35.6 (s, 1C, C$^{4''}$-*C*HMe$_A$Me$_B$, Trip), 35.7 (s, 1C, C$^{4'}$-*C*HMe$_A$Me$_B$, Trip), 90.5 (s, 5C, C_5H_5), 120.9 (s, 1C, *C$^{5''}$*-H, Trip), 121.2 (s, 1C, *C$^{3''}$*-H, Trip), 121.8 (s, 1C, *C$^{3'}$*-H, Trip), 122.8 (s, 1C, *C$^{5'}$*-H, Trip), 129.4 (s, 1C, *C^4*-H, C_6H_3), 130.5 (s, 1C, *C^5*-H, C_6H_3), 131.0 (s, 1C, *C^3* -H, C_6H_3), 137.1 (s, 1C, *C$^{1'}$*, Trip), 137.8 (s, 1C, *C$^{1''}$*, Trip), 139.4 (s, 1C, *C^1*, C_6H_3), 144.4 (s, 1C, *C^6*, C_6H_3), 146.88 (s, 1C, *C$^{2''}$*, Trip), 146.93 (s, 1C, *C^2*, C_6H_3), 146.98 (s, 1C, *C$^{6''}$*, Trip), 148.8 (s, 1C, *C$^{4''}$*, Trip), 149.1 (s, 1C, *C$^{2'}$*, Trip), 149.6 (s, 1C, *C$^{6'}$*, Trip), 150.3 (s, 1C, *C$^{4'}$*, Trip), 161.3 (s, 1C, *C*-Me$_A$), 200.8 (s, 1C, *C*-Me$_B$), 241.1 (s, 1C, *C*O), 245.0 (s, 1C, *C*O).

^{29}Si NMR (59.63 MHz, THF-d_8, 298K, ppm): δ = 135.5 (s).

*Signals marked with an asterisk overlap. The chemical shifts may not be measured directly and are determined from the signals' pattern.

4.2.58 [Cp(CO)$_2$MoSi(C$_6$H$_3$-2,6-Trip$_2$)C(Et)C(Et)] (77)

To a solution of **60** (146 mg, 0.20 mmol) in 5 mL of hexane 3-hexyne was added in a single portion (90 mg, 1.1 mmol). The dark red-brown mixture was stirred for 30 min at 50 °C. The color of the solution changed from red-brown to bright orange. Completion of the reaction was confirmed by IR spectroscopy and then all volatiles were removed *in vacuo*. The resulting solid was dissolved in 2 mL of hexane and the solution was stored for 2 days at −50 °C. The orange crystals of **77** were grown, which were separated by decantation and washed with hexane (2 × 0.5 mL). The obtained bright orange crystals were dried *in vacuo* for 30 min (from −50 °C to ambient temperature). Yield: 180 mg, nearly quantitative. Part of the product was used for X-ray diffraction analysis; the rest was crashed and dried for 2 h at 30 °C to give a bright orange powder. M.p 166−168 °C, decomposes to give a brown-red liquid. Elemental analysis calcd (%) for $C_{49}H_{64}MoO_2Si$ (809.06): C 72.72, H 7.97; found: C 72.56, H 7.83%. IR (hexane, cm^{-1}): 1935 (vs), 1856 (s) [ν(CO)]. IR (Et_2O, cm^{-1}): 1930 (vs), 1851 (s) [ν(CO)].

^{1}H NMR (500.1 MHz, C_6D_6, 298 K, ppm): δ = 0.76 (br, 6H, 2 × CH_2CH_3), 0.95 (br, 3H, CHMe_2, Trip), 1.09 (br, 3H, CHMe_2, Trip), 1.11 (br, 3H, CHMe_2, Trip), 1.23 (br, 15H, 5 × CHMe_2, Trip), 1.35 (br, 2H, CHMe_2, Trip), 1.38 (br, 3H, CHMe_2, Trip), 1.56 (br, 3H, CHMe_2, Trip), 1.73 (br, 3H, CHMe_2, Trip), 2.15 (br, 2H, CH_2CH_3,) 2.18 (q, ^3J(H,H) = 7.4 Hz, 1H, CH_2CH_3), 2.21 (q, ^3J(H,H) = 7.4 Hz, 1H, CH_2CH_3), 2.63 (br, 1H, C*H*Me$_2$, Trip), 2.79 (sept br, ^3J(H,H) = 6.7 Hz, 2H, 2 × C*H*Me$_2$, Trip), 3.34 (br, 2H, 2 × C*H*Me$_2$, Trip), 3.45 (br, 1H, C*H*Me$_2$, Trip), 4.51 (s, 5H, C_5H_5), 7.06 (br, 1H, Ar-H), 7.19 (br, 2H, Ar-H), 7.23 (t, ^3J(H,H) = 7.5 Hz, 1H, C^4-*H*, C_6H_3), 7.25–7.35 (m br, 3H, Ar-H).

^{1}H NMR (300.1 MHz, toluene-d_8, 233 K, ppm): δ = 0.64 (t, ^3J(H,H) = 7.5 Hz, 3H, CH_A,H_A,,Me_A) 0.89 (t, ^3J(H,H) = 7.8 Hz, 3H, CH_B,H_B,,Me_B), 1.00 (d, ^3J(H,H) = 6.7 Hz, 3H, C$^{2'}$-CHMe_AMe$_B$), 1.131 (d, ^3J(H,H) = 6.7 Hz, 3H, C$^{2''}$-CHMe_AMe$_B$, Trip), 1.139 (d, ^3J(H,H) = 6.6 Hz, 3H, C$^{6''}$-CHMe_AMe$_B$, Trip), 1.21 (d, ^3J(H,H) = 6.5 Hz, 3H, C$^{6'}$-CHMe_AMe$_B$, Trip), 1.23 (d, ^3J(H,H) = 6.9 Hz, 3H, C$^{4'}$-CHMe_AMe$_B$, Trip), 1.24 (d, ^3J(H,H) = 6.7 Hz, 3H, C$^{4'}$-CHMe$_A$$Me_B$, Trip), 1.27 (d, ^3J(H,H) = 6.9 Hz, 6H, C$^{4''}$-CHMe_AMe$_B$ and C$^{4''}$-CHMe$_A$$Me_B$,

Trip), 1.38 (d, ^{3}J(H,H) = 6.7 Hz, 3H, C$^{2''}$-CHMe$_A$*Me$_B$*, Trip), 1.41 (d, ^{3}J(H,H) = 6.7 Hz, 3H, C$^{2'}$-CHMe$_A$*Me$_B$*, Trip), 1.60 (d, ^{3}J(H,H) = 6.5 Hz, 3H, C$^{6'}$-CHMe$_A$*Me$_B$*, Trip), 1.79 (d, ^{3}J(H,H) = 6.6 Hz, 3H, C$^{6''}$-CH*Me$_A$*Me$_B$, Trip), 1.70–1.78 (m, 1H, C*H$_B$*H$_B$'Me$_B$), 2.10–2.30 (m, 3H, CH$_B$*H$_B$'*Me$_B$ and C*H$_A$*H$_A$'Me$_A$ and CH$_A$*H$_A$'*Me$_A$), 2.62 (sept, ^{3}J(H,H) = 6.7 Hz, 1H, C$^{2''}$-C*H*Me$_A$Me$_B$, Trip), 2.74 (sept, ^{3}J(H,H) = 6.9 Hz, 1H, C$^{4'}$-C*H*Me$_A$Me$_B$, Trip), 2.77 (sept, ^{3}J(H,H) = 6.9 Hz, 1H, C$^{4''}$-C*H*Me$_A$Me$_B$, Trip), 3.34 (sept, ^{3}J(H,H) = 6.5 Hz, 1H, C$^{6''}$-C*H*Me$_A$Me$_B$, Trip), 3.35 (sept, ^{3}J(H,H) 6.7 Hz, 1H, C$^{2'}$-C*H*Me$_A$Me$_B$, Trip), 3.42 (sept, ^{3}J(H,H) 6.7 Hz, 1H, C$^{6'}$-C*H*Me$_A$Me$_B$, Trip), 4.46 (s, 5H, C$_5$*H$_5$*), 7.07 (d, ^{4}J(H,H) = 1.5 Hz, 1H, C$^{3''}$-*H*, Trip), 7.196 (d, ^{4}J(H,H) = 1.5 Hz, 1H, C$^{3'}$-*H*, Trip), 7.720 (d, ^{4}J(H,H) = 1.5 Hz, 1H, C$^{5'}$-*H*, Trip), 7.24 (dd, ^{3}J(H,H) = 7.5 Hz, ^{3}J(H,H) = 7.6 Hz, 1H, C^{4}-*H*, C$_6$H$_3$), 7.28 (dd, ^{4}J(H,H) = 1.1 Hz, ^{3}J(H,H) = 7.5 Hz, 1H, C^{3}-*H*, C$_6$H$_3$), 7.31 (d, ^{4}J(H,H) = 1.5 Hz, 1H, C$^{5''}$-*H*, Trip), 7.34 (dd, ^{4}J(H,H) = 1.5 Hz, ^{3}J(H,H) = 7.6 Hz, 1H, C^{5}-*H*, C$_6$H$_3$).

^{13}C{H} NMR (75.47 MHz, toluene-*d$_8$*, 233 K, ppm): δ = 14.4 (s, 1C, CH$_2$*Me$_A$*), 15.0 (s, CH$_2$*Me$_B$*,), 22.1 (s, 1C, C$^{2'}$-CHMe$_A$*Me$_B$*), 23.0 (s, 1C, C$^{6''}$-CHMe$_A$*Me$_B$*), 23.1 (s, 1C, C$^{2''}$-CHMe$_A$*Me$_B$*), 23.8 (s, 2C, C$^{4'}$-CHMe$_A$*Me$_B$* and C$^{6'}$-CHMe$_A$*Me$_B$*, Trip), 24.2 (s, 1C, C$^{4''}$-CHMe$_A$*Me$_B$*, Trip), 24.3 (s, 1C, C$^{4'}$-CH*Me$_A$*Me$_B$, Trip), 24.5 (s, 1C, C$^{4''}$-CH*Me$_A$*Me$_B$, Trip), 25.7 (s, 1C, C$^{2'}$-CH*Me$_A$*Me$_B$, Trip), 27.19 (s, 1C, C$^{6''}$-CH*Me$_A$*Me$_B$, Trip), 27.25 (s, 1C, C$^{2''}$-CH*Me$_A$*Me$_B$, Trip), 27.4 (s, 1C, *C*H$_2$Me$_A$), 27.9 (s, 1C, C$^{6'}$-CH*Me$_A$*Me$_B$, Trip), 30.6 (s, 1C, C$^{2''}$-*C*HMe$_A$Me$_B$, Trip), 30.8 (s, 1C, C$^{6''}$-*C*HMe$_A$Me$_B$, Trip), 30.9 (s, 1C, C$^{2'}$-*C*HMe$_A$Me$_B$,Trip), 31.0 (s, 1C, C$^{6'}$-*C*HMe$_A$Me$_B$, Trip), 32.5 (s, 1C, *C*H$_2$Me$_B$), 34.94 (s, 1C, C$^{4'\text{ or }4''}$-*C*HMe$_A$Me$_B$, Trip), 34.96 (s, 1C, C$^{4''\text{ or }4'}$-*C*HMe$_A$Me$_B$, Trip), 90.2 (s, 5C, *C*$_5$H$_5$), 120.0 (s, 1C, *C$^{3''}$*-H, Trip), 120.7 (s, 1C, *C$^{3'}$*-H, Trip), 120.9 (s, 1C, *C$^{5''}$*-H, Trip), 121.8 (s, 1C, *C$^{5'}$*-H, Trip), 128.2 (s, 1C, *C^{4}*-H, C$_6$H$_3$), 129.8 (s, 1C, *C^{5}*-H, C$_6$H$_3$), 131.0 (s, 1C, *C^{3}*-H, C$_6$H$_3$), 136.5 (s, 1C, *C$^{1'}$*, Trip), 137.0 (s, 1C, *C$^{1''}$*, Trip), 137.8 (s, 1C, *C^{1}*, C$_6$H$_3$), 144.1 (s, 1C, *C^{6}*, C$_6$H$_3$), 145.8 (s, 1C, *C$^{2''}$*, Trip), 146.6 (s, 1C, *C^{2}*, C$_6$H$_3$), 146.9 (s, 1C, *C$^{6''}$*, Trip), 148.3 (s, 1C, *C$^{4''}$*, Trip), 148.5 (s, 1C, *C$^{2'}$*, Trip), 149.4 (s, 1C, *C$^{6'}$*, Trip), 149.7 (s, 1C, *C$^{4'}$*, Trip), 167.4 (s, 1C, Et*C$_A$*≡CEt), 208.3 (s, 1C, EtC≡*C$_B$*Et), 240.7 (s, 1C, *C*O), 244.8 (s, 1C, *C*O).

^{29}Si NMR (59.63 MHz, toluene-*d$_8$*, 298K, ppm): δ = 119.7 (s).

4.2.59 [Cp(CO)$_2$MoSi(C$_6$H$_3$-2,6-Trip$_2$)C(NMe$_2$)C(Ph) (78)

To a stirred solution of **60** (146 mg, 0.20 mmol) in 3 mL of hexane PhC≡CNMe$_2$ (64 mg, 0.40 mmol) was added in a single portion. The solution became dark-red and after 5 min red

precipitate was observed. The suspension was further stirred for 15 min at 0 °C and finally 15 min at −20 °C to complete the crystallization. The product was filtered at −20 °C, washed with hexane (3 × 1 mL) and dried *in vacuo* (0.05 mbar) for 1 h at ambient temperature. Yield: 170 mg (0.195 mmol, 94%). Crystals for X-ray analysis have been obtained in a separate experiment, when the reaction mixture was left for crystallization without stirring. M.p 175−176 °C, decomposes to give a black liquid. Elemental analysis calcd (%) for $C_{53}H_{65}MoNO_2Si$ (872.11): C 72.99, H 7.51, N 1.61; found: C 72.90, H 7.57, N 1.47%. IR (hexane, cm^{-1}): 1938 (vs), 1925 (s), 1867 (s), 1854 (m) [*ν*(CO)]. IR (toluene, cm^{-1}): 1933 (vs), 1918 (s), 1857 (s), 1844 (s) [*ν*(CO)].

^{1}H NMR (300.1 MHz, C_6D_6, 298 K, ppm): δ = 0.70 (d br, ^3J(H,H) = 5.5 Hz, 3H, CH*Me*, Trip), 0.92 (d br, ^3J(H,H) = 6.2 Hz, 3H, CH*Me*, Trip), 1.08 (d br, ^3J(H,H) = 6.5 Hz, 3H, CH*Me*, Trip), 1.15–1.30 (m br, 21H, 7 × CH*Me*, Trip), 1.56 (d br, ^3J(H,H) = 6.3 Hz, CH*Me*, 3H, Trip), 1.76 (d br, ^3J(H,H) = 6.1 Hz, 3H, CH*Me*, Trip), 2.55 (s br, 6H, NMe_2), 2.75 (sept br, ^3J(H,H) = 7.0 Hz, 1H, C*H*Me_2, Trip), 2.94 (sept br, ^3J(H,H) = 6.8 Hz, 1H, C*H*Me_2, Trip), 3.27 (sept br, ^3J(H,H) = 6.9 Hz, 1H, C*H*Me_2, Trip), 3.44 (sept br, ^3J(H,H) = 6.3 Hz, 1H, C*H*Me_2, Trip), 3.86 (sept br, ^3J(H,H) = 6.1 Hz, 1H, C*H*Me_2, Trip), 4.64 (s, 5H, C_5H_5), 6.41 (d br, 2H, ^3J(H,H) = 7.4 Hz, C_6H_5), 6.85 (t br, 1H, ^3J(H,H) = 7.3 Hz, C_6H_5), 7.00 (t, ^3J(H,H) = 7.6 Hz, 2H, C_6H_5), 7.10−7.20 (m br, 2H, Ar-H), 7.22−7.35 (m br, 4H, Ar-H), 7.44 (d br, ^3J(H,H) = 6.0 Hz, 1H, Ar-H).

^{1}H NMR (300.1 MHz, toluene-d_8, 233 K, ppm): δ = 0.67 (d, ^3J(H,H) = 6.5 Hz, 3H, C$^{2'}$-CH$Me_A$$Me_B$), 0.95 (d, ^3J(H,H) = 6.5 Hz, 3H, C$^{2'}$-CH$Me_A$$Me_B$, Trip), 1.13 (d, ^3J(H,H) = 6.5 Hz, 3H, C$^{2''}$-CH$Me_A$$Me_B$, Trip), 1.21* (d, ^3J(H,H) = 6.8 Hz, 3H, C$^{4'}$-CH$Me_A$$Me_B$, Trip), 1.22* (d, ^3J(H,H) = 6.8 Hz, 3H, C$^{4'}$-CH$Me_A$$Me_B$, Trip), 1.23 (d, ^3J(H,H) = 6.7 Hz, 3H, C$^{4''}$-CH$Me_A$$Me_B$, Trip), 1.25* (d, ^3J(H,H) = 6.7 Hz, 3H, C$^{4''}$-CH$Me_A$$Me_B$, Trip), 1.26 (d, ^3J(H,H) = 6.4 Hz, 3H, C$^{6''}$-CH$Me_A$$Me_B$, Trip), 1.29 (d, ^3J(H,H) = 6.5 Hz, 3H, C$^{2''}$-CH$Me_A$$Me_B$, Trip), 1.31 (d, ^3J(H,H) = 6.5 Hz, 3H, C$^{6'}$-CH$Me_A$$Me_B$, Trip), 1.61 (d, ^3J(H,H) = 6.5 Hz, 3H, C$^{6'}$-CH$Me_A$$Me_B$, Trip), 1.81 (d, ^3J(H,H) = 6.4 Hz, 3H, C$^{6''}$-CH$Me_A$$Me_B$, Trip), 2.24 (s, 3H, N$Me_A$$Me_B$), 2.71 (sept, ^3J(H,H) = 6.8 Hz, 1H, C$^{4'}$-C*H*$Me_A$$Me_B$, Trip), 2.787* (s, 3H, N$Me_A$$Me_B$), 2.790* (sept, ^3J(H,H) = 6.7 Hz, 1H, C$^{4''}$-C*H*$Me_A$$Me_B$, Trip), 2.95 (sept, ^3J(H,H) = 6.5 Hz, 1H, C$^{2''}$-C*H*$Me_A$$Me_B$, Trip), 3.28 (sept, ^3J(H,H) = 6.5 Hz, 1H, C$^{2'}$-C*H*$Me_A$$Me_B$, Trip), 3.47 (sept, ^3J(H,H) = 6.5 Hz, 1H, C$^{6'}$-C*H*$Me_A$$Me_B$, Trip), 3.93 (sept, ^3J(H,H) = 6.4 Hz, 1H, C$^{6''}$-C*H*$Me_A$$Me_B$, Trip), 4.60 (s, 5H, C_5H_5), 6.37 (d, ^3J(H,H) = 7.4 Hz, 2H, C^{2,6}-*H*, C_6H_5), 6.88 (t, ^3J(H,H) = 7.4 Hz, 1H, C^{4}-*H*, C_6H_5), 7.03 (t, ^3J(H,H) = 7.6 Hz, 2H, C^{3,5}-*H*, C_6H_5), 7.09

(d, ^{4}J(H,H) = 1.3 Hz, 1H, C$^{3'}$-*H*, Trip), 7.14* (s, 1H, C$^{3''}$-*H*, Trip), 7.285* (dd, ^{3}J(H,H) = 7.5 Hz, ^{3}J(H,H) = 7.6 Hz, 1H, C^{4}-*H*, C_6H_3), 7.290 (d, ^{4}J(H,H) = 1.3 Hz, 1H, C$^{5'}$-*H*, Trip), 7.31* (d, ^{4}J(H,H) = 1.4 Hz, 1H, C$^{5''}$-*H*, Trip), 7.32* (dd, ^{4}J(H,H) = 1.0 Hz, ^{3}J(H,H) = 7.6 Hz, 1H, C^{3}-*H*, C_6H_3), 7.48 (dd, ^{4}J(H,H) = 1.0 Hz, ^{3}J(H,H) = 7.5 Hz, 1H, C^{5}-*H*, C_6H_3).

^{13}C{H} NMR (75.47 MHz, toluene-d_8, 233 K, ppm): δ = 21.1 (s, 1C, C$^{2'}$-CH*Me*$_A$Me$_B$), 22.9 (s, 1C, C$^{6''}$-CHMe$_A$*Me*$_B$), 24.0 (s, 1C, C$^{4'}$-CHMe$_A$*Me*$_B$), 24.1* (s, 3C, C$^{4'}$-CH*Me*$_A$Me$_B$ and C$^{4''}$-CH*Me*$_A$Me$_B$ and C$^{6'}$-CHMe$_A$*Me*$_B$, Trip), 24.4 (s, 1C, C$^{2'}$-CH*Me*$_A$Me$_B$, Trip), 24.8 (s, 1C, C$^{4''}$-CHMe$_A$*Me*$_B$, Trip), 25.6 (s, 1C, C$^{2'}$-CHMe$_A$*Me*$_B$, Trip), 26.2 (s, 1C, C$^{6''}$-CH*Me*$_A$Me$_B$, Trip), 27.6 (s, 1C, C$^{6'}$-CH*Me*$_A$Me$_B$, Trip), 28.1 (s, 1C, C$^{2''}$-CHMe$_A$*Me*$_B$, Trip), 30.4 (s, 1C, C$^{2''}$-*C*HMe$_A$Me$_B$, Trip), 30.7 (s, 1C, C$^{2'}$-*C*HMe$_A$Me$_B$, Trip), 30.9 (s, 1C, C$^{6'}$-*C*HMe$_A$Me$_B$,Trip), 32.0 (s, 1C, C$^{6''}$-*C*HMe$_A$Me$_B$, Trip), 34.77 (s, 1C, C$^{4''}$-*C*HMe$_A$Me$_B$, Trip), 34.84 (s, 1C, C$^{4'}$-*C*HMe$_A$Me$_B$, Trip), 46.1 (s, 1C, N*Me*$_A$Me$_B$), 48.2 (s, 1C, NMe$_A$*Me*$_B$), 91.1 (s, 5C, C_5H_5), 120.4 (s, 1C, *C*$^{5''}$-H, Trip), 120.9 (s, 1C, *C*$^{3'}$-H, Trip), 121.1 (s, 1C, *C*$^{3''}$-H, Trip), 122.0 (s, 1C, *C*$^{5'}$-H, Trip), 123.4 (s, 1C, *C*^{4}-H, C_6H_5), 126.7 (s, 2C, *C*^{2,6}-H, C_6H_5), 127.6 (s, 2C, *C*^{3,5}-H, C_6H_5), 128.6 (s, 1C, *C*^{4}-H, C_6H_3), 130.5 (s, 1C, *C*^{5}-H, C_6H_3), 130.7 (s, 1C, *C*^{3}-H, C_6H_3), 137.2 (s, 1C, *C*$^{1'}$, Trip), 137.9 (s, 1C, *C*$^{1''}$, Trip), 140.1 (s, 1C, *C*^{1}, C_6H_5), 142.4 (s, 1C, *C*^{1}, C_6H_3), 144.9 (s, 1C, *C*^{2}, C_6H_3), 145.6 (s, 1C, *C*^{6}, C_6H_3), 147.0 (s, 1C, *C*$^{6''}$, Trip), 147.3 (s, 1C, *C*$^{2''}$, Trip), 148.3 (s, 1C, *C*$^{2'}$, Trip), 148.4 (s, 1C, *C*$^{6'}$, Trip), 148.5 (s, 1C, *C*$^{4''}$, Trip), 148.7 (s, 1C, *C*$^{4'}$, Trip), 159.9 (s, 1C, *C*−Ph), 180.5 (s, 1C, *C*−NMe$_2$), 243.0 (s, 1C, *C*O), 245.3 (s, 1C, *C*O).

^{29}Si NMR (59.63 MHz, toluene-d_8, 298K, ppm): δ = 206.1 (s).

*Signals marked with an asterisk overlap. The chemical shifts may not be measured directly and are determined from the multiplet's pattern.

4.2.60 [Cp(CO)$_2$MoSi(C$_6$H$_3$-2,6-Trip$_2$)C(NMe$_2$)C(NMe$_2$)] (79)

To a stirred solution of **60** (146 mg, 0.20 mmol) in 5 mL of hexane Me$_2$NC≡CNMe$_2$ was added in a single portion (ca. 40 mg, ca. 0.36 mmol) at −60 °C. The solution was allowed to warm up to ambient temperature and stirred further for 20 min. The color changed to dark brown. Completion of the reaction was confirmed by IR spectroscopy and then all volatiles were removed *in vacuo* (1 h, 30 °C). Hexane (2 mL) was added to the residue, and soon after a very dark brown (almost black) microcrystalline precipitate was observed. The Schlenk tube was stored for 1 h at 0 °C and finally 2 h at −30 °C to complete the crystallization. The

product was filtered at −30 °C, washed with hexane (3 × 1 mL) and dried *in vacuo* (0.05 mbar) for 2 h at ambient temperature. Yield: 110 mg (0.131 mmol, 65%). M.p 161–162 °C (dec). Elemental analysis calcd (%) for $C_{49}H_{66}MoN_2O_2Si$ (839.09): C 70.14, H 7.93, N 3.34; found: C 69.90, H 8.01, N 3.16%. IR (hexane, cm^{-1}): 1930 (vs), 1921 (m), 1851 (s), 1842 (m) [*ν*(CO)].

^{1}H NMR (300.1 MHz, C_6D_6, 298 K, ppm): δ = 1.05 (d, ^3J(H,H) = 6.7 Hz, 6H, 2 × CH*Me*, Trip), 1.20–1.33 (m, 21H, 7 × CH*Me*, Trip), 1.39 (d, ^3J(H,H) = 6.8 Hz, 3H, CH*Me*, Trip), 1.67 (d, ^3J(H,H) = 6.6 Hz, 3H, CH*Me*, Trip), 1.74 (d, ^3J(H,H) = 6.6 Hz, CH*Me*, 3H, Trip), 2.16 (s br, 6H, N_AMe_2), 2.52 (s br, 6H, N_AMe_2), 2.75−2.90 (m, 3H, 3 × C*H*Me_2, Trip), 3.33 (sept, ^3J(H,H) = 6.5 Hz, 1H, C*H*Me_2, Trip), 3.38 (sept br, ^3J(H,H) = 6.8 Hz, 1H, C*H*Me_2, Trip), 3.75 (sept, ^3J(H,H) = 6.5 Hz, 1H, C*H*Me_2, Trip), 4.61 (s, 5H, C_5H_5), 7.12 (s br, 1H, Ar-H, Trip), 7.20 (t, 1H, ^3J(H,H) = 7.6 Hz, C_6H_3), 7.20−7.25 (m, 2H, Ar-H), 7.26−7.33 (m, 2H, Ar-H), 7.38 (s br, 1H, Ar-H, Trip).

^{1}H NMR (400.1 MHz, THF-d_8, 298 K, ppm): δ = 0.75 (d, ^3J(H,H) = 6.7 Hz, 3H, C$^{2'}$-CH*Me*$_A$Me$_B$), 0.98 (d, ^3J(H,H) = 6.8 Hz, 3H, C$^{2''}$-CH*Me*$_A$Me$_B$, Trip), 1.09 (d, ^3J(H,H) = 6.6 Hz, 3H, C$^{6''}$-CH*Me*$_A$Me$_B$, Trip), 1.22 (d, ^3J(H,H) = 6.7 Hz, 3H, C$^{6'}$-CH*Me*$_A$Me$_B$, Trip), 1.245 (d, ^3J(H,H) = 6.9 Hz, 3H, C$^{4'}$-CH*Me*$_A$Me$_B$, Trip), 1.250 (d, ^3J(H,H) = 6.9 Hz, 3H, C$^{4'}$-CHMe$_A$*Me*$_B$, Trip), 1.28 (d, ^3J(H,H) = 6.7 Hz, 3H, C$^{6'}$-CHMe$_A$*Me*$_B$, Trip), 1.30 (d, ^3J(H,H) = 6.4 Hz, 3H, C$^{2'}$-CHMe$_A$*Me*$_B$, Trip), 1.320* (d, ^3J(H,H) = 7.0 Hz, 3H, C$^{4''}$-CH*Me*$_A$Me$_B$, Trip), 1.322* (d, ^3J(H,H) = 7.0 Hz, 3H, C$^{4''}$-CHMe$_A$*Me*$_B$, Trip), 1.39 (d, ^3J(H,H) = 6.6 Hz, 3H, C$^{6''}$-CHMe$_A$*Me*$_B$, Trip), 1.41 (d, ^3J(H,H) = 6.8 Hz, 3H, C$^{2''}$-CHMe$_A$*Me*$_B$, Trip), 2.27 (s br, 6H, N_AMe_2), 2.51 (s br, 6H, N_BMe_2), 2.74 (sept, ^3J(H,H) = 6.7 Hz, 1H, C$^{6'}$-C*H*Me$_A$Me$_B$, Trip), 2.88 (sept, ^3J(H,H) = 6.9 Hz, 1H, C$^{4'}$-C*H*Me$_A$Me$_B$, Trip), 2.98 (sept, ^3J(H,H) = 7.0 Hz, 1H, C$^{4''}$-C*H*Me$_A$Me$_B$, Trip), 3.03 (sept, ^3J(H,H) = 6.6 Hz, 1H, C$^{6''}$-C*H*Me$_A$Me$_B$, Trip), 3.27 (sept, ^3J(H,H) = 6.8 Hz, 1H, C$^{2''}$-C*H*Me$_A$Me$_B$, Trip), 3.42 (sept, ^3J(H,H) = 6.7 Hz, 1H, C$^{2'}$-C*H*Me$_A$Me$_B$, Trip), 4.65 (s, 5H, C_5H_5), 7.01 (d, ^4J(H,H) = 1.8 Hz, 1H, C$^{3'}$-*H*, Trip), 7.04 (d, ^4J(H,H) = 1.8 Hz, 1H, C$^{5'}$-*H*, Trip), 7.21 (d, ^4J(H,H) = 1.8 Hz, 1H, C$^{3''}$-*H*, Trip), 7.27* (d, ^4J(H,H) = 1.8 Hz, 1H, C$^{5''}$-*H*, Trip), 7.28* (dd, ^4J(H,H) = 1.2 Hz, ^3J(H,H) = 7.6 Hz, 1H, C^3-*H*, C_6H_3), 7.30 (dd, ^4J(H,H) = 1.2 Hz, ^3J(H,H) = 7.6 Hz, 1H, C^5-*H*, C_6H_3), 7.42 (t, ^3J(H,H) = 7.6 Hz, 1H, C^4-*H*, C_6H_3).

^{13}C{^{1}H} NMR (75.47 MHz, THF-d_8, 298 K, ppm): δ = 23.0 (s, 1C, C$^{2'}$-CHMe$_A$*Me*$_B$), 23.9 (s, 1C, C$^{6'}$-CHMe$_A$*Me*$_B$), 24.17 (s, 1C, C$^{2''}$-CHMe$_A$*Me*$_B$), 24.27 (s, 3C, C$^{4''}$-CH*Me*$_A$Me$_B$, Trip), 24.34 (s, 1C, C$^{6''}$-CHMe$_A$*Me*$_B$, Trip), 24.49 (s, 1C, C$^{4''}$-CHMe$_A$*Me*$_B$, Trip), 24.52 (s,

1C, $C^{4'}$-CHMe$_A$*Me$_B$*, Trip), 24.7 (s, 1C, $C^{4'}$-CH*Me$_A$*Me$_B$, Trip), 25.5 (s, 1C, $C^{2'}$-CH*Me$_A$*Me$_B$, Trip), 26.3 (s, 1C, $C^{2''}$-CH*Me$_A$*Me$_B$, Trip), 27.6 (s, 1C, $C^{6''}$-CH*Me$_A$*Me$_B$, Trip), 28.0 (s, 1C, $C^{6'}$-CH*Me$_A$*Me$_B$, Trip), 31.24 (s, 1C, $C^{6'}$-*C*HMe$_A$Me$_B$, Trip), 31.35 (s, 1C, $C^{2''}$-*C*HMe$_A$Me$_B$, Trip), 31.44 (s, 1C, $C^{6''}$-*C*HMe$_A$Me$_B$,Trip), 31.8 (s, 1C, $C^{2'}$-*C*HMe$_A$Me$_B$, Trip), 35.3 (s, 1C, $C^{4'}$-*C*HMe$_A$Me$_B$, Trip), 35.5 (s, 1C, $C^{4''}$-*C*HMe$_A$Me$_B$, Trip), 42.3 (s br, 2C, N$_A$Me$_2$), 48.2 (s br, 2C, N$_B$Me$_2$), 92.7 (s, 5C, C_5H_5), 121.4* (s, 2C, $C^{3'}$-H and $C^{3''}$-H, Trip), 121.7 (s, 1C, $C^{5'}$-H, Trip), 122.4 (s, 1C, $C^{5''}$-H, Trip), 128.4 (s, 1C, C^4-H, C_6H_3), 131.8 (s, 1C, C^3-H, C_6H_3), 132.3 (s, 1C, C^5-H, C_6H_3), 138.4 (s, 1C, $C^{1''}$, Trip), 139.2 (s, 1C, $C^{1'}$, Trip), 141.6 (s, 1C, C^1, C_6H_3), 145.8 (s, 1C, C^2, C_6H_3), 147.2 (s, 1C, C^6, C_6H_3), 147.65 (s, 1C, $C^{6'}$, Trip), 147.69 (s, 1C, $C^{2'}$, Trip), 147.78 (s, 1C, $C^{2''}$, Trip), 149.2 (s, 1C, $C^{4'}$, Trip), 149.5 (s, 1C, $C^{4''}$, Trip), 149.8 (s, 1C, $C^{6'}$, Trip), 157.1 (s br, 1C, *C*-NMe$_2$), 172.5 (s br, 1C, *C*-NMe$_2$), 245.5 (s, 1C, *C*O), 246.6 (s, 1C, *C*O).

^{29}Si NMR (59.63 MHz, THF-d_8, 298 K, ppm): δ = 134.2 (s).

*Signals marked with an asterisk overlap. The chemical shifts may not be measured directly and are determined from the signals' pattern.

4.2.61 [Cp(CO)$_2$MoSi(C$_6$H$_3$-2,6-Trip$_2$)C(NEt$_2$)C(NEt$_2$)] (80)

To a stirred solution of **60** (146 mg, 0.20 mmol) in 5 mL of hexane Et$_2$NC≡CNEt$_2$ was added in a single portion (67 mg, 0.40 mmol). The dark red-brown mixture was stirred for 60 min at ambient temperature. The color of the solution changed from red-brown to dark violet-brown. Completion of the reaction was confirmed by IR spectroscopy and then all volatiles were removed *in vacuo*. The crude material was dissolved in ca. 0.5 mL of hexane and the solution was stored at −60 °C for 1 week. The brown precipitate was filtered at −78 °C, washed with hexane (1 mL) and dried *in vacuo* (from −78 °C to RT, 2 h). Yield: 116 mg (0.130 mmol, 65%). Elemental analysis calcd (%) for $C_{53}H_{74}MoN_2O_2Si$ (895.19): C 71.11, H 8.33, N 3.13; found: C 70.89, H 8.49, N 3.19%. IR (hexane, cm^{-1}): 1931 (vs), 1919 (s), 1855 (s), 1841 (m) [ν(CO)].

^{1}H NMR (300.1 MHz, C_6D_6, 298 K, ppm): δ = 0.76 (t, ^3J(H,H) = 7.1 Hz, 12H, NCH$_2$C*H$_3$*), 0.85 (d, ^3J(H,H) = 6.5 Hz, 3H, CH*Me*, Trip), 0.99 (d, ^3J(H,H) = 6.6 Hz, 3H, CH*Me*, Trip), 1.11 (d, ^3J(H,H) = 6.7 Hz, 3H, CH*Me*, Trip), 1.22–1.30 (m, 18H, 6 × CH*Me*, Trip), 1.43 (d, ^3J(H,H) = 6.8 Hz, 3H, CH*Me*, Trip), 1.62 (d, ^3J(H,H) = 6.6 Hz, 3H, CH*Me*, Trip), 1.72 (d, ^3J(H,H) = 6.7 Hz, 3H, CH*Me*, Trip), 2.57–2.70 (m br, 4H, NC*H$_2$*CH$_3$), 2.77* (sept, ^3J(H,H) =

7.1 Hz, 1H, C*H*Me$_2$, Trip), 2.81* (sep, ^3J(H,H) = 6.8 Hz, 1H, C*H*Me$_2$, Trip), 2.84* (sept, ^3J(H,H) = 7.0 Hz, 1H, C*H*Me$_2$, Trip), 3.00–3.18 (m br, 2H, NC*H*$_2$CH$_3$), 3.45–3.71 (m br, 2H, NC*H*$_2$CH$_3$), 3.53 (sept, ^3J(H,H) = 6.6 Hz, 1H, C*H*Me$_2$, Trip), 3.57 (sept, ^3J(H,H) = 6.6 Hz, 1H, C*H*Me$_2$, Trip), 3.79 (sept, ^3J(H,H) = 6.6 Hz, 1H, C*H*Me$_2$, Trip), 4.77 (s, 5H, C$_5$*H*$_5$), 7.16–7.25 (m, 5H, Ar-*H*) 7.32 (dd, ^3J(H,H) = 7.1 Hz, ^4J(H,H) = 1.8 Hz, 1H, C$^{3\text{ or }5}$-*H*, C$_6$H$_3$), 7.38 (d, ^4J(H,H) = 1.8 Hz, 1H, C$^{3\text{ or }5}$-*H*, Trip).

^{29}Si NMR (59.63 MHz, THF-d_8, 298 K, ppm): δ = 155.5 (s).

4.2.62 [Cp(CO)$_2$Mo{η^3-Si(C$_6$H$_3$-2,6-Trip$_2$)C(H)C(C$_6$H$_4$-4-OMe)C(H)C(C$_6$H$_4$-4-OMe)}] (81)

To a stirred solution of **60** (146 mg, 0.20 mmol) in 5 mL of petrol ether 4-MeO-C$_6$H$_4$-C≡CH was added in a single portion (80 mg, 0.61 mmol). After 10 min red-brown precipitate was observed. The mixture was stirred further for 2 h at ambient temperature. The product was isolated by filtration, washed with petrol ether by decantation (3×3 mL) and dried *in vacuo* (0.05 mbar, ambient temperature, 30 min) to give red-brown powder. Yield: 160 mg (0.161 mmol, 81%). The product is a mixture of regioisomers with a ratio ca. 5:1, below only data of major product will be given. Crystals for X-ray analysis have been obtained in a separate experiment, when the reaction mixture was left for crystallization without stirring. Elemental analysis calcd (%) for C$_{53}$H$_{74}$MoN$_2$O$_2$Si (991.23): C 73.91, H 7.12; found: C 73.21, H 7.02%. IR (toluene, cm^{-1}): 1919 (vs), 1850 (s), [ν(CO)].

^{1}H NMR (500.1 MHz, C$_6$D$_6$, 298 K, ppm): δ = 1.05–1.15* (br, 12H, 2 × C^2-CH*Me$_A$*Me$_B$ and 2 × C^6-CH*Me$_A$*Me$_B$, Trip), 1.08 (d, ^3J(H,H) = 6.9 Hz, 6H, 2 × C^2-CHMe$_A$*Me$_B$*, Trip) 1.21 (d, ^3J(H,H) = 6.6 Hz, 6H, 2 × C^6-CHMe$_A$*Me$_B$*, Trip), 1.31 (d, ^3J(H,H) = 6.9 Hz, 6H, 2 × C^4-CH*Me$_A$*Me$_B$, Trip), 1.34 (d, ^3J(H,H) = 6.9 Hz, 6H, 2 × C^4-CHMe$_A$*Me$_B$*, Trip), 2.92 (sept, ^3J(H,H) = 6.9 Hz, 2H, 2 × C^4-C*H*Me$_A$Me$_B$, Trip), 3.05* (sept br, ^3J(H,H) = 6.7 Hz, 2H, 2 × C^2-C*H*Me$_A$Me$_B$), 3.08* (sept br, ^3J(H,H) = 6.6 Hz, 2H, 2 × C^6-C*H*Me$_A$Me$_B$), 3.23 (s, 3H, C^4-O*Me*, 2-(C$_6$H$_4$OMe)), 3.30 (s, 3H, C^4-O*Me*, 4-(C$_6$H$_4$OMe)), 4.71 (s, 5H, C$_5$*H*$_5$), 4.98 (d, ^4J(H,H) = 2.0 Hz, 1H, C^5-*H*, C$_4$H$_2$Si), 6.54 (d, ^3J(H,H) = 8.7 Hz, 2H, C^{3,5}-*H*, 4-(C$_6$H$_4$OMe)), 6.67 (d, ^3J(H,H) = 8.8 Hz, 2H, C^{3,5}-*H*, 2-(C$_6$H$_4$OMe)), 6.93 (d, ^3J(H,H) = 8.7 Hz, 2H, C^{2,6}-*H*, 4-(C$_6$H$_4$OMe)), 6.96 (s br, 1H, C^5-*H*, C$_4$H$_2$Si), 7.13 (br, 2H, 2 × C^3-*H*, Trip), 7.17 (t, ^3J(H,H) = 7.6 Hz, 1H, C^4-*H*, C$_6$H$_3$), 7.31 (br, 2H, 2 × C^5-*H*, Trip), 7.33 (d, ^3J(H,H) = 8.8 Hz, 2H, C^{2,6}-*H*, 2-(C$_6$H$_4$OMe)), 7.37 (d, ^3J(H,H) = 7.6 Hz, 2H, C^{3,5} -*H*, C$_6$H$_3$).

$^{13}C\{^1H\}$ NMR (75.47 MHz, C_6D_6, 298 K, ppm): δ = 23.0* (s br, 4C, 2 × C^2-CH*Me*$_A$Me$_B$ and 2 × C^6-CH*Me*$_A$Me$_B$, Trip), 24.39 (s, 2C, 2 × C^4-CHMe$_A$*Me*$_B$, Trip), 24.45 (s, 2C, 2 × C^4-CH*Me*$_A$Me$_B$, Trip), 25.8 (s, 2C, 2 × C^2-CHMe$_A$*Me*$_B$, Trip), 26.0 (s, 2C, 2 × C^6-CHMe$_A$*Me*$_B$, Trip), 30.9 (s, 2C, 2 × C^2-*C*HMe$_A$Me$_B$, Trip), 31.5 (s, 2C, 2 × C^6-*C*HMe$_A$Me$_B$, Trip), 34.8 (s, 2C, 2 × C^4-*C*HMe$_A$Me$_B$,Trip), 54.7 (s, 2C, 2 × C^4-O*Me*), 56.5 (s br, 1C, C^5-H, C_4H_2Si), 80.6 (s br, 1C, C^2-H, C_4H_2Si), 93.2 (s, 5C, C_5H_5), 113.6 (s, 2C, $C^{3,5}$-H, 4-(C_6H_4OMe)), 114.0 (s, 2C, $C^{3,5}$-H, 2-(C_6H_4OMe)), 120.8 (s, 2C, 2 × C^3-H, Trip), 121.6 (s, 2C, 2 × C^5-H, Trip), 126.0 (s, 2C, $C^{2,6}$-H, 2-(C_6H_4OMe)), 127.6 (s, 2C, $C^{2,6}$-H, 4-(C_6H_4OMe)), 129.4 (s, 1C, C^4-H, C_6H_3), 131.7 (s, 2C, $C^{3,5}$-H, C_6H_3), 132.2 (s br, 1C, C^1, C_6H_3), 134.3 (s br, 1C, C^4-H, C_4H_2Si), 140.0 (s, 2C, 2 × C^1, Trip), 142.4 (s br, 1C, C^1, 4-(C_6H_4OMe)), 146.1 (s, C^3-H, C_4H_2Si), 146.9 (s, 2C, 2 × C^2, Trip), 147.3 (s, 2C, 2 × C^6, Trip), 148.9 (s, 2C, 2 × C^4, Trip), 150.0 (s, 2C, $C^{2,6}$-H, C_6H_3), 158.8 (s, 1C, C^4, 2-(C_6H_4OMe)), 159.1 (s, 1C, C^4, 4-(C_6H_4OMe)), 227.8 (s, 1C, *C*O), 244.3 (s, 1C, *C*O).

$^{29}Si\{^1H\}$ NMR (59.63 MHz, C_6D_6, 298K, ppm): δ = −22.0 (s).

*Signals marked with an asterisk overlap. The chemical shifts may not be measured directly and are determined from the signals' pattern.

4.2.63 [(η^5-C_5Me_5)(CO)$_2$CrSi(ISdipp)C(Et)C(Et)][Al(OC(CF$_3$)$_3$)$_4$] (82-Cr)

To a solution of **61-Cr** (65 mg, 0.040 mmol) in 1 mL of fluorobenzene 2 drops of 3-hexyne (excess) were added with a syringe at ambient temperature. An immediate color change was observed from red-brown to grey. The mixture was stirred for 5 min, and then all volatiles were removed under vacuum. The dark residue was treated with ca 1 mL of hexane, a grey crystalline solid was observed. The solid was filtered off and dried *in vacuo* (45 min, RT). Yield – quantitative. IR (fluorobenzene, cm^{-1}): 1937 (vs), 1866 (s) [ν(CO)]. IR (THF, cm^{-1}): 1934 (vs), 1863 (s) [ν(CO)].

^1H NMR (300.1 MHz, THF-d_8, 298 K, ppm):[135] δ = –0.04 (t br, ^3J(H,H) = 7.3 Hz, 3H, CH$_A$H$_B$*CH$_3$*), 1.09 (t br, ^3J(H,H) = 7.4 Hz, 3H, CH$_A$H$_B$*CH$_3$*), 1.35 (d, ^3J(H,H) = 6.6 Hz, 12H, 4 × CH*Me*, Dipp), 1.43 (s, 15H, C_5*Me$_5$*), 1.55 (d, ^3J(H,H) = 6.3 Hz, 6H, 2 × CH*Me*, Dipp), 1.60 (d, ^3J(H,H) = 6.5 Hz, 6H, 2 × CH*Me*, Dipp), 1.9–2.1 (m, 1H, C*H$_A$*H$_B$CH$_3$), 2.4–

[135] Complex **82-Cr** decomposes slowly at ambient temperature in THF-d_8.

2.6(m, 3H, CH_A·H_B·CH_3 + CH_A·,·CH_B·,·CH_3), 3.2–3.5 (m, 4H, 4 × C*H*Me_2, Dipp), 4.5−4.7 (m, 4H, 2 × NCH_AH_B), 7.4–7.6 (m, 6H, 2 × $C^{3,4,5}$-*H*, Dipp).

4.2.64 [(η^5-C_5Me_5)(CO)$_2$CrSi(ISdipp)C(Me)C(Me)][Al(OC(CF_3)$_3$)$_4$] (83-Cr)

A solution of **61-Cr** (163 mg, 0.100 mmol) in 2 mL of fluorobenzene was frozen in a dry ice/isopropanol bath (–78 °C). Several drops of 2-butyne (excess) were added *via* a syringe. The mixture was allowed to warm up slowly to 0 °C in about 10 min. The color of the solution changed rapidly from deep red-brown to less intense green-brown. All volatiles were removed under vacuum at 0 °C (ice-bath) and the dark green-brown residue was dried for 15 min at ambient temperature. An IR spectrum of the solid in fluorobenzene revealed the selective formation of **83-Cr**. The solid was dissolved in ca. 0.5 mL of fluorobenzene, hexane (ca. 1.5 mL) was carefully added, and the solution was stored at –30 °C for a week to complete crystallization.[136] The obtained dark green-grayish (almost black) crystals of **83-Cr** were filtered by decantation, washed with a fluorobenzene/hexane mixture (1:5, 3 × 1 mL) and dried *in vacuo* (0.05 mbar) at ambient temperature for 1 h. Yield: 105 mg (0.062 mmol, 62%). Complex **83-Cr** becomes sticky above 156 °C and turns into a brown liquid at 174–178 °C (dec.). Elemental analysis calcd (%) for $C_{59}H_{59}AlCrF_{36}N_2O_6Si$ (1683.12): C 42.10, H 3.53, N 1.66; found: C 42.08, H 3.64, N 1.60%. IR (fluorobenzene, cm^{-1}): 1942 (vs), 1875 (s) [ν(CO)].

IR (solid, cm^{-1}): ν = 2971 (w), 2912 (vw), 2876 (vw), 1941 (s), 1913 (vw), 1865 (s), 1830 (vw), 1634 (vw), 1588 (vw), 1500 (w), 1463 (w), 1430 (vw), 1389 (w), 1381 (vw), 1351 (w), 1297 (s), 1275 (vs), 1241 (vs), 1211 (vs), 1168 (vs), 1118 (w), 1073 (vw), 1058 (vw), 1049 (vw), 1031 (vw), 1013 (vw), 971 (vs), 926 (w), 880 (vw), 832 (w), 805 (w), 756 (w), 727 (vs), 660 (vw), 643 (w), 614 (w), 601 (w), 561 (m), 537 (m), 520 (m), 496 (w), 442 (s), 395 (w), 386 (w).

^{1}H NMR (300.1 MHz, C_6D_5Cl, 298 K, ppm):[137] δ = 1.10 (d, ^3J(H,H) = 6.6 Hz, 6H, 2 × C^2-CH$Me_A$$Me_B$, Dipp), 1.11 (d, ^3J(H,H) = 6.6 Hz, 6H, 2 × C^6-CH$Me_A$$Me_B$, Dipp), 1.14 (s, 15H, C_5Me_5), 1.30 (s, 3H, =C−Me_A), 1.33 (d, ^3J(H,H) = 6.6 Hz, 6H, 2 × C^6-CH$Me_A$$Me_B$, Dipp), 1.44 (d, ^3J(H,H) = 6.6 Hz, 6H, 2 × C^2-CH$Me_A$$Me_B$, Dipp), 1.96 (s, 3H, =C−Me_B), 2.99 (sept,

[136] Care has to be taken to get the compound **83-Cr** in crystalline form, which tends to precipitate as an oil.

[137] Complex **83-Cr** decomposes slowly at ambient temperature in C_6D_5Cl.

^3J(H,H) = 6.6 Hz, 2H, 2 × C^6-C*H*Me$_A$Me$_B$, Dipp), 3.18 (sept, ^3J(H,H) = 6.6 Hz, 2H, 2 × C^2-C*H*Me$_A$Me$_B$, Dipp), 4.05−4.28 (m, 4H, 2 × NCH_AH_B), 7.10 (d, 2H, 2 × C^5-*H*, Dipp; the signal overlaps with that of the deuterated solvent), 7.13 (d, 2H, 2 × C^3-*H*, Dipp; the signal overlaps with that of the deuterated solvent), 7.25 (t, ^3J(H,H) = 7.7 Hz, 2H, 2 × C^4-*H*, Dipp). ^{1}H NMR (300.1 MHz, C_6D_5Cl, 273 K, ppm):δ = 1.085 (d, ^3J(H,H) = 6.6 Hz, 6H, 2 × C^2-CH*Me$_A$*Me$_B$, Dipp), 1.095 (d, ^3J(H,H) = 6.6 Hz, 6H, 2 × C^6-CH*Me$_A$*Me$_B$, Dipp), 1.12 (s, 15H, C_5*Me$_5$*), 1.26 (s, 3H, =C−*Me$_A$*), 1.32 (d, ^3J(H,H) = 6.6 Hz, 6H, 2 × C^6-CHMe$_A$*Me$_B$*, Dipp), 1.44 (d, ^3J(H,H) = 6.6 Hz, 6H, 2 × C^2-CHMe$_A$*Me$_B$*, Dipp), 1.96 (s, 3H, =C−*Me$_B$*), 2.98 (sept, ^3J(H,H) = 6.6 Hz, 2H, 2 × C^6-C*H*Me$_A$Me$_B$, Dipp), 3.18 (sept, ^3J(H,H) = 6.6 Hz, 2H, 2 × C^2-C*H*Me$_A$Me$_B$, Dipp), 4.03−4.25 (m, 4H, 2 × NCH_AH_B), 7.08 (d, ^3J(H,H) = 7.7 Hz, 2H, 2 × C^5-*H*, Dipp), 7.12 (d, ^3J(H,H) = 7.7 Hz, ^4J(H,H) = 1.3 Hz, 2H, 2 × C^3-*H*, Dipp; the signal overlaps with that of the deuterated solvent), 7.23 (t, ^3J(H,H) = 7.7 Hz, 2H, 2 × C^4-*H*, Dipp).

^{13}C{^{1}H} NMR (75.47 MHz, C_6D_5Cl, 273 K, ppm): δ = 10.0 (s, 5C, C_5*Me$_5$*), 22.1 (s, 1C, =C−*Me$_B$*), 22.6 (s, 2C, 2 × C^2-CHMe$_A$*Me$_B$*, Dipp), 22.8 (s, 2C, 2 × C^6-CHMe$_A$*Me$_B$*, Dipp), 23.2 (s, 1C, =C−*Me$_A$*), 26.5 (s, 2C, 2 × C^2-CH*Me$_A$*Me$_B$, Dipp), 26.7 (s, 2C, 2 × C^6-CH*Me$_A$*Me$_B$, Dipp), 29.1 (s, 2C, 2 × C^6-*C*HMe$_A$Me$_B$, Dipp), 29.6 (s, 2C, 2 × C^2-*C*HMe$_A$Me$_B$, Dipp), 54.9 (s, 2C, 2 × N*C*H$_A$H$_B$), 102.1 (s, 5C, *C$_5$*Me$_5$), 121.9 (q br, ^1J(F,C) = 292 Hz, 12C, 4 × OC(*C*F$_3$)$_3$), 125.34 (s, 2C, 2 × *C^3*-H or 2 × *C^5*-H, Dipp), 125.36 (s, 2C, 2 × *C^3*-H or 2 × *C^5*-H, Dipp), 130.0 (s, 2C, 2 × *C^1*, Dipp), 131.9 (s, 2C, 2 × *C^4*-H, Dipp), 146.4 (s, 2C, 2 × *C^2*-CHMe$_A$Me$_B$, Dipp), 146.9 (s br, 2C, 2 × *C^6*-CHMe$_A$Me$_B$, Dipp), 153.7 (s, 1C, =*C*−Me), 180.1 (s, 1C, N*C*N), 199.9 (s, 1C, =*C*−Me), 250.1 (s, 1C, *C*O), 252.3 (s, 1C, *C*O); the signal of *C*(CF$_3$)$_3$ group of the anion [Al(OC(CF$_3$)$_3$)$_4$]$^-$ was not observed.

^{29}Si{^{1}H} NMR (59.63 MHz, C_6D_5Cl, 298K, ppm): δ = 71.6 (s).

4.2.65 [(η^5-C$_5$Me$_5$)(CO)$_2$MoSi(ISdipp)C(Me)C(Me)][Al(OC(CF$_3$)$_3$)$_4$] (83-Mo)

To a solution of **61-Mo** (200 mg, 0.120 mmol)[138] in 1 mL of fluorobenzene a –50 °C several drops of 2-butyne (ca 20 mg, excess) were added *via* a syringe. The mixture was allowed to warm up slowly to RT in about 10 min. The color of the solution changed from deep brown to

[138] Complex **61-Mo** was prepared by an analogoues procedure to that of **61-Cr**. M. Speer, *Bachelor thesis*, University of Bonn, **2011**.

red-brown. The mixture was stirred 10 min at RT and then all volatiles were removed *in vacuo*. The dark brown residue was dried at ambient temperature and turned into a brown powder by two freeze-pump cycles. Yield: quantitative. IR (fluorobenzene, cm^{-1}): 1948 (vs), 1876 (s) [ν(CO)].

^{1}H NMR (300.1 MHz, C_6D_5Cl, 298 K, ppm): δ = 1.10 (d, ^{3}J(H,H) = 6.6 Hz, 6H, 2 × C^{2}-CHMe_AMe$_B$, Dipp), 1.11 (d, ^{3}J(H,H) = 6.6 Hz, 6H, 2 × C^{6}-CHMe_AMe$_B$, Dipp), 1.31 (s, 15H, C_5Me_5), 1.33 (d, ^{3}J(H,H) = 6.6 Hz, 6H, 2 × C^{6}-CHMe$_A$$Me_B$, Dipp), 1.42 (d, ^{3}J(H,H) = 6.6 Hz, 6H, 2 × C^{2}-CHMe$_A$$Me_B$, Dipp), 1.47 (s, 3H, =C−Me_A), 1.94 (s, 3H, =C−Me_B), 2.95 (sept, ^{3}J(H,H) = 6.6 Hz, 2H, 2 × C^{6}-CHMe$_A$Me$_B$, Dipp), 3.10 (sept, ^{3}J(H,H) = 6.6 Hz, 2H, 2 × C^{2}-CHMe$_A$Me$_B$, Dipp), 4.02−4.22 (m, 4H, 2 × NCH_AH_B), 7.06–7.13 (m, 4H, 2 × C^{3}-H + 2 × C^{5}-H, Dipp; the signal overlaps with that of the deuterated solvent), 7.24 (t, ^{3}J(H,H) = 7.8 Hz, 2H, 2 × C^{4}-H, Dipp).

^{13}C{^{1}H} NMR (75.47 MHz, C_6D_5Cl, 298 K, ppm): δ = 10.5 (s, 5C, C_5Me_5), 22.3 (s br, 1C, =C−Me_B), 22.8 (s, 2C, 2 × C^{2}-CHMe$_A$$Me_B$, Dipp), 23.1 (s, 2C, 2 × C^{6}-CHMe$_A$$Me_B$, Dipp), 24.8 (s br, 1C, =C−Me_A), 26.2 (s, 2C, 2 × C^{2}-CHMe_AMe$_B$, Dipp), 26.5 (s, 2C, 2 × C^{6}-CHMe_AMe$_B$, Dipp), 29.2 (s, 2C, 2 × C^{6}-CHMe$_A$Me$_B$, Dipp), 29.6 (s, 2C, 2 × C^{2}-CHMe$_A$Me$_B$, Dipp), 54.9 (s, 2C, 2 × NCH$_A$H$_B$), 105.7 (s, 5C, C_5Me$_5$), 121.9 (quartet br, ^{1}J(F,C) = 293 Hz, 12C, OC(CF$_3$)$_4$), 125.45 (s, 2C, 2 × C^{3}-H or 2 × C^{5}-H, Dipp), 125.48 (s, 2C, 2 × C^{3}-H or 2 × C^{5}-H, Dipp), 129.9 (s, 2C, 2 × C^{1}, Dipp), 132.0 (s, 2C, 2 × C^{4}-H, Dipp), 146.5 (s, 2C, 2 × C^{2}-CHMe$_A$Me$_B$, Dipp), 146.8 (s, 2C, 2 × C^{6}-CHMe$_A$Me$_B$, Dipp), 152.9 (s, 1C, =C−Me), 179.7 (s, 1C, NCN), 199.6 (s, 1C, =C−Me), 241.1 (s, 1C, CO), 243.9 (s, 1C, CO); the signal of C(CF$_3$)$_3$ group of the anion [Al(OC(CF$_3$)$_3$)$_4$]$^-$ was not observed.

^{29}Si{^{1}H} NMR (59.63 MHz, C_6D_5Cl, 298K, ppm): δ = 61.2 (s)

4.2.66 [Cp(CO)$_2$Fe–Ge(C$_6$H$_3$-2,6-Trip$_2$)] (84)

A stirred suspension of GeCl(C$_6$H$_3$-2,6-Trip$_2$) (195 mg, 0.331 mmol)[139] in 10 mL of pentane was treated with a solution of K[CpFe(CO)$_2$] in 2.5 mL of THF (0.5 mmol)[140] at ambient temperature. The color of the reaction mixture turned immediately green. The mixture was

[139] Donated by Kai W. Stumpf.

[140] Prepared *in situ* from [CpFe(CO)$_2$]$_2$ with two equivalents of KC$_8$ in THF at ambient temperature. IR (THF, cm^{-1}): 1971 (vs), 1795 (s), 1774 (s) [ν(CO)].

stirred for 5 min and all volatilities were removed *in vacuo*. The residue was treated with 2 mL of pentane, the solvent was evaporated and the residue was dried *in vacuo* (1.5 h, RT). The resulting green powder was extracted with a mixture of 5 mL of toluene and 3 mL of pentane. The suspension filtered from a brown powder. The filtrate was concentrated *in vacuo* to about 1 mL; 5 mL of pentane were added and the solution was left for crystallization at ambient temperature for 1 h, then for 3 h at 5 °C. The green crystals were filtered at 0 °C (ice bath), washed with pentane (3 × 1 mL) and dried *in vacuo* (0.5 h, RT). Yield 165 mg (0.226 mmol, 68%). The crystals were suitable for X-ray diffraction analysis. Mp. 260 °C (dec). IR (hexane, cm^{-1}): 1989 (s), 1942 (vs) [ν(CO)]. IR (toluene, cm^{-1}): 1984 (s), 1936 (vs) [ν(CO)]. IR (Et_2O, cm^{-1}): 1986 (s), 1939 (vs) [ν(CO)]. IR (THF, cm^{-1}): 1983 (s), 1935 (vs) [ν(CO)].

^{1}H NMR (300.1 MHz, C_6D_6, 298 K, ppm): δ = 1.10 (d br, ^3J(H,H)=6.7 Hz, 6H, 2 × C^2-CH*Me$_A$*Me$_B$, Trip), 1.17 (d, ^3J(H,H)=6.9 Hz, 12H, 2 × C^4-CH*Me$_A$Me$_B$*), 1.26 (d br, ^3J(H,H)=6.7 Hz, 6H, 2 × C^6-CH*Me$_A$*Me$_B$, Trip), 1.43 (d, ^3J(H,H)=6.7 Hz, 12H, 2 × C^{2,6}-CHMe$_A$*Me$_B$*, Trip), 2.73 (sept, ^3J(H,H)= 6.9 Hz, 2H, 2 × C^4-C*H*Me$_A$Me$_B$, Trip), 3.50 (sept br, ^3J(H,H)=6.7 Hz, 2H, 2 × C^2-C*H*Me$_A$Me$_B$, Trip), 3.63 (sept, ^3J(H,H)=6.7 Hz, 2H, 2 × C^6-C*H*Me$_A$Me$_B$, Trip), 3.90 (s, 5H, C_5H_5), 7.00 (s br, 2H, 2 × C^3-*H*, Trip), 7.15 (s br, 2H, 2 × C^5-*H*, Trip),[141] 7.33–7.37 (m, 2H, C^{3,5}-*H*, C_6H_3), 7.43–7.47 (m, 1H, C^4-*H*, C_6H_3).

^{13}C{^{1}H} NMR (75.47 MHz, C_6D_6, 298 K, ppm): δ = 23.1 (s, 2C, 2 × C^6-CHMe$_A$*Me$_B$*), 23.5 (s, 2C, 2 × C^2-CHMe$_A$*Me$_B$*), 24.0 (s, 2C, 2 × C^4-CH*Me$_A$*Me$_B$), 24.3 (s, 2C, 2 × C^4-CHMe$_A$*Me$_B$*), 26.8 (s, 2C, 2 × C^2-CH*Me$_A$*Me$_B$), 28.0 (s, 2C, 2 × C^6-CH*Me$_A$*Me$_B$), 30.8 (s, 2C, 2 × C^6-*C*HMe$_A$Me$_B$), 31.4 (s, 2C, 2 × C^2-*C*HMe$_A$Me$_B$), 34.8 (s, 2C, 2 × C^4-*C*HMe$_A$Me$_B$), 85.9 (s, 5C, C_5H_5), 120.9 (s br, 2C, 2 × *C*^{3}-H, Trip), 122.4 (s br, 1C, 2 × *C*^{5}-H, Trip), 127.6 (s, 1C, *C*^{4}-H, C_6H_3), 129.4 (s, 2C, *C*^{3,5}-H, C_6H_3), 133.9 (s, 2C, 2 × *C*^{1}, Trip), 141.4 (s, 2C, *C*^{2,6}, C_6H_3), 146.4 (s br, 2C, *C*^{2}, Trip), 147.9 (s br, 2C, 2 × *C*^{6}, Trip), 149.0 (s, 2C, 2 × *C*^{4}, Trip), 177.3 (s, 1C, *C*^{1}, C_6H_3), 212.4 (s, 2C, 2 × *C*O).

After the measurements 50 mg of pyridine were added to the NMR sample. The mixture was degassed and then irradiated for 30 min at ca. 40 °C with a 125W high-pressure mercury UV lamp from ca. 5 cm distance. Subsequently recorded ^{1}H NMR spectrum showed no apparent reaction.

[141] Overlaps with the signal of the deuterated solvent benzene-*d*$_6$.

4.2.67 [Cp(CO)$_2$Fe–Ge(IMe$_4$)(C$_6$H$_3$-2,6-Trip$_2$)] (85)

To a stirred suspension of **84** (54 mg, 0.074 mmol) in 2 mL of diethyl ether a solution of 1,3,4,5-tetramethyimidazol-2-ylidene (ca. 9 mg, 0.07 mmol) in the same solvent was added dropwise. The color of the reaction mixture changed immediately from green to brown-purple. The reaction was monitored by *in situ* IR spectra. The addition of carbene was stopped after conversion of the starting material was complete. The mixture was stirred for additional 5 min and then the solvent was removed *in vacuo*. The residue was extracted with 1 mL of hexane; the filtrate was filtered. The product started to crystallize soon after the filtration. The mixture was stored for 2 h at 0 °C and then overnight at –30 °C. The precipitate was filtered at –30 °C, washed with hexane (2 × 0.5 mL) and dried *in vacuo*. Yield 35 mg (0.041 mmol, 55%), brown-purple crystalline solid. IR (hexane, cm^{-1}): 1943 (vs), 1890 (vs) [*ν*(CO)]. IR (Et$_2$O, cm^{-1}): 1942 (vs), 1889 (vs) [*ν*(CO)].

^{1}H NMR (300.1 MHz, C$_6$D$_6$, 298 K, ppm):[142] δ = 1.03–1.20 (s br, 6H, 2 × CH*Me*), 1.15 (d, ^3J(H,H)=6.7 Hz, 6H, 2 × CH*Me*), 1.23–1.30 (d br, 6H, 2 × CH*Me*), 1.30 (d, ^3J(H,H)=7.0 Hz, 12H, 4 × CH*Me*), 1.39 (s, 6H, C^{4,5}-*Me*, IMe$_4$), 1.73 (d br, ^3J(H,H)=6.7 Hz, 6H, 2 × CH*Me*), 2.87 (sept, ^3J(H,H)=6.8 Hz, 4H, 2 × C^{2,6}-C*H*Me$_2$), 3.20 (s br, 6H, N^{1,3}-*Me*, IMe$_4$), 3.60 (s, ^3J(H,H)=6.7 Hz, 2H, 2 × C^4-C*H*Me$_2$)4.20 (s, 5H, C$_5$*H*$_5$), 7.03–7.12 (m br, 5H, C^{3,4,5}-*H*, C$_6$H$_3$ + 2 × C$^{3\text{ or }5}$-*H*, Trip), 7.26 (s br, 2H, 2 × C$^{5\text{ or }3}$-*H*, Trip).

4.2.68 [(η^5-C$_5$Me$_5$)(CO)$_2$Ru–Ge(C$_6$H$_3$-2,6-Trip$_2$)] (86)

A mixture of [(η^5-C$_5$Me$_5$)Ru(CO)$_2$]$_2$ (65 mg, 0.11 mmol) and KC$_8$ (40 mg, 0.30 mmol, 2.7 eq) was treated with 2 mL of THF at ambient temperature. The mixture was stirred for 10 h and then filtered; the black residue was additionally washed with some of THF. A quantitative formation of K[(η^5-C$_5$Me$_5$)Ru(CO)$_2$] was assumed (0.22 mmol).[143] GeCl(C$_6$H$_3$-2,6-Trip$_2$) (118 mg, 0.200 mmol)[139] was added to the filtrate at ambient temperature in a single portion. The color of the reaction mixture turned immediately green. The IR spectrum revealed selective formation of a product. The suspension was filtered; the filtrate was evaporated *in vacuo*. The residue was extracted with 2 mL of hexane and filtered, the filtrate was evaporated again and the residue was dried *in vacuo*. The resulting solid was dissolved in 1 mL of

[142] Complex **85** is unstable at ambient temperature. The spectrum displayed also decomposition products in ca. 20% quantity.

[143] IR of K[(η^5-C$_5$Me$_5$)Ru(CO)$_2$] in THF, cm^{-1}: 1876 (vs), 1866 (vs), 1792 (s), 1770 (s) [*ν*(CO)].

pentane, the solution was concentrated to about 0.5 mL and stored at –60 °C for 3 days. The dark green crystals obtained were filtered at –78 °C, washed with petrol ether (2 × 0.5 mL) and dried *in vacuo* (30 min, RT). Yield: ca. 50 mg (0.06 mmol, 30%), dark green crystals. Crystallization from pentane at –60 °C afforded green crystals of **86**·pentane solvate that were suitable for X-ray diffraction analysis. IR (hexane, cm^{-1}): 1996 (s), 1944 (vs) [*v*(CO)]. IR (THF, cm^{-1}): 1991 (s), 1937 (vs) [*v*(CO)].

^{1}H NMR (300.1 MHz, C_6D_6, 298 K, ppm): δ = 1.15–1.25 (d br, 12H, 2 × $C^{2,6}$-CH*Me*), 1.22 (d, ^3J(H,H)=6.9 Hz, 12H, 2 × C^4-CHMe_2, Trip), 1.43 (s, 15H, C_5Me_5), 1.46 (d, ^3J(H,H)=6.8 Hz, 12H, 4 × $C^{2,6}$-CH*Me*), 2.77 (sept, ^3J(H,H)= 6.9 Hz, 2H, 2 × C^4-C*H*Me_AMe_B, Trip), 3.60 (sept br, ^3J(H,H)=6.7 Hz, 4H, 2 × $C^{2,6}$-C*H*Me_AMe_B, Trip), 7.05 (s br, 4H, 2 × $C^{3,5}$-*H*, Trip), 7.23–7.25 (m, 2H, $C^{3,5}$-*H*, C_6H_3), 7.34–7.40 (m, 1H, C^4-*H*, C_6H_3).

^{13}C{^{1}H} NMR (75.47 MHz, C_6D_6, 298 K, ppm): δ = 9.7 (s, 5C, C_5Me_5), 24.2 (s br, 8C, 2 × C^4-CHMe_2 + 2 × $C^{2,6}$-CH*Me*), 26.5 (s br, 2C, 2 × $C^{2\text{ or }6}$-CH*Me*), 27.3 (s br, 2C, 2 × $C^{2\text{ or }6}$-CH*Me*), 31.1 (s, 4C, 2 × $C^{2,6}$-*C*HMe_AMe_B), 34.8 (s, 2C, 2 × C^4-*C*HMe_2), 101.3 (s, 5C, C_5Me_5), 121.0 (s br, 2C, 2 × $C^{3\text{ or }5}$-H, Trip), 122.5 (s br, 1C, 2 × $C^{5\text{ or }3}$-H, Trip), 127.0 (s, 1C, C^4-H, C_6H_3), 129.9 (s, 2C, $C^{3,5}$-H, C_6H_3), 135.3 (s, 2C, 2 × C^1, Trip), 140.8 (s, 2C, $C^{2,6}$, C_6H_3), 146.8 (s br, 2C, $C^{2\text{ or }6}$, Trip), 147.7 (s br, 2C, 2 × $C^{6\text{ or }2}$, Trip), 148.4 (s, 2C, 2 × C^4, Trip), 176.9 (s, 1C, C^1, C_6H_3), 202.4 (s, 2C, 2 × *C*O).

4.2.69 [(η^5-C_5(CH=(2-IMe_4)Me_4)(CO)$_2$Ru–GeH$_2$(C_6H_3-2,6-Trip$_2$)] (88)

To a solution of **86** (30 mg, 0.035 mmol) in 0.5 mL of C_6D_6 1,3,4,5-tetramethyimidazol-2-ylidene (6 mg, 0.05 mmol) was added in a single portion. The color of the solution turned immediately red. An NMR spectrum recorded 3 h and 6 h after the addition showed the selective formation of an intermediate product, which was decomposing slowly.[144] After one week of standing at ambient temperature the solution became yellow. NMR spectra were

[144] ^{1}H NMR spectrum of the intermediate product (300.1 MHz, C_6D_6, 298 K, ppm): δ = 1.2 (d br, ^3J(H,H)=6.3 Hz, 12H, 4 × $C^{2,6}$-CH*Me*, Trip), 1.33(d, ^3J(H,H)=6.9 Hz, 12H, 4 × C^4-CH*Me*, Trip), 1.38 (d br, 12H, 4 × $C^{2,6}$-CH*Me*, Trip), 1.52 (s, 6H, 2 × C*Me*, IMe_4), 1.55 (s, 15H, C_5Me_5), 2.89 (sept, ^3J(H,H)=6.9 Hz, 2H, C^4-C*H*Me_2, Trip), 3.28 (s, 6H, 2 × N*Me*, IMe_4), 3.38 (s br, 4H, $C^{2,6}$-C*H*Me_2, Trip), 7.07–7.17 (m, 4–5H, Ar-*H*, the signal overlaps with that of the deuterated benzene); on the basis of the integral intensity, 2 or 3 protons are missing in the aromatic region, probably due to broadness.

recorded and they revealed selective transformation leading to complex **88**. Diffusion of hexane in the C_6D_6 solution at ambient temperature afforded large yellow crystals of **88**.

IR (toluene, cm^{-1}): 1998 (s), 1990 (s), 1939 (vs) [ν(CO)].

^{1}H NMR (400.1 MHz, C_6D_6, 298 K, ppm): δ = 1.22 (d, ^3J(H,H)=6.8 Hz, 12H, 2 × $C^{2,6}$-CHMe_AMe$_B$, Trip), 1.35 (d, ^3J(H,H)=6.9 Hz, 12H, 2 × C^4-CHMe_2, Trip), 1.36 (s br, 6H, $C^{4,5}$-*Me*, IMe_4), 1.61 (s, 6H, $C^{2,5}$-*Me*, C_5Me_4), 1.63 (d, ^3J(H,H)=6.8 Hz, 12H, 2 × $C^{2,6}$-CHMe$_A$$Me_B$, Trip), 1.64 (s, 6H, $C^{3,4}$-*Me*, C_5Me_4), 2.21 (s br, 3H, N-*Me*, IMe_4), 2.53 (s br, 3H, N-*Me*, IMe_4), 2.94 (sept, ^3J(H,H)= 6.9 Hz, 2H, 2 × C^4-C*H*Me$_2$, Trip), 3.29 (sept, ^3J(H,H)=6.8 Hz, 4H, 2 × $C^{2,6}$-C*H*Me$_A$Me$_B$, Trip), 3.33 (s, 1H, –C*H*=IMe_4), 3.75 (s, 2H, GeH_2), 7.23–7.26 (m, 3H, $C^{3,4,5}$-*H*, C_6H_3), 7.28 (s, 4H, 2 × $C^{3,5}$-*H*, Trip).

^{13}C{^{1}H} NMR (100.6 MHz, C_6D_6, 298 K, ppm): δ = 8.6 (s br, 2C, $C^{4,5}$-*Me*, IMe_4), 10.0 (s, 2C, $C^{3,4}$-Me, C_5Me_4), 11.1 (s, $C^{2,5}$-Me, C_5Me_4), 23.7 (s, 4C, 2 × $C^{2,6}$-CHMe$_A$$Me_B$, Trip), 24.5 (s, 4C, 2 × C^4-CHMe_2, Trip), 26.5 (s, 4C, 2 × $C^{2,6}$-CHMe_AMe$_B$, Trip), 29.3 (s br, 1C, N-*Me*, IMe_4),[145] 31.1 (s, 4C, 2 × $C^{2,6}$-*C*HMe$_A$Me$_B$, Trip), 31.9 (s br, 1C, N-*Me*, IMe_4),[145] 35.0 (s, 2C, 2 × C^4-*C*HMe$_2$, Trip), 50.1 (s, 1C, –*C*H=IMe_4), 93.0 (s, 2C, $C^{2,5}$, C_5Me_4), 97.1 (s, 2C, $C^{3,4}$, C_5Me_4), 114.9 (s, 1C, C^1, C_5Me_4), 116.0 (s br, 2C, $C^{4,5}$, IMe_4),[145] 120.9 (s, 4C, 2 × $C^{3,5}$-H, Trip), 126.1 (s, 1C, C^4-H, C_6H_3), 129.9 (s, 2C, $C^{3,5}$-H, C_6H_3), 140.4 (s, 2C, 2 × C^1, Trip), 145.3 (s, 1C, Ge-C^1, C_6H_3), 146.8 (s, 4C, 2 × $C^{2,6}$, Trip), 147.6 (s, 2C, 2 × C^4, Trip), 147 (s, 2C, $C^{2,6}$, C_6H_3), 151.7 (s, 1C, CN_2, IMe_4), 205.2 (s, 2C, 2 × *C*O).

4.2.70 $FeCl_2(IMes)_2$ (89-Cl)

A mixture of iron dichloride (101 mg, 0.797 mmol) and 1,3-bis(2,4,6-trimethylphenyl)-imidazol-2-ylidene (510 mg, 1.68 mmol, 2.11 eq) was treated with 20 mL of toluene. The mixture was stirred overnight at ambient temperature (ca. 14 h) to produce an almost clear, slightly brown solution. The solution was filtered through a cannula. The filtrate was concentrated *in vacuo* to about 5 mL and stored at 5 °C for crystallization. After 16 h colorless crystals were filtered off, washed with hexane (2 × 2 mL) and dried in *vacuo* (1 h, RT). Yield 440 mg (0.598 mmol, 75%), colorless crystals. Elemental analysis calcd (%) for $C_{42}H_{48}Cl_2FeN_4$ (735.61): C 68.58, H 6.58, N 7.62; found: C 68.63, H 6.55, N 7.48%. IR (Nujol, KBr-windows, cm^{-1}): ν = 3135 (w), 1606 (w), 1294 (w), 1259 (m), 1214 (w), 1093

[145] A very broad signal.

(w), 1036 (w), 927 (m), 854 (m), 749 (m), 740 (m), 731 (m), 691 (w). Mossbauer spectrum: I.S. 0.81 cm^{-1}; Q.S. 1.97 cm^{-1}. ^{1}H NMR (300.1 MHz, C_6D_6, 298 K, ppm): δ = 2.22 (s br, 12H, $\Delta\nu_{1/2}$ = 8 Hz, 4 × C^4-C*H*$_3$, Mes), 3.70 (s br, 24H, $\Delta\nu_{1/2}$ = 88 Hz, 4 × $C^{2,6}$-C*H*$_3$, Mes), 5.67 (s br, 8H, $\Delta\nu_{1/2}$ = 17 Hz, 4 × $C^{3,5}$-*H*, Mes), 27.49 (s br, 4H, $\Delta\nu_{1/2}$ = 27 Hz, 4 × NC*H*). [146]

4.2.71 $FeBr_2(IMes)_2$ (89-Br)

A mixture of iron dibromide (108 mg, 0.797 mmol) and 1,3-bis(2,4,6-trimethylphenyl)-imidazol-2-ylidene (510 mg, 1.68 mmol, 2.11 eq) was treated with 20 mL of toluene. The mixture was stirred for 1 h at ambient temperature to produce an almost clear yellow solution; after 1.5 h a white precipitate was observed. The mixture was concentrated *in vacuo* to about 5 mL and stored at −30°C for crystallization for 16 h. The crystallized product was filtered off, washed twice with a hexane/toluene mixture (2:1, 2 × 2 mL) and dried *in vacuo* (1.5 h, 50 °C). Yield: 350 mg (0.424 mmol, 85%), white microcrystalline solid. ^{1}H NMR (300.1 MHz, C_6D_6, 298 K, ppm): δ = 1.43 (s br, 12H, $\Delta\nu_{1/2}$ = 5 Hz, 4 × C^4-C*H*$_3$, Mes), 3.64 (s br, 24H, $\Delta\nu_{1/2}$ = 67 Hz, 4 × $C^{2,6}$-C*H*$_3$, Mes), 4.68 (s br, 8H, $\Delta\nu_{1/2}$ = 13 Hz, 4 × $C^{3,5}$-*H*, Mes), 26.63 (s br, 4H, $\Delta\nu_{1/2}$ = 22 Hz, 4 × NC*H*).[146]

4.2.72 $FeCl_2$(IDipp) (90)

A mixture of iron dichloride (75 mg, 0.592 mmol) and 1,3-bis(2,6-diisopropylphenyl)-imidazol-2-ylidene (500 mg, 1.29 mmol, 2.18 eq) in 20 mL of toluene was heated at 60 °C for 14 h. The mixture was filtered from a small amount of an insoluble residue and the filtrate was concentrated *in vacuo* to about 10 mL. 10 mL of hexane were added on the top of the solution carefully in order to set a two-layer system for slow diffusion. The crystallization was completed after 1 d of standing at ambient temperature. A mixture of large brown crystals and brownish powder was obtained. The precipitate was filtered off, washed with hexane and dried *in vacuo* (1 h, RT): The large brown crystals were separated from the mixture with a spatula. Yield: 150 mg (0.291 mmol, 46%). Elemental analysis calcd (%) for $C_{27}H_{36}Cl_2FeN_2$ (515.34): C 62.93, H 7.04, N 5.44; found: C 63.35, H 7.11, N 5.41%. ^{1}H NMR (300.1 MHz, C_6D_6, 298 K, ppm): δ = −3.40 (s br, 2H, $\Delta\nu_{1/2}$ = 18 Hz, 2 × NC*H* or 2 × C^4-*H*, Dipp), −2.80 (s br, 12H, $\Delta\nu_{1/2}$ = 13 Hz, 4 × CH*Me*$_A$Me$_B$, Dipp), −1.95 (s br, 4H, $\Delta\nu_{1/2}$ = 22 Hz, 2 × $C^{3,5}$-*H*,

[146] The compound is paramagnetic. Signal assignment was performed using the integral ratio of the signals.

Dipp), 0.39 (s br, 4H, $\Delta\nu_{1/2}$ = 200 Hz, 4 × C*H*Me$_A$Me$_B$, Dipp), 1.89 (s br, 2H, $\Delta\nu_{1/2}$ = 19 Hz, 2 × C^4-*H*, Dipp or 2 × NC*H*), 8.29 (s br, 12H, $\Delta\nu_{1/2}$ = 71 Hz, 4 × CHMe$_A$*Me$_B$*, Dipp).[147]

4.2.73 Fe $(CH_3)_2(IMes)_2$ (91)

To a solution of 0.89 mL 1.6 M MeLi in Et_2O (1.42 mmol, 2.0 eq) in 20 mL Et_2O at −78 °C a solution of **89-Cl** (524 mg, 0.712 mmol) in 20 mL of toluene was added dropwise in 10 min to produce a yellow solution. After the addition was complete the mixture was kept at –30 °C for 10 min., the color turned to brown-red. Then the temperature was increased to –20 °C and the mixture was kept at this temperature for 10 min, the color changed to orange-red. The cooling bath was replaced then by a water bath and the mixture was brought to ambient temperature. The solvents were removed *in vacuo* to give an orange solid residue. The residue was extracted with 35 mL of toluene and the extract was filtered. The filtrate was concentrated *in vacuo* to about 10 mL; an orange precipitate was observed. The mixture was stored at –60 °C for 30 min for crystallization. The orange crystals were filtered off at –60 °C, washed with hexane (3 × 5 mL, last time the mixture was stirred for 30 min) and dried in *vacuo* (12 h, RT). Yield: 380 mg (0.547 mmol, 77%). The material is sufficiently pure according to ^{1}H NMR spectroscopy, however it was recrystallized from toluene at −60°C for elemental analysis with significant lost of material. Elemental analysis calcd (%) for $C_{44}H_{54}FeN_4$ (694.77): C 76.06, H 7.83, N 8.07; found: C 75.83, H 7.68, N 7.98%.Mossbauer spectroscopy: I.S. 0.273 cm^{-1}; Q.S 4.750 cm^{-1}. ^{1}H NMR (300.1 MHz, C_6D_6, 298 K, ppm): δ = –31.8 (s br, 1H, $\Delta\nu_{1/2}$ = 230 Hz), –3.5(s br, 3H, $\Delta\nu_{1/2}$ = 250 Hz), –2.1 (s br, 12H, $\Delta\nu_{1/2}$ = 360 Hz), 1.9 (s br, 6H, $\Delta\nu_{1/2}$ = 980 Hz), 6.2 (s br, 2H, $\Delta\nu_{1/2}$ = 930 Hz).[148]

4.2.74 $FeCl(IMes)_2$ (92)

A solution of **89-Cl** was prepared *in situ* from 1,3-bis(2,4,6-trimethylphenyl)imidazol-2-ylidene (1.69 g, 5.55 mmol, 2.09 eq) and iron dichloride (0.336 g, 2.65 mmol) in 50 mL of toluene as described above. To this solution sodium amalgam (3.50 mL 0.515% wt., 10.6 mmol of sodium, 4 eq) was added at ambient temperature and the mixture was stirred

[147] The compound is paramagnetic. Signal assignment was performed using the integral ratio of the signals.

[148] The compound is paramagnetic. Due to large broadness of the signals, the chemical shifts, integral intensities and $\Delta\nu_{1/2}$ should be taken as approximate.

for 24 h. During the stirring the amalgam became a fine grey "powder". The ^{1}H NMR spectrum of an aliquot of the reaction mixture revealed total conversion of the starting material to a new product. 30 mL of hexane were added to the reaction and the suspension was allowed to settle down. The supernatant was carefully filtered with help of a filter cannula which was kept above the mercury level. The very dark purple-brown filtrate was concentrated *in vacuo* to about 20 mL. 30 mL of hexane were added slowly under stirring to precipitate the product. The mixture was stored at –30 °C for 16 h to complete the crystallization. The crystals were filtered off, washed with 10 mL of hexane at −30°C, then with 10 mL of hexane at ambient temperature and dried *in vacuo* (3 h, 40 °C). Yield: 1.22 g (1.74 mmol, 66% based on $FeCl_2$), purple-black crystalline solid, which becomes brown if milled. Elemental analysis calcd (%) for $C_{42}H_{48}ClFeN_4$ (700.16): C 72.05, H 6.91, N 8.00; found: C 72.65, H 6.89, N 7.80%. IR (Nujol, KBr-windows): ν = 3123 (w), 1608 (w), 1488 (m), 1386 (m), 1349 (w), 1256 (s), 1210 (w), 1168 (w), 1050 (s), 962 (m), 924 (m), 850 (m), 709 (m), 573 (m), 416 (w). Mossbauer spectroscopy: I.S. 0.65 cm^{-1}; Q.S. 2.63 cm^{-1}. ^{1}H NMR (300.1 MHz, C_6D_6, 298 K, ppm): δ = −12.42 (s br, 8H, 4 × $C^{3,5}$-*H*, Mes), −12.30 (s br, 12H, 4 × C^4-*Me*, Mes), 7.66 (s br, 24H, $\Delta\nu_{1/2}$ = 170 Hz, 4 × $C^{2,6}$-*Me*, Mes), 51.09 (s br, 4H, $\Delta\nu_{1/2}$ = 39 Hz, 2 × NC*H*).[149]

4.2.75 FeCl(C_6H_3-2,6-Mes_2-NC)$_2$(IMes) (93)

To a mixture of **92** (200 mg, 0.286 mmol) and 2,6-bis(2,4,6-trimethylphenyl)-phenylisocyanide (192 mg, 0.572 mmol) 10 mL of toluene were added. The color immediately changed from brown to purple. The reaction mixture was stirred for 40 min, and the solvent was removed *in vacuo*. The dark violet residue was extracted with 80 mL of warm (40 °C) hexane in portions.[150] Extracts were combined, concentrated *in vacuo* to ca. 5 mL and kept at 0 °C for 40 min for crystallization. The precipitate was filtered off and dried *in vacuo* to give 280 mg of the product. The solid was additionally stirred with 4 mL of hexane at 40 °C, filtered after cooling to 0 °C and dried *in vacuo* to give a brown-purple powder. Yield: 240 mg (0.223 mmol, 78%). Elemental analysis calcd (%) for $C_{71}H_{74}ClFeN_4$ (1074.67): C 79.35, H 6.94, N 5.21; found: C 79.51, H 7.04, N 5.21%. ^{1}H NMR (300.1 MHz, C_6D_6, 298 K, ppm): δ = 1.66 (s br, 12H, $\Delta\nu_{1/2}$ = 25 Hz), 2.0–2.5 (several s br, 38H), 3.27 (s br, 6H, $\Delta\nu_{1/2}$ =

[149] The compound is paramagnetic. Signal assignment was performed using the integral ratio of the signals. Signals at –12.42 and –12.30 ppm overlap, $\Delta\nu_{1/2}$ of the resulting signal is 52 Hz.

[150] Smaller amount of hexane could be used.

15 Hz), 5.97 (s br, 6H, $\Delta\nu_{1/2}$ = 42 Hz), 6.54 (s br, 4H, $\Delta\nu_{1/2}$ = 42 Hz), 6.82 (s br, 4H, $\Delta\nu_{1/2}$ = 23 Hz), 26.16 (s br, 2H, $\Delta\nu_{1/2}$ = 29 Hz), 36.07 (s br, 2H, $\Delta\nu_{1/2}$ = 74 Hz).[151]

4.2.76 [CpMo(CO)$_2$(PMe$_3$)–SiHCl(C$_6$H$_3$-2,6-Mes$_2$)] (94)

20 mL of toluene were added to a mixture of Si(C$_6$H$_3$-2,6-Mes$_2$)HCl$_2$ (130 mg, 0.315mmol) and Li[CpMo(CO)$_2$(PMe$_3$)] (160 mg, 0.539 mmol, 1.7 eq). The mixture was heated in an oil bath at 110 °C for 1 h, until most of the solid dissolved and solution became light brown. The mixture was filtered, the filtrate was evaporated *in vacuo* and the solid residue was extracted with 5 mL of hexane at 60 °C. The filtrate was stored at −60 °C for crystallization. A white precipitate was formed, which was filtered at –60 °C, washed with hexane (2 × 0.5 mL) and dried *in vacuo* (1 h, RT). Yield: 105 mg (0.156 mmol, 50%), colorless microcrystalline powder. IR (hexane, cm^{-1}): 1931 (s), 1858 (vs) [ν(CO)]. IR (toluene, cm^{-1}): 1925 (s), 1848 (vs) [ν(CO)].[152]

^{1}H NMR (300.1 MHz, C$_6$D$_6$, 298 K, ppm): δ = 0.88 (d, 9H, ^3J(P,H) = 9.4 Hz, P(CH$_3$)$_3$), 2.19 (s, 6H, 2 × C^4-*Me*, Mes), 2.39 (s, 6H, 2 × C^2-*Me*, Mes), 2.44 (s, 6H, 2 × C^6-*Me*, Mes), 4.36 (d, ^3J(P,H) = 1.1 Hz, 5H, C$_5$*H*$_5$), 6.29 (d, ^1J(Si,H) = 223.6 Hz, ^{3}J(P,H) = 1.7 Hz, 1H, Si*H*Cl), 6.89 (s, 2H, 2 × C^5-*H*, Mes), 6.95 (s, 2H, 2 × C^3-*H*, Mes), 6.99 (d, ^3J(H,H) = 7.6 Hz, C^{3,5}-*H*, 2H, C$_6$H$_3$), 7.25 (t, ^3J(H,H) = 7.6 Hz, 1H, C^4-*H*, C$_6$H$_3$).

^{13}C{^{1}H} NMR (75.5 MHz, C$_6$D$_6$, 298 K, ppm): δ = 20.1 (d, ^1J(P,C) = 126.0 Hz, 3C, P(*C*H$_3$)$_3$), 21.2 (s, 2C, 2 × C^4-*Me*, Mes), 22.1 (s, 2C, 2 × C^6-*Me*, Mes), 22.2 (s br, 2C, 2 × C^2-*Me*, Mes), 91.6 (s, 5C, *C*$_5$H$_5$), 128.5 (s br, 2C, 2 × *C*^{3}-H, Mes), 128.6 (s, 2C, 2 × *C*^{5}-H, Mes), 129.7 (s br, 2C, *C*^{3,5}-H, C$_6$H$_3$), 129.8 (s, 1C, *C*^{4}-H, C$_6$H$_3$) 136.1 (s, 2C, 2 × *C*^{6}, Mes), 136.6 (s, 2C, 2 × *C*^{4}, Mes), 139.8 (d, ^3J(P,C) = 1.3 Hz, 1C, *C*^{1}, C$_6$H$_3$), 141.8 (s br., 2C, 2 × *C*^{1}, Mes), 149.3 (s, 2C, *C*^{2,6}, C$_6$H$_3$), 230.8 (d, ^2J(P,C) = 26.8 Hz, 1C, *C*O), 234.4 (d, ^2J(P,C) = 25.2 Hz, 1C, *C*O). The *C*^{2}(Mes) signal is not observed.

^{29}Si{^{1}H} NMR (59.6 MHz, C$_6$D$_6$, 298 K, ppm): δ = 42.9 (d, ^2J(P,Si) = 20.7 Hz).

^{31}P{^{1}H} NMR (121.5 MHz, C$_6$D$_6$, 298 K, ppm): δ = 25.0 (s, 1P, P(CH$_3$)$_3$).

---

[151] The compound is paramagnetic and thermolabile.

[152] The intensity of the band at 1848 cm^{-1}exceded the limit of the measurement, therefore the value should be taken as approximate (±3 cm^{-1}).

4.2.77 [CpMo(CO)$_2$(PMe$_3$)–SiHCl(C$_6$H$_3$-2,6-Trip$_2$)] (95)

25 mL of toluene were added to a mixture of Si(C$_6$H$_3$-2,6-Trip$_2$)HCl$_2$ (500 mg, 0.859 mmol) and Li[(η^5-C$_5$Me$_5$)Mo(CO)$_2$(PMe$_3$)] (300 mg, 1.01 mmol, 1.18 eq). The mixture was heated at 110 °C for 24 h. During heating most of the solid dissolved and the mixture became light brown. The suspension was filtered; the filtrate was evaporated *in vacuo*. The residue was extracted with 10 mL of pentane, the extract was filtered and the filtrate was stored at –30 °C for crystallization. A white solid precipitated which was filtered, washed with hexane at -30°C (2 × 1 mL) and dried *in vacuo*. Yield: 130 mg. The combined filtrate and washings were stored for several weeks at –60 °C to give a second crop of the product, which was isolated at –60 °C by filtration, washed with hexane at –60 °C (2 × 0.5 mL) and dried *in vacuo*. Yield: 0.350 g. Combined yield: 480 mg (0.572 mmol, 67%), white microcrystalline powder. Crystals suitable for the X-ray diffraction analysis were grown cooling of a hexane solution of **95** to –60 °C. Elemental analysis calcd (%) for C$_{46}$H$_{64}$ClMoO$_2$PSi (839.45): C 65.82, H 7.68; found: C 65.80, H 7.62 %. IR (pentane, cm^{-1}): 1928 (s), 1852 (vs) [ν(CO)] IR (toluene, cm^{-1}): 1922 (s), 1845 (vs) [ν(CO)].

^{1}H NMR (400.1 MHz, C$_6$D$_6$, 298 K, ppm): δ = 0.88 (d, ^2J(P,H) = 9.3 Hz 9H, P(C*H$_3$*)$_3$), 1.0–1.3 (br, 6H, 2 × CH*Me*), 1.22 (d br, ^3J(H,H) = 6.6 Hz, 6H, 2 × CH*Me*), 1.28 (d, ^3J(H,H) = 6.8 Hz, 6H, 2 × C^4-CH*Me$_A$*Me$_B$), 1.29 (d, ^3J(H,H) = 6.9 Hz, 6H, 2 × C^4-CHMe$_A$*Me$_B$*), 1.58 (br, 12H, 4 × CH*Me*), 2.89 (d, ^3J(H,H) = 6.9 Hz, 2H, 2 × C^4-C*H*Me$_2$), 3.47 (br, 4H, 2 × C^{2,6}-C*H*Me$_2$), 4.34 (d, ^3J(P,H) = 1.1 Hz, 5H, C$_5$*H$_5$*), 6.49 (d, ^1J(Si,H) = 226 Hz, ^3J(P,H) = 1.9 Hz, 1H, Si*H*Cl), 7.15 (t, ^3J(C,H) = 7.4 Hz, 1H, C^4-*H*, C$_6$H$_3$),[153] 7.20–7.23 (m, 2H, C^{3,5}-*H*, C$_6$H$_3$), 7.31 (s, 4H, C^{3,5}-*H*, Trip).

4.2.78 [Cp*Mo(CO)$_2$(PMe$_3$)–SiHCl(C$_6$H$_3$-2,6-Mes$_2$)] (96)

20 mL of toluene were added to a mixture of Si(C$_6$H$_3$-2,6-Mes$_2$)HCl$_2$ (0.286 g, 0.692 mmol) and Li[(η^5-C$_5$Me$_5$)Mo(CO)$_2$(PMe$_3$)] (0.244 g, 0.762 mmol, 1.10 eq). The mixture was heated to reflux for 3 h. During heating most of the solid dissolved and the mixture became orange-brown. The suspension was filtered, the filtrate was evaporated *in vacuo*, and to the residue 5 mL of hexane were added. A white crystalline precipitate was observed immediately. The mixture was refluxed for 5 min and then cooled to 0 °C for 30 min. The precipitate was filtered off, washed with hexane at 0 °C (2 × 5 mL) and dried *in vacuo* (30 min, 40 °C) to give

[153] The signal overlaps with the signal of the deuterated solvent.

an almost white microcrystalline powder. Yield 0.402 g (0.542 mmol, 78%). [*ν*(CO)] IR (toluene, cm^{-1}): 1925 (s), 1842 (vs) [*ν*(CO)]

^{1}H NMR (300.1 MHz, C_6D_6, 298 K, ppm): δ = 1.08 (d, ^{2}J(P,H) = 8.8 Hz 9H, P(C*H*$_3$)$_3$), 1.45 (s, 15H, C_5*Me*$_5$), 2.21 (s, 3H, C$^{2'}$-*Me*), 2.28 (s, 3H, C$^{4''}$-*Me*), 2.30 (s, 3H, C$^{4'}$-*Me*), 2.38 (s, 3H, C$^{2''}$-*Me*), 2.256 (s, 3H, C$^{6''}$-*Me*), 2.562 (s, 3H, C$^{6'}$-*Me*), 6.21 (d, ^{1}J(Si,H) = 205 Hz, ^{3}J(P,H) = 0.8 Hz, 1H, Si*H*Cl), 6.80 (s, 1H, C$^{3'}$-*H*, Mes), 6.94 (m, 2H, C$^{3''}$-*H*, Mes and C$^{3\text{ or }5}$-*H*, C_6H_3), 6.98 (s, 1H, C$^{5''}$-*H*, Mes), 6.99 (m, 1H, C$^{3\text{ or }5}$-*H*, C_6H_3), 7.01 (s, 1H, C$^{5'}$-*H*, Mes), 7.25 (t, ^{3}J(C,H) = 7.5 Hz, 1H, C^{4}-*H*, C_6H_3).

^{13}C{^{1}H} NMR (75.47 MHz, C_6D_6, 298 K, ppm): δ = 10.3 (s, 5C, C_5*Me*$_5$), 19.3 (d, ^{1}J(P,C) = 29.1 Hz, 3C, P(*C*H$_3$)$_3$), 21.2 (s, 1C, C$^{4''}$-*Me*, Mes), 21.3 (s, 1C, C$^{4'}$-*Me*, Mes), 21.7 (s, 1C, C$^{2''}$-*Me*, Mes), 21.9 (s, 1C, C$^{6''}$-*Me*, Mes), 23.3 (s, 1C, C$^{6'}$-*Me*, Mes), 23.8 (s, 1C, C$^{2'}$-*Me*, Mes), 103.1 (s, 5C, *C*$_5$Me$_5$), 127.7 (s, 1C, *C*$^{5''}$-H, Mes), 128.1 (s, 1C, *C*$^{3'}$-H, Mes), 128.4 (s, 1C, *C*$^{3''}$-H, Mes), 129.1 (s, 1C, *C*$^{3\text{ or }5}$-H, C_6H_3), 129.2 (s, 1C, *C*$^{5'}$-H, Mes), 129.5 (s, 1C, *C*^{4}-H, C_6H_3), 130.4 (s, 1C, *C*$^{3\text{ or }5}$-H, C_6H_3), 135.5 (s, 1C, *C*$^{4''}$, Mes), 135.8 (s, 1C, *C*$^{4'}$, Mes), 135.9 (s, 1C, *C*$^{2''}$, Mes), 136.2 (s, 1C, *C*$^{2'}$, Mes), 137.9 (s, 1C, *C*$^{6''}$, Mes), 138.4 (s, 1C, *C*$^{6'}$, Mes), 141.1 (d, ^{3}J(P,C) = 1.3 Hz, 1C, *C*^{1}, C_6H_3), 142.1 (s, 1C, *C*$^{1'}$, Mes), 143.0 (s, 1C, *C*$^{1''}$, Mes), 149.0 (s, 1C, *C*$^{2\text{ or }6}$, C_6H_3), 150.2 (s, 1C, *C*$^{2\text{ or }6}$, C_6H_3), 230.9 (d, ^{2}J(P,C) = 27.5 Hz, 1C, *C*O), 237.3 (d, ^{2}J(P,C) = 25.2 Hz, 1C, *C*O).

^{29}Si{^{1}H} NMR (59.63 MHz, C_6D_6, 298K, ppm): δ = 54.1 (d, ^{2}J(P,Si) = 15.6 Hz, *Si*HCl).

^{31}P{^{1}H} NMR (121.5 MHz, C_6D_6, 298K, ppm): δ = 23.5 (s, 1P, *P*(CH$_3$)$_3$).

4.2.79 [Cp*Mo(CO)$_2$(PMe$_3$)–SiHCl(C$_6$H$_3$-2,6-Trip$_2$)] (97)

15 mL of toluene were added to a mixture of Si(C$_6$H$_3$-2,6-Trip$_2$)HCl$_2$ (0.290 g, 0.499 mmol) and Li[(η^5-C$_5$Me$_5$)Mo(CO)$_2$(PMe$_3$)] (0.200 g, 0.541 mmol, 1.08 eq). The mixture was heated to reflux for 24 h. During heating most of the solid dissolved and the mixture became orange-brown. The suspension was filtered, the filtrate was evaporated *in vacuo*. 15 mL of hexane were added to the residue, the resulting solution was kept at –60 °C for 2 days for crystallization. The precipitate was filtered at –60 °C and dried *in vacuo* (2 h, 40 °C) to give slightly brown microcrystalline powder. Yield 0.402 g, (0.542 mmol, 78%) IR (hexane, cm^{-1}): 1927 (s), 1853 (vs) [*ν*(CO)]. IR (toluene, cm^{-1}): 1923 (s), 1848 (vs) [*ν*(CO)].

^{1}H NMR (300.1 MHz, C_6D_6, 298 K, ppm): δ = 0.87 (d, ^{2}J(P,H) = 8.7 Hz, 9H, P(CH_3)$_3$), 1.08 (d, ^{3}J(H,H) = 6.6 Hz, 3H, C$^{2'}$-CHMe_AMe$_B$), 1.11 (d, ^{3}J(H,H) = 6.7 Hz, 3H, C$^{2''}$-CHMe_AMe$_B$), 1.15 (d, ^{3}J(H,H) = 6.6 Hz, 3H, C$^{6'}$-CHMe_AMe$_B$), 1.21 (d, ^{3}J(H,H) = 6.8 Hz, 3H, C$^{6''}$-CHMe_AMe$_B$), 1.31 (d, ^{3}J(H,H) = 6.9 Hz, 3H, C$^{4'}$-CHMe_AMe$_B$), 1.32 (d, ^{3}J(H,H) = 6.9 Hz, 3H, C$^{4'}$-CHMe$_A$$Me_B$), 1.349 (d, ^{3}J(H,H) = 6.9 Hz, 3H, C$^{4''}$-CHMe_AMe$_B$), 1.353 (d, ^{3}J(H,H) = 6.9 Hz, 3H, C$^{4''}$-CHMe$_A$$Me_B$), 1.45 (d, ^{3}J(H,H) = 6.6 Hz, 3H, C$^{2'}$-CHMe$_A$$Me_B$), 1.46 (d, ^{4}J(P,H) = 0.4 Hz, 15H, C_5Me_5), 1.52 (d, ^{3}J(H,H) = 6.7 Hz, 3H, C$^{2''}$-CHMe$_A$$Me_B$), 1.69 (d, ^{3}J(H,H) = 6.8 Hz, 3H, C$^{6''}$-CHMe$_A$$Me_B$), 1.80 (d, ^{3}J(H,H) = 6.6 Hz, 3H, C$^{6'}$-CHMe$_A$$Me_B$), 2.87 (sept, ^{3}J(H,H) = 6.9 Hz, 1H, C$^{4'}$-CHMe$_A$Me$_B$), 2.91 (sept, ^{3}J(H,H) = 6.6 Hz, 1H, C$^{2'}$-CHMe$_A$Me$_B$), 2.94 (sept, ^{3}J(H,H) = 6.9 Hz, 1H, C$^{4''}$-CHMe$_A$Me$_B$), 3.27 (sept, ^{3}J(H,H) = 6.7 Hz, 1H, C$^{2''}$-CHMe$_A$Me$_B$), 3.52 (sept, ^{3}J(H,H) = 6.6 Hz, 1H, C$^{6''}$-CHMe$_A$Me$_B$), 3.89 (sept, ^{3}J(H,H) = 6.6 Hz, 1H, C$^{6'}$-CHMe$_A$Me$_B$), 6.40 (d, ^{3}J(P,H) = 0.6 Hz, ^{1}J(Si,H) = 206 Hz, 1H, SiHCl), 7.10 (d, ^{4}J(H,H) = 1.8 Hz, 1H, C$^{3'}$-*H*, Trip), 7.11 (t, ^{3}J(H,H) = 7.4 Hz, 1H, C^{4}-*H*, C_6H_3), 7.19 (m, 1H, C^{3}-*H*, C_6H_3), 7.23 (d, ^{4}J(H,H) = 1.8 Hz, 1H, C$^{3''}$-*H*, Trip), 7.24 (m, 1H, C^{5}-*H*, C_6H_3), 7.31 (d, ^{4}J(H,H) = 1.8 Hz, 1H, C$^{5'}$-*H*, Trip) 7.33 (d, ^{4}J(H,H) = 1.8 Hz, 1H, C$^{5''}$-*H*, Trip).

^{13}C{^{1}H} NMR (75.47 MHz, C_6D_6, 298 K, ppm): δ = 10.43 (s, 5C, C_5Me_5), 19.7 (d, ^{2}J(H,H) = 29.7 Hz, 3C, P(*C*H$_3$)$_3$), 22.9 (s, 1C, C$^{6'}$-CHMe$_A$$Me_B$), 23.4 (s, 1C, C$^{2'}$-CHMe$_A$$Me_B$), 23.6 (s, 1C, C$^{2''}$-CHMe$_A$$Me_B$), 23.8 (s, 1C, C$^{6''}$-CHMe$_A$$Me_B$), 24.4 (s, 1C, C$^{4'}$-CH$Me_AMe_B$), 24.6 (s, 1C, C$^{4'}$-CHMe$_A$$Me_B$), 24.6 (s, 1C, C$^{4''}$-CH$Me_AMe_B$), 24.7 (s, 1C, C$^{4''}$-CHMe$_A$$Me_B$), 25.9 (s, 1C, C$^{2''}$-CH$Me_AMe_B$), 26.2 (s, 1C, C$^{6''}$-CH$Me_AMe_B$), 27.5 (s, 1C, C$^{2'}$-CH$Me_AMe_B$), 27.6 (s, 1C, C$^{4'}$-CH$Me_AMe_B$), 30.6 (s, 1C, C$^{2''}$-*C*HMe$_AMe_B$), 30.8 (s, 1C, C$^{2'}$-*C*HMe$_AMe_B$), 31.4 (s, 1C, C$^{6''}$-*C*HMe$_AMe_B$), 31.8 (s, 1C, C$^{6'}$-*C*HMe$_AMe_B$), 34.7 (s, 1C, C$^{4'}$-*C*HMe$_AMe_B$), 35.0 (s, 1C, C$^{4''}$-*C*HMe$_AMe_B$), 103.1 (s, 5C, *C*$_5Me_5$), 120.3 (s, 1C, *C*$^{3''}$-H, Trip), 120.9 (s, 1C, *C*$^{5''}$-H, Trip), 121.0 (s, 1C, *C*$^{3'}$-H, Trip), 121.9 (s, 1C, *C*$^{5'}$-H, Trip), 126.0 (s, 1C, *C*^{4}-H, C_6H_3), 131.4 (s, 1C, *C*^{5}-H, C_6H_3), 133.7 (s, 1C, *C*^{3}-H, C_6H_3), 141.4 (s, 1C, *C*$^{1'}$, Trip), 142.7 (s, 1C, *C*$^{1''}$, Trip), 144.1 (d, ^{3}J(P,C) = 1.0 Hz, 1C, *C*^{1}, C_6H_3), 145.6 (s, 1C, *C*$^{2'}$, Trip), 147.21 (s, 1C, *C*^{3}, C_6H_3), 147.25 (s, 1C, *C*$^{4'}$, Trip), 147.4 (s, 1C, *C*$^{4''}$, Trip), 147.8 (s, 1C, *C*$^{2'}$, Trip), 147.9 (s, 2C, *C*$^{6''}$, Trip + *C*^{6}, C_6H_3), 233.7 (d, ^{2}J(P,C) = 28.8 Hz, 1C, *C*O), 235.9 (d, ^{2}J(P,C) = 25.5 Hz, 1C, *C*O).

^{29}Si{^{1}H} NMR (59.63 MHz, C_6D_6, 298K, ppm): δ = 55.4 (d, ^{2}J(P,Si) = 13 Hz, *Si*HCl).

^{31}P{^{1}H} NMR (121.5 MHz, C_6D_6, 298K, ppm): δ = 24.5 (s, 1P, *P*(CH$_3$)$_3$).

4.3 Improved syntheses of certain starting materials

4.3.1 $SiBr_4$

The original procedure was slightly modified.[154] A mixture of 24.0 g (0.854 mol) of well grinded silicon powder and 1.2 g of copper powder (19 mmol) was distributed among Al_2O_3 wool (about 300 cm^3, just enough to fill the tube cross-section). The wool was inserted into a quartz tube, which was placed in an electric oven and heated up in a slow argon flow. At a temperature of 1025 °C addition of bromine was started dropwise at the higher end of the assembly. The rate was adjusted in such a way that no or only a little of bromine was observed in the condensate in the receiving flask. After a total of 88 mL (274 g, 1.71 mol, 2.0 eq) of bromine was added the color of the downcoming product became slightly orange. The crude product (orange-brown liquid) was distilled under argon at ambient pressure with ca. 3 g of copper powder (for bromine removal). The colorless fraction boiling at 155–156 °C was collected, stirred over a mixture of K_2CO_3 (to remove traces of HBr) and copper powder (to remove traces of Br_2) for 1 h and filtered to give the pure product as a colorless mobile liquid. Yield 210 g (0.604 mol, 71%). ^{29}Si NMR (59.63 MHz, C_6D_6, 298K, ppm): δ = –90.8 (s).

4.3.2 SiI_4

The original procedure was slightly modified.[216] In the preparation the same apparatus was used as for synthesis of $SiBr_4$. The reaction was carried out at 780 °C. Iodine (110 g, 0.433 mol) was added in portions from a flask, connected through a knee, to the upper end of the tube, containing a mixture of silicon (12.2 g, 0.434 mol) and 1.2 g (19 mmol) of copper powder, distributed among Al_2O_3 wool (about 300 cm^3, just enough to fill the tube cross-section). Fine grinding of silicon, thorough distribution of silicon powder over the alumina wool and appropriate rate of addition are crucial for getting a good yield of the product. In the beginning of the reaction, the condensate in the receiver flask had light purple-brown color. The reaction was stopped when the product become contaminated with substantial amount of iodine (dark purple colored). To the crude purple-brown solid material a sufficient amount of copper was added and the mixture was refluxed in toluene (250 mL) until the solution

[154] Handbook of Preparative Inorganic Chemistry – Vol 1, 2nd edition, Ed. G. Brauer, 1963, Academic press inc. pp 686-687.

decolorized and then filtered hot through P3 sintered glass filter. The clear light yellow filtrate was concentrated *in vacuo* to ca. 20 mL, during which most of the product crystallized as a white solid. The mixture was stored overnight at –30 °C and filtered at –30 °C. The product was dried *in vacuo* (1 h, RT). Yield: 51.8 g (62%); white microcrystalline powder. The product is light sensitive and becomes slightly pink if it is stored unprotected from light.

4.3.3 1,3,4,5-tetramethyimidazol-2-ylidene (IMe_4)

A 2 L round-bottom flask, equipped with a magnetic stirring bar and a metal reflux condenser with a mercury bubbler and an inert gas inlet was charged with 1,3,4,5-tetramethylimidazol-2-thione[217],[155] (59.5 g, 0.381 mol) of and potassium metal (37.1 g, 0.949 mol, 2.5 eq).[156] 1.5 L of dry degassed THF was added to the mixture, and the suspension was heated under reflux for 15 h. During this time the potassium metal was consumed, formation of a grey-blue precipitate was observed and the color of the stirred mixture changed from violet initially to blue at the end of the reaction. Completion of the reaction was verified by ^{1}H NMR spectroscopy before work-up. The precipitate was allowed to settle down, the clear yellow supernatant solution was decanted *via* cannula and the precipitate was washed once with 300 mL of THF. The THF washing was combined with the filtrate and evaporated to dryness *in vacuo*. The residue was extracted with warm toluene (ca. 250 mL, 80 °C) and the light brown extract was filtered hot (ca. 70 °C). The filtrate was concentrated *in vacuo* to ca. 60 mL, during this some of the product precipitated. The resulting slurry was cooled to 0 °C for ca. 10 min. The precipitate was collected by filtration, washed with a toluene/hexane mixture (1:3, 3 × 20 mL, 0 °C) and dried *in vacuo* to give the product as beige, crystalline powder. Yield 33.8 g (0.27 mol, 72%). A second crop (ca. 2 g) can be isolated from the combined mother liquor and the washings upon crystallization at –30 °C. The second crop was not as pure as the first crop, but can be used for different syntheses. ^{1}H NMR (300.1 MHz, C_6D_6, 298 K, ppm): δ = 1.58 (s, 6H, $C^{4,5}$–CH_3), 3.36 (s, 6H, $N^{1,3}$–CH_3). ^{13}C{^{1}H} NMR

[155] The synthesis of the thione was repeated twice on a large scale and the yields were 56 and 64% respectively. ^{1}H NMR of the 1,3,4,5-tetramethylimidazol-2-thione (300.1 MHz, C_6D_6, 298 K, ppm): δ = 1.24 (s, 6H, 2 × $C^{4,5}$-CH_3), 3.15 (s, 6H, 2 × $N^{1,3}$-CH_3).

[156] Extreme care is necessary while working with potassium metal.

(75.47 MHz, C_6D_6, 298 K, ppm): δ = 8.8 (s, 2C, $C^{4,5}$–CH_3), 35.1 (s, 2C, $N^{1,3}$–CH_3), 122.5 (s, 2C, $C^{4,5}$).[157]

4.3.4 1,3-bis(2,4,6-trimethylphenyl)imidazol-2-ylidene (IMes)

To a suspension of [IMesH]Cl[218] (13.2 g, 38.7 mmol) in 200 mL of Et_2O a solution of $NaN(TMS)_2$ (7.45 g, 40.6 mmol, 1.05 eq) in 50 mL of Et_2O was added in 2 min at ambient temperature.[158] Upon addition most of the solid dissolved. The suspension was stirred for 1 h at ambient temperature to give a slightly brown solution, containing a brown precipitate (NaCl). The mixture was filtered with a filter cannula and the filtrate was concentrated in vacuum to about 20 mL. A white precipitate was observed. The mixture was cooled with an ice-bath, filtered and the precipitate washed with cold (−30 °C) ether (2×7 mL). The product was dried in *vacuo* (2 h, 50 °C) to give a white, crystalline powder. Yield 9.60 g (31.5 mmol, 81%). Elemental analysis calcd (%) for $C_{21}H_{24}N_2$ (304.4): C 82.85, H 7.95, N 9.20; found: C 82.43, H 8.03, N 9.02%. ^{1}H NMR (300.1 MHz, C_6D_6, 298 K, ppm): δ = 2.14 (s, 12H, 2 × $C^{2,6}$-*Me*, Mes), 2.15 (s, 6H, 2 × C^4-*Me*, Mes), 6.49 (s, 2H, $C^{4,5}$-*H*), 6.80 (m, 4H, 2 × $C^{3,5}$-*H*, Mes). $^{13}C\{^1H\}$ NMR (75.5 MHz, C_6D_6, 298 K, ppm): δ = 18.0 (s, 4C, 2 × $C^{2,6}$-*Me*, Mes), 21.0 (s, 2C, 2 × C^4-*Me*, Mes), 120.5 (s, 2C, $C^{4,5}$), 129.1 (s, 4C, 2 × $C^{3,5}$-H, Mes), 135.4 (s, 4C, 2 × $C^{2,6}$, Mes), 137.2 (s, 2C, 2 × C^4, Mes), 139.2 (s, 2C, 2 × C^1, Mes), 219.3 (s, 1C, CN_2). IR (nujol, KBr-windows, cm^{-1}): ν = 3146 (m), 3118 (m), 3077 (w), 2732 (w), 1733 (w), 1657 (w), 1610 (w), 1560 (w) 1489 (s), 1251 (s), 1087 (w), 1064 (w), 1030 (w), 1012 (w), 962 (w), 927 (m), 887 (w), 852 (s), 743 (w), 735 (m), 635 (w), 570 (w), 461 (w).

4.3.5 1,3-bis-(2,6-diisopropylphenyl)imidazol-2-ylidene (IDipp)

To a mixture of [IDippH]Cl (106.9 g, 0.251 mol)[218] and $NaNTMS_2$ (48.4 g, 0.264 mol, 1.05 eq.) 1 L of THF was added at –30 °C.[158] The cooling bath was removed, and the mixture was stirred for 30 min at ambient temperature to give an orange suspension, containing a white precipitate (NaCl). The mixture was placed in an ultrasonic bath for 2 min and then further stirred 25 min at 30 °C. All volatiles were removed and the residue was dried *in vacuo*

[157] No attempts were undertaken to detect the C^2 (carbene-carbon) resonance, which appears according to the literature at δ = 212.7 ppm in C_6D_6.

[158] A modified procedure, originally reported by A. Tudose, A. Demonceau, L. Delaude, *J. Organomet. Chem.* **2006**, *691*, 5356.

(12 h, 50 °C).[159] To the solid brownish crystalline material 2 L of dry diethyl ether was added and the mixture was stirred well. After a major part of the NaCl settled down, the supernatant was decanted and filtered through a Celite pad. The precipitate was suspended in some additional diethyl ether and filtered at last. The clear light brown filtrate was concentrated *in vacuo* to about 400 mL, during this a lot of the product precipitated. The suspension was cooled to –10 °C and filtered, the precipitate was washed with diethyl ether at –10 °C (200 mL in total) and dried *in vacuo* (8 h, 50 °C) to give the product as a white, microcrystalline solid. Yield 70.3 g (0.181 mol, 72%). The mother liquor and washings were combined, concentrated to about 50 mL and stored at 0 °C. The precipitate was filtered off, washed with diethyl ether at 0 °C (2 × 20 mL) and dried *in vacuo* (2 h, 60 °C) to give a second crop of the product. Yield 8.5 g (22 mmol, 9%). ^{1}H NMR (300.1 MHz, C_6D_6, 298 K, ppm): δ = 1.18 (d, ^{3}J(H,H) = 6.9 Hz, 12H, 4 × CHMe_AMe$_B$), 1.27 (d, ^{3}J(H,H) = 6.9 Hz, 12H, 4 × CHMe$_A$$Me_B$), 2.95 (sept, ^{3}J(H,H) = 6.9 Hz, 4H, 4 × CHMe$_A$Me$_B$), 6.62 (s, 2H, C^{4,5}-H), 7.18 (m, 4H, 2 × C^{3,5}-H, Dipp), 7.29 (m, 2H, 2 × C^{4}-H, Dipp). ^{13}C{^{1}H} NMR (75.5 MHz, C_6D_6, 298 K, ppm): δ = 23.6 (s, 4C, 4 × CHMe_AMe$_B$), 24.8 (s, 4C, 4 × CHMe$_A$$Me_B$), 28.7 (s, 4C, 4 × CHMe$_AMe_B$), 121.5 (s, 2C, 2 × C^{4}-H, Dipp), 123.7 (s, 4C, 2 × $C^{3,5}$-H, Dipp), 129.0 (s, 4C, 2 × $C^{2,6}$, Dipp), 138.9 (s, 2C 2 × C^{1}, Dipp), 146.2 (s, 2C, 2 × C^{4}-H, Dipp), 220.6 (s, 1C, CN$_2$). IR (nujol, KBr-windows, cm^{1}): ν = 3142 (m), 3059 (m), 1467 (s), 1389 (s), 1361 (m), 1330 (w), 1095 (m), 935 (m), 807 (m), 801 (m), 769 (m), 765 (m), 745 (s).

4.3.6 1,3-bis-(2,6-diisopropylphenyl)imidazolin-2-ylidene (ISdipp)

Deprotonation of [ISdippH]Br with KH.[121]

Advantages: very clean reaction, cheap base.

Disadvantages: long reaction time, incomplete conversion

To a mixture of [ISdippH]Br[160] (50.3 g, 0.107 mol), a spatula of dibenzo-18-crown-6 and KH (8.1 g, 0.20 mol, 1.9 eq.) 800 mL of THF was added. The suspension was stirred for 5 days at ambient temperature with a mercury pressure release bubbler. The mixture was placed from time to time in an ultrasonic bath. During the stirring the amount of the insoluble material decreased and hydrogen evolution weakened, but not stopped. After 5 days the

[159] Complete removal of TMS_2NH seems to ease subsequent filtration.

[160] Prepared by a slightly modified procedure reported by E. L. Kolychev, I. A. Portnyagin, V. V. Shuntikov, V. N. Khrustalev, M. S. Nechaev; *J. Organomet. Chem*. **2009**, *694*, 2454.

solvent was removed and the white residue was dried *in vacuo* (30 min, RT). The solid was extracted with diethyl ether in portions (total of 700 mL) and the extracts were filtered through a Celite pad. The clear light brown filtrate was concentrated under reduced pressure to about 300 mL and part of the product crystallized. The mixture was heated to reflux to dissolve the carbene and then slowly cooled down to ambient temperature (1 h), then to 0 °C (0.5 h) and finally concentrated to 100 mL *in vacuo*. The crystallization was completed at -40 °C, the product was filtered off, washed with diethyl ether (2 × 50 mL) at –40 °C and dried *in vacuo* (from –40 °C to 40 °C, 2 h at 40 °C) to give the product as a floppy white microcrystalline solid. Yield 26.9 g (68.9 mmol, 64%).[161] ^{1}H NMR (300.1 MHz, C_6D_6, 298 K, ppm): δ = 1.28 (d, ^3J(H,H) = 6.8 Hz, 12H, 2 × C^{2,6}-CHMe_AMe$_B$, Dipp), 1.33 (d, ^3J(H,H) = 6.8 Hz, 12H, 2 × C^{2,6}-CHMe$_A$$Me_B$, Dipp), 3.28 (sept, ^3J(H,H) = 6.9 Hz, 4H, 2 × C^{2,6}-CHMe$_A$Me$_B$, Dipp), 3.37 (s, 4H, 2 × NCH_2), 7.16−7.20 (m, 4H, 2 × C^{3,5}-H, Dipp), 7.24−7.29 (m, 2H, 2 × C^4-H, Dipp). ^{13}C{^{1}H} NMR (75.47 MHz, C_6D_6, 298 K, ppm): δ = 23.6 (s, 4C, 2 × C^{2,6}-CHMe_AMe$_B$, Dipp), 25.4 (s, 4C, 2 × C^{2,6}-CHMe$_A$$Me_B$, Dipp), 28.9 (s, 4C, 2 × C^{2,6}-CHMe$_A$Me$_B$, Dipp), 53.7 (s, 4C, 2 × NCH$_2$), 124.0 (s, 4C, 2 × $C^{3,5}$-H, Dipp), 128.3* (s, 2C, 2 × C^4-H, Dipp), 139.4 (s, 2C, 2 × C^1, Dipp), 147.4* (s, 4C, 2 × $C^{2,6}$, Dipp), 244.1 (s, 1C, CN$_2$). The signals marked with an asterisk were incorrectly assigned in reference [121].

Deprotonation of [ISdippH]Br with NaNTMS$_2$.[162]

Advantages: short reaction time.

Disadvantages: formation of a byproduct, expensive base.

To a mixture of [ISdippH]Br[163] (34.0 g, 72.1 mmol) and NaNTMS$_2$ (14.0 g, 76.3 mmol, 1.06 eq.) 400 mL of diethyl ether was added. The suspension was stirred for 3 h at ambient temperature. During the stirring most of the solid dissolved. The suspension was filtered through a Celite pad. The clear light brown filtrate was concentrated under reduced pressure to about 250 mL and part of the product crystallized. The mixture was heated to reflux to dissolve the carbene and then slowly cooled down and stirred at ambient temperature (2 h), then at 0 °C (0.5 h) and finally stored at –30 °C overnight. The product was filtered off,

[161] Longer reaction time should increase the yield. Heating or refluxing might be appropriate.

[162] M. Iglesias, D. J. Beetstra, J. C. Knight, L.-L. Ooi, A. Stasch, S. Coles, L. Male, M. B. Hursthouse, K. J. Cavell, A. Dervisi, I. A. Fallis, *Organometallics* **2008**, *27*, 3279.

[163] Prepared by a slightly modified procedure reported by E. L. Kolychev, I. A. Portnyagin, V. V. Shuntikov, V. N. Khrustalev, M. S. Nechaev; *J. Organomet. Chem*. **2009**, *694*, 2454.

washed with diethyl ether (2 × 30 mL) at –30 °C and dried *in vacuo* (from –30 °C to 60 °C, several hours at 60 °C) to give the carbene as a floppy white microcrystalline solid. Yield 16.0 g (40.9 mmol, 57%). The product was shown by ^{1}H NMR spectroscopy to be pure.

The crude reaction mixture contains about 20% of CH_2=CH−N(Dipp)−CH=N−Dipp (**25**) which was isolated in pure form from the mother liquor. The Et_2O filtrate and washings were combined, concentrated to ca 50 mL and stored at –30 °C for a week to produce a mixture of small crystals of ISdipp and large stars of **25**. The carbene was removed as a suspension in diethyl ether, the by-product was washed with a small amount of acetone and dried *in vacuo* (30 min, RT). Yield ca. 1g, 4%. ^{1}H NMR (300.1 MHz, C_6D_6, 298 K, ppm): δ = 1.14 (d br, ^{3}J(H,H) = 6.8 Hz, 6H, 2 × CHMe_AMe$_B$, Dipp), 1.19 (d, ^{3}J(H,H) = 6.8 Hz, 6H, 2 × CHMe$_A$$Me_B$, Dipp), 1.24 (d, ^{3}J(H,H) = 6.8 Hz, 12H, 2 × CHMe_2, Dipp), 3.18 (sept, ^{3}J(H,H) = 6.8 Hz, 2H, 2 × C*H*Me$_2$, Dipp), 3.37 (sept br, ^{3}J(H,H) = 6.8 Hz, 2H, 2 × C*H*Me$_2$, Dipp), 3.88 (d br, ^{3}J(H,H) = 15.5 Hz, 1H, CH=CH_AH$_B$), 4.18 (s br, 1H, CH=CH$_A$$H_B$)*, 7.06−7.22 (several multiplets, 6H, 2 × C$_6H_3$, Dipp), 8.17 (s br, 1H, NC*H*N). The signal marked with an asterisk was tentatively assigned, and one C*H* signal is probably hidden under the signals of the aromatic protons. The compound appears to be the product of a Hoffmann-like elimination of HBr from [ISdippH]Br. The structure was solved by X-ray crystallography.

4.3.7 [CpCr(CO)$_3$H]

$Cr(CO)_6$ (35.7 g, 162 mmol) and NaCp (14.7 g, 167 mmol, 1.03 equiv) were mixed and 700 mL of dimethoxyethane were added.[164] The stirred mixture was heated under reflux for 36 h. The completion of the reaction was controlled by IR spectroscopy. The resulting yellow-brown solution of Na[CpMo(CO)$_3$] was cooled to –30 °C and a degassed solution of HCl (37%, 14.0 mL, ρ = 1.19 g/cm^3, 0.169 mol) was added dropwise. The color brightened and a precipitate was observed (NaCl). The mixture was allowed to warm up to ambient temperature and the solvents were removed *in vacuo*. The residue was extracted with about 500 mL of diethyl ether and the mixture was filtered, the yellow-green filtrate was evaporated to dryness *in vacuo*. The product was extracted with about 500 mL of hexane and the extract was filtered. The yellow filtrate with a slight green touch was evaporated under reduced

[164] The procedures are based on the previously reported a) T. S. Piper, J. Wilkinson, *J. Inorg. Nucl. Chem.* **1956**, *3*, 104; b) E. O. Fischer; *Inorg. Synth*. **1963**, *7*, 136.

pressure and the product was dried *in vacuo* (1 h, RT) to give the product.[165] Yelow-green microcrystalline powder, yield 16.7 g (82.6 mmol, 51% from $Cr(CO)_6$). IR (hexane, cm^{-1}): 2018 (s), 1946(m), 1937 (vs) [*v*(CO)].

4.3.8 [CpMo(CO)$_3$H]

$Mo(CO)_6$ (40.0 g, 152 mmol) and NaCp (14.50 g, 165 mmol) were mixed and 450 mL of dimethoxyethane were added.[164] The stirred mixture was heated under reflux for 24 h. The completion of the reaction was controlled by IR spectroscopy.[166] The resulting yellow-brown solution of $Na[CpMo(CO)_3]$ was cooled to –30 °C and a degassed solution of HCl (37%, 14.0 mL, ρ = 1.19 g/cm^3, 0.169 mol) was added dropwise. The color brightened and a precipitate was observed (NaCl). The mixture was allowed to warm up to ambient temperature and the solvents were removed *in vacuo*. The residue was extracted with 400 mL of diethyl ether and the mixture was filtered, the brown filtrate was evaporated to dryness *in vacuo*. The product was extracted with hexane in portions (250 mL + 2 × 50 mL) and the extracts were filtered from some of a brown oily residue. The combined filtrates were evaporated under reduced pressure and the product was dried *in vacuo* (1 h, RT). Yellow microcrystalline powder, yield 30.6 g (0.124 mol, 82% based on $Mo(CO)_6$). IR (pentane, cm^{-1}): 2030 (s), 1945(vs), [*v*(CO)].^{1}H NMR (300.13 MHz, C_6D_6, 298 K, ppm): δ = –5.48 (s, 1H, Mo-*H*), 4.55 (s, 5H, C_5H_5).

4.3.9 [Cp*Cr(CO)$_3$H]; [Cp*Mo(CO)$_3$H]

$Cr(CO)_6$ (9.82 g, 44.6 mmol) and LiCp* (6.66 g, 46.8 mmol) were mixed and 250 mL of dimethoxyethane were added.[164] The stirred mixture was heated under reflux for 72 h. The completion of the reaction was controlled by IR spectroscopy. The resulting light brown-yellow suspension (white precipitate of excess of LiCp*) was cooled to –60 °C and degassed HCl (37%, 4.14 mL, ρ = 1.19 g/cm^3, 50 mmol) was added dropwise.[167] The mixture was

---

[165] Careful, the product is thermally unstable and decomposes at RT to give the green dimer $[CpCr(CO)_3]_2$.

[166] $Mo(CO)_6$: IR (DME, cm^{-1}): 1980 cm^{-1}, [*v*(CO)]. $Na[CpMo(CO)_3]$: IR (DME, cm^{-1}): 1897 (vs), 1780(vs), 1750 (s, sh), [*v*(CO)].

[167] Glacial acetic acid can be more conveniently used for Protonation. B. Baars, *Diploma thesis*, University of Bonn, **2012**. See also the synthesis of $[Cp^*W(CO)_3H]$, p. 260.

allowed to warm up to RT. The color brightened and a precipitate was observed (NaCl). The solvents were removed *in vacuo* and the dried residue was extracted with about 200 mL of hexane and the extract was filtered. The yellow filtrate was concentrated under vacuum to about about 20 mL, a yellow precipitate was observed. The mixture was stored at –60 °C for 1 h and then the yellow precipitate was collected by filtration, washed with hexane at –60 °C and dried *in vacuo* for 1 h at RT. Yellow microcrystalline powder, yield 9.64 g (35.4 mmol, 79% based on $Cr(CO)_6$). IR (hexane, cm^{-1}): 2001(s), 1928(s), 1921(vs) [ν(CO)]. IR (Et_2O, cm^{-1}): 1998(s), 1916(vs) [ν(CO)]. ^{1}H NMR (300.13 MHz, C_6D_6, 298 K, ppm): δ = –5.54 (s, 1H, Cr-*H*), 1.54 (s, 15H, C_5*Me*$_5$). $^{13}C\{^1H\}$ NMR (74.5 MHz, C_6D_6, 298 K, ppm): δ = 10.4 (s, 5C, C_5*Me*$_5$), 99.9 (s, 5C, *C*$_5$Me$_5$), 237.6 (s, 3C, *C*O).

Complex [Cp*Mo(CO)$_3$H] was prepared in a similar way upon refluxing in DME LiCp* and $Mo(CO)_6$ for 46 h, subsequent protonation with 37% wt. HCl and crystallization from hexane at –30 °C in 71% yield.[167] IR (hexane, cm^{-1}): 2015(s), 1931(vs) [ν(CO)].^{1}H NMR (300.13 MHz, C_6D_6, 298 K, ppm): δ = –5.00 (s, 1H, Cr-*H*), 1.67 (s, 15H, C_5*Me*$_5$). M. Speer, *Bachelor thesis*, University of Bonn, 2011.

4.3.10 [Cp*W(CO)$_3$H]

$W(CO)_6$ (7.04 g, 20.0 mmol) and LiCp* (2.99 g, 21 mmol) were mixed and 90 mL of dimethoxyethane were added.[164] The stirred mixture was heated under reflux for 25 h. The completion of the reaction was controlled by IR spectroscopy.[168] The resulting brown suspension (white precipitate of excess of LiCp*) was cooled to –30 °C and degassed glacial acetic acid (1.3 mL, ρ = 1.05 g/cm^3, 1.37 g, 23 mmol) was added dropwise. The mixture was allowed to warm up to RT. The color brightened and a precipitate was observed (LiOAc). The solvents were removed *in vacuo* and the residue was dried *in vacuo* for 1 h at 30 °C. The resulting light brown solid was extracted with petrol ether at +30 °C (70 + 2 × 10 mL) and the extract was filtered. The yellow filtrate was concentrated under vacuum to about about 10 mL, a yellow precipitate was observed. The mixture was stored at –60 °C for 30 min and then the yellow precipitate was collected by filtration, washed with petrol ether at –60 °C (2 × 7 mL) and dried *in vacuo* for 20 min at RT. Yellow microcrystalline powder, yield 6.82 g (16.9 mmol, 84% based on $W(CO)_6$). IR (petrol ether, cm^{-1}): 2013(m), 1924(vs) [ν(CO)]. ^{1}H NMR (300.13 MHz, C_6D_6, 298 K, ppm): δ = –6.52 (s, ^1J(W,H) = 39.9 Hz, 1H, W-*H*), 1.74 (s,

[168] Li[Cp*W(CO)$_3$]; IR (DME, cm^{-1}): 1885 (vs), 1787 (vs), 1762 (m), 1715 (s) [ν(CO)].

15H, C_5Me_5). $^{13}C\{^1H\}$ NMR (74.5 MHz, C_6D_6, 298 K, ppm): δ = 11.1 (s, 5C, C_5Me_5), 103.2 (s, J(W,C) = 5.8 Hz, 5C, C_5Me_5), 221.7 (s, 3C, *C*O).

4.3.11 Li[CpCr(CO)$_3$]

To a well stirred suspension of [CpCr(CO)$_3$H] (1.60 g, 7.92 mmol) in 30 mL of hexane a solution of 2.5 M *n*-BuLi in hexane (3.15 mL, 7.88 mmol) was added dropwise at –78 °C and the mixture was allowed to warm up to RT (the reaction can be conveniently carried out also at 0 °C).[169] A beige precipitate was observed. The resulting suspension was stirred for 1 h at ambient temperature. The precipitate was filtered off, washed with hexane (2 × 10 mL) and dried *in vacuo* (0.5 h, 40 °C) to give a fine beige powder. Yield 1.68 g, quantitative. IR (THF, cm^{-1}): 1902(s), 1804(vs), 1779(m), 1717(s) [ν(CO)]. ^{1}H NMR (400.1 MHz, CD_3CN, 298 K, ppm): δ = 4.41 (s, 5H, C_5H_5).

4.3.12 Li[CpMo(CO)$_3$]

To a well stirred solution of [CpMo(CO)$_3$H] (14.2 g, 57.7 mmol) in 150 mL of hexane a solution of 2.5 M *n*-BuLi in hexane (23.1 mL, 57.8 mmol) was added dropwise in 10 min at 0 °C (a needle in the septum was used for pressure release).[169] A beige precipitate was observed and the mixture warmed up substantially (a needle in the septum was used for pressure release). The resulting suspension was stirred for 1.5 h at ambient temperature. The precipitate was filtered off, washed with hexane (2 × 75 mL) and dried *in vacuo* (10 h, RT) to give fine beige powder. Yield 11.8 g (46.8 mmol, 81%). IR (THF, cm^{-1}): 1906(s), 1898(m sh), 1806(vs), 1782(m), 1717(s) [ν(CO)]. ^{1}H NMR (400.1 MHz, CD_3CN, 298 K, ppm): δ = 5.06 (s, 5H, C_5H_5). $^{13}C\{^1H\}$ NMR (100.6 MHz, CD_3CN, 298 K, ppm): δ = 87.1 (s, 5C, C_5H_5), 236.6 (s, 3C, 3 × CO).

4.3.13 K[CpW(CO)$_3$]

A mixture of W(CO)$_6$ (1.62 g, 4.60 mmol) and KCp (0.488 g, 4.68 mmol) was refluxed in 30 mL of DME for 40 h. The reaction completion was confirmed by IR spectroscopy. The mixture was filtered and the orange filtrate was evaporated to dryness. The residue was

[169] Similar to the procedure reported by K. M. Waltz, J. F. Hartwig, *J. Am. Chem. Soc.* **2000**, *122*, 11358.

treated with 10 mL of hexane, the resulting suspension immersed for 15 min in an ultrasonic bath, and then the solvent removed *in vacuo*. The obtained solid was dried *in vacuo* (50 °C, 4 h, 0.05 mbar) to give K[CpW(CO)$_3$]·0.05DME as a brownish powder. Yield – quantitative. IR (THF, cm^{-1}): 1888(s), 1776(vs), 1756(vs) [ν(CO)].^{1}H NMR (300.13 MHz, THF-d_8, 298 K, ppm): δ = 5.03 (s, 5H, C$_5H_5$).

4.3.14 Li[Cp*M(CO)$_3$]; M = Cr, Mo, W

To a well stirred solution of [Cp*Cr(CO)$_3$H] (9.64 g, 35.4 mmol) in 100 mL of hexane a solution of 2.5 M *n*-BuLi in hexane (14.9 mL, 37.3 mmol, 1.05 equiv) was added dropwise in 5 min at RT (water bath, a needle in the septum was used for pressure release).[169] A yellow precipitate was observed, the resulting suspension was stirred for 1 h at ambient temperature. The precipitate was filtered off, washed with hexane (3 × 30 mL) and dried *in vacuo* (2 h, RT) to give a fine yellow powder. Yield 8.69 g (31.2 mmol, 88%). IR (THF, cm^{-1}): 1887(vs), 1793(vs), 1768(m), 1703(s) [ν(CO)]. ^{1}H NMR (300.1 MHz, CD$_3$CN, 298 K, ppm): δ = 1.83 (s, 15H, C$_5Me_5$). ^{13}C{^{1}H} NMR (75.47 MHz, CD$_3$CN, 298 K, ppm): δ = 11.7 (s, 5C, C$_5Me_5$), 95.0 (s, 5C, *C*$_5$Me$_5$), 249.1 (s, 3C, 3 × CO).

Complex Li[Cp*Mo(CO)$_3$] was obtained by essentially the same procedure. IR (THF, cm^{-1}): 1892(vs), 1795(vs), 1768(m), 1702(s) [ν(CO)]. ^{1}H NMR (300.1 MHz, CD$_3$CN, 298 K, ppm): δ = 1.98 (s, 15H, C$_5Me_5$). ^{13}C{^{1}H} NMR (75.47 MHz, CD$_3$CN, 298 K, ppm): δ = 12.1 (s, 5C, C$_5Me_5$), 100.6 (s, 5C, *C*$_5$Me$_5$), 239.8 (s, 3C, 3 × CO). M. Speer, *Bachelor thesis*, University of Bonn, **2011**.

Complex Li[Cp*W(CO)$_3$] was obtained by essentially the same procedure. IR (THF, cm^{-1}): 1887(s), 1790(vs), 1766(w), 1701(s) [ν(CO)]. ^{1}H NMR (300.1 MHz, CD$_3$CN, 298 K, ppm): δ = 2.07 (s, 15H, C$_5Me_5$). ^{13}C{^{1}H} NMR (75.47 MHz, CD$_3$CN, 298 K, ppm): δ = 11.9 (s, 5C, C$_5Me_5$), 99.5 (s, 5C, J(W,C) = 4.5 Hz, *C*$_5$Me$_5$), 232.2 (s, ^1J(W,C) = 199.5 Hz, 3C, 3 × CO).

4.3.15 Si(C$_6$H$_3$-2,6-Mes$_2$)HCl$_2$ (26)

A solution of Li(C$_6$H$_3$-2,6-Mes$_2$) (5.25 g, 16.4 mmol) in 50 mL of diethyl ether was added dropwise under vigorous stirring to SiHCl$_3$ (5.0 mL, 6.7 g, 50 mmol, 3.0 eq.) at –78 °C. [170]

[170] Originally reported by R. S. Simons, S. T. Haubrich, B. V. Mork, M. Niemeyer, P. P. Power, *Main Group Chemistry* **1998**, *2*, 275.

Precipitation of LiCl was observed. The mixture was allowed to warm up to room temperature and stirred then for 30 min. All volatilities were removed *in vacuo* and the residue (white) was dried (1 h, RT). The solid was extracted with 80 mL of toluene at 70 °C and filtered hot. The clear colorless[172] filtrate was concentrated *in vacuo* to about 10 mL, a white precipitate was observed. Hexane (10 mL) was added and the mixture was stirred at –30 °C for 30 min. The precipitate was filtered off at –30 °C, washed with hexane (2 × 5 mL) and dried *in vacuo* (1 h, RT) to give a white microcrystalline solid. Yield 6.17 g (14.9 mmol, 91%). The product was shown by ^{1}H NMR spectroscopy to be pure.

4.3.16 Si(C$_6$H$_3$-2,6-Trip$_2$)HCl$_2$ (27)

A suspension of (C$_6$H$_3$-2,6-Trip$_2$)I (15.0 g, 24.6 mmol) in 150 mL of diethyl ether was treated with 2.5 M solution of *n*-BuLi in hexane (10.5 mL, 26.3 mmol, 1.07 eq.) at –78 °C under stirring.[170] The mixture was allowed to slowly warm up to room temperature (ca. 30 min) producing a clear colorless solution. All volatilities were removed *in vacuo* and the residue was dried (30 min, RT). The solid was dissolved in 150 mL of diethyl ether and treated with 2.5 M solution of *n*-BuLi in hexane (0.7 mL, 1.8 mmol, 0.07 eq.) at –78 °C under stirring.[171] The solution was allowed to slowly warm up to room temperature (ca. 30 min) and then was added dropwise under vigorous stirring to SiHCl$_3$ (7.5 mL, 10.1 g, 74.3 mmol, 3.0 eq.) at –78 °C. Precipitation of LiCl was observed. The mixture was allowed to warm up to room temperature and stirred then for 30 min. All volatilities were removed *in vacuo* and the residue (white) was dried (1 h, 40 °C). The solid was extracted with 100 mL of toluene at 100 °C and filtered hot. The clear colorless filtrate was concentrated *in vacuo* to about 20 mL, during this most of the product crystallizes.[172] Hexane (30 mL) was added and the mixture was stirred in an ice-bath for 10 min. The precipitate was filtered off at 0 °C, washed with hexane (2 × 10 mL) and dried *in vacuo* (30 min, 50 °C) to give a white microcrystalline solid. Yield 13.4 g (23.0 mmol, 94%). The product was shown by ^{1}H NMR spectroscopy to be pure.

---

[171] The second addition of *n*-BuLi is necessary to complete the conversion of ArI.

[172] The filtrate is pink, has the air leaked in. Notably, the originally reported procedure claimed, that the product was extracted with hexane. Following the procedure as described resulted in ridiculous yield, because the product is practically insoluble in hexane.

4.4 List of compounds prepared according to the established procedures

Compound	Experimenter	Reference
$(C_6H_3\text{-}2,6\text{-}Mes_2)I$; $(C_6H_3\text{-}2,6\text{-}Trip_2)I$	G. Hofer	[219]
$(C_6H_3\text{-}2,6\text{-}Dipp_2)I$	O. Chernov	[219]
NaC_5H_5	n/a	[216]
LiCp*; KCp*	O. Chernov	[220]
$FeCl_2$; $FeBr_2$	B. Beile/O. Chernov	[221]
$SiHI_3$	O. Chernov	[216]
IMe_2iPr_2	O. Chernov/K. W. Stumpf	[217]
$Ge(C_6H_3\text{-}2,6\text{-}Trip_2)Cl$	K. W. Stumpf	[222]
$(C_6H_3\text{-}2,6\text{-}Mes_2)NC$	G. Hofer	[21x]
$Li[Al(OC(CF_3)_3)_4]$	O. Chernov/Y. Lebedev	[223]
$Na[B(C_6H_3\text{-}3,5\text{-}CF_3)_4]$	N. Weidemann	[224]
$B(C_6F_5)_3$	O. Chernov	[225]
$Li[B(C_6F_5)_4]\cdot 2.5Et_2O$	U. Chakraborty/ O. Chernov	[226]
$Ru_3(CO)_{12}$; $[Cp^*Ru(CO)_2]_2$	O. Chernov	[227]
Pme_3	G. Hofer	[228]
$[Li(THF)_4][CPh_3]$	M. Speer	122
(2,4,6-trimethylphenyl)-phosphane	K. Kühnel-Lysek	–
$(Et_4N)N_3$	P. Portius	[229]
$[CpCo(C_2H_4)_2]$	O. Chernov/Y. Lebedev	[230]

4.5 List of commercially available reagents

Compound	Supplier	Purification
*n*BuLi (2.5 M in hexane)	ChemMetall	–
MeLi (1.6 M in Et_2O)	ChemMetall	–
Mg turnings	Aldrich	–
Li	ChemMetall	Washed with petrol ether
Na	n/a	Washed with petrol ether
K, 98%	Aldrich	Washed with petrol ether
Fe (powder)	Fluka	–
2,6-diisopropylaniline, 90+%	Alfa Aesar	–
2,4,6-trimethylaniline, 98%	Alfa Aesar	–
Glyoxal (40 wt% in water)	Acros	–
$(CH_2O)_n$	n/a	–
Trimethylsilyl chloride	Merck	–
$SiHCl_3$, 97%	ABCR	Neutralized with K_2CO_3
Hexamethyldisilazane, 98.5%	ABCR	–
N-Ethyldiisopropylamine, 99%	Alfa Aesar	–
C_6F_5Br; 99%	FluoroChem	–
$(CF_3)_3COH$, 97%	FluoroChem	–
Me_4NCl	Aldrich	Dried at 200 °C in vacuum
$LiAlH_4$	Aldrich	Extracted with Et_2O
$BF_3(Me_2O)$	n/a	–
C_2H_2 (in acetone)	Praxair	Passed through a condenser at – 78 °C
C_2H_4 (3.5)	Praxair	–

2-butyne, 98%	ABCR	Dried over CaH_2 and recondenced
3-hexyne, 99%	Aldrich	Dried over CaH_2 and recondenced
DCl, 98 atom% (4 M in 1,4-dioxane)	Aldrich	–
D_2O	Aldrich	Degassed prior to use
Br_2 (p.a.)	Merck	–
I_2	Grüssing	–
KPF_6	Aldrich	–
NH_3 (0.5 M in 1,4-dioxane)	Aldrich	–
$Cr(CO)_6$, 98%	Ventron	–
$Mo(CO)_6$ (p.a.)	Ventron/Fluka	–
$W(CO)_6$, 99%	Acros	–
HCl (37% in water)	Merck	–
CH_3COOH, 99–100%	Riedel-de-Haen	Degassed prior to use
N,N'-dimethylthiourea, 99%	Acros	–
N,N'-diisopropylthiourea, 99%	Aldrich	–
Triethyl orthoformate, ≥98%	Fluka	–
Acetoine, >96%	SAFC	–
1,2-dibromoethane	n/a	Distilled prior to use

5 Appendices

5.1 Crystallographic Data of Compounds

5.1.1 $[SiBr_3(IDipp)]Br \cdot 3CH_2Cl_2$ (15)

Empirical formula	$C_{30}H_{42}Br_4Cl_6N_2Si$	
Formula weight	991.09	
Temperature	123(2) K	
Wavelength	0.71073 Å	
Crystal system, space group	Triclinic, P –1	
Unit cell dimensions	a = 10.7906(8) Å	α = 114.572(3)°
	b = 13.9075(12) Å	β = 94.728(5)°
	c = 15.6922(13) Å	γ = 106.658(5)°
Volume	1996.1(3) $Å^3$	
Z, Calculated density	2, 1.649 $Mg \cdot m^{-3}$	
Absorption coefficient	4.488 mm^{-1}	
F(000)	984	
Crystal size	0.60 × 0.40 × 0.20 mm	
θ range for data collection	3.28 to 25.25°	
Limiting indices	$-12 \le h \le 12, -16 \le k \le 16, -18 \le l \le 18$	
Reflections collected / unique	18741 / 7135 [R(int) = 0.1480]	
Completeness to θ = 25.25	98.7%	
Absorption correction	Semi-empirical from equivalents	
Max. and min. transmission	0.489 and 0.201	
Refinement method	Full-matrix least-squares on F^2	
Data / restraints / parameters	7135 / 0 / 396	
Goodness-of-fit on F^2	1.008	
Final R indices [I>2sigma(I)]	$R_1 = 0.0699$, $wR_2 = 0.1597$	
R indices (all data)	$R_1 = 0.1276$, $wR_2 = 0.1840$	
Largest diff. peak and hole	1.000 and –1.443 $e \cdot Å^{-3}$	

5.1.2 $SiBr_2(IDipp)$ (16)

Empirical formula	$C_{27}H_{36}Br_2N_2Si$
Formula weight	576.49
Temperature	100(2) K
Wavelength	0.71073 Å

Crystal system, space group	Monoclinic, P 21/n		
Unit cell dimensions	a = 10.0268(4) Å	α = 90°	
	b = 19.3415(8) Å	β = 99.290(2)°	
	c = 14.7139(6) Å	γ = 90°	
Volume	2816.1(2) $Å^3$		
Z, Calculated density	4, 1.360 $Mg·m^{-3}$	Absorption coefficient	2.938 mm^{-1}
F(000)	1184		
Crystal size	0.60 × 0.32 × 0.04 mm		
θ range for data collection	1.75 to 28.00°		
Limiting indices	$-13 \le h \le 13$, $-25 \le k \le 25$, $-19 \le l \le 19$		
Reflections collected / unique	88994 / 6798 [R(int) = 0.1430]		
Completeness to θ = 28.00	100.0%		
Absorption correction	Semi-empirical from equivalents		
Max. and min. transmission	0.75902 and 0.35470		
Refinement method	Full-matrix least-squares on F^2		
Data / restraints / parameters	6798 / 0 / 297		
Goodness-of-fit on F^2	1.064		
Final R indices [I>2sigma(I)]	R_1 = 0.0471, wR_2 = 0.0851		
R indices (all data)	R_1 = 0.0685, wR_2 = 0.0949		
Largest diff. peak and hole	0.457 and –1.054 $e·Å^{-3}$		

5.1.3 $SiBr_2$(ISdipp) (20)

Empirical formula	$C_{27}H_{38}Br_2N_2Si$		
Formula weight	578.50		
Temperature	123(2) K		
Wavelength	0.71073 Å		
Crystal system, space group	Orthorhombic, P b c a		
Unit cell dimensions	a = 19.0176(3) Å	α = 90°	
	b = 19.4966(4) Å	β = 90°	
	c = 30.1211(4) Å	γ = 90°	
Volume	11168.3(3) $Å^3$		
Z, Calculated density	16, 1.376 $Mg·m^{-3}$		
Absorption coefficient	2.963 mm^{-1}		
F(000)	4768		
Crystal size	0.22 × 0.16 × 0.12 mm		
θ range for data collection	2.74 to 28.00°		
Limiting indices	$-25 \le h \le 21$, $-25 \le k \le 23$, $-39 \le l \le 39$		
Reflections collected / unique	76484 / 13459 [R(int) = 0.0803]		
Completeness to θ = 28.00	99.9%		

Absorption correction	Semi-empirical from equivalents
Max. and min. transmission	0.69192 and 0.58002
Refinement method	Full-matrix least-squares on F^2
Data / restraints / parameters	13459 / 0 / 593
Goodness-of-fit on F^2	0.874
Final R indices [I>2sigma(I)]	$R_1 = 0.0335$, $wR_2 = 0.0558$
R indices (all data)	$R_1 = 0.0745$, $wR_2 = 0.0618$
Largest diff. peak and hole	0.685 and –0.959 e·Å^{-3}

5.1.4 Si(C_6H_3-2,6-Mes_2)(IMe_4)Cl (28)

Empirical formula	$C_{69}H_{82}Cl_2N_4Si_2$	
Formula weight	1094.47	
Temperature	123(2) K	
Wavelength	0.71073 Å	
Crystal system, space group	Monoclinic, P 21/n	
Unit cell dimensions	a = 13.6805(3) Å	α = 90°
	b = 15.2312(3) Å	β = 100.972(2)°
	c = 30.2805(7) Å	γ = 90°
Volume	6194.2(2) Å^3	
Z, Calculated density	4, 1.174 Mg·m^{-3}	
Absorption coefficient	0.187 mm^{-1}	
F(000)	2344	
Crystal size	0.60 × 0.60 × 0.30 mm	
θ range for data collection	3.68 to 28.00°	
Limiting indices	$-17 \le h \le 18$, $-20 \le k \le 20$, $-39 \le l \le 39$	
Reflections collected / unique	76866 / 14893 [R(int) = 0.0567]	
Completeness to θ = 28.00	99.7%	
Absorption correction	Semi-empirical from equivalents	
Max. and min. transmission	0.9460 and 0.8960	
Refinement method	Full-matrix least-squares on F^2	
Data / restraints / parameters	14893 / 0 / 715	
Goodness-of-fit on F^2	1.055	
Final R indices [I>2sigma(I)]	$R_1 = 0.0447$, $wR_2 = 0.1305$	
R indices (all data)	$R_1 = 0.0582$, $wR_2 = 0.1362$	
Largest diff. peak and hole	0.808 and –0.294 e·Å^{-3}	

5.1.5 Si(C_6H_3-2,6-$Trip_2$)(IMe_4)Cl (29)

Empirical formula	$C_{46}H_{64}ClN_2Si$

Formula weight	708.53	
Temperature	123(2) K	
Wavelength	0.71073 Å	
Crystal system, space group	Monoclinic, P 21/n	
Unit cell dimensions	a = 12.5583(2) Å	α = 90°
	b = 16.2448(3) Å	β = 101.4300(9)°
	c = 21.2224(4) Å	γ = 90°
Volume	4243.65(13) $Å^3$	
Z, Calculated density	4, 1.109 $Mg·m^{-3}$	
Absorption coefficient	0.150 mm^{-1}	
F(000)	1540	
Crystal size	0.60 × 0.60 × 0.60 mm	
θ range for data collection	2.51 to 27.00°	
Limiting indices	$-16 \leq h \leq 16, -20 \leq k \leq 20, -27 \leq l \leq 26$	
Reflections collected / unique	60746 / 9246 [R(int) = 0.0761]	
Completeness to θ = 27.00	99.9%	
Absorption correction	Semi-empirical from equivalents	
Max. and min. transmission	0.9151 and 0.9151	
Refinement method	Full-matrix least-squares on F^2	
Data / restraints / parameters	9246 / 6 / 467	
Goodness-of-fit on F^2	1.058	
Final R indices [I>2sigma(I)]	R_1 = 0.0574, wR_2 = 0.1536	
R indices (all data)	R_1 = 0.0732, wR_2 = 0.1661	
Largest diff. peak and hole	1.612 and –0.632 $e·Å^{-3}$	

5.1.6 Si_2(ISdipp)$_2$ (21)

Empirical formula	$C_{54}H_{76}N_4Si_2$	
Formula weight	837.37	
Temperature	123(2) K	
Wavelength	0.71073 Å	
Crystal system, space group	Monoclinic, P 21/c	
Unit cell dimensions	a = 12.9429(8) Å	α = 90°
	b = 14.5144(10) Å	β = 118.791(4)°
	c = 15.2506(8) Å	γ = 90°
Volume	2510.8(3) $Å^3$	
Z, Calculated density	2, 1.108 $Mg·m^{-3}$	
Absorption coefficient	0.109 mm^{-1}	
F(000)	912	
Crystal size	0.20 × 0.08 × 0.02 mm	

θ range for data collection	2.81 to 28.00°
Limiting indices	$-13 \leq h \leq 17, -17 \leq k \leq 19, -20 \leq l \leq 17$
Reflections collected / unique	17399 / 5943 [R(int) = 0.0661]
Completeness to θ = 28.00	98.2%
Absorption correction	Semi-empirical from equivalents
Max. and min. transmission	0.9978 and 0.9786
Refinement method	Full-matrix least-squares on F^2
Data / restraints / parameters	5943 / 2 / 280
Goodness-of-fit on F^2	0.910
Final R indices [I>2sigma(I)]	$R_1 = 0.0448$, $wR_2 = 0.0943$
R indices (all data)	$R_1 = 0.0943$, $wR_2 = 0.1068$
Extinction coefficient	0.0039(7)
Largest diff. peak and hole	0.249 and –0.261 e·Å^{-3}

5.1.7 $[Si(IMe_4)_3]I_2 \cdot 2CH_2Cl_2$ (23)

Empirical formula	$C_{23}H_{40}Cl_4I_2N_6Si$	
Moiety formula	$C_{21}H_{36}N_6Si$, 2(CH_2Cl_2), 2(I)	
Formula weight	824.30	
Temperature	100(2) K	
Wavelength	0.71073 Å	
Crystal system, space group	Monoclinic, P 21/c	
Unit cell dimensions	a = 16.5785(6) Å	alpha = 90°.
	b = 11.8636(4) Å	beta = 99.1360(10)°.
	c = 17.3146(5) Å	gamma = 90°.
Volume	3362.25(19) Å^3	
Z, Calculated density	4, 1.628 Mg·m^{-3}	
Absorption coefficient	2.247 mm^{-1}	
F(000)	1632	
Crystal size	0.60 × 0.10 × 0.08 mm	
θ angle for data collection	2.49 to 28.00°.	
Limiting indices	$-21 \leq h \leq 21, -15 \leq k \leq 15, -22 \leq l \leq 15$	
Reflections collected / unique	31346 / 8086 [R(int) = 0.0392]	
Completeness to θ = 28.00	99.7 %	
Absorption correction	Semi-empirical from equivalents	
Max. and min. transmission	0.8407 and 0.3458	
Refinement method	Full-matrix least-squares on F^2	
Data / restraints / parameters	8086 / 0 / 337	
Goodness-of-fit on F^2	1.040	
Final R indices [I>2σ(I)]	$R_1 = 0.0311$, $wR_2 = 0.0677$	

R indices (all data)	$R_1 = 0.0442$, $wR_2 = 0.0740$	
Largest diff. peak and hole	1.573 and –0.626 e·A^{-3}	

5.1.8 [Si(C$_6$H$_3$-2,6-Mes$_2$)(IMe$_4$)]$_2$ (32)

Empirical formula	$C_{66}H_{84}N_4OSi_2$	
Formula weight	1005.55	
Temperature	123(2) K	
Wavelength	0.71073 Å	
Crystal system, space group	Monoclinic, C 2/c	
Unit cell dimensions	a = 19.2385(7) Å	α = 90°
	b = 12.1820(3) Å	β = 103.745(3)°
	c = 25.1160(10) Å	γ = 90°
Volume	5717.7(3) Å^3	
Z, Calculated density	4, 1.168 Mg·m^{-3}	
Absorption coefficient	0.108 mm^{-1}	
F(000)	2176	
Crystal size	0.38 × 0.26 × 0.09 mm	
θ range for data collection	3.66 to 26.00°	
Limiting indices	–21 ≤ h ≤ 23, –15 ≤ k ≤ 13, –30 ≤ l ≤ 30	
Reflections collected / unique	19764 / 5589 [R(int) = 0.0548]	
Completeness to θ = 26.00	99.5%	
Absorption correction	Integration	
Max. and min. transmission	0.9786 and 0.9281	
Refinement method	Full-matrix least-squares on F^2	
Data / restraints / parameters	5589 / 28 / 361	
Goodness-of-fit on F^2	1.099	
Final R indices [I>2sigma(I)]	$R_1 = 0.0778$, $wR_2 = 0.2102$	
R indices (all data)	$R_1 = 0.1003$, $wR_2 = 0.2193$	
Extinction coefficient	0.0019(4)	
Largest diff. peak and hole	0.620 and –0.443 e·Å^{-3}	

5.1.9 [K$_2$(IMe$_4$)$_3$][SiHR$_2$]$_2$ (34), "Mes"

Empirical formula	$C_{69}H_{86}K_2N_6Si_2$	
Formula weight	1133.82	
Temperature	123(2) K	
Wavelength	0.71073 Å	
Crystal system, space group	Monoclinic, C 2/c	
Unit cell dimensions	a = 24.6003(7) Å	α = 90°

	b = 13.7698(3) Å	β = 129.580(2)°
	c = 24.2194(6) Å	γ = 90°
Volume	6323.2(3) Å^3	
Z, Calculated density	4, 1.191 Mg·m^{-3}	
Absorption coefficient	0.233 mm^{-1}	
F(000)	2432	
Crystal size	0.584 × 0.178 × 0.174 mm	
θ range for data collection	2.89 to 28.00°	
Limiting indices	$-32 \le h \le 32$, $-16 \le k \le 18$, $-31 \le l \le 31$	
Reflections collected / unique	22227 / 7618 [R(int) = 0.0486]	
Completeness to θ = 28.00	99.7%	
Absorption correction	Integration	
Max. and min. transmission	0.9663 and 0.8730	
Refinement method	Full-matrix least-squares on F^2	
Data / restraints / parameters	7618 / 0 / 373	
Goodness-of-fit on F^2	0.909	
Final R indices [I>2sigma(I)]	R_1 = 0.0394, wR_2 = 0.0988	
R indices (all data)	R_1 = 0.0571, wR_2 = 0.1032	
Extinction coefficient	0.00156(18)	
Largest diff. peak and hole	0.307 and –0.417 e·Å^{-3}	

5.1.10 $[K(THF)]_2[SiHR_2]_2 \cdot C_6H_{14}$ (35), "Trip"

Empirical formula	$C_{92}H_{140}K_2O_2Si_2$	
Formula weight	1414.44	
Temperature	100(2) K	
Wavelength	0.71073 Å	
Crystal system, space group	Triclinic, P –1	
Unit cell dimensions	a = 11.4911(4) Å	α = 76.9710(10)°
	b = 12.1400(4) Å	β = 74.5290(10)°
	c = 16.4617(5) Å	γ = 73.2300(10)°
Volume	2091.49(12) Å^3	
Z, Calculated density	1, 1.123 Mg·m^{-3}	
Absorption coefficient	0.188 mm^{-1}	
F(000)	776	
Crystal size	0.4 × 0.24 × 0.08 mm	
θ range for data collection	2.36 to 26.00°	
Limiting indices	$-14 \le h \le 11$, $-13 \le k \le 14$, $-20 \le l \le 18$	
Reflections collected / unique	10532 / 7730 [R(int) = 0.0679]	
Completeness to θ = 26.00	94.1%	

Absorption correction	Semi-empirical from equivalents
Refinement method	Full-matrix least-squares on F^2
Data / restraints / parameters	7730 / 88 / 480
Goodness-of-fit on F^2	1.079
Final R indices [I>2sigma(I)]	R_1 = 0.0750, wR_2 = 0.2121
R indices (all data)	R_1 = 0.1012, wR_2 = 0.2325
Largest diff. peak and hole	1.038 and –0.860 e·Å^{-3}

5.1.11 Si(C_6H_3-2,6-Mes_2)H(1-CH_2-IMe_4–2-(PF_5))F·Et_2O·0.5C_6H_{14} (36)

Empirical formula	$C_{50}H_{78}F_6N_2OPSi$	
Formula weight	896.20	
Temperature	100(2) K	
Wavelength	0.71073 Å	
Crystal system, space group	Triclinic, P –1	
Unit cell dimensions	a = 9.3342(7) Å	α = 91.933(2)°
	b = 12.6877(10) Å	β = 99.631(3)°
	c = 22.5398(19) Å	γ = 106.054(2)°
Volume	2520.1(3) Å^3	
Z, Calculated density	2, 1.181 Mg·m^{-3}	
Absorption coefficient	0.137 mm^{-1}	
F(000)	966	
Crystal size	0.32 × 0.28 × 0.06 mm	
θ range for data collection	2.38 to 28.00°	
Limiting indices	-9 ≤ h ≤ 12, –16 ≤ k ≤ 11, –29 ≤ l ≤ 29	
Reflections collected / unique	37226 / 12012 [R(int) = 0.0771]	
Completeness to θ = 28.00	98.6%	
Absorption correction	Semi-empirical from equivalents	
Max. and min. transmission	0.9918 and 0.9575	
Refinement method	Full-matrix least-squares on F^2	
Data / restraints / parameters	12012 / 0 / 569	
Goodness-of-fit on F^2	0.971	
Final R indices [I>2sigma(I)]	R_1 = 0.0595, wR_2 = 0.1312	
R indices (all data)	R_1 = 0.1326, wR_2 = 0.1555	
Extinction coefficient	0.0026(8)	
Largest diff. peak and hole	1.044 and –0.360 e·Å^{-3}	

5.1.12 [(SiCl(C_6H_3-2,6-$Trip_2$)(IMe_4)){P_4}(Si(C_6H_3-2,6-$Trip_2$)(IMe_4))]Cl (37)

Empirical formula	$C_{74}H_{98}Cl_2N_4O_3P_4Si_2$

Formula weight	1342.52	
Temperature	100(2) K	
Wavelength	0.71073 Å	
Crystal system, space group	Triclinic, P –1	
Unit cell dimensions	a = 11.9481(3) Å	α = 68.072(2)°
	b = 16.3583(4) Å	β = 81.887(2)°
	c = 20.3076(5) Å	γ = 82.765(2)°
Volume	3633.52(16) $Å^3$	
Z, Calculated density	2, 1.227 $Mg·m^{-3}$	
Absorption coefficient	0.259 mm^{-1}	
F(000)	1432	
Crystal size	0.48 × 0.48 × 0.14 mm	
θ range for data collection	1.09 to 28.00°	
Limiting indices	$-15 \leq h \leq 14, -18 \leq k \leq 21, -24 \leq l \leq 23$	
Reflections collected / unique	19158 / 14783 [R(int) = 0.0943]	
Completeness to θ = 28.00	84.3%	
Absorption correction	Semi-empirical from equivalents	
Max. and min. transmission	0.95 and 0.90	
Refinement method	Full-matrix least-squares on F^2	
Data / restraints / parameters	14783 / 90 / 822	
Goodness-of-fit on F^2	1.119	
Final R indices [I>2sigma(I)]	R_1 = 0.0946, wR_2 = 0.2776	
R indices (all data)	R_1 = 0.1434, wR_2 = 0.3202	
Largest diff. peak and hole	4.157 and –1.693 $e·Å^{-3}$	

5.1.13 [CpCo{Si(C_6H_3-2,6-$Trip_2$)Cl(IMe_4)}] (38)

Empirical formula	$C_{101}H_{144}Cl_2Co_2N_4Si_2$	
Formula weight	1659.14	
Temperature	100(2) K	
Wavelength	0.71073 Å	
Crystal system, space group	Triclinic, P –1	
Unit cell dimensions	a = 15.1333(18) Å	α = 97.635(4)°
	b = 16.8965(19) Å	β = 95.937(4)°
	c = 20.961(2) Å	γ = 115.375(3)°
Volume	4722.1(9) $Å^3$	
Z, Calculated density	2, 1.167 $Mg·m^{-3}$	
Absorption coefficient	0.480 mm^{-1}	
F(000)	1788	
Crystal size	0.60 × 0.30 × 0.10 mm	

θ range for data collection	1.81 to 26.00°
Limiting indices	$-18 \le h \le 18, -20 \le k \le 19, -25 \le l \le 25$
Reflections collected / unique	39580 / 18038 [R(int) = 0.0711]
Completeness to θ = 26.00	97.2%
Absorption correction	Empirical
Max. and min. transmission	0.7458 and 0.6244
Refinement method	Full-matrix least-squares on F^2
Data / restraints / parameters	18038 / 0 / 1034
Goodness-of-fit on F^2	0.912
Final R indices [I>2sigma(I)]	$R_1 = 0.0497$, $wR_2 = 0.1196$
R indices (all data)	$R_1 = 0.0999$, $wR_2 = 0.1411$
Largest diff. peak and hole	0.770 and –0.575 e·Å^{-3}

5.1.14 [CpMo(CO)$_2$=Si(C$_6$H$_3$-2,6-Trip$_2$)(IMe$_4$)]·PhMe (42)

Empirical formula	$C_{57}H_{74}MoN_2O_2Si$	
Formula weight	943.21	
Temperature	100(2) K	
Wavelength	0.71073 Å	
Crystal system, space group	Monoclinic, P21/n	
Unit cell dimensions	a = 11.1325(4) Å	α = 90°
	b = 27.7444(10) Å	β = 91.5660(10)°
	c = 33.0433(12) Å	γ = 90°
Volume	10202.1(6) Å^3	
Z, Calculated density	8, 1.228 Mg·m^{-3}	
Absorption coefficient	0.323 mm^{-1}	
F(000)	4016	
Crystal size	0.60 × 0.12 × 0.12 mm	
θ range for data collection	0.96 to 27.00°	
Limiting indices	$-14 \le h \le 13, -35 \le k \le 35, -41 \le l \le 42$	
Reflections collected / unique	79759 / 22261 [R(int) = 0.0343]	
Completeness to θ = 27.00	99.9%	
Max. and min. transmission	0.9623 and 0.8299	
Refinement method	Full-matrix-block least-squares on F^2	
Data / restraints / parameters	22261 / 157 / 1267	
Goodness-of-fit on F^2	1.071	
Final R indices [I>2sigma(I)]	$R_1 = 0.0559$, $wR_2 = 0.1407$	
R indices (all data)	$R_1 = 0.0688$, $wR_2 = 0.1494$	
Largest diff. peak and hole	3.089 and –0.858 e·Å^{-3}	

5.1.15 [{Si(C_6H_3-2,6-$Trip_2$)H(1-CH_2-IMe_3)}$_2$][CpMo(CO)$_3$]$_2$ (46)

Empirical formula	$C_{226}H_{290}MoN_8O_{13}Si_4$	
Formula weight	3822.78	
Temperature	123(2) K	
Wavelength	0.71073 Å	
Crystal system, space group	Monoclinic, C 2/c	
Unit cell dimensions	a = 29.6269(3) Å	α = 90°
	b = 25.8034(4) Å	β = 90.5500(8)°
	c = 26.8059(3) Å	γ = 90°
Volume	20491.5(4) Å^3	
Z, Calculated density	4, 1.239 Mg·m^{-3}	
Absorption coefficient	0.324 mm^{-1}	
F(000)	8120	
Crystal size	0.48 × 0.32 × 0.32 mm	
θ range for data collection	2.34 to 28.00°	
Limiting indices	$-39 \le h \le 39$, $-31 \le k \le 34$, $-35 \le l \le 35$	
Reflections collected / unique	94897 / 24449 [R(int) = 0.0652]	
Completeness to θ = 28.00	98.8%	
Absorption correction	Semi-empirical from equivalents	
Max. and min. transmission	0.9034 and 0.8600	
Refinement method	Full-matrix least-squares on F^2	
Data / restraints / parameters	24449 / 283 / 1250	
Goodness-of-fit on F^2	1.044	
Final R indices [I>2sigma(I)]	R_1 = 0.0687, wR_2 = 0.1888	
R indices (all data)	R_1 = 0.1007, wR_2 = 0.2153	
Largest diff. peak and hole	2.060 and –1.897 e·Å^{-3}	

5.1.16 [CpCr(CO)$_2$=SiBr(ISdipp)]·0.5C_6H_{14} (49)

Empirical formula	$C_{37}H_{50}BrCrN_2O_2Si$	
Moiety formula	$C_{34}H_{43}BrCrN_2O_2Si$,·0.5(C_6H_{14})	
Formula weight	714.79	
Temperature	100(2) K	
Wavelength	0.71073 Å	
Crystal system, space group	Orthorhombic, P b c a	
Unit cell dimensions	a = 14.6096(7) Å	α = 90°
	b = 18.6056(8) Å	β = 90°
	c = 26.0831(9) Å	γ = 90°
Volume	7089.9(5) Å^3	
Z, Calculated density	8, 1.339 Mg·m^{-3}	

Absorption coefficient	1.518 mm^{-1}
F(000)	3000
Crystal size	0.60 × 0.12 × 0.10 mm
θ range for data collection	2.32 to 28.00°
Limiting indices	$-19 \le h \le 19$, $-24 \le k \le 23$, $-22 \le l \le 34$
Reflections collected / unique	45591 / 8551 [R(int) = 0.0683]
Completeness to θ = 28.00	99.8%
Absorption correction	Empirical
Max. and min. transmission	0.8630 and 0.4629
Refinement method	Full-matrix least-squares on F^2
Data / restraints / parameters	8551 / 22 / 405
Goodness-of-fit on F^2	1.032
Final R indices [I>2sigma(I)]	R_1 = 0.0453, wR_2 = 0.1076
R indices (all data)	R_1 = 0.0776, wR_2 = 0.1219
Largest diff. peak and hole	1.002 and –0.696 e·$Å^{-3}$

5.1.17 [(C_5Me_5)Mo(CO)$_2$=SiI(IDipp)] (53-Mo)

Empirical formula	$C_{39}H_{51}IMoN_2O_2Si$	
Formula weight	830.75	
Temperature	123(2) K	
Wavelength	0.71073 Å	
Crystal system, space group	Monoclinic, C 2/c	
Unit cell dimensions	a = 31.7443(7) Å	α = 90°
	b = 13.7342(3) Å	β = 109.3840(13)°
	c = 19.4194(4) Å	γ = 90°
Volume	7986.6(3) $Å^3$	
Z, Calculated density	8, 1.382 Mg·m^{-3}	
Absorption coefficient	1.164 mm^{-1}	
F(000)	3392	
Crystal size	0.60 × 0.60 × 0.04 mm	
θ range for data collection	2.52 to 27.00°	
Limiting indices	$-40 \le h \le 40$, $-17 \le k \le 17$, $-24 \le l \le 24$	
Reflections collected / unique	69917 / 8711 [R(int) = 0.0584]	
Completeness to θ = 27.00	99.9%	
Absorption correction	Semi-empirical from equivalents	
Max. and min. transmission	0.83034 and 0.54749	
Refinement method	Full-matrix least-squares on F^2	
Data / restraints / parameters	8711 / 12 / 428	
Goodness-of-fit on F^2	1.065	

Final R indices [I>2sigma(I)]	1 = 0.0325, wR_2 = 0.0843
R indices (all data)	1 = 0.0438, wR_2 = 0.0901
Largest diff. peak and hole	1.322 and –0.564 e·Å^{-3}

5.1.18 [*trans*-CpMo(CO)$_2$(PMe$_3$)SiI$_2$]$_2$ (48)

Empirical formula	$C_{28}H_{44}I_4Mo_2O_6P_2Si_2$	
Formula weight	1294.23	
Temperature	123(2) K	
Wavelength	0.71073 Å	
Crystal system, space group	Monoclinic, P 21/c	
Unit cell dimensions	a = 15.8677(5) Å	α = 90°
	b = 12.0815(2) Å	β = 102.4940(12)°
	c = 21.8470(6) Å	γ = 90°
Volume	4089.01(18) Å^3	
Z, Calculated density	4, 2.102 Mg·m^{-3}	
Absorption coefficient	3.806 mm^{-1}	
F(000)	2456	
Crystal size	0.25 × 0.16 × 0.10 mm	
θ range for data collection	2.45 to 28.00°	
Limiting indices	–20 ≤ h ≤ 18, –15 ≤ k ≤ 14, –28 ≤ l ≤ 22	
Reflections collected / unique	26769 / 9588 [R(int) = 0.0498]	
Completeness to θ = 28.00	97.3%	
Absorption correction	Semi-empirical from equivalents	
Max. and min. transmission	0.66378 and 0.59241	
Refinement method	Full-matrix least-squares on F^2	
Data / restraints / parameters	9588 / 180 / 449	
Goodness-of-fit on F^2	0.956	
Final R indices [I>2sigma(I)]	R_1 = 0.0330, wR_2 = 0.0668	
R indices (all data)	R_1 = 0.0527, wR_2 = 0.0724	
Largest diff. peak and hole	1.366 and –1.369 e·Å^{-3}	

5.1.19 [CpCr(CO)$_2$Si(IMe$_2$*i*Pr$_2$)Br] (55)

Empirical formula	$C_{35}H_{51}BrCrN_4O_2Si$
Moiety formula	$C_{29}H_{45}BrCrN_4O_2Si$, C_6H_6
Formula weight	719.80
Temperature	123(2) K
Wavelength	0.71073 Å
Crystal system, space group	Monoclinic, P 21/c

Unit cell dimensions	a = 10.8143(3) Å	α = 90°
	b = 11.8568(3) Å	β = 96.0620(10)°
	c = 27.4144(7) Å	γ = 90°
Volume	3495.50(16) $Å^3$	
Z, Calculated density	4, 1.368 $Mg·m^{-3}$	
Absorption coefficient	1.541 mm^{-1}	
F(000)	1512	
Crystal size	0.24 × 0.10 × 0.02 mm	
θ range for data collection	3.27 to 28.00°	
Limiting indices	$-14 \leq h \leq 14$, $-15 \leq k \leq 15$, $-36 \leq l \leq 22$	
Reflections collected / unique	26685 / 8425 [R(int) = 0.0326]	
Completeness to θ = 28.00	99.8%	
Absorption correction	Empirical	
Max. and min. transmission	0.9698 and 0.7086	
Refinement method	Full-matrix least-squares on F^2	
Data / restraints / parameters	8425 / 2 / 409	
Goodness-of-fit on F^2	1.007	
Final R indices [I>2sigma(I)]	R_1 = 0.0392, wR_2 = 0.1242	
R indices (all data)	R_1 = 0.0479, wR_2 = 0.1299	
Largest diff. peak and hole	0.870 and –1.221 $e·Å^{-3}$	

5.1.20 [Cp(CO)Cr(μ-COSi(IMe$_2$*i*Pr$_2$)$_2$)$_2$Cr(CO)Cp][B(C$_6$F$_5$)$_4$]$_2$·C$_6$H$_5$F (57)

Empirical formula	$C_{112}H_{95}B_2Cr_2F_{41}N_8O_4Si2$	
Moiety formula	$C_{58}H_{90}Cr_2N_8O_4Si_2$, $2(C_{24}BF_{20})$, C_6H_5F	
Formula weight	2577.76	
Temperature	100(2) K	
Wavelength	0.71073 Å	
Crystal system, space group	Triclinic, P –1	
Unit cell dimensions	a = 13.1338(7) Å	α = 87.404(3)°
	b = 13.5459(8) Å	β = 81.489(2)°
	c = 15.9070(8) Å	γ = 84.110(3)°
Volume	2782.8(3) $Å^3$	
Z, Calculated density	1, 1.538 $Mg·m^{-3}$	
Absorption coefficient	0.343 mm^{-1}	
F(000)	1310	
Crystal size	0.60 × 0.20 × 0.02 mm	
θ range for data collection	1.58 to 28.00°	
Limiting indices	$-17 \leq h \leq 17$, $-17 \leq k \leq 17$, $0 \leq l \leq 21$	
Reflections collected / unique	45652 / 13152 [R(int) = 0.0833]	

Completeness to θ = 28.00	97.9%
Absorption correction	Empirical
Max. and min. transmission	0.9932 and 0.8207
Refinement method	Full-matrix least-squares on F^2
Data / restraints / parameters	30192 / 10 / 788
Goodness-of-fit on F^2	1.048
Final R indices [I>2sigma(I)]	R_1 = 0.0642, wR_2 = 0.1274
R indices (all data)	R_1 = 0.1020, wR_2 = 0.1459
Largest diff. peak and hole	0.576 and –0.768 e·Å^{-3}

5.1.21 [(η^5-(C$_6$F$_5$)$_3$B-C$_5$H$_4$)Mo(CO)$_2$(μ-H)=SiAr^{Trip}(IMe$_4$)]·2PhMe (59)

Empirical formula	$C_{82}H_{82}BF_{15}MoN_2O_2Si$	
Formula weight	1547.34	
Temperature	123(2) K	
Wavelength	0.71073 Å	
Crystal system, space group	Triclinic, P –1	
Unit cell dimensions	a = 13.2916(4) Å	α = 99.9559(18)°
	b = 17.1779(5) Å	β = 94.242(2)°
	c = 17.1780(5) Å	γ = 104.9980(16)°
Volume	3702.29(19) Å^3	
Z, Calculated density	2, 1.388 Mg·m^{-3}	
Absorption coefficient	0.280 mm^{-1}	
F(000)	1600	
Crystal size	0.32 × 0.31 × 0.27 mm	
θ range for data collection	2.29 to 28.00°	
Limiting indices	–17 ≤ h ≤ 17, –22 ≤ k ≤ 21, –20 ≤ l ≤ 22	
Reflections collected / unique	42460 / 17313 [R(int) = 0.1016]	
Completeness to θ = 28.00	96.8%	
Absorption correction	Semi-empirical from equivalents	
Max. and min. transmission	0.9292 and 0.9152	
Refinement method	Full-matrix least-squares on F^2	
Data / restraints / parameters	17313 / 60 / 959	
Goodness-of-fit on F^2	1.024	
Final R indices [I>2sigma(I)]	R_1 = 0.0497, wR_2 = 0.1204	
R indices (all data)	R_1 = 0.0768, wR_2 = 0.1323	
Largest diff. peak and hole	1.721 and –1.142 e·Å^{-3}	

5.1.22 [CpMo(CO)$_2$≡Si(C$_6$H$_3$-2,6-Trip$_2$)]·C$_5$H$_{12}$ (60)

Empirical formula	$C_{48}H_{66}MoO_2Si$	
Formula weight	799.04	
Temperature	100(2) K	
Wavelength	0.71073 Å	
Crystal system, space group	Monoclinic, P 21/c	
Unit cell dimensions	a = 9.4075(3) Å	α = 90°
	b = 17.9074(7) Å	β = 95.966(2)°
	c = 26.8309(11) Å	γ = 90°
Volume	4495.6(3) Å^3	
Z, Calculated density	4, 1.181 Mg·m^{-3}	
Absorption coefficient	0.353 mm^{-1}	
F(000)	1704	
Crystal size	0.36 × 0.06 × 0.04 mm	
θ range for data collection	2.74 to 28.00°	
Limiting indices	$-12 \le h \le 10$, $-23 \le k \le 23$, $-35 \le l \le 35$	
Reflections collected / unique	64226 / 10821 [R(int) = 0.0647]	
Completeness to θ = 28.00	99.6%	
Absorption correction	Semi-empirical from equivalents	
Max. and min. transmission	0.9860 and 0.8834	
Refinement method	Full-matrix least-squares on F^2	
Data / restraints / parameters	10821 / 0 / 481	
Goodness-of-fit on F^2	1.046	
Final R indices [I>2sigma(I)]	R_1 = 0.0421, wR_2 = 0.0922	
R indices (all data)	R_1 = 0.0671, wR_2 = 0.1015	
Largest diff. peak and hole	0.677 and –0.671 e·Å^{-3}	

5.1.23 [Cp*Cr(CO)$_2$≡Si(ISdipp)][B(C$_6$H$_2$-3,5-(CF$_3$)$_2$)$_4$] (62-Cr)

Empirical formula	$C_{71}H_{65}BCrF_{24}N_2O_2Si$	
Moiety formula	$C_{39}H_{53}CrN_2O_2Si$, $C_{32}H_{12}BF_{24}$	
Formula weight	1525.15	
Temperature	100(2) K	
Wavelength	0.71073 Å	
Crystal system, space group	Monoclinic, P 21/c	
Unit cell dimensions	a = 19.4621(8) Å	α = 90°
	b = 19.0087(8) Å	β = 101.686(2)°
	c = 19.6420(8) Å	γ = 90°
Volume	7115.9(5) Å^3	
Z, Calculated density	4, 1.424 Mg·m^{-3}	

Absorption coefficient	0.286 mm^{-1}
F(000)	3120
Crystal size	0.40 × 0.36 × 0.08 mm
θ range for data collection	2.37 to 28.00°.
Limiting indices	–25≤h≤25, –24≤k≤25, –25≤l≤23
Reflections collected / unique	97939 / 17056 [R(int) = 0.0570]
Completeness to θ = 28.00	99.4%
Absorption correction	Empirical
Max. and min. transmission	0.9775 and 0.8941
Refinement method	Full-matrix least-squares on F^2
Data / restraints / parameters	17056 / 133 / 988
Goodness-of-fit on F^2	1.031
Final R indices [I>2σ(I)]	R_1 = 0.0610, wR_2 = 0.1349
R indices (all data)	R_1 = 0.1033, wR_2 = 0.1497
Largest diff. peak and hole	0.827 and –0.729 $e \cdot A^{-3}$

5.1.24 [Cp(CO)$_2$Mo(μ-H)=Si(C$_6$H$_3$-2,6-Trip$_2$)(NH$_2$)] (66)

Empirical formula	$C_{43}H_{57}MoNO_2Si$	
Formula weight	743.93	
Temperature	123(2) K	
Wavelength	0.71073 Å	
Crystal system, space group	Monoclinic, P 21/n	
Unit cell dimensions	a = 14.457(2) Å	α = 90°.
	b = 11.5555(19) Å	β = 102.280(5)°.
	c = 24.088(4) Å	γ = 90°.
Volume	3932.0(11) $Å^3$	
Z, Calculated density	4, 1.257 $M \cdot gm^{-3}$	
Absorption coefficient	0.399 mm^{-1}	
F(000)	1576	
Crystal size	0.48 × 0.20 × 0.16 mm	
θ range for data collection	2.54 to 28.00°.	
Limiting indices	-18 ≤ h ≤ 19, -15 ≤ k ≤ 15, -31 ≤ l ≤ 30	
Reflections collected / unique	83261 / 9482 [R(int) = 0.0388]	
Completeness to θ = 28.00	99.9 %	
Absorption correction	Empirical	
Max. and min. transmission	0.9389 and 0.8315	
Refinement method	Full-matrix least-squares on F^2	
Data / restraints / parameters	9482 / 9 / 457	
Goodness-of-fit on F^2	1.040	

Final R indices [I>2sigma(I)]	$R_1 = 0.0250$, $wR_2 = 0.0604$
R indices (all data)	$R_1 = 0.0316$, $wR_2 = 0.0633$
Largest diff. peak and hole	0.426 and –0.400 e·A^{-3}

5.1.25 [CpMo(CO)$_2${η^2-(P,Si)-MesPH–SiH(C$_6$H$_3$-2,6-Trip$_2$)}·2.5C$_6$H$_{14}$ (69)

Empirical formula	$C_{67}H_{102}MoO_2PSi$	
Moiety formula	$C_{52}H_{67}MoO_2PSi$, 2.5(C_6H_{14})	
Formula weight	1094.49	
Temperature	123(2) K	
Wavelength	0.71073 Å	
Crystal system, space group	Triclinic, P –1	
Unit cell dimensions	a = 13.1554(6) Å	α = 67.972(3)°
	b = 16.5886(12) Å	β = 85.358(4)°
	c = 16.8440(13) Å	γ = 69.325(3)°
Volume	3182.5(4) Å^3	
Z, Calculated density	2, 1.142 Mg·m^{-3}	
Absorption coefficient	0.290 mm^{-1}	
F(000)	1182	
Crystal size	0.48 × 0.32 × 0.24 mm	
θ range for data collection	3.12 to 28.00°	
Limiting indices	–17 ≤ h ≤ 17, –21 ≤ k ≤ 21, –22 ≤ l ≤ 22	
Reflections collected / unique	54753 / 15018 [R(int) = 0.2946]	
Completeness to θ = 28.00	97.7%	
Absorption correction	Semi-empirical from equivalents	
Max. and min. transmission	0.9336 and 0.8732	
Refinement method	Full-matrix least-squares on F^2	
Data / restraints / parameters	15018 / 124 / 674	
Goodness-of-fit on F^2	0.966	
Final R indices [I>2sigma(I)]	$R_1 = 0.0989$, $wR_2 = 0.2363$	
R indices (all data)	$R_1 = 0.2280$, $wR_2 = 0.2960$	
Largest diff. peak and hole	1.748 and –0.839 e·Å^{-3}	

5.1.26 [NMe$_4$][CpMo(CO)2=SiCl(C$_6$H$_3$-2,6-Trip$_2$)] (70-Cl)

Empirical formula	$C_{54}H_{74}ClMoNO_2Si$
Formula weight	928.62
Temperature	123(2) K
Wavelength	0.71073 Å
Crystal system, space group	Triclinic, P –1

Unit cell dimensions	a = 10.3003(18) Å	α = 63.729(5)°
	b = 16.703(3) Å	β = 73.721(6)°
	c = 17.346(2) Å	γ = 77.256(6)°
Volume	2552.7(7) $Å^3$	
Z, Calculated density	2, 1.208 $Mg·m^{-3}$	
Absorption coefficient	0.371 mm^{-1}	
F(000)	988	
Crystal size	0.48 × 0.12 × 0.04 mm	
θ range for data collection	2.16 to 26.00°	
Limiting indices	$-12 \le h \le 12, -18 \le k \le 20, 0 \le l \le 21$	
Reflections collected / unique	10003 / 10003 [R(int) = 0.0790]	
Completeness to θ = 26.00	99.6%	
Absorption correction	Semi-empirical from equivalents	
Max. and min. transmission	0.9709 and 0.9162	
Refinement method	Full-matrix least-squares on F^2	
Data / restraints / parameters	10003 / 25 / 557	
Goodness-of-fit on F^2	1.013	
Final R indices [I>2sigma(I)]	R_1 = 0.0567, wR_2 = 0.1283	
R indices (all data)	R_1 = 0.0971, wR_2 = 0.1415	
Largest diff. peak and hole	1.117 and –1.239 $e·Å^{-3}$	

5.1.27 [NEt_4][$CpMo(CO)_2$=$Si(N_3)(C_6H_3$-2,6-$Trip_2)$] (71-N_3)

Empirical formula	$C_{65}H_{90}MoN_4O_2Si$	
Formula weight	1083.44	
Temperature	123(2) K	
Wavelength	0.71073 Å	
Crystal system, space group	Triclinic, P –1	
Unit cell dimensions	a = 11.7975(9) Å	α = 84.691(3)°
	b = 15.1247(12) Å	β = 85.949(3)°
	c = 19.0876(15) Å	γ = 71.201(3)°
Volume	3207.3(4) $Å^3$	
Z, Calculated density	2, 1.122 $Mg·m^{-3}$	
Absorption coefficient	0.265 mm^{-1}	
F(000)	1160	
Crystal size	0.6 × 0.38 × 0.1 mm	
θ range for data collection	1.83 to 25.25°	
Limiting indices	$-14 \le h \le 14, -17 \le k \le 18, -19 \le l \le 22$	
Reflections collected / unique	34396 / 11582 [R(int) = 0.0533]	
Completeness to θ = 25.25	99.8%	

Absorption correction	Semi-empirical from equivalents
Refinement method	Full-matrix least-squares on F^2
Data / restraints / parameters	11582 / 0 / 709
Goodness-of-fit on F^2	1.028
Final R indices [I>2sigma(I)]	$R_1 = 0.0663$, $wR_2 = 0.1732$
R indices (all data)	$R_1 = 0.1015$, $wR_2 = 0.1887$
Largest diff. peak and hole	2.307 and –0.693 e·Å^{-3}

5.1.28 [μ-Li(Et$_2$O)$_2$)]$_2$[CpMo(CO)$_2$=Si(C$_6$H$_3$-2,6-Trip$_2$)Me]$_2$·Et$_2$O (72)

Empirical formula	$C_{108}H_{164}Li_2Mo_2O_9Si_2$	
Moiety formula	$C_{104}H_{154}Li_2Mo_2O_8Si_2$, $C_4H_{10}O$	
Formula weight	1868.33	
Temperature	123(2) K	
Wavelength	0.71073 Å	
Crystal system, space group	Triclinic, P –1	
Unit cell dimensions	a = 13.2613(3) Å	α = 81.5123(18)°
	b = 13.3119(5) Å	β = 78.841(2)°
	c = 16.6015(6) Å	γ = 67.901(2)°
Volume	2655.03(15) Å^3	
Z, Calculated density	1, 1.169 Mg·m^{-3}	
Absorption coefficient	0.311 mm^{-1}	
F(000)	1002	
Crystal size	0.24 × 0.24 × 0.04 mm	
θ range for data collection	2.51 to 27.00°	
Limiting indices	$-16 \le h \le 16$, $-16 \le k \le 17$, $-21 \le l \le 19$	
Reflections collected / unique	30273 / 11505 [R(int) = 0.0539]	
Completeness to θ = 27.00	99.4%	
Absorption correction	Semi-empirical from equivalents	
Max. and min. transmission	0.9877 and 0.9291	
Refinement method	Full-matrix least-squares on F^2	
Data / restraints / parameters	11505 / 58 / 594	
Goodness-of-fit on F^2	1.019	
Final R indices [I>2sigma(I)]	$R_1 = 0.0379$, $wR_2 = 0.0923$	
R indices (all data)	$R_1 = 0.0549$, $wR_2 = 0.0978$	
Largest diff. peak and hole	0.537 and –0.730 e·Å^{-3}	

5.1.29 Li$_2$(DME)$_2$[CpMo(CO)$_2$Si(C$_6$H$_3$-2,6-Trip$_2$)Me$_2$]·1.5Et$_2$O (73)

Empirical formula	$C_{118}H_{190}Li_4Mo_2O_{15}Si_2$

Moiety formula	$C_{106}H_{160}Li_4Mo_2O_{12}Si_2,·3(C_4H_{10}O)$	
Formula weight	2124.52	
Temperature	100(2) K	
Wavelength	0.71073 Å	
Crystal system, space group	Triclinic, P –1	
Unit cell dimensions	a = 12.6214(18) Å	α = 93.260(4)°
	b = 15.353(2) Å	β = 90.946(4)°
	c = 16.018(3) Å	γ = 106.560(4)°
Volume	2968.7(8) $Å^3$	
Z, Calculated density	1, 1.188 $Mg·m^{-3}$	
Absorption coefficient	0.289 mm^{-1}	
F(000)	1142	
Crystal size	0.40 × 0.30 × 0.08 mm	
θ range for data collection	2.77 to 28.00°	
Limiting indices	$–16 \leq h \leq 16, –20 \leq k \leq 20, 0 \leq l \leq 21$	
Reflections collected / unique	31796 / 14190 [R(int) = 0.0534]	
Completeness to θ = 28.00	98.9%	
Absorption correction	Empirical	
Max. and min. transmission	0.9772 and 0.8930	
Refinement method	Full-matrix least-squares on F^2	
Data / restraints / parameters	14190 / 26 / 679	
Goodness-of-fit on F^2	1.163	
Final R indices [I>2sigma(I)]	$R_1 = 0.0421$, $wR_2 = 0.1179$	
R indices (all data)	$R_1 = 0.0484$, $wR_2 = 0.1203$	
Largest diff. peak and hole	0.969 and $–0.786\ e·Å^{-3}$	

5.1.30 $[K(DME)]_2[CpMo(CO)_2\text{-}SiR_3]$ (74)

Empirical formula	$C_{204}H_{292}K_8Mo_4O_{22}Si_4$	
Formula weight	3905.30	
Temperature	296(2) K	
Wavelength	0.71073 Å	
Crystal system, space group	Triclinic, P –1	
Unit cell dimensions	a = 12.5582(10) Å	α = 87.235(5)°
	b = 20.2469(17) Å	β = 84.697(4)°
	c = 20.3662(16) Å	γ = 86.380(4)°
Volume	5141.3(7) $Å^3$	
Z, Calculated density	1, 1.261 $Mg·m^{-3}$	
Absorption coefficient	0.484 mm^{-1}	
F(000)	2068	

Crystal size	0.60 × 0.12 × 0.12 mm
θ range for data collection	1.01 to 25.25°
Limiting indices	–14 ≤ h ≤ 15, –24 ≤ k ≤ 24, 0 ≤ l ≤ 24
Reflections collected / unique	56332 / 17427 [R(int) = 0.0961]
Completeness to θ = 25.25	93.6%
Absorption correction	Empirical
Max. and min. transmission	0.7461 and 0.3330
Refinement method	Full-matrix least-squares on F^2
Data / restraints / parameters	21268 / 120 / 1115
Goodness-of-fit on F^2	1.014
Final R indices [I>2sigma(I)]	R_1 = 0.0846, wR_2 = 0.2126
R indices (all data)	R_1 = 0.1227, wR_2 = 0.2416
Largest diff. peak and hole	1.977 and –1.105 e·Å^{-3}

5.1.31 [Cp(CO)$_2$Mo{SiC(Me)C(Me)(C$_6$H$_3$-2,6-Trip$_2$)}] (76)

Empirical formula	$C_{47}H_{60}MoO_2Si$	
Formula weight	780.98	
Temperature	123(2) K	
Wavelength	0.71073 Å	
Crystal system, space group	Triclinic, P –1	
Unit cell dimensions	a = 11.0549(2) Å	α = 107.1320(9)°
	b = 13.3974(2) Å	β = 98.8837(10)°
	c = 16.2495(3) Å	γ = 108.3700(10)°
Volume	2099.99(6) Å^3	
Z, Calculated density	2, 1.235 Mg·m^{-3}	
Absorption coefficient	0.376 mm^{-1}	
F(000)	828	
Crystal size	0.60 × 0.60 × 0.60 mm	
θ range for data collection	2.54 to 28.00°	
Limiting indices	–14 ≤ h ≤ 14, –17 ≤ k ≤ 17, –21 ≤ l ≤ 21	
Reflections collected / unique	40382 / 10070 [R(int) = 0.0571]	
Completeness to θ = 28.00	99.1%	
Absorption correction	Semi-empirical from equivalents	
Max. and min. transmission	0.8056 and 0.8056	
Refinement method	Full-matrix least-squares on F^2	
Data / restraints / parameters	10070 / 329 / 496	
Goodness-of-fit on F^2	1.067	
Final R indices [I>2sigma(I)]	R_1 = 0.0361, wR_2 = 0.0893	
R indices (all data)	R_1 = 0.0483, wR_2 = 0.0945	

Extinction coefficient	0.0025(7)
Largest diff. peak and hole	0.719 and –0.910 e·Å^{-3}

5.1.32 [Cp(CO)$_2$Mo{SiC(Ph)C(Me)(C$_6$H$_3$-2,6-Trip$_2$)}] (78)

Empirical formula	$C_{53}H_{65}MoNO_2Si$	
Formula weight	872.09	
Temperature	100(2) K	
Wavelength	0.71073 Å	
Crystal system, space group	Triclinic, P –1	
Unit cell dimensions	a = 11.978(4) Å	α = 106.104(9)°
	b = 18.167(5) Å	β = 96.273(9)°
	c = 22.715(7) Å	γ = 90.282(9)°
Volume	4718(2) Å^3	
Z, Calculated density	4, 1.228 Mg·m^{-3}	
Absorption coefficient	0.343 mm^{-1}	
F(000)	1848	
Crystal size	0.2 × 0.18 × 0.02 mm	
θ range for data collection	0.94 to 25.25°	
Limiting indices	$-14 \le h \le 14$, $-21 \le k \le 20$, $0 \le l \le 27$	
Reflections collected / unique	48510 / 15640 [R(int) = 0.1213]	
Completeness to θ = 25.25	91.0%	
Absorption correction	Empirical	
Max. and min. transmission	0.99 and 0.93	
Refinement method	Full-matrix least-squares on F^2	
Data / restraints / parameters	15640 / 306 / 1046	
Goodness-of-fit on F^2	1.081	
Final R indices [I>2sigma(I)]	R_1 = 0.0737, wR_2 = 0.1928	
R indices (all data)	R_1 = 0.1368, wR_2 = 0.2372	
Largest diff. peak and hole	1.368 and –1.278 e·Å^{-3}	

5.1.33 [Cp(CO)$_2$Mo{η^3-Si(C$_6$H$_3$-2,6-Trip$_2$)C(H)C(C$_6$H$_4$-4-OMe)C(H)C(C$_6$H$_4$-4-OMe)}] (81)

Empirical formula	$C_{61}H_{70}MoO_4Si$	
Formula weight	991.20	
Temperature	123(2) K	
Wavelength	0.71073 Å	
Crystal system, space group	Orthorhombic, P n a 21	
Unit cell dimensions	a = 29.8964(9) Å	α = 90°

	b = 11.8178(3) Å	β = 90°
	c = 14.9937(4) Å	γ = 90°
Volume	5297.4(3) $Å^3$	
Z, Calculated density	4, 1.243 $Mg·m^{-3}$	
Absorption coefficient	0.316 mm^{-1}	
F(000)	2096	
Crystal size	0.37 × 0.18 × 0.12 mm	
θ range for data collection	2.73 to 25.99°	
Limiting indices	$-33 \leq h \leq 36, -14 \leq k \leq 13, -18 \leq l \leq 18$	
Reflections collected / unique	28738 / 10377 [R(int) = 0.0530]	
Completeness to θ = 25.99	99.4%	
Absorption correction	Integration	
Max. and min. transmission	0.9540 and 0.8402	
Refinement method	Full-matrix least-squares on F^2	
Data / restraints / parameters	10377 / 25 / 624	
Goodness-of-fit on F^2	0.968	
Final R indices [I>2sigma(I)]	R_1 = 0.0485, wR_2 = 0.1121	
R indices (all data)	R_1 = 0.0639, wR_2 = 0.1187	
Absolute structure parameter	-0.01(3)	
Largest diff. peak and hole	0.465 and –0.431 $e·Å^{-3}$	

5.1.34 $[(\eta^5\text{-}C_5Me_5)(CO)_2CrSi(ISdipp)C(Me)C(Me)][Al(OC(CF_3)_3)_4]$ (83-Cr)

Empirical formula	$C_{59}H_{59}AlCrF_{36}N_2O_6Si$	
Moiety formula	$C_{43}H_{59}CrN_2O_2Si$, $C_{16}AlF_{36}O_4$	
Formula weight	1683.15	
Temperature	123(2) K	
Wavelength	0.71073 A	
Crystal system, space group	Orthorhombic, P 21 21 21	
Unit cell dimensions	a = 17.8878(4) Å	alpha = 90°.
	b = 19.3120(4) Å	beta = 90°.
	c = 20.3643(5) Å	gamma = 90°.
Volume	7034.8(3) $Å^3$	
Z, Calculated density	4, 1.589 gcm^3	
Absorption coefficient	0.337 mm^{-1}	
F(000)	3400	
Crystal size	0.30 x 0.30 x 0.20 mm	
θ range for data collection	2.91 to 28.00°.	
Limiting indices	$-23 \leq h \leq 19, -25 \leq k \leq 23, -25 \leq l \leq 26$	
Reflections collected / unique	32928 / 16968 [R(int) = 0.0525]	

Completeness to θ= 28.0	99.8%
Absorption correction	integration
Max. and min. transmission	0.9469 and 0.9220
Refinement method	Full-matrix least-squares on F^2
Data / restraints / parameters	6968 / 0 / 970
Goodness-of-fit on F^2	0.812
Final R indices [I>2σ(I)]	R_1 = 0.0443, wR_2 = 0.0423
R indices (all data)	R_1 = 0.0821, wR_2 = 0.0483
Absolute structure parameter	012(13)
Largest diff. peak and hole	0301 and –0.340 e·A^{-3}

5.1.35 [$Cp(CO)_2Fe–Ge(C_6H_3$-2,6-$Trip_2)$] (84)

Empirical formula	$C_{43}H_{54}FeGeO_2$	
Formula weight	731.30	
Temperature	123(2) K	
Wavelength	0.71073 Å	
Crystal system, space group	Orthorhombic, P n m a	
Unit cell dimensions	a = 14.6376(3) Å	α = 90°
	b = 23.9730(6) Å	β = 90°
	c = 10.8195(2) Å	γ = 90°
Volume	3796.64(14) $Å^3$	
Z, Calculated density	4, 1.279 Mg·m^{-3}	
Absorption coefficient	1.208 mm^{-1}	
F(000)	1544	
Crystal size	0.60 × 0.40 × 0.12 mm	
θ range for data collection	2.78 to 27.99°	
Limiting indices	$–17 \le h \le 19$, $–31 \le k \le 27$, $–14 \le l \le 12$	
Reflections collected / unique	35027 / 4678 [R(int) = 0.0706]	
Completeness to θ = 27.99	99.8%	
Absorption correction	Semi-empirical from equivalents	
Max. and min. transmission	0.8686 and 0.5310	
Refinement method	Full-matrix least-squares on F^2	
Data / restraints / parameters	4678 / 2 / 261	
Goodness-of-fit on F^2	1.007	
Final R indices [I>2sigma(I)]	R_1 = 0.0400, wR_2 = 0.1017	
R indices (all data)	R_1 = 0.0647, wR_2 = 0.1100	
Extinction coefficient	0.0042(4)	
Largest diff. peak and hole	0.715 and –0.608 e·$Å^{-3}$	

5.1.36 [Cp*(CO)$_2$Ru–Ge(C$_6$H$_3$-2,6-Trip$_2$)] (86)

Empirical formula	$C_{53}H_{76}GeO_2Ru$	
Formula weight	918.80	
Temperature	123(2) K	
Wavelength	0.71073 Å	
Crystal system, space group	Monoclinic, P 21/c	
Unit cell dimensions	a = 11.3110(5) Å	α = 90°
	b = 40.8113(11) Å	β = 111.449(3)°
	c = 11.5777(5) Å	γ = 90°
Volume	4974.3(3) Å^3	
Z, Calculated density	4, 1.227 Mg·m^{-3}	
Absorption coefficient	0.944 mm^{-1}	
F(000)	1944	
Crystal size	0.20 × 0.20 × 0.14 mm	
θ range for data collection	2.94 to 26.00°	
Limiting indices	$-13 \le h \le 13$, $-50 \le k \le 48$, $-14 \le l \le 14$	
Reflections collected / unique	40195 / 9740 [R(int) = 0.0923]	
Completeness to θ = 26.00	99.8%	
Absorption correction	Semi-empirical from equivalents	
Max. and min. transmission	1.1067 and 0.7629	
Refinement method	Full-matrix least-squares on F^2	
Data / restraints / parameters	9740 / 50 / 533	
Goodness-of-fit on F^2	0.905	
Final R indices [I>2sigma(I)]	R_1 = 0.0426, wR_2 = 0.0884	
R indices (all data)	R_1 = 0.0753, wR_2 = 0.0968	
Largest diff. peak and hole	0.516 and –0.565 e·Å^{-3}	

5.1.37 [(η^5-C$_5$(CH=(2-IMe$_4$)Me$_4$)(CO)$_2$Ru–GeH$_2$(C$_6$H$_3$-2,6-Trip$_2$)] (88)

Empirical formula	$C_{55}H_{76}GeN_2O_2Ru$	
Moiety formula	$C_{55}H_{76}GeN_2O_2Ru$	
Formula weight	970.84	
Temperature	123(2) K	
Wavelength	0.71073 Å	
Crystal system, space group	Monoclinic, P 21/n	
Unit cell dimensions	a = 16.8010(6) Å	α = 90°
	b = 16.2013(3) Å	β = 91.1843(13)°
	c = 18.6650(7) Å	γ = 90°
Volume	5079.5(3) Å^3	
Z, Calculated density	4, 1.270 Mg·m^{-3}	

Absorption coefficient	0.930 mm^{-1}
F(000)	2048
Crystal size	0.60 × 0.32 × 0.28 mm
θ range for data collection	2.52 to 28.00°
Limiting indices	$-16 \le h \le 22$, $-21 \le k \le 20$, $-19 \le l \le 24$
Reflections collected / unique	32035 / 11926 [R(int) = 0.0780]
Completeness to θ = 28.00	97.2%
Absorption correction	Semi-empirical from equivalents
Max. and min. transmission	0.7808 and 0.6055
Refinement method	Full-matrix least-squares on F^2
Data / restraints / parameters	11926 / 0 / 578
Goodness-of-fit on F^2	0.876
Final R indices [I>2sigma(I)]	R_1 = 0.0391, wR_2 = 0.0738
R indices (all data)	R_1 = 0.0906, wR_2 = 0.0859
Largest diff. peak and hole	0.951 and –1.221 e·$Å^{-3}$

5.1.38 [Fe(IMes)$_2$Cl$_2$] (89-Cl)

Empirical formula	$C_{42}H_{48}Cl_2FeN_4$	
Formula weight	735.59	
Temperature	123(2) K	
Wavelength	0.71073 Å	
Crystal system, space group	Triclinic, P –1	
Unit cell dimensions	a = 9.7165(3) Å	α = 79.434(2)°
	b = 10.6639(3) Å	β = 79.589(2)°
	c = 19.8371(6) Å	γ = 70.322(2)°
Volume	1886.81(10) $Å^3$	
Z, Calculated density	2, 1.295 Mg·m^{-3}	
Absorption coefficient	0.576 mm^{-1}	
F(000)	776	
Crystal size	0.60 × 0.15 × 0.10 mm	
θ range for data collection	2.05 to 28.00°	
Limiting indices	$-12 \le h \le 12$, $-14 \le k \le 14$, $-26 \le l \le 26$	
Reflections collected / unique	32619 / 9100 [R(int) = 0.1009]	
Completeness to θ = 28.00	99.9%	
Absorption correction	Integration	
Max. and min. transmission	0.9542 and 0.8092	
Refinement method	Full-matrix least-squares on F^2	
Data / restraints / parameters	9100 / 0 / 454	
Goodness-of-fit on F^2	1.027	

Final R indices [I>2sigma(I)]	$R_1 = 0.0399$, $wR_2 = 0.0980$
R indices (all data)	$R_1 = 0.0487$, $wR_2 = 0.1006$
Largest diff. peak and hole	0.758 and –0.746 e·Å^{-3}

5.1.39 [Fe(IDipp)Cl(μ-Cl)]$_2$·2C$_6$D$_6$ (90)

Empirical formula	$C_{78}H_{96}Cl_4Fe_2N_4$	
Formula weight	1343.09	
Temperature	123(2) K	
Wavelength	0.71073 Å	
Crystal system, space group	Triclinic, P –1	
Unit cell dimensions	a = 10.5915(3) Å	α = 70.8523(16)°
	b = 12.3124(2) Å	β = 88.7243(15)°
	c = 16.0115(4) Å	γ = 66.5959(16)°
Volume	1796.10(7) Å^3	
Z, Calculated density	1, 1.242 Mg·m^{-3}	
Absorption coefficient	0.597 mm^{-1}	
F(000)	712	
Crystal size	0.53 × 0.46 × 0.45 mm	
θ range for data collection	2.65 to 28.00°	
Limiting indices	$-13 \le h \le 13$, $-16 \le k \le 16$, $-21 \le l \le 21$	
Reflections collected / unique	22958 / 8408 [R(int) = 0.0426]	
Completeness to θ = 28.00	97.0%	
Absorption correction	Semi-empirical from equivalents	
Max. and min. transmission	0.88126 and 0.75082	
Refinement method	Full-matrix least-squares on F^2	
Data / restraints / parameters	8408 / 0 / 406	
Goodness-of-fit on F^2	1.033	
Final R indices [I>2sigma(I)]	$R_1 = 0.0313$, $wR_2 = 0.0792$	
R indices (all data)	$R_1 = 0.0411$, $wR_2 = 0.0825$	
Extinction coefficient	0.0040(7)	
Largest diff. peak and hole	0.332 and –0.441 e·Å^{-3}	

5.1.40 [Fe(IMes)$_2$(CH$_3$)$_2$] (91)

Empirical formula	$C_{44}H_{54}FeN_4$
Formula weight	694.76
Temperature	123(2) K
Wavelength	0.71073 Å
Crystal system, space group	Monoclinic, C 2/c

Unit cell dimensions	a = 20.7807(3) Å	α = 90°
	b = 20.7862(4) Å	β = 107.5810(10)°
	c = 18.8908(3) Å	γ = 90°
Volume	7778.8(2) $Å^3$	
Z, Calculated density	8, 1.186 $Mg·m^{-3}$	
Absorption coefficient	0.422 mm^{-1}	
F(000)	2976	
Crystal size	0.26 × 0.14 × 0.07 mm	
θ range for data collection	2.92 to 27.51°	
Limiting indices	$-26 \le h \le 26$, $-26 \le k \le 26$, $-24 \le l \le 24$	
Reflections collected / unique	34380 / 8921 [R(int) = 0.1052]	
Completeness to θ = 27.51	99.7%	
Absorption correction	Semi-empirical from equivalents	
Refinement method	Full-matrix least-squares on F^2	
Data / restraints / parameters	8921 / 0 / 457	
Goodness-of-fit on F^2	0.631	
Final R indices [I>2sigma(I)]	R_1 = 0.0258, wR_2 = 0.0297	
R indices (all data)	R_1 = 0.1266, wR_2 = 0.0560	
Largest diff. peak and hole	0.296 and –0.817 $e·Å^{-3}$	

5.1.41 [Fe(IMes)$_2$Cl] (92)

Empirical formula	$C_{42}H_{48}ClFeN_4$	
Formula weight	700.14	
Temperature	123(2) K	
Wavelength	0.71073 Å	
Crystal system, space group	Monoclinic, P 21	
Unit cell dimensions	a = 10.6941(4) Å	α = 90°
	b = 13.0816(4) Å	β = 102.186(3)°
	c = 13.9966(5) Å	γ = 90°
Volume	1913.95(11) $Å^3$	
Z, Calculated density	2, 1.215 $Mg·m^{-3}$	
Absorption coefficient	0.497 mm^{-1}	
F(000)	742	
Crystal size	0.40 × 0.30 × 0.05 mm	
θ range for data collection	2.15 to 28.00°	
Limiting indices	$-14 \le h \le 14$, $-17 \le k \le 17$, $-18 \le l \le 18$	
Reflections collected / unique	24682 / 9094 [R(int) = 0.0732]	
Completeness to θ = 28.00	100.0%	
Absorption correction	Semi-empirical from equivalents	

Max. and min. transmission	0.97562 and 0.82913
Refinement method	Full-matrix least-squares on F^2
Data / restraints / parameters	9094 / 1 / 445
Goodness-of-fit on F^2	0.955Final R indices [I>2sigma(I)] R_1 = 0.0505, wR_2 = 0.1137
R indices (all data)	R_1 = 0.0666, wR_2 = 0.1181
Absolute structure parameter	0.026(16)
Largest diff. peak and hole	1.320 and –0.259 e·Å^{-3}

5.2 List of Abbreviations

*n*Bu	*n*-butyl
*t*Bu	*tert*-butyl
BDE	bond dissociation energy
ca.	circa
Cp	η^5-cyclopentadienyl (C_5H_5)
Cp*	η^5-pentamethylcyclopentadienyl (C_5Me_5)
Cg	center of gravity
$\Delta\nu_{½}$	half height width
dec.	decomposition
depe	1,2-bis(diethylphosphino)ethane
DFT	density functional theory
Dipp	2,6-diisopropylphenyl
dmpe	1,2-bis(diethylphosphino)ethane
EPR	electron paramagnetic resonance
eq.	equivalents
Et_2O	diethyl ether
et al.	and others
h	hour
IDipp	1,3-bis(2,6-diisopropylphenyl)imidazol-2-ylidene
in situ	in place (Latin)
in vacuo	under vacuum
IMe_4	1,3,4,5-tetramethylimidazol-2-ylidene
IMe_2iPr_2	1,3-diisopropyl-4,5-dimethylimidazol-2-ylidene
IR	infra red
ISdipp	1,3-bis(2,6-diisopropylphenyl)imidazolidin-2-ylidene

Mes	2,4,6-trimethylphenyl
m.p.	melting point
NMR	nuclear magnetic resonance
ppm	parts per million
RT	room temperature
THF	tetrahydrofuran
TMS	trimethylsilyl
Trip	2,4,6-triisopropylphenyl
vide infra	see below (Latin)
vide supra	see above (Latin)
WBI	Wiberg bond index

5.3 Scientific Contributions from this work

Journal articles

- Chromium–Silicon Multiple Bonds: The Chemistry of Terminal N-Heterocyclic-Carbene-Stabilized Halosilylidyne Ligands. A. C. Filippou, O. Chernov, G. Schnakenburg, *Chemistry - A European Journal*, **2011**, *17*, 13574.
- Metal–silicon triple bonds: Nucleophilic addition and redox reactions of the silylidyne complex [$Cp(CO)_2Mo{\equiv}Si–R$]. A. C. Filippou, O. Chernov, G. Schnakenburg, *Angewandte Chemie*, **2011**, *123*, 1154. *Angewandte Chemie International Edition*, **2011**, *50*, 1122.
- Metal–silicon triple bonds: The molybdenum silylidyne complex [$Cp(CO)_2Mo{\equiv}Si–R$]. A. C. Filippou, O. Chernov, K. W. Stumpf, G. Schnakenburg, *Angewandte Chemie*, **2010**, *122*, 3368. *Angewandte Chemie International Edition*, **2010**, *49*, 3296.
- Stable N-Heterocyclic carbene adducts of arylchlorosilylenes and their germanium homologues. A. C. Filippou, O. Chernov, B. Blom, K. W. Stumpf, G. Schnakenburg, *Chemistry – A European Journal*, **2010**, *16*, 2866.
- $SiBr_2$(IDipp): A stable N-Heterocyclic carbene adduct of dibromosilylene. A. C. Filippou, O. Chernov, G. Schnakenburg, *Angewandte Chemie* **2009**, *121*, 5797. *Angewandte Chemie International Edition*, **2009**, *48*, 5687.

Poster sessions

- Metal–Silicon Triple Bonds: the First Silylidyne Complex. A. C. Filippou, O. Chernov, K. W. Stumpf, G. Schnakenburg, 3rd EuCheMS Chemistry Congress, 08–09.2010, Nürnberg, Germany

Lectures

- Recent advances in the chemistry of low-valent silicon compounds. Inorganic chemistry colloquium at Institute of Inorganic Chemistry, University of Bonn, 2011.

This page was intentionally left blank

Other publications

- Metal Activation of a Germylenoid, a New Approach to Metal−Germanium Triple Bonds: Synthesis and Reactions of the Germylidyne Complexes $[Cp(CO)_2M{\equiv}Ge{-}C(SiMe_3)_3]$ (M = Mo, W). A. C. Filippou, K. W. Stumpf, O. Chernov, G. Schnakenburg. *Organometallics* **2012**, *31*, 748.
- In search for a pentacoordinated monoorgano stannyl cation. M. S. Nechaev, O. V. Chernov, I. A. Portnyagin, V. N. Khrustalev, R. R. Aysin, V. V. Lunin. *Journal of Organometallic Chemistry*, **2010**, *695*, 365.
- Heteroleptic tin(II) dialkoxides stabilized by intramolecular coordination $Sn(OCH_2CH_2NMe_2)(OR)$ (R = Me, Et, *i*Pr, *t*Bu, Ph). Synthesis, structure and catalytic activity in polyurethane synthesis. O. V. Chernov, A. Yu. Smirnov, I. A. Portnyagin, V. N. Khrustalev, M. S. Nechaev. *Journal of Organometallic Chemistry*, **2009***, 694,* 3184.
- Heteronuclear bonding between heavier Group 14 elements and transition metals: novel trioxystannate–iron complex $\{[Li][(Me_2NCH_2CH_2O)_3Sn\text{-}Fe(CO)_4]\}_2$ with unusual stannate fragment. V. N. Khrustalev, I. A. Portnyagin, O. V. Chernov, M. S. Nechaev, R. R. Aysin, S. S. Bukalov, *Dalton Transactions*, **2008**, 1140.

5.4 Oath of Compliance with the Principles of Scientific Integrity

I hereby affirm that this dissertation was prepared independently at the Institute of Inorganic Chemistry, University of Bonn under the guidance of Prof. Dr. A. C. Filippou, and that all references and additional sources have been appropriately cited.

Oleg Chernov

Bonn, April 2012.

5.6 References

[1] P. Müller, *Pure Appl. Chem.* **1994**, *66*, 1077.

[2] G. P. Moss, P. A. S. Smith, D. Tavernier, *Pure Appl. Chem.* **1995**, *67*, 1307.

[3] a) J. Sauer, P. Carsky, R. Zahradnik, *Collect. Czech. Chem. Commun. 1982, 47, 1149-1168* **1982**, *47*, 1149; b) Y. Apeloig, *The Chemistry of Organic Silicon Compounds, Vol. 1*, Wiley, Chichester, **1989**; c) M. Karni, Y. Apeloig, J. Kapp, P. v. R. Schleyer, *The Chemistry of Organic Silicon Compounds, Vol. 3*, Wiley, Chichester, **2001**.

[4] a) M. J. S. Dewar, C. Jie, *Organometallics* **1987**, *6*, 1486; b) W. S. Scheldrick, *The Chemistry of Organic Silicon Compounds, Vol. 3*, Wiley, Chichester, **1989**.

[5] P. L. Timms, R. A. Kent, T. C. Ehlert, J. L. Margrave, *J. Am. Chem. Soc.* **1965**, *87*, 2824.

[6] J. C. Thompson, J. L. Margrave, *Science* **1967**, *155*, 669.

[7] R. Schwarz, G. Pietsoh, *Z. Anorg. Allg. Chem.* **1937**, *232*, 249.

[8] R. K. Asundi, M. Karim, R. Samuel, *Proc. Phys. Soc.* **1938**, *50*, 581.

[9] W. H. Atwell, D. R. Weyenberg, *Angew. Chem.* **1969**, *81*, 485.

[10] O. M. Nefedow, M. N. Manakow, *Angew. Chem.* **1966**, *78*, 1039.

[11] C.-S. Liu, T.-L. Hwang, *Adv. Inorg. Chem. Radiochem.* **1985**, *29*, 1.

[12] H. Schäfer, J. Nickl, *Z. Anorg. Allg. Chem.* **1953**, *274*, 250.

[13] E. Wolf, C. Herbst, *Z. Anorg. Allg. Chem.* **1966**, *347*, 113.

[14] M. Schmeißer, K. Friederich, *Angew. Chem.* **1964**, *76*, 782.

[15] H. Schäfer, B. Morcher, *Z. Anorg. Allg. Chem.* **1957**, *290*, 279.

[16] V. I. Zubkov, M. V. Tikhomirov, K. A. Andrianov, S. A. Golubtzov, *Proc. Acad. Sci. USSR, Chem. Sec. (engl. translation)* **1964**, *159*, 599.

[17] P. S. Skell, E. J. Goldstein, *J. Am. Chem. Soc.* **1964**, *86*, 1442.

[18] E. Sirtl, K. Reuschel, *Z. Anorg. Allg. Chem.* **1964**, *332*, 113.

[19] M. Schmeißer, K. P. Ehlers, *Angew. Chem.* **1964**, *76*, 781.

[20] a) W. H. Atwell, D. R. Weyenberg, *J. Organomet. Chem.* **1966**, *5*, 594; b) W. H. Atwell, D. R. Weyenberg, *J. Am. Chem. Soc.* **1968**, *90*, 3438; I. M. T. Davidson, K. J. Hughes, S. Ijadi-Maghsoodi, c) *Organometallics* **1987**, *6*, 639.

[21] H. Schäfer, *Z. Anorg. Allg. Chem.* **1953**, *274*, 265.

[22] a) O. P. Strausz, K. Obi, W. K. Duholke, *J. Am. Chem. Soc.* **1968**, *90*, 1359; b) K. Obi, A. Clement, H. E. Gunning, O. P. Strausz, *J. Am. Chem. Soc.* **1969**, *91*, 1622.

[23] a) G. R. Gillette, G. H. Noren, R. West, *Organometallics* **1989**, *8*, 487; b) C. A. Arrington, J. T. Petty, S. E. Payne, W. C. K. Haskins, *J. Am. Chem. Soc.* **1988**, *110*, 6240; c) M. A. Pearsall, R. West, *J. Am. Chem. Soc.* **1988**, *110*, 7228; d) W. Ando, A. Sekiguchi, K. Hagiwara, A. Sakakibara, H. Yoshida, *Organometallics* **1988**, *7*, 558; e) G. Levin, P. K. Das, C. L. Lee, *Organometallics* **1988**, *7*, 1231; f) W. Ando, K. Hagiwara, A. Sekiguchi, *Organometallics* **1987**, *6*, 2270; g) G. R. Gillette, G. H. Noren, R. West, *Organometallics* **1987**, *6*, 2617.

[24] N. Takeda, H. Suzuki, N. Tokitoh, R. Okazaki, S. Nagase, *J. Am. Chem. Soc.* **1997**, *119*, 1456.

[25] U. Herzog, R. Richter, E. Brendler, G. Roewer, *J. Organomet. Chem.* **1996**, *507*, 221.

[26] F. Meyer-Wegner, A. Nadj, M. Bolte, N. Auner, M. Wagner, M. C. Holthausen, H.-W. Lerner, *Chem. Eur. J.* **2011**, *17*, 4715.

[27] a) G. Sawitzki, H. G. V. Schnering, *Chem. Ber.* **1976**, *109*, 3728; b) D. Kummer, H. Köster, *Angew. Chem. Int. Ed. Engl.* **1969**, *8*, 878.

[28] S. Herzog, F. Krebs, *Zeitschrift für Chemie* **1968**, *8*, 149.

[29] A. G. MacDiarmid, P. M. Broudy, J. Chu, C. M. Mikulski, P. J. Russo, B. B. Wayland, D. Weber, Univ. Coll., Dublin, Dep. Chem., **1974**, pp. 2.24a.

[30] a) G. D. Cooper, A. R. Gilbert, *J. Am. Chem. Soc.* **1960**, *82*, 5042; b) L.-P. Müller, W.-W. D. Mont, J. Jeske, P. G. Jones, *Chem. Ber.* **1995**, *128*, 615; c) W.-W. du Mont, L. Müller, R. Martens, P. M. Papathomas, B. A. Smart, H. E. Robertson, D. W. H. Rankin, *Eur. J. Inorg. Chem.* **1999**, 1381.

[31] J. Heinicke, B. Gehrhus, S. Meinel, *J. Organomet. Chem.* **1994**, *474*, 71.

[32] W.-W. du Mont, T. Gust, E. Seppälä, C. Wismach, P. G. Jones, L. Ernst, J. Grunenberg, H. C. Marsmann, *Angew. Chem.* **2002**, *114*, 3977.

[33] G. P. Moss, P. A. S. Smith, D. Tavernier, *Pure Appl. Chem.* **1995**, *67*, 1307.

[34] N. Wiberg, W. Niedermayer, *J. Organomet. Chem.* **2001**, *628*, 57.

[35] M. E. Lee, H. M. Cho, M. S. Ryu, C. H. Kim, W. Ando, *J. Am. Chem. Soc.* **2001**, *123*, 7732.

[36] Z. Wang, in *Comprehensive Organic Name Reactions and Reagents*, John Wiley & Sons, Inc., **2010**.

[37] R. A. Benkeser, *Acc. Chem. Res.* **1971**, *4*, 94.

[38] R. A. Benkeser, S. Dunny, P. R. Jones, *J. Organomet. Chem.* **1965**, *4*, 338.

[39] R. A. Benkeser, W. E. Smith, *J. Am. Chem. Soc.* **1968**, *90*, 5307.

[40] a) R. A. Benkeser, K. M. Foley, J. M. Gaul, G. S. H. Li, *J. Am. Chem. Soc.* **1970**, *92*, 3232; b) R. A. Benkeser, G. S. Li, E. C. Mozdzen, *J. Organomet. Chem.* **1979**, *178*, 21; c) R. A. Benkeser, K. M. Foley, J. M. Gaul, G. S. H. Li, W. E. Smith, *J. Am. Chem. Soc.* **1969**, *91*, 4578; d) R. A. Benkeser, W. E. Smith, *J. Am. Chem. Soc.* **1969**, *91*, 1556.

[41] R. A. Benkeser, J. M. Gaul, W. E. Smith, *J. Am. Chem. Soc.* **1969**, *91*, 3666.

[42] R. A. Benkeser, D. C. Snyder, *J. Organomet. Chem.* **1982**, *225*, 107.

[43] R. A. Benkeser, K. M. Voley, J. B. Grutzner, W. E. Smith, *J. Am. Chem. Soc.* **1970**, *92*, 697.

[44] a) H.-H. Karsch, P. Schlueter, **1997**, DE19711154A1; b) H. H. Karsch, P. A. Schlueter, F. Bienlein, M. Herker, E. Witt, A. Sladek, M. Heckel, *Z. Anorg. Allg. Chem.* **1998**, *624*, 295.

[45] a) R. S. Ghadwal, H. W. Roesky, S. Merkel, J. Henn, D. Stalke, *Angew. Chem.* **2009**, *121*, 5793; b) R. S. Ghadwal, H. W. Roesky, S. Merkel, J. Henn, D. Stalke, *Angew. Chem. Int. Ed.* **2009**, *48*, 5683.

[46] a) N. J. Hill, R. West, *J. Organomet. Chem.* **2004**, *689*, 4165; b) K. Mitsuo, *J. Organomet. Chem.* **2004**, *689*, 4475; M. Asay, C. Jones, M. Driess, *Chem. Rev.* **2011**, *111*, 354; c) M. Weidenbruch, *Coord. Chem. Rev.* **1994**, *130*, 275; d) S. Yao, Y. Xiong, M. Driess, *Organometallics* **2011**, *30*, 1748.

[47] B. Gehrhus, M. F. Lappert, *J. Organomet. Chem.* **2001**, *617-618*, 209.

[48] P. Jutzi, U. Holtmann, D. Kanne, C. Krüger, R. Blom, R. Gleiter, I. Hyla-Kryspin, *Chem. Ber.* **1989**, *122*, 1629.

[49] P. Jutzi, A. Mix, B. Rummel, W. W. Schoeller, B. Neumann, H.-G. Stammler, *Science* **2004**, *305*, 849.

[50] P. Jutzi, K. Leszczynska, A. Mix, B. Neumann, B. Rummel, W. Schoeller, H.-G. Stammler, *Organometallics* **2010**, *29*, 4759.

[51] P. Jutzi, A. Mix, B. Neumann, B. Rummel, H.-G. Stammler, *J. Chem. Soc., Chem. Commun.* **2006**, 3519.

[52] a) H. H. Karsch, U. Keller, S. Gamper, G. Müller, *Angew. Chem. Int. Ed. Engl.* **1990**, *29*, 295; b) H. H. Karsch, U. Keller, S. Gamper, G. Müller, *Angew. Chem.* **1990**, *102*, 297.

[53] A. J. Arduengo, R. L. Harlow, M. Kline, *J. Am. Chem. Soc.* **1991**, *113*, 361.

[54] M. Veith, E. Werle, R. Lisowsky, R. Köppe, H. Schnöckel, *Chem. Ber.* **1992**, *125*, 1375.

[55] M. Denk, R. Lennon, R. Hayashi, R. West, A. V. Belyakov, H. P. Verne, A. Haaland, M. Wagner, N. Metzler, *J. Am. Chem. Soc.* **1994**, *116*, 2691.

[56] M. Denk, J. C. Green, N. Metzler, M. Wagner, *J. Chem. Soc., Dalton Trans.* **1994**, 2405.

[57] T. A. Schmedake, M. Haaf, Y. Apeloig, T. Müller, S. Bukalov, R. West, *J. Am. Chem. Soc.* **1999**, *121*, 9479.

[58] a) B. Gehrhus, M. F. Lappert, J. Heinicke, R. Boese, D. Blaser, *J. Chem. Soc., Chem. Commun.* **1995**, 1931; b) J. Heinicke, A. Oprea, M. K. Kindermann, T. Karpati, L. Nyulászi, T. Veszprémi, *Chem. Eur. J.* **1998**, *4*, 541; B. c) Gehrhus, P. B. Hitchcock, M. F. Lappert, *Z. Anorg. Allg. Chem.* **2005**, *631*, 1383.

[59] B. Gehrhus, P. B. Hitchcock, M. F. Lappert, *J. Chem. Soc., Dalton Trans.* **2000**, 3094.

[60] W. Marco Boesveld, B. Gehrhus, P. B. Hitchcock, M. F. Lappert, P. von R. Schleyer, *J. Chem. Soc., Chem. Commun.* **1999**, 755.

[61] M. Driess, S. Yao, M. Brym, C. van Wüllen, D. Lentz, *J. Am. Chem. Soc.* **2006**, *128*, 9628.

[62] Y. Xiong, S. Yao, M. Driess, *J. Am. Chem. Soc.* **2009**, *131*, 7562.

[63] C.-W. So, H. W. Roesky, J. Magull, R. B. Oswald, *Angew. Chem.* **2006**, *118*, 4052.

[64] C.-W. So, H. W. Roesky, J. Magull, R. B. Oswald, *Angew. Chem. Int. Ed.* **2006**, *45*, 3948.

[65] S. S. Sen, H. W. Roesky, D. Stern, J. Henn, D. Stalke, *J. Am. Chem. Soc.* **2009**, *132*, 1123.

[66] a) M. Kira, S. Ishida, T. Iwamoto, C. Kabuto, *J. Am. Chem. Soc.* **1999**, *121*, 9722; b) M. Kira, T. Iwamoto, S. Ishida, *Bull. Chem. Soc. Jpn.* **2007**, *80*, 258.

[67] a) A. Sekiguchi, T. Tanaka, M. Ichinohe, K. Akiyama, S. Tero-Kubota, *J. Am. Chem. Soc.* **2003**, *125*, 4962; b) M. C. Holthausen, W. Koch, Y. Apeloig, *J. Am. Chem. Soc.* **1999**, *121*, 2623; c) T. Tanaka, M. Ichinohe, A. Sekiguchi, *Chem. Lett.* **2004**, *33*, 1420.

[68] Y. Wang, Y. Xie, P. Wei, R. B. King, H. F. Schaefer, P. von R. Schleyer, G. H. Robinson, *Science* **2008**, *321*, 1069.

[69] K. Suzuki, T. Matsuo, D. Hashizume, K. Tamao, *J. Am. Chem. Soc.* **2011**, *133*, 19710.

[70] E. O. Fisher, A. Maasböl, *Angew. Chem.* **1964**, *76*, 645.

[71] R. R. Schrock, *J. Am. Chem. Soc.* **1974**, *96*, 6796.

[72] The Nobel Prize in Chemistry, **2005**. Y. Chauvin, R. H. Grubbs, R. R. Schrock. http://www.nobelprize.org/nobel_prizes/chemistry/laureates/2005/

[73] The Nobel Prize in Chemistry, **2010**. R. F. Heck, E. Negishi, A. Suzuki. http://www.nobelprize.org/nobel_prizes/chemistry/laureates/2010/

[74] a) H. K. Sharma, K. H. Pannell, *Chem. Rev.* **1995**, *95*, 1351; b) F. Gauvin, J. F. Harrod, H. G. Woo, *Adv. Organomet. Chem.* **1998**, *42*, 363; c) J. Y. Corey, *Adv. Organomet. Chem.* **2004**, *51*, 1; d) T. D. Tilley, *Comments Inorg. Chem.* **1990**, *10*, 37.

[75] P. B. Glaser, T. D. Tilley, *J. Am. Chem. Soc.* **2003**, *125*, 13640.

[76] G. Schnakenburg, Ph. D thesis, University of Bonn **2008**.

[77] R. Waterman, P. G. Hayes, T. D. Tilley, *Acc. Chem. Res.* **2007**, *40*, 712.

[78] a) C. Zybill, G. Müller, *Angew. Chem.* **1987**, *99*, 683; b) C. Zybill, G. Müller, *Angew. Chem. Int. Ed.* **1987**, *26*, 669.

[79] D. A. Straus, T. D. Tilley, A. L. Rheingold, S. J. Geib, *J. Am. Chem. Soc.* **1987**, *109*, 5872.

[80] K. Ueno, H. Tobita, M. Shimoi, H. Ogino, *J. Am. Chem. Soc.* **1988**, *110*, 4092.

[81] D. A. Straus, S. D. Grumbine, T. D. Tilley, *J. Am. Chem. Soc.* **1990**, *112*, 7801.

[82] a) P. B. Glaser, P. W. Wanandi, T. D. Tilley, *Organometallics* **2004**, *23*, 693; b) S. R. Klei, T. D. Tilley, R. G. Bergman, *Organometallics* **2002**, *21*, 4648; c) S. K. Grumbine, G. P. Mitchell, D. A. Straus, T. D. Tilley, A. L. Rheingold, *Organometallics* **1998**, *17*, 5607; d) G. P. Mitchell, T. D. Tilley, *J. Am. Chem. Soc.* **1998**, *120*, 7635; e) P. W. Wanandi, T. D. Tilley, *Organometallics* **1997**, *16*, 4299; f) S. D. Grumbine, T. D. Tilley, A. L. Rheingold, *J. Am. Chem. Soc.* **1993**, *115*, 358; g) S. D. Grumbine, T. D. Tilley, F. P. Arnold, A. L. Rheingold, *J. Am. Chem. Soc.* **1993**, *115*, 7884; h) D. A. Straus, C. Zhang, G. E. Quimbita, S. D. Grumbine, R. H. Heyn, T. D. Tilley, A. L. Rheingold, S. J. Geib, *J. Am. Chem. Soc.* **1990**, *112*, 2673.

[83] S. K. Grumbine, T. D. Tilley, F. P. Arnold, A. L. Rheingold, *J. Am. Chem. Soc.* **1994**, *116*, 5495.

[84] M. Haaf, T. A. Schmedake, R. West, *Acc. Chem. Res.* **2000**, *33*, 704.

[85] J. D. Feldman, G. P. Mitchell, J.-O. Nolte, T. D. Tilley, *J. Am. Chem. Soc.* **1998**, *120*, 11184.

[86] B. V. Mork, T. D. Tilley, A. J. Schultz, J. A. Cowan, *J. Am. Chem. Soc.* **2004**, *126*, 10428.

[87] a) B. V. Mork, T. D. Tilley, *Angew. Chem. Int. Ed.* **2003**, *42*, 357; b) B. V. Mork, T. D. Tilley, *Angew. Chem.* **2003**, *115*, 371.

[88] A. Shinohara, J. McBee, T. D. Tilley, *Inorg. Chem.* **2009**, *48*, 8081.

[89] B. V. Mork, T. D. Tilley, *J. Am. Chem. Soc.* **2001**, *123*, 9702.

[90] B. V. Mork, T. D. Tilley, *J. Am. Chem. Soc.* **2004**, *126*, 4375.

[91] T. Watanabe, H. Hashimoto, H. Tobita, *Angew. Chem.* **2004**, *116*, 220.

[92] P. G. Hayes, R. Waterman, P. B. Glaser, T. D. Tilley, *Organometallics* **2009**, *28*, 5082.

[93] M. Ochiai, H. Hashimoto, H. Tobita, *Angew. Chem.* **2007**, *119*, 8340.

[94] a) P. G. Hayes, C. Beddie, M. B. Hall, R. Waterman, T. D. Tilley, *J. Am. Chem. Soc.* **2005**, *128*, 428; b) P. B. Glaser, T. D. Tilley, *Organometallics* **2004**, *23*, 5799.

[95] a) J. D. Feldman, J. C. Peters, T. D. Tilley, *Organometallics* **2002**, *21*, 4065; b) J. C. Peters, J. D. Feldman, T. D. Tilley, *J. Am. Chem. Soc.* **1999**, *121*, 9871.

[96] a) G. P. Mitchell, T. D. Tilley, *Angew. Chem.* **1998**, *110*, 2602; b) G. P. Mitchell, T. D. Tilley, *Angew. Chem. Int. Ed.* **1998**, *37*, 2524.

[97] a) H. Hashimoto, A. Matsuda, H. Tobita, *Chem. Lett.* **2005**, *34*, 1374; b) H. Tobita, A. Matsuda, H. Hashimoto, K. Ueno, H. Ogino, *Angew. Chem.* **2004**, *116*, 223.

[98] H. Hashimoto, J. Sato, H. Tobita, *Organometallics* **2009**, *28*, 3963.

[99] a) E. Suzuki, T. Komuro, Y. Kanno, M. Okazaki, H. Tobita, *Organometallics* **2010,** *29*, 5296; b) E. Suzuki, T. Komuro, M. Okazaki, H. Tobita, *Organometallics* **2009**, *28*, 1791.

[100] E. Suzuki, M. Okazaki, H. Tobita, *Chem. Lett.* **2005**, *34*, 1026.

[101] N. Nakata, T. Fujita, A. Sekiguchi, *J. Am. Chem. Soc.* **2006**, *128*, 16024.

[102] E. O. Fischer, G. Kreis, C. G. Kreiter, J. Mülle, G. Huttner, H. Lorenz, *Angew. Chem.* **1973**, *85*, 618.

[103] J. H. Wengrovius, J. Sancho, R. R. Schrock, *J. Am. Chem. Soc.* **1981**, *103*, 3932.

[104] R. S. Simons, P. P. Power, *J. Am. Chem. Soc.* **1996**, *118*, 11966.

[105] L. Pu, B. Twamley, S. T. Haubrich, M. M. Olmstead, B. V. Mork, R. S. Simons, P. P. Power, *J. Am. Chem. Soc.* **2000**, *122*, 650.

[106] A. C. Filippou, A. I. Philippopoulos, P. Portius, D. U. Neumann, *Angew. Chem. Int. Ed.* **2000**, *39*, 2778.

[107] A. C. Filippou, P. Portius, A. I. Philippopoulos, *Organometallics* **2002**, *21*, 653.

[108] a) A. C. Filippou, P. Portius, A. I. Philippopoulos, H. Rohde, *Angew. Chem. Int. Ed.* **2003**, *42*, 445; b) A. C. Filippou, A. I. Philippopoulos, G. Schnakenburg, *Organometallics* **2003**, *22*, 3339; c) A. C. Filippou, H. Rohde, G. Schnakenburg, *Angew. Chem. Int. Ed.* **2004**, *43*, 2243; d) A. C. Filippou, N. Weidemann, G. Schnakenburg, H. Rohde, A. I. Philippopoulos, *Angew. Chem. Int. Ed.* **2004**, *43*, 6512; e) A. C. Filippou, N. Weidemann, A. I. Philippopoulos, G. Schnakenburg, *Angew. Chem. Int. Ed.* **2006**, *45*, 5987; f) A. C. Filippou, N. Weidemann, G. Schnakenburg, *Angew. Chem. Int. Ed.* **2008**, *47*, 5799.

[109] A. C. Filippou, G. Schnakenburg, A. I. Philippopoulos, N. Weidemann, *Angew. Chem. Int. Ed.* **2005**, *44*, 5979.

[110] U. Chakraborty, poster, Wöhlertagung, Freiburg, **2010**.

[111] B. Blom, *Dissertation*, University of Bonn, **2011**.

[112] D. Geiß, *Diploma thesis*, University of Bonn, **2011**.

[113] P. Jutzi, C. Leue, *Organometallics* **1994**, *13*, 2898.

[114] S. Inoue, M. Driess, *Organometallics* **2009**, *28*, 5032.

[115] C. Jones, R. P. Rose, A. Stasch, *Dalton Trans.* **2008**, 2871.

[116] H. Lei, J.-D. Guo, J. C. Fettinger, S. Nagase, P. P. Power, *Organometallics* **2011**.

[117] S. D. Grumbine, R. K. Chadha, T. D. Tilley, *J. Am. Chem. Soc.* **1992**, *114*, 1518.

[118] N. Takagi, K. Yamazaki, S. Nagase, *Bull. Korean Chem. Soc.* **2003**, *24*, 832.

[119] K. K. Pandey, A. Lledos, *Inorg. Chem.* **2009**, *48*, 2748.

[120] a) T. Pilati, M. Simonetta, *Acta Cryst.* **1984**, *C40*, 1407; b) F. E. Hahn, L. Wittenbecher, D. Le Van, R. Fröhlich, *Angew. Chem. Int. Ed.* **2000**, *39*, 541.

[121] a) A. J. Arduengo, R. Krafczyk, R. Schmutzler, H. A. Craig, J. R. Goerlich, W. J. Marshall, M. Unverzagt, *Tetrahedron* **1999**, *55*, 14523.

[122] T. Iijima, H. Jimbo, M. Taguchi, *J. Mol. Struct.* **1986**, *144*, 191.

[123] R. S. Ghadwal, S. S. Sen, H. W. Roesky, G. Tavcar, S. Merkel, D. Stalke, *Organometallics* **2009**, *28*, 6374.

[124] a) A. C. Filippou, O. Chernov, G. Schnakenburg, *Angew. Chem. Int. Ed.* **2009**, *48*, 5687; b) A. C. Filippou, O. Chernov, G. Schnakenburg, *Angew. Chem.* **2009**, *121*, 5797.

[125] Y. Xiong, S. L. Yao, M. Driess, *Chem. – Asian J.* **2010**, *5*, 322.

[126] a) A. G. Brook, S. C. Nyburg, F. Abdesaken, B. Gutekunst, G. Gutekunst, R. Krishna, M. R. Kallury, Y. C. Poon, Y. M. Chang, W. N. Winnie, *J. Am. Chem. Soc.* **1982**, *104*, 5667; b) N. Wiberg, G. Wagner, G. Muller, *Angew. Chem.* **1985**, *24*, 229; c) D. Bravo-Zhivotovskii, R. Dobrovetsky, D. Nemirovsky, V. Molev, M. Bendikov, G. Molev, M. Botoshansky, Y. Apeloig, *Angew. Chem.* **2008**, *120*, 4415.

[127] V. Jonas, G. Frenking, M. T. Reetz, *J. Am. Chem. Soc.* **1994**, *116*, 8741.

[128] D. Seyferth, *Organometallics* **2001**, *20*, 4978.

[129] a) B. E. Eichler, L. Pu, M. Stender, P. P. Power, *Polyhedron* **2001**, *20*, 551; b) L. Pu, M. M. Olmstead, P. P. Power, B. Schiemenz, *Organometallics* **1998**, *17*, 5602; c) R. S. Simons, L. Pu, M. M. Olmstead, P. P. Power, *Organometallics* **1997**, *16*, 1920.

[130] R. Pietschnig, R. West, D. R. Powell, *Organometallics* **2000**, *19*, 2724.

[131] a) H. Cui, Y. Shao, X. Li, L. Kong, C. Cui, *Organometallics* **2009**, *28*, 5191; b) Y. H. Gao, J. Y. Zhang, H. F. Hu, C. M. Cui, *Organometallics* **2010**, *29*, 3063.

[132] C. Cui, H. Cui, Y. Shao, X. Li, L. Kong, J. Zhang, **2009**, Patent CN 101602774 (A)

[133] R. S. Simons, S. T. Haubrich, B. V. Mork, M. Niemeyer, P. P. Power, *Main Group Chem.* **1998**, *2*, 275.

[134] N. Weidemann, G. Schnakenburg, A. C. Filippou, *Z. Anorg. Allg. Chem.* **2009**, *635*, 253.

[135] A. C. Filippou, O. Chernov, B. Blom, K. W. Stumpf, G. Schnakenburg, *Chem. Eur. J.* **2010**, *16*, 2866.

[136] a) R. D. Baechler, K. Mislow, *J. Am. Chem. Soc.* **1970**, *92*, 3090; b) A. Rauk, J. D. Andose, W. G. Frick, R. Tang, K. Mislow, *J. Am. Chem. Soc.* **1971**, *93*, 6507.

[137] G. C. Levy, D. M. White, J. D. Cargioli, *J. Magn. Reson.* **1972**, *8*, 280.

[138] J. Braddock-Wilking, Y. Zhang, J. Y. Corey, N. P. Rath, *J. Organomet. Chem.* **2008**, *693*, 1233.

[139] J. Yang, I. Guzei, J. G. Verkade, *J. Organomet. Chem.* **2002**, *649*, 276.

[140] P. Jutzi, D. Kanne, M. Hursthouse, A. J. Howes, *Chem. Ber.* **1988**, *121*, 1299.

[141] a) A. Schmidpeter, S. Lochschmidt, K. Karaghiosoff, W. S. Sheldrick, *J. Chem. Soc., Chem. Commun.* **1985**, 1447; b) K. Hensen, T. Stumpf, M. Bolte, C. Näther, H. Fleischer, *J. Am. Chem. Soc.* **1998**, *120*, 10402; c) N. Furukawa, S. Sato, *Heteroat. Chem.* **2002**, *13*, 406; d) J. D. Burton, R. M. K. Deng, K. B. Dillon, P. K. Monks, R. J. Olivey, *Heteroat. Chem.* **2005**, *16*, 447; e) J. L. Dutton, H. M. Tuononen, M. C. Jennings, P. J. Ragogna, *J. Am. Chem. Soc.* **2006**, *128*, 12624; f) D. Vidovic, M. Findlater, A. H. Cowley, *J. Am. Chem. Soc.* **2007**, *129*, 8436; g) P. A. Rupar, V. N. Staroverov, K. M. Baines, *Science* **2008**, *322*, 1360.

[142] P. A. Rupar, V. N. Staroverov, P. J. Ragogna, K. M. Baines, *J. Am. Chem. Soc.* **2007**, *129*, 15138.

[143] J. J. Weigand, K.-O. Feldmann, F. D. Henne, *J. Am. Chem. Soc.*, *132*, 16321.

[144] M. Driess, S. Yao, M. Brym, C. van Wüllen, *Angew. Chem.* **2006**, *118*, 6882.

[145] A. Bondi, *J. Phys. Chem.* **1964**, *68*, 441.

[146] P. A. Rupar, M. C. Jennings, K. M. Baines, *Organometallics* **2008**, *27*, 5043.

[147] P. Pyykkö, M. Atsumi, *Chem. Eur. J.* **2009**, *15*, 186.

[148] T. Yamaguchi, A. Sekiguchi, M. Driess, *J. Am. Chem. Soc.* **2010**, *132*, 14061.

[149] Y. Liu, D. Ballweg, T. Müller, I. A. Guzei, R. W. Clark, R. West, *J. Am. Chem. Soc.* **2002**, *124*, 12174.

[150] a) S. P. Downing, A. A. Danopoulos, *Organometallics* **2006**, *25*, 1337; b) P. L. Arnold, S. T. Liddle, *Organometallics* **2006**, *25*, 1485.

[151] a) M. Gartner, H. Gorls, M. Westerhausen, *Acta Cryst.* **2007**, *E63*, m2289; b) X. He, B. C. Noll, A. Beatty, R. E. Mulvey, K. W. Henderson, *J. Am. Chem. Soc.* **2004**, *126*, 7444.

[152] A. J. Arduengo III, F. Davidson, R. Krafczyk, W. J. Marshall, R. Schmutzler, *Monatshefte für Chemie* **2000**, *131*, 251.

[153] a) Y. Xiong, S. Yao, M. Brym, M. Driess, *Angew. Chem.* **2007**, *119*, 4595; b) J. D. Masuda, W. W. Schoeller, B. Donnadieu, G. Bertrand, *Angew. Chem.* **2007**, *119*, 7182; c) Y. Peng, H. Fan, H. Zhu, H. W. Roesky, J. Magull, C. E. Hughes, *Angew. Chem.* **2004**, *116*, 3525.

[154] a) A. C. Filippou, O. Chernov, G. Schnakenburg, *Angew. Chem. Int. Ed.* **2011**, *50*, 1122; b) A. C. Filippou, O. Chernov, G. Schnakenburg, *Angew. Chem.* **2011**, *123*, 1154.

[155] A. C. Filippou, A. I. Philippopoulos, P. Portius, G. Schnakenburg, *Organometallics* **2004**, *23*, 4503.

[156] M. Hirotsu, T. Nunokawa, K. Ueno, *Organometallics* **2006**, *25*, 1554.

[157] S. H. A. Petri, D. Eikenberg, B. Neumann, H.-G. Stammler, P. Jutzi, *Organometallics* **1999**, *18*, 2615.

[158] S. B. Clendenning, B. Gehrhus, P. B. Hitchcock, D. F. Moser, J. F. Nixon, R. West, *J. Chem. Soc., Dalton Trans.* **2002**, 484.

[159] A. C. Filippou, D. Wössner, G. KociokKohn, I. Hinz, *J. Organomet. Chem.* **1997**, *541*, 333.

[160] a) A. C. Filippou, O. Chernov, K. W. Stumpf, G. Schnakenburg, *Angew. Chem.* **2010**, *122*, 3368; b) A. C. Filippou, O. Chernov, K. W. Stumpf, G. Schnakenburg, *Angew. Chem. Int. Ed.* **2010**, *49*, 3296.

[161] N. Kuhn, T. Kratz, D. Bläser, R. Boese, *Chem. Ber.* **1995**, *128*, 245.

[162] P. Pyykkö, M. Atsumi, *Chem. Eur. J.* **2009**, *15*, 12770.

[163] T. A. Schmedake, M. Haaf, B. J. Paradise, A. J. Millevolte, D. R. Powell, R. West, *J. Organomet. Chem.* **2001**, *636*, 17.

[164] G. N. Glavee, B. R. Jagirdar, J. J. Schneider, K. J. Klabunde, L. J. Radonovich, K. Dodd, *Organometallics* **1992**, *11*, 1043.

[165] B. Rees, A. Mitschler, *J. Am. Chem. Soc.* **1976**, *98*, 7918.

[166] A. C. Filippou, O. Chernov, G. Schnakenburg, *Chem. Eur. J.* **2011**, *17*, 13574.

[167] K. Takanashi, V. Y. Lee, T. Yokoyama, A. Sekiguchi, *J. Am. Chem. Soc.* **2009**, *131*, 916.

[168] K. Ueno, S. Asami, N. Watanabe, H. Ogino, *Organometallics* **2002**, *21*, 1326.

[169] a) S. H. A. Petri, B. Neumann, H.-G. Stammler, P. Jutzi, *J. Organomet. Chem.* **1998**, *553*, 317; b) T. S. Koloski, D. C. Pestana, P. J. Carroll, D. H. Berry, *Organometallics* **1994**, *13*, 489.

[170] C. Ackerhans, P. Böttcher, P. Müller, H. W. Roesky, I. Usón, H.-G. Schmidt, M. Noltemeyer, *Inorg. Chem.* **2001**, *40*, 3766.

[171] a) A. Sekiguchi, R. Kinjo, M. Ichinohe, *Science* **2004**, *305*, 1755; b) Y. Murata, M. Ichinohe, A. Sekiguchi, *J. Am. Chem. Soc.* **2010**, *132*, 16768.

[172] a) H. Fan, D. Adhikari, A. A. Saleh, R. L. Clark, F. J. Zuno-Cruz, G. Sanchez Cabrera, J. C. Huffman, M. Pink, D. J. Mindiola, M.-H. Baik, *J. Am. Chem. Soc.* **2008**, *130*, 17351; b) G. N. Glavee, B. R. Jagirdar, J. J. Schneider, K. J. Klabunde, L. J. Radonovich, K. Dodd, *Organometallics* **1992**, *11*, 1043; c) B. R. Jagirdar, K. J. Klabunde, R. Palmer, L. J. Radonovich, *Inorg. Chim. Acta* **1996**, *250*, 317; d) B. R. Jagirdar, R. Palmer, K. J. Klabunde, L. J. Radonovich, *Inorg. Chem.* **1995**, *34*, 278.

[173] a) T. Watanabe, H. Hashimoto, H. Tobita, *Organometallics* **2004**, *23*, 4150; b) G. I. Nikonov, L. G. Kuzmina, S. F. Vyboishchikov, D. A. Lemenovskii, J. A. K. Howard, *Chem. Eur. J.* **1999**, *5*, 2947; c) K. Y. Dorogov, E. Dumont, N.-N. Ho, A. V. Churakov, L. G. Kuzmina, J.-M. Poblet, A. J. Schultz, J. A. K. Howard, R. Bau, A. Lledos, G. I. Nikonov, *Organometallics* **2004**, *23*, 2845; d) M. Theil, P. Jutzi, B. Neumann, A. Stammler, H.-G. Stammler, *Organometallics* **2000**, *19*, 2937.

[174] A. C. Filippou, D. Wössner, B. Lungwitz, G. KociokKohn, *Angew. Chem. Int. Ed. Engl.* **1996**, *35*, 876.

[175] R. Gleiter, D. B. Werz, F. Rominger, E. Zhutov, N. S. Zefirov, M. V. Proskurnina, *European Journal of Organic Chemistry* **2007**, *2007*, 5834.

[176] L. H. Doerrer, A. J. Graham, D. Haussinger, M. L. H. Green, *J. Chem. Soc., Dalton Trans.* **2000**, 813.

[177] A. C. Esqueda, S. Conejero, C. Maya, E. Carmona, *Organometallics* **2010**

29, 5481; J. L. McBee, T. D. Tilley, *Organometallics* **2009**, *28*, 5072.

[178] H. Sakaba, S. Watanabe, C. Kabuto, K. Kabuto, *J. Am. Chem. Soc.* **2003**, *125*, 2842.

[179] a) Yusuke Tanabe, Yoshiyuki Mizuhata, N. Tokitoh, *Pure Appl. Chem.* **2010**, *82*, 879; b) F. Delpech, S. Sabo-Etienne, B. Donnadieu, B. Chaudret, *Organometallics* **1998**, *17*, 4926; c) N. Peulecke, A. Ohff, P. Kosse, A. Tillack, A. Spannenberg, R. Kempe, W. Baumann, V. V. Burlakov, U. Rosenthal, *Chem. Eur. J.* **1998**, *4*, 1852.

[180] S. M. I. Al-Rafia, A. C. Malcolm, R. McDonald, M. J. Ferguson, E. Rivard, *Chem. Comm.* **2012**, *48*, 1308.

[181] A. C. Filippou, K. W. Stumpf, O. Chernov, G. Schnakenburg, *Organometallics* **2012**, *31*, 748.

[182] M. Falk, E. Whalley, *J. Chem. Phys.* **1961**, *34*, 1554.

[183] a) N. V. Belkova, E. I. Gutsul, O. A. Filippov, V. A. Levina, D. A. Valyaev, L. M. Epstein, A. Lledos, E. S. Shubina, *J. Am. Chem. Soc.* **2006**, *128*, 3486.

[184] A. C. Filippou, P. Portius, J. G. Winter, G. Kociok-Kohn, *J. Organomet. Chem.* **2001**, *628*, 11.

[185] G. A. Carriedo, V. Riera, M. L. Rodriguez, J. C. Jeffery, *J. Organomet. Chem.* **1986**, *314*, 139.

[186] W. Malisisch, R. Lankat, O. Fey, J. Reising, S. Schmitzer, *J. Chem. Soc., Chem. Commun.* **1995**, 1917.

[187] a) M. Denk, R. K. Hayashi, R. West, *J. Am. Chem. Soc.* **1994**, *116*, 10813; b) S. S. Zigler, K. J. Haller, R. West, M. S. Gordon, *Organometallics* **1989**, *8*, 1656.

[188] G. R. Fulmer, A. J. M. Miller, N. H. Sherden, H. E. Gottlieb, A. Nudelman, B. M. Stoltz, J. E. Bercaw, K. I. Goldberg, *Organometallics* **2010**, *29*, 2176.

[189] M. Weinmann, G. Rheinwald, L. Zsolnai, O. Walter, M. Büchner, B. Schiemenz, G. Huttner, H. Lang, *Organometallics* **1998**, *17*, 3299.

[190] a) J. E. Ellis, *Organometallics* **2003**, *22*, 3322; b) J. E. Ellis, *Inorg. Chem.* **2006**, *45*, 3167; c) J. E. Ellis, F. G. A. Stone, R. West, *Adv. Organomet. Chem.* **1990**, *31*, 1.

[191] G. M. Bodner, L. J. Todd, *Inorg. Chem.* **1974**, *13*, 1335.

[192] a) R. R. Schrock, *Polyhedron* **1995**, *14*, 3177; b) T. J. Katz, J. McGinnis, *J. Am. Chem. Soc.* **1975**, *97*, 1592.

[193] a) M. R. Churchill, J. W. Ziller, J. H. Freudenberger, R. R. Schrock, *Organometallics* **1984**, *3*, 1554; b) J. H. Freudenberger, R. R. Schrock, M. R. Churchill, A. L. Rheingold, J. W. Ziller, *Organometallics* **1984**, *3*, 1563.

[194] M. R. Churchill, J. W. Ziller, L. McCullough, S. F. Pedersen, R. R. Schrock, *Organometallics* **1983**, *2*, 1046.

[195] F. H. Allen, O. Kennard, D. G. Watson, L. Brammer, A. G. Orpen, R. Taylor, *Journal of the Chemical Society, Perkin Transactions 2* **1987**, S1.

[196] a) J. Braddock-Wilking, J. Y. Corey, K. A. Trankler, K. M. Dill, L. M. French, N. P. Rath, *Organometallics* **2004**, *23*, 4576; b) J. Braddock-Wilking, T. Bandrowsky, N. Praingam, N. P. Rath, *Organometallics* **2009**, *28*, 4098.

[197] a) W. P. Freeman, T. D. Tilley, A. L. Rheingold, *J. Am. Chem. Soc.* **1994**, *116*, 8428; b) J. M. Dysard, T. D. Tilley, *J. Am. Chem. Soc.* **1998**, *120*, 8245; c) J. M. Dysard, T. D. Tilley, *J. Am. Chem. Soc.* **2000**, *122*, 3097.

[198] M. G. B. Drew, V. Félix, I. S. Goncalves, C. C. Romao, B. Royo, *Organometallics* **1998**, *17*, 5782.

[199] Y. Zhang, B. Wang, S. Xu, X. Zhou, *Organometallics* **2001**, *20*, 3829.

[200] a) L. Lange, B. Meyer, W.-W. du Mont, *J. Organomet. Chem.* **1987**, *329*, C17; b) W. P. Neumann, *Chem. Rev.* **1991**, *91*, 311.

[201] M.-Z. Chen, H.-M. Sun, W.-F. Li, Z.-G. Wang, Q. Shen, Y. Zhang, *J. Organomet. Chem.* **2006**, *691*, 2489.

[202] J. Louie, R. H. Grubbs, *J. Chem. Soc., Chem. Commun.* **2000**, 1479.

[203] Y. Ohki, T. Hatanaka, K. Tatsumi, *J. Am. Chem. Soc.* **2008**, *130*, 17174.

[204] L. LePichon, D. W. Stephan, *Inorg. Chem.* **2001**, *40*, 3827.

[205] S. A. Llewellyn, M. L. H. Green, J. C. Green, A. R. Cowley, *Dalton Trans.* **2006**, 2535.

[206] M. Tilset, I. Fjeldahl, J.-R. Hamon, P. Hamon, L. c. Toupet, J.-Y. Saillard, K. Costuas, A. Haynes, *J. Am. Chem. Soc.* **2001**, *123*, 9984.

[207] E. J. Hawrelak, W. H. Bernskoetter, E. Lobkovsky, G. T. Yee, E. Bill, P. J. Chirik, *Inorg. Chem.* **2005**, *44*, 3103.

[208] a) P. R. Edwards, C. E. Jonson, *J. Chem. Phys.* **1967**, *47*, 2074; b) J. E. Barclay, G. J. Leigh, A. Houlton, J. Silver, *Dalton Trans.* **1988**, 2865.

[209] a) J. M. Smith, A. R. Sadique, T. R. Cundari, K. R. Rodgers, G. Lukat-Rodgers, R. J. Lachicotte, C. J. Flaschenriem, J. Vela, P. L. Holland, *J. Am. Chem. Soc.* **2005**, *128*, 756; b) P. L. Holland, *Acc. Chem. Res.* **2008**, *41*, 905.

[210] S. A. Stoian, J. Vela, J. M. Smith, A. R. Sadique, P. L. Holland, E. Münck, E. L. Bominaar, *J. Am. Chem. Soc.* **2006**, *128*, 10181.

[211] Y. Nakajima, Y. Nakao, S. Sakaki, Y. Tamada, T. Ono, F. Ozawa, *J. Am. Chem. Soc.* **2010**, *132*, 9934.

[212] a) Y. Yu, A. R. Sadique, J. M. Smith, T. R. Dugan, R. E. Cowley, W. W. Brennessel, C. J. Flaschenriem, E. Bill, T. R. Cundari, P. L. Holland, *J. Am. Chem. Soc.* **2008**, *130*, 6624; b) S. A. Stoian, Y. Yu, J. M. Smith, P. L. Holland, E. L. Bominaar, E. Münck, *Inorg. Chem.* **2005**, *44*, 4915.

[213] W. Malisch, R. Lankat, S. Schmitzer, R. Pikl, U. Posset, W. Kiefer, *Organometallics* **1995**, *14*, 5622.

[214] U.M.Tripathi, G.L.Wegner, A.Schier, A.Jockisch, H.Schmidbaur, *Z. Naturforsch.* **1998**, *53 b*, 939.

[215] R. Schwesinger, H. Schlemper, *Angew. Chem. Int. Ed. Engl.* **1987**, *26*, 1167.

[216] G. Brauer, *Handbuch der Präparativen Anorganischen Chemie*, Stuttgart, **1975**.

[217] N. Kuhn, T. Kratz, *Synthesis* **1993**, 561.

[218] L. Hintermann, *Beilstein Journal of Organic Chemistry* **2007**, *3*, 22.

[219] a) C. J. F. Du, H. Hart, K. K. D. Ng, *J. Org. Chem* **1986**, *51*, 3162; b) B. Schiemenz, P. P. Power, *Organometallics* **1996**, *15*, 958.

[220] O. T. Beachley, R. Blom, M. R. Churchill, K. Faegri, J. C. Fettinger, J. C. Pazik, L. Victoriano, *Organometallics* **1989**, *8*, 346.

[221] G. Winter, *Inorg. Synth.* **1973**, *14*, 102.

[222] N. Weidemann, *Dissertation*, Humbolt University of Berlin, **2008**.

[223] I. Krossing, *Chem. Eur. J.* **2001**, *7*, 490; I. Krossing, A. Reisinger, *Coord. Chem. Rev.* **2006**, *250*, 2721.

[224] a) N. A. Yakelis, R. G. Bergman, *Organometallics* **2005**, *24*, 3579; b) D. L. Reger, C. A. Little, J. J. S. Lamba, K. J. Brown, *Inorg. Synth.* **2004**, *34*, 5.

[225] J. L. W. Pohlmann, F. E. Brinckmann, *Z. Naturforschung B.* **1965**, *20*, 5.

[226] J. B. Lambert, S. Zhang, S. M. Ciro, *Organometallics* **1994**, *13*, 2430.

[227] a) M. Faure, L. Maurette, B. Donnadieu, G. Lavigne, *Angew. Chem. Int. Ed.* **1999**, *38*, 518; b) M. Faure, L. Maurette, B. Donnadieu, G. Lavigne, *Angew. Chem.* **1999**, *111*, 539; c) G. O. Nelson, C. E. Sumner, *Organometallics* **1986**, *5*, 1983.

[228] M. L. Luetkens, A. P. Sattelberger, H. H. Murray, J. D. Basil, J. P. Fackler, *Inorg. Synth.* **1989**, *26*, 7.

[229] R. E. Palermo, R. Singh, J. K. Bashkin, R. H. Holm, *J. Am. Chem. Soc.* **1984**, *106*, 2600.

[230] J. K. Cammack, S. Jalisatgi, A. J. Matzger, A. NegrÃ³n, K. P. C. Vollhardt, *J. Org. Chem* **1996**, *61*, 4798.